TESIS DE DOCTORADO

TRANSITION METAL PROMOTED TRANSFORMATIONS OF ALKYLIDENECYCLOPROPANES

Felipe Ignacio Verdugo Leal

ESCUELA DE DOCTORADO INTERNACIONAL

PROGRAMA DE DOCTORADO EN CIENCIA Y TECNOLOGÍA QUÍMICA

SANTIAGO DE COMPOSTELA

2020

USC
UNIVERSIDADE
DE SANTIAGO
DE COMPOSTELA

DECLARACIÓN DEL AUTOR DE LA TESIS

Transition Metal Promoted Transformations of Alkylidenecyclopropanes

D. Felipe Ignacio Verdugo Leal

Presento mi tesis, siguiendo el procedimiento adecuado al Reglamento, y declaro que:

1) *La tesis abarca los resultados de la elaboración de mi trabajo.*
2) *En su caso, en la tesis se hace referencia a las colaboraciones que tuvo este trabajo.*
3) *La tesis es la versión definitiva presentada para su defensa y coincide con la versión enviada en formato electrónico.*
4) *Confirmo que la tesis no incurre en ningún tipo de plagio de otros autores ni de trabajos presentados por mí para la obtención de otros títulos.*

En Santiago de Compostela, 11 de Febrero de 2020

Fdo. Felipe Ignacio Verdugo Leal

USC
UNIVERSIDADE
DE SANTIAGO
DE COMPOSTELA

AUTORIZACIÓN DEL DIRECTOR / TUTOR DE LA TESIS

Transition Metal Promoted Transformations of Alkylidenecyclopropanes

D. José Luis Mascareñas Cid

D. Fernando López García

INFORMA/N:

Que la presente tesis, corresponde con el trabajo realizado por D. ***Felipe Ignacio Verdugo Leal****, bajo mi dirección, y autorizo su presentación, considerando que reúne los requisitos exigidos en el Reglamento de Estudios de Doctorado de la USC, y que como director de ésta no incurre en las causas de abstención establecidas en Ley 40/2015.*

En Santiago de Compostela, 11 de Febrero de 2020

Fdo. José Luis Mascareñas Cid

Fdo. Fernando López García

USC
UNIVERSIDADE
DE SANTIAGO
DE COMPOSTELA

Aknowledgments

Me gustaría agradecer en primer lugar, a mis directores de tesis José Luis Mascareñas y Fernando López, por aceptarme en el grupo y guiarme durante estos años. A ambos los considero profesionales y personas excepcionales, y me honra haber trabajado con ustedes. También un agradecimiento especial a la Prof. Cristina Nevado de la Universidad de Zürich, por abrirme un espacio en su grupo y permitirme conocer a toda esa gente maravillosa. Fue una experiencia que nunca voy a olvidar. Muchas gracias. Y por supuesto también agradecer al Dr. Moisés Gulías, quien me apoyó durante estos años de trabajo, en particular en la gestión de mi viaje a Zürich.

A los Prof. Victor Kesternich y Marcia Pérez-Fehrmann que, de no haber sido por su apoyo incondicional, no habría podido llegar hasta aquí. Gracias por creer en mí. A mi amigo Ronald Nelson, quien me ha ayudado en cada paso que he dado como químico. Estoy seguro de que nos espera mucho trabajo juntos en el futuro.

Quiero también *sentidamente* agradecer, *y pedir perdón*, a mi hijo Vicente. Sé que para obtener cosas en la vida hay que dar algo a cambio, y para realizar este doctorado, tuve que sacrificar mi tiempo contigo. Tiempo que no se puede recuperar. Desde que naciste, has sido un motor fundamental para todas las cosas que he hecho. Te quiero como no te imaginas hijo. Siempre voy a estar aquí, para lo que necesites. También me gustaría agradecer a Gabriela Salazar. Por cuidar de nuestro hijo durante estos años, y permitirme estar siempre a su lado. Te lo agradeceré siempre.

Extiendo también este agradecimiento a toda mi familia. Nico, nos hicimos mucha falta, pero ese tiempo se puede recuperar. Siempre puedes contar conmigo hermano <3. A mi hermana Francisca, quien siempre ha estado ahí en momentos de dificultad. Has cumplido tu rol de hermana mayor de manera impecable, te quiero mucho. A mi hermano Gonzalo, que siempre ha estado presente en mi vida, en momentos buenos y malos. A mi Papá, por su amor incondicional de padre. No sé si podría haber tenido un mejor papá. De ti aprendí mucho. Te quiero y admiro. Y finalmente, y no menos importante, a mi querida Madre. Siempre nos llevamos mal, porque somos iguales. De ti aprendí el rigor, la constancia y la dedicación a lo que uno hace. Te quiero mucho, mamá.

También me gustaría agradecer especialmente a Tania, por quererme y *aguantarme*. Se que soy una persona un poco difícil, y aun así no me has dejado solo en ningún momento. Desde que te conocí, todo se ha hecho más fácil y llevadero. Espero que me sigas aguantando un poco más. Te quiero mucho <3.

Quiero también agradecer a todas las personas que hicieron posible mi supervivencia fuera de Chile. A mi BFF local, Jaime Fernández, por hacerme perder el tiempo tantas veces, haciéndome significativamente menos eficiente (a veces no es bueno trabajar tanto). A mi amigo Marc Font, a quien considero referente como químico y como persona, y que siempre está ahí para aconsejarme. A mi hermanita Federica Novelli a quien quiero mucho (aunque se le vaya la olla muchísimo). Sé que nuestra amistad va a durar muuuucho

tiempo. A Andrés Seoane, que, aunque tu amistad implique un ejercicio de paciencia constante, vale mucho la pena. A Popi y a Laia, que siempre han sido un bálsamo para desintoxicarme un poco de esta gente que solo habla de química. Y a tres mujeres quienes admiro mucho profesionalmente. A Soraya Learte, no solo por ser parte fundamental del eje del mal, sino que también por ser una amiga y científica excepcional. A Eva Rivera. Siempre lo he dicho: nuestro grupo perdió una científica de primer nivel al dejarte ir. A Sandra Arias, por ser una persona maravillosa y profesional excelente. *El mundo -científico- necesita mujeres fuertes como ustedes.*

Also I would like to thank to all the people that I met during my stay in Zürich. First, to my dear friends Alexandre Genoux, Cédric Hervieu and Hélène Beucher. I had an amazing time in Zürich because of you. Thank you for everything guys <3. To Andrea Schmidt and Céline Friedrich for reciving me at their home and for being so wonderful with me. To Roopender Kumar, who teached me "the arts" of gold chemistry. Thanks for your guide. To Giulia, Tamara, Andres, Felix, Sven, Gianna and all the people that I met in Zürich. Thank you for everything.

A mis compis de laboratorio. Todos, sin excepción, han colaborado de alguna manera a hacerme sentir acogido. En primer lugar, a Ricardo Rodiño (gracias por aguantarme durante el TFM) y Eduardo Da Concepción. Muchas gracias por su colaboración en el laboratorio, me siento honrado de compartir trabajos con ustedes. Especial agradecimiento también a María Rey (gracias por la eterna paciencia) y a Adrián Jiménez. También a los investigadores senior María Tomás, Cristian Vidal y Jose Couceiro. Siempre es un gusto ver gente tan comprometida y con tanto talento. También agradecer a mis compañeros David Fernandez, Ivan Varela, Borja Cendón, Andy Arribas, Xandro Vidal, Joan Ávila, Noelia Casanova, Helio Faustino, David Cagiao, Alejandro Gutierrez y José González con quienes compartí mucho tiempo de laboratorio. En las familias hay momentos buenos y malos, y como grupo siempre hemos sido una gran familia (a veces un poco disfuncional).

Desde que dejé la carrera de ingeniería y me cambié a química, ha sido un viaje largo y difícil, pero también muy revelador. Siempre me he considerado una persona privilegiada por haber descubierto la química a tiempo, por haber encontrado algo que me apasionara y me impulsara siempre adelante. Se ganan cosas, se aprende mucho, pero también se pierden otras que pueden ser igual o más valiosas. Cuando ya está todo hecho, solo queda aceptar el resultado y pensar que las decisiones tomadas fueron las correctas.

Muchas gracias a TODAS las personas que he conocido durante estos 6 años. A todos ustedes, mis agradecimientos.

Thank you very much to ALL the people that I met during these 6 years. To all of you, my deep aknowledgments.

Dedicated to my son, Vicente.

USC
UNIVERSIDADE
DE SANTIAGO
DE COMPOSTELA

Table of contents

USC
UNIVERSIDADE
DE SANTIAGO
DE COMPOSTELA

Abbreviations and acronyms

Ac	Acetyl/CH_3CO-
ACP	Alkylidenecyclopropane
AcOH	Acetic acid
BAr^F	Tetrakis[3,5-bis(trifluoromethyl)phenyl] borate
BINAP	2,2′-Bis(diphenylphosphino)-1,1′-binaphthalene
BINOL	1,1′-Bi(2-naphthol)
Bn	Benzyl/$C_6H_5CH_2$
Boc	*tert*-Butyloxycarbonyl
br	Broad
BrettPhos	2-(Dicyclohexylphosphino) 3,6-dimethoxy-2′,4′,6′-triisopropyl-1,1′-biphenyl
BzO	Benzoyl/C_6H_5CO-
BzOH	Benzoic acid
COD	1,5-cyclooctadiene
Cy	Cyclohexyl
d	Doublet
dd	Double doublet
ddd	Doublet of doublet of doublets
dq	Doublet of quartet
dt	Doublet of triplets
dba	dibenzylideneacetone
DAD	Diode array detector
DBU	1,8-Diazabicyclo[5.4.0]undec-7-ene
DCE	1,2-dichloroethane
DFT	Density functional theory
DMAP	4-dimethylaminopyridine
DME	Dimethoxy ethane
DMEDA	N,N′-Dimethylethylene diamine
DMF	*N,N*-dimethyl formamide
DMSO	Dimethyl sulfoxide
dr	Diastereomeric ratio
DTBP	2,6-di-*tert*-butyl pyridine
DuPhos	(−)-1,2-Bis[(2*R*,5*R*)-2,5-dimethylphospholano]-benzene
EDG	Electron-donating group
ee	Enantiomeric excess
eq/equiv	Equivalents
er	Enantiomeric ratio
ESI	Electrospray
EWG	Electron-withdrawing group
GC-MS	Gas chromatography mass spectrometry
HOMO	Highest occupied molecular orbital
HPLC	High performance liquid chromatography
HRMS	High resolution mass spectra
IPr	1,3-Bis(2,6-diisopropylphenyl)imidazol-2-ylidene
JohnPhos	(2-Biphenyl)di-tert-butylphosphine
LRMS	Low resolution mass spectra
LUMO	Lowest unoccupied molecular orbital
m	Multiplet
MCP	Methylenecyclopropane
min	Minute/s
Ms	Methanesulfonyl/Mesyl
MS	Molecular sieves
MTBE	Methyl-*tert*-butyl ether
n.a.	Not available
nOe	Nuclear Overhauser effect
NTf_2	bis(trifluoromethanesulfonyl) imide
NHC	*N*-heterocyclic carbene
NMR	Nuclear magnetic resonance
p	Pentet
PDC	Pyridinium dichromate
PG	Protecting group
phen	1,10-phenanthroline
PivO	Pivaloyl/$(CH_3)_3CCO$-
$P(O\text{-}o\text{-}biPh)_3$	tris(2-phenylphenyl)phosphite
p-TsOH	*para*-toluenesulfonic acid
Pyr	Pyridine
q	Quartet
qd	Quartet of doublets
rt	Room temperature

RuPhos	2-Dicyclohexylphosphino-2′,6′-diisopropoxybiphenyl
s	Singlet
SOMO	Singly occupied molecular orbital
SPhos	2-Dicyclohexylphosphino-2′,6′-dimethoxybiphenyl
SPINOL	2,2',3,3'-tetrahydro-1,1'-spirobi[indene]-7,7'-diol
t	Triplet
t	time
T	Temperature
ta	"Temperatura ambiente"
TBDPS	*tert*-butyldiphenylsilyl
TBS	*tert*-butyldimethylsilyl
tBuBrettPhos	2-(Di-tert-butylphosphino)-2′,4′,6′- triisopropyl-3,6-dimethoxy-1,1′-biphenyl
tBuXPhos	2-Di-tert-butylphosphino-2′,4′,6′-triisopropylbiphenyl
td	Triple doublet
TFA	Trifluoroacetic acid
Tf	Trifluoromethanesulfonyl
THF	Tetrahydrofuran
THP	Tetrahydropyran
TIPS	Triisopropylsilyl
TLC	Thin layer chromatography
TMS	Trimethylsilyl
TMM	Trimethylenemethane
Tol	Tolyl
Ts	*para*-toluenesulfonyl/Tosyl
VAPOL	2,2′-Diphenyl-(4-biphenanthrol)
VANOL	3,3′-Diphenyl-2,2′-bi-1-naphthalol
VCP	Vinylcyclopropane
Xantphos	4,5-Bis(diphenylphosphino)-9,9-dimethylxanthene
XPhos	2-Dicyclohexylphosphino-2′,4′,6′-triisopropylbiphenyl

Disclaimer

Throughout this thesis, when referring to cycloadditions we use the Huisgen notation, using parenthesis, where the numbers refer to the atoms involved in the forming ring (for instance in (4+3), (4+2), (2+2) cycloadditions) to distinguish from the Woodward-Hoffman notation, using brackets, where the numbers refer to the electrons involved in bonding changes.[1] However, in some specific examples we use the brackets notation that is also acceptable.

[1] (a) R. Huisgen, *Angew. Chemie Int. Ed.* **1968**, *7*, 321. (b) J. Limanto, K. S. Khuong, K. N. Houk, M. L. Snapper, *J. Am. Chem. Soc.* **2003**, *125*, 16310.

USC
UNIVERSIDADE
DE SANTIAGO
DE COMPOSTELA

Preface

USC
UNIVERSIDADE
DE SANTIAGO
DE COMPOSTELA

Synthetic Chemistry in the XXI century

Science is the language that allows us to understand the architecture and functioning of the universe. Chemistry is, in particular, the branch of science responsible for studying the structure, properties and transformations of matter at a molecular level. Progress in this field has had an enormous influence in our life, and it is among the disciplines that has most contributed to increase our life span and quality.

Living entities are composed by organic molecules made by a bunch of atoms (C, H, O, N, P, S halogens and few others) which, with different distributions and configurations, provide infinite molecular possibilities. Many biologically important organic molecules, either natural or not, exhibit frequently complex polycyclic scaffolds, featuring several heteroatoms and stereogenic centers (Figure 1).[2,3] To further study the properties and applications of these molecules, it is extremely important to develop synthetic methodologies that allow to assemble their skeletons in a rapid and practical manner. These methodologies should also allow to make different analogs and scale up the protocols in order to prepare relatively high amounts of these compounds.

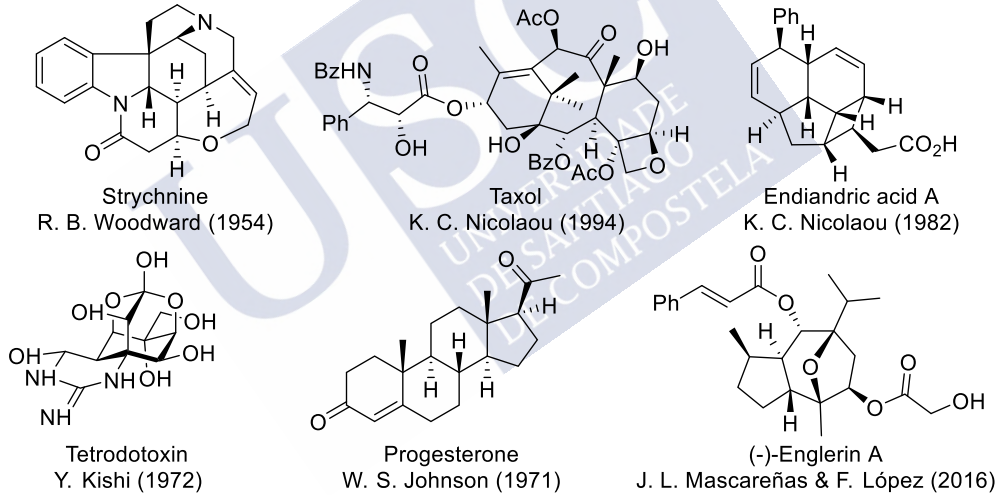

Figure 1. Examples of cyclic natural products with an important biological activity.

In this context, modern synthetic chemistry demands the development of processes that allow to increase the target-associated skeletal complexity in an efficient and sustainable way.[4] Indeed, we face a change in paradigm, and in the XXI century the development of synthetic processes that are efficient and green is mandatory. Thus, there are many aspects that must be considered in a synthetic programme, such as the use of cheap, non-toxic and readily

[2] (a) K. C. Nicolaou, E. J. Sorensen, *Classics in Total Synthesis: targets, strategies, methods*, Wiley-VCH, **1996**. (b) K. C. Nicolaou, S. A. Snyder, *Classics in Total Synthesis II: more targets, strategies, methods*, Wiley-VCH, **2003**. (c) E. J. Corey, J. J. Li, *Total Synthesis of Natural Products: At the Frontiers of Organic Chemistry*, Springer, **2012**.
[3] R. Nelson, M. Gulías, J. L. Mascareñas, F. López, *Angew. Chemie - Int. Ed.* **2016**, *55*, 14359.
[4] (a) P. A. Wender, B. Miller, *Nature* **2009**, *460*, 197. (b) P. A. Wender, *Tetrahedron* **2013**, *69*, 7529. (c) P. A. Wender, *Nat. Prod. Rep.* **2014**, *31*, 433. (d) T. Gaich, P. S. Baran, *J. Org. Chem.* **2010**, *75*, 4657. (e) T. Hudlicky, M. G. Natchus, *Organic synthesis: Theory and Applications*, Vol. 2, Ed.: JAI, Greenwich, CT, **1993**.

accessible starting materials and solvents, temperatures and pressures near to atmospheric values and the minimization of the amounts of waste. From the point of view of efficiency, the synthetic transformations should allow to increase molecular complexity with high overall yields and high structural control, leading to products that maximize the number of atoms transferred from the starting materials to the products, concept known as *atom economy*.

In this context, **Organometallic Chemistry** provides an impressive number of tools in the pursuit for the optimal organic synthesis. Traditional, metal free chemistry is somewhat limited by the stereoelectronic features of the reagents, and the reactivity modes are pre-established. The use of metals offers the possibility to overcome these boundaries by providing new activation paths for unreactive systems, particularly when using sub-stoichiometric amounts of transition metal complexes, the so-called **organometallic catalysis**.[5]

1. Organometallic catalysis

1.1. Introduction

Organometallic reagents provide an alternative for overcoming the limitations of the traditional reactivity, owing to the possibility of activating the substrates by metal coordination. The potential of metal-based reagents lies not only in the inherent reactivity of the metal, but also in the wide possibilities for fine tuning their electronic and steric features depending on the structure and properties of their ancillary ligands. On the other hand, the ability of transition metals to easily change between oxidation states allows to unlock redox pathways, which in many cases are critical for implementing catalytic cycles.

The relevance in metal-catalyzed transformations and their impact on the advance of science has been widely recognized with the award of several Nobel Prizes during the last two decades (Figure 2). For instance, in 2001 the Nobel prize was divided, one half jointly to W. S. Knowles and R. Noyori "for their work on chirally catalysed hydrogenation reactions" and the other half to K. B. Sharpless "for his work on chirally catalysed oxidation reactions".[6] Later, in 2005, T. Chauvin, R. Grubbs and R. Schrock were also awarded for their work in the development of the alkene metathesis, a strategy that allows to "*cut and sew*" olefins with the help of a transition metal catalyst.[7] Finally in 2010, the recognition was given to the pioneers of metal-catalyzed cross-coupling methodologies, between organic halides and diverse reaction partners such as: activated alkenes (R. Heck), organozinc compounds (E. Negishi) or organoboronic acids (A. Suzuki).[8] Nowadays, these methodologies have relevant applications in synthetic chemistry ,pharmaceutical industry and material sciences.

---

[5] (a) L. S. Hegedus, B. C. G. Söderberg, *Transition Metals in the Synthesis of Complex Organic Molecules*, 2nd Ed. University Science Books: Sausalito, California, **1999**. (b) D. Astruc, *Organometallic Chemistry and Catalysis*, Springer-Verlag, **2007**.

[6] https://www.nobelprize.org/nobel_prizes/chemistry/laureates/2001/

[7] https://www.nobelprize.org/nobel_prizes/chemistry/laureates/2005/

[8] https://www.nobelprize.org/nobel_prizes/chemistry/laureates/2010/

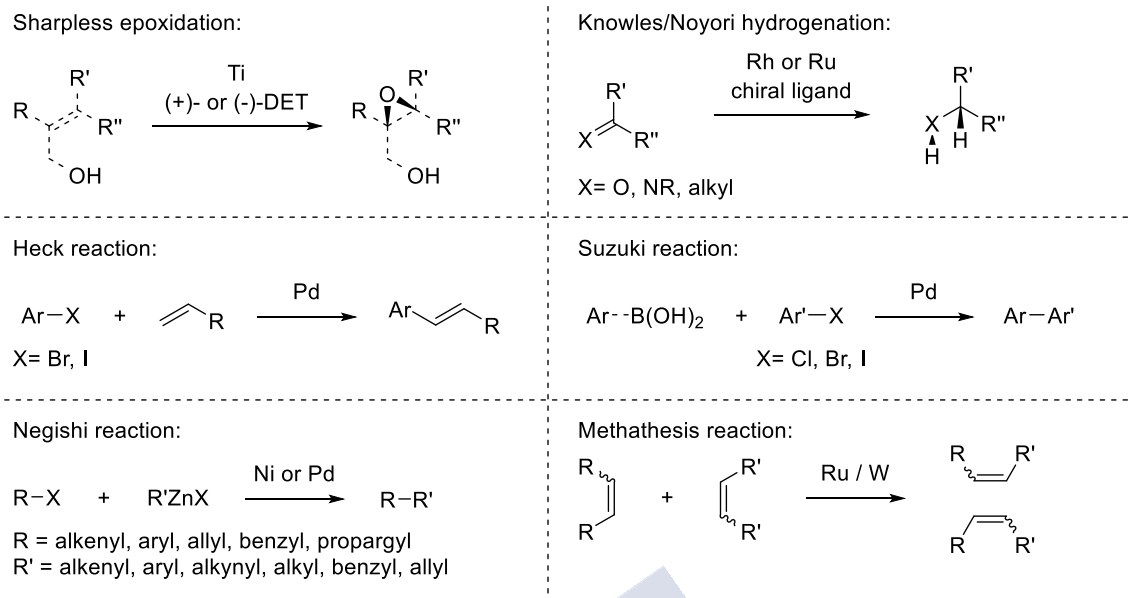

Figure 2. Transition metal catalyzed reactions awarded with a Nobel Prize.

1.2. Transition metal catalyzed cycloadditions

Many interesting molecules are constituted by complex polycyclic cores. Therefore, the rapid assembly of these scaffolds in a low number of steps is one of the main challenges in the design of efficient synthesis of these products. In this regard, cycloaddition reactions are especially appealing transformations due to their potential for generating various bonds in one operational step, and for assembling complex tridimensional structures from simple acyclic starting materials. Moreover, cycloaddition processes generally show excellent degrees of selectivity and atom economy.

Classical cycloadditions can be classified as *allowed* or *forbidden*, in a simplified way, considering the Woodward-Hoffman rules and Fukui´s frontier orbital theory (Figure 3).[9] The *allowed* reactions can *a priori* take place spontaneously or by heating and, on the other hand, the so called *forbidden* transformations require photochemical conditions, radical initiators or other kind of adjuvants.[10] Arguably, in a historical context, Diels-Alder reaction is the quintessential cycloaddition which, in a [4π + 2π] process, is able to straightforwardly assemble a six-membered cycle in one step, generating up to four contiguous stereogenic centers.[11]

[9] S. Inagaki, H. Fujimoto, K. Fukui, *J. Am. Chem. Soc.* **1976**, *98*, 4693.
[10] M. Lautens, W. Klute, W. Tam, *Chem. Rev.* **1996**, *96*, 49.
[11] (a) O. Diels, K. Alder, *Justus Liebigs Ann. Chem.* **1928**, *460*, 98. For representative reviews see: (b) F. Fringuelli, A. Taticchi, The Diels-Alder Reaction: Selected Practical Methods; Wiley, **2002**. (c) J. P. Miller, Advances in Chemistry Research. Volume 18 - Recent Advances in Asymmetric Diels-Alder Reactions; Taylor, J. C., Ed.; Nova Science Publishers, Inc., **2013**, 18, 179. (d) K. P. C. Vollhardt, N. E. Schore, Organic Chemistry, W.H. Freeman & Co Ltd, **1998**.

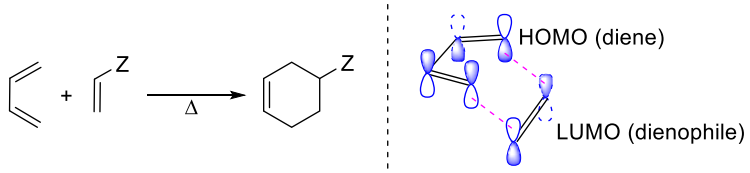

Figure 3. Diels-Alder reaction.

An example of the application of this cycloaddition in modern synthetic chemistry was described by Rychnovsky in 2019,[12] in the total synthesis of (±)-illisimonin A (Scheme 1). In this report, the complex polycyclic core of the natural compound is assembled through an intramolecular (4+2) cycloaddition between an electronically-activated alkene and a cyclopentadiene that is formed *in-situ*. The reaction selectively generates four new chiral centers with good yield.

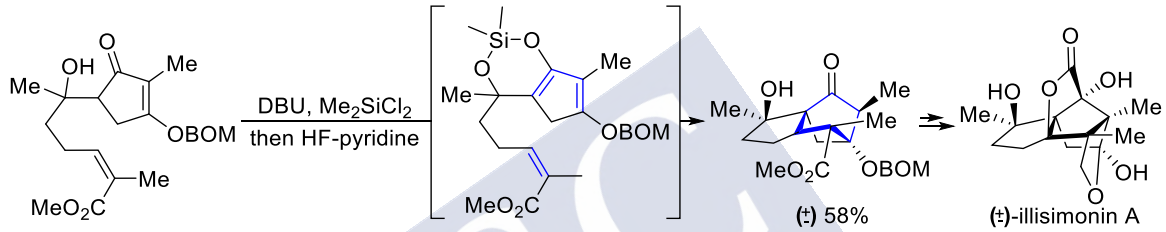

Scheme 1. Total synthesis of (±)-illisimonin A.

Despite the great impact of Diels-Alder and other thermal cycloadditions in synthetic chemistry, the requirement of electronically matched reaction counterparts restricts their synthetic applicability. In this regard, transition metal reagents, by being able to activate a wide range of otherwise unreactive functional groups, can open impressive opportunities to achieve new type of formal cycloadditions.[13]

The power of transition metals in catalysis is further enhanced by the possibility of modifying the oxidation state and stereoelectronic properties of the metal center by playing with the ancillary ligands. Moreover, the use of chiral ligands might allow a chirality transfer from the metal environment to the substrate, which eventually provides for *asymmetric catalytic transformations*.[14]

A good example of the groundbreaking potential of transition metal catalysis (TMC) in cycloaddition reactions is the synthesis of cyclooctatetraene from acetylene (Scheme 2). While the classic route to cyclooctatetraene involved 13 steps and a poor 1-2% overall yield, the nickel catalyzed cycloaddition of acetylene reported by Reppe`s group in 1948,[15] provides the target molecule in one step with an outstanding 90% yield.

[12] A. S. Burns, S. D. Rychnovsky, *J. Am. Chem. Soc.* **2019**, *141*, 13295–13300.
[13] A. C. Jones, J. A. May, R. Sarpong, B. M. Stoltz, *Angew. Chemie - Int. Ed.* **2014**, *53*, 2556.
[14] E. N. Jacobsen, A. Pfaltz, H. Yamamoto, *Comprehensive Asymmetric Catalysis I-III*, Springer-Verlag, **2000**.
[15] W. Reppe, O. Schlichting, K. Klager, T. Toepel, *Justus Liebigs Ann. Chem.* **1948**, *560*.

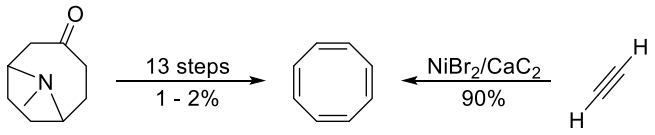

Scheme 2. Comparative synthesis of cyclooctadiene.

Another pioneer example, reported by Wender in 1985,[16] involves the nickel catalyzed (4+4) intramolecular cycloaddition of conjugated dienes, a process that delivers 5,8-bicyclic products in good yields and excellent diastereoselectivity (Scheme 3). Remarkably, in the absence of the metal catalyst, under thermal conditions, none of these cycloadditions proceed, which highlights the power of metal catalysts to unveil new formal cycloaddition processes.

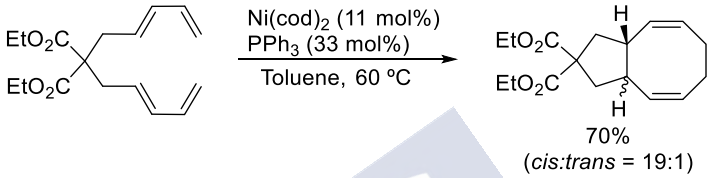

Scheme 3. Nickel catalyzed (4+4) cycloaddition.

Another elegant example developed by Wender involved an intramolecular (4+2) cycloaddition between alkynes and dienes, promoted by a Ni(0)/phosphite catalyst (Scheme 4).[17] The non-catalyzed reaction requires 150 ºC to take place, whereas the metal promoted process proceeds at room temperature in excellent yield and complete diastereoselectivity.

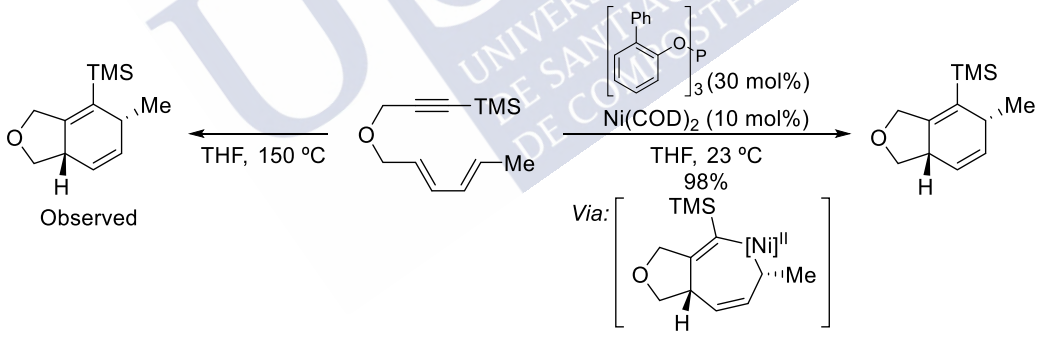

Scheme 4. Nickel catalyzed (4+2) cycloaddition.

[16] P. A. Wender, N. C. Ihle, *J. Am. Chem. Soc*. **1986**, 108, 4678–4679.

[17] P. A. Wender, T. E. Jenkins, *J. Am. Chem. Soc.* **1989**, *111*, 6432.

2. Asymmetric catalysis

Most naturally occurring organic molecules and bioactive compounds are chiral; therefore the development of methods that allow to assemble these molecules in an enantioselective fashion is of enormous relevance.[18] There are several ways of inducing asymmetry in a synthetic process. Below, we describe the most relevant approaches.[19]

2.1. Diastereoselective reactions

If a catalytic chemical transformation is applied over a chiral substrate, the chirality of this starting material can induce asymmetry on the new chiral center, as a consequence of steric interactions developed during the process, leading to diastereoselective processes (Scheme 5). Obtaining complete diastereoselectivities is not always easy, and the formation or availability of the original chiral starting material might be also not trivial. [20]

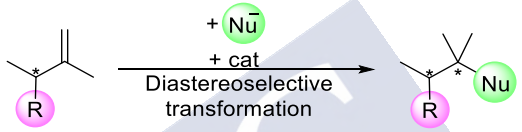

Scheme 5. Example of a diastereoselective reaction.

Asymmetric induction using chiral auxiliaries

Chiral auxiliaries are widely used in asymmetric synthesis, as they can be *"pasted and removed"* in the substrate (Scheme 6). This strategy is usually efficient in terms of chirality transfer, and depending on the configuration of the auxiliary, both enantiomers might be synthesized. Nevertheless, the requirement of stoichiometric amounts of the chiral auxiliary and the addition of two extra operational steps (insertion and eventual removal of the auxiliary), are important practical limitations.[21]

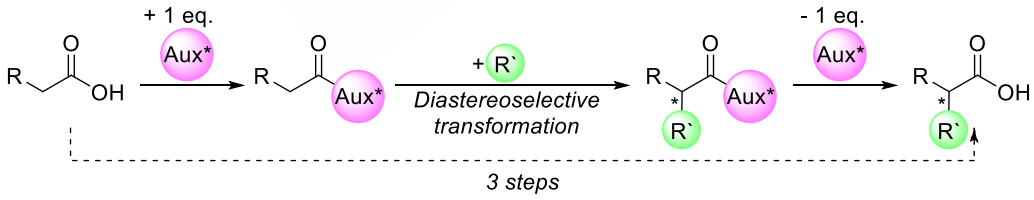

Scheme 6. Example of asymmetric induction by achiral auxiliary.

[18] Mohr, J. T.; Krout, M. R.; Stoltz, B. M. *Nature* **2008**, *455*, 323.
[19] For a review of the use of asymmetric catalysis in total synthesis, see: Mohr, J. T.; Krout, M. R.; Stoltz, B. M. *Nature* **2008**, *455*, 323.
[20] For an example of a diastereoselective synthesis, see: Mitchell, H. J.; Nelson, A.; Warren, S. *J. Chem. Soc., Perkin Transactions 1*. **1999**, 1899.
[21] For an example of synthesis using chiral auxiliaries, see: (a) Bull, S. D.; Davies, S. G.; Fox, D. J.; Garner, A. C.; Sellers, T. G. *Pure and Applied Chemistry* **1998**, *70*, 1501. (b) Geary, L. M.; Hultin, P. G. *Tetrahedron: Asymm.* **2009**, *20*, 131.

Asymmetric induction using chiral catalysts

Undoubtedly, the most attractive way of achieving asymmetric transformations consist of using chiral reagents in sub-stoichiometric amounts. In the case of organometallic catalysis, the reagent could be chiral due to the inherent chirality of its metal center or by the presence of chiral ancillary ligands (Scheme 7). The enantioselectivity is usually a consequence of interactions between the chiral environment of the catalyst and the substrate (either covalent or non-covalent) which precede the formation of a new stereogenic center. Many factors might influence the efficiency of the asymmetric induction, and usually it is very challenging the development and understanding of highly enantioselective reactions based on this strategy. However, because of their catalytic nature, these approaches are the mostly desirable.[22]

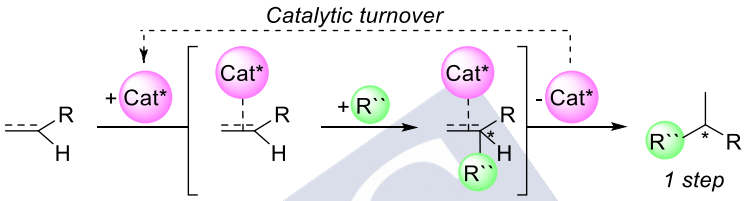

Scheme 7. Catalytic asymmetric induction

Usually the development of **metal-catalyzed enantioselective transformations** is preceded by a deep study to understand the nature of the transformation, including the stereoelectronic requirements of the ligand and the metal, as this allows a more rational design of the chiral catalyst.[23]

Currently, the portfolio of chiral compounds employed as metal ancillary ligands is very broad. Bidentate ligands are the most commonly used, and many of them exhibit axial chirality with C_2 symmetry. Their ability to chelate the metal center provides a rigid environment by fixing the conformation of the complex, which can be very important for obtaining good results (Figure 4a).[24] For these reasons, chiral monodentate ligands have been largely ignored in the field; however, they have attracted significant attention in the last two decades, and even several applications in industrial processes are now available with this type of ligands (Figure 4b).[25]

[22] For a review about chiral catalysis, see: Yoon, T. P.; Jacobsen, E. N. *Science* **2003**, *299*, 1691.
[23] Traverse, J. F.; Snapper, M. L. *Drug Discovery Today* **2002**, *7*, 1002.
[24] (a) Ojima, I. *Catalytic Asymmetric Synthesis* Wiley, New York, **2000**. (b) Brunner, H.; Zettlmeier, W. *Handbook of Enantioselective Catalysis* Wiley, New York, **1993**.
[25] (a) Tang, W. J.; Zhang, X. M. *Chem. Rev.* **2003**, *103*, 3029. (b) Lagasse, F.; Kagan, H. B. *Chem. Pharm. Bull.* **2000**, *48*, 315. (c) Feringa, B. L. *Acc. Chem. Res.* **2000**, *33*, 346.

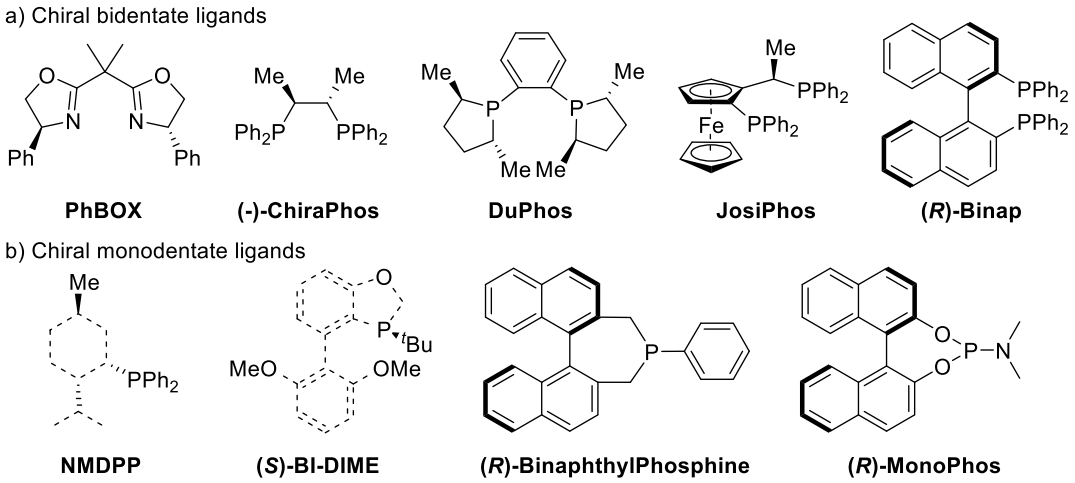

Figure 4. Chiral mono- and bidentate ligands.

The stereoelectronic properties of a metal center can be significantly influenced by their ligands. In this regard, phosphorus-based compounds are privileged due to the possibility to manage their electronic properties with the substituents, varying from strong *σ*-donor phosphines to *π*-acceptor phosphites (Figure 5). In this context, a relatively young family of monodentate chiral ligands introduced by Feringa are the so called chiral *phosphoramidites*. These ligands are generally stable and easy to synthesize, just by combining a diol, an amine and a simple phosphorus precursor. Chiral phosphoramidites are obtained when either a chiral diol or an amine is employed. Hence, many phosphoramidites can be straightforwardly synthesized expanding the significantly the palette of new chiral ligands.

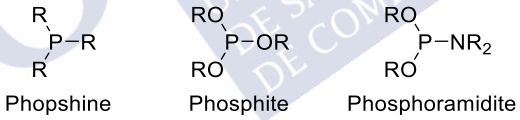

Figure 5. Examples of phosphorus-based ligands.

After the initial developments, they have been extensively used in several metal-catalyzed asymmetric applications (Scheme 8).[26] For instance, some representative examples involve copper and rhodium catalyzed conjugated additions of organometallic reagents to Michael acceptors,[27] rhodium catalyzed asymmetric hydrogenations,[28] copper or iridium catalyzed asymmetric allylic alkylations,[29] and even synthetically challenging cycloadditions.[30]

[26] J. F. Teichert, B. L. Feringa, *Angew. Chemie - Int. Ed.* **2010**, *49*, 2486–2528.
[27] B. L. Feringa, M. Pineschi, L. A. Arnold, R. Imbos, A. H. M. De Vries, *Angew. Chemie (International Ed. English)* **1997**, *36*, 2620–2623.
[28] M. Van den Berg, A. J. Minaard, E. P. Schudde, J. Van Esch, A. H. De Vries, *J. Am. Chem. Soc.* **2000**, *122*, 11539-11540
[29] H. Malda, A. W. Van Zijl, L. A. Arnold, B. L. Feringa, *Org. Lett.* **2001**, *3*, 1169–1171.
[30] I. Alonso, B. Trillo, F. López, S. Montserrat, G. Ujaque, L. Castedo, A. Lledós, J. L. Mascareñas, *J. Am. Chem. Soc.* **2009**, *131*, 13020–13030.

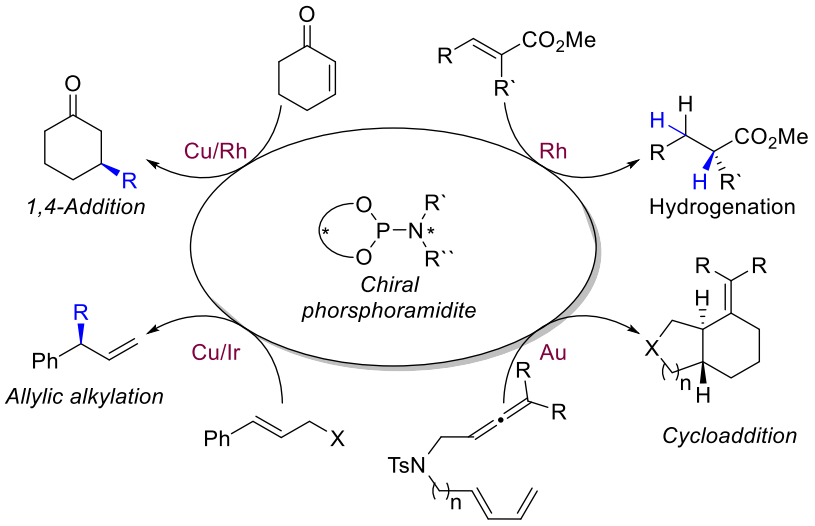

Scheme 8. Chiral phosphoramidites in metal catalysis.

An illustrative example of the use of phosphoramidites in asymmetric cycloaddition reactions was the reported by the Trost group in 2006,[31] and later in 2011,[32] consisting of a palladium catalyzed (3+2) intermolecular cycloaddition between a trimethylenemethane precursor (TMM) and a Michael acceptor (Scheme 9). The use of a strained phosphoramidites in combination with $Pd(dba)_2$ allowed to carry out the reaction under mild conditions, giving access to five-membered carbocyclic compounds in good to excellent yields and enantioselectivities.

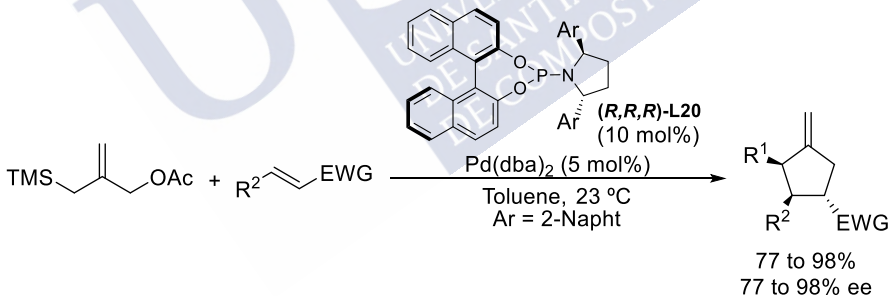

Scheme 9. Pd-catalyzed enantioselective (3+2) reaction between TMM precursors and alkenes.

[31] B. M. Trost, J. P. Stambuli, S. M. Silverman, U. Schwörer, *J. Am. Chem. Soc.* **2006**, *128*, 13328–13329.
[32] B. M. Trost, S. M. Silverman, J. P. Stambuli, *J. Am. Chem. Soc.* **2011**, *133*, 19483–19497.

Metal-catalyzed cycloadditions of alkylidenecyclopropanes

1. Pioneering examples of transition metal-catalyzed formal cycloadditions of methylenecyclopropanes

Methylenecyclopropanes (MCPs) and alkylidenecyclopropanes (ACPs) are among of the most strained cyclic structures (38.8 kcal/mol compared with 29.0 kcal/mol of cyclopropane). This is a consequence of the presence of the cyclopropane-fused double bond, which induces a wider angle at the cyclopropyl sp^2 carbon and an increased length of distal C-C bond (Figure 6a).[33] Additionally, the presence of this double bond allows coordination of transition metals, therefore facilitating the participation of these scaffolds in many TM-promoted transformations, including the activation and cleavage of their C-C bonds.[34] These characteristics, together with their remarkable stability (they are even found in natural products, Figure 6a), and ready accessibility, makes them **privileged structures for the development of novel transition metal catalyzed transformations**.

Methylenecyclopropanes can react as 2C synthons through the exocyclic alkene, participating in processes such as hydrofunctionalizations,[35] 1,3-dipolar additions,[36] or cycloadditions[37] (Figure 6b). More importantly, they also can participate as 3C synthons in reactions that involve the opening of the cyclopropane ring, especially cycloaddition processes, something very attractive for the assembly of complex carbocyclic cores.[38]

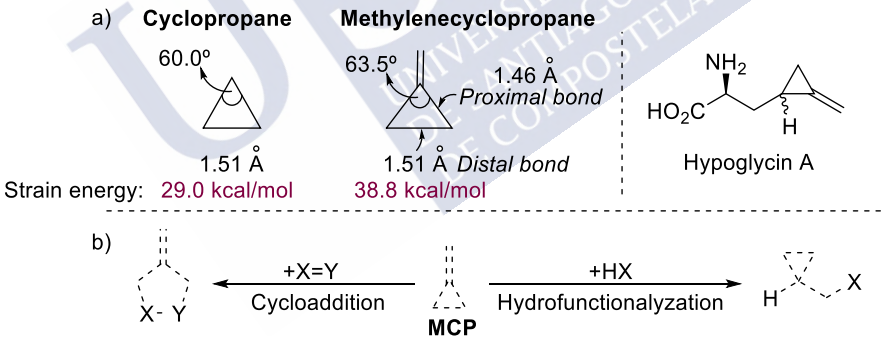

Figure 6. Structural differences between cyclopropanes and methylenecyclopropanes.

On this regard, methylene- and alkylidenecyclopropanes have been described to participate in a wide range of different TMC cycloaddition reactions as 3C synthons.[39] From an energetic perspective, these transformations are favored by the release of strain energy associated to the

[33] Laurie, V. W.; Stigliani, W. M. *J. Am. Chem. Soc.* **1970**, *92*, 1485.
[34] (a) Masarwa, A.; Marek, I., *Chemistry,* **2010**, *16* (32), 9712-21. (b) L. Z. Yu, M. Shi, *Chem. - A Eur. J.* **2019**, *25*, 7591–7606. (c) Pellissier, H., *Tetrahedron* **2010,** *66* (43), 8341-8375. (d) Pellissier, H., *Tetrahedron* **2014,** *70* (34), 4991-5031.
[35] J. C. Timmerman, B. D. Robertson, R. A. Widenhoefer, J. C. Timmerman, B. D. Robertson, *Angew. Chemie - Int. Ed.* **2015**, *54*, 2251–2254. (b) J. C. Timmerman, R. A. Widenhoefer, *Adv. Synth. Catal.* **2015**, *357*, 3703–3706.
[36] K. Estieu, J. Ollivier, J. Salau, F. M. Cordero, A. Goti, A. Brandi, *Communications* **1997**, *3263*, 8276–8277.
[37] I. Nakamura, T. Nemoto, Y. Yamamoto, M. De Armin, *Angew. Chemie - Int. Ed.* **2006**, *45*, 5176–5179.
[38] P. Chen, B. A. Billett, T. Tsukamoto, G. Dong, *ACS Catal.* **2017**, *7*, 1340–1360.
[39] (a) Binger, P.; Buech, H. M. *Top. Curr. Chem.* **1987**, *135*, 77. (b) Lautens, M.; Klute, W.; Tam, W. *Chem. Rev.* **1996**, *96*, 49. (c) Chan, D. M. T. *Comprehensive Organic Synthesis* ed. Trost, B. M.; Pergamon: Oxford, **1991**, *4*, 217.

cleavage of one of their C-C bonds. In presence of metal complexes of Ni, Pd, Ru, Ir or Rh, the C-C activation process generally involves an oxidative mechanism, wherein the nature of the metal complex determines whether the proximal (C_1-C_2) or the distal (C_2-C_3) bond are cleaved (Scheme 10).[40] Depending on the type of scission, two different metallacyclobutanic intermediates are obtained that, in presence of unsaturated partners, can participate in migratory insertion/reductive elimination sequences to give different cyclopentanic products.

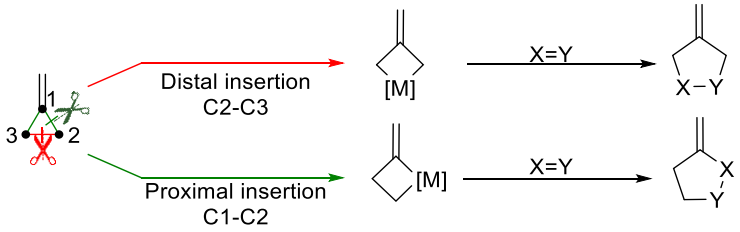

Scheme 10. Distal and proximal cleavage of methylenecyclopropane

The first studies on the reactivity of MCPs as 3C synthons in cycloaddition reactions were reported by Noyori[41] and Binger,[42] and demonstrated that ancillary ligands can determine whether a distal or a proximal C-C bond rupture occurs. In general, while $Ni(COD)_2$ or $Ni(acn)_2$ induce a selective proximal cleavage (Scheme 11a), the use of the same nickel precursors in combination with phosphine or phosphite ligands preferentially promotes a distal cleavage (Scheme 11b).

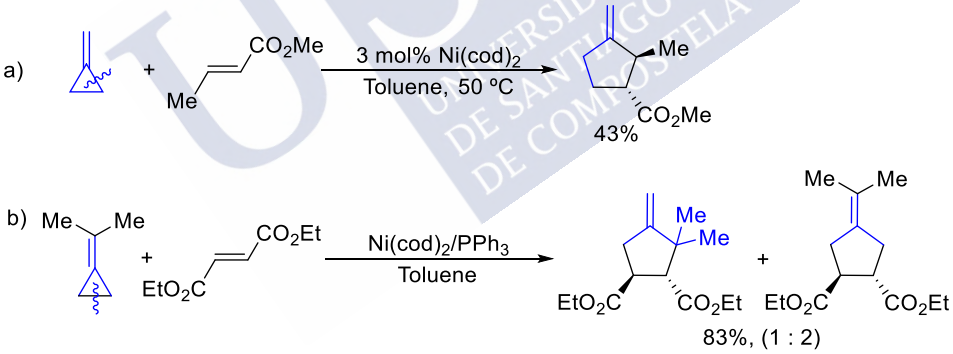

Scheme 11. Proximal (a) and distal (b) insertions using Ni (0) catalysts.

The detection of transient nickelacycle intermediates of type **A** and **B** by NMR experiments allowed Binger to propose a third mechanistic scenario, consisting of a first formation of the metallacyclopentane **A** through an oxidative cyclization mechanism, followed by a *β*-carboelimination leading to intermediate **B** (scheme 11). Overall, the transformation involves a formal cleavage of the MCP C-C proximal bond.[42]

[40] (a) Nakamura, I.; Yamamoto, Y. *Adv. Synth. Catal.* **2002**, *344*, 111. (b) Rubin, M.; Rubina, M.; Gevorgyan, V. *Chem. Rev.* **2007**, *107*, 3117.
[41] Noyori, R.; Yamakawa, M.; Takaya, H. *Tetrahedron Lett.* **1978**, *19*, 4823.
[42] (a) Binger, P.; Doyle, M. J.; Benn, R. *Chem. Ber.* **1983**, *116*, 1. (b) Binger, P.; Brinkmann, A.; Wedemann, P. *Chem. Ber.* **1983**, *116*, 2920.

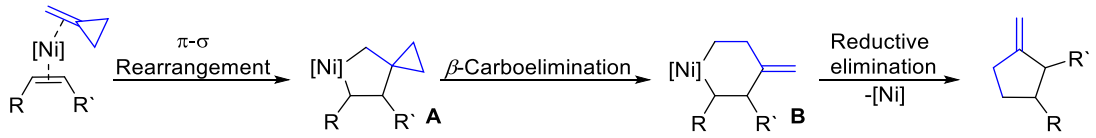

Scheme 12. Alternative mechanism of Ni (0) proximal insertion.

Palladium catalysts can also promote the cycloaddition of MCPs with different type of alkenes through the selective cleavage of the C-C distal bond of the cyclopropane. A pioneer example was described by Binger, who showed that a catalyst formed by Et_2AlOEt/ $Pd(acac)_2$/ P^iPr_3 is able to promote a (3+2) cycloaddition between MCP and norbornene to yield fused tricyclic products (Scheme 13).[43] The authors proposed an initial oxidative addition over the C-C distal bond to give the metallacyclobutane **A**. This species undergoes the migratory insertion of the alkene delivering the palladacyclohexane **B**, which is in equilibrium with its corresponding π-allylic form **C**. Finally, a reductive elimination would provide the fused carbocyclic product.

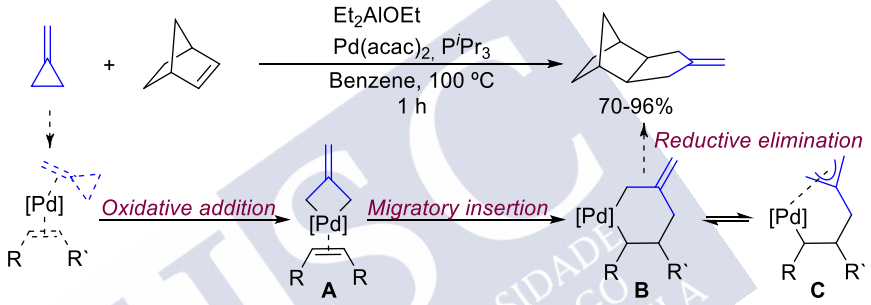

Scheme 13. Palladium catalyzed (3+2) between MCP and unactivated alkene.

Motherwell carried out an comparative study of the reactivity of alkynyl-tethered MCP derivatives under Pd and Ni catalysis (Scheme 14).[44] Interestingly, while the use of $Ni(COD)_2$ leads to the cleavage of the proximal C-C bond to give bicyclo [4.2.1] nonane scaffolds, a palladium-phosphite catalyst promoted the cleavage of the C-C distal bond, to provide bicyclo[4.3.0]nonanes with somewhat higher efficiency.

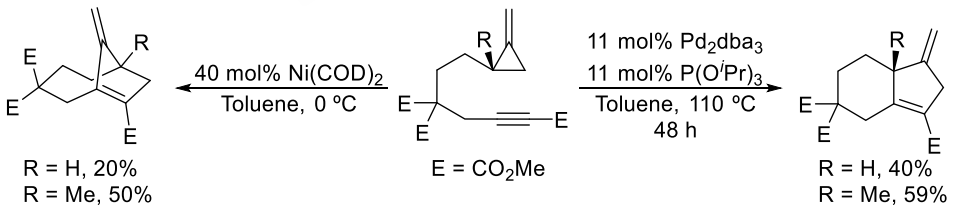

Scheme 14. Divergent behavior of MCPs in presence of palladium or nickel.

[43] (a) Binger, P.; Schuchardt, U. *Chem. Ber.* **1980**, *113*, 1063. (b) Binger, P.; Schuchardt, U. *Chem. Ber.* **1980**, *113*, 3334. (c) Binger, P.; Schuchardt, U. *Chem. Ber.* **1981**, *114*, 3313. (d) Binger, P.; Schuchardt, U. *Angew. Chem., Int. Ed. Engl.* **1977**, *16*, 249.

[44] Bapuji, S. A.; Motherwell, W. B.; Shipman, M. *Tetrahedron Lett.* **1989**, *30*, 7107.

Related palladium catalyzed (3+2) cycloadditions of similar substrates with chiral stereocenters were developed by Lautens in 1996 (Scheme 15).[45] When two different diastereoisomers of the cycloaddition precursor **1** were treated with the Pd catalyst, the products were obtained with complete stereospecificty. These results allowed to propose a palladacyclobutane intermediate **A**, which preserves the stereochemical information of the parent precursor.

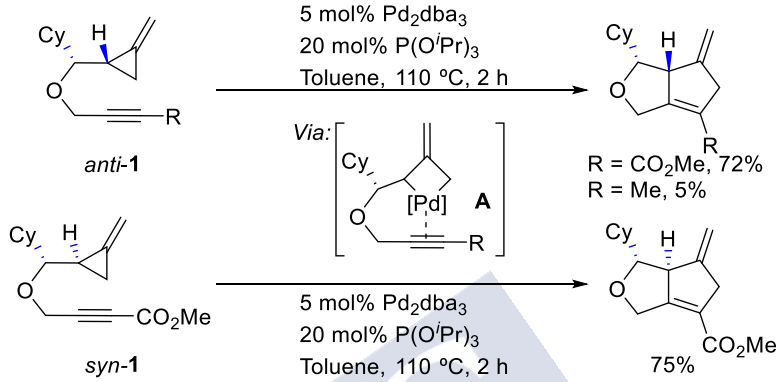

Scheme 15. Diastereospecificity of the (3+2) cycloaddition with alkynes.

A similar comparative experiment using electronically-activated alkenes, instead alkynes, was also reported by the same group. In this case, the transformation has an extra challenge due the formation of two new stereocenters in the process (Scheme 16). A palladium (0)-phosphine catalyst successfully provided the corresponding cycloadducts, alebit the substrate stereochemistry influenced the configuration of the newly formed stereocenters. Thus, while the isomer *anti*-**2** provided with complete diastereoselectivity the (3+2) cycloadduct, the isomer *syn*-**2** provided a mixture of epimers in a good 87% overall yield, with a ratio of products 1:1.

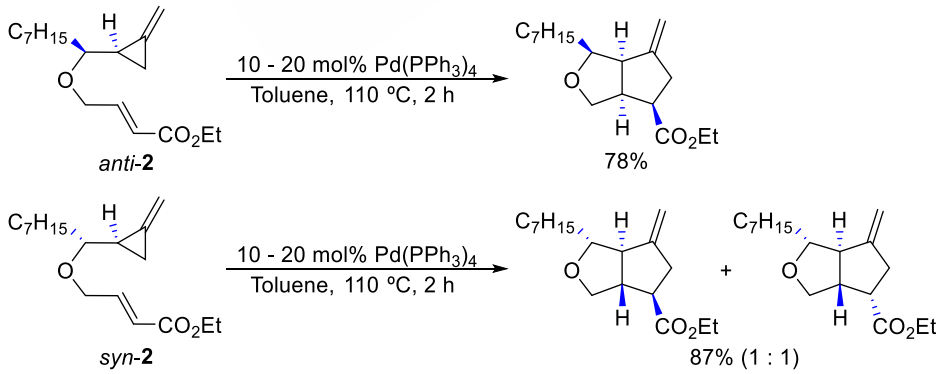

Scheme 16. Diastereospecificity of the (3+2) cycloaddition with alkenes.

[45] (a) Lautens, M.; Ren, Y.; Delanghe, P. H. M. *J. Am. Chem. Soc*. **1994**, *116*, 8821. (b) Lautens, M.; Ren, Y.; Delanghe, P. H. M. *J. Am. Chem. Soc*. **1996**, *118*, 9597. (c) Lautens, M.; Ren, Y. *J. Am. Chem. Soc*. **1996**, *118*, 10668.

2. Transition metal-catalyzed cycloadditions of alkylidenecyclopropanes to assemble carbocyclic adducts

Alkylidenecyclopropanes have also an interesting cycloaddition reactivity, in the presence of transition metals. [46] From a synthetic point of view this is relevant because they are easier to make and, in general, are more stable. In this context, our group as well as those of Evans, Saito and others have explored the potential of alkylidenecyclopropanes in transition metal catalyzed cycloaddition reactions, demonstrating that they can be converted into a wide variety of synthetically challenging polycarbocyclic scaffolds (Figure 7).[47] The reaction manifold depends on which bond, either proximal or distal, is cleaved, as well as on the potential incorporation of one or more unsaturated C-C partners. Thus, these powerful synthetic precursors serve for the construction of several small-to-medium sized carbocyclic systems.[48]

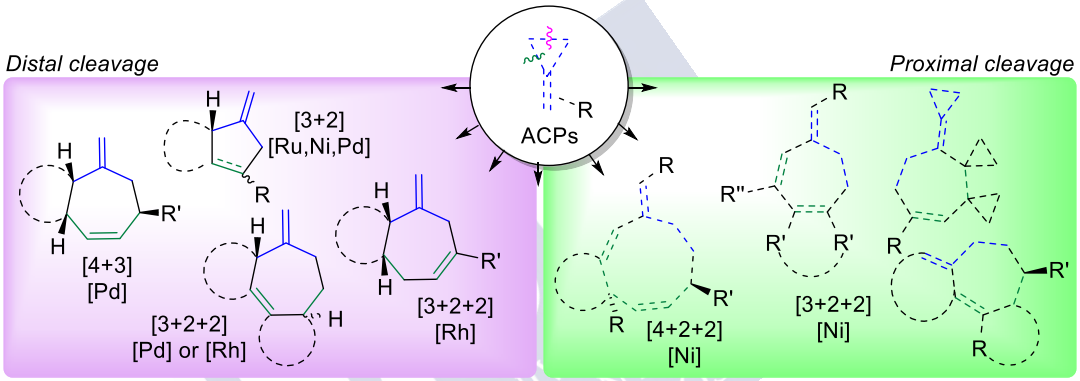

Figure 7. TMC cycloadditions of alkylidenecyclopropanes.

2.1. Construction of five-membered carbocycles

(3+2) Cycloadditions

In 2003, our group described the first examples of an intramolecular (3+2) cycloaddition between alkylidenecyclopropanes and alkynes using a palladium (0)-phosphite catalyst.[49] In general, the reaction provides the cycloadducts with good to excellent yields regardless of the type of substituents at the alkyne moiety. But interestingly, contrary to the work of Lautens,[50] alkynes bearing an electron withdrawing carboxylic esters were not reactive (Scheme 17)

[46] Suzuki, T.; Fujimoto, H. *Inorg. Chem.* **2000**, *39*, 1113.
[47] (a) M. Gulías, F. López, J. L. Mascareñas, *Pure Appl. Chem.* **2011**, *83*, 495–506. (b) G. Fumagalli, S. Stanton, J. F. Bower, *Chem. Rev.* **2017**, *117*, 9404–9432. (c) M. Shi, J. M. Lu, Y. Wei, L. X. Shao, *Acc. Chem. Res.* **2012**, *45*, 641–652.
[48] (a) L. Souillart, N. Cramer, *Chem. Rev.* **2015**, *115*, 9410–9464. (b) P. Chen, B. A. Billett, T. Tsukamoto, G. Dong, *ACS Catal.* **2017**, *7*, 1340–1360.
[49] (a) Delgado, A.; Rodríguez, J. R.; Castedo, L.; Mascareñas, J. L. *J. Am. Chem. Soc.* **2003**, *125*, 9282. (b) López, F.; Delgado, A.; Rodríguez, J. R.; Castedo, L.; Mascareñas, J. L. *J. Am. Chem. Soc.* **2004**, *126*, 10262.
[50] (a) Lautens, M.; Ren, Y.; Delanghe, P. H. M. *J. Am. Chem. Soc.* **1994**, *116*, 8821. (b) Lautens, M.; Ren, Y.; Delanghe, P. H. M. *J. Am. Chem. Soc.* **1996**, *118*, 9597. (c) Lautens, M.; Ren, Y. *J. Am. Chem. Soc.* **1996**, *118*, 10668.

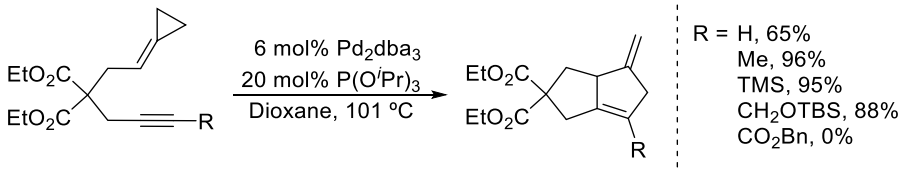

Scheme 17. Pd catalyzed intramolecular (3+2) cycloaddition between ACPs and alkynes.

The analysis of different phosphites and phosphoramidite ligands, allowed to find out that a catalyst prepared in situ from Pd_2dba_3 and the phosphite ligand **L1** is significantly more efficient than the one from $P(O^iPr)_3$. Indeed, the reaction proceeds well with just 1 mol% of Pd_2dba_3 and 2 mol% of **L1** (Scheme 18).[51]

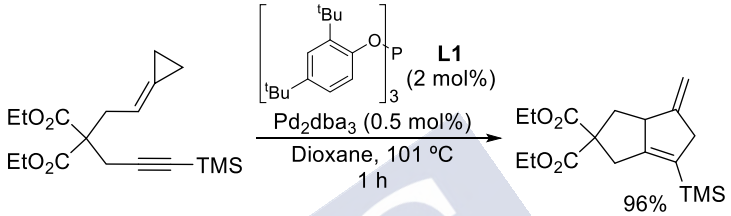

Scheme 18. Pd catalyzed (3+2) cycloaddition with low catalytic loads.

DFT studies carried out in collaboration with Prof. Cárdenas suggested three possible mechanistic scenarios (Scheme 19).[52] P*athway 1* starts with the oxidative addition of the metal center over the distal position of the cyclopropane moiety generating the palladacyclobutane **B**, that can further isomerize through a Pd-TMM like transition state towards the species **C**. This intermediate would evolve to palladacyclohexane **D** by migratory insertion and finally, after reductive elimination, provides the corresponding (3+2) cycloadduct **E**.

In *Pathway 2* palladacyclobutane **B** evolves directly to the intermediate **D** through a concerted metalloene rearrangement.

The *pathway 3* proposed an oxidative cyclization between the substrate and the metal complex leading to the intermediate **F**, which after a *β*-carboelimination leads to the formation of the common intermediate **D**.

The calculations suggested that *pathway 3* is energetically disfavored due the high energy barrier of the oxidative cyclization, compared with the processes that involves a C-C oxidative addition. Albeit *pathway 1* would be the most favored scenario, *pathway 2* could not be discarded due the small difference in energies between both processes. Complementary, calculations also evidenced that the step with higher activation barrier for *pathway 1* is the carbometallation, whereas for *pathway 2* it would be the metalloene rearrangement.

The calculations also offered a plausible explanation about the reluctance to alkynes bearing EWGs to participate in the cycloaddition. In this case, a Michael-type addition of the double

[51] Durán, J.; Gulías, M.; Castedo, L.; Mascareñas, J. L. *Org. Lett.* **2005**, *7*, 5693.
[52] (a) García-Fandiño, R.; Gulías, M.; Castedo, L.; Granja, J. R.; Mascareñas, J. L.; Cárdenas, D. J. *Chem. Eur. J.* **2008**, 14, 272.

bond of the alkylidenecyclopropane over the *a,β*-unsaturated system would generate the allenoate intermediate **G**, which does not progress towards the desired cycloadduct.

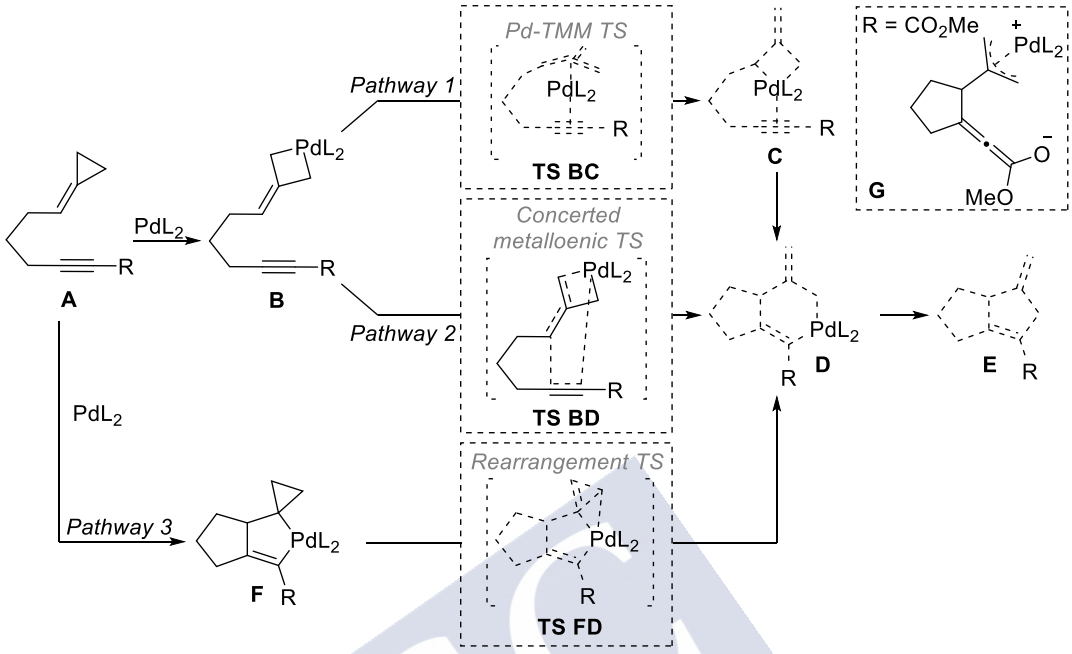

Scheme 19. Mechanistic hypothesis for the Pd catalyzed (3+2) cycloaddition with alkynes.

In 2006 our group extended this chemistry by developing an intramolecular (3+2) cycloaddition between alkylidenecyclopropanes and alkenes.[53] The annulation provides the products with high yields and excellent diastereocontrol, particularly considering the simultaneous formation of up to three chiral centers. Phosphites demonstrated to be the ligands of choice for this reaction (Table 1). In particular, using $P(OiPr)_3$ or **L1** , the cycloadduct **4a** was obtained with complete diastereoselectivity and good yield, (entry 1 and 2). Mechanistically significant, when the cycloaddition of the *cis* isomer ***Z-3a*** using $P(OiPr)_3$ as ligand, provided the expected product **4** in 72% yield, as a single isomer (entry 3). However, when the bulkier phosphite **L1** was used, a mixture of the epimeric product **4`** and compound **4``** were obtained (entry 3).

[53] M. Gulías, R. García, A. Delgado, L. Castedo, J. L. Mascareñas, *J. Am. Chem. Soc.* **2006**, *128*, 384–385.

Table 1. Pd catalyzed intramolecular (3+2) cycloaddition between ACPs and alkenes.

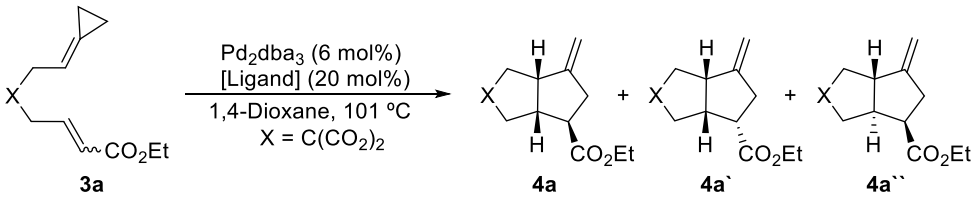

Entry	*E* / *Z*	Ligand	Product	Yield (%)
1	*E*	$P(O^iPr)_3$	**4a**	74
2	*E*	**L1**	**4a**	82
3	*Z*	$P(O^iPr)_3$	**4a**	72
4	*Z*	**L1**	**4a`** + **4a``**	87 (5.3 : 1)

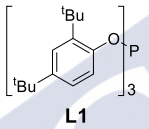

Importantly, substrates bearing non-activated alkenes such as **5a** (R = H) or **5b** (R = Me) did not provide the desired cycloadducts with $P(OiPr)_3$ as ligand, but instead, a mixture of products of type **6** and **7** (Scheme 20). Interestingly, the use of the bulkier ligand **L1** successfully provide the corresponding cyclic product, but as a mixture of *cis*- and *trans*- fused cycloadducts type **4** and **5**.

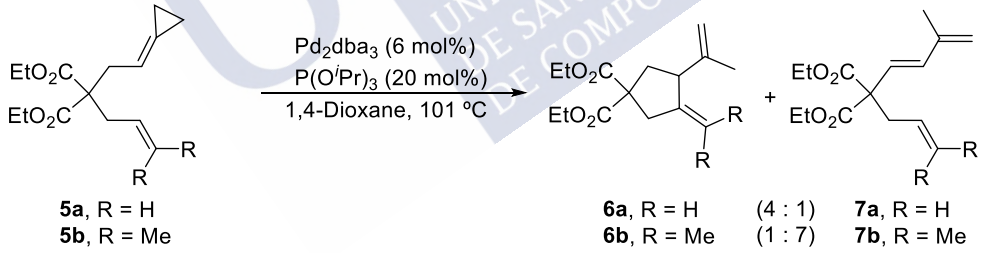

Scheme 20. Reaction outcome using non-activated alkenes with $Pd_2dba_3/P(^iOPr)_3$ catalyst.

To understand this experimental outcome, DFT studies were carried out in collaboration with Prof. Cárdenas and Dr. Rebeca García-Fandiño (Scheme 21).[54] PH_3 was used as model ligand and **A1** (R = H, not activated alkene) or **A2** (R = CO_2Me, activated alkene) as cycloaddition precursors. The reaction begins with the oxidative addition of the distal C–C bond of the ACP forming the palladacyclobutane **B**. From this intermediate, three potential scenarios were analyzed:

Pathway 1, in which **B** evolves towards its isomer **C** through a Pd-TMM type of transition state. Then, a carbometallation of the alkene leads to the palladacyclohexane **D**, which can deliver the desired cycloadduct **E** after reductive elimination. Alternatively, the undesired side-

[54] R. Garcia-Fandino, M. Gulías, J. L. Mascareñas, D. J. Cárdenas, *Dalt. Trans.* **2012**, *41*, 9468–9481.

product **G** could be generated when the alkene is terminal or bearing non-electronwithrawing alkyl substituents.

Pathway 2 implies the direct evolution of the palladacycle **B** towards **D** through a metalloene rearrangement.

Pathway 3 is only energetically feasible when R = EWG, and involves a Michael-type addition of the double bond of the alkylidenecyclopropane to the *a,β*-unsaturated ester, to yield the zwitterionic intermediate **F**, which could further evolve towards the palladacycle **D** or directly to the cycloadduct **E**.

It is important to remark that *Pathway 3* allows to explain the formation of epimers **4** and **4`** from (*Z*)-**3a,** when **L1** is used (Table 1, entry 4), since intermediate enolate **F** can rotate along its adjacent C-C bond losing the stereospecificity. Comparing the energetic barriers of the addition step (Michael addition) explains the exclusive formation of **4** from substrate *E*. In general, the energetic results obtained suggests that the preferred pathway is highly dependent in structural features of the substrate and in the type and number of ligands attached to the metal.

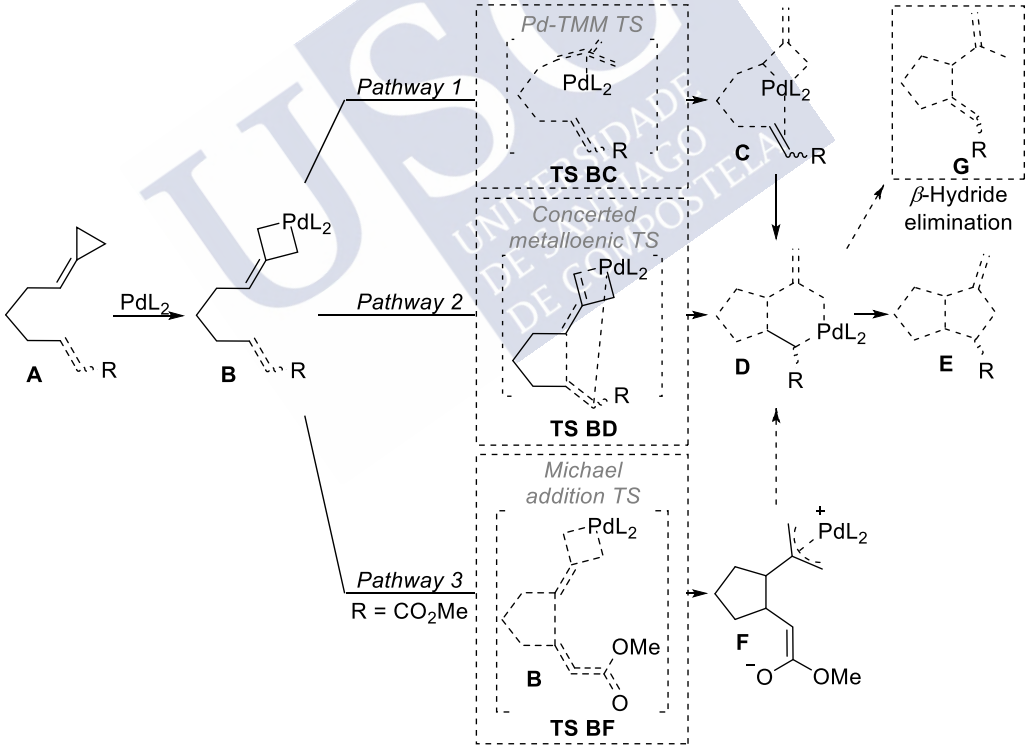

Scheme 21. Mechanistic hypothesis for the Pd catalyzed (3+2) cycloaddition with alkenes.

Another article published in 2006 showed that allenes are also suitable reaction counterparts (Scheme 22). In this case, only a 2 mol% of Pd_2dba_3 and 5 mol% of **L1** was necessary to afford the corresponding fused bicyclic systems with high diastereoselectivity and good yields.

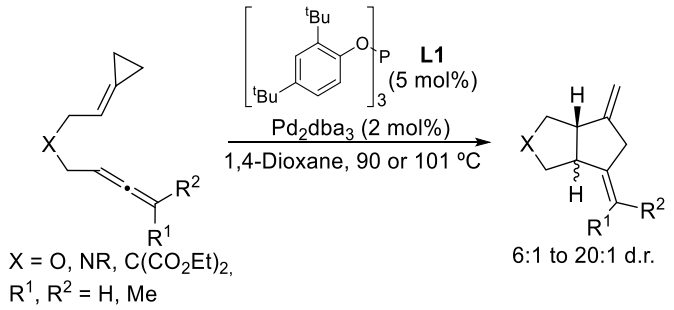

Scheme 22. Pd catalyzed intramolecular (3+2) cycloaddition between ACPs and allenes.

Alkylidenecyclopropanes can also participate in (3+2) cycloadditions in presence of nickel catalysts. In this regard, a seminal work published by Binger in 1987 showed that alkylidenecyclopropanes can intermolecularly react with activated alkenes, leading to five-membered carbocycles (Scheme 23).[55] In most of the cases, the reactions give complex isomeric mixtures of products arising from distal or proximal cleavage of the cyclopropane, depending highly in the substrates and the reaction conditions used.

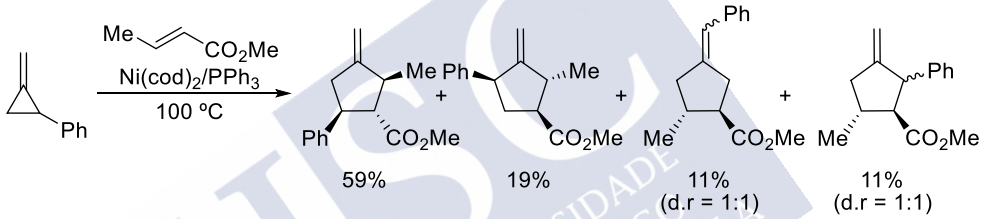

Scheme 23. Ni catalyzed intermolecular (3+2) cycloaddition between ACPs and alkenes.

A further work published by Zhang in 2011 showed that ACPs can react intramolecularly with alkynes, using a 5 mol% a $Ni(cod)_2$ and a 20 mol% of PPh_3, affording polycyclic systems in moderate yields (Scheme 24).[56] The proposed mechanism involves a cleavage of the proximal C-C bond of the ACP (**A**) and further migratory insertion of the alkyne to yield the nickelacyclohexane **B**. Finally, after reductive elimination, the polycyclic compounds are obtained.

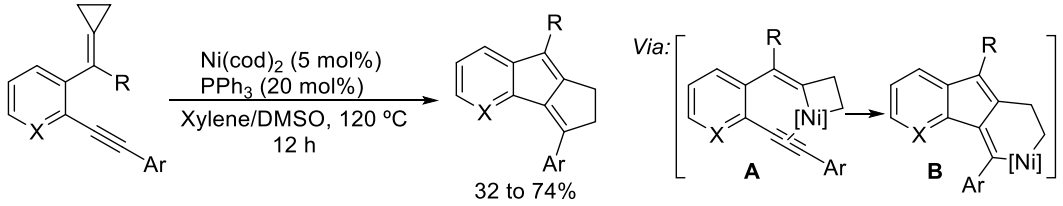

Scheme 24. Ni catalyzed intramolecular (3+2) cycloaddition between ACPs and alkynes.

A related reactivity had been previously observed by our group during the development of a (3+2+2) annulation between ACPs and an external activated alkenes. In particular, a five-membered carbocycle resulting from an intermolecular (3+2) cycloaddition between the ACP

[55] P. Binger, H. M. Büch, *Top. Curr. Chem*. **1987**, 77–151.
[56] B. Yao, Y. Li, Z. Liang, Y. Zhang, *Org. Lett.* **2011**, *13*, 640–643.

and the alkene was detected as side product (Scheme 25).[57] Curiously, control experiments showed that in the absence of the alkyne tethered to the ACP, the intermolecular (3+2) cycloaddition does not occur, suggesting that the triple bond might assist the formation of this byproduct. Later, similar experimental observations were reported by Bhargava, in a Ni-catalyzed (3+2) cycloaddition of bis-alkylidenecyclopropanes.[58]

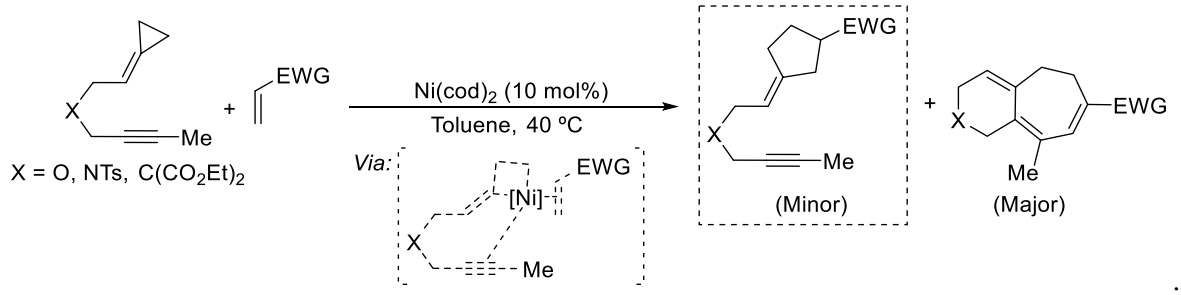

Scheme 25. Ni catalyzed intermolecular (3+2+2) cycloaddition between ACPs and alkenes.

(2+2+1) Cycloadditions

In 2016 Tanaka showed that electron deficient ACPs can behave as 1C synthons in a Rh catalyzed (2+2+1) annulation with 1,6-diynes, yielding highly substituted fused-fulvenes (Scheme 26).[59] The authors proposed a C-C activation of the proximal bond of the cyclopropane to yield an intermediate **A** that evolves to the rhodium vinylidene **B,** through a *β*-carboelimination that releases ethylene. At this point, the incorporation of the diyne through a (2+2) process with the vinylidene generates the rhodacyclobutene **C** that further inserts the pendant alkyne forming the rhodacycle **D**. Finally, the fulvene is afforded after reductive elimination.

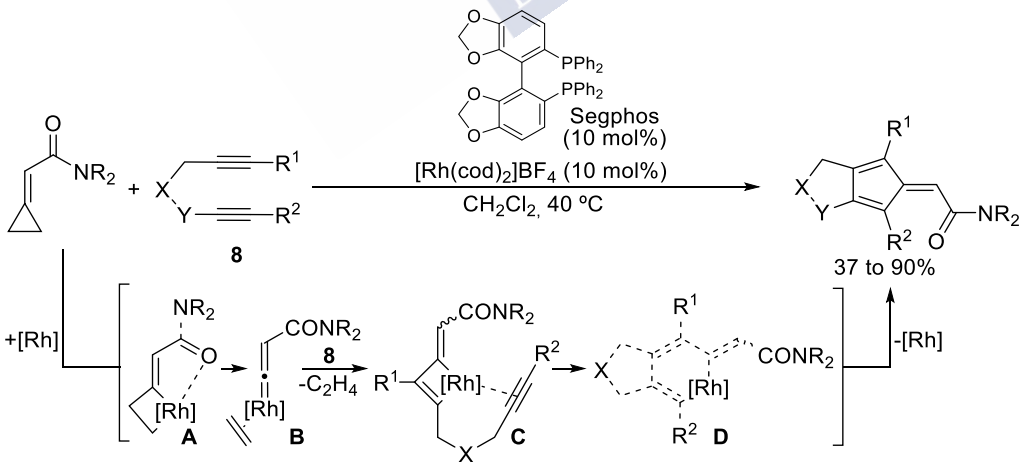

Scheme 26. Rh catalyzed intermolecular (2+2+1) cycloaddition between ACPs and diynes.

[57] L. Saya, G. Bhargava, M. A. Navarro, M. Gulías, F. López, I. Fernández, L. Castedo, J. L. Mascareñas, *Angew. Chemie - Int. Ed.* **2010**, *49*, 9886–9890.
[58] B. Kuila, D. Mahajan, P. Singh, G. Bhargava, *Tetrahedron Lett.* **2015**, *56*, 1307–1311.
[59] S. Yoshizaki, Y. Shibata, K. Tanaka, *Angew. Chemie - Int. Ed.* **2017**, *56*, 3590–3593.

In summary, alkylidenecyclopropanes can participate in a variety of (3+2) and related to formal cycloadditions, leading five-membered carbocycles. Nevertheless, there were no precedents on enantioselective approaches.

2.2. Construction of seven-membered carbocycles

The construction of seven-membered carbocycles through transition metal catalyzed cycloadditions of ACPs can be attained by using formal (4+3) or (3+2+2) annulations in which the ACP participates as 3C synthon.[60] Interestingly, while only a few examples of (4+3) annulations were described, a wide variety of multicomponent (3+2+2) annulations have been developed, using alkenes, alkynes, or allenes as reaction counterparts.

(4+3) Cycloadditions

The first example of a (4+3) annulation involving a MCP was that reported by Binger in 1987,[55] and consisted of an intermolecular palladium catalyzed cycloaddition with dimethylmuconate that yielded the corresponding seven-membered carbocycle in good yield, albeit as a mixture of diastereoisomers (Scheme 27). The reaction is proposed to proceed through C-C activation of the distal position to generate a **Pd-TMM** intermediate, which is the species undergoing the (4+3) annulation with the dimethyl muconate. Nevertheless, is important to highlight that this single example was indicated in a review article, but the experimental result was never published.

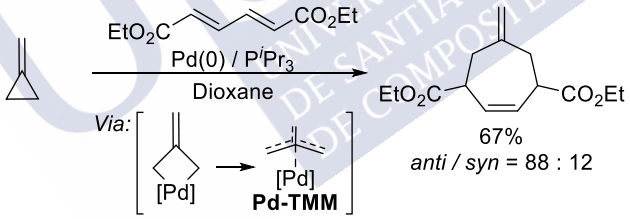

Scheme 27. Pd catalyzed intermolecular (4+3) cycloaddition between MCP and dienes.

It is worth to mention the similarities of this work by Binger with that developed by Trost on intermolecular (4+3) annulation between a TMM precursor and dimethylmuconate (Scheme 28).[61] Albeit similar types of **Pd-TMM** are proposed to be involved, the reaction outcomes are totally different as, in the case reported by Trost, using $Pd(PPh_3)_4$ and dppe as ligand, a regioisomeric mixture of the seven and five-membered carbocycles were obtained.

[60] (a) P. A. Inglesby, P. A. Evans, *Chem. Soc. Rev.* **2010**, *39*, 2791–2805. (b) G. Fumagalli, S. Stanton, J. F. Bower, *Chem. Rev.* **2017**, *117*, 9404–9432. (c) P. Chen, B. A. Billett, T. Tsukamoto, G. Dong, *ACS Catal.* **2017**, *7*, 1340–1360.
[61] B. M. Trost, T. N. Nanninga, D. M. T. Chan, *Organometallics* **1982**, *1*, 1543–1545.

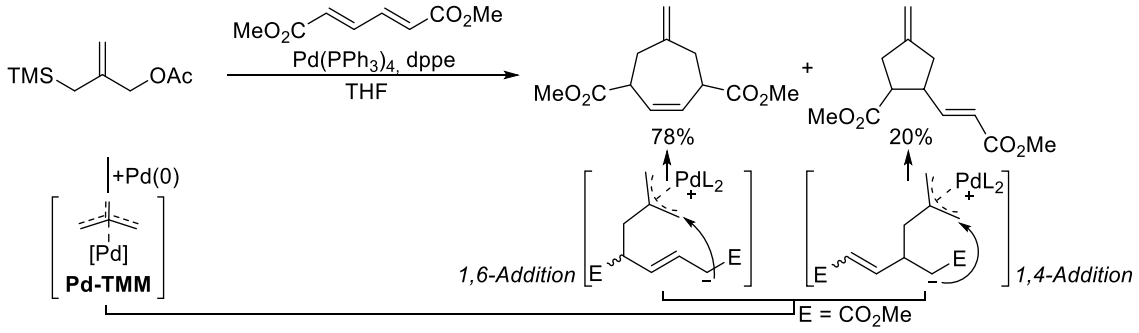

Scheme 28. Pd catalyzed intermolecular (4+3) cycloaddition between TMM precursors and dienes.

The first example of a (4+3) cycloaddition of ACPs and dienes was published by our group in 2007.[62] Using substrates of type **9**, Pd_2dba_3 and the phosphoramidite **L2** as ligand, fused seven-membered carbocycles were obtained with complete diastereoselectivity and good yields. Usually, very good (4+3)/(3+2) selectivity was observed when dienes bearing EWGs at their terminal position are used (ratios higher than 10:1). However, the lack of these substituents or the incorporation of alternative groups at the diene might affect this selectivity (Scheme 29). Remarkably, a preliminary evaluation using the chiral phosphoramidite **(*R*)-L3** showed that the reaction can be carried out enantioselectively, albeit with modest results. Nonetheless, this constituted the first report of an intramolecular asymmetric (4+3) cycloaddition of ACPs (See page 48).

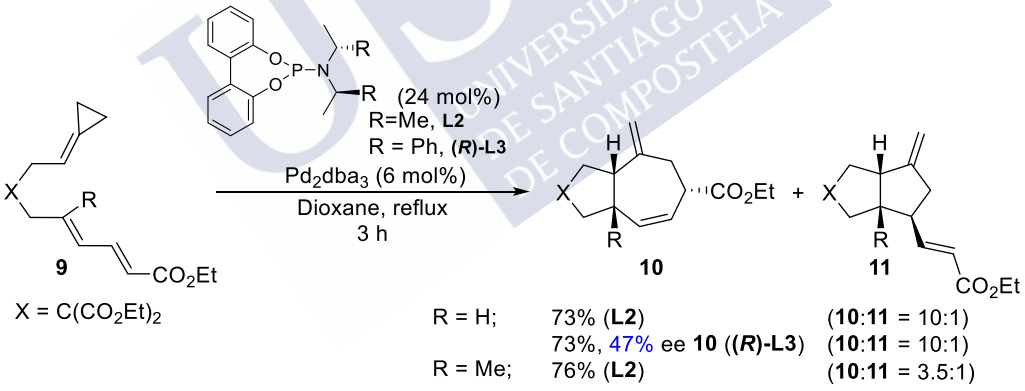

Scheme 29. Pd catalyzed intramolecular (4+3) cycloaddition between ACPs and dienes.

The proposed reaction mechanism involves the formation of a palladacyclobutane **A** that inserts the internal double bond of the conjugated diene delivering the palladacyclohexane intermediate **B**, which might be considered as as σ- or π-allyl complex. A reductive elimination from this intermediate could afford both the (3+2) or, from the isomeric form **C**, the (4+3) adduct (Scheme 30).

[62] M. Gulías, J. Durán, F. López, L. Castedo, J. L. Mascareñas, *J. Am. Chem. Soc.* **2007**, *129*, 11026–11027.

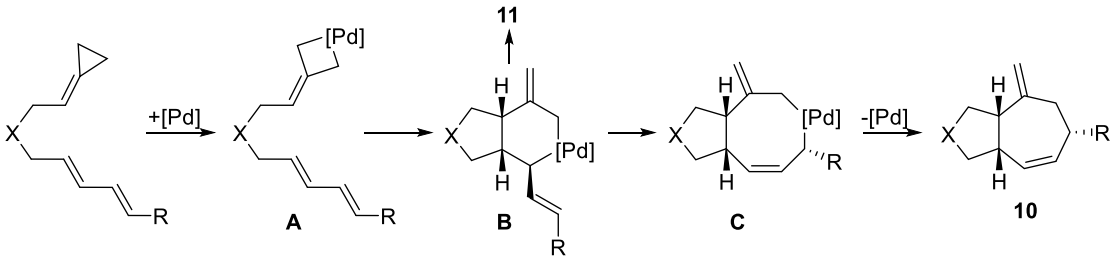

Scheme 30. Mechanistic proposal for the Pd catalyzed (4+3) annulation.

Saito showed that ACPs bearing a carboxylic ester can participate in intermolecular (4+3) annulations with conjugated dienes, under nickel (0)-phosphite catalysis (Scheme 31).[63] Two types of regioisomeric cycloadducts **12** and **12`**, products of the proximal cleavage of the ACP are obtained with poor selectivity. Moreover, subtle modifications at the diene severely decrease the product selectivity. The reaction proceeds through an oxidative cyclization between the metal and the diene delivering intermediate **A**, which insert the ACP leading to a spirocyclic intermediate **B**. A β-carboelimination and a final reductive elimination delivers the seven-membered cycloadducts.

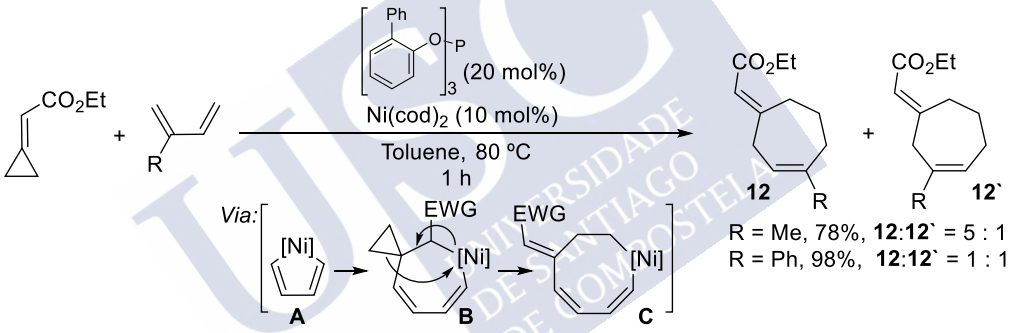

Scheme 31. Ni catalyzed intermolecular (4+3) cycloaddition between ACPs and dienes.

(3+2+2) Cycloadditions

An alternative way to generate seven membered carbocycles is based on multicomponent (3+2+2) cycloadditions. Saito and coworkers reported a pioneer example, namely an intermolecular Ni-catalyzed (3+2+2) cycloaddition between the ACPs and alkynes (Scheme 32). The first report in 2004, involves the use of a single type of alkyne, so two identical units of the alkyne are incorporated into the final cycloheptane product of type **13**.[64] However, in 2006, the same group demonstrated that it was also possible to carry out the reaction with two different alkynes, to obtain products like **14** in good yields and complete regioselectivity.[65] The reaction mechanism would be similar to that abovementioned proposed for dienes.[63]

[63] S. Saito, K. Takeuchi, *Tetrahedron Lett.* **2007**, *48*, 595–598.
[64] S. Saito, M. Masuda, S. Komagawa, *J. Am. Chem. Soc.* **2004**, *126*, 10540–10541.
[65] S. Komagawa, S. Saito, *Angew. Chemie - Int. Ed.* **2006**, *45*, 2446–2449.

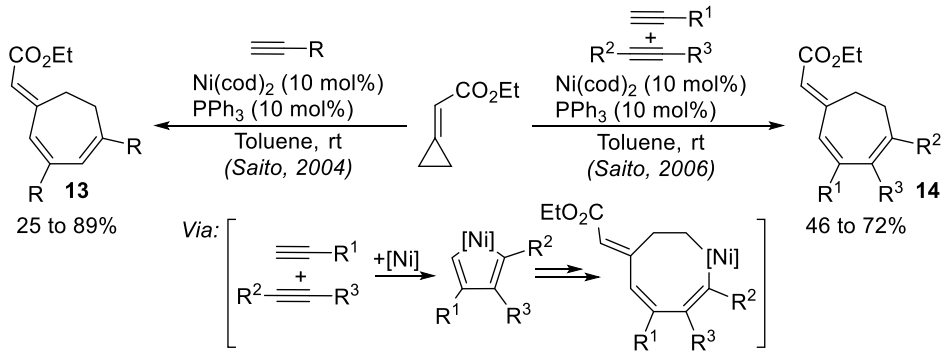

Scheme 32. Ni catalyzed intermolecular (3+2+2) cycloaddition between ACPs and alkynes.

As previously introduced in the context of the (3+2) annulations, in 2010 our group showed that nickel catalysts can promote semi-intermolecular (3+2+2) annulations between ACPs and alkenes bearing EWGs, to assemble seven-membered carbocycles of type **15** (Scheme 33).[66] The reaction, which is promoted by $Ni(cod)_2$, affords 6-7 fused bicycles with good to complete (3+2+2)/(3+2) selectivity (**15**:**16** ratios from 4:1 to 1:0). The mechanism, supported by DFT calculations, begins with the C-C insertion at the proximal bond of the cyclopropane to afford a nickelacyclobutanic intermediate **A** that evolves by migratory insertion of the tethered alkyne to the nickelacycle **B.** Then, a regioselective coordination and migratory insertion (**C**) of the external alkene leads, after a reductive elimination, to the observed cycloadduct.

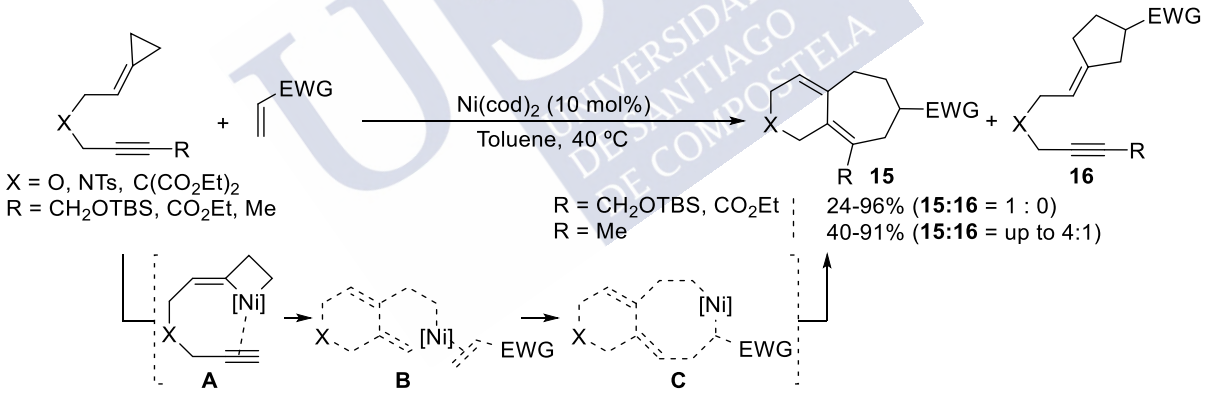

Scheme 33. Ni-catalyzed intermolecular (3+2+2) cycloaddition between ACPs and alkenes.

Later on, in 2015, Tanaka described a Rh catalyzed intermolecular annulation between an amide- containing ACPs and a 1,6-diyne, providing fused-cycloheptadienic products in good yields, but after long reaction times (Scheme 34).[67] The reaction take place under mild conditions and shows a good functional group tolerance in the alkynes.. The reaction starts with an oxidative cyclization between the alkyne and the catalyst leading intermediate rhodacycle **A** evolving to spirocycle **B** after migratory insertion. This intermediate evolves

[66] L. Saya, G. Bhargava, M. A. Navarro, M. Gulías, F. López, I. Fernández, L. Castedo, J. L. Mascareñas, *Angew. Chemie - Int.* **2010**, 9886–9890.
[67] T. Yoshida, Y. Tajima, M. Kobayashi, K. Masutomi, K. Noguchi, K. Tanaka, *Angew. Chemie - Int. Ed.* **2015**, *54*, 8241–8244.

through a β-carboelimination to rhodacycle **C** which eventually provides the fused seven-membered product.

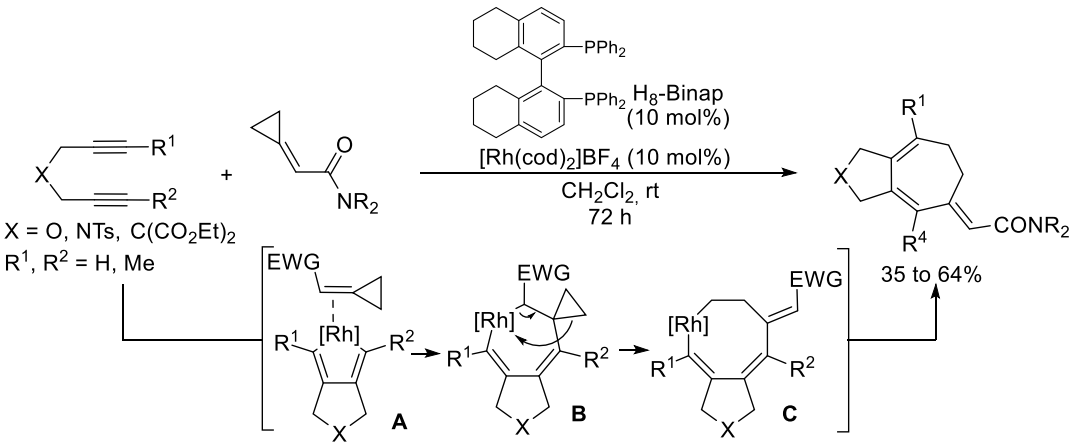

Scheme 34. Rh(I)-catalyzed (3+2+2) cycloaddition between ACPs and alkynes.

Evans and coworkers exploited alternative types of Rh-catalyzed (3+2+2) cycloadditions by using alkene- and alkyne-tethered ACPs (Scheme 35). In the first report of 2008, the authors described the intermolecular reaction between ACPs and electronically-activated alkynes, so that isomeric mixtures of adducts **18** and **18`** were obtained in good yields and moderate to excellent selectivities, in favor of the regioisomer **18**.[68] The authors proposed an oxidative addition over the distal C-C bond of the ACP, forming intermediate **A**. This species undergoes the insertion of the alkene leading to the formation of *π*-allylic rhodium (III) species of type **B,** which reacts with the alkyne regioselectively. As consequence, *π*-allylic rhodium (III) species **C** are generated, which after reductive elimination, provides the product **18**. This mechanistic proposal was further supported by a study published in 2014, where the *π*-allylic form of a rhodium (III) complex of type **B** was isolated and characterized by X-ray crystallography. [69]

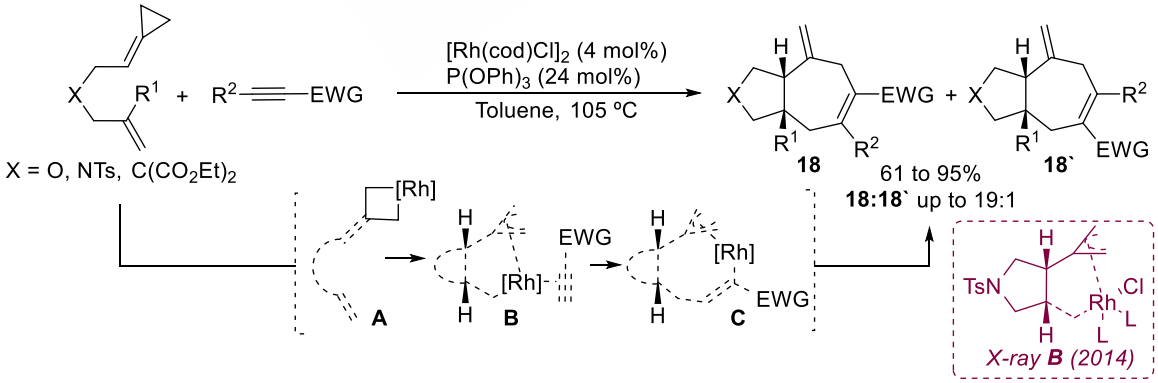

Scheme 35. Rh(I)-catalyzed intermolecular (3+2+2) cycloaddition between ACPs and alkynes.

[68] P. A. Evans, P. A. Inglesby, *J. Am. Chem. Soc.* **2008**, *130*, 12838.
[69] P. A. Inglesby, J. Bacsa, D. E. Negru, P. A. Evans, *Angew. Chemie - Int. Ed.* **2014**, *53*, 3952–3956.

In 2015, Evans showed that allenes were also competent reaction partners, providing for the regio- and diastereoselective assembly of 5-7 bicyclic products in good to excellent yields (Scheme 36). The reaction shows a high tolerance to functional groups in the tether of the ACP when electronically activated allenes are used as counterparts. Mechanistically, the reaction is proposed to follow the same course than those indicated previously.

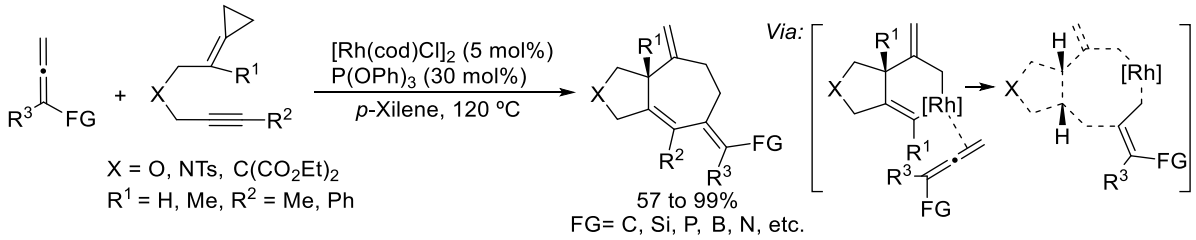

Scheme 36. Rh(I)-catalyzed intermolecular (3+2+2) cycloaddition between ACPs and allenes.

Our group reported in 2014 a related fully intermolecular Rh-catalyzed (3+2+2) annulations between ACPs, alkynes and alkenes to generate complex tricyclic products (Scheme 37).[70] The reaction uses a rhodium (I) – phosphine catalyst when the alkene is monosubstituted, whereas for trisubstituted alkenes is necessary the use of a phosphoramidite ligand. The products are obtained in good yields and, in most of the cases, with total *syn* selectivity. DFT calculations suggests that the reaction mechanism would involve the formation of a π-allylic - rhodium (III) complex **A**, similar to the described by Evans, which selectively inserts the pendant alkene forming species **B**, leading to the products after reductive elimination. Noteworthy, a previous report of our group showed that this reaction can be carried out using a palladium (0) – phosphite catalyst, but with lower efficiency.[71]

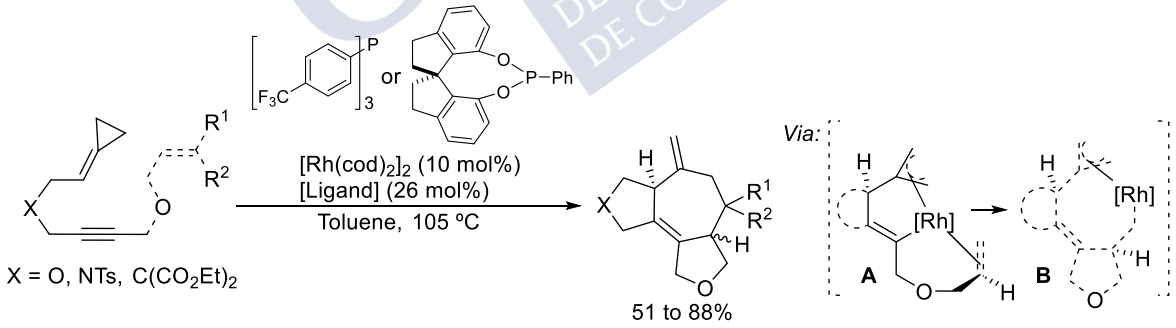

Scheme 37. Rh(I)-catalyzed intramolecular (3+2+2) cycloaddition between ACPs with alkynes and allenes.

Therefore, a number of cycloadditions of ACPs have been reported to yield seven-membered carbocycles through (3+2+2) and (4+3) with different unsaturated partners. However, enantioselective versions are clearly underdeveloped. On this regard, the palladium catalyzed (4+3) intramolecular cycloaddition between ACPs and dienes developed by our group is the only one that has shown the potential to be carried out in an enantioselective manner.[62]

[70] M. Araya, M. Gulías, I. Fernández, G. Bhargava, L. Castedo, J. L. Mascareñas, F. López, *Chem. - A Eur. J.* **2014**, *20*, 10255–10259.
[71] G. Bhargava, B. Trillo, M. Araya, F. López, L. Castedo, J. L. Mascareñas, *Chem. Commun.* **2010**, *46*, 270–272.

3. Heterocycloaddition reactions of alkylidenecyclopropanes

As indicated, alkylidenecyclopropanes are powerful 3C building blocks for the construction of small-to-medium sized mono- or polycarbocyclic systems, particularly with an odd number of carbons.[72] The development of related cycloadditions to provide heterocyclic systems could be *a priori* achieved by using unsaturated carbon-heteroatom reaction partners, such as aldehydes or imines.[73] However, only a few examples of transition metal catalyzed heterocycloadditions using alkylidenecyclopropanes have been developed so far, and all of them involved important limitations. The most relevant examples are described in the chapter 2 of this manuscript (See pages 69-77). Moreover, high order heterocycloaddition reactions using APCs are still no reported.

Considering the potential of ACPs for promoting reactions through the activation of C-C bonds, their easy accessibility, and the precedents indicated in the previous sections, my PhD work was focused on solving some of the limitations of these metal-based catalytic technologies while discovering new, relevant reactivities that can impact the field of synthetic chemistry.

In particular, most of the work has been focused to the development of enantioselective variants of previous reactions, and to the discovery of intramolecular heterocycloadditions with C=X partners, owing to their synthetic potential and the lack of precedents. On the other hand, we also describe part of the work carried out in collaboration with Dr. Cristina Nevado, in two short stays at the University of Zurich.

The work has been summarized in the following three chapters:

Chapter I: Enantioselective palladium-catalyzed [3C + 2C] and [4C + 3C] intramolecular cycloadditions of alkylidenecyclopropanes

Chapter II: Palladium-catalyzed (3+2) heterocycloadditions of alkylidenecyclopropanes

Chapter III: Cyclometallated alkenyl-gold (III) species by proximal ring-opening of ortho-(cyclopropylidenemethyl)pyridines

[72] (a) M. Shi, J. M. Lu, Y. Wei, L. X. Shao, *Acc. Chem. Res.* **2012**, *45*, 641–652. (b) G. Fumagalli, S. Stanton, J. F. Bower, *Chem. Rev.* **2017**, *117*, 9404–9432. (c) P. Chen, B. A. Billett, T. Tsukamoto, G. Dong, *ACS Catal.* **2017**, *7*, 1340–1360. (d) L. Z. Yu, M. Shi, *Chem. - A Eur. J.* **2019**, *25*, 7591–7606.
[73] L. Yu, M. Liu, F. Chen, Q. Xu, *Org. Biomol. Chem.* **2015**, *13*, 8379–92.

USC
UNIVERSIDADE
DE SANTIAGO
DE COMPOSTELA

CHAPTER I: Enantioselective palladium-catalyzed (3C + 2C) and (4C + 3C) cycloaddition of alkylidenecyclopropanes

USC
UNIVERSIDADE
DE SANTIAGO
DE COMPOSTELA

1. Introduction

Transition metal-catalyzed enantioselective cycloadditions

Many of the existing bioactive molecules exhibit cyclic cores and relatively complex tridimensional structures. It is well known that the chemistry that govern biological systems is chiral, therefore the specific activity of bioactive molecules is highly dependent on their optical activity (Figure 8). The generation of these complex polycarbocyclic structures in an enantioselective form is highly relevant. Thus, a mayor challenge in current synthetic chemistry consists of the development of methodologies that allow the straightforward assembly of complex polycyclic scaffolds in an enantioselective manner, from readily available achiral precursors.[74]

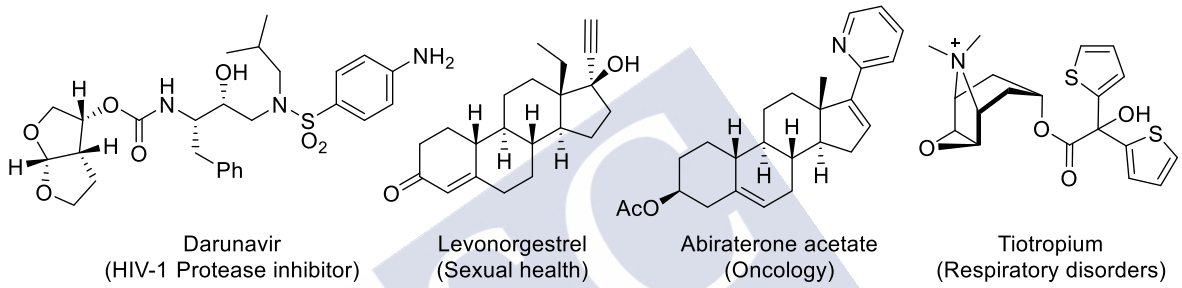

Figure 8. Biologically relevant chiral polycyclic molecules.

In this context, intramolecular cycloaddition reactions are powerful synthetic tools because they have the potential of enabling the transformation of simple linear starting materials into complex polycyclic molecules. If the reaction involves the use of C-C unsaturated systems, the formation of C-C bonds bearing sp^3 stereocenters can occur. Thus, in a single operational step, polycyclic cores bearing new chiral centers can be assembled.

While non-catalyzed enantioselective reactions rely on the use of enantioenriched starting materials, catalytic processes only require substoichiometric amounts of a chiral organic or organometallic molecule, potentially improving the reaction efficiency. In this regard, chiral organometallic catalysts based on the use of chiral ancillary ligands offer a broad range of opportunitie,s considering the availability of different types of metals and ligands.

1.1. Transition metal catalyzed cycloadditions leading to five-membered carbocycles

Despite a considerable number of transition metal catalyzed (3+2) enantioselective formal cycloadditions have been reported, most examples involve intermolecular annulations and

[74] (a) J. J. Li, E. J. Corey, *Total Synthesis of Natural Products: At the Frontiers of Organic Chemistry*, Springer, **2012.** (b) K. C. Nicolaou, E. J. Sorensen, *Classics in Total Synthesis: targets, strategies, methods*, Wiley-VCH, **1996**. (c) K. C. Nicolaou, S. A. Snyder, *Classics in Total Synthesis II: more targets, strategies, methods*, Wiley-VCH, **2003**. (d) K. C. Nicolaou, J. S. Chen, *Classics in total synthesis III: Further targets, strategies, methods*, Wiley-VCH, **2011.** (e) J. H. Rigby, *Studies in Natural Products Chemistry*, Vol. 12, Elsevier, Amsterdam, **1988**.

lead to monocyclic products. In contrast, the development of intramolecular variants, which would lead to more complex polycyclic scaffolds, are still underdeveloped, either using (2+2+1) or (3+2) annulation strategies. The most relevant inter and intramolecular enantioselective cycloaddition examples, relevant to this PhD work, are summarized in the following sections.

(2+2+1) Cycloadditions

One of the first examples of an intramolecular enantioselective transition metal-catalyzed cycloaddition for the construction of a five-membered carbocycle consisted of a Pauson-Khand reaction reported by Buchwald and coworkers in 1996 (Scheme 38).[75] In this work, the use a chiral titanium catalyst in the presence of CO allows to transform a variety of enynes into different bicyclic cyclopentanones, with high yields and remarkable enantioselectivities. Unfortunately, for the most challenging substrates, high catalytic loadings were required. The proposed mechanism is based on the formation of titanacyclopropene **A**, which evolves via enantiodetermining migratory insertion of the alkene towards the species **B**. At this point, a CO molecule gets inserted between the Csp^2-Ti bond leading to **C** which finally, after a reductive elimination, affords the cyclopentanone.

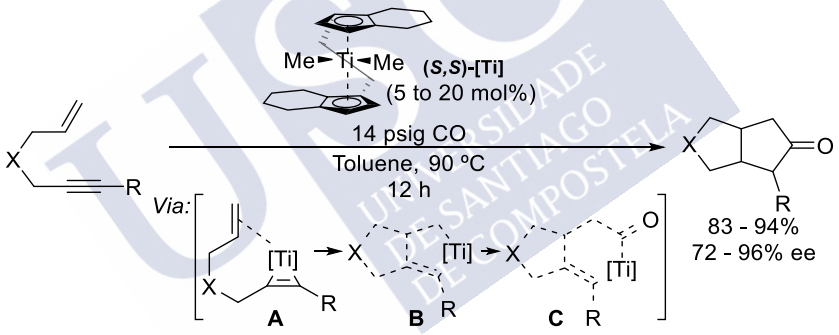

Scheme 38. Ti(IV)-catalyzed enantioselective Pauson-Khand reaction.

A related work was published by Verdaguer and Riera in 2015 using, in this case, a cationic rhodium catalyst and a small wide-angle bisphosphine chiral ligand (Scheme 39).[76] This transformation takes place under milder conditions, using lower temperatures and CO at atmospheric pressure. Nevertheless, the scope is still limited, the yields and enantioselectivities are moderate and competitive (2+2+2) cycloadducts are observed in significant yields.

[75] F. A. Hicks, S. L. Buchwald, *J. Am. Chem. Soc.* **1996**, *118*, 11688–11689.
[76] A. R. Constantino, A. Grabulosa, A. Riera, X. Verdaguer, **2015**, *Organometallics*, *34*, 4989-4993.

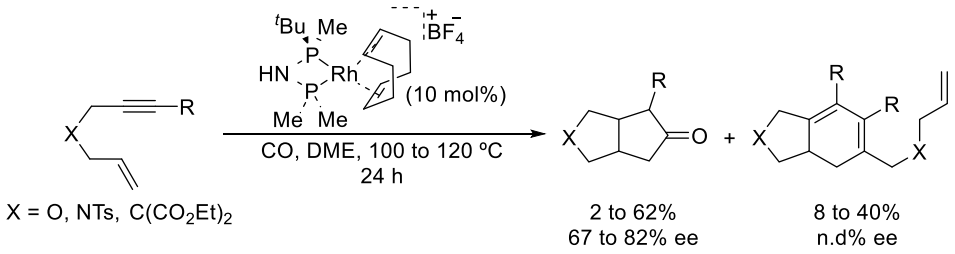

Scheme 39. Rh(I)-catalyzed enantioselective Pauson-Khand reaction.

Intermolecular (3+2) Cycloadditions

Probably one of the most explored enantioselective cycloadditions for the construction of five-membered carbocycles is based on the generation of chiral Pd-TMM species. The first report on this asymmetric reaction was published in 2006, but it was not until 2011 when ligand optimization studies allowed to enhance the enantioselectivity of the process, reaching high yields and enantiomeric excesses.[77] The TMM precursors reacts with a Pd complex bearing the chiral phosphoramidite **(*R,R,R*)-L20** to yield a Pd-TMM that undergoes a highly enantioselective annulation with a Michael acceptor (Scheme 40). More recently, a new variant of TMM precursors bearing nitrile groups seems to be more efficient. After these works were published, related enantioselective technologies were additionally described by this group using different TMM precursors and reaction counterparts.[78]

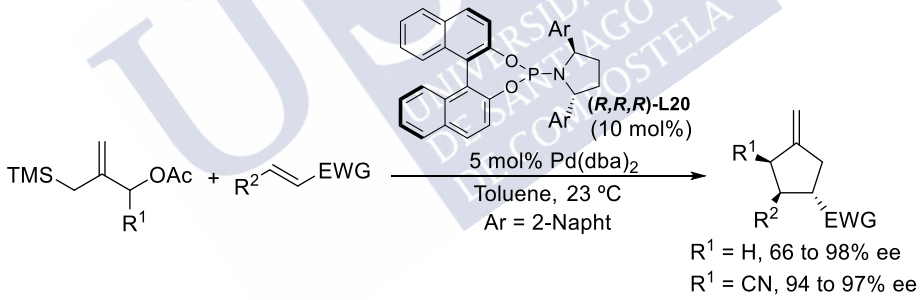

Scheme 40. Pd-catalyzed enantioselective (3+2) reaction between TMM precursors and alkenes.

Enantioselective annulations based on C-C activation are very appealing from a synthetic point of view, because they generally involve high degrees of atom economy. In this regard, vinylcyclopropanes (VCPs) are very versatile building blocks in the enantioselective construction of carbocyclic systems.

[77] B. M. Trost, S. M. Silverman, J. P. Stambuli, *J. Am. Chem. Soc.* **2011**, *133*, 19483–19497.
[78] (a) B. M. Trost, T. M. Lam, *J. Am. Chem. Soc.* **2012**, *134*, 11319–11321. (b) B. M. Trost, A. Maruniak, *Angew. Chemie - Int. Ed.* **2013**, *52*, 6262–6264. (c) B. M. Trost, Y. Wang, *Angew. Chemie - Int. Ed.* **2018**, *57*, 11025–11029. (d) B. M. Trost, Z. Jiao, C.-I. J. Hung, *Angew. Chemie Int. Ed.* **2019**, *58*, 15154–15158.

An elegant example using vinylcyclopropanes and *a,β*-unsaturated aldehydes as reaction partners was reported by Jørgensen in 2016 (Scheme 41).[79] The reaction takes place through synergistic action of a palladium (0) catalyst, to activate the cyclopropane leading to intermediate **A**, and an organocatalyst (Hayashi-Jørgensen prolinol), to generate a suitable electrophilic iminium partner **B**. The reaction evolves through a nucleophilic *1,4*-addition of the stabilized malonic anion over the iminium, followed by a ring closing of the generated enamine **C**.

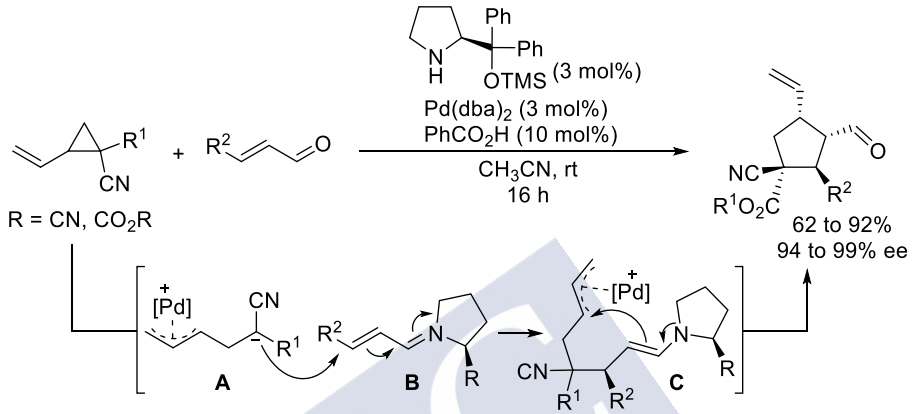

Scheme 41. Synergistic enantioselective (3+2) reaction between VCPs and *a,β*-unsaturated aldehydes.

In 2018, Shi reported a mechanistically related (3+2) cycloaddition between VCP and indoles to yield fused polycyclic cores bearing up to three new stereogenic centers (Scheme 42).[80] The transformation, promoted by a palladium (0) - chiral phosphoramidite catalyst takes place under mild conditions to provide good overall yields and good to excellent enantioselectivities, but poor diastereoselectivities.

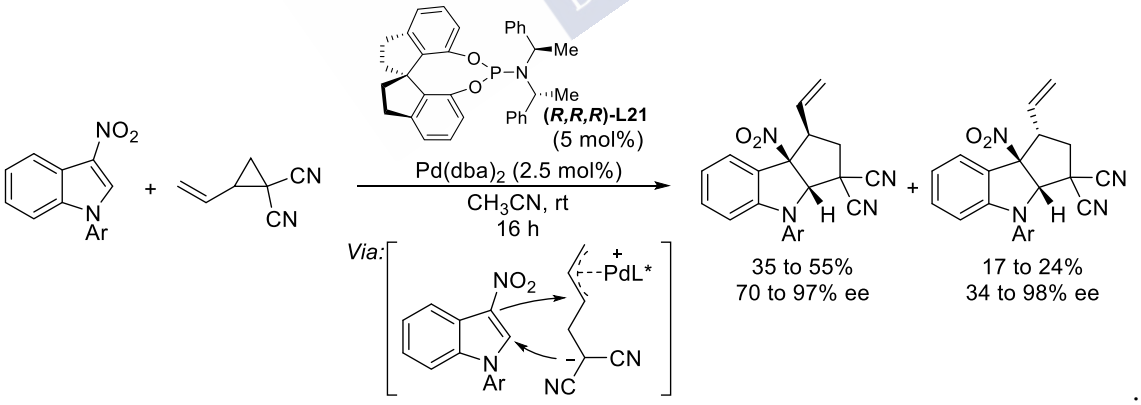

Scheme 42. Pd-catalyzed enantioselective (3+2) between VCPs and indoles.

[79] K. S. Halskov, L. Næsborg, F. Tur, K. A. Jørgensen, *Org. Lett.* **2016**, *18*, 2220–2223.
[80] M. Sun, Z. Q. Zhu, L. Gu, X. Wan, G. J. Mei, F. Shi, *J. Org. Chem.* **2018**, *83*, 2341–2348.

Intramolecular (3+2) Cycloadditions

Yu and coworkers demonstrated that vinylcyclopropanes (VCPs) can react intramolecularly with tethered alkynes in presence of a cationic rhodium (I) catalyst prepared in situ from $[Rh(CO)_2Cl]_2$, $AgSbF_6$ and H_8- BINAP. The reaction provides fused 5,5 bicyclic scaffolds with a vinyl group at the ring fusion, in good yields and with excellent enantioselectivities (Scheme 43).[81] The reaction mechanism, which is supported with DFT studies, entails initial coordination of the metal to the double bond of the VCP (**A**), followed by the ring opening of the cyclopropane to generate the rhodium π-allylic species **B**. A migratory insertion step of the tethered alkyne leads to the rhodacyclohexene **C** that provides the bicyclic products after reductive elimination.

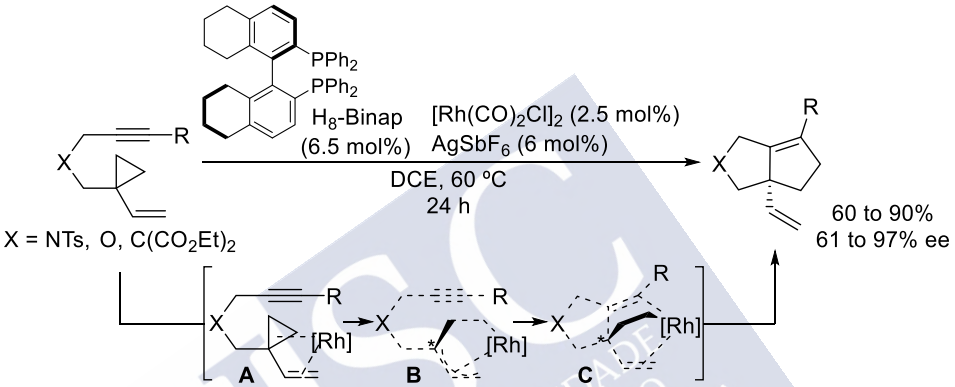

Scheme 43. Rh(I)-catalyzed enantioselective (3+2) reaction between VCPs precursors and alkynes.

Despite the important number of TMC annulations using alkylidenecyclopropanes as 3C partners, the development of enantioselective variants remained elusive prior to the development of the current PhD work. Some of preliminary work in the group had indeed confirmed the difficulties of achieving the required asymmetric annulation. [82] Given that the racemic transformation involved the use of phosphite ligands (scheme 44),[83] these previous attempts were carried out using electronically similar, readily accessible phosphoramidite ligands. Contrary to phosphites, which are usually prone to oxidation processes, phosphoramidites are highly robust and have been shown very effective in different types of TMC reactions, including Pd catalyzed cycloadditions.[84]

[81] M. Lin, G. Y. Kang, Y. A. Guo, Z. X. Yu, *J. Am. Chem. Soc.* **2012**, *134*, 398–405.
[82] Preliminary enantioselective studies carried out by Dr. Juan Durán Verdasco (**2011**) and Dr. Lara Villarino Palmaz (**2013**), *Doctoral Thesis*.
[83] M. Gulías, R. García, a Delgado, L. Castedo, J. L. Mascareñas, *J. Am. Chem. Soc.* **2006**, *128*, 384–385.
[84] B. M. Trost, S. M. Silverman, J. P. Stambuli, *J. Am. Chem. Soc.* **2011**, *133*, 19483–19497. (b) B. M. Trost, S. M. Silverman, *J. Am. Chem. Soc.* **2012**, *134*, 4941–4954. (c) B. M. Trost, A. Maruniak, *Angew. Chemie - Int. Ed.* **2013**, *52*, 6262–6264. (d) B. M. Trost, G. Mata, *Angew. Chemie - Int. Ed.* **2018**, *57*, 12333–12337.

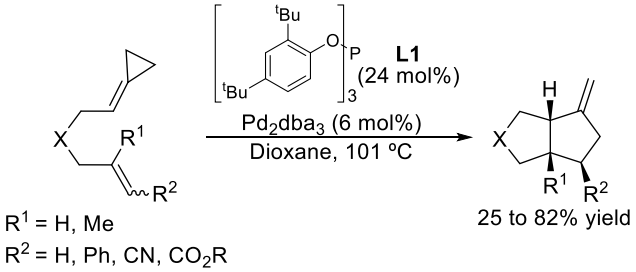

Scheme 44. Racemic Pd-catalyzed intramolecular (3+2) between ACPs and alkenes.

Initial efforts carried out by the group involve the use of BINOL-based phosphoramidite **L2**, using **3b** as model precursor (Scheme 45).[85] Under the same reaction conditions than the racemic transformation, the isomer **(*R*,*R*,*R*)-L4** provided the cycloadduct in a moderate -48% ee, whereas the diastereoisomer **(*S*,*R*,*R*)-L4** achieved a poor 6% ee. It is important to highlight that regardless the configuration of the ligand, the reaction showed total diastereoselectivity. Interestingly, the use of a ligand bearing phenyl groups at 3,3` positions of the BINOL core showed strongly improve the ee. While **(*S*,*S*,*S*)-L5** lead to a poor 26% ee, the isomer **(*S*,*R*,*R*)-L5** lead to the major formation of the opposite enantiomer, in a promising 74% ee.

The use of a phosphoramidite with an achiral diisopropylamine (**(*S*)-L6**) confirmed the importance of amine chirality for enantioinduction (31%ee). On the other hand, the use of a conformationally more restricted pyrrolidine phosphoramidites (**(*R*,*R*,*R*)-L7** and **(*S*,*R*,*R*)-L7**) led to lower ee values of 45% and 17%, respectively. These results confirmed that the amine used in the phosphoramidite contributes considerably to the asymmetric induction of the process. Curiously, **(*S*,*R*,*R*)-L8**, an structural analogue to **(*S*,*R*,*R*)-L5,** but bearing a VAPOL core instead of BINOL, provided the cycloadduct with a good 67% yield, and a similar ee than **(*S*,*R*,*R*)-L5** (74% ee).

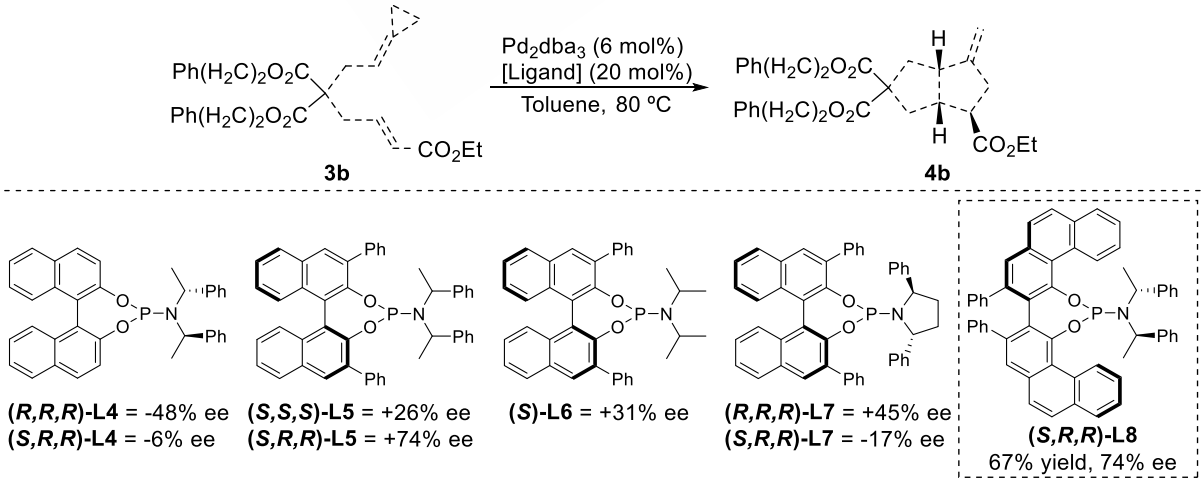

Scheme 45. Preliminary screening of chiral ligands for the enantioselective (3+2) reaction. NOTE: The sign "+ or – " is used to indicate whether they provide the same or opposite major enantiomer"

[85] J. F. Teichert, B. L. Feringa, *Angew. Chemie - Int. Ed.* **2010**, *49*, 2486–2528.

Further optimization carried out by Dr. Lara Villarino showed that changing the palladium precatalyst from Pd_2dba_3 to $CpPd(\eta^3\text{-}1\text{-}PhC_3H_4)$ significantly improved the reaction rate and yield (Table 2). Thus, the reaction promoted by $CpPd(\eta^3\text{-}1\text{-}PhC_3H_4)$ and ***(S,R,R)*-L6** provided the product in 88% yield after only two hours of reaction, with the same 75% ee (entry 1 *vs* 2). Additionally, the decrease in the catalytic load of the ligand from 20 mol% to 12.5 mol% did not affect the reaction efficiency (entry 3).

Curiously, a remarkably enhancement of the enantioselectivity was observed when the temperature was raised from 80 to 110 ºC, so that **4b** was obtained in an 88% yield and 84% ee (entry 4). This temperature-dependence of the ee is not very usual. Related reports in literature associate this enhancement of the selectivity at higher temperatures to reactions with a large entropic contribution to the diastereomeric transition state energies at the enantiodetermining step.[86] Finally, it was possible to decrease the catalytic load down to a 5 mol% of $CpPd(\eta^3\text{-}1\text{-}PhC_3H_4)$ and a 6 mol% of **(*S,R,R*)-L8** without affecting the reaction efficiency (94%, 83% ee, entry 5).

Table 2. Optimization of the enantioselective (3+2) cycloaddition.

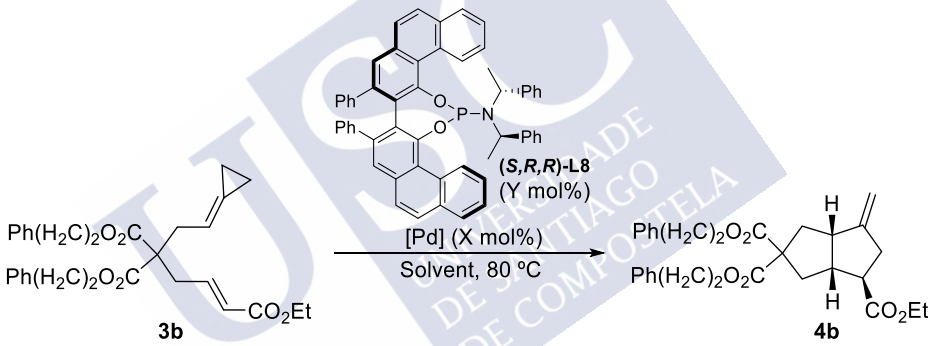

Entry	[Pd] (mol%)	L (mol%)	T (ºC)	t (h)[a]	4b (%)[b]	ee (%)[c]
1	$Pd_2(dba)_3$ (6)	20	80	8	67	75
2	$CpPd(\eta^3\text{-}1\text{-}PhC_3H_4)$ (10)	20	80	2	88	75
3	$CpPd(\eta^3\text{-}1\text{-}PhC_3H_4)$ (10)	12.5	80	3	85	76
4	$CpPd(\eta^3\text{-}1\text{-}PhC_3H_4)$ (10)	12.5	110	1.5	88	84
5	$CpPd(\eta^3\text{-}1\text{-}PhC_3H_4)$ (5)	6	110	4	94	83

[86] For other works related with temperature-dependent enantioinductive processes, see: (a) R. Saito, S. Naruse, K. Takano, K. Fukuda, A. Katoh, Y. Inoue, *Org. Lett.* **2006**, *8*, 2067–2070. (b) Y. Sohtome, B. Shin, N. Horitsugi, K. Noguchi, K. Nagasawa, *Chem. - An Asian J.* **2011**, *6*, 2463–2470. (c) G. Pandey, S. Rajender, *Chem. - A Eur. J.* **2011**, *17*, 6304–6308. (d) G. Storch, O. Trapp, *Angew. Chemie - Int. Ed.* **2015**, *54*, 3580–3586. (e) M. K. Ilg, L. M. Wolf, L. Mantilli, C. Farès, W. Thiel, A. Fürstner, *Chem. - A Eur. J.* **2015**, *21*, 12279–12284. (f) I. Méndez, R. Rodríguez, V. Polo, V. Passarelli, F. J. Lahoz, P. García-Orduña, D. Carmona, *Chem. - A Eur. J.* **2016**, *22*, 11064–11083. (g) S. Wang, J. Xiao, J. Li, H. Xiang, C. Wang, X. Chen, R. G. Carter, H. Yang, *Chem. Commun.* **2017**, *53*, 4441–4444.

Once the temperature, catalytic loading, solvent and concentration were optimized, a final tuning of the ligand was carried out (Scheme 46). In particular, two phosphoramidites **(*S,R,R*)-L9** and **(*S,R,R*)-L10**, bearing a bis[(R)-(+)-(1-naphthyl)ethyl]amine instead of the bis[(R)-(+)-1-phenylethyl]amine were prepared and tested in the model reaction. This change resulted in a substantial improvement of enantioselectivities. For the BINOL-based ligands, ee changed from 78% ee to an 87% ee (entry 1 and 2), whereas for the VAPOL derivate the ee reached an excellent 94% ee (entry 3 and 4). Therefore, with these promising results in hand, the study of the scope of this process was the next objective, which was tackled in this Chapter 1 of the thesis (see Objective, page 49)

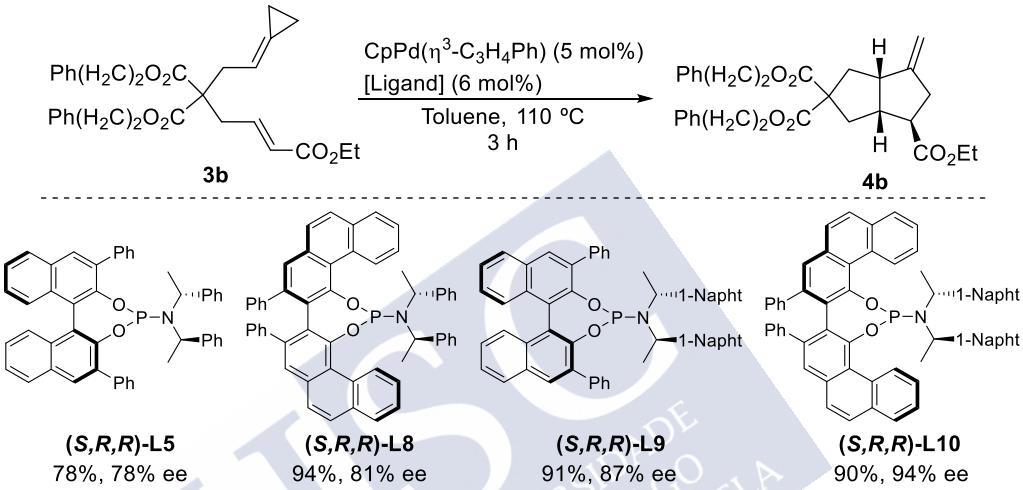

Scheme 46. Secondary screening of chiral ligands for the enantioselective (3+2) reaction.

1.2. Enantioselective TMC intramolecular cycloadditions leading to seven-membered carbocycles

The formation of larger cyclic systems is, in general, significantly more difficult.[60] In the context of enantioselective transition metal catalyzed cycloadditions leading to seven-membered carbocycles, only a few cases, mostly intramolecular (5+2) and (4+3) annulations have been reported.

(5+2) Cycloadditions

The first example of a (5+2) cycloaddition was reported by Wender in 1998 and consisted of a rhodium catalyzed intramolecular cycloaddition of VCPs and alkenes (Scheme 47).[87] Albeit the racemic transformation was almost exclusively explored in this work, the authors provided one example using CHIRAPHOS as ligand, which led a moderate 63% ee. In 2006, the same group showed that this (5+2) annulation using a cationic rhodium (I) – BINAP complex leads to fused products with full *syn*-selectivity at the ring fusion and, in many cases, good or excellent enantioselectivities.[88] Nevertheless, the scope is not very broad and the highest

[87] P. A. Wender, C. O. Husfeld, E. Langkopf, J. A. Love, N. Pleuss, *Tetrahedron* **1998**, *54*, 7203–7220.
[88] P. A. Wender, L. O. Haustedt, J. Lim, J. A. Love, T. J. Williams, J. Y. Yoon, *J. Am. Chem. Soc.* **2006**, *128*, 6302–6303.

enantioselectivities are only achieved when malonates are used in the connecting tether. The proposed mechanism involves the initial formation of the six-membered rhodacycle **A**, followed by the migratory insertion of the pending alkene and a reductive elimination in the resulting rhodalacyclooctene intermediate **B**.

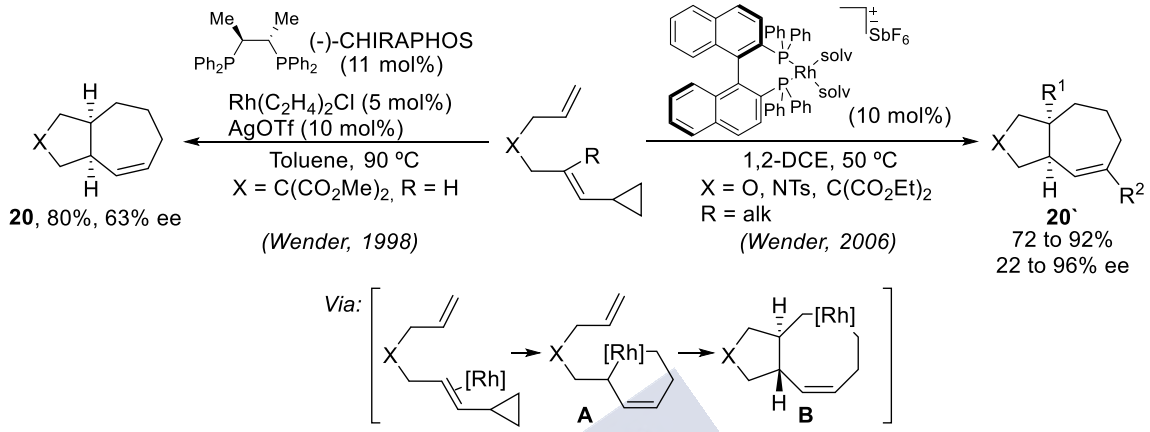

Scheme 47. Rh(I)-catalyzed intramolecular (5+2) between VCPs and alkenes.

Few years later, Hayashi and co-workers developed the enantioselective intramolecular variant using VCPs tethered to alkynes (Scheme 48).[89] The catalytic system, composed by a 5 mol% of $[RhCl(C_2H_4)_2]_2$, 7.5 mol% of phosphoramidite ***(S,R,R)*-L4** and 6 mol% of $NaBAr^F_4$, provides the fused bicyclic products bearing one chiral center in good enantioselectivities, regardless the type of functional group in the connecting tether. Moreover, alkynes bearing aromatic, aliphatic or even terminal alkynes are well tolerated.

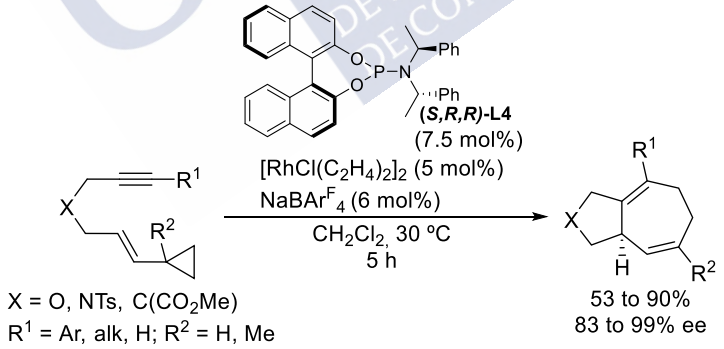

Scheme 48. Rh(I)-catalyzed intramolecular (5+2) between VCPs and alkynes.

(4+3) Cycloadditions

In 2011, our group described an enantioselective intramolecular gold catalyzed (4+3) annulation of allenedienes, reaction that gives access to fused 5-7 bicyclic scaffolds with full *anti* selectivity in the ring junction (Scheme 49).[90] The use of a cationic gold (I) complex, generated *in situ* from a bulky BINOL based phosphoramidite gold(I) chloride complex and

[89] R. Shintani, H. Nakatsu, K. Takatsu, T. Hayashi, *Chem. - A Eur. J.* **2009**, *15*, 8692–8694.
[90] Alonso, H. Faustino, F. López, J. L. Mascareñas, *Angew. Chemie - Int. Ed.* **2011**, *50*, 11496–11500.

an silver(I) salt, provides the products with high efficiency, reaching excellent yields and enantioselectivities, of up to 98% ee. Experimental evidence and DFT calculations suggest that the reaction starts through the activation of the allene by the gold complex, followed by the formation of the cationic π-allylic species **A** that further evolves through a concerted [4C(4 π) + 3C(2 π)] with the diene towards the gold carbene **B**. At this point an 1,2-hydride migration, with concomitant elimination of the gold(I) species, provides the corresponding fused seven-membered carbocycles.

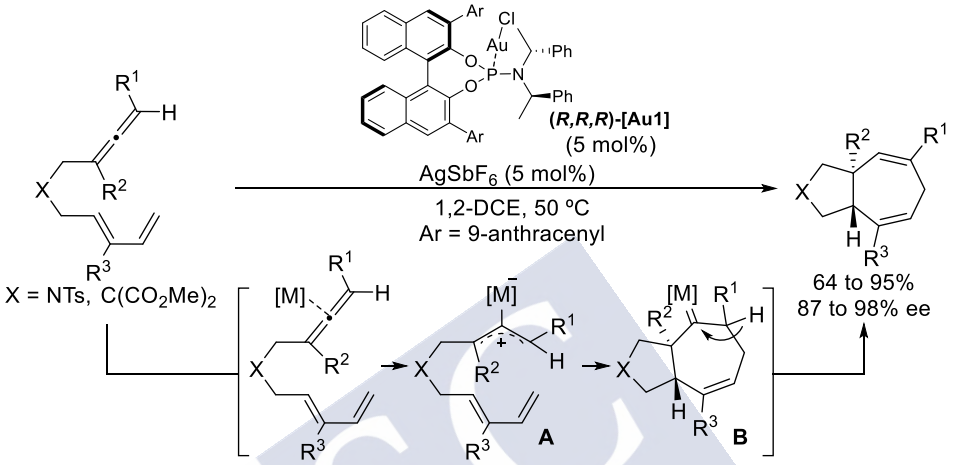

Scheme 49. Au(I)-catalyzed intramolecular (4+2) of allenedienes.

In 2007 our group also reported the palladium catalyzed intramolecular (4+3) cycloaddition between ACPs and dienes, to yield bicyclo [5.3.0] decane of type **10** (Scheme 50).[62] By using a simple chiral phosphoramidite ligand such as **(*R*)-L3**, the viability of an asymmetric reaction was also demonstrated. Thus, enantioselectivities of 45%, 47% and 64% ee were reported for three isolated cases. These examples constituted the first cases of asymmetric induction in a (4+3) annulation involving ACPs . Moreover, the indicate that that a highly enantioselective version could be reachable by fine tuning the catalyst and reaction conditions.

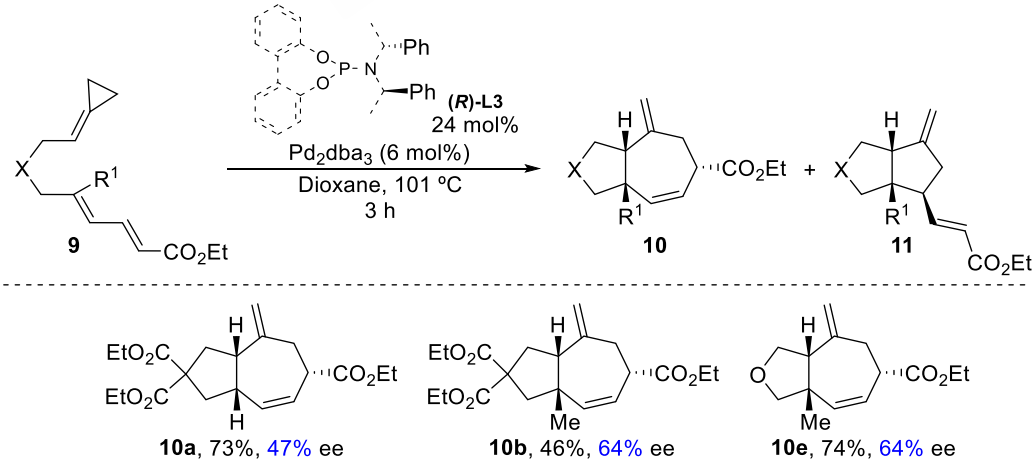

Scheme 50. Pd-catalyzed intramolecular (4+3) between ACPs and dienes.

2. Objectives

Based on the prior work developed by former PhD students Juan Durán and Lara Villarino in the development of palladium catalyzed enantioselective (3+2) cycloaddition reaction of alkylidenecyclopropanes and alkenes (see Scheme 46, page 53), our first goal consisted on assessing the viability and scope of this methodology. This required the preparation of several alkene-tethered alkylidenecyclopropane analogues with different structural features, such as different tethers or substituents at the ACP and the alkene.

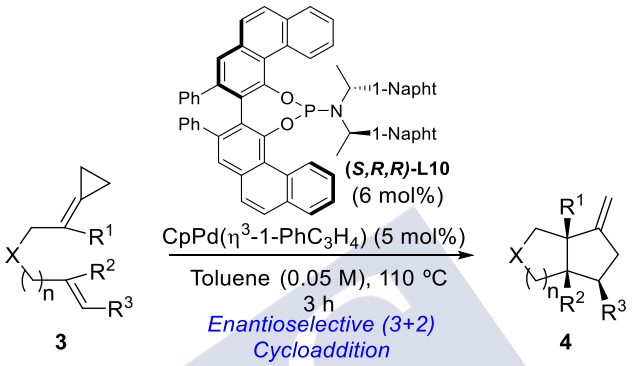

Scheme 51. Evaluation of the scope of the enantioselective (3+2) cycloaddition.

In addition, we planned the development of highly enantioselective variants of the palladium catalyzed intramolecular (4+3) cycloaddition between alkylidenecyclopropanes and conjugated dienes (Scheme 52). To develop the asymmetric reaction, we will assess the performance of precursor **9a** using several chiral ligands. Once optimal conditions can we developed, we will study the scope of the reaction.

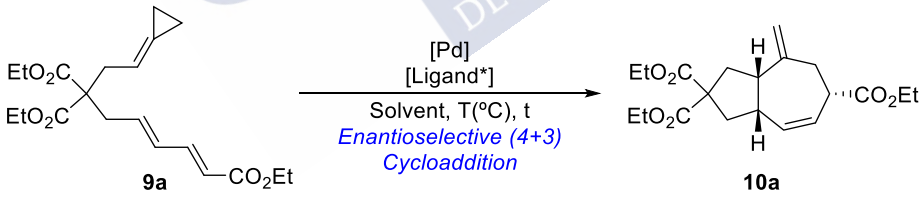

Scheme 52. Development of the enantioselective (4+3) cycloaddition.

3. Results and discussion

3.1. Enantioselective (3+2) cycloaddition between ACPs and alkenes

To evaluate the reaction, we first needed the preparation of different ACP precursors (Figure 9). Substrates **3b**, **3c** are direct analogues of the model substrate **3a** and allow to evaluate the influence of subtle modifications in the reaction efficiency. To compare the reactivity of precursors bearing different electron withdrawing groups in the alkene, we will prepare amide (**3h**) or a ketone (**3g**) derivative.

Precursors bearing a methyl substituent in the alkylidenecyclopropane (**3d**) or at the β-position of the ester (**3e**) are especially interesting, as they would allow to build bicycles with challenging quaternary chiral centers at the ring fusion. To evaluate whether the length of the tether is relevant, substrate **3f** with an additional methylene unit will also be tested. Furthermore, we also plan to make precursors with heteroatoms at the tether, such as the ether **3k**, amine **3i** and tosylamide **3j**, as well as other containing unactivated double bonds. In this regard, bisalkylidenecyclopropane **3m** and derivatives like **3n** or allene **3o** will also be evaluated.

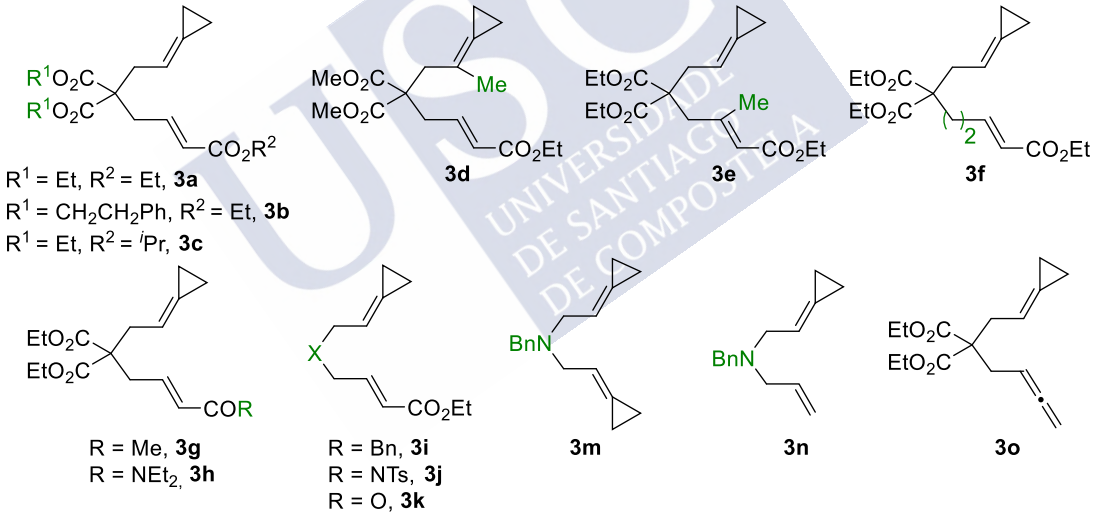

Figure 9. Substrates synthesized for the reaction scope.

3.1.1. Synthesis of precursors

The model precursor **3a** was readily synthesized in two steps. Alkylation of diethylmalonate under palladium catalyzed conditions with the tosylate **21** leads to **22** in a 57%yield. A subsequent alkylation using NaH and ethyl 4-bromocrotonate provided the desired model precursor **3a** in an 80% yield (Scheme 53).

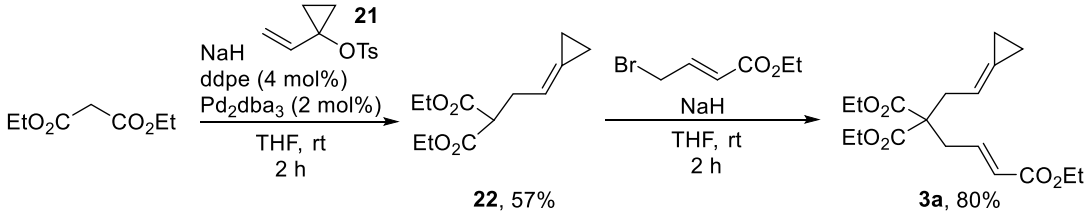

Scheme 53. Synthesis of substrates **3a** (model).

Using the same synthetic route, we also prepared the methyl-substituted analogue **3d**. The palladium catalyzed alkylation was carried out with the ether **23** as surrogate of the tosylate **21**, affording the malonate **24** in 50% yield. After a second alkylation with ethyl 4-bromocrotonate, malonate **3d** was obtained in a good 73% yield (Scheme 54).

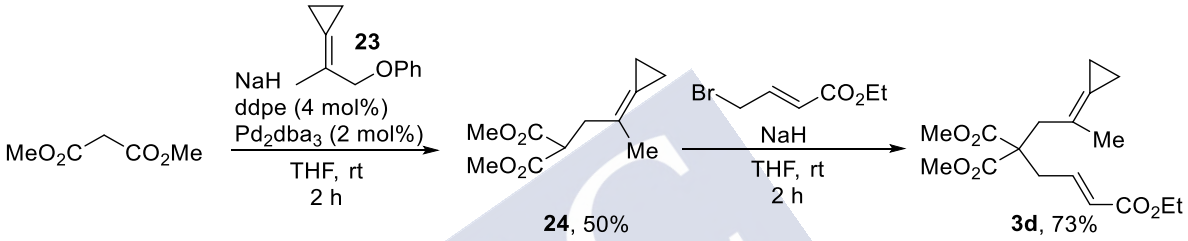

Scheme 54. Synthesis of substrate **3d**.

Ester **3c**, amide **3h** and ketone **3h** where synthesized starting from malonate **22**, which was alkylated with 2-bromo-1,1-dimethoxyethane using NaH as base, followed by an *in situ* hydrolysis, affording **48a** in a 60% yield (two steps). The treatment of this aldehyde with different phosphorus ylides leads to the precursors **3c**, **3g** and **3h** in good yields (Scheme 55).

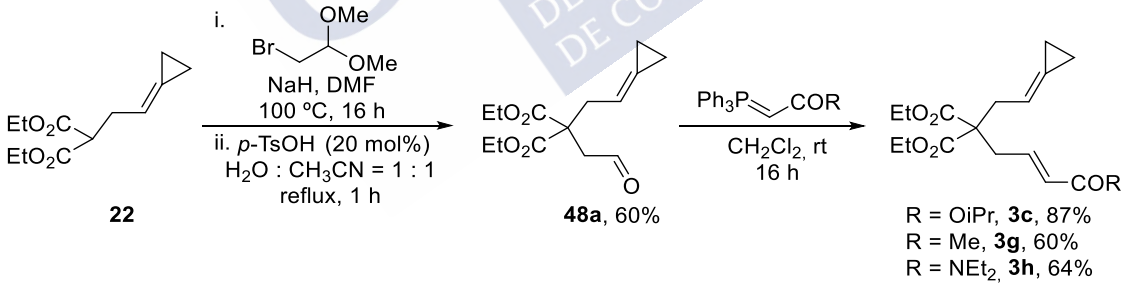

Scheme 55. Synthesis of substrates **3c**, **3h** and **3h**.

Precursor **3f** was also synthesized in two steps from **22,** through a Michael addition to acrolein (80% yield) and a subsequent Wittig reaction, using the (carbethoxymethylene) triphenylphosphorane (85% yield, Scheme 56).

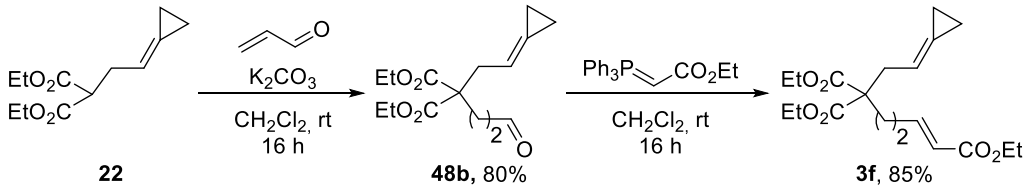

Scheme 56. Synthesis of substrate **3f**.

An oxygenated-tethered precursor was prepared through an initial Tsuji-Trost reaction between ethyleneglycol and tosylate **21**, to yield the alcohol **26** in 59% yield. Then, a Swern oxidation and subsequent Wittig reaction produced **3k** in a 48% yield (two steps, Scheme 57).

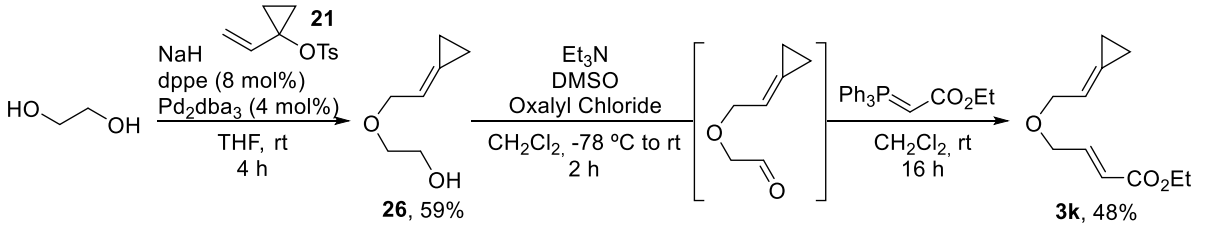

Scheme 57. Synthesis of substrate **3k**.

N-Benzyl analogue **3m** was also synthesized from the tosylate **21** upon treatment with benzyl amine, $Pd_2(dba)_3$ and PPh_3. Besides the e bisalkylidenecyclopropane **3m** (20% yield), the mono alkylated product **27** was also obtained in 69% yield (Scheme 58).

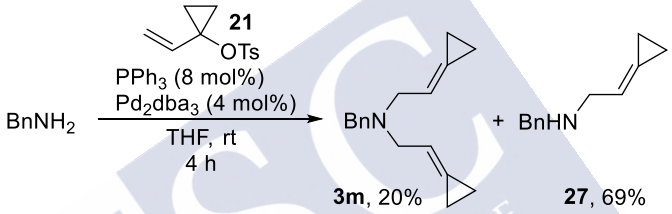

Scheme 58. Synthesis of substrate **20** and precursor **27**.

Treatment of this monoalkylated amine **27** with K_2CO_3 and either ethyl *trans*-4-bromo-2-butenoate or allyl bromide, led to precursors **3i** and **3n** in good yields (Scheme 59).

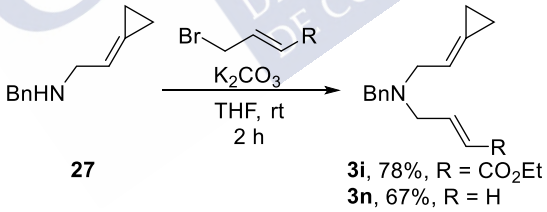

Scheme 59. Synthesis of substrates **3j** and **3n**.

Using a similar strategy, the *N*-tosyl analogue **3j** was synthesized by a Pd-catalyzed allylic alkylation of NH(Ts)Boc with tosylate **21**, followed by removal of the Boc group and treatment of the resulting sulfonamide with NaH and ethyl 4-bromocrotonate (55% yield, Scheme 60).

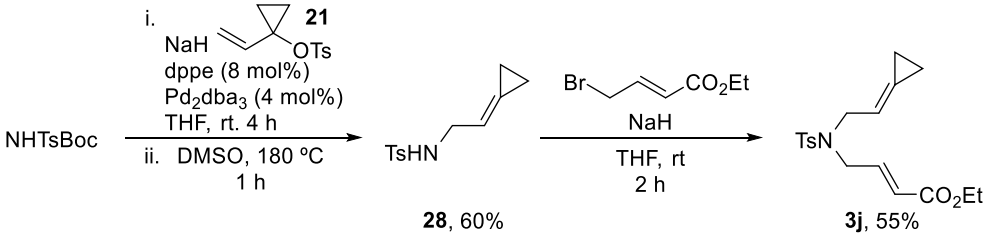

Scheme 60. Synthesis of substrate **3j**.

Finally, the allene **3o** was synthesized by treatment of the propargylic alcohol **19** alkyne with $LiAlH_4$ (49% yield) followed by mesylation of the resulting alcohol **29** and subsequent alkylation with **22** (22% yield over the two steps, Scheme 61).

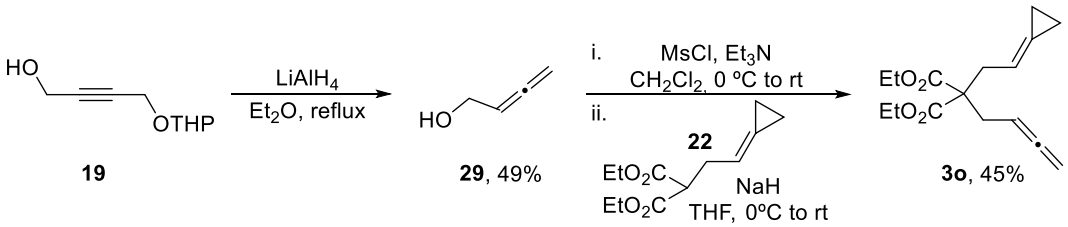

Scheme 61. Synthesis of substrate **3o**.

3.1.2. Ligand synthesis

Considering that the most promising preliminary results were obtained using the bulky phosphoramidite derived from VAPOL, **(*S*,*R*,*R*)-L10**, and that the synthesis of this ligand was problematic and lacked reproducibility, we first focused on optimizing its preparation.

The original procedure used stoichiometric amounts of the amine and PCl_3 for the first step (Scheme 62), so we envisioned that the non-quantitative formation of the dichloride intermediate **17** could be responsible for the low yields and poor reproducibility.

Therefore, to ensure the quantitative formation of the intermediate **17**, we added an excess of PCl_3 (10 eq.) and Et_3N (10 eq.) in the first step of the reaction. Once the intermediate **17** has been successfully formed, the excess of PCl_3 was removed under high vacuum, and the crude was washed with CH_2Cl_2. This process was repeated twice. Once the PCl_3 was fully removed, the resulting solid was dissolved in CH_2Cl_2, and Et_3N (10 eq.) was added. The mixture was cooled at 0 ºC and a mixture of (*S*)-VAPOL (1 eq.) in CH_2Cl_2 with Et_3N (10 eq.) was added dropwise, and the reaction was stirred at room temperature for 16 h. These modifications in the protocol allowed to drastically improve the reaction yields, obtaining the ligand **(*S*,*R*,*R*)-L10** in an excellent 90% yield. This optimized protocol was also used in the synthesis of a wide variety of other bulky phosphoramidites.[91]

[91] ***Previous protocol***: Chiral amine (1 eq.), Et_3N (1.2 eq.) and PCl_3 (1 eq.) in toluene (0.08 M), then 6 h at 70 ºC. Then rt and add Et_3N (2.2 eq.). Cool to -78 ºC and add (*S*)-VAPOL (1 eq.) in toluene (0.5 M), then 12 h at rt. 48% yield.
New protocol: Chiral amine (1.1 eq.),Et_3N (4 eq.) in dry CH_2Cl_2 (0.5 M) at 0 ºC, then PCl_3 (10 eq.), then 2h at rt. Extract the volatiles (3 times) dissolve in dry CH_2Cl_2 (0.1 M) and add Et_3N (4 eq.) at 0 ºC. Add (*S*)-VAPOL (1 eq.), Et_3N (4 eq.) in dry CH_2Cl_2 (0.1 M), then 16 h at rt. 90% yield.

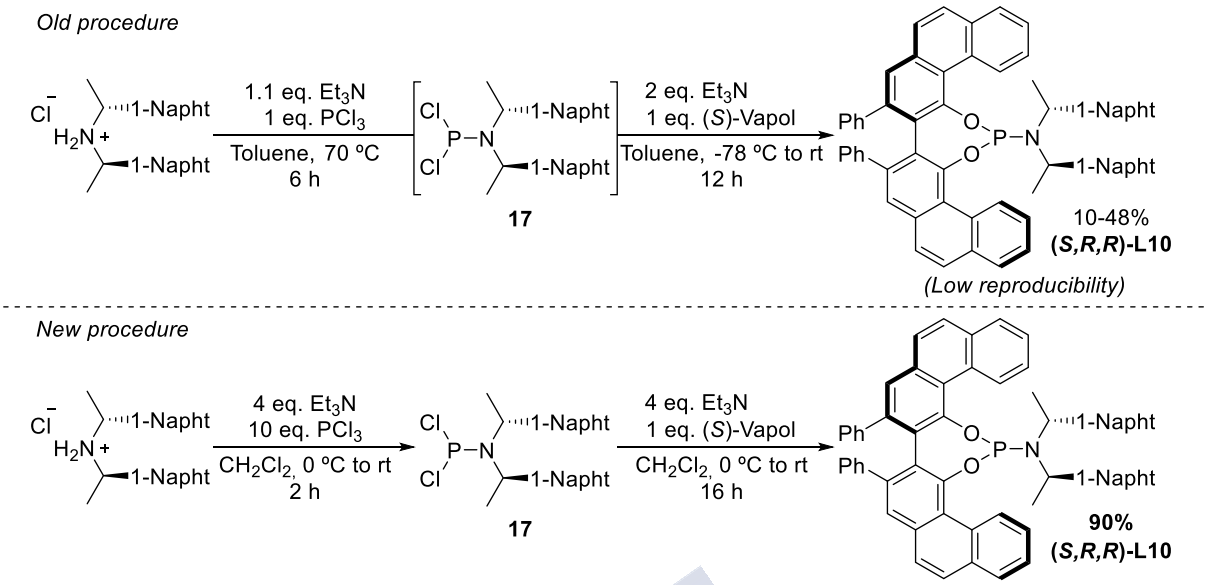

Scheme 62. Synthesis of chiral phosphoramidite **(*S*,*R*,*R*)-L10**.

3.1.3. Study of the enantioselective (3+2) cycloaddition

We first repeated the experiments previously carried out in the group, using the model precursor **3a** (Scheme 63). Thus, this ACP was refluxed in toluene in the presence of CpPd(η³-1-PhC$_3$H$_4$) (5 mol%) and phosphoramidite **(*S*,*R*,*R*)-L10** (6 mol%) for 3h. The reaction gave the expected cycloadduct **4a** with a 94% ee, albeit the yield was 70% instead of 90%, due to an incomplete conversion (entry 1). After several control experiments evaluating the purity of the reagents, quality of solvents etc., we identified that the presence of oxygen traces was important for an optimal reaction.

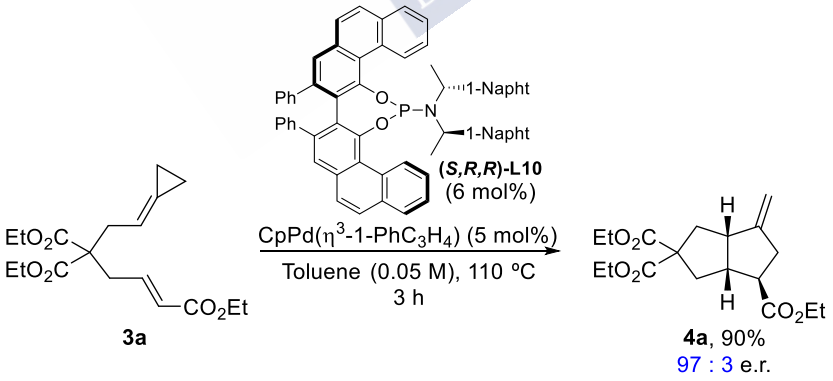

Scheme 63. Optimized reaction conditions reported by Dr. Lara Villarino.

Thus, the catalytic experiment was repeated using argon bubbling as deoxygenation method, which allowed to reach full conversion after 4h, and obtain the product **4a** in 77% yield (Table 3, entry 2). A different degassing method was also used, which consist in three freeze/vacuum pump cycles prior to equilibration at room temperature before heating (immediate heating after cycles can lead to overpressure). Using this procedure, the reaction was complete after 3 h, and gave the product in 85% yield and 92% ee (entry 3). Finally, we raised the catalytic

loading of the ligand from a 6 to 10%, to warrant the availability of non-oxidized form of the ligand in the reaction media. Gratifyingly, using these conditions, we were able to obtain the product after 3 h in a 90% yield and 94% ee (entry 4). Using these conditions, the reaction proved to be highly reproducible.

Table 3. Reproducibility tests of the described asymmetric conditions.

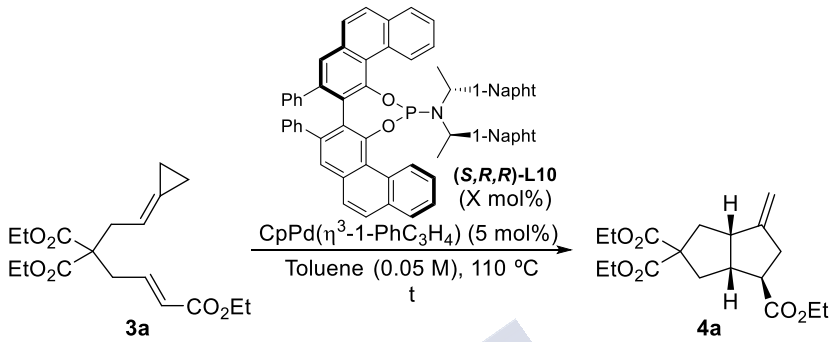

Entry	Ligand (mol %)	Conv (%)	t (h)[b]	4a (%)[c]	ee (%)
1	6	78	6	70	92
2[d]	6	100	4	85	92
3[e]	6	100	3	90	92
4[e]	10	100	3	90	94

Reaction conditions: **3a** (0.15 mmol), CpPd(η³-1-PhC₃H₄) (5 mol%), **(*S*,*R*,*R*)-L10** (6 - 10 mol%), freshly distilled toluene [0.05 M], reflux. [b] Full conversion of **3a** was observed at the specified time, unless otherwise noted. [c] Isolated yield. [d] Degasified by argon bubbling. [e] Degasified by argon-freezing

3.1.4. Reaction scope

Once the optimal conditions were established, we evaluated the scope of the method (Scheme 64). The reaction of the cycloaddition precursor **4a**, bearing an ethyl malonate at the tether also provided a good yield (89%) and an excellent 94% ee. Likewise, the 2-phenylethyl malonate derivative **4b** also afforded a 90% yield and a 93% ee. Interestingly, the use of an isopropyl carboxylic ester in the alkene **4c** was possible, providing the expected adduct with complete diastereoselectivity, 90% yield and an excellent 90% ee.

Interestingly, the method is also effective to make bicycles bearing quaternary chiral centers at the ring fusion. Using the methyl-substituted alkylidenecyclopropane the desired cycloadduct **4d** was obtained in 85% yield and with excellent 92% ee. On the other hand, when the methyl was introduced at the *β*-position of the alkene, the cycloadduct **4e** was also obtained with high diastereoselectivity (d.r > 12 : 1), albeit the enantioselectivity was notably affected (44% ee).

Moreover, the use of precursors with extended connecting tethers, such as **3f**, which holds an additional methylene moiety at chain, is also possible. The expected 6,5 bicyclic adduct **4f** is

obtained in an excellent 90% yield, but as a mixture of diastereoisomers (d.r = 1.1 : 1). The isomer with the *cis* fusion showed a moderate 56% ee.[92]

We also evaluated the effect of having different EWGs at the alkene. Therefore, the alkenylketone participated in the cycloaddition to give **4g** in an excellent 87% yield, moderate enantioselectivity (56% ee). If the substituent is a diethyl amide the reaction is less efficient, 50% conversion and 15% of overall yield (**4h**), as a mixture of isomers with a modest diastereomeric ratio. In this case, we couldn't determine the enantioselectivity with our current analytic techniques. Nonetheless, these two latter results demonstrate that the alkene architecture plays an important role in determining yields and enantioselectivities.

We next checked whether the reaction tolerates heteroatoms at the connecting tether, so that the construction of fused-bicyclic tetrahydrofurans and pyrrolidines could be achieved. Gratifyingly, the *N*-Benzyl derivative **3i** provided the corresponding pyrrolidine **4i** in 70% yield and a 94% ee. Likewise, the *N*-tosyl analogue could be transformed to the expected cycloadduct, albeit the product **4j** is obtained with slightly lower ee. (74% ee). Finally, the oxygenated precursor **4k** provided the corresponding tetrahydrofuranic product in 55% yield and a similar 78% ee.

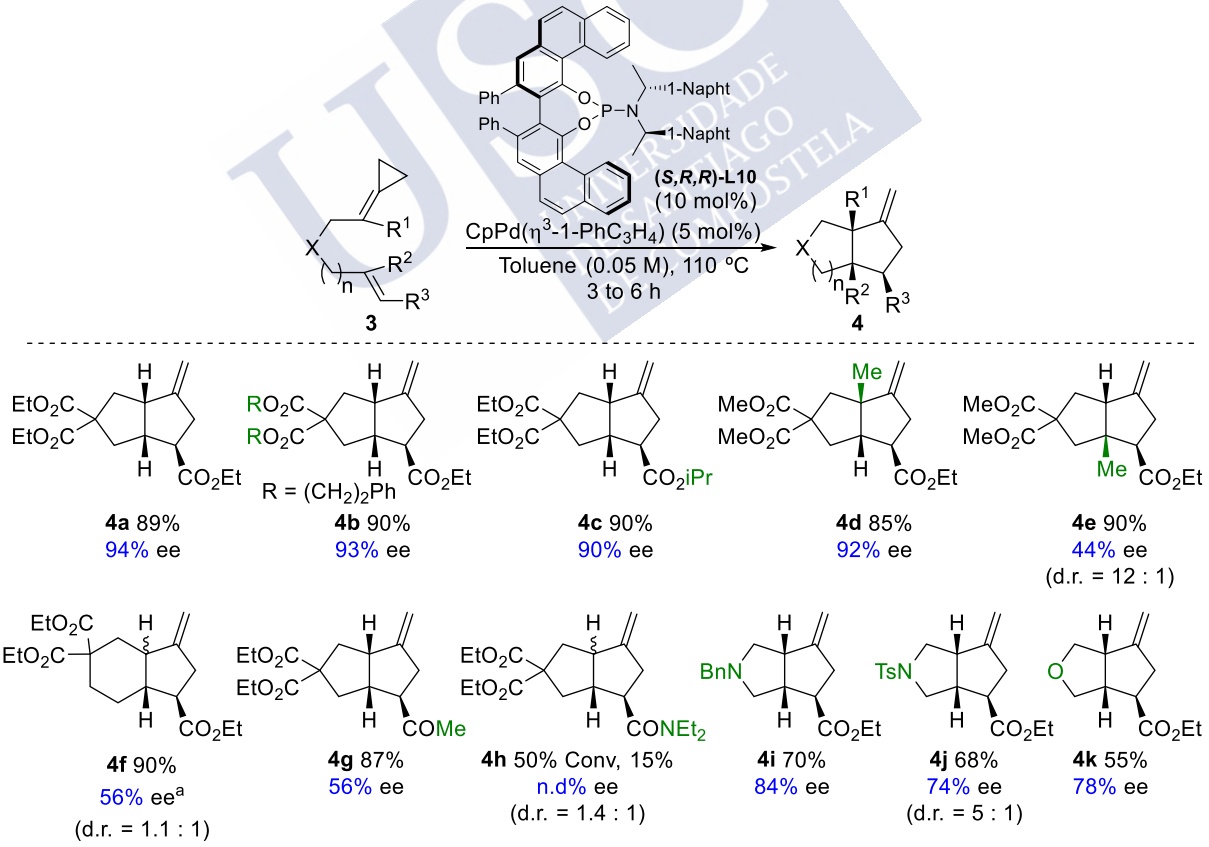

Scheme 64. Scope of the enantioselective (3+2) cycloaddition of activated alkenes.

[92] Enantioselectivity of *trans*-**4f** isomer couldn't be measured due no chromatographic conditions were found.

Non-activated alkenes are also suitable cycloaddition partners (Figure 10). Therefore, the N-Benzyl spirocyclic **4m** was obtained with complete diastereoselectivity, albeit moderate conversion (75% conversion, 50% yield) and enantioinduction of 50% ee. On the other hand, ACPs precursors containing terminal alkene groups also underwent the reaction in moderate yield (e.g. **4n**); however, the ee could not be determined. Finally, allenes are also competent reaction partners. Thus, the cycloadduct **4o** was obtained as a mixture of diastereoisomers (d.r = 1.1 : 1) in 60% yield, albeit with a low 24% ee.

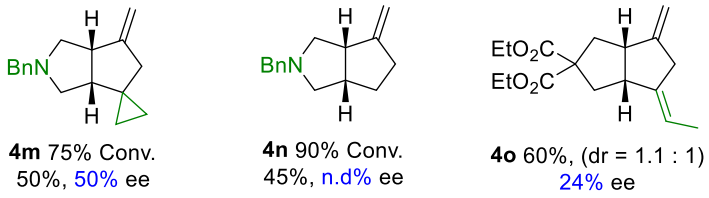

Figure 10. Scope of the enantioselective (3+2) cycloaddition of unactivated alkenes.

The synthetic potential of the resulting 5-5 byciclic systems was preliminary analyzed (Scheme 65). The substrate **4a** can be efficiently converted into the ketone **4ac** with an ozonolysis reaction (95% yield). On the other hand, treatment of the adducts **4a**, **4i** and **4j** with excess of $LiAlH_4$ provided the corresponding alcohols in good yields.

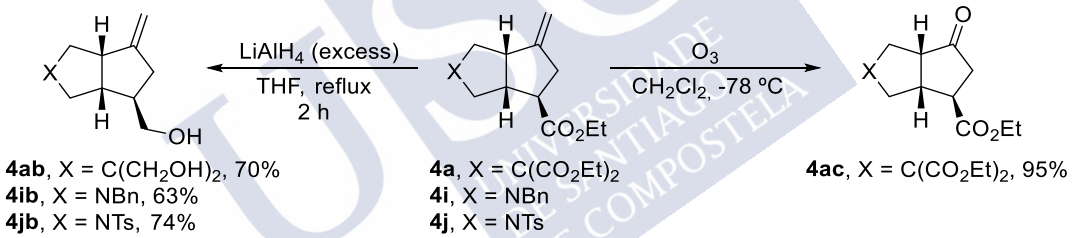

Scheme 65. Synthetic derivatization of products **4a**, **4i** and **4j**.

To determine the absolute configuration of the cycloadducts, we prepared the 3,5-dinitrobenzoyl ester **30** from the alcohol **4jb** (Scheme 66). Its crystallization from a CH_2Cl_2:Heptane mixture allowed to determine that its absolute configuration as 3a*S*, 4*R* and 6a*S*. Alternatively, we could also obtain crystals suitable for X-ray diffraction from the alcohol derivative **4ab**, which confirmed the same absolute configuration (Figure 11).

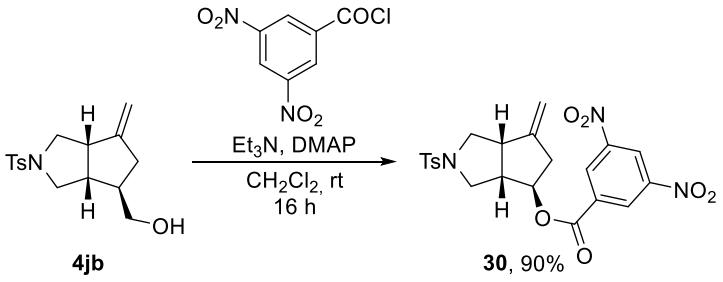

Scheme 66. Synthetic derivatization of alcohol **4jb**.

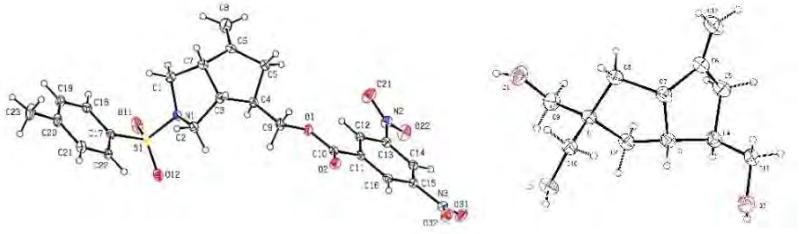

Figure 11. Crystal structure of **30** and **4ab**.

Summarizing, we have developed a palladium catalyzed enantioselective (3+2) cycloaddition that constitutes the first example of an enantioselective TMC annulation of alkylidenecyclopropanes. The reaction allows the construction of bicyclic structures with excellent diastereoselectivities and very high enantioselectivities for a number of cases in which three new stereocenters are generated. However, the levels of enantioinduction have been shown to be highly dependent on the substituents at the alkene partner, and on the type of connecting tether. Nonetheless, it is important to remark that the method is one of the very few enantioselective intramolecular TMC cycloadditions that allows the formation of 5,5-bicarbocyclic systems.

3.2. Enantioselective (4+3) cycloaddition between ACPs and dienes

*3.2.1. Optimization with model precursor **9a***

The model substrate **9a**, was prepared following a procedure previously described by our group (Scheme 67).[62] Briefly, malonate **22** was alkylated with the tosylate **31**, and the resulting product was treated with *n*BuLi and ethyl chloroformiate to give the corresponding ester derivative **32** (60% overall yield for the two steps). Finally, treatment of this alkyne with stoichiometric amounts of PPh_3 and PhOH promoted an isomerization to the conjugated diene **9a**, which was obtained in 59% yield.

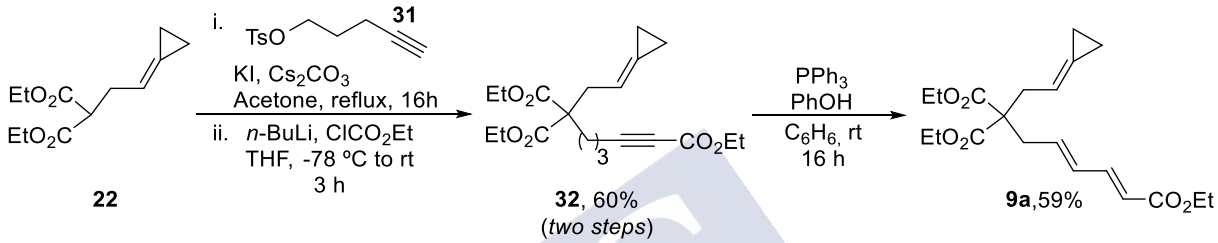

Scheme 67. Synthesis of substrate **9a**.

First, we analyzed the performance of the catalyst that provided the best results in the enantioselective (3+2) cycloaddition (Table 4, entry 1). Unfortunately, heating a solution of **9a** at 110 °C, in the presence of CpPd(η^3-1-PhC_3H_4) (5 mol%) and **(*S*,*R*,*R*)-L10** (10 mol%) led to a poor conversion after 12 h, providing a 5:1 mixture of the desired adduct **10a** and the (3+2) byproduct **11a** , in low overall yield. However, since the enantioselectivity of the desired (4+3) adduct was high (88% ee, entry 1), we explored the possibility of increasing the efficiency at higher temperatures. Thus, carrying out the reaction at 150 °C allowed to reach full conversion, and a 5 : 1 mixture of **10a** and **11a** was obtained in an overall good 75% yield (entry 2). Interestingly, the ee was slightly higher, of 92%. Despite this very good enantioselectivity, the moderate (4+3)/(3+2) ratio led us to further explore alternative combinations of Pd(0) precursors and chiral phosphoramidite ligands.

Thus, we found that the less bulky ligand **(*S*,*R*,*R*)-L8**, under otherwise identical reaction conditions, provided a 74% combined yield of **10a** and **11a**, with lower selectivity (3:1 ratio), but a similar ee (entry 1 *vs* 3). Changing the chiral backbone of the ligand from VAPOL to the less bulky VANOL **(*S*,*R*,*R*)-L11** allowed to reach full conversions under reflux (110 °C, 12 h reaction), while keeping the same enantioselectivity; however, the (4+3)/(3+2) ratio was not improved (entry 4).

At this point, we evaluated the effect of the chirality in the amine using the phosphoramidite **(*S*)-L12**, which bears a bis(diisopropyl) amine. Interestingly, the reaction time was drastically improved as well as the ratio of products, but the enantioselectivity dropped severely (entry 5), demonstrating that the contribution of a chiral amine is crucial for the enantioinduction.

Thus, we tested alternative chiral backbones, keeping the bis[(R)-1-phenylethyl]amine as chiral amine unit. Curiously, the use of the BINOL-derived phosphoramidite **(*S,R,R*)-L4** led lower (4+3)/(3+2) ratios and poor yields (entry 7). On the other hand, biphenol derivate **(*R*)-L13** which is similar to the previously reported **(*R*)-L3,**[62] but bearing phenyl groups at the 3,3` positions of the biphenol, did provide significantly lower selectivities (entries 7 and 8). Moreover, the use of an analogue with a conformationally restricted pyrrolidine amine, such as **(*S,R,R*)-L14,** showed a similar reaction outcome (entry 9).

Table 4. Screening of chiral phosphoramidite ligands in model substrate **9a**.

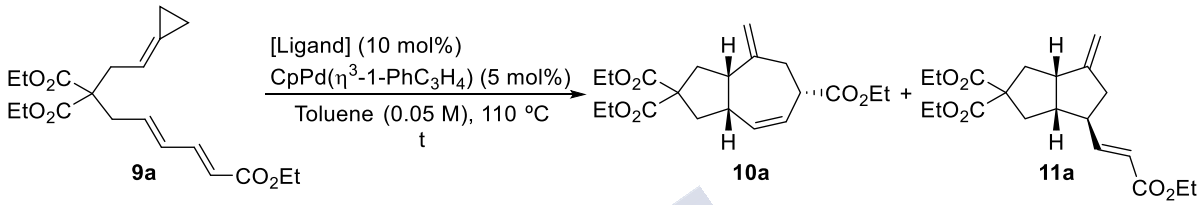

Entry	Ligand	t (h)[b]	Conv. (%)	4a:5a	4a (%)[c]	4a, ee (%)
1	(*S,R,R*)-**L10**	12	56	5 : 1	37	88
2[a]	(*S,R,R*)-**L10**	6	100	5 : 1	75	92
3	(*S,R,R*)-**L8**	6	74	3 : 1	38	88
4	(*S,R,R*)-**L11**	12	100	3 : 1	68	88
5	(*S*)-**L12**	4	100	8 : 1	75	56
6	(*S,R,R*)-**L4**	6	100	1 : 2	13	n.d
7	(*R*)-**L3**	4	100	19 : 1	86	70
8	(*R*)-**L13**	6	80	2 : 1	38	56
9	(*R,R*)-**L14**	6	82	5 : 1	33	74

[a] *Reaction conditions*: **9a** (0.15 mmol), CpPd(η3-1-PhC3H4) (5 mol%), [Ligand] (10 mol%), freshly distilled toluene [0.05 M], reflux. [b] Full conversion of **9a** was observed at the specified time, unless otherwise noted. [c] Isolated yield. [d] Carried out at 130 ºC in a sealed tube.

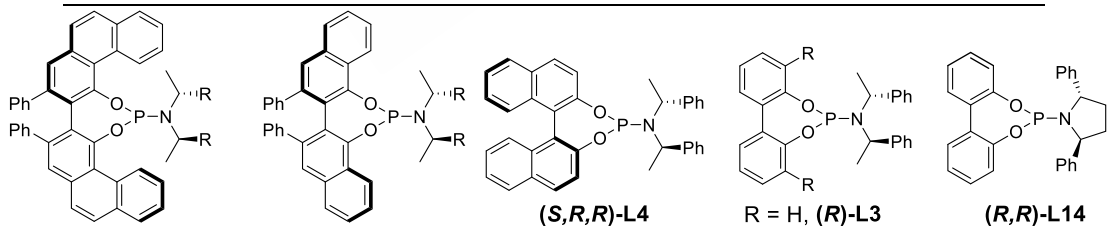

R=Ph, **(*S,R,R*)-L8**
R=1-Napht, **(*S,R,R*)-L10**

R=Ph, **(*S,R,R*)-L11**
R=Me, **(*S*)-L12**

(*S,R,R*)-L4

R = H, **(*R*)-L3**
R = Ph, **(*R*)-L13**

(*R,R*)-L14

With these results in hand, we decided to check the influence of alternative reaction parameters, using **(*S,R,R*)-L8** as model ligand (Table 5). Interestingly, the reaction rate and selectivity were drastically improved by using dioxane as solvent instead toluene, so that full conversion were obtained after refluxing for 5 h, while the (4+3)/(3+2) selectivity was significantly enhanced (10:1 vs 3:1; table 5, entry 1 *vs* 2). In addition, changing the precatalyst from CpPd(η3-1-PhC3H4) to Pd_2dba_3 allowed to reach the full conversions in 3 h, leading to the desired cycloadduct in a promising 81% yield, very good selectivity (10 : 1) and an excellent

90 ee (entry 3). Based on these new conditions, we reevaluated the performance of other ligands (entries 3-6). Thus, we detected that the reaction using the BINOL -phosphoramidite **(*S,R,R*)-L4** provides full selectivity towards the seven-membered carbocycle, which was obtained in 90% yield and with 86% ee (entry 4). Interestingly, the use of an 8H-BINOL phosphoramidite analogue **(*S,R,R*)-L16** led to a significantly lower yield, product selectivity and enantioselectivity (entry 5). Particularly surprising, **(*S,R,R*)-L15,** which bears a 1-naphthyl groups instead phenyl at the chiral amine, led to lower reaction yields and selectivity, contrary to that observed in the (3+2) cycloadditions (entry 6).

Finally, we confirmed that the configuration **(*S,R,R*)** of **L4** corresponded to a matched situation. Thus, using the diastereoisomer **(*R,R,R*)-L4** under otherwise identical reaction conditions, the product selectivity as well as the enantioselectivity of the (4+3) cycloadduct were significantly lower (82% yield, **10a**:**11a** = 5.5 : 1, 56% ee **10a**, entry 8).

Table 5. Secondary screening and optimization of the reaction.

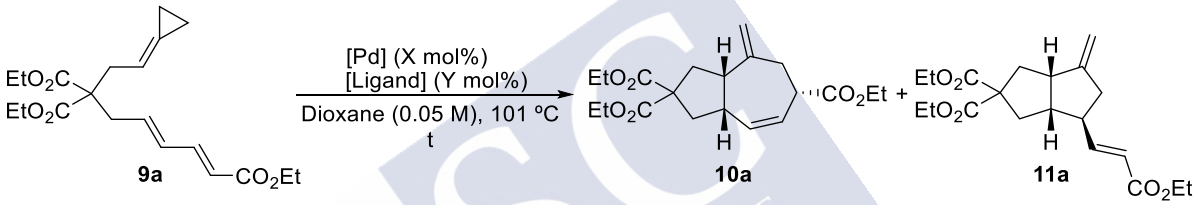

Entry	[Pd] (%)	Ligand (%)	t (h)[b]	4a:5a	4a (%)[c]	4a, ee (%)
1[e]	$CpPd(\eta^3\text{-}1\text{-}PhC_3H_4)$(5)	**(*S,R,R*)-L8** (10)	12	3 : 1	68	88
2	$CpPd(\eta^3\text{-}1\text{-}PhC_3H_4)$(5)	**(*S,R,R*)-L8** (10)	5	10 : 1	70	90
3	Pd_2dba_3(5)	**(*S,R,R*)-L8** (14)	3	10 : 1	81	90
4	Pd_2dba_3(5)	**(*S,R,R*)-L4** (14)	3	>20 : 1	90	86
5	Pd_2dba_3(5)	**(*S,R,R*)-L16** (14)	4	4 : 1	28(40)[d]	n.d
6	Pd_2dba_3(5)	**(*S,R,R*)-L15** (14)	4	8 : 1	74	72
7	Pd_2dba_3(5)	**(*R,R,R*)-L4** (14)	3	5.5 : 1	82	56

[a] *Reaction conditions*: **9a** (0.15 mmol), [Pd] (X mol%), [Ligand] (Y mol%), freshly distilled dioxane [0.05 M], reflux. [b] Full conversion of **9a** was observed at the specified time, unless otherwise noted. [c] Isolated yield. [d] Value of conversion under parenthesis. [e] Carried out in toluene.

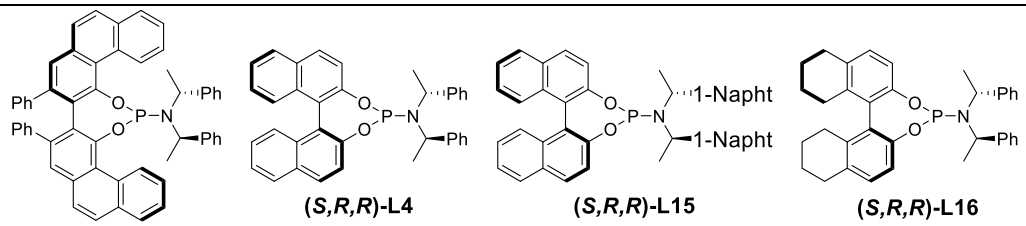

The effect of the temperature in the enantioselectivity was also explored in the oxygenated precursor **9e** (Scheme 68). Under optimized conditions, the compound **10e** was obtained in 74% yield and 60% ee (entry 4). Carrying out the reaction at 130 ºC showed the same enantioselectivity than at 101 ºC (entry 3 *vs* 4), whereas at 80 ºC, after 16 h, the reaction was low yielding, and also worst in terms of regio and enantioselectivity (entry 5). This behavior

is similar to the observed in the (3+2) cycloaddition, in which the enantioselectivity increases with the temperature, reaching a limit above reflux conditions. As abovementioned in the (3+2) section, this enhancement in the selectivity at higher temperatures has been related to reactions with a large entropic contribution to the diastereomeric transition state energies at the enantiodetermining step. [86]

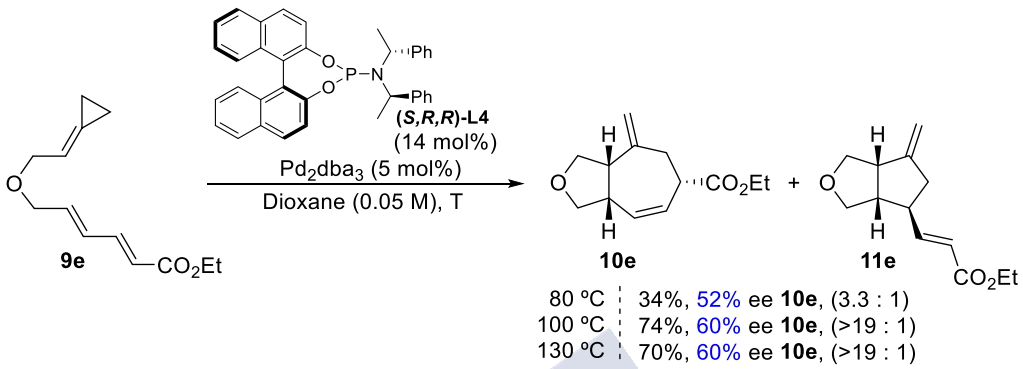

Scheme 68. Temperature effect on the (4+3) cycloaddition.

3.2.2. Reaction scope

In addition to the abovementioned oxygenated precursor **9e**, we also synthesized different substrates such as the methyl-substituted analogues **9b** and **9c**, which would deliver synthetically challenging bicyclic systems bearing quaternary centers at the ring fusion. Also, substrate **9d,** which bears a non-activated diene was synthesized (Figure 12).

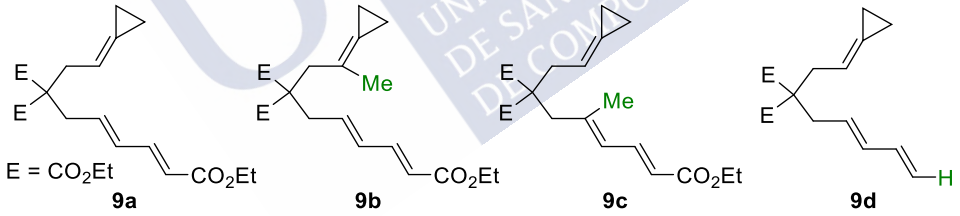

Figure 12. Synthesis to evaluate the scope.

The preparation of **9b** was carried out following the same route as for **9a**, starting in this case from malonate **24.** The final product was obtained in an overall yield of 58%, for the three steps (Scheme 69)**.**

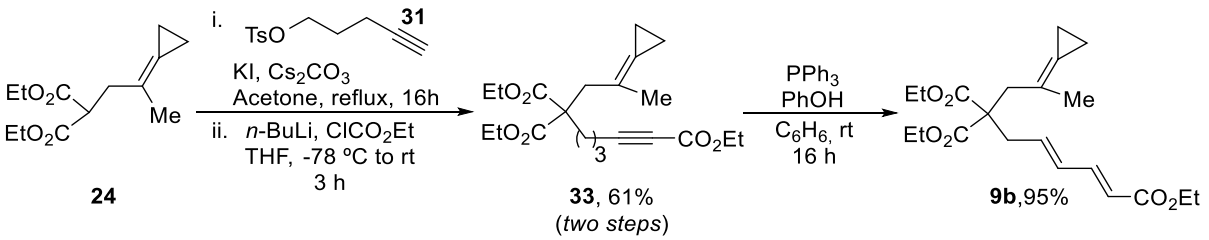

Scheme 69. Synthesis of substrate **9b**.

The δ-methylated analogue **9c** was synthesized starting from the alcohol **34**, using a Heck coupling with ethyl acrylate catalyzed by $PdCl_2(PPh_3)$. Mesylation of the resulting alcohol with $MsCl/Et_3N$ directly led to the allylic chloride **35**, which was isolated in 28% overall yield (two steps). Finally, an alkylation of **22** with this dienyl chloride afforded the cycloaddition precursor **9c** in 63% yield (Scheme 70).

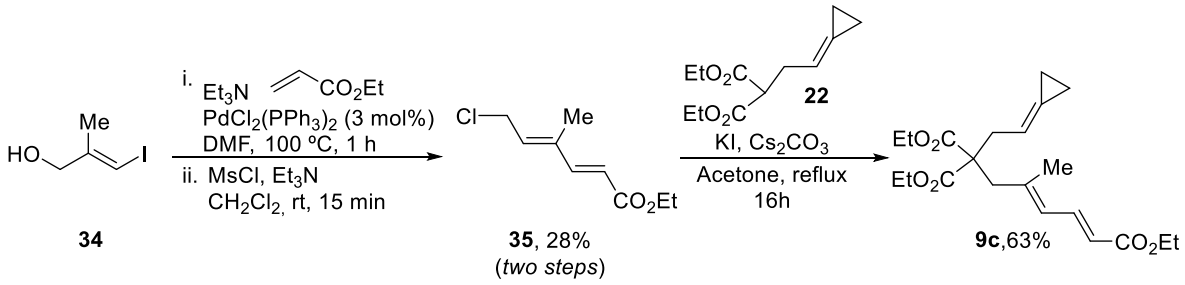

Scheme 70. Synthesis of substrate **9c**.

Ether **9e** was synthesized starting from alcohol **36**, by alkylation with tosylate **21** using palladium catalysis, and treatment of the crude with TBAF to afford alcohol **37** in a 68% overall yield for the two steps. The oxidation of **37** using PCC allowed to afford the *E* isomer of the corresponding α, β-unsaturated aldehyde, which isomerized under these reaction conditions. Finally, after a Wittig reaction, product **9e** was obtained in a 55% yield for these two steps (Scheme 71).

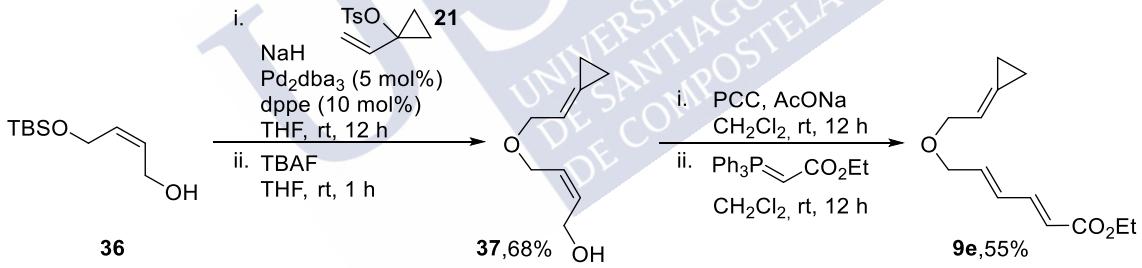

Scheme 71. Synthesis of substrate **9e**.

The precursor with a non-activated diene **9d** was prepared from 1,4-pentadien-3-ol, by treatment with HCl at room temperature, and the addition of the resulting diene (*E*-5-chloropenta-1,3-diene **38**) over a solution of the malonic anion formed by the combination of malonate **22** and NaH in THF (81% yield, Scheme 72).

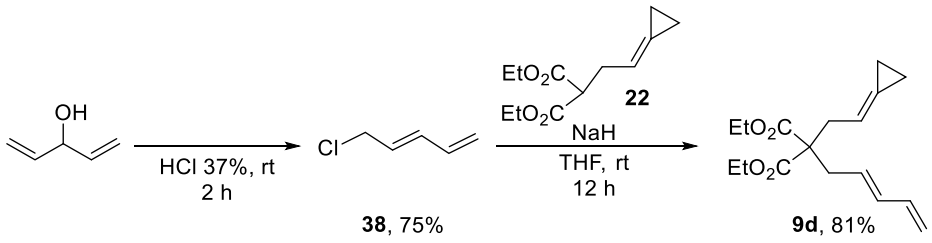

Scheme 72. Synthesis of substrate **9d**.

With these substrates at hand, we explored the scope of the reaction (Scheme 73 and 74). The racemic samples of the cycloadducts used as reference for the determination of the enantioselectivities were obtained carrying out the corresponding reactions with the phosphoramidite **L2**. As previously reported, this small ligand leads to the seven-membered carbocycle with moderate to good selectivities in several cases. Nevertheless, the reaction showed to be much more efficient with **(*S*,*R*,*R*)-L4**. For instance, substrate **9b** under racemic conditions using **L2**, lead to the (3+2) adduct **11b** as major product. However, using as ligand **(*S*,*R*,*R*)-L4** the desired cycloheptene cycloadduct **10b** was obtained in 72% yield and an excellent 94% ee.

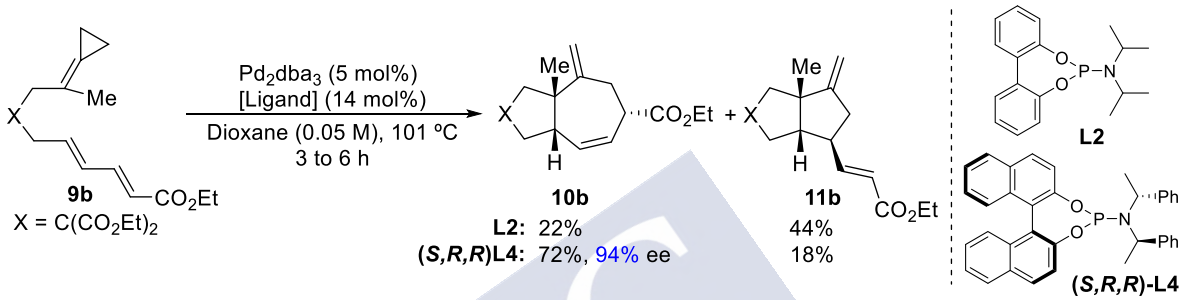

Scheme 73. Comparison between racemic and asymmetric conditions.

Other malonate tethered substrates bearing dienes with terminal carboxylic esters provided also remarkable results. As previously mentioned, under optimized conditions, the model substrate **9a** reacted selectively to give the desired product in an excellent 90% yield and 86% ee (**10a**:**11a** = 20 : 1); whereas the analogue obtained from a *δ*-methyl diene (**10c**) provided an excellent 90% yield and 82% ee, but the product selectivity was significantly eroded (**10c**:**11c** = 2.4 : 1). Importantly, the absence of the carboxylic ester as activating group affected the reaction efficiency. Thus, albeit the reaction of the precursor 9d led to the (4+3) cycloadduct **10d** with complete selectively (**10d**:**11d** = 1 : 0), and moderate 64% yield, the enantioselectivity turned out to be modest, of 54%. Finally, as previously shown in Scheme 68, the cycloaddition of the oxygenated precursor **9e** selectively produced the fused tetrahydrofuran **10e** in 75% yield and 60% ee.

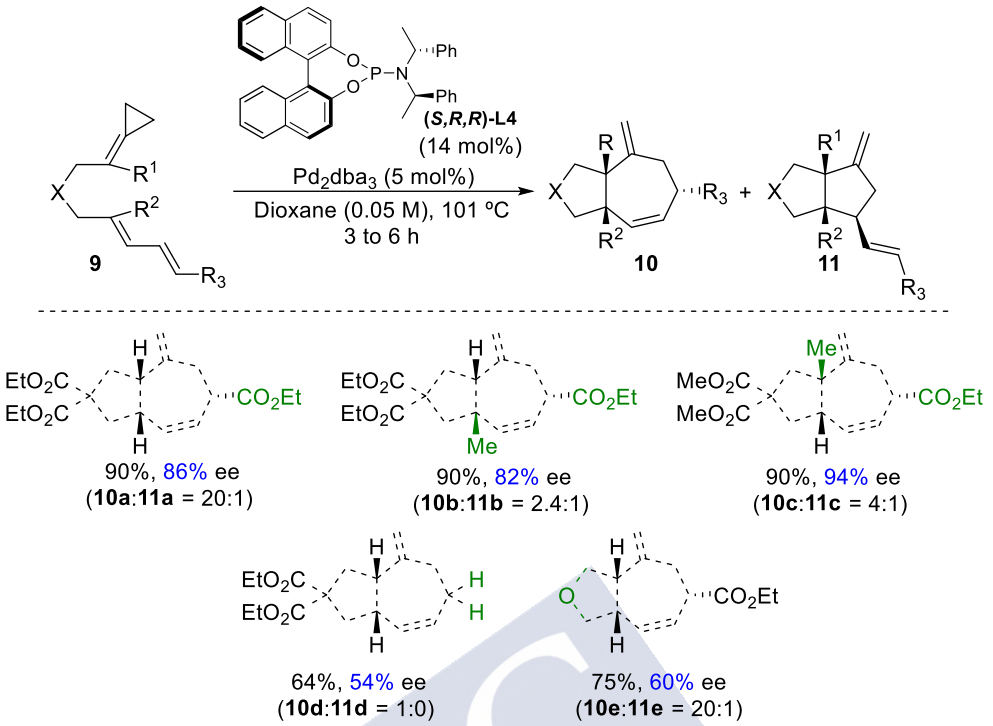

Scheme 74. Scope of the enantioselective (4+3) cycloaddition reaction.

4. Conclusions

In conclusion, we have evaluated the scope of the enantioselective palladium catalyzed (3+2) cycloaddition reaction between ACPs and activated alkenes (Scheme 75). The reaction proved to be highly diastereo- and enantioselective when a sterically demanding phosphoramidite was used in combination with the Pd(II) precursor CpPd(η^3-1-PhC$_3$H$_4$). The cycloaddition provides a straightforward access to synthetically appealing enantioenriched bicyclo[3.3.0]octanes.

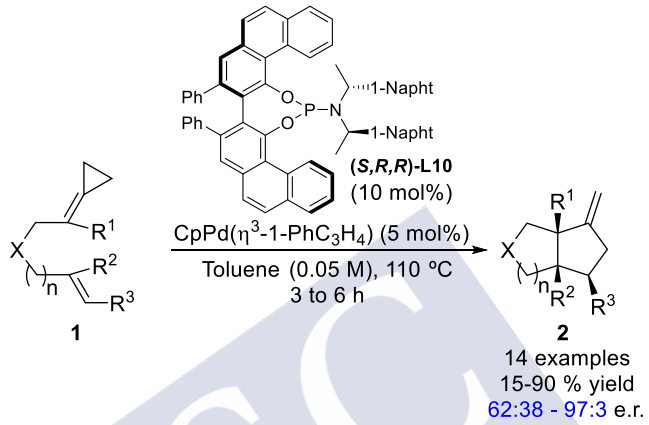

Scheme 75. Palladium catalyzed enantioselective (3+2) cycloaddition reaction.

The reaction efficiency depends on the substrate. The best enantioselectivities were observed when the alkene bears a carboxylic ester as activating group and the precursor presents a geminal diester in the connecting tether (94% ee). The construction of challenging products bearing quaternary chiral centers at the ring fusion was also possible. Cycloaddition precursors, bearing heteroatoms at the connecting tether provided good yields and moderate to high enantioselectivities (Figure 13).

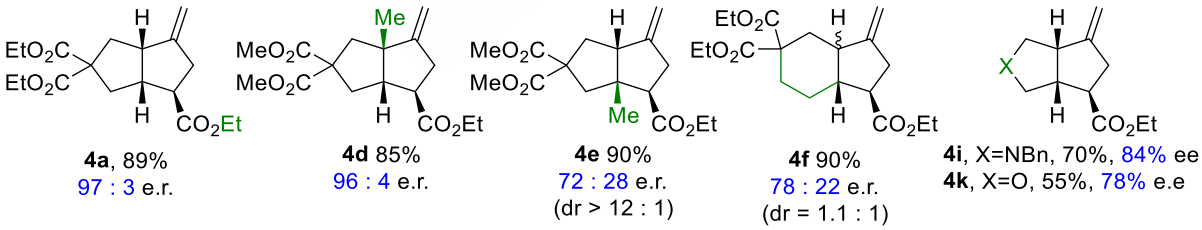

Figure 13. Reaction scope of the enantioselective (3+2) cycloaddition with activated alkenes.

The use of alkenes without electron activating groups, as well as with allenes is also viable, albeit the conditions might need to be further re-optimized to obtain better results (Figure 14).

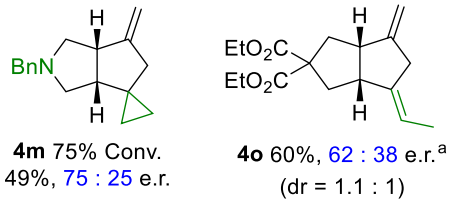

Figure 14. Reaction scope of the enantioselective (3+2) cycloaddition with unactivated alkenes.

In addition, we have developed an enantioselective palladium catalyzed intramolecular (4+3) cycloaddition between alkylidenecyclopropanes and dienes (Scheme 76). For this reaction, the use of $Pd_2(dba)_3$ and a less sterically demanding phosphoramidite was required to obtain (4+3) cycloadducts with high selectivity (versus competitive (3+2) adducts), and excellent degrees of stereocontrol.

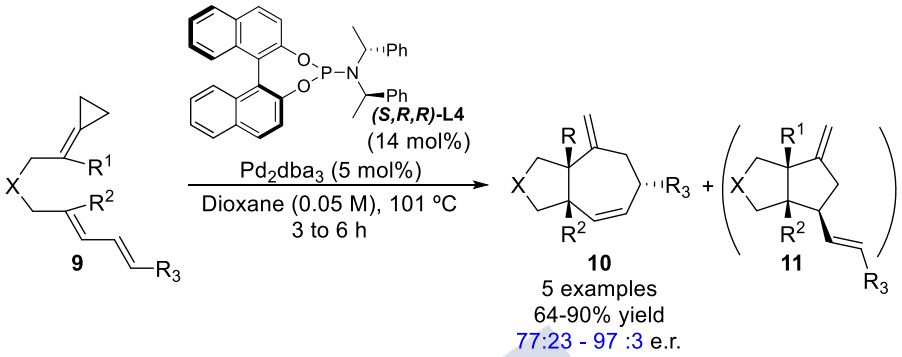

Scheme 76. Palladium catalyzed enantioselective (4+3) cycloaddition reaction.

The transformation showed similar electronic requirements than the (3+2) cycloaddition (Figure 15). Electronically activated dienes bearing ester groups exhibit the best results when a malonate was used at the connecting tether, reaching a 90% yield and 94% ee Moreover, challenging bicycles bearing quaternary stereocenters at the ring fusion could also be obtained. The reaction also tolerates the presence of heteroatoms at the tether, albeit lower selectivities are observed. Finally, non-activated dienes can also participate in the asymmetric reaction, but provide lower yield and ee.

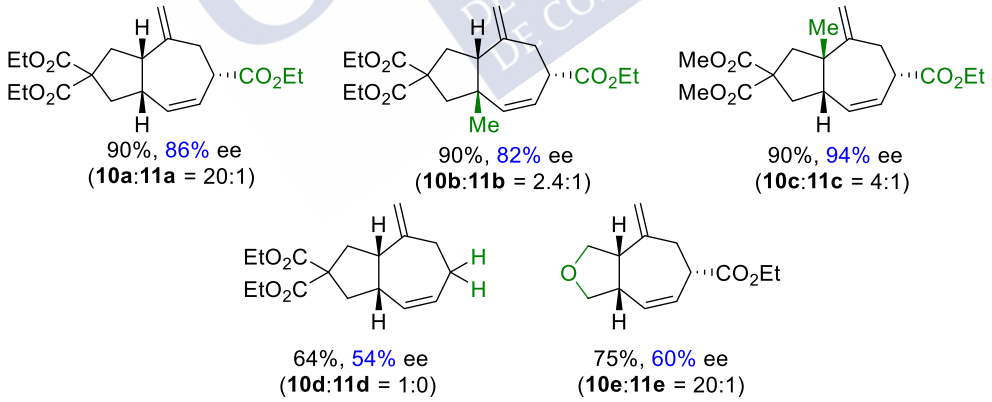

Figure 15. Reaction scope of the enantioselective (4+3) cycloaddition with dienes.

USC
UNIVERSIDADE
DE SANTIAGO
DE COMPOSTELA

CHAPTER II: Palladium catalyzed (3 + 2) heterocycloadditions of alkylidenecyclopropanes

USC
UNIVERSIDADE
DE SANTIAGO
DE COMPOSTELA

1. Introduction

Relevance of five-membered heterocyclic systems

The stereoselective and efficient construction of heterocyclic systems is still one of the most relevant challenges in synthetic organic chemistry, especially because of the great number of compounds with pharmaceutical or agrochemical applications that exhibit this kind of scaffolds.[93] Heteroatoms modify the polarization of a molecule but, more importantly, allow the substrate to interact with their receptor through their lone pair of electrons. Thus, the combination of all these features and the rigidity provided by a cyclic structure can strongly determine the physicochemical properties of these compounds. [94]

Five-membered heterocycles such as tetrahydrofurans an pyrrolidines are among the most prevalent heterocyclic systems in bioactive molecules (Figure 16). In this regard, many synthetic strategies have been developed for the selective construction of these scaffolds. However, and despite important milestones achieved, the development of catalytic, versatile and efficient methods towards these scaffolds is still a major goal. Especially attractive, are those reactions that are based on the use of transition metal-based strategies since they can provide the cyclic systems from readily available acyclic precursors. In the following section, we summarized the most relevant examples related to the work of this chapter.[95]

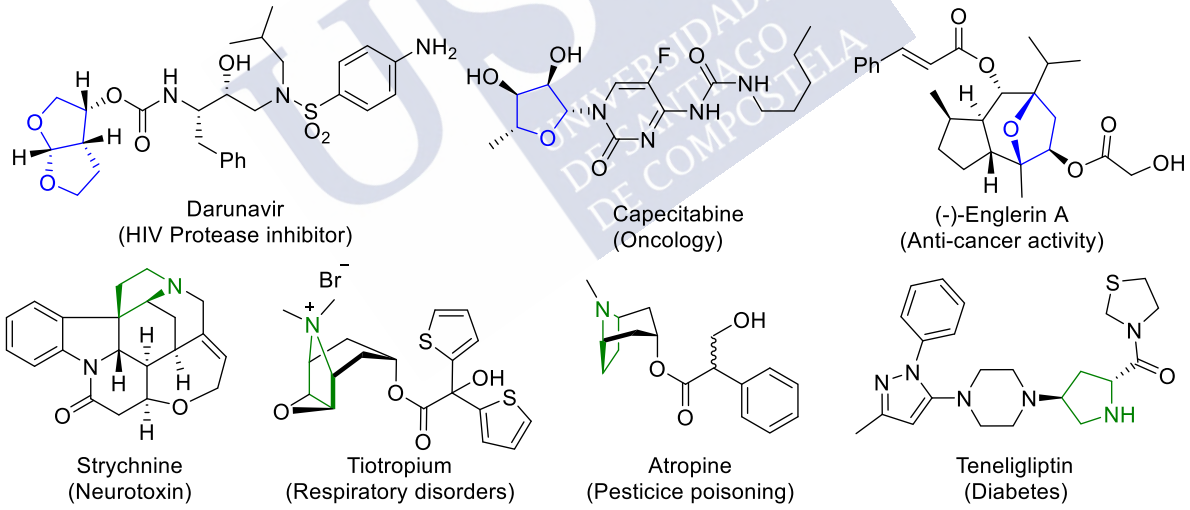

Figure 16. Biologically relevant molecules containing tetrahydrofuran and pyrrolidine scaffolds.

[93] D. C. Blakemore, L. Castro, I. Churcher, D. C. Rees, A. W. Thomas, D. M. Wilson, A. Wood, *Nat. Chem.* **2018**, *10*, 383–394.
[94] (a) J. Dinges, C. Lamberth in: *The Significance of Heterocycles for Pharmaceuticals and Agrochemicals*. J. Dinges, C. Lamberth (ed.), *Bioactive Heterocyclic Compound Classes*. Chapter 1, pages 3-20. Wiley-VCH, **2012**. (b) D. C. Blakemore, L. Castro, I. Churcher, D. C. Rees, A. W. Thomas, D. M. Wilson, A. Wood, *Nat. Chem.* **2018**, *10*, 383–394.
[95] I. Nakamura, Y. Yamamoto, *Chem. Rev.* **2004**, *104*, 2127–2198.

1.1. Metal catalyzed cycloadditions for the construction of tetrahydrofurans and related five-membered oxacyclic systems

(3+2) Cycloadditions

In 1990, Trost reported one of the pioneering reports on the assembly of THFs by TMC cycloadditions (Scheme 77).[96] In particular, he describe how various silicon or tin allylic reagents could participate in a hetero- (3`+2) cycloaddition with different aldehydes, using the catalyst generated in situ from $Pd(OAc)_2$ and triphenylphospine, in combination with a trialkyl tin acetate as cocatalyst. Despite the novelty, the process faced several limitations, such as the complicate synthesis of the starting materials, the moderate yields of the cycloaddition, poor diastereoselectivities, as well as the requirement of toxic tin additives. The reaction was proposed to begin with the formation of the isomeric forms of Pd-TMM **A** and **A`**, wich undergoes a 1,2 addition to the aldehyde generating the corresponding tin alkoxides **B** or **B`**, which intramolecularly reacts with the electrophilic p-allyl-Pd species providing the regioisomeric mixture of tetrahydrofurans.

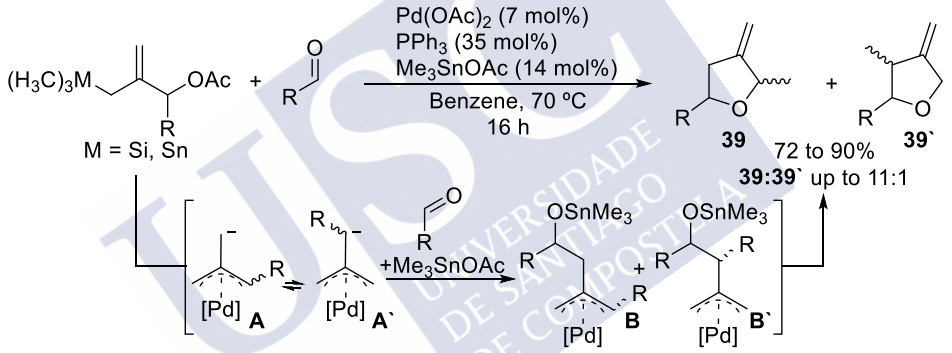

Scheme 77. Pd-catalyzed (3+2) cycloaddition between TMM precursors and aldehydes.

Two decades later, in 2011, the same group showed that this reaction can be carried out enantioselectively and milder conditions (Scheme 78).[97] The use of a catalyst formed by $Pd(dba)_2$, chiral phosphoramidite ligand **(*R,R,R*)-L22** and $In(acac)_3$, that act as Lewis acid activator for the aldehyde, promotes the (3+2) cycloaddition between TMM precursors and aldehydes, providing both good yields and enantioselectivities. The reaction tolerates the use of aromatic, heteroaromaric and cynammaldehydes, but only two examples show enantioselectivities above 90%.

[96] B. M. Trost, S. a King, *J. Am. Chem. Soc.* **1990**, *112*, 408–422.
[97] B. M. Trost, D. A. Bringley, S. M. Silverman, *J. Am. Chem. Soc.* **2011**, 7664–7667. [1] B. M. Trost, D. A. Bringley, S. M. Silverman, *J. Am. Chem. Soc.* **2011**, 7664–7667.

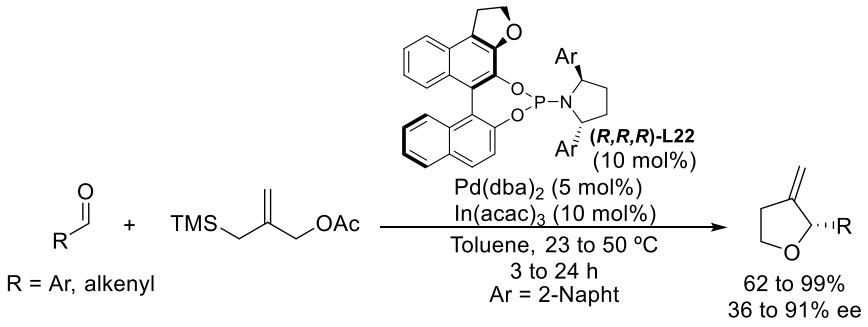

Scheme 78. Pd-catalyzed enantioselective (3+2) cycloaddition between TMM precursors and aldehydes.

Subsequent reports extended the scope to ketones, which efficiently react with TMM precursors in racemic and enantioselective fashion (Scheme 79a).[98] Particularly, in 2013 tetrahydrofurans of type **40** were obtained with excellent enantioselectivities using a Pd(0) catalyst *in situ* generated from CpPd(η^3-C_3H_5) and **(*S*,*R*,*R*)-L22**. Few years later, in 2018, the group extended the scope to the use of 2,2,2-trifluoromethyl ketones,[99] just by using a TMM precursor that bears a CN group instead of the TMS moiety. Interestingly in this case, dihydrofurans of type **40`**, resulting from the isomerization of the *exo*-methylene (product of type **40**), are obtained. All three examples (aldehydes, ketones and fluorinated ketones) follow the same mechanistic principles (Scheme 79b), albeit the generation of the Pd-TMM intermediate depends on the substrate used. In the latter case, a trialkylsilane group is not requiered since the pKa of the hydrogens adjacent to the CN group is sufficient low to allow the deprotonation by the *tert*-butoxide generated from the Boc group, after Pd oxidative insertion.

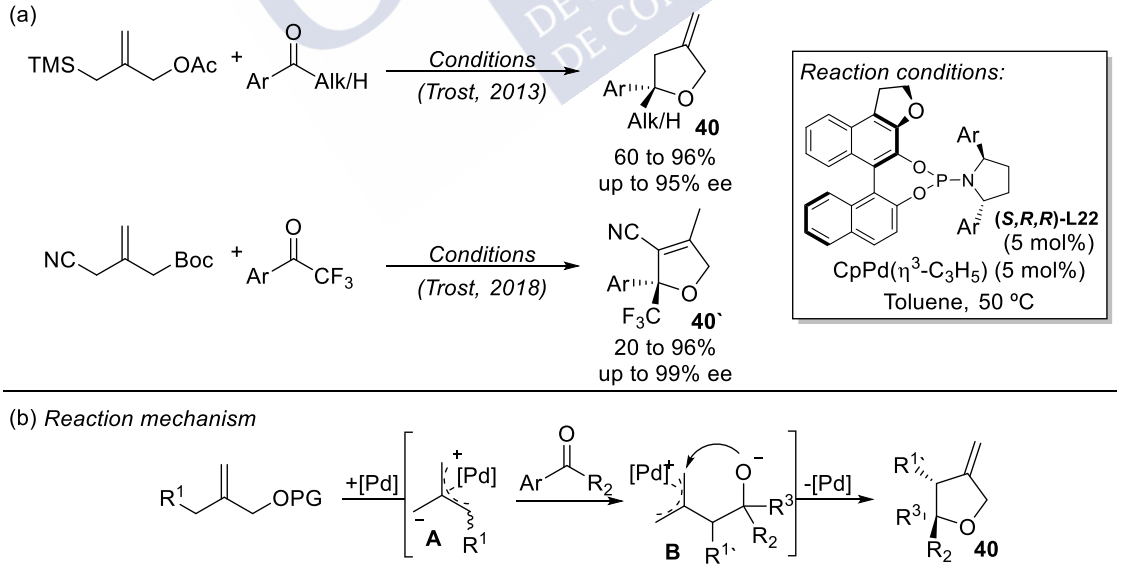

Scheme 79. Pd-catalyzed (3+2) cycloaddition between TMM precursors and ketones or fluorinated ketones.

[98] B. M. Trost, D. A. Bringley, *Angew. Chemie - Int. Ed.* **2013**, *52*, 4466–4469.
[99] B. M. Trost, G. Mata, *Angew. Chemie - Int. Ed.* **2018**, *57*, 12333–12337.

Donor-acceptor cyclopropanes are also suitable precursors for the construction of five-membered oxacycles through metal promoted ring opening/cycloaddition processes (Scheme 80).[100] An interesting example published by Johnson in 2009 employs a chiral magnesium pybox catalyst that is able to promote dynamic kinetic asymmetric cycloaddition between the racemic cyclopropanes and aldehydes, to obtain the corresponding tetrahydrofurans with high diastereoselectivity and excellent enantioselectivities.[101] Nevertheless, the reaction requires long reaction times, the use of CCl_4 as solvent and aromatic substituents at the cyclopropane to facilitate the equilibration to the postulated carbocationic intermediate.

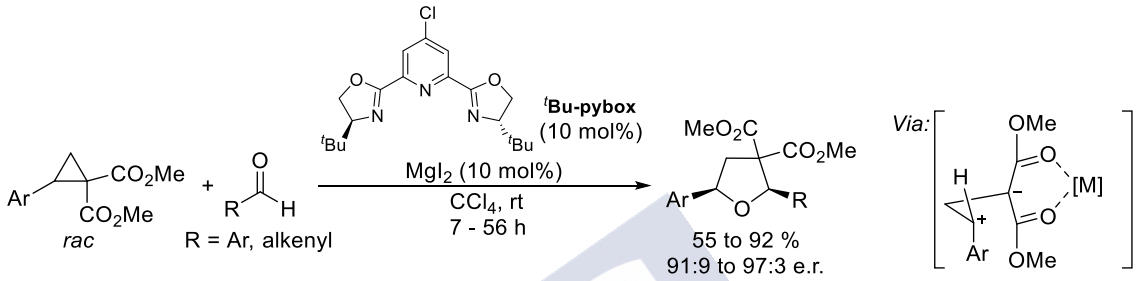

Scheme 80. Mg-catalyzed (3+2) cycloaddition between donor-acceptor cyclopropanes and aldehydes.

Relevant to this PhD work, Yamamoto described the first example of a transition metal catalyzed (3+2) cycloaddition between alkylidenecyclopropanes and aldehydes (Scheme 81).[102] The method allows the assembly of functionalized tetrahydrofurans, but only works with aromatic aldehydes. Ketones do not participate in the process, and most of the examples have been reported with symmetrically disubstituted ACPs. When a non-symmetrically substituted ACP is used, a negligible d.r is obtained (d.r = 1.3:1), whereas with monosubstituted ACP the yields are low. The proposed reaction mechanism involves a metalloene rearrangement between palladacyclobutane and the aldehyde, leading to a π-allylic intermediate, which affords the product after reductive elimination.

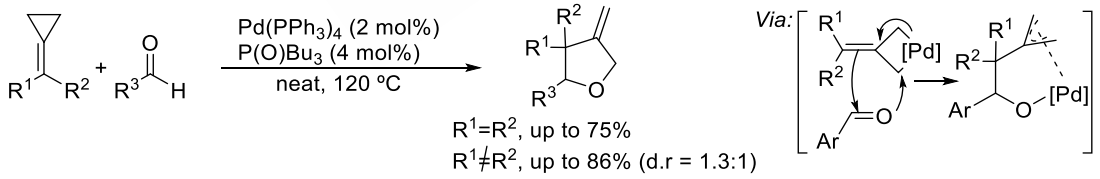

Scheme 81. Pd-catalyzed intermolecular (3+2) cycloaddition between ACPs and aldehydes.

As we have revised, versatile and rapid TMC methods for the assembly of functionalized tetrahydrofuranes efficiently, with high selectivity, good reaction yield and broad scope are scarce. Regarding the use of ACPs, only one intermolecular reaction has been reported, and holds severe limitations. Notably, there are not precedents on related intramolecular reactions that could afford fused-tetrahydrofuran structures.

---

[100] T. F. Schneider, J. Kaschel, D. B. Werz, *Angew. Chemie - Int. Ed.* **2014**, *53*, 5504–5523.
[101] A. T. Parsons, J. S. Johnson, *J. Am. Chem. Soc.* **2009**, *131*, 3122–3123.
[102] I. Nakamura, B. H. Oh, S. Saito, Y. Yamamoto, *Angew. Chemie - Int. Ed.* **2001**, *40*, 1298–1300.

1.2. Metal-catalyzed cycloadditions for the construction of pyrrolidines and related five-membered azacyles

(3+2) Cycloadditions

In 1993, the Trost group demonstrated that Pd-TMM cycloadditions are also useful for the construction of pyrrolidines (Scheme 82).[103] The use of the TMM precursor and N-Tosyl imines in the presence of a palladium (0)-phosphite catalyst allowed the formation of the corresponding pyrrolidines in good yields. The proposed mechanism is homolog to that previously shown for the cycloaddition with carbonyls.

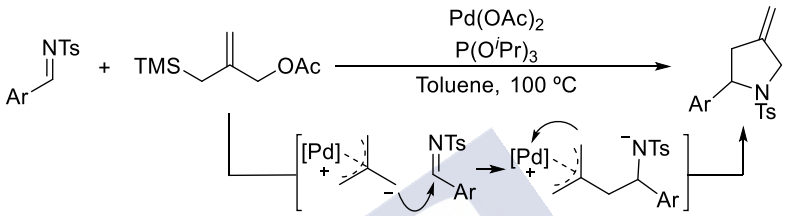

Scheme 82. Pd-catalyzed intermolecular (3+2) between TMM precursors and imines.

The same group developed enantioselective variants of this reaction (Scheme 83). In a first case, the authors demonstrate that a chiral Pd catalyst prepared from CpPd(η^3-C_3H_5) and the phosphoramidite **(*R*,*R*,*R*)-L20** was able to promote highly enantioselective (3+2) cycloadditions between *N*-Boc imines and the same type of TMM precursors.[104] Later on, in 2012, the authors employed the TMM precursors that bear a nitrile group, in combination of N-tosyl imines.[105] Significantly, the use of ketimines was tolerated, leading to pyrrolidines bearing appealing chiral quaternary centers.

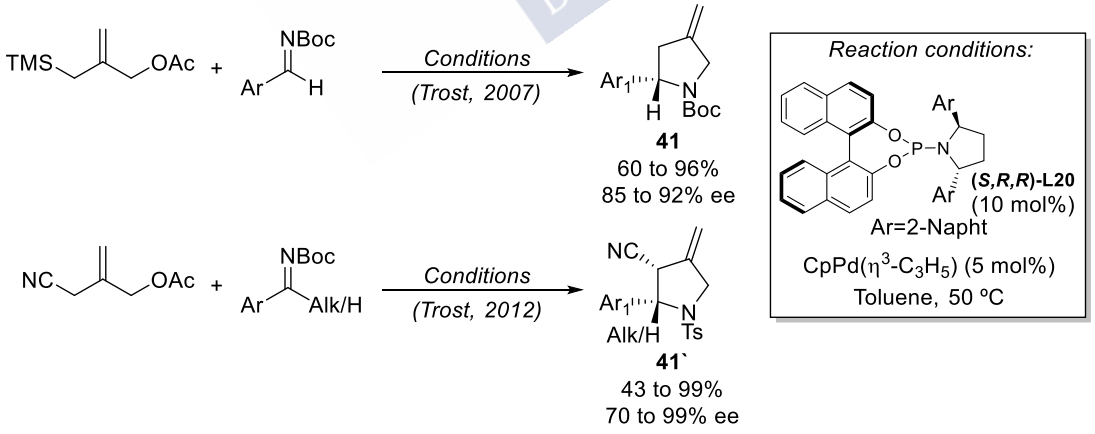

Scheme 83. Pd-catalyzed enantioselective (3+2) between TMM precursors and imines.

[103] B. M. Trost, C. M. Marrs, *J. Am. Chem. Soc.* **1993**, *115*, 6636–6645.
[104] B. M. Trost, S. M. Silverman, J. P. Stambuli, *J. Am. Chem. Soc.* **2007**, *129*, 12398–12399.
[105] B. M. Trost, S. M. Silverman, *J. Am. Chem. Soc.* **2012**, *134*, 4941–4954.

Aziridines have also been used as partner in TMC cycloadditions leading to pyrrolidines (Scheme 84). [106] Thus, Zhang reported in 2016 a Rh-catalyzed stereospecific formal (3+2) cycloaddition between vinyl aziridines and allenes.[107] When monosubstituted allenamides are used as starting materials, pyrrolidines of type **42** are efficiently obtained. In contrast, when 1,3-disubstituted allenes are used, pyrrolidines bearing an *exo*-alkene at the alpha position of type **42`** are obtained. Both reactions are highly efficient, nevertheless, the requirement of enantioenriched starting materials is an important drawback for the reaction. The proposed mechanism starts with the formation of the intermediate **A** through an initial C-N activation. Then, depending on the allene used, the migratory insertion can take place between the Rh-C or Rh-N bonds. In the first case, intermediates like **B** are obtained, eventually providing pyrrolidines of type **42**. Contrary, when 1,3-disubstituted allenes are used, the formation of intermediates of type **B`** leads to isomeric adducts **42`,** after a reductive elimination step.

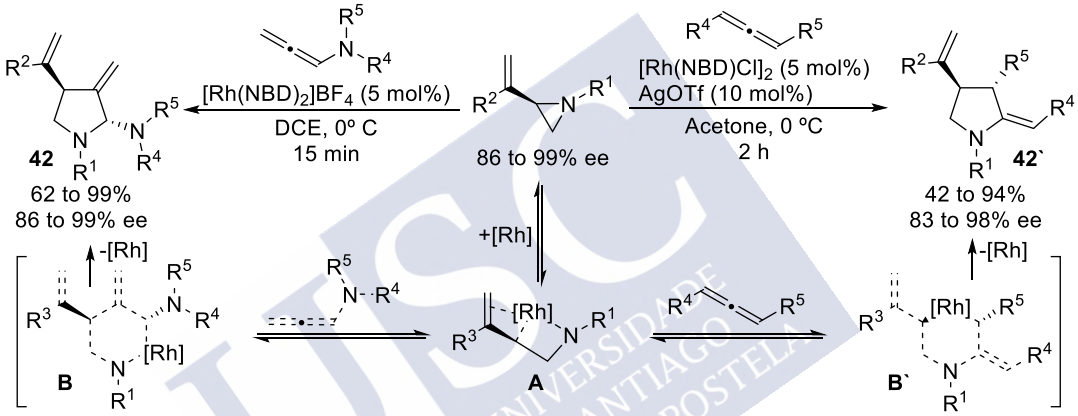

Scheme 84. Rh(I)-catalyzed enantiospecific (3+2) between aziridines and allenes.

Regarding the use of cyclopropanic precursors, Liu reported in 2019 a palladium catalyzed intermolecular (3+2) annulation between donor-acceptor vinylcyclopropanes and imines (Scheme 85).[108] In this report, a combination of $Pd(dba)_2$ and the chiral phosphoramidite ligand **(*S*)-L23** is key to promote the annulation with the isatin derivates, whereas **(*S*,*R*,*R*)-L24** is required for the reaction with aldimines. The reaction leads to the corresponding pyrrolidines in good yields an enantioselectivities, but with modest diastereoselectivities.

[106] A. L. Cardoso, T. M. V. D. Pinho E Melo, *European J. Org. Chem.* **2012**, 6479–6501.
[107] T.-Y. Lin, C.-Z. Zhu, P. Zhang, Y. Wang, H.-H. Wu, J.-J. Feng, J. Zhang, *Angew. Chemie Int. Ed.* **2016**, 1–6.
[108] X. B. Huang, X. J. Li, T. T. Li, B. Chen, W. D. Chu, L. He, Q. Z. Liu, *Org. Lett.* **2019**, *21*, 1713–1716.

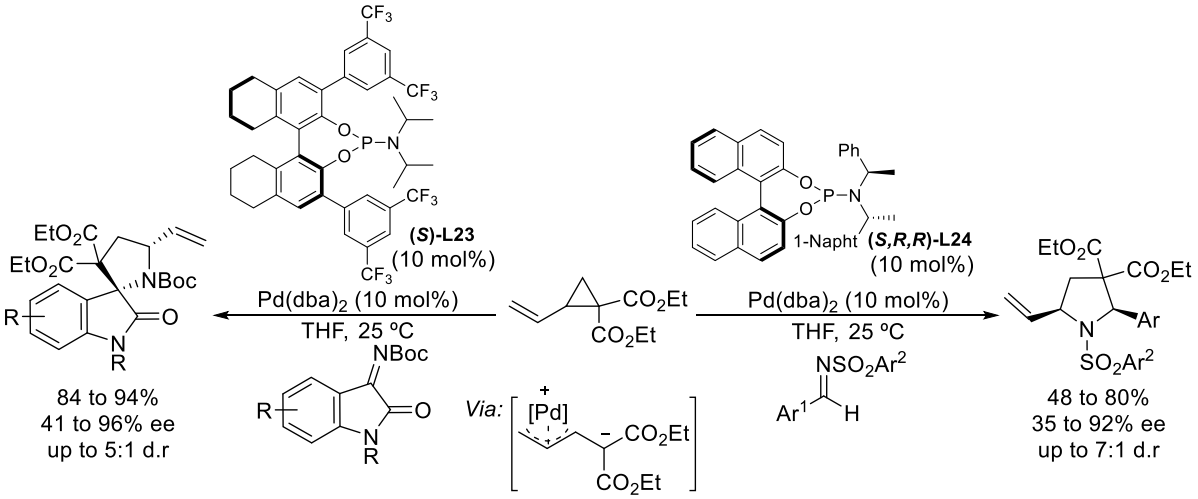

Scheme 85. Rh(I)-catalyzed enantioselective (3+2) between VCPs and imines.

Wu and coworkers reported in 2011 a formal (3+2) annulattion that takes place by mixing ACPs like 1-(cyclopropylidenemethyl)-2-ethynylbenzene with azides in presence of a copper catalyst, to give fused tricyclic pyrrolidines (Scheme 86).[109] The reaction proceeds under mild conditions, but the scope is limited and the obtained yields are moderate. The reaction starts through a an initial copper catalyzed click annulation, generating the intermediate **A**, that further eliminates a molecule of N_2 forming the ketenimine **B**. This intermediate evolves through a 6π-cyclization and finally an intramolecular rearrangement (**C**) forms the final product. Thus, the metal only promotes the formation triazolic intermediate, but is not *a priori* related with the cyclization process itself.

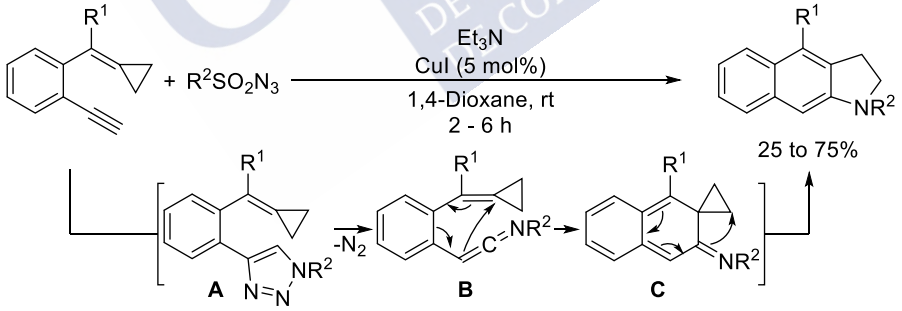

Scheme 86. Cu(I)-promoted formal (3+2) between ACPs and alkynes.

A formal (3+2) cycloaddition using imines as counterparts was also described by Yamamoto in 2001 (Scheme 87).[110] This seminal work shows that catalytic amounts of $Pd(PPh_3)_4$ in combination with triphenylphosphine oxide can promote the (3+2) heterocycloaddition between tosyl imines and ACPs equipped with two alkyl substituents at the alkene, to give synthetically appealing functionalized pyrrolidines. Nevertheless, the scope of the reaction is

[109] (a) S. Li, Y. Luo, J. Wu, *Org. Lett.* **2011**, *13*, 3190–3193. (b) S. Li, Z. Li, J. Wu, *Adv. Synth. Catal.* **2012**, *354*, 3087–3094.

[110] (a) B. H. Oh, I. Nakamura, S. Saito, Y. Yamamoto, *Tetrahedron Lett.* **2001**, *42*, 6203–6205. (b) B. H. Oh, I. Nakamura, S. Saito, Y. Yamamoto, *Heterocycles.* **2003**, *61*, 247-257.

very limited, since only aromatic imines and alkyl disubstituted ACPs participate in the process. Moreover, when different substituents at the ACPs are used, a complete lack of diastereoselectivity is observed. The proposed mechanism is similar to that shown for the cycloaddition with aldehydes, and involves the formation of π-Allyl-Pd intermediate from a metalloene rearrangement, which evolves to the observed pyrrolidines.

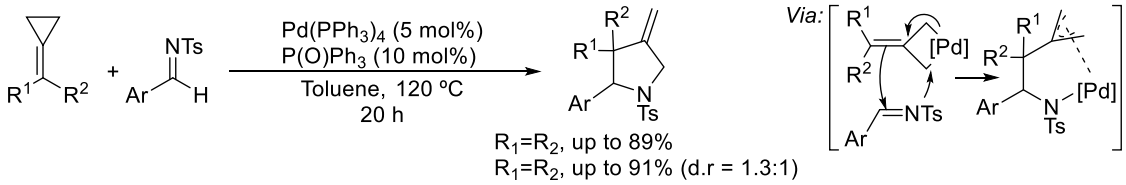

Scheme 87. Pd-catalyzed intermolecular (3+2) between ACPs and imines.

A second report was published by the same group in 2004, using in this case 1,2-diazines as counterpart (Scheme 88).[111] Interestingly, the commonly obtained exo-methylene cyclic scaffold is not obtained, but instead the reaction produces the fused pyrroles. The scope of the reaction is very limited, and take place under harsh conditions. Mechanistically, the authors proposed an initial C-C bond cleavage of the distal position of the cyclopropane, followed by coordination of the diazine. Then, an *1,2*-addition over the C=N bond (**A**) leads to the allyl-Pd species **B**, which further evolves to **C,** which bears the *exo* double bond. An eventual oxidation and aromatization towards the 5-azaindolizines would then take place, albeit details of this process are not provided.

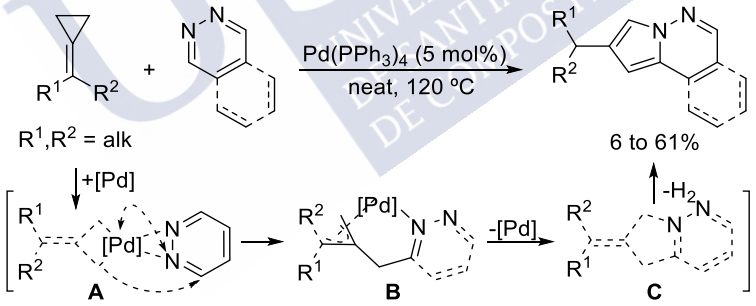

Scheme 88. Pd-catalyzed intermolecular (3+2) between ACPs and 1,2-diazines.

The most recent report was published by Bhargava in 2019, who showed that bis-alkylidenecyclopropanes can react intermolecularly with azocarboxylates in presence of a Ni(0) catalyst to assemble pyrazole-1,2-dicarboxylates (Scheme 89).[112] The reaction requires a large excess (10 eq.) of DIAD or DEAD as reaction counterparts, leading to the heterocyclic products in moderate yields and narrow scope. Mechanistically,[113] the reaction involves the insertion of the metal at the proximal position of the ACP, followed by a migratory insertion

[111] A. I. Siriwardana, I. Nakamura, Y. Yamamoto, *J. Org. Chem.* **2004**, *69*, 3202–3204.
[112] B. Kuila, R. Naikoo, D. Mahajan, P. Singh, G. Bhargava, *Synlett*, **2020**, *31*, 65–68.
[113] (a) L. Saya, G. Bhargava, M. A. Navarro, M. Gulías, F. López, I. Fernández, L. Castedo, J. L. Mascareñas, *Angew. Chemie - Int. Ed.* **2010**, *49*, 9886–9890. (b) B. Kuila, D. Mahajan, P. Singh, G. Bhargava, *Tetrahedron Lett.* **2015**, *56*, 1307–1311.

of the diazocarboxylate partner, leading to the corresponding products after reductive elimination.

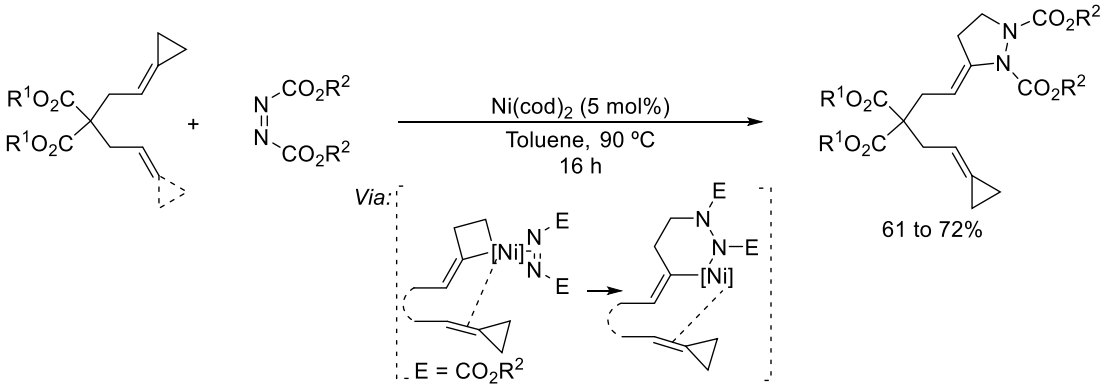

Scheme 89. Ni-catalyzed intermolecular (3+2) cycloaddition between ACPs and azocarboxylates.

(4+1) Cycloadditions

Shi reported in 2006 a formal gold catalyzed (4+1) annulation between ACPs and primary tosyl amines, promoted by a cationic gold (I) complex (Scheme 90). [114] The reaction is restricted to the use of aryl substituded ACPs at the terminal position of the alkene, leading to the pyrrolidinic products in moderate yields. The reaction proceeds through a π-activation of the alkylidenecyclopropane (**A**) by gold, followed by an intramolecular hydroamination process that provides the alkenylamide **B** and, after protodeauration, the homoallylic amide **C**. Then, a second activation of the alkene by the metal center, followed by an intramolecular cyclization and further protodeauration (**D**) leads to the corresponding pyrrolidines .

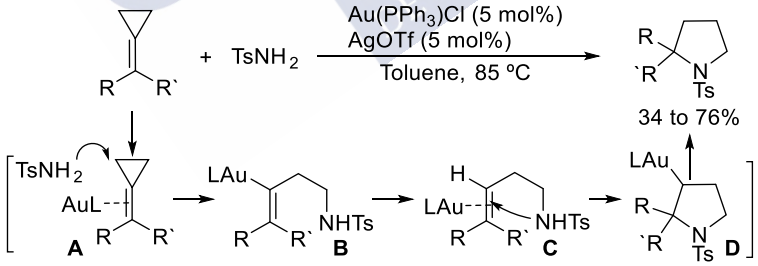

Scheme 90. Au(I)-catalyzed intermolecular (4+1) annulation between ACPs and tosylamides.

The presented precedents are the most representative related examples of TMC processes for synthesis of pyrrolidines. Albeit they are important contributions, most of them shows important limitations. In addition, enantioselective annulations for the assembly of enantioenriched pyrrolidines are very scarce, whereas synthetically useful intramolecular cycloadditions remain still unprecedented.

[114] M. Shi, L. P. Liu, J. Tang, *Org. Lett.* **2006**, *8*, 4043–4046.

2. Objectives

Considering the challenges associated to building small-sized heterocycles and the limited precedents of intramolecular (3+2) heterocycloadditions of alkylidenecyclopropanes, we proposed the development of intramolecular palladium catalyzed cycloadditions between ACPs and a carbon-heteroatom unsaturated reaction partners, such as imines and carbonyls in order to obtain highly substituted fused- pyrrolidines and tetrahydrofurans (Scheme 91).

The process is not obvious, given that it is well known that Csp^3-X reductive eliminations are less favorable than the homolog C-C processes. Moreover, at least two different β-hydride elimination process could compete delivering produces such as **47** or **47``**, further difficulting the cycloaddition event.

In the specific case of the annulation with imines, additional challenges regarding the inherent stability and reactivity of imines must also be overcomed. For instance, aliphatic imines are not stable when they have enolizable positions, so that formation of enamines and Mannich type products can occur. Additionally, it is well known that imines can coordinate metal complexes, potentially inhibiting their catalytic activity.

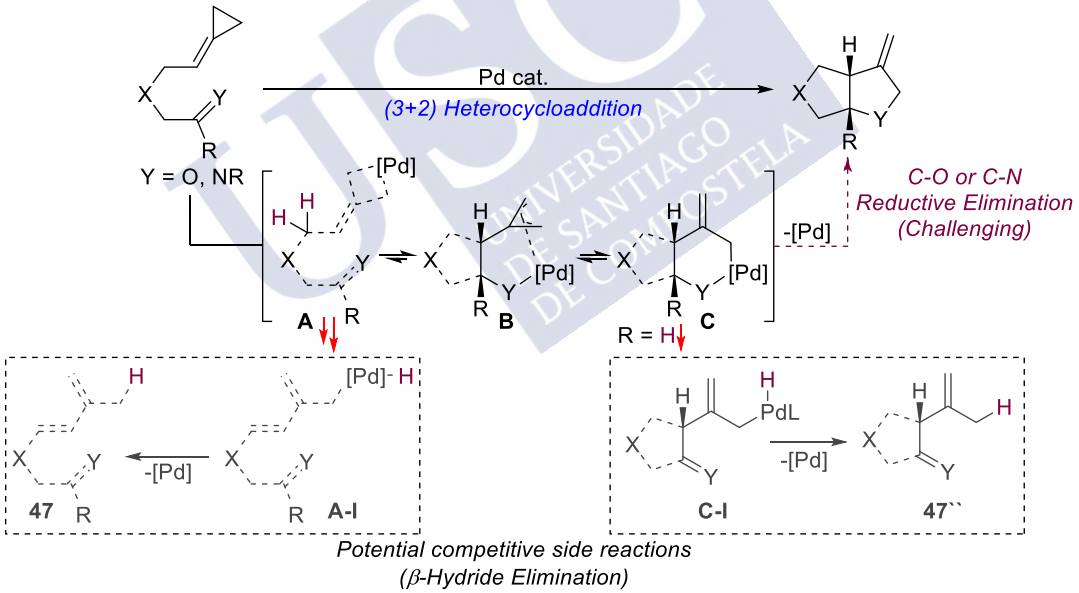

Scheme 91. New palladium catalyzed (3+2) heterocycloaddition reactions.

3. Results and discussion

3.1. Metal-catalyzed (3+2) heterocycloadditions of ACPs. Access to five-membered azacycles

3.1.1. Study of the intramolecular (3+2) cycloaddition

To evaluate the viability of the intramolecular annulation with nitrogenated reaction partners, we synthesized the *tert*-butyl sulfinyl imine derivative **43**, since it is known that this type of aliphatic imines might be reasonably stable, even when bearing adjacent hydrogens, susceptible of enolization. The synthesis was carried out by treating the aldehyde **48a**[62] with 2-methyl-2-propanesulfinamide and catalytic amounts of antranilic acid, which produces the imine in a 61% yield, in its pure isomeric *E* form (Scheme 92).

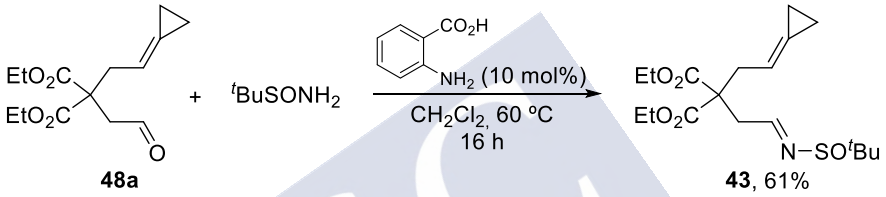

Scheme 92. Synthesis of substrates **43**.

We then checked the reactivity of **43** when submitted to the optimal conditions found for the (3+2) cycloadditions between alkylidenecyclopropanes and alkenes, consisting of the use of a 6 mol% of Pd_2dba_3 and the phosphite **L1** (24 mol%).[53] Unfortunately, despite full conversion was observed after 3 h in refluxing dioxane, the desired cycloadduct type **44** was not detected (Scheme 93).

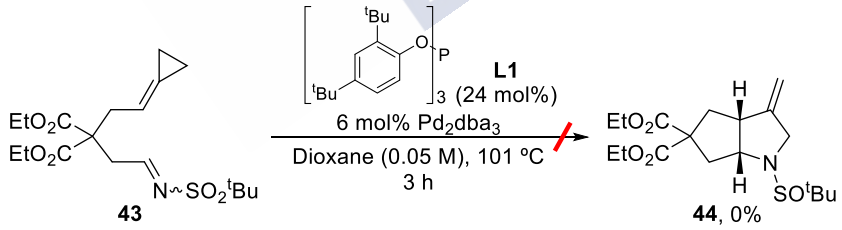

Scheme 93. Preliminary testing of imines in (3+2) cycloaddition.

We next explored other type of nitrogenated unsaturated partners (Scheme 94). A recent work reported by our group showed that oxime ethers and esters are suitable reaction counterparts in gold catalyzed cycloaddition reactions that were not feasible with related imines.[115] Indeed, oxime ethers and esters bearing enolizable adjacent carbons are perfectly stable but still readily accessible. Moreover, the lower Lewis basicity of their nitrogen atom, compared to analog imines, makes them more compatible with metal catalysts, so inhibition by strong coordination to the metal is less easy. Finally, it is also important to consider that *E* and *Z*

[115] D. C. Marcote, I. Varela, J. Fernández-Casado, J. L. Mascarenas, F. López, *J. Am. Chem. Soc.* **2018**, *140*, 16821–16833.

isomers of oximes are configurationally stable, so variable *Z/E* mixtures are usually obtained in their synthesis.

On these basis, we synthesized the oxime ethers **45a** and **45b** from the aldehyde **48a**, by condensation with the corresponding hydroxylamines under basic conditions **45a** (R = OBn, 72%, *E*/*Z* = 2 : 1) and **45b** (R = OMe, 75%, *E*/*Z* = 2 : 1). Moreover, the condensation with simple hydroxylamine under equal conditions delivered the oxime **45h** (R = OH, 79%, *E*/*Z* = 1 : 1), **45i**, which was transformed into the corresponding benzoyl ester by treatment with BzCl and Et_3N (R=OBz, 20%, *E*/*Z* = 2 : 1).

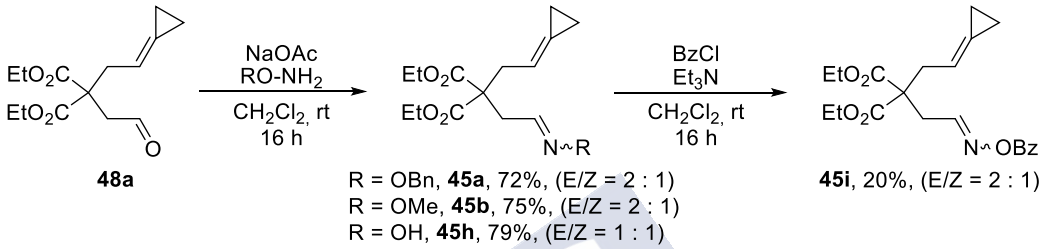

Scheme 94. Screening of unsaturated carbon-nitrogen reaction counterparts.

Considering that oxime ethers were obtained with variable *E/Z* ratios, we used samples with *E/Z* = 1.1:1, in order to obtain comparable results. Interestingly under the standard reaction conditions, using phosphite **L1** as ligand (Table 6), the O-benzoyl oxime **45i** is converted into the debenzoylated product **45i`**, which was isolated in a 20%yield (entry 1). This result can be explained considering the ability of Pd(0) complex to oxidatively insert into N-OR bonds (Scheme 95). Moreover, the oxime derivative **45h** did not afford the desired adduct probably due the deactivation of the catalyst by the OH group (entry 2). To our delight, the *O*-benzyl oxime **45a** provided the cycloadduct **46a** as major product in a promising 50% yield, with full *syn* selectivity at the ring fusion (Table 6). A small amount of the diene side product **47** was also obtained (entry 3). The formation of this diene can be explained by a *β*-hydride elimination in the metallacyclobutane **A** , which is followed by a C-H reductive elimination at **B**.

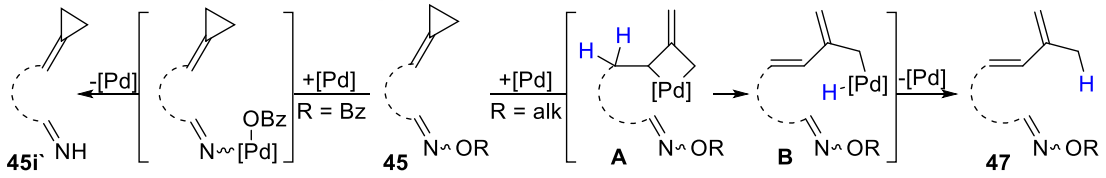

Scheme 95. Mechanistic explanation for the formation of **47** and **45i`**.

The use of a less bulky phosphite such as $(iPrO)_3P$ led to a poor conversion and the desired product was not observed (entry 4), whereas with the phosphoramidite **L2** the desired adduct **46a** was obtained in a poor 11% yield (entry 5). On the other hand, the related O-methyl aldoxime **45b** also participated in the cycloaddition promoted by Pd_2dba_3/**L1,** to give the corresponding cycloadduct in a 47% yield (entry 6).

Table 6. Preliminary evaluation of different oximes ethers and esters.[116]

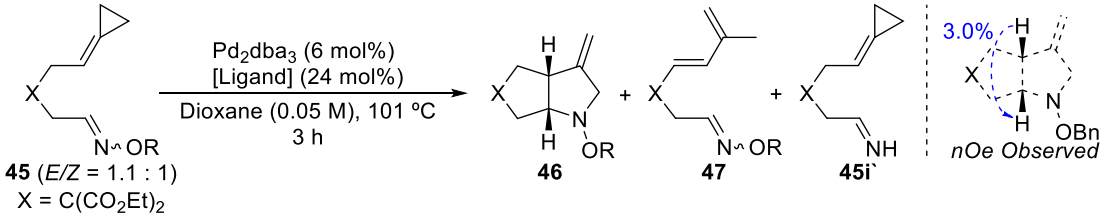

Entry	Ligand	R	Conv. (%)[c]	46 (%)[c]	47 (%)[c]	45i` (%)[c]
1	**L1**	OBz	100	-	-	20
2	**L1**	OH	40	-	5	-
3	**L1**	OBn	100	43[b]	10	-
4	$(iPrO)_3P$	OBn	70	-	10	-
5	**L2**	OBn	100	11	15	-
6	**L1**	OMe	100	45[b]	16	-

[a] *Reaction conditions*: **45** (0.15 mmol), Pd_2dba_3 (6 mol%), [Ligand] (24 mol%), dry 1,4-dioxane [0.05 M], reflux. [b] Isolated yield. [c] Determined by ^{1}H-NMR using 1,3,5-trimethoxybenzene as internal standard.

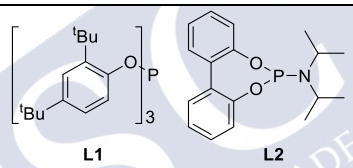

Interestingly, when the cycloaddition of **45a** was repeated using a different batch of substrate with an *E/Z* ratio of 2:1, we noticed an increase in the reaction yield, as **46a** was obtained in a 53% yield (Scheme 96).

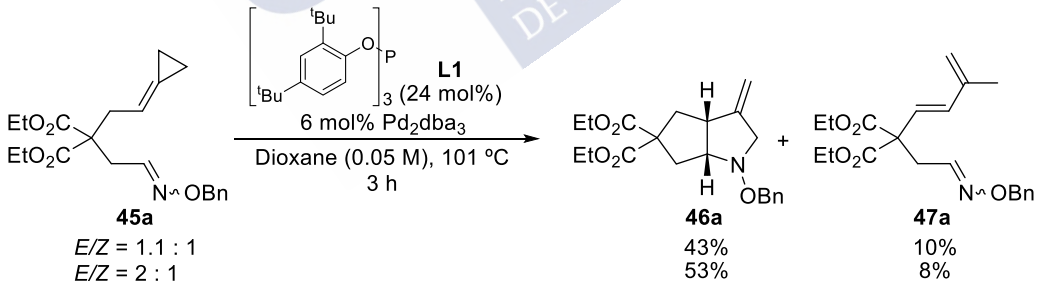

Scheme 96. Different reactivity of *E*/*Z* mixtures.

Considering these results, we evaluated the reactivity of both *E* and *Z* isomers separately (Table 7). When the pure isomer (*E*)-**45a** was submitted to the reaction conditions, **46a** was obtained selectively in 55% yield (entry 1), whereas the sample enriched with the (*Z*)- **45a** isomer (*E*/*Z* = 1 : 5) led to a lower yield and rate, so that a full conversion was not achieved (entry 2). Moreover, an almost equimolar mixture of both products **46a** and **47a** was obtained in low yields. Interestingly, when a mixture with a (*E*/*Z*) = 1 : 1 was used, we obtained a result

[116] Considering that substrates were obtained as isomeric *E*/*Z* mixtures with variable ratios, we used samples with *E*/*Z* = 1.1:1. Thus, the results obtained can be compared.

similar to that resulting from the *E* isomer: a mixture of **46a** in a 43% and diene **47a** in a 10% yield (entry 3). These results suggest that the formation of the cycloadduct of type **46** is favored for the *E*-isomer, whereas the *Z*-isomer led to lower reaction rates, preferentially delivering the undesired byproduct of type **47**.

Table 7. Evaluating the reactivity of *E* and *Z* isomers.

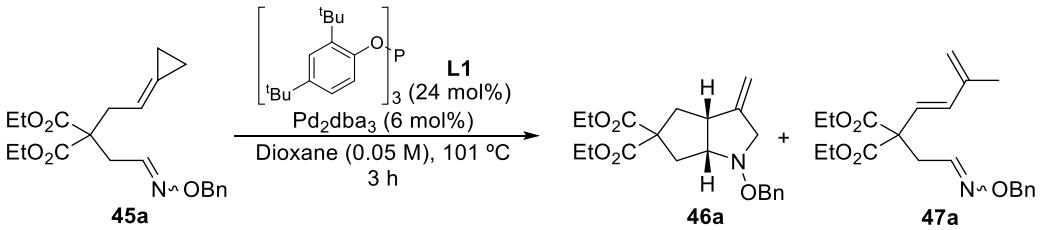

Entry	Conv. (%)	13a` (*E*/*Z*)	46a (%)[b]	47a (%)[b]
1	100	1 : 0	55	<5
2	90	1 : 5	21	30
3	100	1 : 1	43	10

[a] *Reaction conditions*: **45** (0.15 mmol), Pd_2dba_3 (6 mol%), **L1** (24 mol%), dry 1,4-dioxane [0.05 M], reflux. [b] Determined by ^{1}H-NMR using 1,3,5-trimethoxybenzene as internal standard.

We next evaluated different solvents using the oxime **45b** as model precursor (*E*/*Z* = 1.4:1, Table 8). Toluene leads to a similar yield of **46b**, with slightly higher amount of diene **47b** (entries 1 and 2), while protic solvents such as *t*AmOH led exclusively to the dienic product in 65% yield (entry 3). In addition, other solvents such as 1,2-DCE or THF were also suitable, but the reaction provided lower yields of the adduct **46b**, being the diene **47b** the major product (entry 4 and 5).

Table 8. Preliminary screening of solvents.

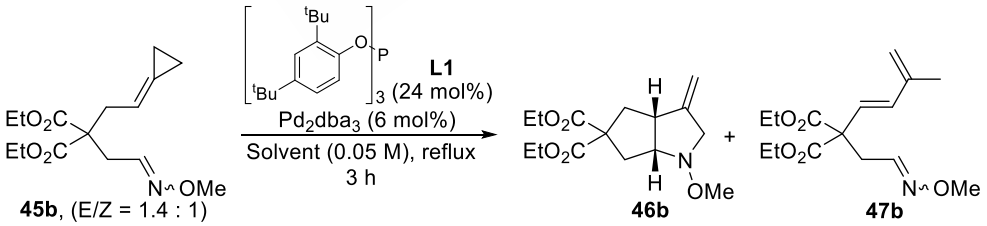

Entry	Solvent	46b (%)[c]	47b(%)[c]
1	1,4-Dioxane	50	20
2	$PhCH_3$	49	36
3	*t*AmOH	-	65
4	1,2-DCE	39	50
5	THF	36	55

[a] *Reaction conditions*: **45** (0.15 mmol), Pd_2dba_3 (6 mol%), **L1** (24 mol%), dry solvent [0.05 M], T (ºC). [b] Isolated yield. [c] Determined by ^{1}H-NMR using 1,3,5-trimethoxybenzene as internal standard.

An additional screening of solvents was carried out using in this case the oxime ether **45b** with a *E/Z* ratio of = 2 : 1 (Table 9).[117] The use of 1,4-dioxane provided a similar result than the previously obtained with analogue **45a** (OBn) with an E/Z = 2 : 1 (53%, Scheme 96), reaching in this case a 50% of isolated yield (entry 1). Gratifyingly, **46b** was obtained in a 70% in toluene (entry 2), whereas using $PhCF_3$ as solvent, a lower conversion and reaction yields were observed (entry 3). Finally, fluorobenzene and *n*-heptane provided just slightly lower yields than toluene (entry 4 and 5 *vs* 2).

Table 9. Secondary screening of solvents.

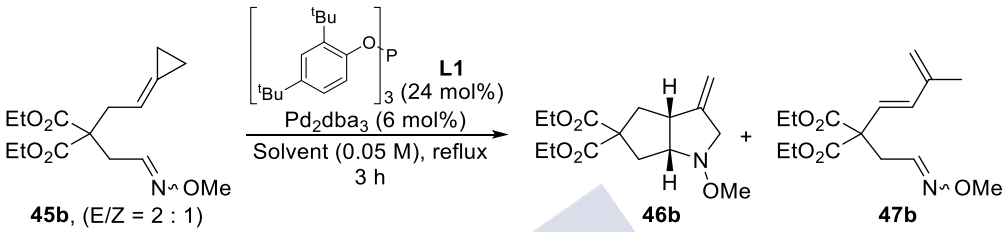

Entry	Solvent	Conv. (%)[c]	14a (%)[c]	15a (%)[c]
1	1,4-dioxane	100	50 [b]	8
2	$PhCH_3$	100	70[b]	28
3	$PhCF_3$	70	40	30
4	C_6H_5F	100	60[b]	40
5	*n*-Heptane	100	66[b]	20

[a] *Reaction conditions*: **45** (0.15 mmol), Pd_2dba_3 (6 mol%), **L1** (24 mol%), dry solvent [0.05 M], T (ºC). [b] Isolated yield. [c] Determined by ^{1}H-NMR using 1,3,5-trimethoxybenzene as internal standard.

Then we evaluated the influence of the temperature in the reaction. Similar yields were observed in the range of temperatures from 70 º to 100 ºC (Table 10, entries 2 - 4), while at 110 ºC the reaction yield decreased and we observed the formation of a black solid, indicative of the decomposition of the catalyst (entry 1). On the other hand, at 60 ºC the conversion is incomplete, and the diene is obtained as major product (entry 5).

[117] Once oxime ethers were established as the most suitable reaction counterpart, the next experiments were carried out using the E/Z mixture originally obtained from the reaction synthesized.

Table 10. Evaluation of the temperature effect in the reaction.

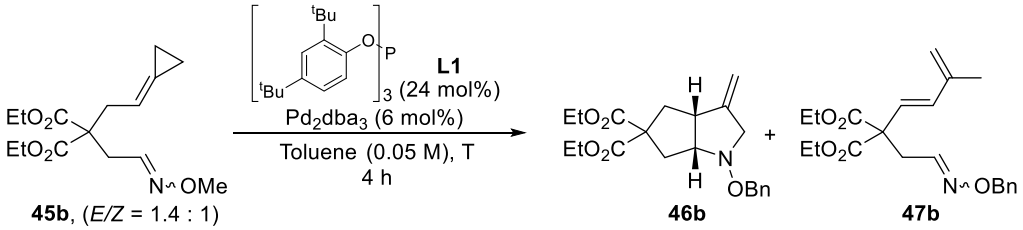

Entry	T (°C)	Conv. (%)[b]	14a (%)[b]	15a (%)[b]
1	110	100	38	23
2	100	100	44	30
3	80	100	45	43
4	70	95	45	45
5	60	85	24	49

[a] *Reaction conditions*: **45** (0.15 mmol), Pd_2dba_3 (6 mol%), **L1** (24 mol%), freshly distilled toluene [0.05 M], T (°C). [b] Determined by ^{1}H-NMR using 1,3,5-trimethoxybenzene as internal standard.

Next, we tried to optimize the catalyst loading (Table 11). A decrease from a 24 mol% of **L1** to a 13 mol%, did not affect the reaction yield (entry 1 *vs* 2), suggesting that only one ligand is linked to the metal center. Additionally, when other Pd (0) sources such as CpPd(η^3-1-PhC_3H_4) or $Pd(PPh_3)_4$ were tested, lower yields were observed (entries 3 and 4).

Table 11. Evaluation of the precatalyst effect in the reaction.

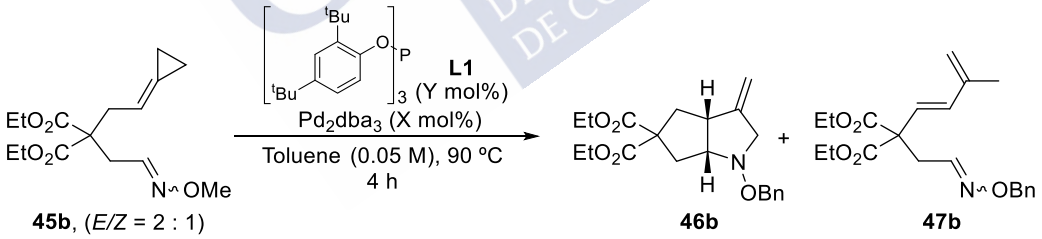

Entry	[Pd] (X mol %)	L1 (Y mol %)	Conv. (%)[b]	46b (%)[b]	47b (%)[b]
1	**Pd_2dba_3 (6)**	24	100	70	18
2	**Pd_2dba_3 (6)**	13	100	70	28
3	**CpPd(η^3-1-PhC_3H_4) (12)**	13	60	32	8
4	**$Pd(PPh_3)_4$ (10)**	13	50	0	<5

[a] *Reaction conditions*: **45** (0.15 mmol), [Pd] (X mol%), **L1** (Y mol%), freshly distilled toluene [0.05 M], 90 °C. [b] Determined by ^{1}H-NMR using 1,3,5-trimethoxybenzene as internal standard.

With most of the variables optimized, a second screening of phosphites and phosphine ligands was carried out. Curiously, less bulky aromatic phosphites like **$P(OPh)_3$** or **L17** provided much lower reaction yields (Table 12, entries 2 and 3). On the other hand, when electron deficient

phosphines such as **L18** and **L19** were used, the exclusive formation of diene **47b** was detected (4 and 5). Interestingly, bulky biaryl phosphines are also suitable ligands for the reaction. Specifically, RuPhos led to a good 60% yield of the cycloadduct **46b** , and the formation of a new type of dienic sideproduct, **47b`** (entry 6). The ligand tBuXPhos provided a similar result (entry 7), while Pd catalysts with biscyclohexyl phosphines XPhos and BrettPhos predominantly afforded the diene **47b`** (entry 8 and 9).

Table 12. Further screening of ligands for the intramolecular cycloaddition with oximes.

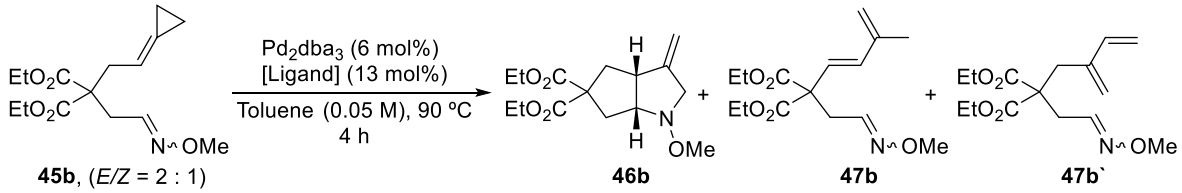

Entry	Ligand	Conv. (%)[b]	46b (%)[b]	47b (%)[b]	47b` (%)[b]
1	**L1**	100	70	28	-
2	**P(OPh)$_3$**	55	<5	42	-
3	**L17**	95	25	35	-
4	**L18**	20	-	10	-
5	**L19**	38	-	15	-
6	RuPhos	100	62	-	25
7	*t*BuXPhos	100	54	-	10
8	XPhos	100	15	-	45
9	BrettPhos	100	4	-	45

[a] *Reaction conditions*: **45** (0.15 mmol), Pd_2dba_3 (6 mol%), [Ligand] (13 mol%), freshly distilled toluene [0.05 M], 90 °C. [b] Determined by ^{1}H-NMR using 1,3,5-trimethoxybenzene as internal standard.

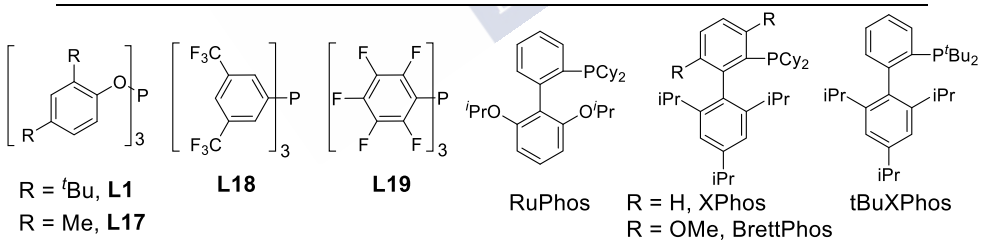

To summarize, the best conditions involve the use of a 6 mol% of Pd_2dba_3, 13 mol% of **L1**, in toluene under reflux. These conditions allowed to obtain the desired cycloadduct in 70% yield. Biaryl phosphines such as Ruphos are also good ligands for the reaction, providing a 62% yield.

3.1.2. Scope of the Pd-catalyzed intramolecular (3+2) cycloaddition between ACPs and oxime ethers

To evaluate the scope of the above reaction we synthesized several cycloaddition precursors. For instance, we prepared the precursor **45c** that exhibits a longer tether, to evaluate whether 6-5 bicyclic systems could also be accessible. Moreover, a ketoxime ether **45d**, was also made, as this could produce fused- pyrrolidines bearing a quaternary stereocenter at the ring fusion. On the other hand, we also studied the influence of heteroatoms at the tether, by preparing precursors bearing an oxygen (**45e**) or a nitrogen (**45f**) atom. Finally, a precursor with a simple aliphatic chain (**45g**), was also synthesized, to determine the real influence of the Thorpe-Ingold effect in these cycloadditions. The synthesis of all the aldoximes was carried out from the aldehydes by treatment with O-benzylhydroxylamine hydrochloride under basic media. The expected oximes were isolated in good yields and with *E/Z* ratios that usually varied from 1.1:1 to 3:1, as shown in the Scheme 97.

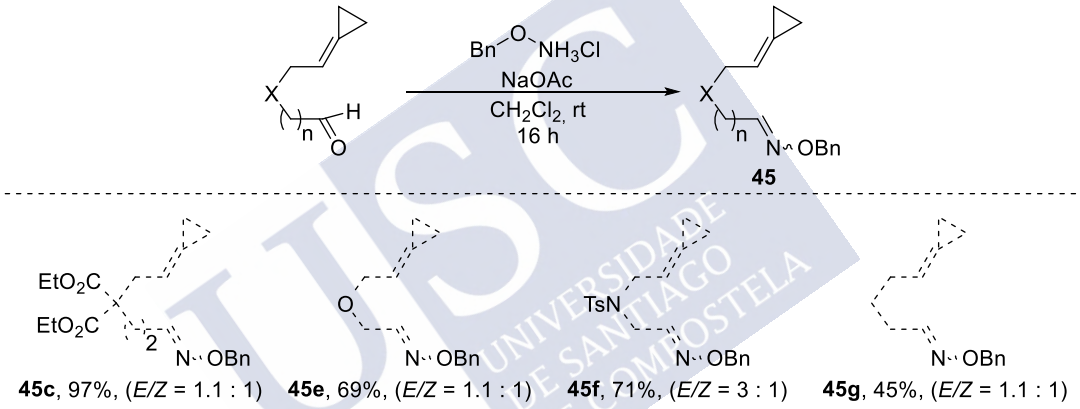

Scheme 97. Synthesis of substrates **45c**, **45e**, **45f** and **45g**.

The synthesis of the ketoxime was achieved in two steps, starting from malonate **56a**, which was submitted to a Tsuji-Trost reaction with tosylate **21** to give the ketone **49a** in 81% yield. Treatment of this compound with O-benzylhydroxylamine under basic conditions led to the oxime **45d** as pure *E* isomer with an 81% yield (Scheme 98).

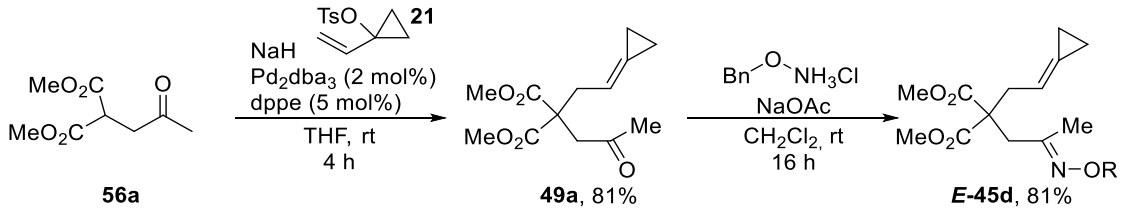

Scheme 98. Synthesis of substrate **45d**.

Treatment of model substrates **45b** (OR^3 =OMe) and **45a** (OR^3 = OBn) with 6 mol% of $Pd_2(dba)_3$ and a 13 mol% of **L1** in toluene at 90º C, provided the respective cycloadducts in 69-70% yield (Scheme 99). Unfortunately, the reaction of **45c**, with the longer connecting tether or that of the ketoxime ether **45d** did not produce the cycloadduct, but only traces of diene products of type

47 and a partial recovery of the starting material. On the other hand, the cycloadditions of precursors with an oxygenated, nitrogenated or non-functionalized tether (**45e-g**) also led to partial conversions, but neither the cycloadduct nor the diene sideproducts could be detected. Similarly, the use of RuPhos instead **L1**, which proof to also be a competent ligand for the cycloaddition, did not provide the desired cycloadducts, leading in most of the cases to uncomplete conversions and major formation of dienes of type **47`** (Page 94, table 12).

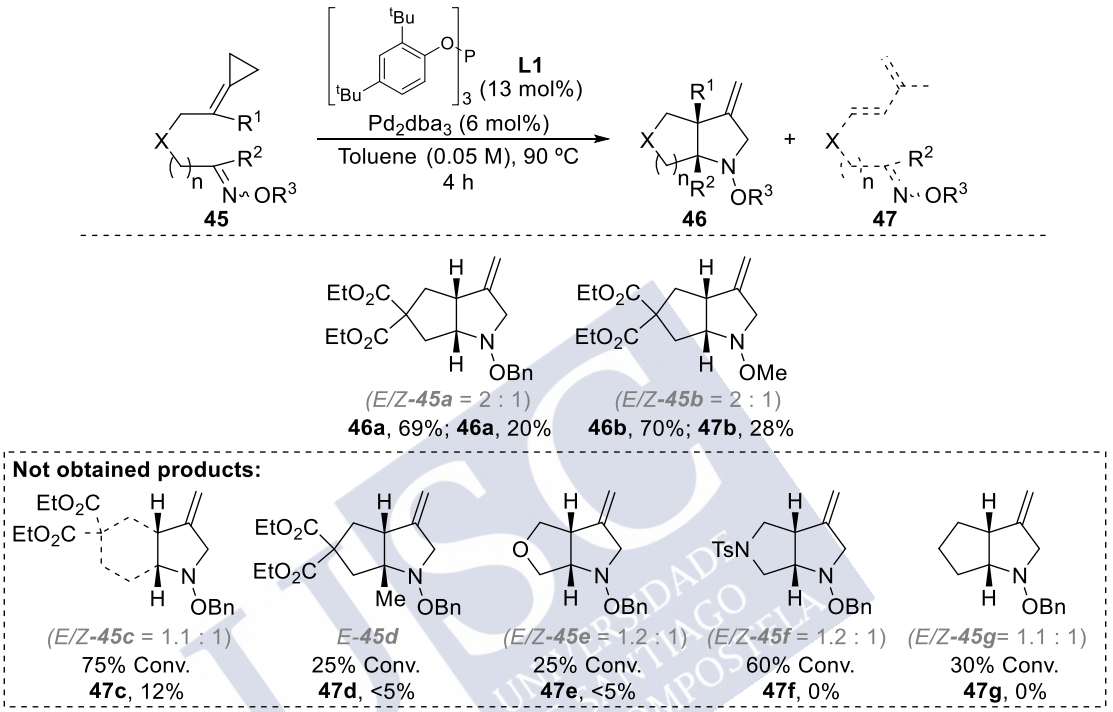

Scheme 99. Reaction scope of the intramolecular (3+2) cycloaddition with oximes.

3.1.3. Enantioselective intramolecular cycloadditions

Parallel to the development of the racemic cycloaddition, we also evaluated the viability of enantioselective variants using **45a** (*E*/*Z* = 10:1) as model substrate, and several chiral ligands. In particular, we explored catalysts prepared from different chiral phosphoramidites (13 mol%) and Pd_2dba_3 (6 mol%) in dry toluene under reflux. To our delight, when the ligand **(*S*,*R*,*R*)-L10** was tested, the desired adduct **46a** was obtained in an excellent 90% yield and 94% ee (Table 13, entry 1)

Unfortunately, this result was not easily reproduced. Since the source of dry toluene was the only parameter that changed throughout these experiments, we reasoned that different levels of dryness in the solvent could be responsible for this lack of reproducibility. Thus, we eventually found that the use of freshly distilled dry toluene, modified by the addition of 5 eq. of water, provides excellent selectivities and yields as well as high ee's (entry 6). Using distilled toluene without any added water led to poorer results (entry 3), whereas higher amounts of water, such as 10 or 15 eq. led to moderate reaction yields but high enantioselectivities for **46a**

(entry 4), with the presence of significant amounts of the diene (10-33% yield, entries 4 and 5).[118] These results suggest that water plays key role in the enantioselective determining step, but it has also a relevant role in the formation of the dienic byproduct.

Table 13. Screening of additives.

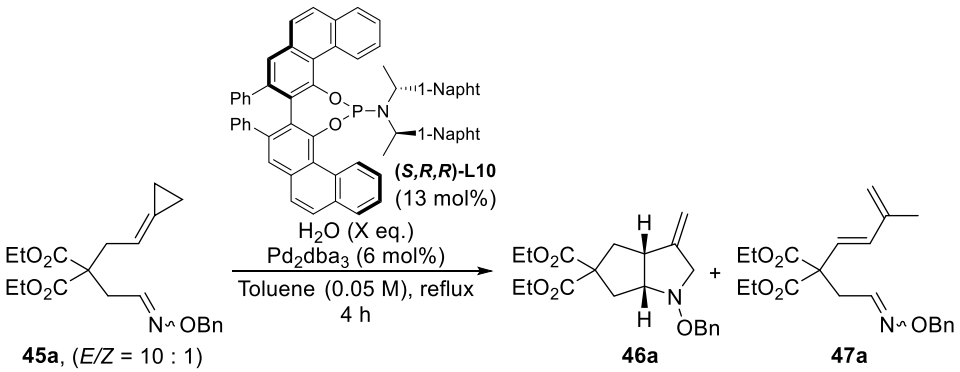

Entry	H_2O (eq.)	46a (%)[b]	47a (%)[c]	ee 46a (%)
1[d]	-	90	<5	94
2[e]	-	24	13	68
3[f]	-	30	30	68
4[f]	15	48	33	88
5[f]	10	70	10	88
6[f]	5	87	<5	88

[a] *Reaction conditions*: **45** (0.15 mmol), Pd_2dba_3 (6 mol%), **(*S*,*R*,*R*)-L10** (13 mol%), freshly distilled toluene [0.05 M], X eq. H_2O, reflux. [b] Isolated yield. [c] Determined by ^{1}H-NMR using 1,3,5-trimethoxybenzene as internal standard. [d] initial result using an "old" open bottle of dry toluene. [e] carried out with a new just opened bottle of dry toluene. [f] Carried out with freshly distilled toluene.

Using the less bulky VAPOL-based ligand **(*S*,*R*,*R*)-L8** we observed lower reaction yields and enantiomeric ratios, indicating that that bulkiness of **(*S*,*R*,*R*)-L10** is very important to achieve high enantioselectivities (Scheme 100).

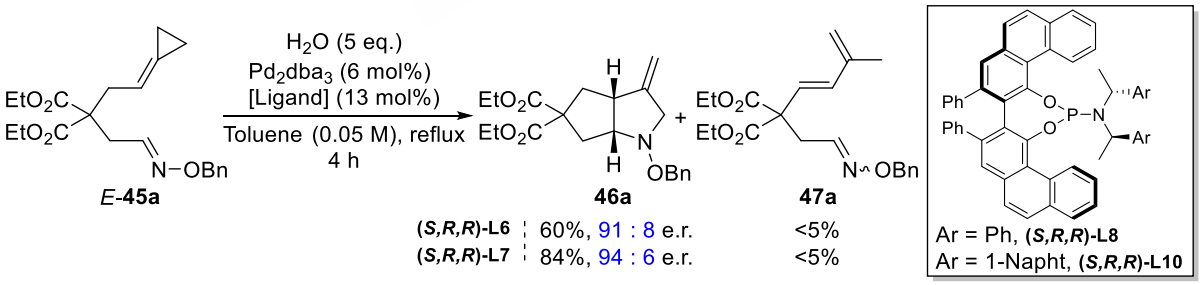

Scheme 100. Screening of chiral ligands for the enantioselective intramolecular cycloaddition with oximes.

[118] Complementary, we also checked the use of alternative solvents but none of them improves the results achieved with toluene (+5 equiv of water). For instance: 1,4-Dioxane (37%, 72% ee), *i*PrOH (40%, 78% ee), DMSO (70%, 76% ee), DMF (73%, 82% ee), NMP (65%, 86% ee) and DMA (60%, 88% ee.).

We next evaluated the reactivity of the Z and E isomers of **45**a, separately. As expected from the results of the racemic reaction, the *E* isomer reacts more efficiently, leading to **46a** in a 85% yield and an outstanding 88% ee The use of the *Z* isomer allows to afford the cyclic product in a moderate 60% yield and surprisingly, in this case, the formation of the opposite enantiomer of **46a** was favored, showing an -40% ee (Scheme 101).

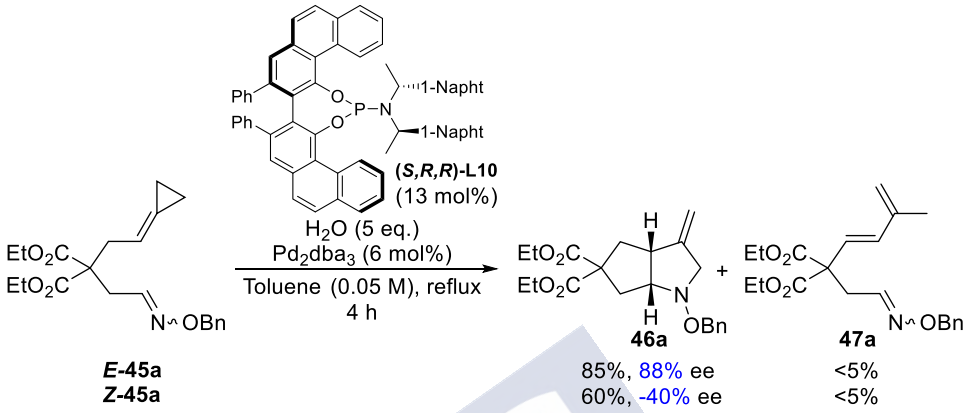

Scheme 101. Evaluation of enantioselective reaction with pure isomers.

At this point, we re-evaluated the reactivity of precursor **45b** bearing a methyl group at the oxime. To our delight, the reaction efficiently provided the cycloadduct **46b** in an excellent 90% yield and 94% ee (Scheme 102).

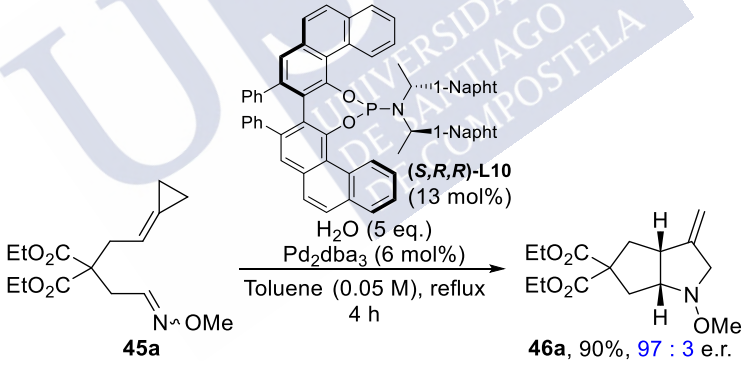

Scheme 102. Optimized reaction for substrate **45b** (OMe).

The absolute configuration of the cycloadduct was determined by the transforming **46a** into the diol **46aa** by treatment with $LiAlH_4$ (70% yield, Scheme 103). Crystallization of this compound from a heptane/dichloromethane mixture, and subsequent X-ray analysis showed a (3a*S*, 6a*S*) configuration at the ring fusion, similar to the observed in the enantioselective cycloaddition with alkenes.[119]

[119] F. Verdugo, L. Villarino, J. Durán, M. Gulías, J. L. Mascareñas, F. López, *ACS Catal.* **2018**, *8*, 6100–6105.

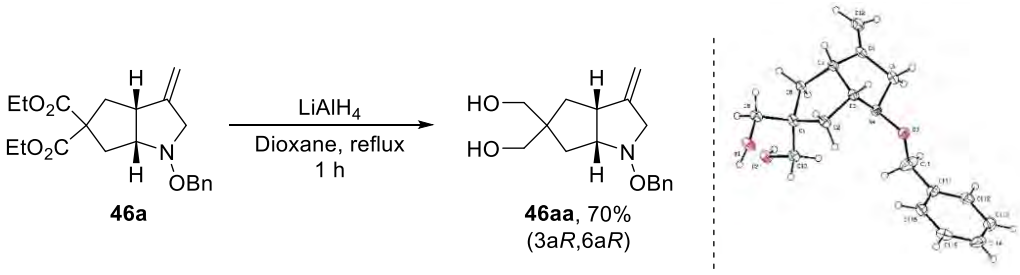

Scheme 103. Reduction of **46a** to the diol **46aa** and crystal structure of **46aa**.

3.1.4. Scope of the Pd-catalyzed enantioselective (3+2) cycloaddition between ACPs and oxime ethers

With the optimized conditions for the enantioselective reaction in hand, we further investigated the scope of the processes using other precursors (Scheme 104). Unfortunately, we observed similar reactivity problems than with the racemic series. Substrates like **45c**, with an extra methylene unit, ketoxime **45d**, or substrates with different connecting tethers (**45e, 45f,** and **45g**) failed to give the desired cycloadducts, providing complex mixtures of products. Moreover, carrying out the reactions at higher temperatures (130º or 150 ºC) only raised the conversion, but again the desired product was not formed.

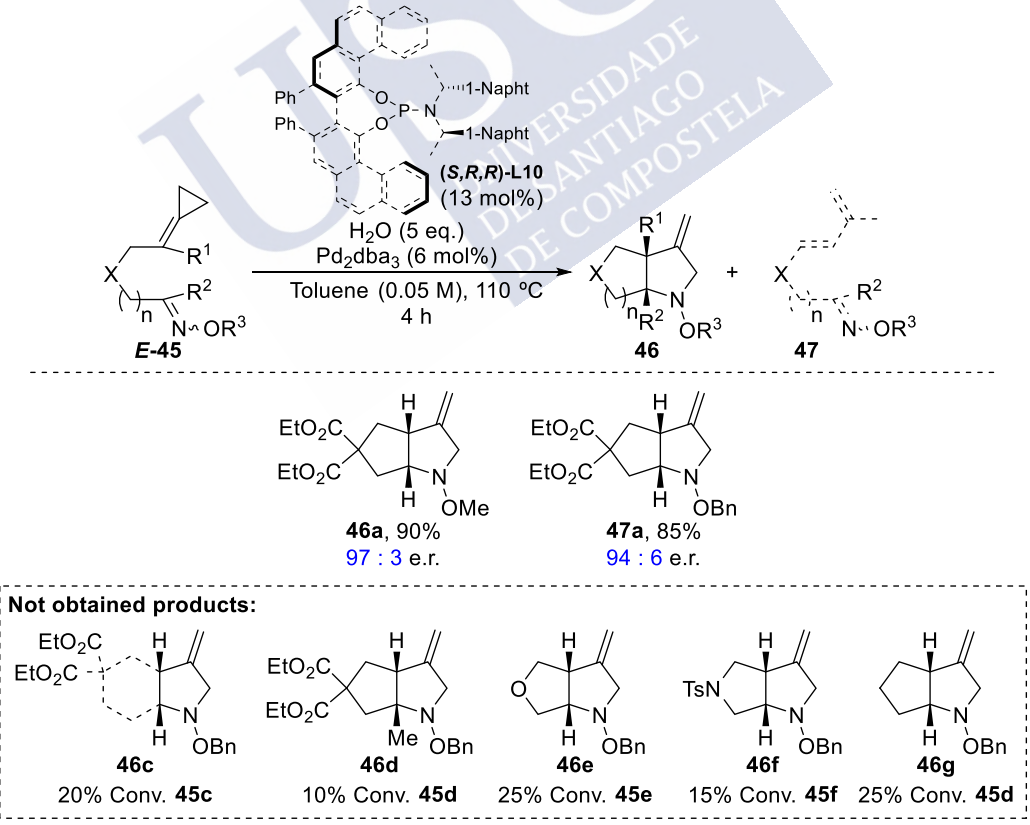

Scheme 104. Reaction scope of the intramolecular (3+2) cycloaddition with oximes.

We were intrigued by the severe limitation of the scope. Thus, we envisioned that increasing the oxime reactivity might favor the reaction. To do this, we ran the reaction in presence of several Lewis and Brønsted acid additives (0.5 eq.). However, under these conditions we observed a drastic decrease in the conversion (Table 14).

Table 14. Screening of Lewis and Brønsted acids.

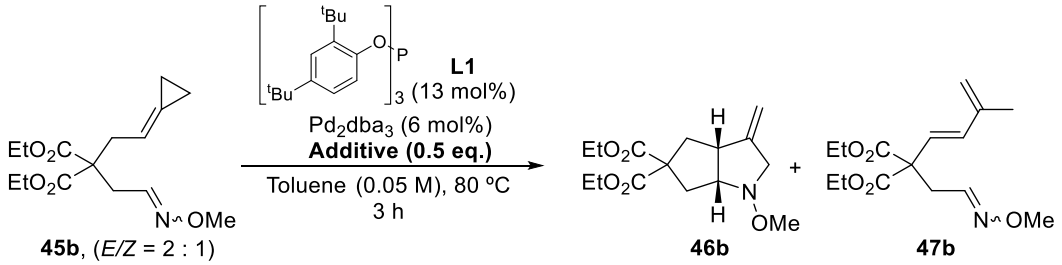

Entry	Additive	Conv. (%)[b]	46b (%)[b]	46b (%)[b]
1	-	75	50	20
2	Thiourea	45	-	-
3	*p*-TsOH·H_2O	20	-	-
4	(*R*)-CPA	12	-	12
5	$ZnCl_2$·(THF)	5	-	-
6	$In(OTf)_3$	33	-	-
7	$B(OMe)_3$	15	-	10

[a] *Reaction conditions*: **45b** (0.15 mmol), Pd_2dba_3 (6 mol%), **L1** (13 mol%), 50 mol% Additive, freshly distilled toluene [0.05 M], reflux. [b] Determined by ^{1}H-NMR using 1,3,5-trimethoxybenzene as internal standard.

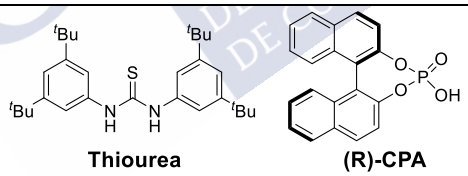

3.1.5. Mechanistic studies

Considering that the (*E*/*Z*) ratio of the starting materials is relevant for the efficiency of the reaction, we studied the isomerization properties of the oxime ethers (Scheme 105). When a sample enriched with the *E* isomer was stirred in $CDCl_3$ for 16 hours, we observed an equilibration to a mixture of isomers (*E*/*Z*) = 1.1 : 1, likely due to the traces of hydrogen chloride that was are present in deuterated chloroform. This demonstrates that these oximes are highly sensitive to the presence of acids.

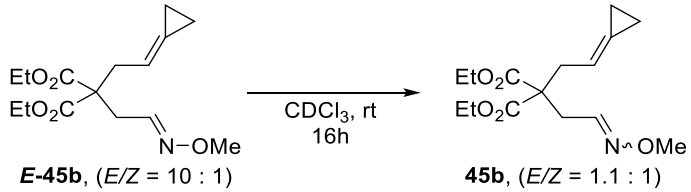

Scheme 105. Isomerization experiment of *E* isomer.

We therefore questioned whether this isomerization could occur during the reaction. Thus, we submitted a sample of ***E*-13a** under reaction conditions for 1h. Interestingly, the recovered starting material showed the same (*E/Z*) ratio, suggesting that the substrate ***E*-13a** doesn´t isomerize during the reaction.

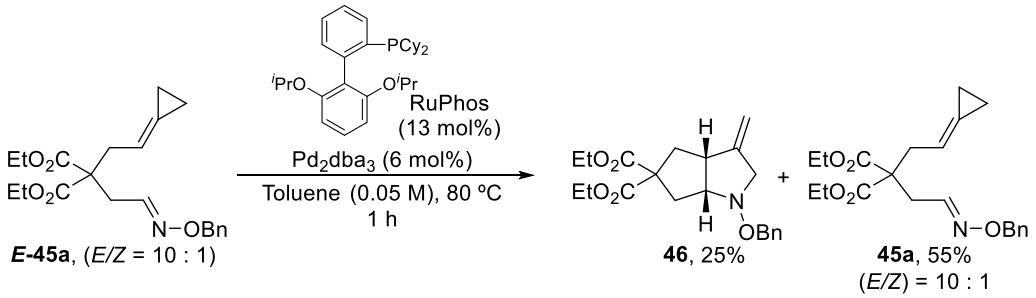

Scheme 106. Evaluation of isomerization of *E* isomer under reaction conditions.

Considering the formation of an unexpected diene **47`,** we carried out experiments using a deuterium labeled substrate ***E*-45b-*d*$_4$** to gain a deeper understanding of the process.[120] As can be deduced from scheme 107, the reaction promoted by a $Pd_2dba_3$/RuPhos provided a mixture of **46b-*d*$_4$,** (57% yield) and **47`-*d*$_4$** (33%).

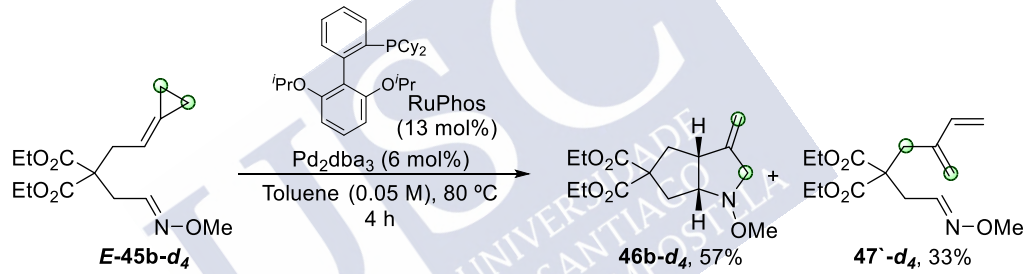

Scheme 107. Deuterium labeling experiment.

Based on these experimental results and precedents of similar reactions, we propose a reaction mechanism involving an initial insertion of the Pd into de distal C-C bond of the ACP leading to the metallacyclobutane **A**, which can isomerize to the intermediate **B**. This intermediate would coordinate the pendant C=N bond and evolve through a carbometallation towards the palladacyclohexane **C**, with a *syn* stereochemistry. As an alternative pathway, intermediate **A** could evolve directly to **C** through a metalloene rearrangement. This common intermediate **V** can produce **46** after reductive elimination. The formation of **47**, observed when **L1** is used as ligand, can be explained starting from the metallacyclobutane intermediate **B**, which could evolve through a *β*-hydride elimination towards the palladium hydride **B-I** which finally produce diene **47**. This type of competitive pathway has been previously observed in related ACP cycloadditions.[121]

On the other hand, to the best of our knowledge, the generation of side products of type **47`** is completely unprecedented in any type of metal-promoted ACP cycloaddition**.** Based on the

[120] Carried out by Ricardo Rodiño Balboa.
[121] (a) M. Gulias, R. Garcia, a Delgado, L. Castedo, J. L. Mascarenas, *J. Am. Chem. Soc.* **2006**, *128*, 384–385. (b) R. Garcia-Fandino, M. Gulias, J. L. Mascarenas, D. J. Cardenas, *Dalt. Trans.* **2012**, *41*, 9468–9481.

previously shown deuterium labeling experiments, we can preliminary propose a metalloene rearrangement (**A-I**) that could proceed in an intramolecular (**Path 1**) or intermolecular (**Path 2**) manner, as depicted in scheme 108. Nonetheless, further experiments and computational studies are needed to fully unveil the real nature of these reaction intermediates.

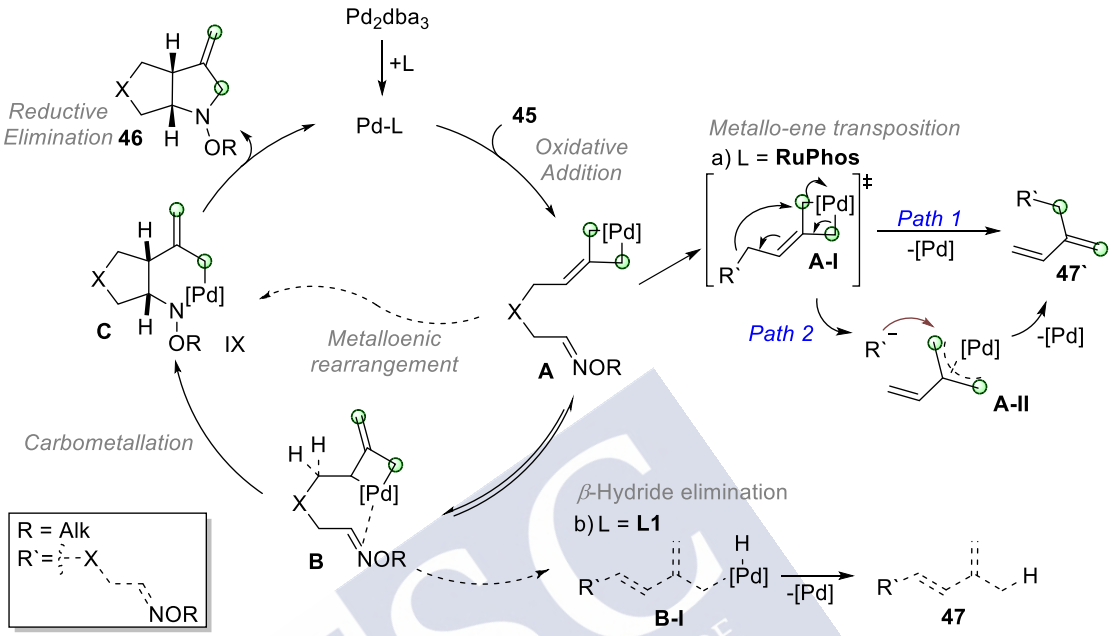

Scheme 108. General reaction mechanism proposed for the (3+2) cycloaddition with oximes.

3.2. Metal-catalyzed (3+2) cycloadditions between ACPs and carbonyls: Access to five-membered oxacycles

To explore the feasibility of carrying out an oxygenated version of the intramolecular (3+2) annulation, we selected the aldehyde **48a** and the corresponding methyl ketone **49a** as model substrates. Aldehyde **48a** was synthesized following reported procedures (Scheme 109).[122]

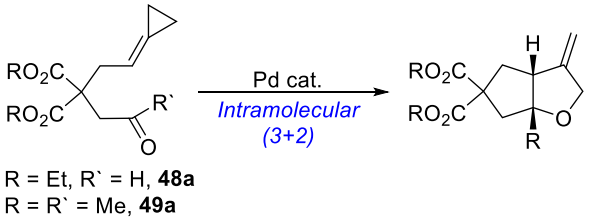

Scheme 109. Models for the study of oxygenated (3+2).

3.2.1. Intramolecular annulations

Intramolecular (3+2) cycloaddition between ACPs and aldehydes

We first tried the optimal reaction conditions used in the (3+2) cycloaddition between ACPs and alkenes, consisting of a 6 mol% Pd_2dba_3 and 24 mol% of phosphite **L1**.[53] Unfortunately, despite observing full conversion, the desired cycloadduct was not detected by ^{1}H-NMR (entry 1). We also tested the conditions described by Yamamoto on intermolecular heterocycloadditions with aldehydes,[102] which involve the use of $Pd(PPh_3)_4$ and different phosphine oxides. Interestingly, in both cases, the desired cycloadduct was formed, but in very poor yields (entry 2 and 3). In order to further improve the yield, we tested the phosphoramidite **L2,** which has been previously used in the (4+3) cycloadditions of ACPs and dienes. We observed full conversion after 3 hours, and isolated the desired compound **50a** in 20% yield**,** together with a 5% yield of the isomerized byproduct. The *cis* configuration at the ring fusion could be confirmed through nOe experiments (Table 15).

Considering that the lack of efficiency could be due to a difficult C-O reductive elimination, we focused our attention on bulky biaryl phosphines ligands that had been shown effective in carbon-heteroatom bond forming reactions involving Pd(II)-Pd(0) reductive eliminations. Gratifyingly, the reaction using RuPhos as ligand provided **50a** as the only product detected, albeit in a moderate yield (45%, entry 5).

[122] M. Gulias, R. Garcia, a Delgado, L. Castedo, J. L. Mascarenas, *J. Am. Chem. Soc.* **2006**, *128*, 384–385.

Table 15. Screening of ligands for the intramolecular cycloaddition with aldehydes.

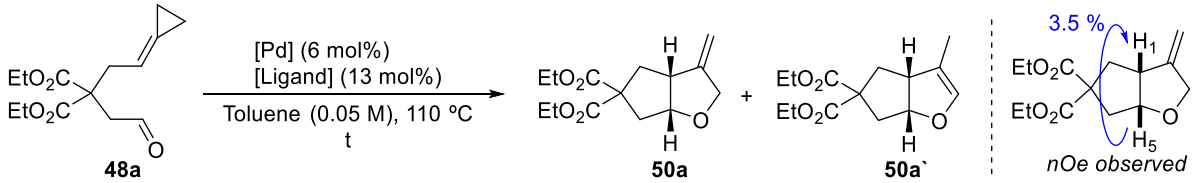

Entry	[Pd]	Ligand	t (h)[b]	Conv. (%)[c]	50a (%)[c]	50a` (%)[c]
1[d]	Pd_2dba_3	**L1**	3	100	-	-
2	$Pd(PPh_3)_4$	$P(O)Bu_3$	8	30	10	-
3	$Pd(PPh_3)_4$	$P(O)Ph_3$	8	35	25	-
4	Pd_2dba_3	**L2**	3	100	20	5
5	Pd_2dba_3	RuPhos	2	100	45	<5

[a] *Reaction conditions*: **48a** (0.15 mmol), Pd_2dba_3 (6 mol%), [Ligand] (13 mol%), freshly distilled toluene [0.05 M], reflux. [b] Full conversion of **48a** was observed at the specified time, unless otherwise noted. [c] Determined by ^{1}H-NMR using 1,3,5-trimethoxybenzene as internal standard. [d] Using 24 mol% of **L1**.

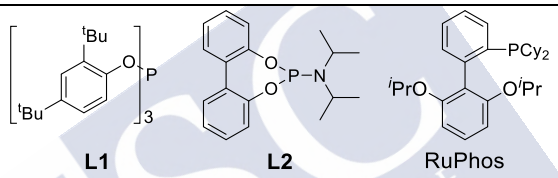

Interestingly, heating at 110 ºC was necessary to achieve full conversions after 3 h (Table 16, entry 1 and 2). We were pleased to observe that with XPhos, under otherwise identical reaction conditions, the desired cycloadduct was produced in a good 71% yield (entry 3). The ligands Brettphos or tBuBrettphos led to the slightly better yields (75% and 71%, entries 4 and 5).

Table 16. Screening of Buchwald ligands for the intramolecular cycloaddition with aldehydes.

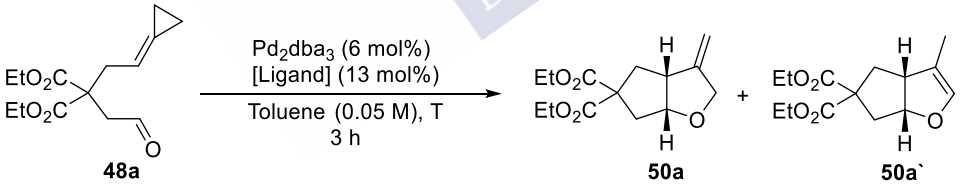

Entry	Ligand	T (°C)	Conv. (%)[b]	50a (%)[b]	50a` (%)[b]
1	RuPhos	100	85	30	<5
2	RuPhos	80	35	0	<5
3	XPhos	110	100	71	<5
4	BrettPhos	110	100	75	<5
5	tBuBrettphos	110	100	71	8

[a] *Reaction conditions*: **48a** (0.15 mmol), Pd_2dba_3 (6 mol%), [Ligand] (13 mol%), freshly distilled toluene [0.05 M], reflux. [b] Determined by ^{1}H-NMR using 1,3,5-trimethoxybenzene as internal standard.

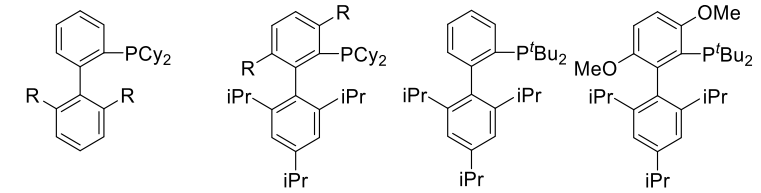

We next investigated the influence of the solvent in the cycloaddition (Table 17). Trifluorotoluene showed an equally good performance in comparison with toluene (entry 1 *vs* 2), whereas the use of heptane also allowed an efficient cycloaddition, albeit in a slightly lower 70% yield (entry 3). Interestingly, the use of 1,4-dioxane, which was the solvent of choice for many cycloadditions of alkylidenecyclopropanes, led to lower yields of mixtures between **50a** (36% yield) and the alkene isomerized product **50a`** (15% yield, entry 4). Finally, the reaction did not take place when 1,2-dichloroethane was employed (entry 5).

Table 17. Screening of solvents for the intramolecular cycloaddition with aldehydes.

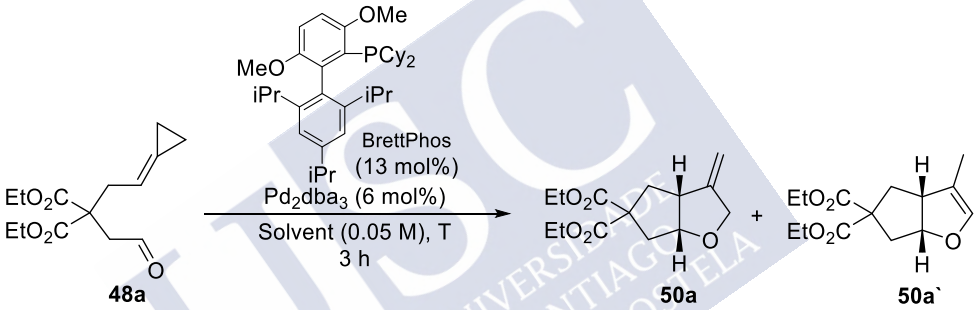

Entry	Ligand	T (°C)	Conv. (%)[b]	50a (%)[b]	50a` (%)[b]
1	PhMe	110	100	75	<5
2	$PhCF_3$	102	100	77	<5
3	Heptane	98	100	70	<5
4	Dioxane	101	100	36	15
5	1,2-Dichloroethane	83	20	0	<5

[a] *Reaction conditions*: **48a** (0.15 mmol), Pd_2dba_3 (6 mol%), BrettPhos (13 mol%), dry solvent [0.05 M], reflux. [b] Determined by ^{1}H-NMR using 1,3,5-trimethoxybenzene as internal standard.

We also evaluated the type of palladium precatalyst used in the reaction (Table 18). When CpPd(η^3-1-PhC_3H_4 was used, a significant decrease in the reaction yield was observed (entry 2). We repeated this particular reaction in the presence of an 18 mol% of dba, and the yield remained invariable, indicating that the poorer performance of CpPd(η^3-1-PhC_3H_4) is not due to the lack of dba in the media (entry 3). The use of other precatalysts such as $[PdCl(C_3H_5)]_2$ or $Pd(PPh_3)_4$ also provided the desired product, but with poorer yields and lower conversions than Pd_2dba_3 (entry 4 and 5).

Table 18. Screening of precatalysts for the intramolecular cycloaddition with aldehydes.

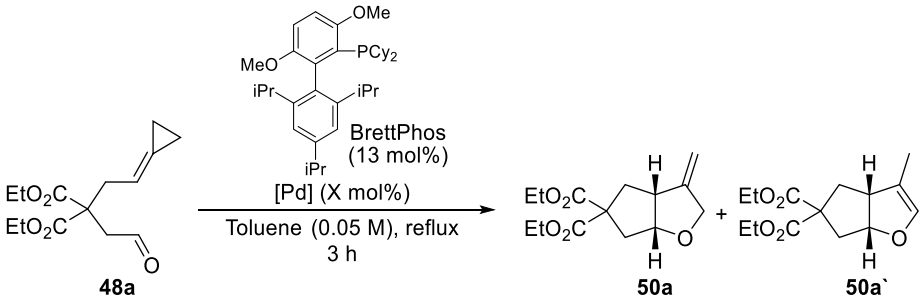

Entry	[Pd] (mol%)	Conv. (%)[b]	50a (%)[b]	50a` (%)[b]
1	Pd_2dba_3 (6)	100	75	<5
2	$CpPd(\eta^3\text{-}1\text{-}PhC_3H_4)$ (12)	100	54	<5
3[c]	$CpPd(\eta^3\text{-}1\text{-}PhC_3H_4)$ (12)	100	58	<5
4	$[PdCl(C_3H_5)]_2$ (6)	60	10	<5
5	$Pd(PPh_3)_4$ (6)	60	30	<5

[a] *Reaction conditions*: **48a** (0.15 mmol), [Pd] (X mol%), BrettPhos (13 mol%), freshly distilled toluene [0.05 M], reflux. [b] Determined by ^{1}H-NMR using 1,3,5-trimethoxybenzene as internal standard. [c] Carried out adding an 18 mol% of dba.

Finally, we explored the possibility of reducing the catalyst loading. Thus, we found that using only a 3 mol% of Pd_2dba_3 and a 7 mol% of BrettPhos, the reaction proceeds with the same efficiency, leading to **50a** in a good 74% yield (Scheme 110).

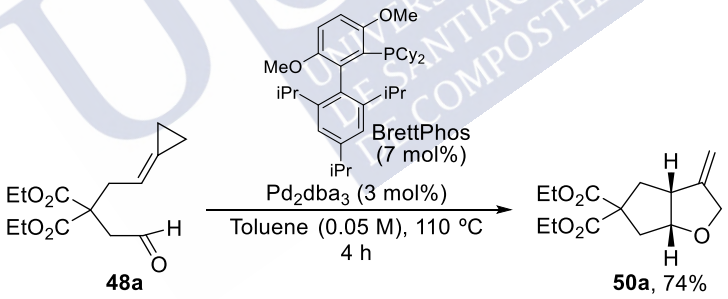

Scheme 110. Catalysis using 1 mol% of Pd_2dba_3.

To analyze the scope of the method, we synthesized several cycloaddition precursors with different structural features, indicated in figure 17.

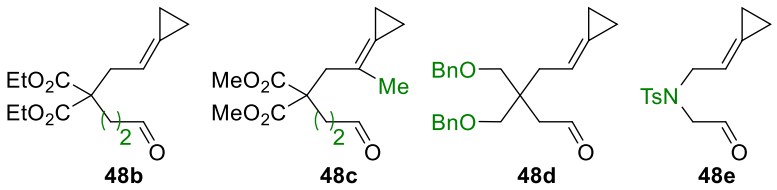

Figure 17. Aldehydes synthesized for the scope evaluation.

The synthesis of substrates **48b** and **48c,** which exhibit extended tethers, was carried out through a Michael addition of the corresponding malonates **22** and **24** to acrolein, furnishing the aldehydes **48b** in 63% yield and **48c** in 42% yield (Scheme 111).

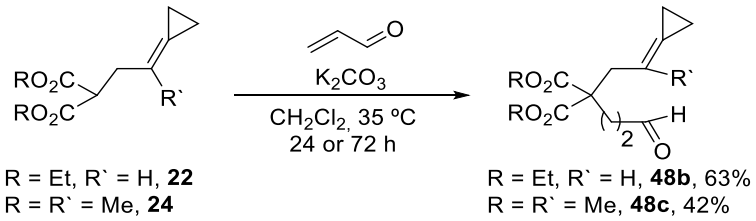

Scheme 111. Synthesis of substrate **48b** and **48c**.

The aldehyde **48d** was synthesized from malonate **52**, upon reduction with $LiAlH_4$, and benzylation to yield the acetal **53** in 70% yield (two steps). Subsequent hydrolysis under acidic conditions led to the desired cycloaddition precursor in 50% yield (Scheme 112).

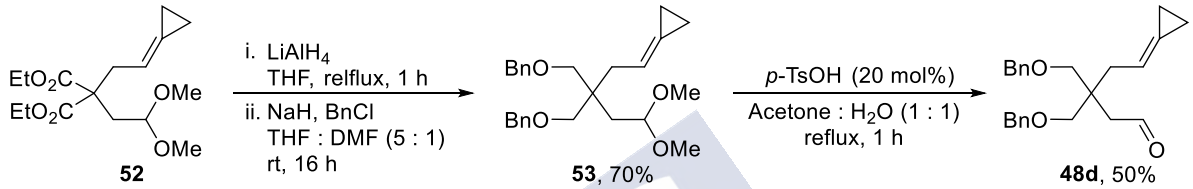

Scheme 112. Synthesis of substrate **48d**.

The N-Tosyl analogue **48e** was easily synthesized by treatment of **54** with NaH and further addition of 2-bromo-1,1-dimethoxyethane, affording the acetal **55** in a 75% yield. Finally, the hydrolysis of this compound using *p*-TsOH generated the aldehyde **48e** in an 80% yield (Scheme 113).

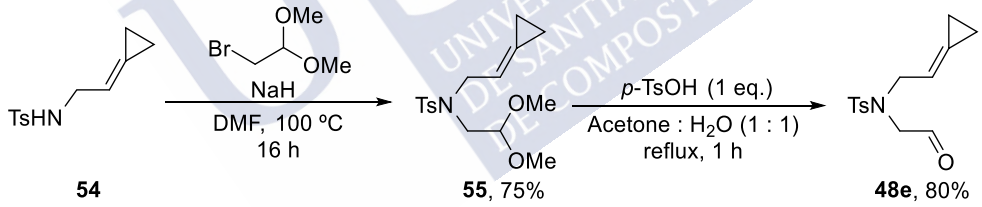

Scheme 113. Synthesis of substrate **48e**.

With these different substrates in hand, we evaluated the scope of the aldehyde-containing substrates (Scheme 114). Gratifyingly, the cyclohexane-fused tetrahydrofuran **50b** was obtained in an excellent 90% yield, as a *cis:trans* isomeric mixture (d.r = 3.3 : 1). The annulation could also be carried out with an aldehyde precursor that bears a methyl group at the internal alkene position of the ACP, to afford **50c,** which bears a quaternary stereocenter at the ring fusion, in a 86% (d.r = 1 : 1). Related to others 5-5 bicyclic systems, the cycloaddition is not limited to substrates bearing *gem*-diesters at the connecting tether, so we could obtain tetrahydrofurans like **50d** (75% yield), or the pyrrolidine-fused derivative **50e** (60%) in a fully diastereoselective manner.

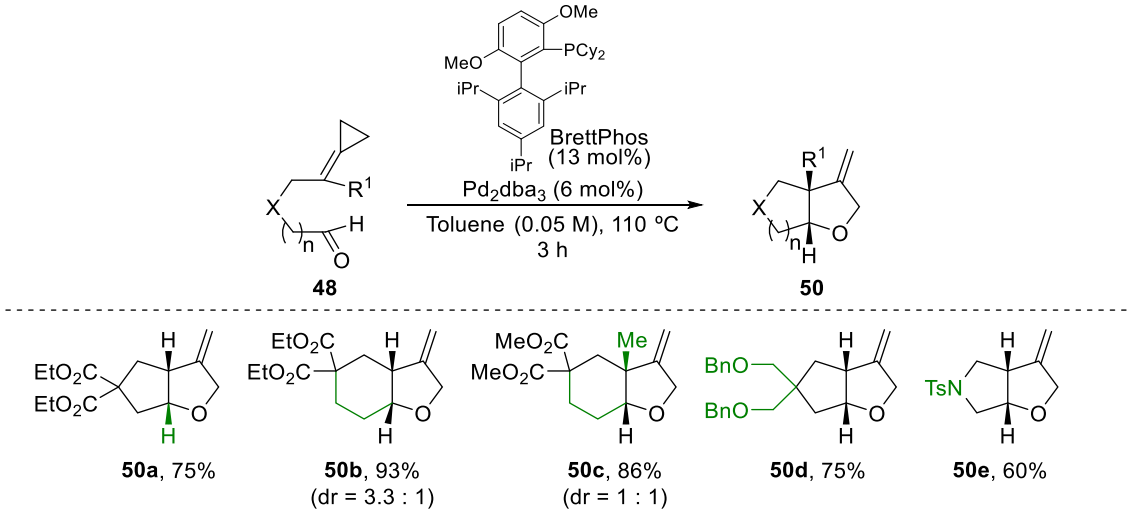

Scheme 114. Reaction scope of the intramolecular (3+2) cycloaddition with aldehydes.

Intramolecular (3+2) cycloaddition between ACPs and ketones

Based on the good results obtained with aldehydes, we moved to explore the viability of cycloadditions with ketones, instead of aldehydes (Scheme 115). This transformation is more challenging due the reduce electrophilicity of ketones and the higher steric hindrance of the system. To carry out this study, we synthesized the precursor **49a** in two steps consisting of an alkylation of dimethyl malonate with 2-chloroacetone and a subsequent Tsuji-Trost reaction between the obtained product (**56a**, 60% yield) and the tosylate **21**, a reaction that proceeded in a good 80% yield.

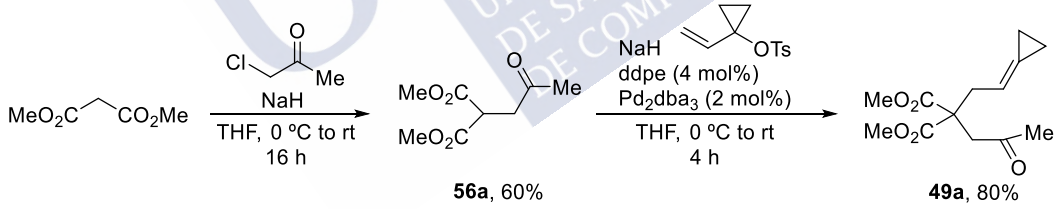

Scheme 115. Synthesis of model substrate **49a**.

We first tried the optimal conditions previously found for aldehyde-based precursors. To our delight, the catalyst generated from 6 mol% of Pd_2dba_3 and 13 mol% of Brettphos efficiently promoted the cycloaddition in refluxing toluene, so that the desired tetrahydrofuran **51a** was isolated in a good 65% yield. nOe experiments confirmed the *syn* configuration at the ring fusion, similar to the observed for aldehyde series (Scheme 116). In an attempt to further improve the reaction yield, we evaluated other related Buchwald´s biaryl phosphines. Ligands SPhos and XPhos promoted the reaction with a similar efficiency than Brettphos, whereas the use of tBuXPhos led to a significant improvement of the yield, up to 80%. interestingly, RuPhos, which provided a moderate performance for aldehyde-bearing substrates led to the product in an excellent 90% yield. Importantly, the reaction can be carried out with the same efficiency and yield, using just 1 mol% of Pd_2dba_3 and 3 mol% of Ruphos.

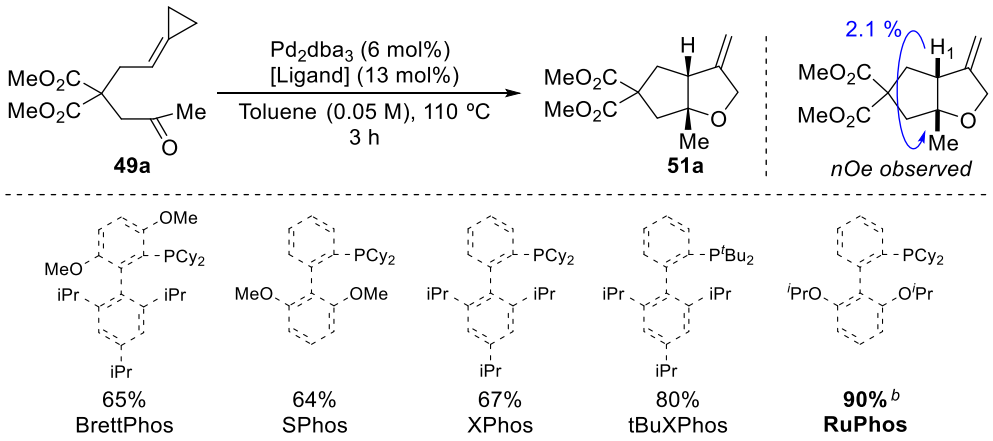

Scheme 116. Screening of different Buchwald phosphines.

Therefore, we evaluated the scope of the reaction using Pd_2dba_3 (6 mol%) and RuPhos (13 mol%) as the optimal catalyst. We synthesized several cycloaddition precursors bearing different structural features, as indicated in the figure 18. In order to evaluate the diastereoselectivity of the reaction, a substrate which exhibit a chiral center was also synthesized (**49j**).

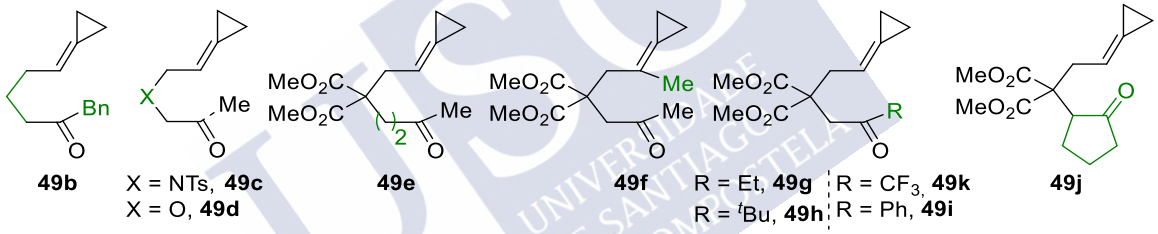

Figure 18. Substrates to evaluate the reaction scope.

Using the same route than for the model substrate **49a**, the synthesis of several ketones begun with alkylation of dimethylmalonate with 2-bromo- or 2-chloro-ketones, leading to the corresponding ketones in moderate yields. The second alkylation, with the tosylate **21**, was carried using these ketones under Tsuji-Trost conditions, and afforded the desired ACP precursors bearing an ethyl, *t*-butyl or a phenyl ketone (Scheme 117).

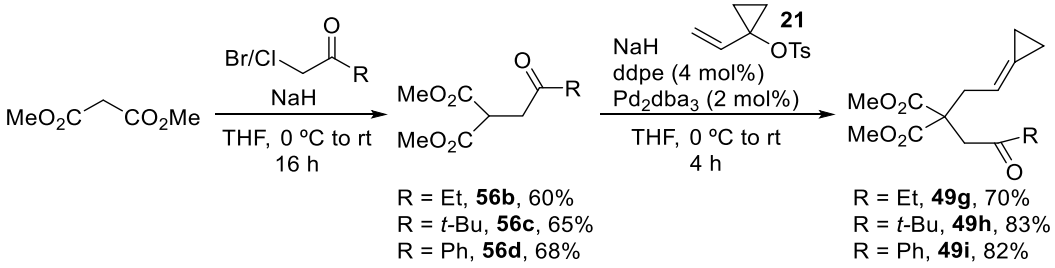

Scheme 117. Synthesis of substrates **49(g-i)**.

In a similar manner, a substrate exhibiting a cyclic ketone **49j** was also synthesized using the malonate **56e** (Scheme 118). On the other hand, the precursors with heteroatoms in the connecting tether were rapidly synthesized by the Pd-catalyzed allylic alkylation of tosylate

21. The N-Ts tethered compound **49c** was obtained in 84% yield, whereas the oxygenated analogue **49d**, was obtained in a modest 30% yield.

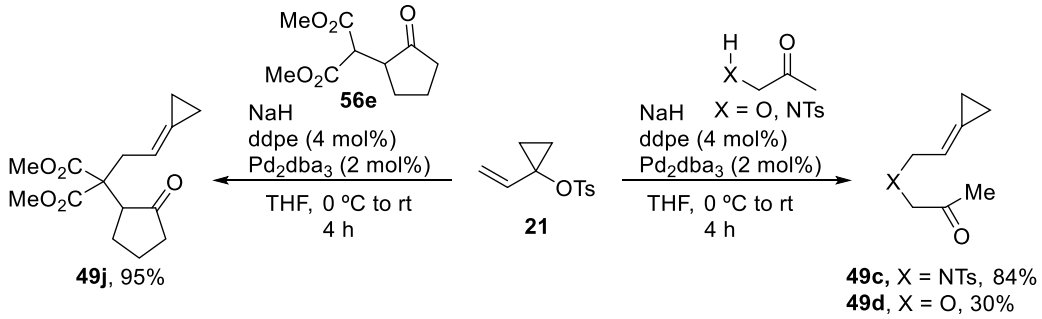

Scheme 118. Synthesis of substrates **49j**, **49c** and **49d**.

On the other hand, the substrate bearing a methyl group at the internal position of the ACP (**49f**) was made from the ketone **56a** by a Pd-catalyzed allylic alkylation using the ether **23** as surrogate of the commonly used tosylate **21** (Scheme 119).

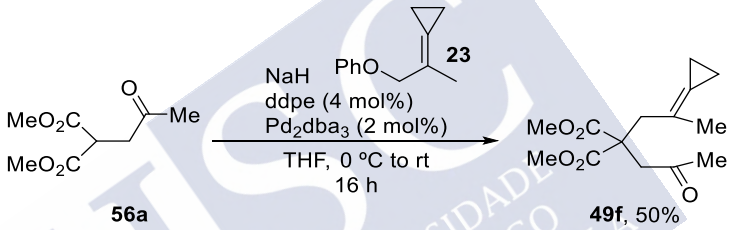

Scheme 119. Synthesis of substrate **49f**.

To evaluate the effect of having electron deficient ketones, trifluoromethyl ketone **49k** was synthesized in a two-step sequence consisting of a first addition of "CF_3-"to the aldehyde **48a** (66% yield) and a subsequent oxidation of the resulting alcohol (50% yield, Scheme 120).

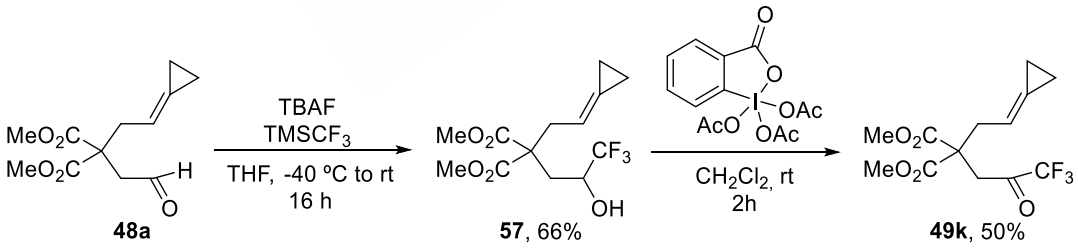

Scheme 120. Synthesis of substrate **49k**.

The ketone **49e** which exhibits an additional methylene moiety at the connecting tether was made using standard protocols previously described for aldehyde precursors, as indicated in scheme 121.

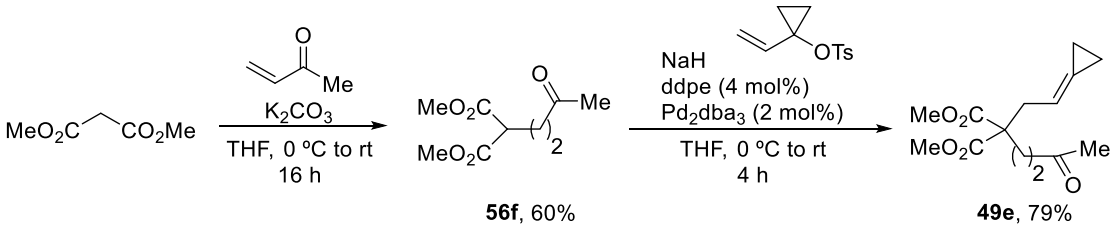

Scheme 121. Synthesis of substrate **49e**.

Finally, we prepared a precursor containing a non-functionalized carbonated tether, in 4 steps from δ-valerolactone. First, the Weinreb amide **58** resulting from the aminolysis of the lactone was submitted to a Swern oxidation, followed by a Wittig reaction with cyclopropyltriphenylphosphonium bromide to afford the alkylidenecyclopropane **59** in 25% overall yield. Treatment of this Weinreb amide with benzylmagesiumbromide produced the ketone **49b**, which was isolated in 75% yield (Scheme 122).

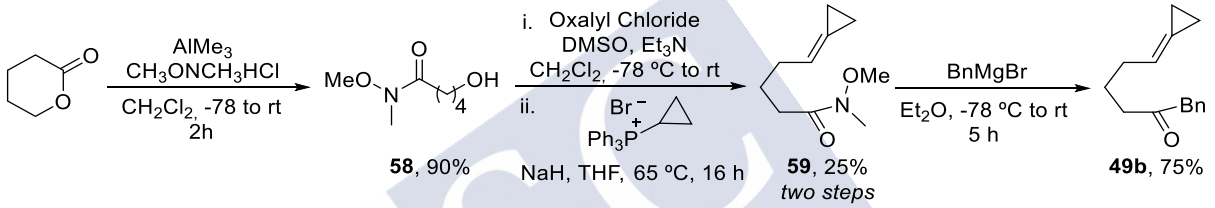

Scheme 122. Synthesis of substrates **49b**.

The cycloaddition reaction showed an excellent scope. As can be seen in scheme 123, a variety of five-membered fused tetrahydrofuranes were obtained in good to excellent yields. For instance, fused-cyclopentane (**51b**, 40%), pyrrolidine (**51c**, 80%) or tetrahydrofuran (**51d**, 90%) derivative were obtained with complete diastereoselectivity and good to excellent yields. The length of the connecting tether can also be increased in one-methylene unit, to produce the hexane-fused tetrahydrofuran **51e** with an excellent 94% yield (*cis:trans* ratio 10:1). The related ketone precursor bearing a methyl-substituted ACP also participated in the cycloaddition to deliver a fused-tetrahydrofuran with two quaternary centers at the fusion (**51f**). Importantly, the intramolecular cycloaddition is not limited to methyl ketones. Related, ethyl , benzyl, and even a t-butyl ketone participated in the cycloadditions providing the adducts in moderate to good yields (**51b**, **51h**, 40 – 90% yield). Moreover, a phenyl ketone also provides a good yield of the corresponding product (**51i**, 60%). We also tested the cycloaddition of a substrate **49j** bearing the ACP tethered to a cyclopentanone moiety, delivering the tricyclic adduct **51j**, which holds three consecutive stereocenters, in excellent yield and complete diastereoselectivity. Unfortunately, when the trifluoromethylated substrate **49k** was tested, we observed an immediate formation of a black precipitate (palladium black), recovering the staring material.

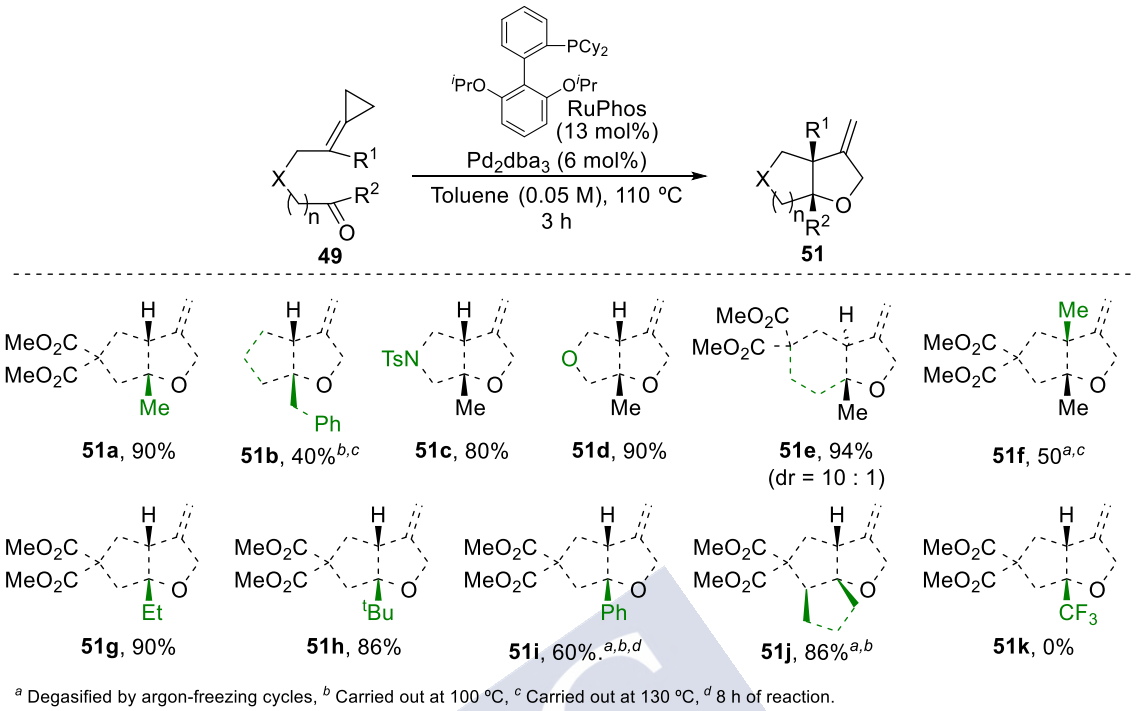

[a] Degasified by argon-freezing cycles, [b] Carried out at 100 °C, [c] Carried out at 130 °C, [d] 8 h of reaction.

Scheme 123. Reaction scope of the intramolecular (3+2) cycloaddition with ketones.

In all cases, NMR experiments were carried out to determine the relative configuration of cycloadducts (nOe and NOESY). Moreover, compounds **51f**, **51h** and **51j** are solids that could be crystallized from heptane/CH_2Cl_2 mixtures. Their structures were further determined by X-ray crystallography analysis (Figure 19).

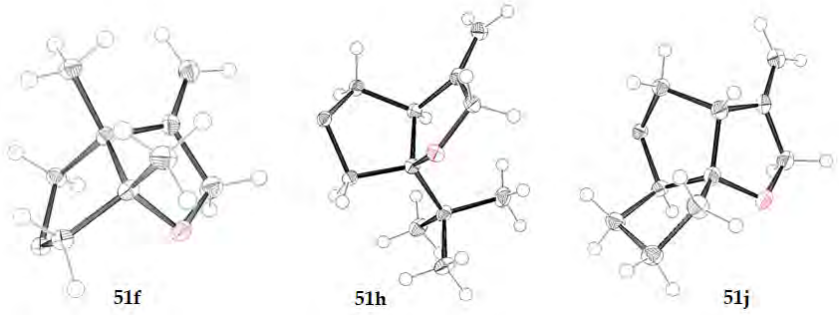

Figure 19. *Structure of **51a**, **51f** and **51j** obtained by X-ray crystallography.*

Based on the previous studies on TMC (3+2) cycloadditions between ACPs and C-C unsaturated bonds, out initial mechanistic hypothesis consists of the oxidative addition of Pd the distal C-C bond of the cyclopropane to give a metallacyclobutane such as **A** (Scheme 124). From this intermediate, two possibilities can be envisioned. First, **A** would evolve through a Pd-TMM type transition state towards its *exo*-methylene isomer **B**, which can evolve through a carbometallation to provide the oxapalladacyclohexane intermediate **C**. The second alternative would involve the direct evolution from metallacyclobutane **A** towards the intermediate **C** through a metalloenic rearrangement, a pathway that has been previously suggested for the intramolecular (3+2) cycloaddition between ACPs and electronically-

activated alkenes.[52,102] To shed light on the viability of these pathways as well as on the nature of the intermediate species of type **C`**, the PhD student from our group Ricardo Rodiño, carried out preliminary DFT calculations using a model system consisting of a methyl-ketone containing ACP (R = Me, Scheme 124) and PH_3 as ligand. The results suggest that the pathway that involves the metalloene rearrangement is energetically favored. Moreover, these theoretical results also indicate that both types of isomers with π-allyl-Pd complex **C`** and the σ- allyl Od complex **C** are feasible, but the reductive elimination occurs from the π-allyl species with a significantly lower energy barrier. Nonetheless, these studies are still under development, and the final conclusions will be further reported by Ricardo Rodiño.

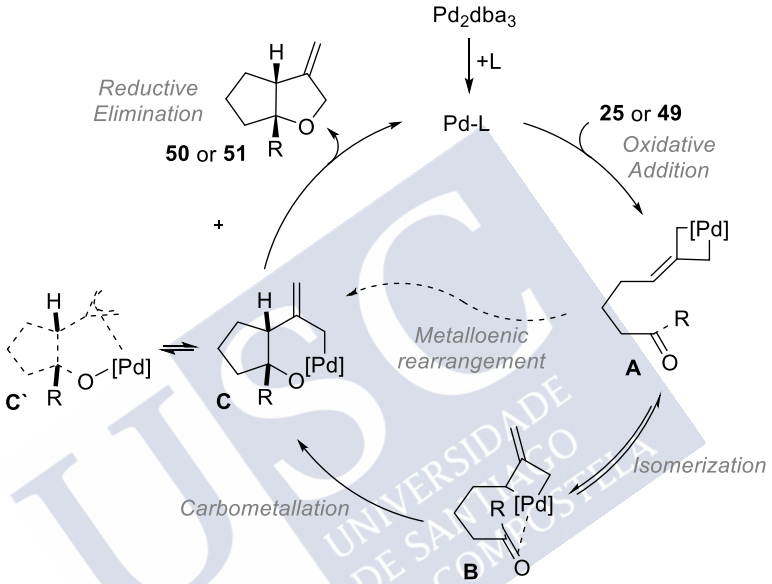

Scheme 124. General reaction mechanism proposed for the (3+2) cycloaddition reactions.

We next investigated the synthetic potential of these tetrahydrofurans. Using the adduct **51a** as model adduct, we found that its exocyclic methylene can be easily hydrogenated under rhodium catalysis, leading to **60a** as a 6:1 mixture of diastereoisomers, in an excellent 90% yield. The major isomer (drawn in scheme 125) could be independently isolated and its relative configuration was determined through nOe and 2D-NMR experiments

Moreover, the products can be manipulated by different oxidation reactions. Using ruthenium catalysis, the ketone **62a** was obtained in 60% yield, whereas the treatment of **51a** with an excess of CrO_3 and 3,5-dimethylpyrazole led to the synthetically appealing α-methylene γ-butyrolactone **63a** in 66% yield. The same reaction conditions applied to more complex products such as **51e** and **51j** worked with similar efficiency, leading to lactones **63e** and **63j** in 71 and 70% yield, respectively. Finally, treatment of **51a** with an excess of SeO_2 led to the double oxidized lactones **61a** (50% yield), together with its epimeric aldehyde (**61a`** , X% yield) and traces of and **63a,** under unoptimized conditions. The stereochemistry the bicyclic lactone **61a** was confirmed by nOe experiments, and that of the aldehyde **61a`** by X-ray crystallography (Figure 20). Curiously, the configuration of the carbon bearing a hydroxyl

group is opposite to that of the same carbon at the cycloadduct **61a**. This result would indicate that the allylic oxidation at the ring fusion is not diastereoselective.

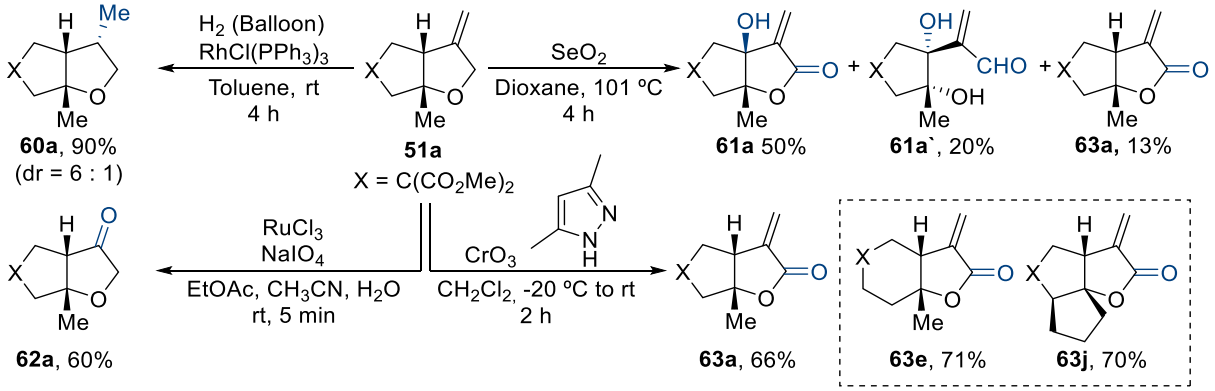

Scheme 125. Synthetic derivatization of **51a, 51e** and **51j**.

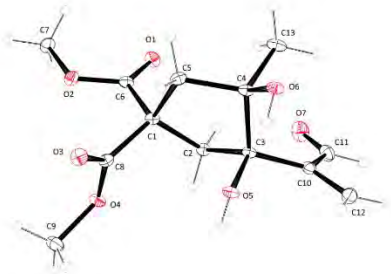

Figure 20. Structure of aldehyde **61a`** confirmed by X-ray crystallography.

In summary, we have developed a highly diastereoselective Pd-catalyzed intramolecular (3+2) between ACPs and aldehydes or ketones that delivers fused-bicyclic tetrahydrofurans. The appropriate selection of Pd ligands showed to be key to obtain good yields and selectivities. Moreover, several synthetically appealing modifications of the resulting fused-tetrahydrofurans were demonstrated, including the highly selective oxidation to α-methylene-γ-butyrolactones.

3.2.2. Intermolecular (3+2) cycloadditions with trifluoromethyl ketones

The exploration of the intermolecular reaction was carried out in collaboration with PhD student Eduardo Da Concepción (Scheme 126). At the outset, we selected the readily accessible alkylidenecyclopropane **65a** as the model cycloaddition precursor. This compound was synthesized in two steps consisting of the TBDPS monoprotection of ethyleneglycol and a subsequent Pd-catalyzed allylic etherification with the tosylate **21**. The desired alkylidenecyclopropane **65a** was obtained in an overall 72% yield (two steps).

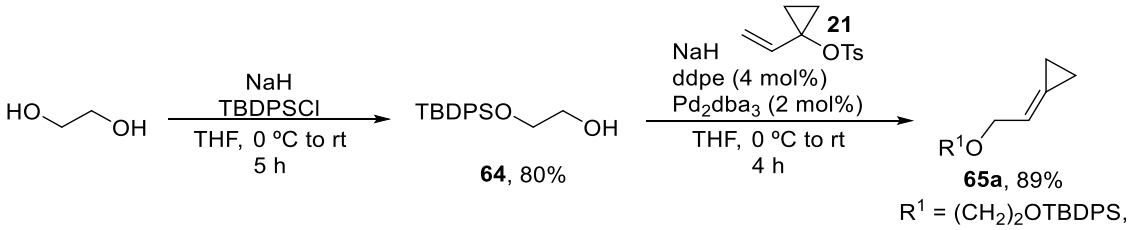

Scheme 126. Synthesis of substrate **65a**.

We first carried out a preliminary screening with the model ACP **65a** and several carbonyl partners (e.g. benzaldehyde, acetophenone, ethyl benzoate, benzoyl chloride, among others), using the optimal conditions previously found for the intramolecular (3+2) cycloadditions with carbonyls (Scheme 127). Generally, full conversion of the starting ACP was observed, albeit we did not detect signals of cycloadducts in the complex mixtures observed by NMR analysis of the crude reaction mixtures. However, we found that 2,2,2-trifluoroacetophenone react smoothly with **65a**, to produce the corresponding (3+2) cycloadducts **66a** and **66a'** in excellent overall yield, and with a diastereomeric ratio of 1.3:1. The major diastereoisomer was assigned by analogy with other cases (vide infra), and holds the CF_3 group and the α-hydrogen in *cis* disposition. Despite the requirement of a trifluoromethylated ketones might be seen as a limitation, the result is very appealing from a mechanistic perspective and also because these type of fluorinated THF derivatives are relevant in the field of drug discovery.[123]

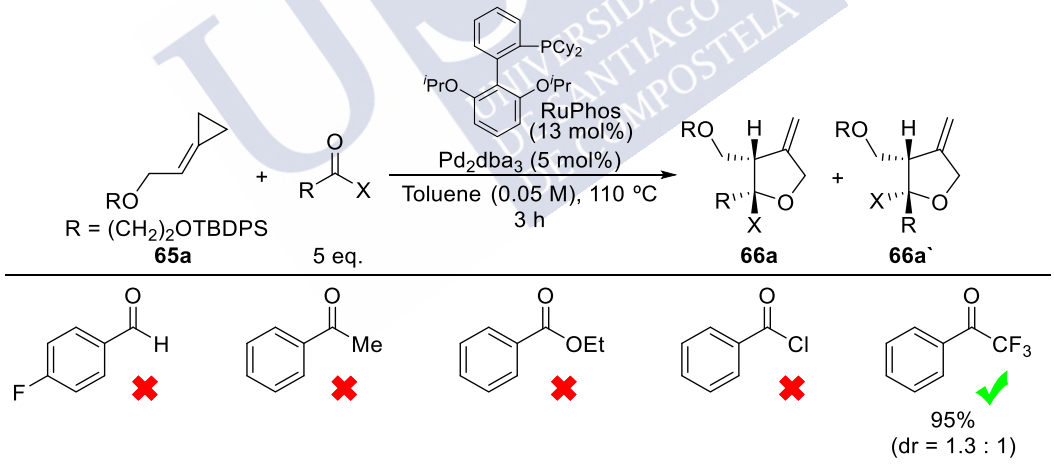

Scheme 127. Screening of carbonylic counterparts for the intermolecular reaction.

At this point, we evaluated different Buchwald ligands to check whether the diastereoselectivity could be improved. Unfortunately, despite the excellent overall yields observed in most cases, only moderate improvements of the diastereomeric ratio were observed (Scheme 128). The best ratio, of (1.7: 1) was obtained with tBuBrettphos. Nonetheless, subsequent optimization studies were carried out with **RuPhos,** due to its lower cost. Interestingly, with **RuPhos,** the catalytic load can be significantly decreased to a 2 mol%

[123] a) B. M. Trost, G. Mata, *Angew. Chem. Int. Ed.* **2018**, *57*, 12333-12337. (b) B. M. Trost, D. A. Bringley, *Angew. Chem. Int. Ed.* **2013**, *52*, 4466-4469.

Pd_2dba_3 and 5 mol% Ruphos, without losing efficiency, even when 2 eq. of 2,2,2-trifluoroacetophenone was employed.

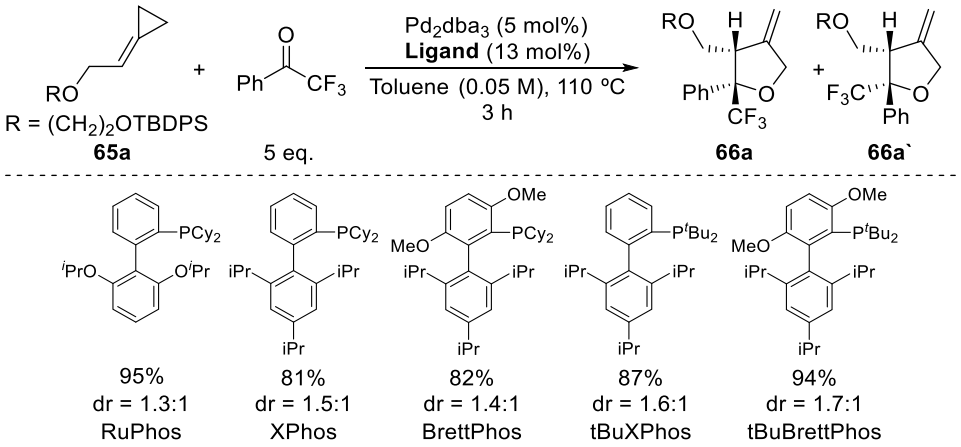

Scheme 128. Screening of different Buchwald phosphines.

Once we have established the optimal reaction conditions, we evaluated the scope testing different alkylidenecyclopropanes as starting materials (Scheme 129). The synthesis of -OTBS analogues **65b-c** was carried by the reduction of α,β-unsaturated esters **68a-b**,[124] with DIBAL-H followed by treatment with NaH and TBSCl.

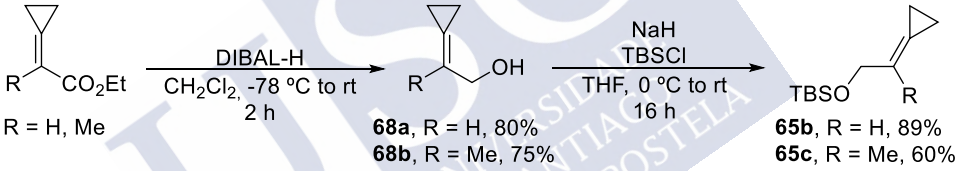

Scheme 129. Synthesis of substrate **65b** and **65c**.

The cycloadducts **66a** and **66b** were obtained in good overall yields as mixtures of diastereoisomers with similar low diastereoselectivity. On the other hand, the ACP bearing a carbonated chain **65d** or the methyl-substituted precursor **65c** were also good cycloaddition partners, showing a slightly better diastereoselectivity (74% yield, 1.8:1). In the latter case the reaction proceeded efficiently at 130 ºC to provide the corresponding tetrahydrofuran bearing two adjacent chiral quaternary centers in a good 60% yield. Interestingly in this case, the major isomer exhibits a *trans* relative configuration of the formed stereocenters (Scheme 130).

[124] H. Hori, S. Arai, A. Nishida, *Adv. Synth. Catal.* **2017**, *359*, 1170–1176.

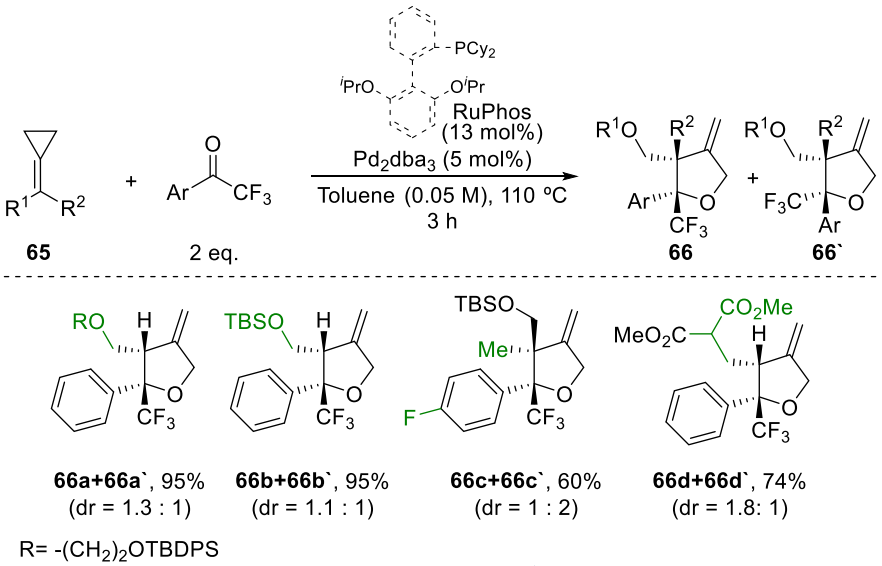

Scheme 130. Reaction scope of the intermolecular (3+2) cycloaddition with fluorinated ketones.

By 1H-NMR we could characterize the stereochemistry of the major isomer of the malonate adducts **66d** (Figure 21). Thus, 1D-nOe experiments showed that *syn* adduct is obtained preferentially, similarly to the intramolecular reaction. By analogy the diastereomeric ratio could also be determined for other examples.

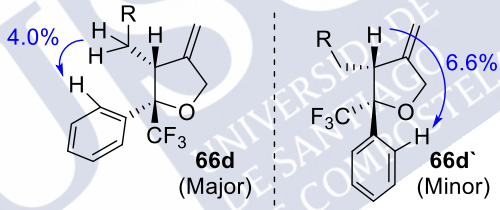

Figure 21. Determination of the relative configuration of diastereoisomers **66d** and **66d`**.

Therefore, ACPs react efficiently with 2,2,2-trifluoroketones in a formal (3+2) cycloaddition to afford highly functionalized tetrahydrofurans. Nevertheless, the diastereoselectivity remains as an important limitation for this reaction, as consequence of the higher conformational freedom compared with the intramolecular reactions. In the future, the group will undertake further studies to improve the diastereoselectivity of these transformations, as well as the development of their corresponding enantioselective versions.

4. Addendum: Palladium catalyzed Tandem cycloisomerization reactions of alkylidenecyclopropanes

During a very preliminary exploration of the viability of an enantioselective version of the cycloaddition between ACPs and carbonyl groups, we discovered some unexpected, interesting results (Scheme 131). In particular, when the aldehyde **48a** was treated with $Pd_2(dba)_3$ and the chiral monophosphine ligand (S)-BI-DIME, we obtained together with the expected fused-tetrahydrofuran (15% yield, ee not determined) a monocyclic product that was eventually identified as the alcohol **69a**. Although the precise mechanism by which this product might be generated is not trivial, the participation of zwitterionic species of type **A** seems plausible**.**

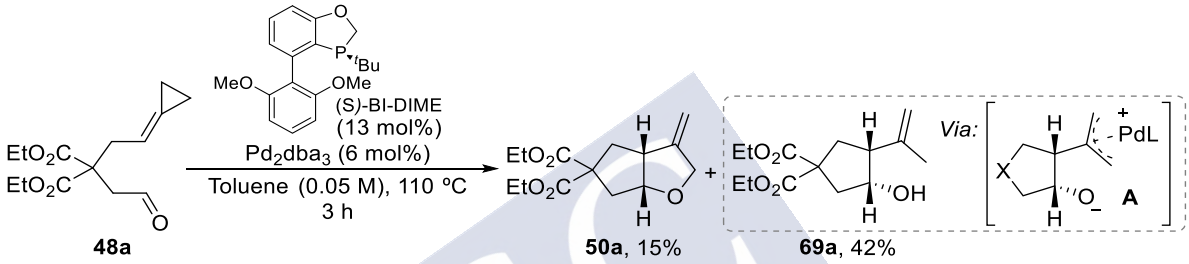

Scheme 131. Screening using chiral ligands in the intramolecular cycloaddition with aldehydes.

Curiously, the cycloaddition of the methyl ketone **49a** in presence of a related Pd-phosphoramidite catalyst composed by a 6 mol% of Pd_2dba_3 and 13 mol% of phosphoramidite **(*S,R,R*)-L4**, led to the formation of the bicyclic lactone **70a** (25 % yield), whereas the (3+2) adduct was not observed (Scheme 132). The formation of this lactone is compatible with the presence of a zwitterionic intermediate like **A** that, in this case, would evolve through a transesterification with a germinal ester to yield intermediate **B**. The formation of the product from this intermediate would require a hydride source, albeit it is not clear yet its origin and nature of this species.

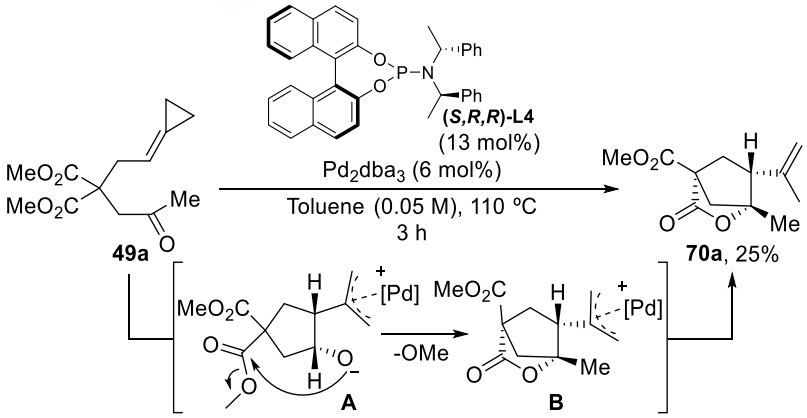

Scheme 132. Hypothesis for new cyclization reactions.

Based on these unexpected results, we hypothesized whether it would be possible to further exploit the reactivity of these zwitterionic species, by its in situ trapping with different types of nucleophiles (Scheme 133).

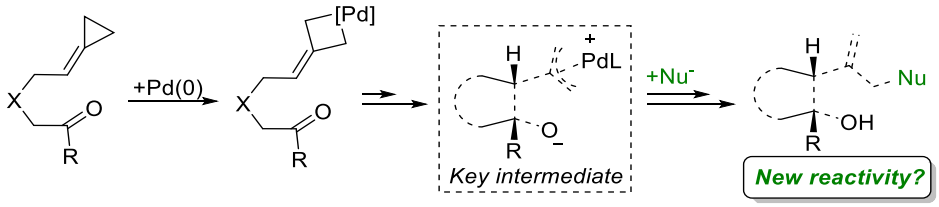

Scheme 133. Hypothesis for new cyclization reactions.

To the best of our knowledge, this reactivity of alkylidenecyclopropanes is unprecedented. The only report that shows some similarity is the work published by Shi in 2017, which explores the reactivity of keto-vinylidenecyclopropanes (VDCP) and terminal alkynes, through a synergistic cycloisomerization/cross coupling reaction (Scheme 134).[125] The transformation, which uses a 2.5 mol% of $[Rh(cod)_2]_2$, 6 mol% of $AgNTf_2$ and 6 mol% of chiral ligand (*R*)-SDP, affords functionalized piperidines bearing a new chiral center. Despite its novelty, the reaction shows important limitations, such as the restriction to N-tosyl tethered substrates, exclusively bearing aromatic ketones. Moreover, the alkynes must have an aromatic substituent to ensure the efficiency of the process. The proposed mechanism involves the formation of the metallacyclobutane **A that,** after migratory insertion of the ketone leads to the π-allyl-Rh species **B**, which further transmetallate the alkyne from the silver alkynyl species **C**. Finally, the piperidine is obtained after a C-C reductive elimination.

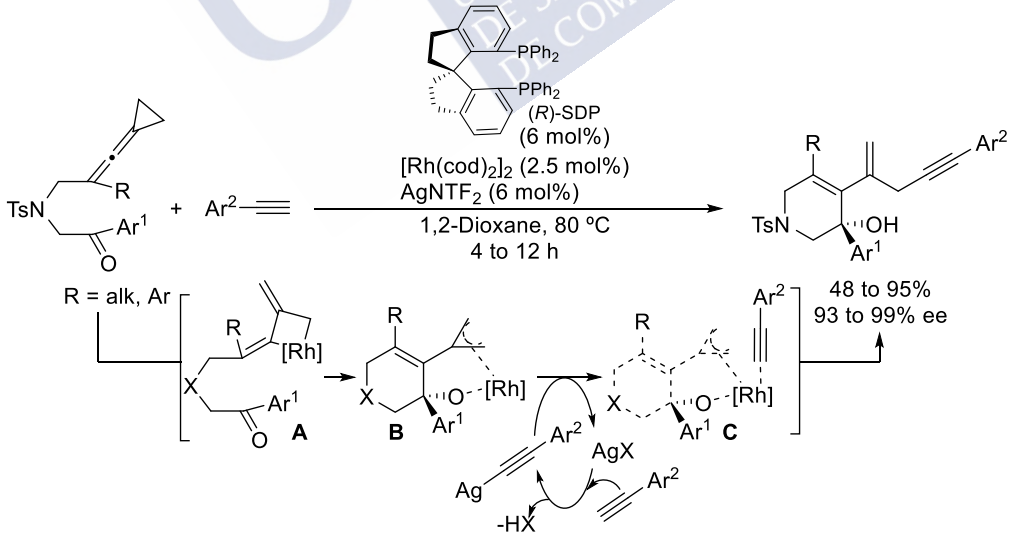

Scheme 134. Rh/Ag synergistic cycloisomerization/cross coupling reaction of VCPs.

More recently Shi´s group extended this methodology to the incorporation of indoles and related secondary amines as nucleophiles, using a similar preformed rhodium catalyst, but

[125] S. Yang, K. H. Rui, X. Y. Tang, Q. Xu, M. Shi, *J. Am. Chem. Soc.* **2017**, *139*, 5957–5964.

with a different counterion.[126] The products are obtained in good to excellent yields and superb enantioselectivities, albeit the use of VCPs tethered to aromatic ketones through an N-Ts linker is still a requisite (Scheme 135).

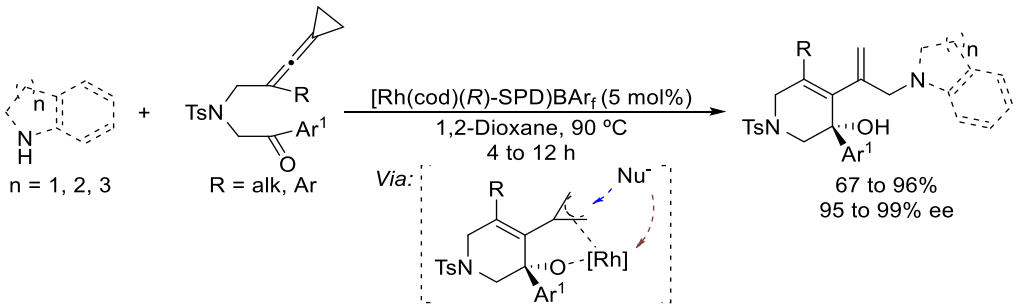

Scheme 135. Rh catalyzed hydroamination of VCPs.

In the following section, we describe our preliminary efforts to exploit the reactivity of the palladium π-allyl intermediates generated from the ACPs.

4.1. Objective

Considering the enormous potential boronic acids as nucleophiles in Suzuki-Miyaura couplings, we tested them as π-allyl trapping nucleophiles (Scheme 136). Ideally, the boronic acid would be activated by the alkoxide of intermediate **A** generating a boronate (**B**) that could participate in an intramolecular transmetallation to generate a new π-allyl-Pd-aryl intermediate **C**. A reductive elimination would then provide a product of type **72**, formally resulting from a tandem cycloisomerization of **49** coupled to an allyl-aryl Suzuki-like cross coupling reaction. The whole process generates one cycle, two stereocenters and two new C-C bonds. On the other hand, the use of alternative nucleophiles typically employed in Pd-catalyzed allylic substitution, such as sulfonamides, phenols or activated methylene compounds, will also be explored.

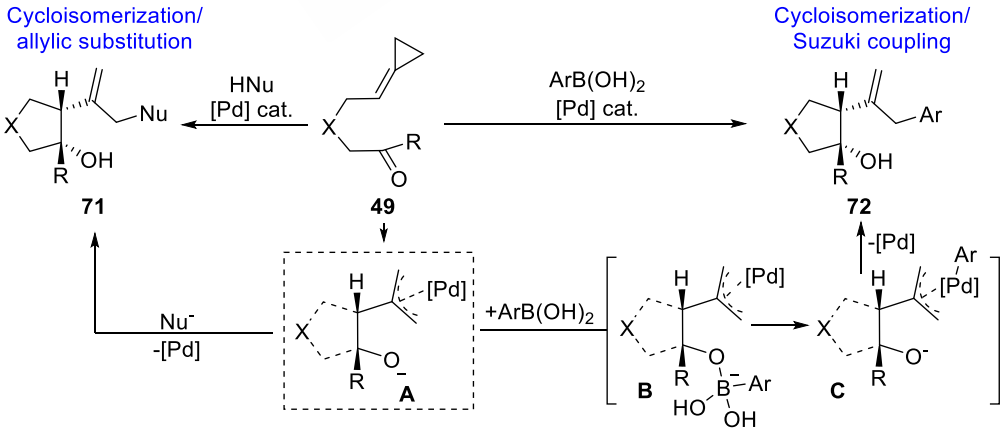

Scheme 136. New tandem cycloisomerization of alkylidenecyclopropanes.

[126] S. Yang, Q. Z. Li, C. Xu, Q. Xu, M. Shi, *Chem. Sci.* **2018**, *9*, 5074–5081.

Precedents of trapping intermediate π-allyl metal intermediates

TMC reactions that combines the formation of a transient π-allyl-Pd species with a cross-coupling reaction in a tandem process are not very common. One representative example was described by Sigman in 2009, which explores the hydroarylation of dienes using boronic esters in presence of a Pd (II) catalyst (Scheme 137).[127] The reaction starts with the formation of a catalytically active Pd hydride after the oxidation of the alcohol used as solvent, followed by the selective hydrometallation of the diene at the terminal position forming the π-allyl-Pd species **A**. This intermediate reacts through transmetallation with the boronic ester forming intermediate **B**, which after reductive elimination affords the branched products in good yields.

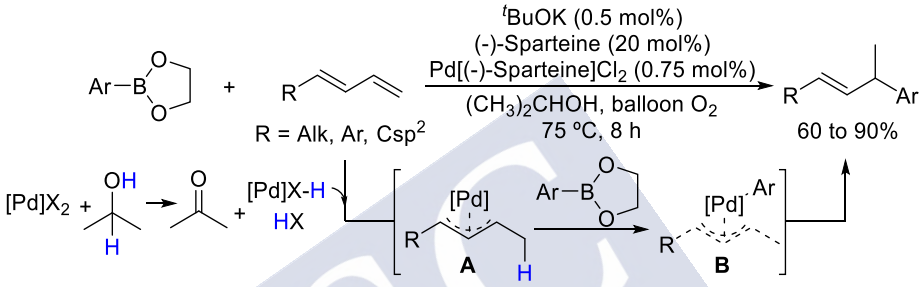

Scheme 137: Pd catalyzed hydroarylation of dienes.

A more commonly used strategy is based on different palladium sources in combination with allylic acetates (Scheme 138).[128] A report published by Fernandes in 2016 shows how the reaction of γ-vinyl-lactones with different aryl boronic acids, using $Pd(OAc)_2$/TMEDA as catalyst, provides different arylated products.[129] The reaction involves an oxidative addition to generate the π-allyl-Pd species **A**, which transmetallate the boronic acid to **B** and, after reductive elimination, gives products of type **74**. Interestingly, using a larger excess of the boronic acids (3 eq.) in presence of oxygen, diarylated products of type **74`** are obtained.

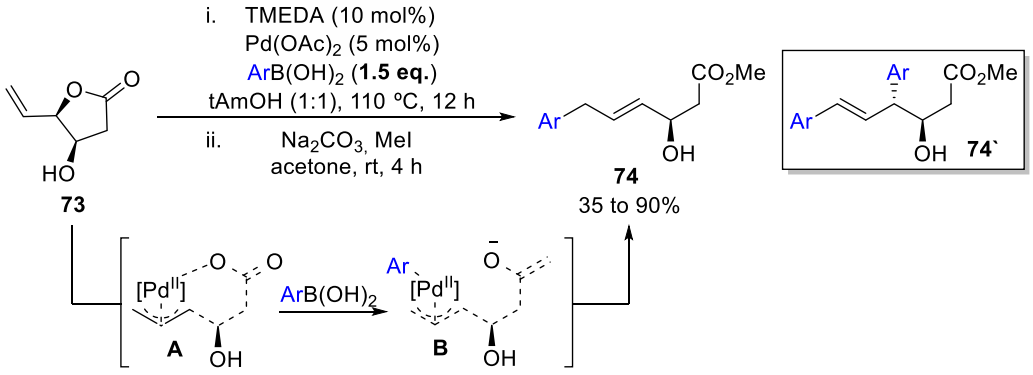

Scheme 138: Pd catalyzed cross-coupling of γ-vinyl-lactone.

[127] L. Liao, M. S. Sigman, *J. Am. Chem. Soc.* **2010**, *132*, 10209–10211.
[128] (a) H. Ohmiya, Y. Makida, T. Tanaka, M. Sawamura, *J. Am. Chem. Soc.* **2008**, *51*, 17276–17277. (b) C. Li, J. Xing, J. Zhao, P. Huynh, W. Zhang, P. Jiang, Y. J. Zhang, *Org. Lett.* **2012**, *14*, 390–393.
[129] J. L. Nallasivam, R. A. Fernandes, *J. Am. Chem. Soc.* **2016**, *138*, 13238–13245.

4.2. Results and discussion

4.2.1 Tandem cycloisomerization/Suzuki-like coupling

We first tested the cyclization and subsequent cross-coupling reaction using boronic acids, selecting the ACP-ketone **49a** as model substrate (Scheme 139). To our delight, when a mixture of **49a** and *p*-methoxy boronic acid (2 eq.) was refluxed in dioxane in the presence of 6 mol% of Pd_2dba_3 and 13 mol% of the phosphoramidite **(*S*,*R*,*R*)-L4**, a complete conversion towards a new single product **72aa** was observed after just 1 h reaction, with complete stereoselectivity, as confirmed by nOe experiments.[130] The formation of this product is compatible with our initial hypothesis, and implies the formation of the π-allyl-Pd-Aryl intermediate **A** after an intramolecular transmetallation.

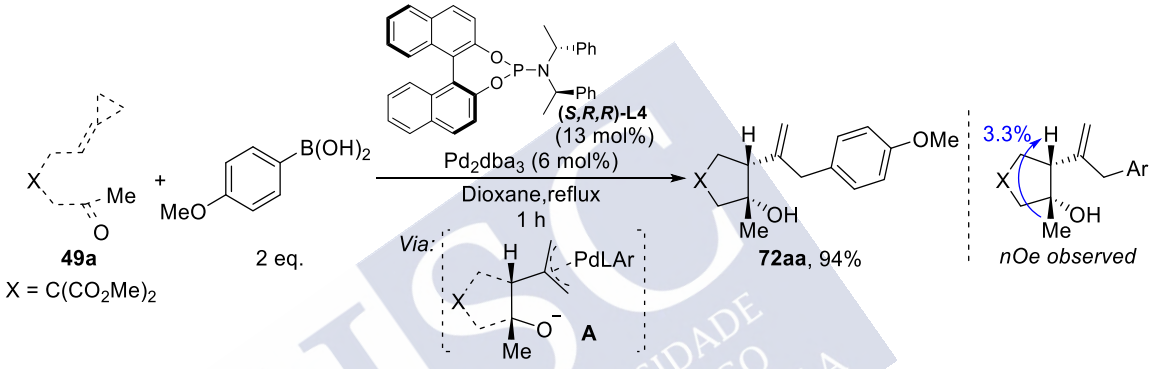

Scheme 139. Cyclization- cross coupling reaction.

Control experiments indicated that the reaction is highly dependent on the nature of the ligand (Table 19). In general, the catalysts generated from Pd_2dba_3 and electron deficient monodentate ligands such as phosphoramidites **(*S*,*R*,*R*)-L4** or **L2** (entry 1 and 2), phosphite **L1** (entry 3), or the bis-trifluoromethyl phosphine **L18** (entry 4) were able to promote the reaction efficiently leading to **72aa** in excellent yields in all cases. In contrast, the use of more electron-rich phosphines such as PPh_3 (entry 5) does not promote the reaction. Particularly interesting is the use of RuPhos, which produced the (3+2) adduct **51a** in 90% yield (entry 6), exactly the same result that is obtained in the absence of boronic acid (entry 7). This result clearly suggests that the nature of the intermediate after migratory insertion of the carbonyl is very dependent on the nature of the ancillary ligand. However, when the reaction catalyzed by Pd_2dba_3/**(*S*,*R*,*R*)-L4** was carried out in absence of the boronic acid, no significative formation of any product was observed (entry 8).

[130] Since a chiral ligand was used in the reaction, we measured the ee and it turned to be of 64:26.

Table 19. Screening of ligands.

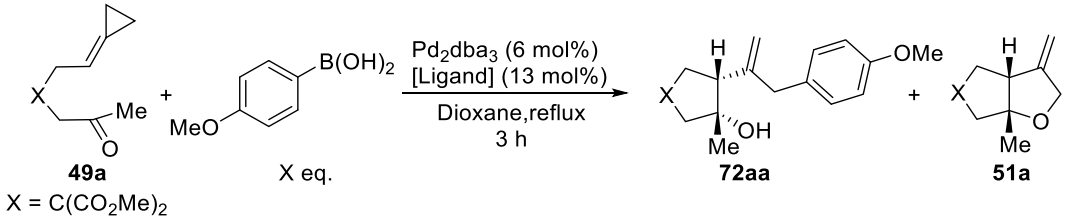

Entry	Ligand	X (eq.)	Conv. (%)[b]	72aa (%)[b]	51a (%)[b]
1	**(*S*,*R*,*R*)-L4**	2	100	90	<5
2	**L1**	2	100	90	<5
3	**L2**	2	100	90	<5
4	**L18**	2	100	90	<5
5	**PPh_3**	2	15	-	-
6	**RuPhos**	2	100	-	90
7	**RuPhos**	0	100	-	90
8	**(*S*,*R*,*R*)-L4**	0	70	-	<5

[a] *Reaction conditions*: **49a** (0.15 mmol), Pd_2dba_3 (6 mol%), [Ligand] (13 mol%), 2 eq. Boronic acid, dry 1,4-dioxane [0.05 M], reflux. [b] Determined by ^{1}H-NMR using 1,3,5-trimethoxybenzene as internal standard.

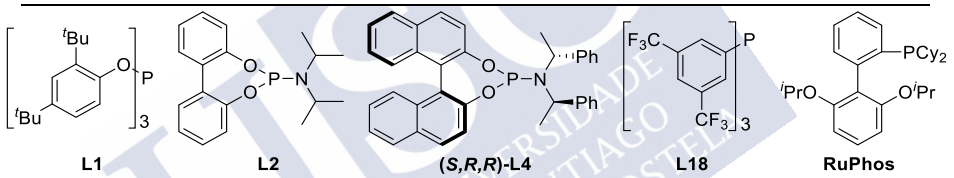

The influence of the solvent on the efficiency of the reaction was checked using the achiral phosphoramidite ligand **L2** (Table 20). We observed that polar solvents are more appropriate, reaching an excellent 90% yield using dioxane and also *t*-amyl alcohol, which is a not a conventional solvent for palladium catalysis with ACPs (entry 1 and 2). Toluene and 1,2-dichloroethane are also suitable solvents, but lower yields are obtained (entry 3 and 4). On the other hand, acetonitrile inhibits the reaction probably due its strong coordinating character (entry 5).

Table 20. Influence of different solvents in the reaction.

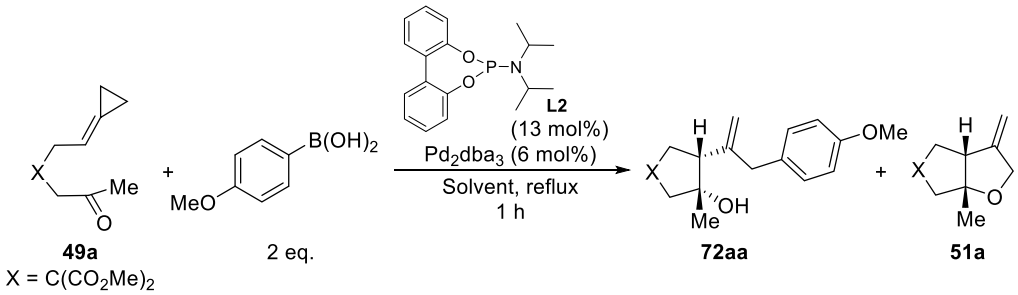

Entry	Solvent	Conv. (%)[b]	72aa (%)[b]	51a (%)[b]
1	Dioxane	100	90	<5
2	^{t}AmOH	100	90	<5
3	Toluene	100	78	10
4	$Cl(CH_2)_2Cl$	55	31	<5
5	CH_3CN	5	-	-

[a] *Reaction conditions*: **49a** (0.15 mmol), Pd_2dba_3 (6 mol%), **L2**(13 mol%), 2 eq. Boronic acid, dry solvent [0.05 M], reflux. [b] Determined by ^{1}H-NMR using 1,3,5-trimethoxybenzene as internal standard.

A final optimization was carried out with different Pd(0) sources and reevaluating the palladium to ligand ratio, using **L2** as model ligand (Table 21). The use of palladium (II) precursors that can be *in situ* converted to Pd(0) species after reduction, such as $Pd(OAc)_2$ or $[(C_3H_5)PdCl]_2$, led to poor conversions (entry 1 and 2), while $CpPd(\eta^3\text{-}1\text{-}PhC_3H_4)$ provided a mixture of **72aa** and **51a** in an excellent overall yield, albeit showing the preferential formation of the (3+2) cycloadduct (entry 3). Regarding other Pd (0) sources, the use of $Pd(PPh_3)_4$ did not induce the desired reactivity (entry 4). Therefore, Pd_2dba_3 turned out to be the most efficient Pd(0) source, and indeed, the catalytic loading could be reduced to a 2 mol% of Pd_2dba_3 and a 5 mol% of **L2**, without affecting the yield, whereas the amount of boronic acid could be reduced to 1.5 equivalents (entry 6). Thus, we selected a catalytic loading of 4 mol% of Pd_2dba_3 and 9% of ligand for subsequent studies.

Table 21. Evaluating palladium sources and stoichiometry of the reaction.

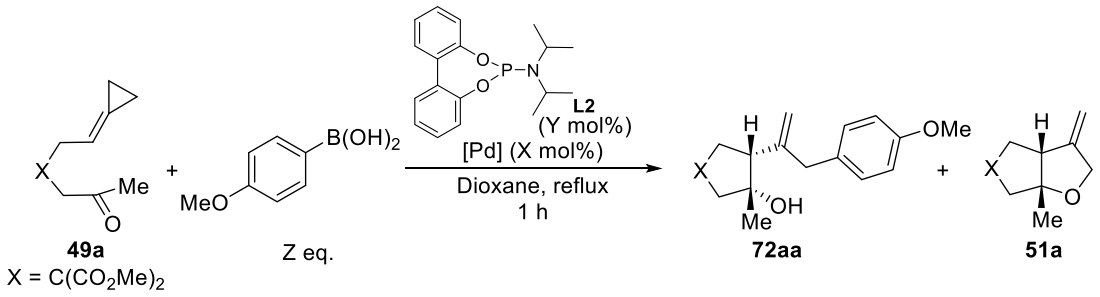

Entry	[Pd] (x mol%)	Y (mol%)	Z (eq.)	Conv. (%)[b]	72aa (%)[b]	51a (%)[b]
1	$PdOAc_2$ (12)	24	2	70	5	25
2	$[(C_3H_5)PdCl]_2$ (6)	12	2	5	-	-
3	$CpPd(\eta^3\text{-}1\text{-}PhC_3H_4)$ (12)	13	2	100	30	60
4	$Pd(PPh_3)_4$ (12)	13	2	5	-	-
5	Pd_2dba_3 (6)	13	2	100	90	<5
6	Pd_2dba_3 (2)	5	1.5	100	90	<5

[a] *Reaction conditions*: **49a** (0.15 mmol), Pd_2dba_3 (X mol%), **L2** (Y mol%), Z eq. Boronic acid, dry 1,4-dioxane [0.05 M], reflux. [b] Determined by ^{1}H-NMR using 1,3,5-trimethoxybenzene as internal standard.

Thus, we next tested other boronic acids as coupling partners (Scheme 140). Curiously, *p*-F-phenylboronic acid did not provide the product when **L2** was employed as ligand, probably due to a slower transmetallation of this electron-poor boronic acid.[131] However, using phosphine **L18** the reaction can be performed in an efficient way, leading to **72ac** in an excellent 96% yield.

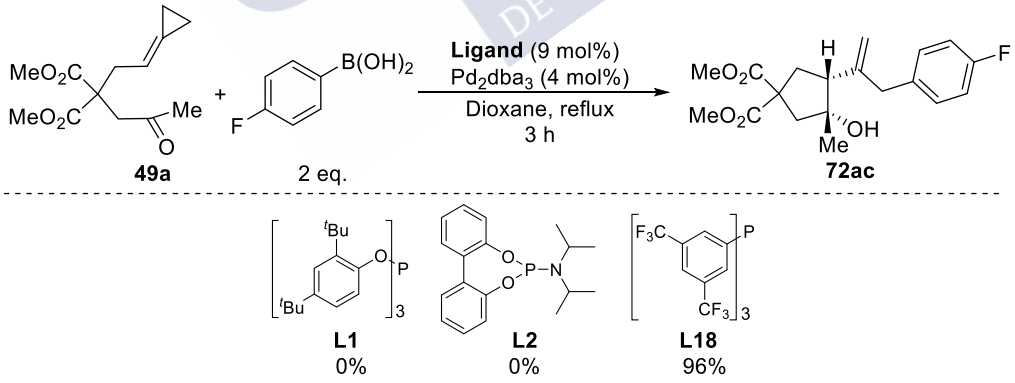

Scheme 140. Secondary evaluation of ligands for the cycloisomerization/cross coupling reaction.

We next tried a non-aromatic boronic acids such as the cyclopentene-1-ylboronic acid. Under standard conditions, we observed a poor 25% conversion (after 3h), but the product was not detected in the crude mixture (entry 1). Considering that probably the generated alkoxide could not be enough to activate this boronic acid, we tested the addition of different external bases (Table 22). To our delight, adding K_2CO_3, we obtained a 60% of conversion and a 40% of

[131] S. Zhao, T. Gensch, B. Murray, Z. L. Niemeyer, M. S. Sigman, M. R. Biscoe, *Science*. **2018**, *362*, 670–674.

yield of **72ae** (entry 2), while with K_3PO_4 we obtained a mixture of **72ae** and the lactone **70ae,** in an excellent 94% overall yield (entry 3). The formation of the latter might be explained assuming an intramolecular transesterification of the initially formed **72ae**, under basic conditions. Finally, the use of an organic base such as DBU did not lead to the desired products (entry 4).

Table 22 Evaluating bases for cross-coupling reaction.

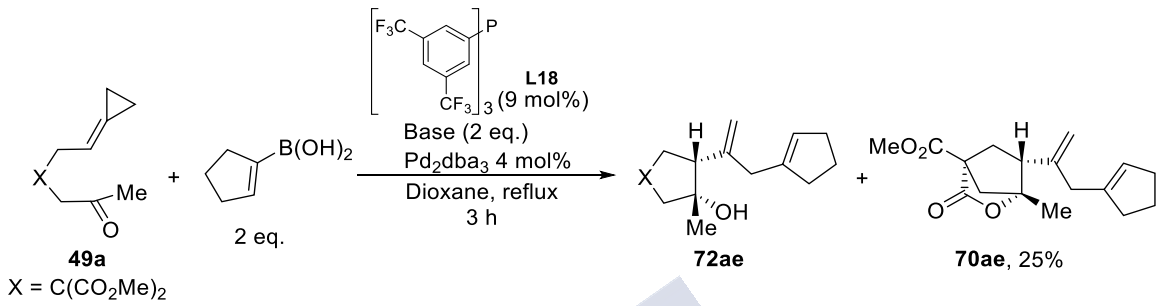

Entry	Base	Conv. (%)[b]	72ae (%)[b]	70ae (%)[b]
1	-	25	-	-
2	K_2CO_3	60	40	
3	K_3PO_4	100	36	58
4	DBU	20	-	-

[a] *Reaction conditions*: **49a** (0.15 mmol), Pd_2dba_3 (6 mol%), **L18** (13 mol%), 2 eq. Boronic acid, dry solvent [0.05 M], reflux. [b] Determined by ^{1}H-NMR using 1,3,5-trimethoxybenzene as internal standard.

With the optimal reaction conditions in hand, we evaluated the scope of the reaction (Scheme 141). First, we tested the reactivity of **49a** with different boronic acids. The reaction tolerates arylboronic acids bearing different substituents at *para*-position (**72aa**, **77ab** and **72ac**), providing yields above 90%. When 1-phenylvinyl boronic acid was used as coupling partner, the corresponding product, **72ad** was obtained in an excellent 88% yield. As previously commented, when cyclopenten-1-ylboronic acid was used in combination with **49a**, a side product arising from a transesterification was isolated, together with the expected product (Table 22). This process does not occur when the N-Tosyl precursor **49c** is used, so the desired product **72ce** could be obtained in a higher yield (63% yield). The use of *p*-OMe-phenyl boronic acid with the N-Ts derivative provided pyrrolidine **7ca** in an excellent 90% yield. To our delight, the reaction is not restricted to the use of the ACPs precursors **49a** and **49c**. Indeed, a precursor lacking functional groups in the connecting tether also provided the desired product (**72ba**) in a good 50%yield, whereas an oxygenated ACP lead to tetrahydrofuran **72da** in good yield (63%). Finally, a substrate bearing a preformed chiral center provided the fused bicyclic product **72ja** in 90% yield. Remarkably, all the cycloadducts were obtained diastereoselectively, where the H and Me groups of the new chiral centers formed shows a *syn*- distribution.

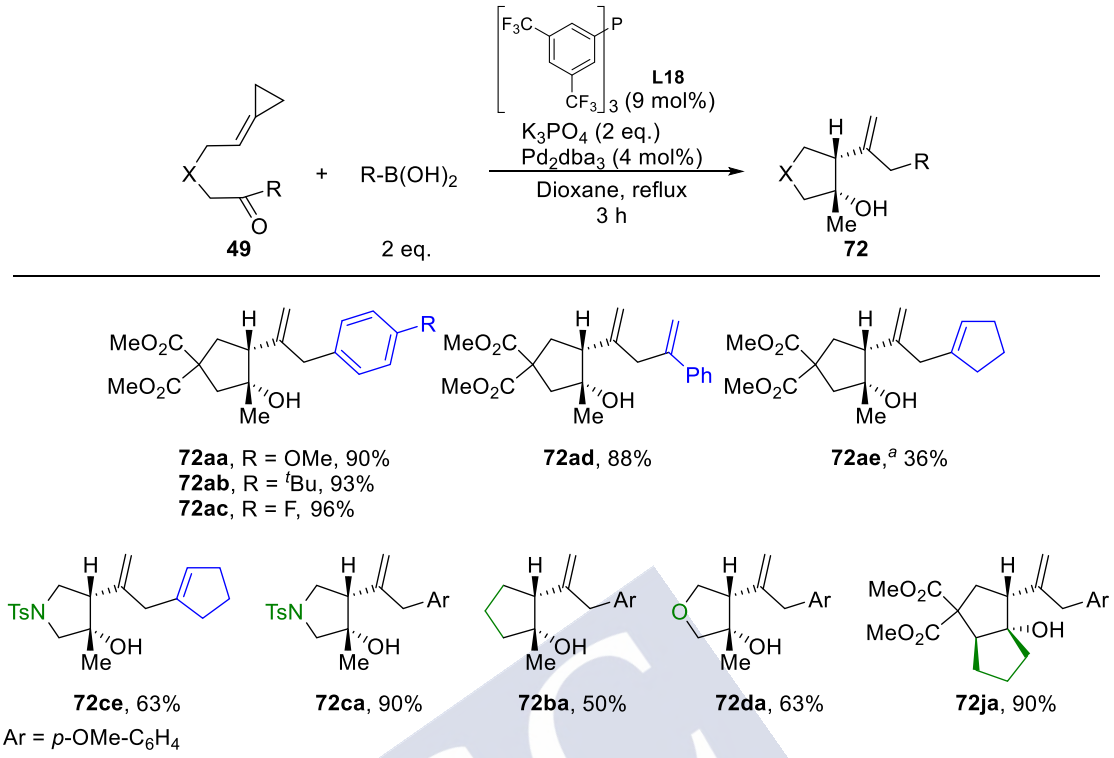

[a]*Lactone* ***70ae*** *was obtained as major byproduct (Table 12). The re-optimization of the reaction conditions (temperature, base) could lead to a better result.*

Scheme 141. Scope of tandem cycloisomerization/cross coupling between ACPs and boronic acids.

We also tested an alkyl-boronic acid to evaluate whether we can form Csp^3-Csp^3 bonds, which are known to be more challenging (Scheme 142). Unfortunately, the use of *n*-butylboronic acid only lead to the proto-demetallated product **70a** in 70% yield. Albeit further studies are required to understand the process, a priori, **70a** could be the results of a *β*-hydride elimination in intermediate A, a process that delivers the Pd-hydride intermediate B, which could undergo reductive elimination to produce **70a**.

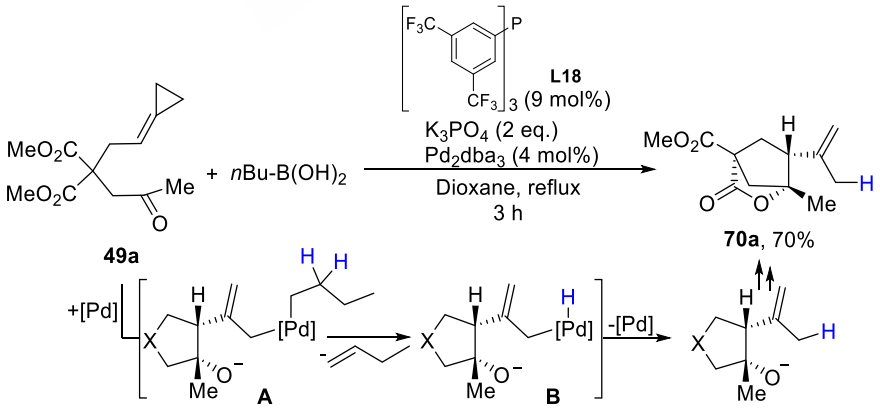

Scheme 142. Reaction between **49a** and *n*BuB(OH)$_2$.

To conclude, we have developed a stereoselective cycloisomerization/tandem Suzuki coupling between carbonyl-tethered ACP's and boronic acids. In the future, the scope of the

process will be fully investigated, including the development of an enantioselective version. Moreover, mechanistic studies will be carried out to shed light on the particular features of this rare process.

4.2.2. Tandem cycloisomerization /allylic substitution

Once the viability of a tandem cycloisomerization/allylic Suzuki-type coupling was shown, we next explored the possibility of trapping the generated π-allyl-Pd intermediate with alternative nucleophiles, which could be eventually generated in situ by deprotonation with the generated alkoxide, as shown in scheme 143.

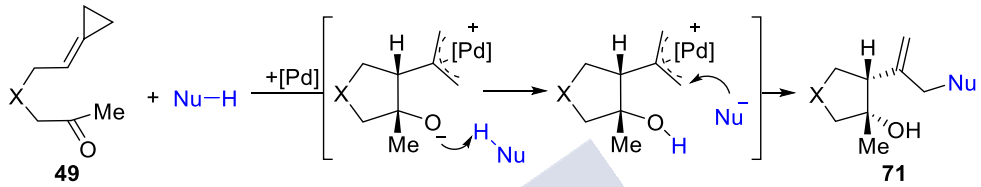

Scheme 143. Cyclization-nucleophilic addition reaction.

We initially selected the reaction of **49a** in the presence of dimethylmalonate (Scheme 144). Unfortunately, treatment of **49a** and methyl malonate with Pd_2dba_3 and L2, , did not afford the expected product, but a complex mixture of products (50% conversion after 3h at reflux).

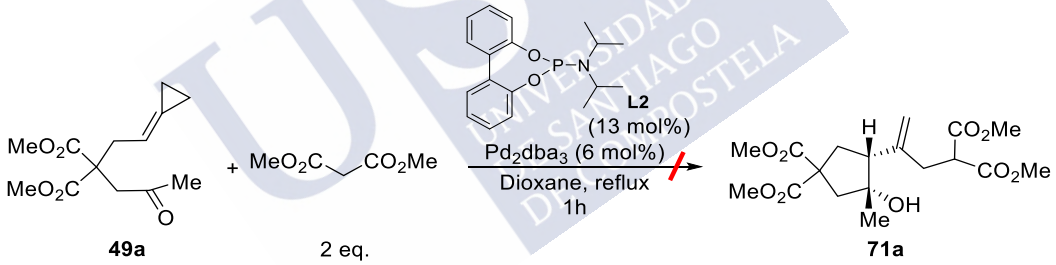

Scheme 144. Cyclization-allylic substitution with malonates.

Then we tested different bases. Gratifyingly, when K_2CO_3 was used under otherwise identical reaction conditions, the expected product **71a** was obtained in an excellent 90% yield. And more interestingly, when K_3PO_4 was used as base, a new bicyclic lactone **75a** was obtained with complete selectivity, in an excellent 88% yield (Scheme 145).

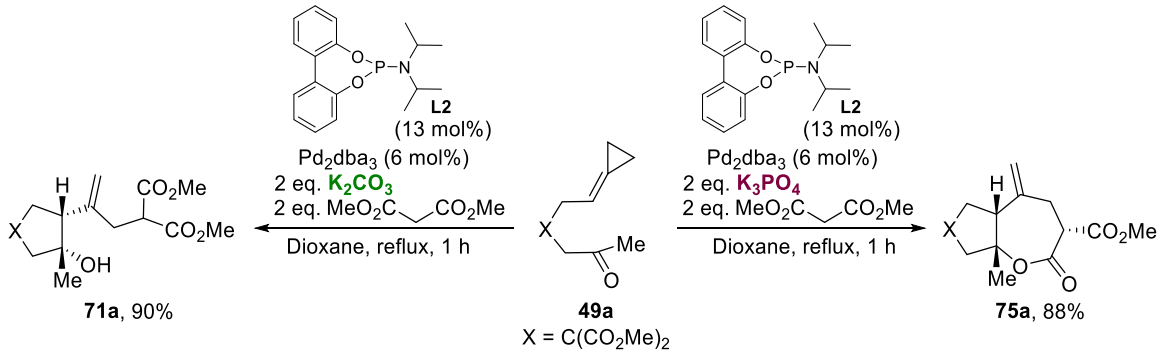

Scheme 145. Tandem cycloisomerization with addition of malonates.

This formal (3+2+2) annulation could be explained through the intramolecular transesterification of malonate **71a** towards **75a** (Scheme 146). To test this hypothesis, a control experiment was carried out by mixing malonate **71a** with 2 eq. of K_3PO_4 in dioxane and refluxing 3 hours. Indeed, the lactonization occurs with complete diastereoselectivity, leading to **75a** in a moderate 40% of yield. This low yield might indicate that the product is not stable for long reaction times, therefore, it will be an important aspect to consider in the future for further development of this reaction.

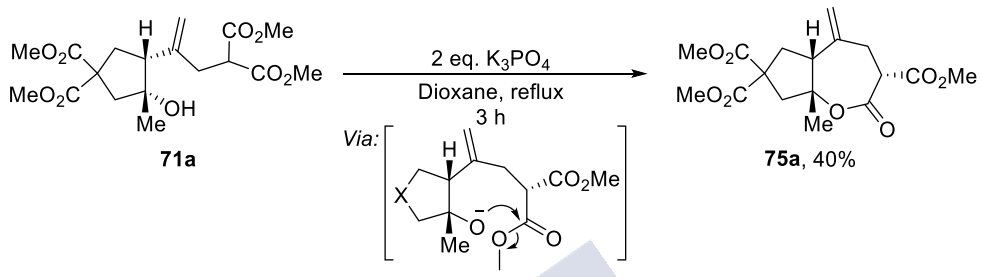

Scheme 146. Control experiment of the intramolecular transesterification.

In summary, we have preliminary explored the reactivity of a new *β*-alcoxy Allyl-Pd zwitterionic species **III** formed as intermediates in the C-C activation of 5-oxo-alkylidenecyclopropane. We have demonstrated that boronic acids are excellent nucleophiles for the reaction, but malonic enolates can also be used. Moreover, the use of K_3PO_4 as base leads to the formation of appealing seven-membered lactones through a novel formal (3+2+2) cycloaddition.

These new tandem cycloisomerization/allylic substitution reactions are still in an optimization phase, and we are attempting to extend it to other challenging nucleophiles and develop enantioselective versions. It represents a very simple and powerful strategy to increase skeletal and functional complexity in metal-catalyzed reactions.

5. Conclusions

In conclusion, an intramolecular racemic and enantioselective (3+2) heterocycloaddition with oxime ethers has been developed (Scheme 147). When the model precursors **45a** and **45b** were studied, the corresponding bicyclic pyrrolidines were obtained with complete diastereoselectivity in good yields with the racemic catalyst generated from Pd_2dba_3 and phosphite L1. Moreover, when a chiral phosphoramidite such as **L10** is used instead of **L1**, both excellent yields and enantioselectivities were obtained. Unfortunately, when the scope of this method was evaluated, the reaction showed to be limited to these model substrates. Our efforts to overcome these limitations did not provide yet the desired results.

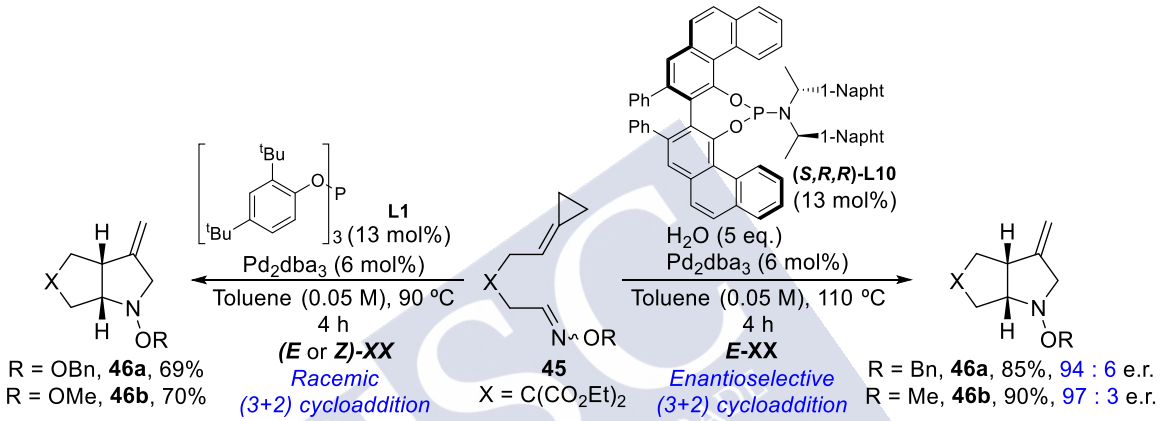

Scheme 147. Racemic and enantioselective intramolecular (3+2) cycloaddition of ACPs with oximes.

Additionally, we have successfully developed new palladium catalyzed intramolecular (3+2) heterocycloadditions between alkylidenecyclopropanes and carbonyls (aldehydes and ketones, Scheme 148). The scope of the reaction proved to be quite broad, enabling the synthesis of a wide variety of fused-tetrahydrofurans with good to excellent yields and a very good diastereoselectivities. Interestingly, the use of bulky biaryl phosphine ligands was key for an efficient cycloaddition, being Brettphos the ligand of choice for aldehyde-bearing substrates while the homologous ketones required the sterically less hindered RuPhos ligand.

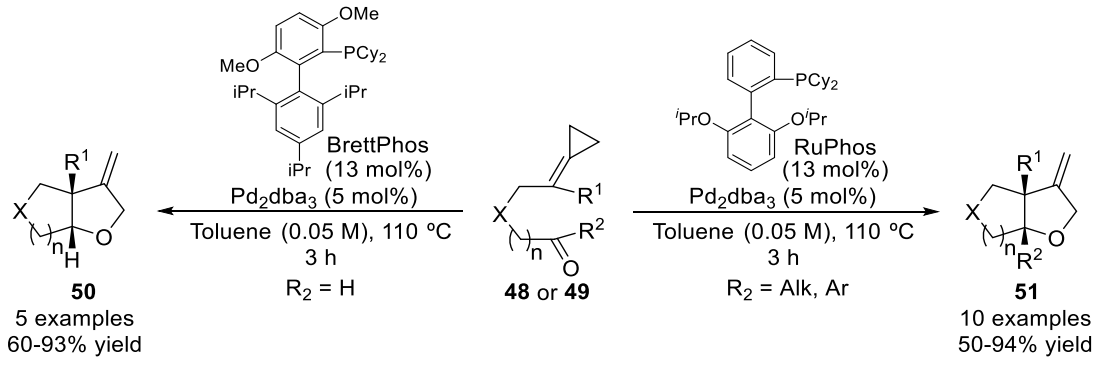

Scheme 148. Intramolecular (3+2) cycloaddition with aldehydes or ketones.

In addition, an intermolecular variant was also developed by using trifluoromethyl ketones as carbonyl partners (Scheme 149). The reaction provides access to appealing functionalized fluorinated tetrahydrofurans of type **66+66`,** bearing quaternary stereocenters, in good to excellent yields and moderate stereocontrol.

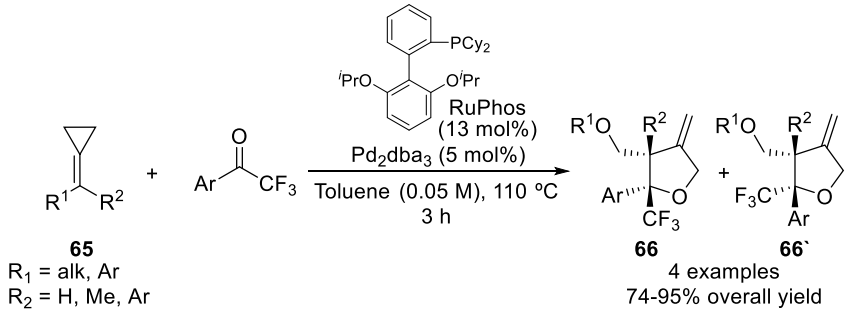

Scheme 149. Intermolecular (3+2) cycloaddition with fluorinated ketones.

CHAPTER III: Cyclometallated alkenyl-gold (III) species by proximal ring-opening of 2-(cyclopropylidenemethyl)pyridines

USC
UNIVERSIDADE
DE SANTIAGO
DE COMPOSTELA

1. Introduction

1.1 Catalysis by gold(I) and gold(III) complexes

Since many centuries ago, gold is considered among the most valuable and prescious metals. This metal is found in nature in the stable gold (0) oxidation form, a characteristic shared with only few other elements (e.g. Cu, Ag, Hg, Zn, etc.). From a chemical perspective, the stability and intrinsic inertness of gold(0) led to the notion that it was not catalytically competent. However, the dicovery almost two decades ago, that of gold(III) and most in particularly gold(I) complexes hold an unique and extremelly rich reactivity, led to an exponential surge of novel catalytic applications that nowadays constitute a whole new area of catalysis, which constitutes the core of **carbophilic catalysis**.[132]

Gold complexes can act as soft lewis acids to selectively activate C-C unsaturated π-systems, such as those of alkynes, alkenes or allenes. This carbophilicity is significantly higher for gold (I) complexes than for gold(III) counterparts. This is associated to the "relativistic effects", highly significant in Au and Pt (Figure 22).[133] From an electronic point of view, it has been postulated that the contraction of the *6s* leads to a relatively low-lying lowest unoccupied molecular orbital (LUMO), and therefore the strong Lewis acidity confers gold a superior potential to coordinate C-Cunsaturated systems likealkenes, alkynes or allenes. On the other hand, the relativistically expanded *5d*, with a decreased electron/electron repulse in the diffuse orbital, result in a less nucleophilic metal that is less prone to undergo to oxidative processes. Accordingly, Au and Pt dos not commonly participate in 2e- redox chemistry, like more common transition metals (e.g. Pd, Ni, Rh, Ru, etc.).

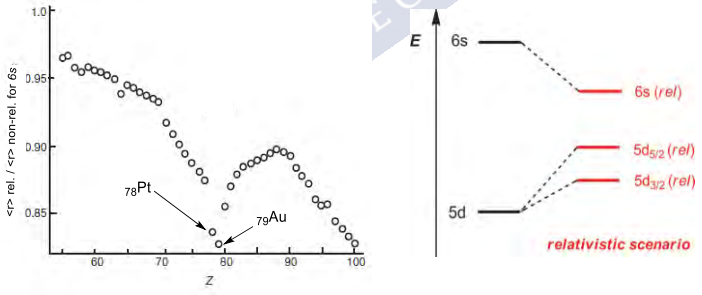

Figure 22. Calculation of the relativistic contraction of *6s* orbitals. Figure reproduced from ref. 133.

Gold chemistry is also popular due their simplicity from a experimental point of view. Initially, AuCl or $AuCl_3$ salts where used as catalyst, but later complexes of type LAuCl proved to be much more competent in homogeneous catalysis. They exhibit a linear conformation mode L-Au-X (e.g. PPh_3AuCl , Figure 23),[134] and the reactivity of the catalyst can be easily modulated by the type ancilliary ligand (L = (phosphines, N-Heterocyclic carbenes, phosphites and

[132] A. S. K. Hashmi, F. D. Toste, *Modern Gold Catalyzed Synthesis*, Wiley-VCH, **2012**.
[133] D. J. Gorin, F. D. Toste, *Nature* **2007**, *446*, 395–403.
[134] A. Fürstner, P. W. Davies, *Angew. Chemie - Int. Ed.* **2007**, *46*, 3410

phopsphoramidites, among others). On the other hand, gold (III) complexes, d^8 systems of generally 16 electron, hold their ancilliary ligands in a squared planar arragement..

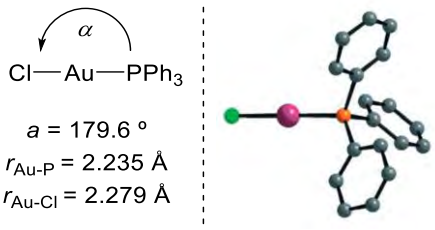

Figure 23. Crystal structure of PPh_3AuCl.

Due the linear coordination of neutral gold(I) complexes, as exemplified with PPh_3AuCl, it is necessary to abstact the X ligand (Cl) in order to generate a vancance for coordination of the substrate. Indeed, most of the gold(I) catalyst are used in their cationic form, after the abstraction of the chloride counteranion with equimolar ammounts of a scavenger, such as a silver (I) salt (Figure 24).[135]

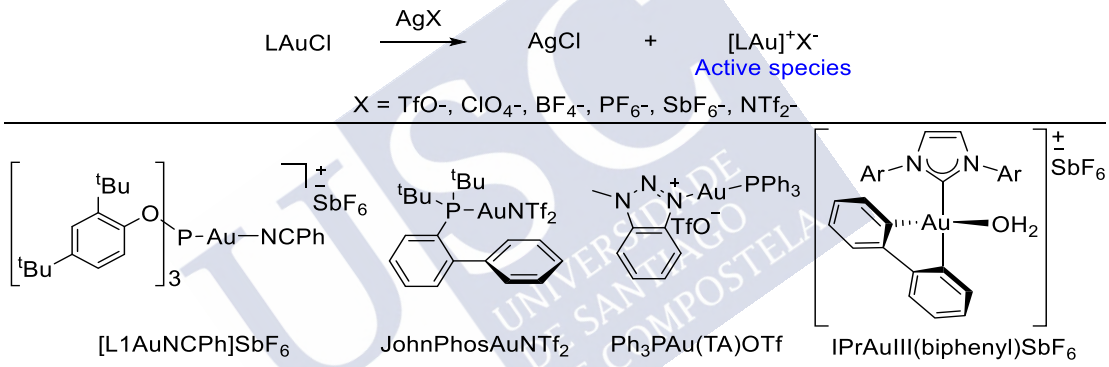

Figure 24. General formation of active gold(I) species and some of the most common gold(I) catalysts.

1.1.1. Gold(I) catalysis

The accepted mechanism that rules the gold activation of unsaturated C-C bonds of alkenes, alkynes or allenes consists of the coordination of the metal to the π-system through a $[LAu]^+$-$\pi_{C\text{-}C}$ intermediate (**A**). This interaction conferes an electronic defficiency to the C-C unsaturated system, making them susceptible to the addition of diverse nucleophiles such as alcohols, amines, amides andeven other C-C systems unsaturated systems.[136] Once the nucleophilic addition takes place, a *trans*-alk(en)yl gold complex **B** is formed, and this can further evolve by interception with an electrophile (usually a proton), releasing the corresponding product (**C)** and regenerating the catalytic cationic gold (I) species (Scheme 150).[137]

[135] (a) C. Nevado, A. M. Echavarren, *Chem. Eur. J.* **2005**, *11*, 3155. (b) A. Homs, I. Escofet, A. M. Echavarren, *Org. Lett.* **2013**, *15*, 5782.
[136] E. Jiménez-Núñez, A. M. Echavarren, *Chem. Rev.* **2008**, *108*, 3326.
[137] (a) M. Kumar, G. B. Hammond, B. Xu, *Org. Lett.* **2014**, *16*, 3452. (b) A. Grirrane, E. Álvarez, H. García, A. Corma, *Angew. Chemie - Int. Ed.* **2014**, *53*, 7253.

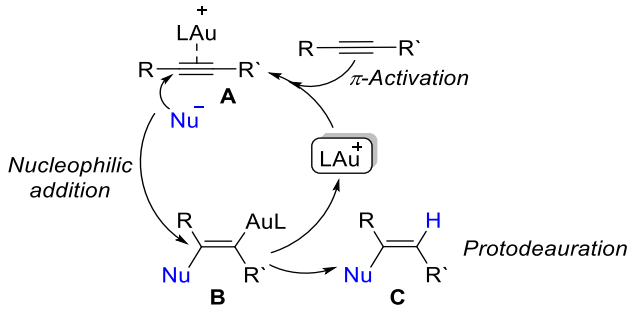

Scheme 150. Activation of triple or double C-C bonds by gold(I) complexes.

One of the model reactions of gold (I) catalysts that exemplifies very well the field of carbophilic catalysis, is the intramolecular cycloisomerization of enynes, pioneered by Echavarren.[138] The reaction takes place under mild conditions, leading divergently to many different cyclic scaffolds depending on the conditions, additive or ligands at gold. Gold(I) species usually activates the alkyne of the enyne, followed by an intramolecular nucleophilic addition of the alkene. For terminal alkynes, the addition occurs via *5-exo-dig*, whereas enynes bearing substituted alkynes usually evolve through a *6-endo-dig* pathway (Scheme 151).

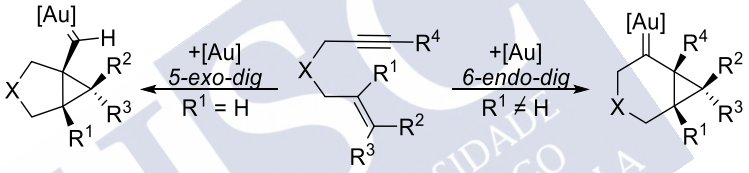

Scheme 151. Gold(I) cyclization of enynes.

1.1.2. Gold(III) catalysis

A seminal work reported by Hashmi and coworkers in 2000 demonstrated that gold (III) salts can also promote intramolecular cycloisomerization reactions. In particular, the authors described a gold-catalyzed (4+2) annulation of furfuryl-tethered alkynes that delivers fused-phenols (Scheme 152).[139] The transformation is proposed to be initiated by the activation of the alkyne and subsequent cyclopropanation forming the strained gold carbene **A**. A ring opening process would deliver the *a,β*-unsaturated intermediate **B** that, after a tandem cyclization/aromatization furnishes the product.

[138] (a) C. Nieto-Oberhuber, M. P. Muñoz, E. Buñuel, C. Nevada, D. J. Cárdenas, A. M. Echavarren, *Angew. Chemie - Int. Ed.* **2004**, *43*, 2402–2406. (b) E. Jímenez-Núñez, A. M. Echavarren, *Chem. Commun.* **2007**, 333.
[139] (a) A. S. K. Hashmi, T. M. Frost, J. W. Bats, *J. Am. Chem. Soc.* **2000**, *122*, 11553. (b) A. S. K. Hashmi, M. Rudolph, J. P. Weyrauch, M. Wölfle, W. Frey, J. W. Bats, *Angew. Chemie - Int. Ed.* **2005**, *44*, 2798.

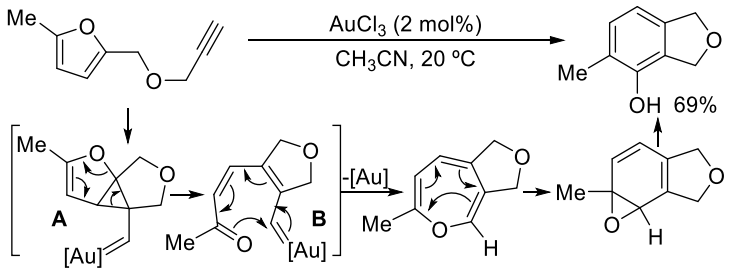

Scheme 152. Au(I)-catalyzed formal (4+2) of furfuryl alkynes.

In general, gold (III) complexes are more commonly used as oxophilic Lewis acids, rather than as carbophilic catalysts. An elegant example of this dichotomy was reported by Toste 2015. The authors showed how two related NHC-gold complexes ,with different oxidation states, **78** and **78'** (Scheme 153), exhibit a totally opposite selectivity.[140] Thus, the NHC-gold(I) complex **78** selectively provided the 1,2-addition of an enolsilyl ether to cinnamaldehyde, to give the corresponding aldol adduct. On the contrary, the NHC-gold (III) counterpart **78`** selectively promoted the 1,4-addition, under otherwise identical reaction conditions. Interestingly, the gold (III) complex **78`** was easily synthesized from the NHC gold (I) complex **78**, through a C-C activation of biphenylene.

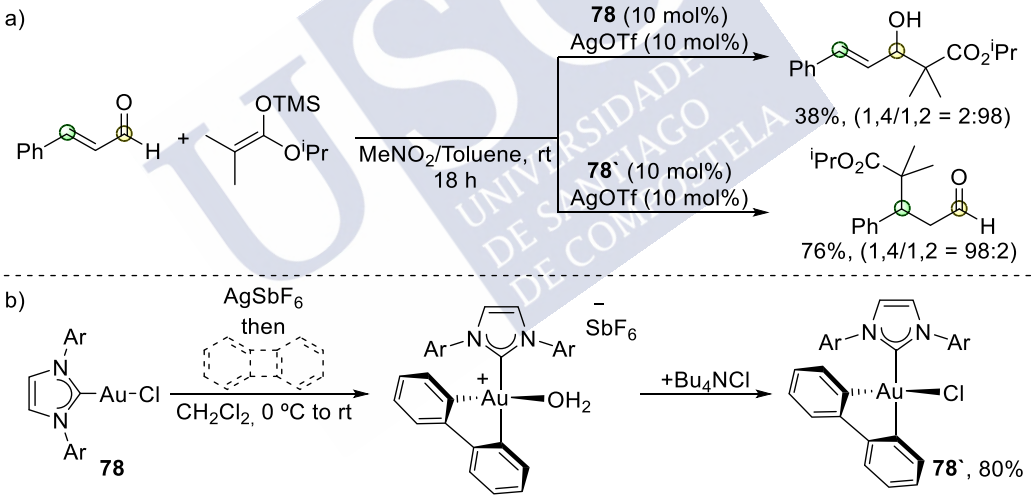

Scheme 153. (a) Au-catalyzed *1,2*- and *1,4*-addition of sylylenolates to *a,β*-unsaturated aldehydes (b) Synthesis of gold (III) complex through C-C activation.

[140] C.-Y. Wu, T. Horibe, C. B. Jacobsen, F. D. Toste, *Nature* **2015**, *517*, 449–454.

1.2. Gold catalyzed reactions of alkylidenecyclopropanes

The reactivity of ACPs in presence of gold(I) complexes is governed by the high carbophilicity of this metal, which can strongly activate the C-C double bond. Depending on the strength of the activation, a simple hydrofunctionalizations or a ring expansion might occur. [141] Next, we revise some of the most representative examples of reactions of alkylidenecyclopropanes catalyzed by gold complexes.

1.2.1 Ring expansions of ACPs

Activation of the C-C double bond of ACPs by a carbophilic metal might facilitate a ring expansion, namely a 1,2-carbon shift, that releases the strain while generating a metal carbene intermediate. The first examples of such a reactivity with a carbophilic catalyst were reported by Fürstner and coworkers in 2006, and consisted of a $PtCl_2$ catalyzed ring expansion of alkylidenecyclopropanes, to deliver highly substituted cyclobutenes (Scheme 154).[142] The proposed reaction mechanism involves an initial π-activation of the double bond that triggers a 1,2-carbon shift leading to a platinum carbene, which after a 1,2-hydrogen shift affords the cyclobutenic products.

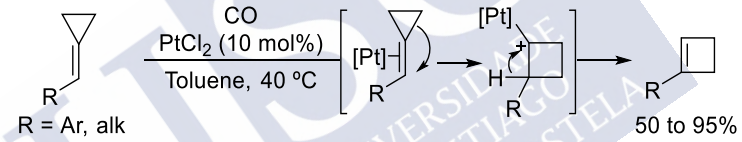

Scheme 154. Pt-catalyzed ring expansion of ACPs.

Echavarren demonstrated in 2014 that the gold-catalyzed ring expansion of alkylidenecyclopropanes to yield cyclobutenes can be coupled to a subsequent cyclopropanation with a gold carbene generated in situ from a retro-Buchner reaction (Scheme 155).[143] The formal (4+1) reaction is catalyzed by a cationic gold(I)/JohnPhos complex, leading to cyclopentenic products in moderate to good yields. Despite the elegance of the process, the reaction requires high temperatures and sealed tube conditions, and is restricted to the use of cycloheptatrienes bearing aromatic substitutions. The reaction mechanism involves the ring expansion of the ACP promoted by gold (**A**) and, in parallel, the generation of a gold carbene of type **B** from the cycloheptatriene. Both intermediates reacts through a cyclopropanation process, leading to the fused bicyclo [2,1,0] pentane derivates **C**, which undergo a ring opening towards the a putative cyclopentane **D** that finally leads to the formation of the cyclopentenes.

[141] D. H. Zhang, X. Y. Tang, M. Shi, *Acc. Chem. Res.* **2014**, *47*, 913–924.
[142] A. Fürstner, C. Aïssa, *J. Am. Chem. Soc.* **2006**, *128*, 6306–6307.
[143] (a) Y. Wang, M. E. Muratore, Z. Rong, A. M. Echavarren, *Angew. Chemie - Int. Ed.* **2014**, *53*, 14022–14026, (b) Y. Wang, M. E. Muratore, Z. Rong, A. M. Echavarren, *Angew. Chemie - Int. Ed.* **2014**, *53*, 14022–14026.

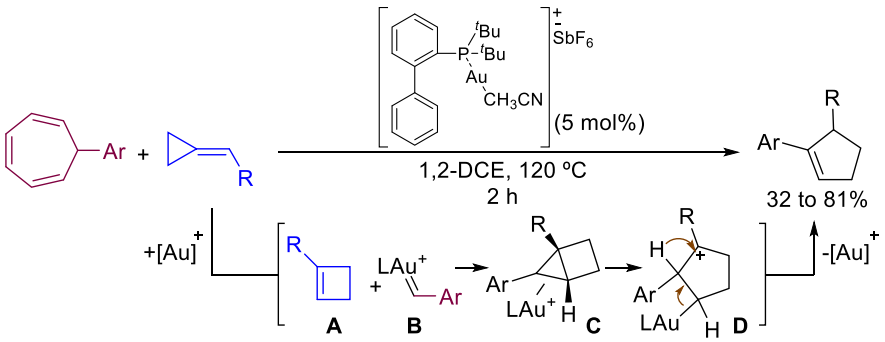

Scheme 155. Au(I)-catalyzed formal (4+2) between ACPs and 1,3,5-cyclohepta-triene.

In 2009, Mascareñas and Esteruelas reported a related ring expansion of ACPs promoted by cationic osmium or ruthenium species (Scheme 156).[144] Albeit the reaction is not catalytic, it highlights the possibility of using directing groups such as pyridines to facilitate the coordination of a metal, to trigger a subsequent activation of the ACP. In this case, the resulting cyclobutylcarbenes were obtained in excellent yields.

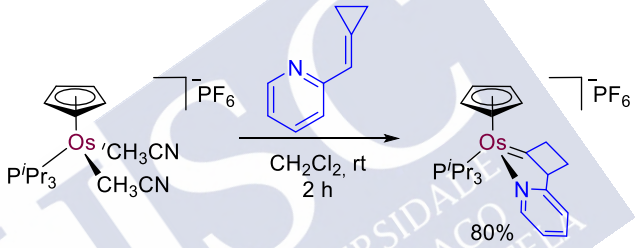

Scheme 156. Os(II)-promoted ring expansion of ACPs.

The reaction is not limited to the use of pyridines as chelating groups, since carboxylic esters also proved to be competent, leading to the same type of metal carbenes with more moderate yield (Scheme 157).

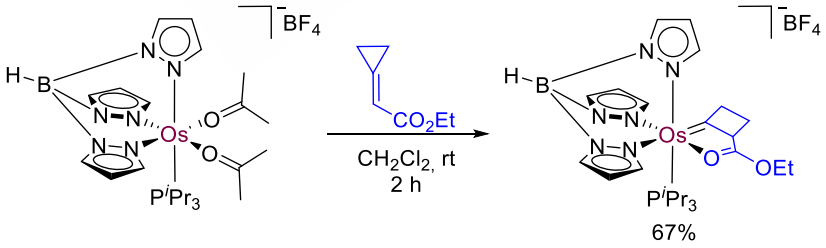

Scheme 157. Os(II) and Ru(II)-promoted ring expansion of ACPs.

In contrast with the previous redox-neutral ring expansion reactions, DFT calculations supports that the formation of the metal carbene involves changes in the oxidation states of the metal (Scheme 158). In particular, the coordination of the metal to the pyridine and the C-

[144] R. Castro-Rodrigo, M. A. Esteruelas, S. Fuertes, A. M. López, F. López, J. L. Mascareñas, S. Mozo, E. Oñate, L. Saya, L. Villarino, *J. Am. Chem. Soc.* **2009**, *131*, 15572–15573.

C double bond (**A**) triggers an oxidative cyclization to an osmium (IV) intermediate **B**, which undergoes a 1,2-carbon shift leading to the corresponding metal carbene **C**.

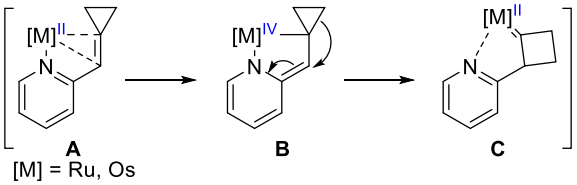

Scheme 158. Mechanistic proposal for the Os(II)-promoted ring expansion of ACPs.

1.2.2. Ring-opening reactions of ACPs

In 2010, Shi and coworkers reported a gold catalyzed diacetoxylation of alkylidenecyclopropanes that involves the distal cleavage of the cyclopropanic ring (Scheme 159).[145] The reaction uses a gold (I) species in presence of an excess of an hypervalent iodine in an acidic media, leading to the oxidized product in moderate to good yields. The proposed mechanism starts with the formation of the catallytically active L-Au-OAc complex, wich reacts with ACP through a nucleophilic addition of an acetate, leading to an intermediate **A**. This complex is further oxidized by the (diacetoxyiodo)benzene to a bis-acetate gold (III) intermediate **B** which, after reductive elimination, provides the diacetoxylated products.

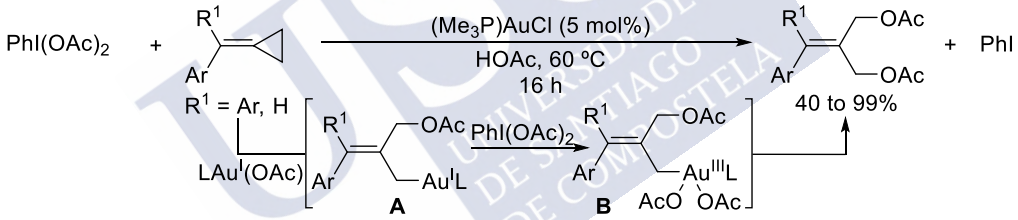

Scheme 159. Au-catalyzed cyclization diacetoxylation of ACPs.

In 2017, the same group reported an oxidative annulation of ACPs which involves the **proximal cleavage** of the cyclopropane to yield polycyclic aromatic hydrocarbons in good yields (Scheme 160).[146] The reaction is promoted by a gold(I)/ JohnPhos complex and stoichiometic amounts of a pyridine N-oxide as oxidant. The reaction starts with the activation of the triple bond by gold (**A**), followed by the intramolecular cyclization with the alkene of the ACP, generating the spirocyclic intermediate **B**. This species traps a pyridine oxide molecule, evolving towards the intermediate **C**, cleaving the proximal bond of the alkylidenecyclopropane during the process. Finally, after an elimination and further protodeauration, the policyclic aldehydes are obtained.

[145] D. H. Zhang, L. Z. Dai, M. Shi, *European J. Org. Chem.* **2010**, 5454–5459.
[146] L.-Z. Yu, Y. Wei, M. Shi, *ACS Catal.* **2017**, *7*, 4242–4247.

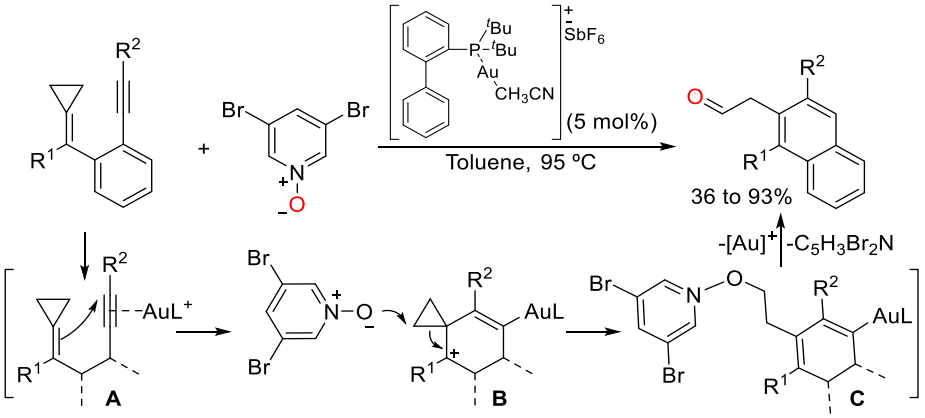

Scheme 160. Au(I)-catalyzed oxidative cyclization of alkynylidenecyclopropanes.

1.2.3. Reactions preserving the cyclopropyl ring

Alkylidenecyclopropanes can also react as simple activated alkenes, without compromising the integrity of the cyclopropanic scaffold. An ilustrative example was reported by Widenhoefer in 2015,[35] and consits of an *anti*-markovnikov hydroamination reaction with cyclic ureas. Control experiments have shown that the observed selectivity is exclusive for the ACP moiety, since dimethyl substituted or alkylidenecyclobutanes afford the Markovnikov product. The reaction provides the cyclopropanic products in good yields, and with high diastereoselecties (Scheme 161).

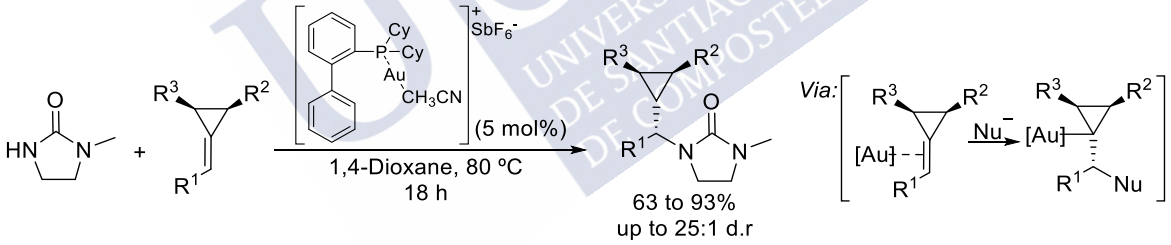

Scheme 161. Au(I)-catalyzed Anti-Markovnikov hydroamination of ACPs.

Another interesting work, developed by Gagné and coworkers reports an enantioselective Cope rearragement catalyzed by gold ,using alkenylidenecyclopropanes (Scheme 162).[147] The reaction takes place with a bimetallic gold (I) complex, (S)-3,5-xylyl-PHANEPHOS(AuCl)2 and provides diverse spirocyclic vinylcyclopropanes in good yields and moderate to excellent enantioselectivities. DFT calculations suggest that the reaction starts by the activation of the double bond of the ACP (**A**), and a subsequent attack by the pendant alkene to give the carbocationic intermediate **B**, which finally evolves to spirocyclic product.

[147] R. J. Felix, D. Weber, O. Gutierrez, D. J. Tantillo, M. R. Gagné, *Nat. Chem.* **2012**, *4*, 405–409.

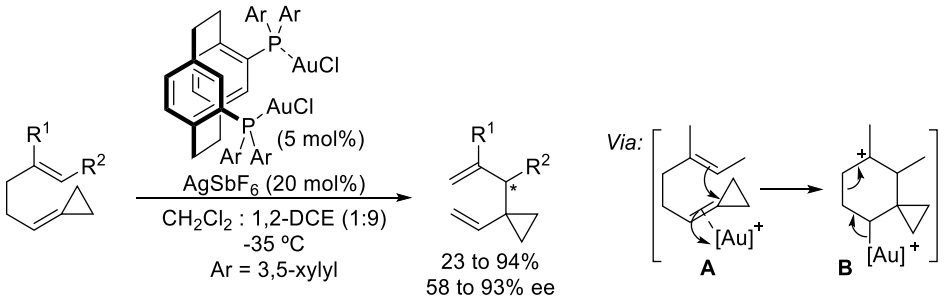

Scheme 162. Au(I)-catalyzed enantioselective Cope rearrangement of ACPs.

1.3. Pyridine as chelation assistant directing group in transition metal catalyzed C-C bond activations

The activation of Csp^3-Csp^3 bonds faces many challenges and, compared to the activation of C-H bonds is less developed. This is mainly due to the inertness of C-C bonds and their high directionality, which disfavor the interaction with metals. A strategy used to overcome this problem consists of anchoring directing groups (DGs) to the substrate, that drives the metal to the reacting site favoring the reaction (Figure 25). In some cases, functional groups of the substrates can be used as directing groups (carboxylic acids, alcohols, etc.) representing an ideal scenario, but this is not very common.

Thus, the incorporation of directing groups is a well-known strategy in C-C activation processes, where a chelating ligand located close to the target bond result in an energy release through the formation of stabilized metalacyclic complexes.[148] Meanwhile the use of permanent directing groups such as pyridine or 8-acylquinoline has been explored,[149] a more practical and desirable use of transient directing groups are still underdeveloped.

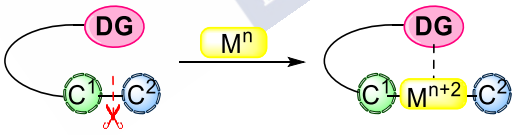

Figure 25. Directed intramolecular metal promoted C-C activation.

An example of the use of pyridine as permanent directing group was reported by Matsuda, in 2016 (Scheme 163).[150] Using (2-pyridylmethylene)cyclobutenes and different alkynes in presence of a rhodium (I)/PPh_3 catalyst, different aromatic rings can be assembled through a formal (4+2) annulation. The reaction mechanism starts with the pyridine directed C-C cleavage of the cyclobutene (**A**), which is possible only in with the *E* form of the starting

[148] L. Souillart, N. Cramer, *Chem. Rev.* **2015**, *115*, 9410–9464.
[149] (a) J. W. Suggs, C. H. Jun, *J. Chem. Soc. Chem. Commun.* **1985**, 92–93. (b) A. M. Dreis, C. J. Douglas, *J. Am. Chem. Soc.* **2009**, *131*, 412–413. (c) J. Wang, W. Chen, S. Zuo, L. Liu, X. Zhang, J. Wang, *Angew. Chemie - Int. Ed.* **2012**, *51*, 12334–12338.
[150] T. Matsuda, T. Matsumoto, *Org. Biomol. Chem.* **2016**, *14*, 5023–5027.

material. The alkyne is then incorporated through a migratory insertion (**B**), which generates the products after a reductive elimination and further aromatization.

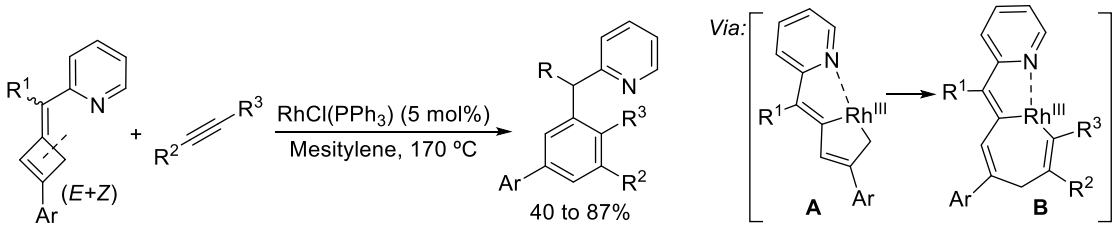

Scheme 163. Rh(I)-catalyzed intermolecular (4+2) annulation of cyclobutenes and alkynes.

Dong and coworkers explored in 2014 the use of 2-amino-pyridines as transient directing groups for a C-C activation/ring-expansion reaction (Scheme 164).[151] This report show how different tethered alkenylcyclobutanones in presence of a rhodium (I) catalyst leads to different fused six-membered carbocycles, in variable yields and diastereoselectivities. The reaction begins with the formation imine which directs the C-C oxidative addition of the rhodium (I) complex leading to the rhodacycle **A.** An intramolecular migratory insertion of the tethered alkene leads to the intermediate which, after reductive elimination and a subsequent hydrolysis, provides bicyclic adduct. A related work of 2019 showed that the reaction can occur in an intermolecular fashion, using indanones and ethylene as reaction counterparts for a 2C ring expansion reaction.[152]

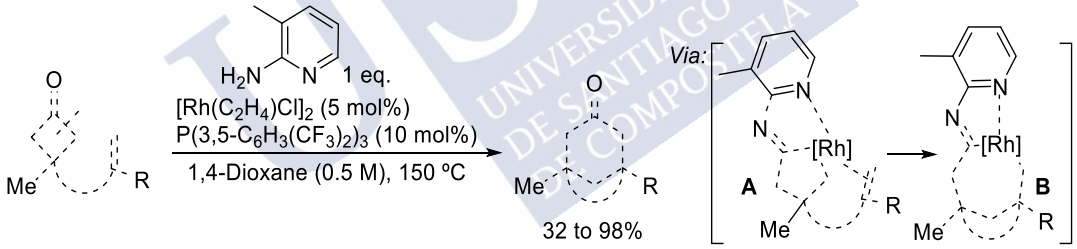

Scheme 164. Rh(I)-catalyzed intramolecular (4+2) annulation of cyclobutanones and alkenes.

[151] H. M. Ko, G. Dong, *Nat. Chem.* **2014**, *6*, 739–744.
[152] Y. Xia, S. Ochi, G. Dong, *J. Am. Chem. Soc.* **2019**, jacs.9b07445.

2. Objectives

In the context of a research stay at the University of Zurich, in the group of Prof. Cristina Nevado, we explored the reactivity of (2-pyridyl)methylenecyclopropanes in presence of different gold species. In particular, we considered that gold (I) complexes could participate in a pyridine directed C-C activation of the proximal bond of the alkylidenecyclopropanes of type **79** through an oxidative addition mechanism. Thus, new bicyclic (N^C^C) gold (III) complexes of type **80** could be obtained. This would be particularly interesting due the lack of C-C activation processes promoted by gold(I) complexes (Scheme 165).[153]

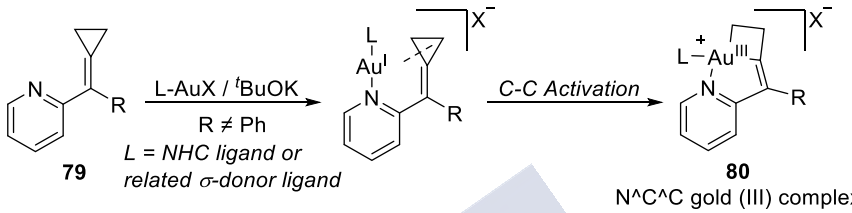

Scheme 165. Initial hypothesis of gold mediated C-C and C-H activation reactions.

On the other hand, we hypothesized that alkylidenecyclopropanes of type **79a** with a phenyl substituent at the alkene, could preferentially react with Au(III) complexes through a redox neutral intramolecular C-H activation, leading to six membered (N^C) gold (III) complexes of type **81**, thus opening new opportunities to explore the catalytic and photophysical properties of these and related Au(III) complexes. In summary, we wanted to explore whether we could use pyridine-substituted ACPs to induce different C-H or C-C activations, depending on the nature of the catalyst and substrate (Scheme 166).

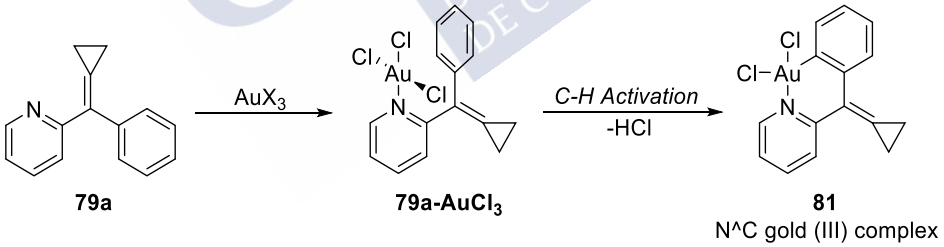

Scheme 166. Initial hypothesis of gold mediated C-C and C-H activation reactions.

[153] For a review of reactivity of gold complexes in organometallic reactions see: M. Joost, A. Amgoune, D. Bourissou, *Angew. Chemie - Int. Ed.* **2015**, *54*, 15022–15045.

3. Results and discussion

For the formation of the new gold (III) complexes we used three different (2-pyridyl)methylenecyclopropanes. Compounds **79(a-c)** bearing a Ph, Me and H substituents were synthesized from their corresponding 2-carbonylpyridines through a Wittig reaction leading to the products in an excellent 90% when (R = Ph), and poor yields when (R = Me, H).

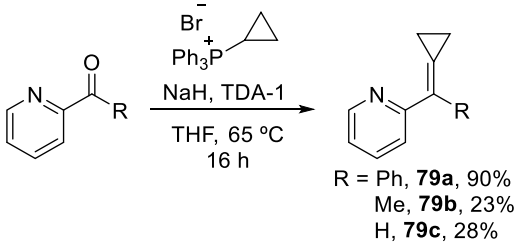

Scheme 167. Synthesis of substrates **79a**, **79b** and **79c**.

3.1. Exploration using gold (III) sources

3.1.1. Cyclometallation reactions

At the outset, we explored the reactivity of **79a** in the presence of **$NaAuCl_4$** as source of gold (III). Thus, we combined equimolar amounts of an acetonitrile solution of the pyridine **79a** with an aqueous solution of $NaAuCl_4$ (solvents ratio 1 :1). After stirring for 5 minutes at room temperature, the formation of an orange solid was noticed, which get slowly dissolved over time. The reaction was stopped after 2 hours, and a mixture of two different products was detected by ^{1}H-NMR.

Surprisingly, instead of the hypothesized product resulting from the C-C activation, a new stable metallacycle **82a** was isolated in a good 75% yield, which structurally determined through X-ray crystallography (Figure 26). Moreover, a second product, eventually identified as the spirocyclic gold complex **83a,** was also observed in 15% yield. Unfortunately, this product could not be isolated due to its lower stability.[154]

The mechanism behind the formation of the major compound **82a**, is not trivial. On the other hand, the formation of the spirocyclic complex **83a** could involve a coordination of gold to give **79a-$AuCl_3$**, and a subsequent activation of the double bond to induce a nucleophilic addition of a chloride ion (direct or through a carbocationic intermediate). This mechanism is similar to the reported by Cinellu (Scheme 173),[155] which uses a methylene group instead of an alkylidenecyclopropane, although in this report harsh reaction condition were required. Thus, despite the formation of this particular complex is not restricted to the presence of the cyclopropilic moiety, it is clear that the energetic demand in our case is significantly lower.

[154] The compound was identified by analogy with other cases (vide infra).
[155] M. A. Cinellu, F. Cocco, G. Minghetti, S. Stoccoro, A. Zucca, M. Manassero, *J. Organomet. Chem.* **2009**, *694*, 2949–2955.

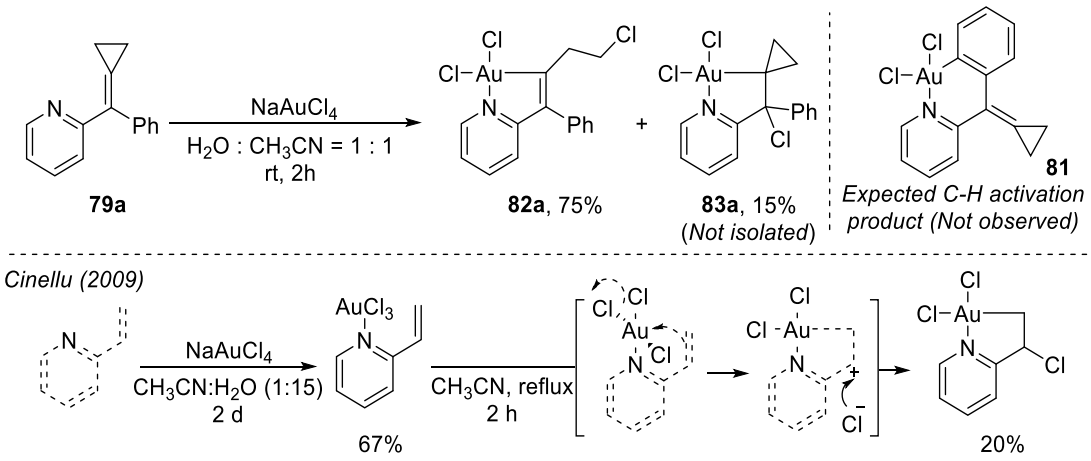

Scheme 168. Cyclometallation reaction of **79a** with $NaAuCl_4$.

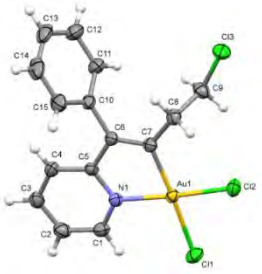

Figure 26. Crystal structure of C^N-Au(III) complex **82a**.

We repeated the reaction under the same conditions, but it was stopped after 15 minutes to isolate the initially formed orange solid. To our delight, we were able to crystallize this solid that turned out to be the gold (III) coordinated to pyridine **79a-AuCl$_3$** which was isolated in a 52% yield.

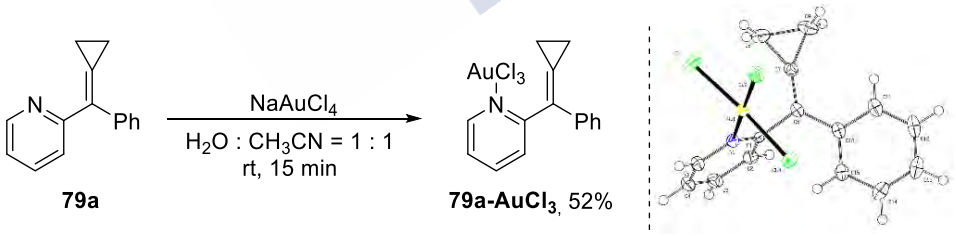

Scheme 169. Synthesis of coordinated complex **79a-AuCl$_3$** and its crystal structure.

Next, we evaluated the same reaction conditions in substrates **79b** and **79c** (R = Me, H). Gratifyingly, metallacycles of type **82** were obtained in good yields R = Me (**82b**), and in 40% yield when R = H (**82c**). On the other hand, spirocyclic compounds where obtained in a 30% yield when R = Me (**83b**), and in a 18% when R = H (**83c**). In this case, the spirocyclic complexes could be isolated and fully characterized. Moreover, the structures of **82b** and **82c** were further confirmed through X-ray crystallography (Scheme 170).

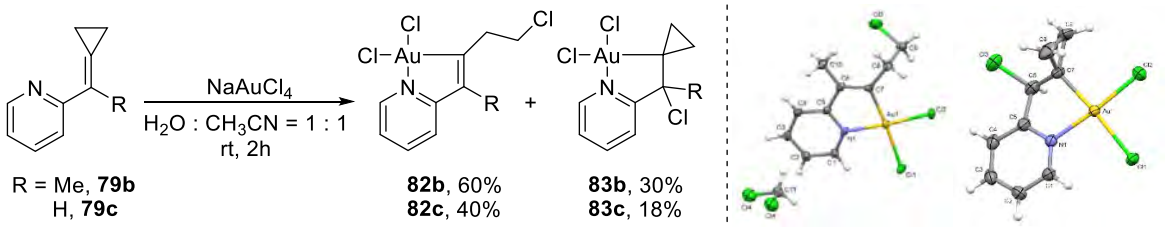

Scheme 170. Cyclometallation reaction for **79b** and **79c**. (b) Crystal structure of **82b** and **82c**.

Using $AuCl_3$ as gold (III) source we also observed the cyclometallation reactions, but in this case the reaction was sluggish, leading to **82a** in 50% yield in combination with a 20% of the coordinated species **79a-AuCl₃** (Table 23, entry 1 vs 2). Interestingly, the more stable $AuBr_3$ showed to be a more competent gold (III) source, leading to **82a`** in an excellent 81% yield (entry 3). Other sources like $Au(OAc)_3$ or $Au(OH)_3$ did not provide the cyclometallated species, even after heating (entry 4 and 5).

Table 23. Cyclometallation with different gold (III) sources.

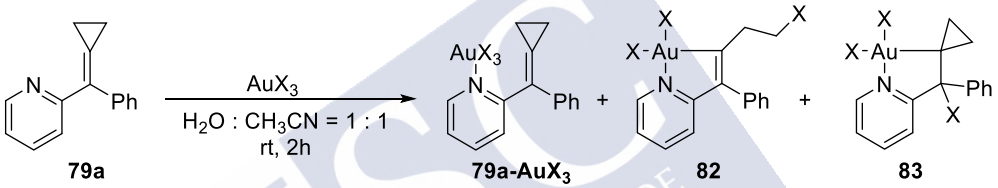

Entry	AuX_3	Conv. (%)[c]	79a-AuX_3 (%)[c]	82 (%)[b]	83 (%)[c]
1	$NaAuCl_4$	100	-	75	15
2	$AuCl_3$	100	20	50	-
3	$AuBr_3$	100	-	81	-
4[a]	$AuOAc_3$	-	-	-	-
5[a]	$AuOH_3$	-	-	-	-

[a] *Reaction conditions*: **79a** (0.15 mmol), AuX_3 (1 eq.), H_2O/CH_3CN (1 : 1) [0.01 M], rt. [b] Isolated yield. [c] Determined by ^{1}H-NMR using 1,3,5-trimethoxybenzene as internal standard.

The reactions of substrates **79b** and **79c** with $AuBr_3$ proceeded smoothly. In particular, the reaction of **79b** (R = Me) selectively provided the metallacycle **82b`** in 60% yield. Curiously, when substrate **79c** (R = H) was used, a mixture of the metallacycle **82c`** and a new cyclobutanic gold complex **84`** was obtained. This product was characterized by X-ray crystallography (Scheme 176).

The formation of the cyclobutanic complex **84`** can be explained based on previous reports of ring expansion reactions of alkylidenecyclopropanes mediated by transition metal complexes.[156] The reaction starts by the coordination of gold by the pyridine moiety leading to

[156] (a) A. Fürstner, C. Aïssa, *J. Am. Chem. Soc.* **2006**, *128*, 6306–6307. (b) M. Shi, L. P. Liu, J. Tang, *J. Am. Chem. Soc.* **2006**, *128*, 7430–7431. (c) R. Castro-rodrigo, M. A. Esteruelas, S. Fuertes, A. M. Lo, F. Lo, L. Mascaren, S. Mozo, E.

complex **79c-AuBr$_3$**, which further activates the π-system of the C=C bond, leading to the cationic species **A**. This cationic species is poorly stabilized, triggering a *1,2*-carbon shift which leads to the more stable intermediate **B**. Finally, a free bromide ion attacks the carbocation leading to the complex **84`**.

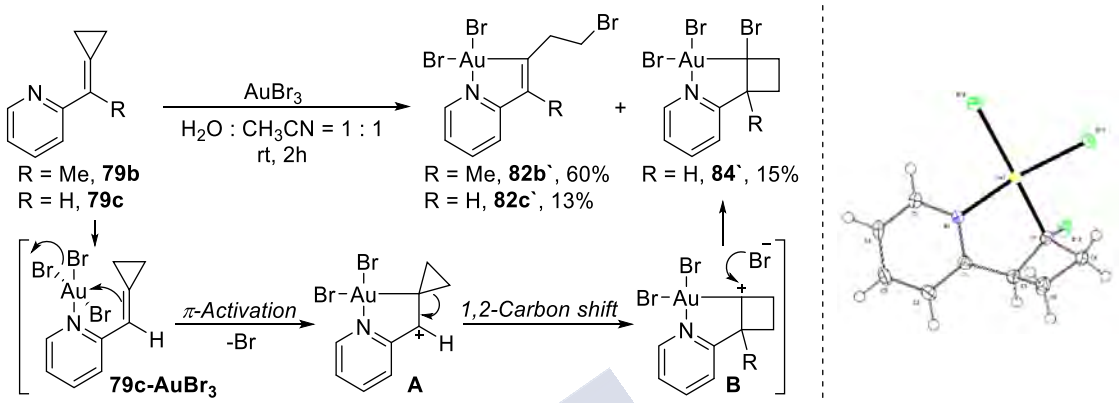

Scheme 171. Cyclometallation reaction of **79b** and **79c** with $AuBr_3$ and the crystal structure of **84`**.

3.1.2. Mechanistic studies to explain the formation of complex **82a**

To the best of our knowledge, the above cyclometallation reaction is unprecedented. Moreover, the formation of cyclometallated (N^C) gold (III) species generally requires the use harsh reagents or reaction conditions.[157] In contrast, this new reaction takes place using only water and acetonitrile as solvents, at room temperature and with short reaction times, providing the cyclometallated complexes in good yields.

To further evaluate the mechanism, we primarily analyzed whether the observed reactivity is exclusive of alkylidenecyclopropanes. We synthesized the analogue **88** bearing two methyl groups instead of the cyclopropane and also the alkylidenecyclobutane **89**. When both compounds were separately submitted to the reaction conditions, none of them led to any cyclometallated species, recovering the starting materials. Thus, the alkylidenecyclopropane moiety is required to obtain the observed reactivity, *suggesting that the reaction is related to a strain release driven process*.

On, L. Villarino, **2009**, 15572–15573. (d) Y. Wang, M. E. Muratore, Z. Rong, A. M. Echavarren, *Angew. Chemie - Int. Ed.* **2014**, *53*, 14022–14026.

[157] R. Kumar, C. Nevado, *Angew. Chemie - Int. Ed.* **2017**, *56*, 1994–2015.

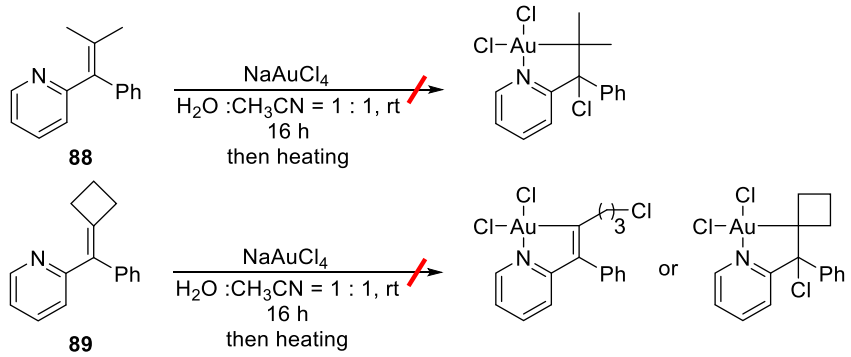

Scheme 172. Control experiments of cyclometallation.

Next, we studied the effect of the solvents in the cyclometallation reaction (Table 24). For this purpose, we monitored the evolution of complex **79a-AuCl$_3$** in different solvents by ^{1}H-NMR. Polar solvents such as H_2O/CH_3CN (1:1) or ^{t}BuOH led to mixtures of cyclometallated species **82a** and **83a** with similar ratios (entry 1 and 2), with uncomplete conversion in the case of the ^{t}BuOH . Interestingly, when anhydrous CH_2Cl_2 was used, the compound **82a** was selectively obtained, *suggesting that polar solvents could favor the formation of* **83a**, *probably through a cationic mechanism*.

Table 24. Solvent effect in cyclometallation reaction.

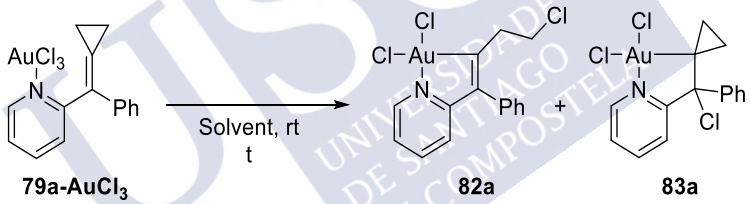

Entry	Solvent	Conv. (%)[b]	82a : 83a [b]
1	H_2O/CH_3CN (1 : 1)	100	4.5 . 1
2	^{t}BuOH	80	3.3 : 1
3	CH_2Cl_2	100	1 : 0

[a] *Reaction conditions*: **79a** (0.05 mmol), solvent [0.01 M], rt. [b] Determined by ^{1}H-NMR using 1,3,5-trimethoxybenzene as internal standard.

We wondered whether the formation of complexes **82a** and **83a** could be mechanistically related. More specifically, we considered the possibility that **83a** could evolve towards **82a** after a ring opening process. For this purpose, we exposed 4 to 1 mixture of a **83a** and **82a** to different conditions, and the changes in the **83a**/**82a** ration were measured by 1H-NMR using 1,3,5-trimethoxybenzene as internal standard.

Since the gold (III) complexes were usually purified by filtration in silica gel, we speculate that the SiO_2 could affect the products ratio. However, when a mixture of **83a** and **82a** (4:1) in CH_2Cl_2 was mixed with SiO_2 and stirred for 2 h at room temperature, the amount of **83a** drop

by half, but no increment of **82a** was observed (Table 25, entry 1). This suggests that SiO_2 promotes the degradation of **83a,** while **82a** is not affected**.**

Next, when the solution (4:1) in CH_2Cl_2 was stirred for 24 h at room temperature, the ratio remained invariable, whereas heating to 80 ºC and 1 h to 120 ºC, we observed a subtle decrease of **83a** but no increment in **82a** (entry 2 - 4). A similar reaction result was observed when a H_2O/CH_3CN (1:1) mixture was used as solvent (entry 5 and 6). All together, these results suggest that both compounds are generated independently and are not mechanistically involved.

Table 25. Control experiments of isomerization reaction.

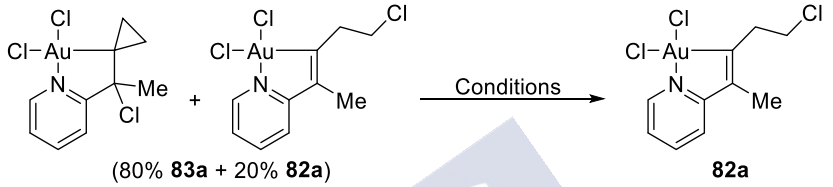

Entry	Solvent	Additive	t (h)	T (°C)	83a : 82a (%)[b]
1	CH_2Cl_2	SiO_2	2	25	40 : 20
2	CH_2Cl_2	-	24	25	80 : 20
3	CH_2Cl_2	-	1	80	85 : 20
4	CH_2Cl_2	-	2	120	70 : 20
5	H_2O/CH_3CN (1 : 1)	-	2	25	85 : 15
6	H_2O/CH_3CN (1 : 1)	-	12	80	80 : 15

[a] *Reaction conditions*: Mixture of **83a** and **82a** (8 : 2) (0.10 mmol), solvent [0.01 M], T (ºC). [b] Determined by ^{1}H-NMR using 1,3,5-trimethoxybenzene as internal standard.

Overall, these experiments confirm that the reaction mechanism is not trivial, so that more information is required in order to make a mechanistic proposal. In this regard, complementary experiments carried out at the University of Zürich have shed light on these mechanistic questions, which will be shortly published.

3.2. Exploration using gold (I) sources

We preliminary explored the reactivity of pyridine **79a** in presence of AuCl as gold (I) source. Using the same abovementioned conditions for the synthesis of cyclometallated gold (III) complexes, full conversion was observed after 2 h. When the crude was analyzed by 1H-NMR, we could identified the product in 55% global yield, and curiously, an 8% yield of the gold (III) cyclometallated complex **82a**.[158] The formation of this complex could be explained assuming a disproportionation of gold (I) into a gold (III) species, under ambient conditions. The resulting

[158] 1,3,5-trimethoxybenzene was used as internal standard.

that can further evolve to complex **82a**. The coordinated complex **79a-AuCl** structure was confirmed by X-Ray crystallography.

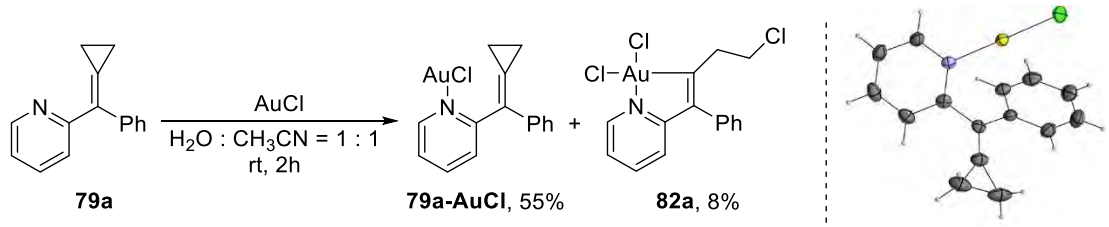

Scheme 173. Synthesis of coordinated complex **79a-AuCl** and its crystal structure.

Importantly, in an attempt to force the C-C activation of the ACP, complex **79a-AuCl** in dry CH_2Cl_2 was heated at 100 °C for 16 h, but unfortunately, no cyclometallated product was found (Scheme 179). Considering the moderate reactivity of neutral **79a-AuCl** we evaluated the reactivity of the corresponding cationic form of this complex. Thus, we tested the performance of **79a-AuCl** , after adding different silver-based chloride scavengers , and followed its evolution through ^{1}H-NMR. At -78 °C we were able to detect a stable cationic coordinated **79a-Au$^+$** species, but in all cases it rapidly decomposed upon increasing the temperature. Moreover, in an attempt to stabilize the formed cationic complex, we added NBu_4Cl but it was unfruitful, only leading to decomposition or in the best case, the liberation of the pyridine **79a**.

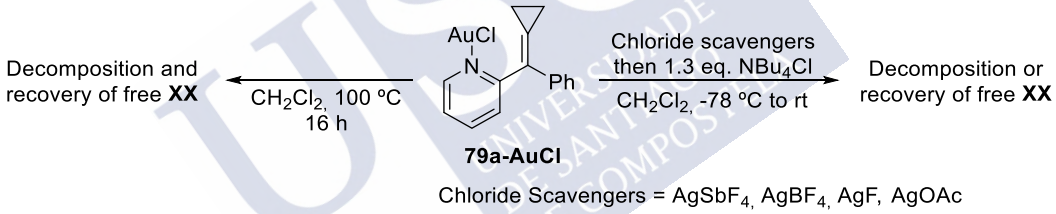

Scheme 174. Chloride abstraction experiments of **79a-AuCl**.

Thus, in a preliminary exploration, we have found that **79a-AuCl** complexes or cationic **79a-Au$^+$** does not promote, *a priori*, a C-C activation process on this 2-(cyclopropylidenemethyl) pyridine moiety. Thus, based on these complications and in the short time available for the research stay, we decided to focus our efforts in the results obtained using gold (III) sources.

3.3. Exploring the reactivity of the cyclometallated (N^C) gold (III) complexes

Based on the promising results obtained in the formation of stable cyclometallated (N^C) gold (III) complexes, we decided to further study the reactivity of complex **82a**. Based on their structure, we envisioned that this type of complex could be used to study elementary steps related to cross-coupling reactions. Thus, we planned a *step-by-step* study of transmetallation and reductive elimination processes.

3.3.1. Transmetallation experiments

We started studying the reactivity of **82a** in the presence of boronic acids with different bases. Considering that electron-poor boronic acids promote slower reductive elimination processes

than their electron-rich homologous, we decided to use 4-fluorophenyl boronic acid as reaction counterpart, in attempts to generate stable intermediates. Thus, these compounds can be eventually isolated and characterized.

At the outset, we mixed complex **82a** and the boronic acid but the formation of any transmetallated complexes was not detected (Table 26, entry 1). The use K_2CO_3 or KOH lead to a full conversion of the starting material, but only complex mixtures were generated (entry 2 and 3). On the contrary, K_3PO_4 was able to promote the transmetallation efficiently, leading to equimolar amounts of the complexes ***cis*-85** and ***trans*-85** (entry 4). Interestingly, when the reaction was carried out at 50 ºC for 16 hours, a mixture of ***trans*-85** with a small portion of bis-transmetallated species **86** was obtained in an excellent overall yield (entry 4).

Table 26. Screening of different bases for the transmetallation reaction.

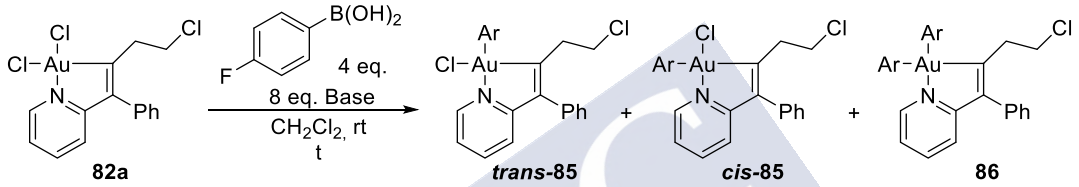

Entry	Base	t (h)	T (ºC)	Conv. (%)[c]	*trans*-85 (%)[c]	*cis*-85 (%)[c]	86 (%)[c]
1	-	5	25	5	-	-	-
2	K_2CO_3	1	25	100	-	-	<5
3	KOH	1	25	100	-	-	-
4	K_3PO_4	1	25	50	25	25	-
5	K_3PO_4	16	50	100	83[b]	-	16

[a] *Reaction conditions*: **82a** (0.10 mmol), Base (8 eq.), Boronic acid (4 eq.), dry CH_2Cl_2 [0.01 M], rt. [b] Isolated yield. [c] Determined by ^{1}H-NMR using 1,3,5-trimethoxybenzene as internal standard.

Gratifyingly, both mono-transmetallated complexes ***cis*-85** and ***trans*-85** were isolated, characterized and further crystallized using CH_2Cl_2/Benzene mixtures. Their crystal structure was confirmed by X-ray crystallography (Figure 27). Unfortunately, the crystallization of bis-transmetallated complex **86** was not possible because it rapidly decomposes.

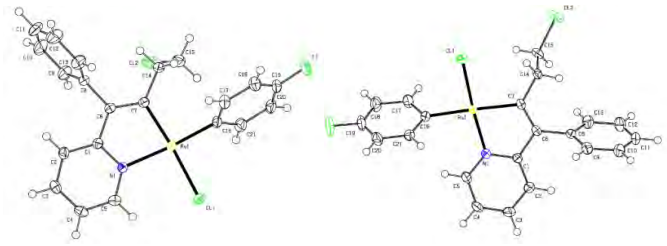

Figure 27. *Structure of monotransmetallated complexes **trans*-85** and **cis*-85** obtained by X-ray crystallography.*

Then we studied the stoichiometry of the reaction (Table 27). Using 1 or 2 eq. of boronic a slow conversion was observed leading to mixtures of mono-transmetallated products in similar

amounts (entry 1 and 2). Interestingly, using an excess of boronic acid (4 eq.), after 4 hours, we could observe the selective formation of ***trans*-85**, which was isolated in a 95% yield (entry 3).

Table 27. Transmetallation experiments modifying stoichiometry.

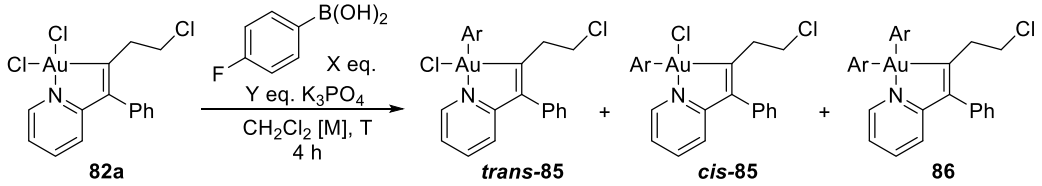

Entry	X (eq.)	Y (eq.)	t (h)	Conv. (%)[c]	*trans*-85 (%)[c]	cis-85 (%)[c]	86 (%)[c]
1	1	2	20	33	6	17	-
2	2	4	20	60	21	25	-
3	4	8	4	100	95[b]	<5	<5

[a] *Reaction conditions*: **82a** (0.10 mmol), Boronic acid (X eq.), K_3PO_4 (Y eq.), dry CH_2Cl_2 [0.01 M], T (ºC). [b] Isolated yield. [c] Determined by ^{1}H-NMR using 1,3,5-trimethoxybenzene as internal standard.

The results exposed in table 27 suggest that the evolution of mono-transmetallated isomers could be related. Therefore, we evaluated whether they could isomerize under reaction conditions through ^{1}H-NMR.[159] Interestingly, ***trans*-85** showed a high stability, and no significative variation was noticed (Scheme 180a). We were surprised to see that compound ***cis*-85** spontaneously isomerized to ***trans*-85**. Moreover, the conversion was significatively faster when the sample was exposed to a Blue LED (Scheme 180b).

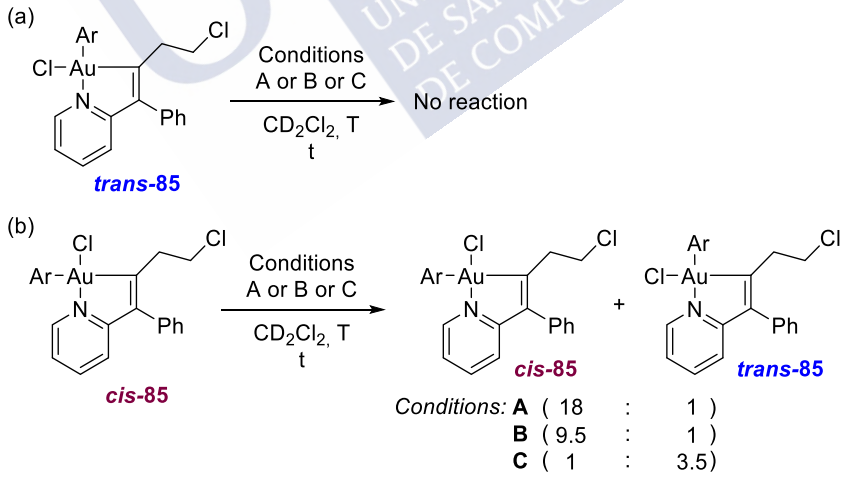

Scheme 175. Stability experiments of mono-transmetallated gold (III) complexes.

Based on this new evidence, we evaluated the transmetallation reaction in the absence of light (Scheme 181). Surprisingly, after 1 hour the major formation of ***cis*-85** was observed and

[159] [a] *Reaction conditions*: ***cis*-85 or *trans*-85** (0.01 M) in $CDCl_2$. The reaction was carried out in an NMR tube. [b] rt, 2 h. [c] 40 ºC, 16 h. [d] rt, Blue LED, 6h.

eventually isolated in 40% yield. After this time, the amounts of ***cis*-85** began slowly to decrease, and the formation of ***trans*-85** was detected by 1H-NMR.

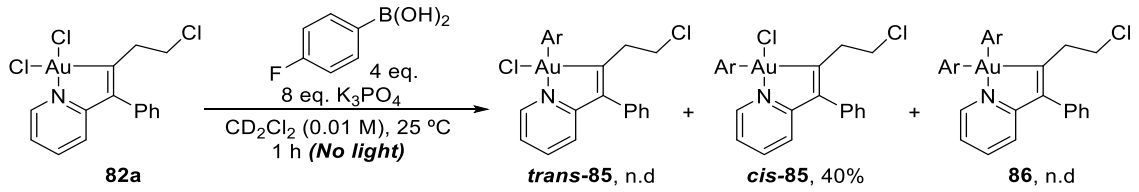

Scheme 181. Transmetallation experiment carried out in absence of light.

On these bases, it seems reasonable to propose that the compound ***cis*-85** is kinetically favored. This is supported by the strong *trans* effect observed in the X-Ray structure of the product **82b** (R=Me). The Au-Cl[1] bond is significantly longer (2.39 Å) than Au-Cl[2] (2.28 Å), facilitating its participation in a transmetallation step.

Regarding the formation of the bis-transmetallated product **86**, similar characteristic was observed in the Au-Cl bond lengths of both mono-transmetallated precursors in solid state (***trans*-85** (2.35 Å) and ***cis*-85** (2.27 Å)). Nevertheless, additional studies are still required to fully understand these processes.

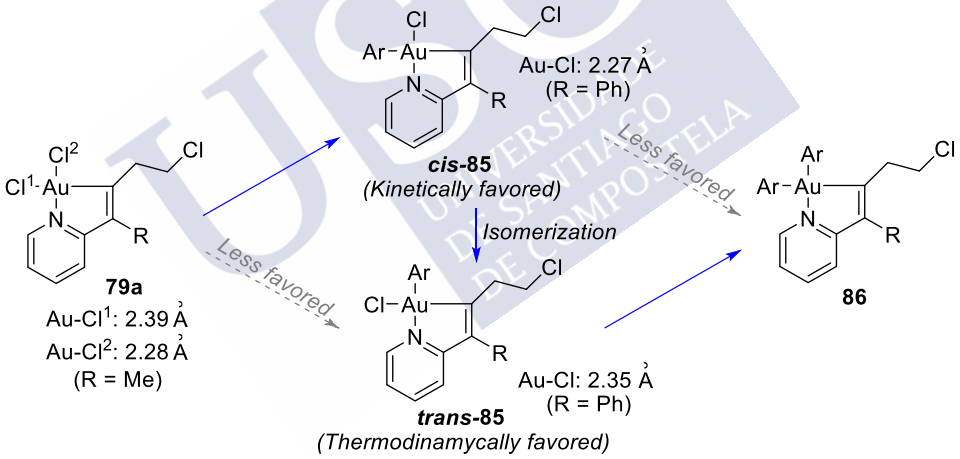

Scheme 176. Putative evolution of transmetallation reactions.

3.3.2. Reductive elimination experiments

We preliminary investigated the reductive elimination step using ***trans*-85** and **86**. We found that ***trans*-85** leads to the desired cross-coupling product **87**, but in a modest 30% yield requiring temperatures of 150 ºC and long reaction times. On the other hand, the bis-transmetallated metallacycle **86** showed to be much more reactive, leading to small portions of the desired product **87** in combination with high amounts of the homo-coupling product 4,4'-difluoro-1,1'-biphenyl.

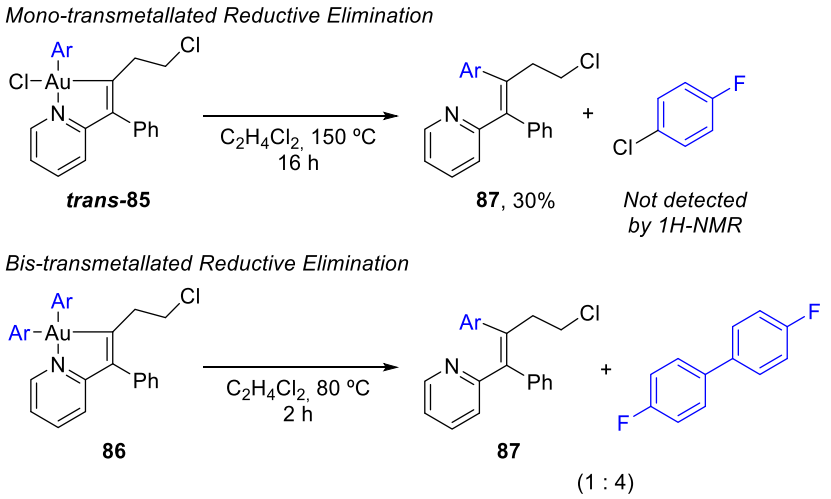

Scheme 177. Reductive elimination experiment for ***trans*-85** and **86** complexes.

As has been presented, the (C^N) gold (III) complexes obtained from the novel cyclometallation reaction of alkylidenecyclopropanes have shown to be competent substrates for transmetallation and reductive elimination processes. Nevertheless, these studies are preliminary, so that their application to the development of catalytic applications has to be further investigated.

4. Conclusions

In conclusion, in collaboration with the group of Prof. Cristina Nevado of the University of Zurich, we have explored the reactivity of 2-(cyclopropylidenemethyl)pyridines in presence of gold (I) and gold (III) species. Unexpectedly, using gold (III) sources we discovered new strain release-promoted cyclometallation reactions, that takes place under mild conditions leading to novel metallacycles in good yields. Thus, three types of complexes were identified, based on C-C, C=C or C-C and C=C bond activations (Scheme 184). Whereas complexes **82** were obtained through a C-C activation process, spirocyclic products **83** would be obtained through a π-activation of the C=C bond of the cyclopropane. A final cyclobutanic complex of type **84**, product of a π- and further C=C activations was also isolated and identified.

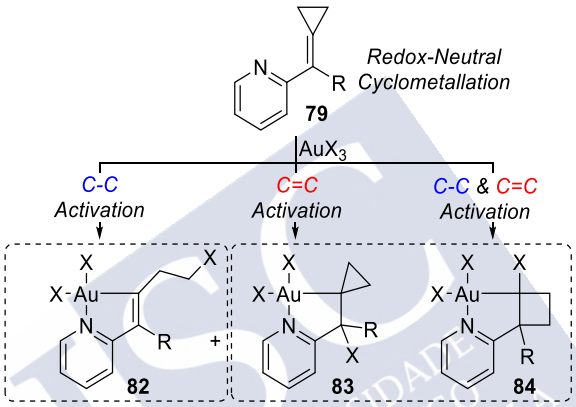

Scheme 178. Cyclometallation reaction of alkylidenecyclopropanes with gold **III** sources.

The reactivity of the complex **82a** was further studied in transmetallation experiments. The combination of this complex with 4-fluorophenylboronic acid and K_3PO_4 lead to different transmetallated species. Experiments suggest that kinetically favored ***cis*-85** complex is formed first and can rapidly isomerizes to thermodynamic product ***trans*-85**. The second transmetallation seems slower, being formed mainly from complex ***trans*-85**. In both transmetallations, the cleavage of the chloride *cis* to the gold atom seems to be favored, which is agrees with the strong *trans*-effect induced by the Csp^2-Au bonded to the metal center. This can be confirmed by the length measured of these corresponding Au-Cl[1] bonds.

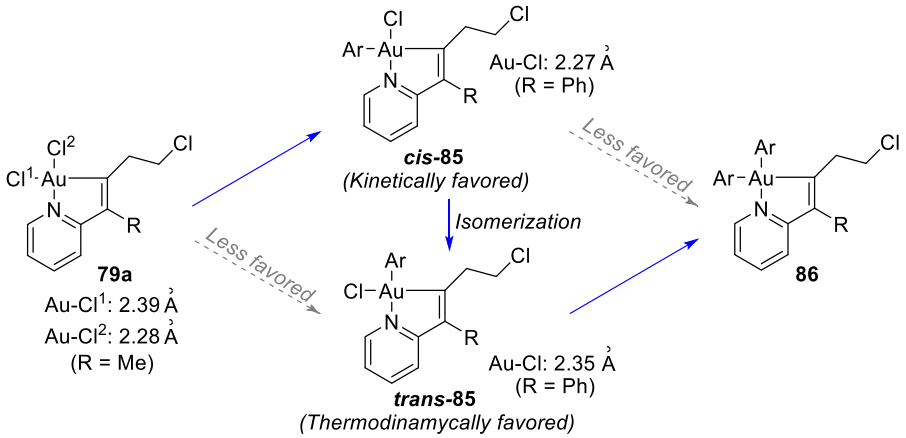

Scheme 179. Evolution of transmetallated species.

Finally, we preliminary evaluate the reductive elimination starting from complexes ***trans-85*** and **86**. In the case of the monotransmetallated complex ***trans-85***, the desired cross coupling product was isolated in a 30% yield as single product but requiring high temperatures and long reaction times. On the other hand, bis-transmetallated complex **86** showed a faster evolution at lower temperature leading also to the desired reductive elimination product **87**, but in combination with the homo-coupling adduct as major product.

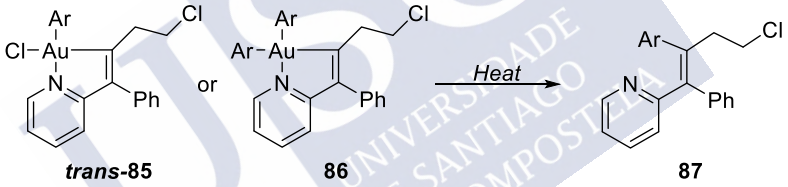

Scheme 180. Reductive elimination experiments.

Experimental part

USC
UNIVERSIDADE
DE SANTIAGO
DE COMPOSTELA

General procedures

Dry solvents were freshly distilled under argon from an appropriate drying agent according to Perrin[160] indications before its use. Toluene, 1,4-Dioxane and THF were dried over Na/benzophenone; CH_2Cl_2, diisopropylamine and Et_3N over CaH_2. Other solvents such as CH_3CN, C_6H_6 and $C_6H_5CF_3$ were obtained commercially dry.

Reagents employed in the synthesis of starting materials were purchased from Sigma Aldrich, Alfa Aesar, TCI or Acros and used without further purification. Substrates **22**,[161] **31**,[163] **16**,[162] **22,**[162] **24**,[175] **48a**,[163] **56a**,[177] **56b**,[164] **56c**,[165] **56d**,[166] **56e**,[167] **79b**,[168] **79c**[168] and cycloaddition precursors **3b**,[161] **3c**,[161] **3g**,[161] **3h**, [161] **3m**, [161] **3n**, [161] **3o**, [161] **9a**,[163] **9b**,[163] **9d**[163] and **9e**[163] are known compounds and were synthesized following reported procedures. Chiral phosphoramidites **L2,**[163] **(*R*,*R*)-L3,**[163] **(*S*,*R*,*R*)-L4,**[169] **(*R*,*R*,*R*)-L4,**[169] **(*S*,*R*,*R*)-L5,**[162] **(*S*)-L6,**[162] **(*S*,*R*,*R*)-L7,**[170] **(*R*,*R*,*R*)-L7,** [177] **(*S*,*R*,*R*)-L8,**[162] **(*S*,*R*,*R*)-L9,**[162] **(*S*,*R*,*R*)-L10,**[162] **(*S*,*R*,*R*)-L11,**[162] **(*S*)-L12,**[171] **(*R*,*R*)-L14,**[172] **(*R*,*R*)-L15,**[173] **(*S*,*R*,*R*)-L16**[162] and **(*S*,*R*,*R*)-L17**[174] are known compounds and were synthesized following reported procedures. Ligands **L1**, RuPhos, BrettPhos, tBuBrettphos, XPhos and tBuXPhos are commercial, and were purchased from Sigma Aldrich and Alfa Aesar. All other reagents used were purchased from Aldrich, Alfa Aesar, TCI or Acros and used without further purification. The glassware used in the reactions was dried in an oven heating at 150 ºC for 4 h, followed by cooling under argon atmosphere. Reactions were conducted in dry solvents under argon atmosphere unless otherwise stated. The abbreviation "rt" refers to reactions carried out approximately at 23 °C. Reaction mixtures were stirred using Teflon-coated magnetic stirring bars. For reactions at high temperatures, Thermowatch-controlled silicone oil baths or aluminum heating plates were used. For reaction at low temperatures, ice baths (0 ºC) and ice/NaCl (-15 ºC) were used. The additions of solutions were carried out via syringe or cannula. The syringes used were plastic (Braun©) and Teflon (Hamilton©), with Sterican® (Braun©) needles. Thin-layer chromatography (*tlc*) was performed on silica gel plates F_{254}

---

160 D. Perrin, W. L. F. Armarego, *Purification of Laboratory Chemicals*, Butterworth-Heinemann, **2003**.
161 M. Gulias, R. Garcia, a Delgado, L. Castedo, J. L. Mascarenas, *J. Am. Chem. Soc.* **2006**, *128*, 384–385.
162 F. Verdugo, L. Villarino, J. Durán, M. Gulías, J. L. Mascareñas, F. López, *ACS Catal.* **2018**, *8*, 6100–6105.
163 M. Gulías, J. Durán, F. López, L. Castedo, J. L. Mascareñas, *J. Am. Chem. Soc.* **2007**, *129*, 11026–11027.
164 S. Mondal, S. Yetra, A. Patra, S. Kunte, R. G. Gonnade, A. T. Biju, *Chem. Comm.*, **2014**, *50*, 14539-14542.
165 S. Bera, R. C. Samanta, C. G. Daniliuc, A. Studer, *Angew. Chem. Int. Ed.*, **2014**, *53*, 9622-9626.
166 R. Watile, A. Bunrit, J. Margalef, S. Akkarasamiyo, R. Ayub, E. Lagerspets, S. Biswas, T. Repo, J. S. M. Samec, *Nat. Comm.*, **2019**, *10*, 1-9.
167 B. Y. Majama, *Am. Jour. Org. Chem.*, **2012**, *2(6)*, 127-131.
168 J. Medina, T. Kang, T. G. Erbay, H. Shao, G. M. Gallego, S. Yang, M. Tran-Dubé, P. F. Richardson, J, Derosa, R. Helsel, R. L. Patman, F. Wang, C. P. Ashcroft, J. F. Braganza, I. McApline, P. Liu, K. M. Engle. *ACS Catal*. **2019**, *9*, 11130-11136.
169 B. L. Feringa, M. Pineschi, L. A. Arnold, R. Imbos, A. H. M. De Vries, *Angew. Chemie (International Ed. English)* **1997**, *36*, 2620–2623.
170 D. R. Tobergte, S. Curtis, *J. Chem. Inf. Model.* **2013**, *53*, 1689–1699.
171 H. Harada, R. K. Thalji, R. G. Bergman, J. A. Ellman. *J. Org. Chem.*, **2008**, *73*, 6772-6779.
172 Juan Durán Verdasco, *Tesis doctoral*, **2011**.
173 C. Monti, C. Gennari, U. Piarulli, Chem. Eur. J. **2007**, *13*, 1547-1558.
174 S. S. Goh, S. Guduguntla, T. Kikuchi, M. Lutz, E. Otten, M. Fujita, B. L. Feringa, *J. Am. Chem. Soc.* **2018**, *140*, 7052–7055.

Merck and components were visualized by observation under UV light (254 nm), and then by treating the plates with *p*-anisaldehyde or cerium nitrate solutions, followed by heating. Flash chromatography was carried out on silica gel 60 (40-63 μm) unless otherwise noted, and as eluent a mixture of hexane/EtOAc (or diethyl ether) in varying proportion depending on the need. The solutions resulting from the elaboration of the different reactions were dried with anhydrous Na_2SO_4 or $MgSO_4$. Concentration refers to the removal of volatile solvents via distillation using a Büchi rotary evaporator followed by residual solvent removal under high vacuum.

NMR spectra were recorded in $CDCl_3$ unless otherwise noted, at spectrometers VARIAN Mercury-300 (300.13 MHz for ^{1}H and 75.47 MHz for ^{13}C), VARIAN innova-400 (399.97 MHz for ^{1}H and 100.58 MHz for ^{13}C) and VARIAN innova-500 or BRUKER DRX-500 (500.13 MHz for ^{1}H, 125.76 MHz for ^{13}C and 202 MHz for ^{31}P). Chemical shifts are expressed in δ (ppm) and coupling constants in Hz. Carbon types and structure assignments were determined from ^{13}C-DEPT-135. The following abbreviations are used to indicate signal multiplicity: s, singlet; d, doublet; t, triplet; q, quartet; p, pentet; dd, double doublet; ddd, doublet of doublet of doublets; td, triple doublet; dt, doublet of triplets; dq, doublet of quartet; qd, quartet of doublets; m, multiplet; br, broad. NMR spectra were analyzed using MestreNova© NMR data processing software (www.mestrelab.com). Low Resolution Mass Spectra (LRMS) were recorded using the chemical ionization technique by a gas chromatography using an Agilent Technologies 6896N, Network GC System, equipped with the HP 190915-433 column and the Agilent 5976 Network Mass Selective Detector in the chemical ionization mode. For electrospray ionization (ESI), an UHPLC-Mass with Bruker AmaZon SL IT-MS detector was used. High Resolution Mass Spectra (HRMS) were carried out at the CACTUS facility of the University of Santiago de Compostela using a Bruker ESI-TOF BIOTOF II. For HPLC analysis, the samples were filtered through Whatman™ syringe filters (13 mm diameter nylon filter membrane, pore size 0.45 μm). Enantioselectivities were determined in an Agilent HPLC 1100 Series with Chiralpak® IA, IB, IC, IE, IF, IA3, OZ-H and AY-H analytical chiral columns.

CHAPTER I: Enantioselective palladium-catalyzed (3C + 2C) and (4C + 3C) cycloaddition of alkylidenecyclopropanes

1.1. Synthesis of chiral phosphoramidite ligands

Procedure exemplified for the ligand **(*S,R,R*)-L10**.

N,N-Bis((R)-1-(naphthalen-1-yl)ethyl)-8,9-diphenyldiphenanthro[4,3-d:3',4'-f][1,3,2]dioxa phosphepin -18-amine (*S,R,R*)-L10

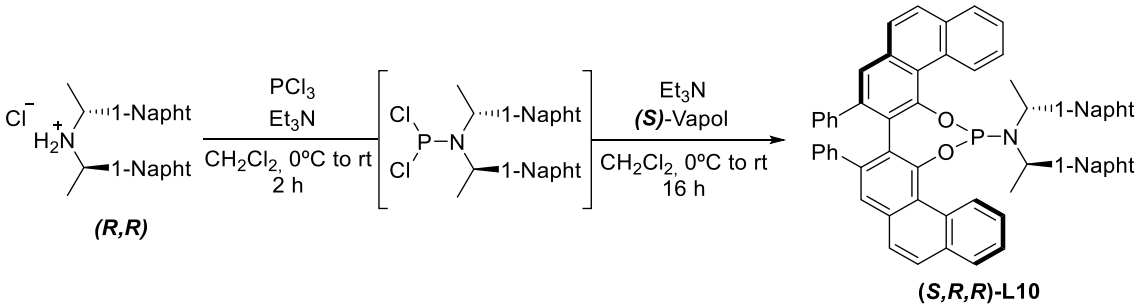

A solution of bis[(*R*)-(−)-(1-naphthyl)ethyl]amine hydrochloride (37 mg, 0.10 mmol, 1.1 eq) and Et_3N (60 µL, 0.42 mmol) in freshly distilled CH_2Cl_2 (1 mL) was added to a dry Schlenck tube containing 3A molecular sieves (300 mg) under Argon. The mixture was cooled down to 0 ºC and PCl_3 (81 µL, 0.93 mmol, 10 eq) was added dropwise. The mixture was stirred at rt for 2 h and the volatiles were carefully removed connecting the Schlenck tube to a high vacuum system. The resulting yellowish solid was dissolved in dry CH_2Cl_2 (1 mL) under argon atmosphere and then volatiles where removed again under vacuum. This procedure was repeated twice in order to remove excess of PCl_3. Then, the resulting residue was dissolved in CH_2Cl_2 (1 mL), Et_3N (60 µL, 0.42 mmol) was added and the mixture was cooled down to 0 ºC. A solution of (*S*)-Vapol (50 mg, 0.09 mmol, 1 eq) and Et_3N (60 µL, 0.42 mmol, 4.5 eq) in freshly distilled dry CH_2Cl_2 (1 mL) was then added dropwise at 0 ºC. The resulting mixture was allowed to warm to rt and stirred for 16 h. The solvent was evaporated and the crude residue was purified by flash chromatography (2 – 3 % EtOAc/ Hexanes) to yield the **L10** (66 mg, 0.07mmol, 80% yield) as a white solid. **^{1}H- NMR** (500 MHz, $CDCl_3$, 25 ºC) δ (ppm): 10.24 (1H, dd, *J* = 8.3, 1.5 Hz), 8.49 (1H, d, *J* = 8.5 Hz), 8.09 (1H, dd, *J* = 7.8, 1.8 Hz), 8.02 (1H, br s), 7.99 – 7.71 (9H, m), 7.69 (1H, s), 7.65 (1H, d, *J* = 8.7 Hz), 7.59 (1H, ddd, *J* = 8.0, 6.8, 1.2 Hz), 7.53 (2H, br s), 7.46 (2H, s), 7.31 (1H, br s), 7.16 – 7.02 (3H, m), 7.02 – 6.88 (5H, m), 6.85 (2H, t, *J* = 7.6 Hz), 6.81 – 6.68 (2H, m), 6.65 - 6.60 (3H, m), 6.40 - 6.31 (2H, m), 5.83 – 5.54 (2H, m), 2.23 – 2.06 (3H, br s), 0.78 – 0.54 (3H, m); **^{13}C- NMR** (126 MHz, $CDCl_3$) δ (ppm): 151.4, 151.3, 150.4, 141.9, 141.2, 140.2, 140.1, 134.6, 134.3, 133.3, 133.0, 130.3, 130.0, 129.7, 129.4, 129.3, 128.7, 128.5, 128.4, 128.4, 128.1, 127.7, 127.5, 127.4, 127.2, 127.1, 127.0, 126.9, 126.8, 126.5, 126.5, 126.4, 126.3, 125.3, 122.6, 122.2, 53.6, 51.0, 19.8. **^{31}P- NMR** (121.5 MHz, $CDCl_3$) δ (ppm): 141.6; **LRMS** (m/z, ESI): 892 (M+H); **HRMS** (ESI-TOF): *m/z* calculated for $C_{64}H_{47}NO_2P$ $[M+H]^+$: *m/z* 892.3316 found 892.3321.

NOTE: In our hands, the use of this procedure is key for the synthesis of highly congested phosphoramidite ligands such as **(*S,R,R*)-L10**. However, less complex phosphoramidites can be equally prepared using simpler, previously reported procedures.

1.2. Synthesis of (3+2) cycloaddition precursors

1-Ethyl 4,4-diphenethyl (E)-6-cyclopropylidenehex-1-ene-1,4,4-tricarboxylate (3a)

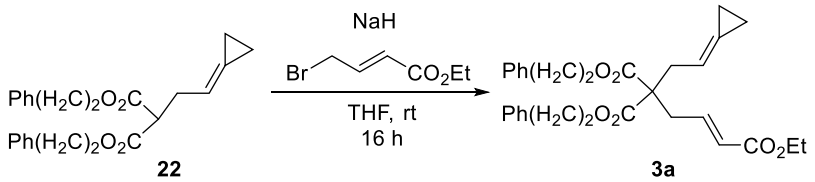

A solution of malonate **22**[161] (575 mg, 1.52 mmol) in THF (10 mL) was added dropwise to a suspension of NaH (60 mg, 1.60 mmol) in THF (6 mL), cooled at 0ºC. After stirring for 30 min, *E*-ethyl 4-bromocrotonate (0.4 ml, 2.23 mmol) was added dropwise. The mixture was stirred overnight at rt, then poured into water and extracted with Et_2O (3x20 mL). The organic phases were dried, filtered and concentrated to give an oily residue that was purified by flash chromatography (5 % Et_2O/hexanes) to yield **3a** (600 mg, 1.22 mmol, 80% yield) as a colourless oil. **^{1}H-NMR** (300 MHz, $CDCl_3$) δ (ppm): 7.31 – 7.16 (10H, m), 6.79 – 6.69 (1H, m), 5.69 (1H, d, *J* = 15.5 Hz), 5.52 -5.45 (1H, m), 4.24 (4H, dt, *J* = 7.0 y 1.7 Hz), 4.16 (2H, q, *J* = 7.1 Hz), 2.85 (4H, t, *J* = 7.0 Hz), 2.75 – 2.67 (4H, m), 1.27 (3H, t, *J* = 7.1 Hz), 1.07 – 0.88 (4H, m); **^{13}C-NMR** (75.4 MHz, $CDCl_3$) *δ* (ppm): 168.3 (C), 163.9 (C), 140.8 (CH), 135.5 (C), 126.9 (CH), 126.6 (CH), 125.0 (CH), 124.7 (CH), 122.9 (CH), 109.5 (CH), 64.0 (CH_2), 58.4 (CH_2), 55.5 (C), 33.3 (CH_2), 33.3 (CH_2), 32.8 (CH_2), 12.3 (CH_3), 1.0 (CH_2), 0.02 (CH_2); **LRMS** (m/z, ESI): 491 (M+H, 7), 341, 209, 133, 105; **HRMS** (ESI-TOF): *m/z* calculated for $C_{30}H_{35}O_6$ $[M+H]^+$: *m/z* 491.2434, found 491.2421

4,4-Diethyl 1-isopropyl (E)-6-cyclopropylidenehex-1-ene-1,4,4-tricarboxylate (3c)

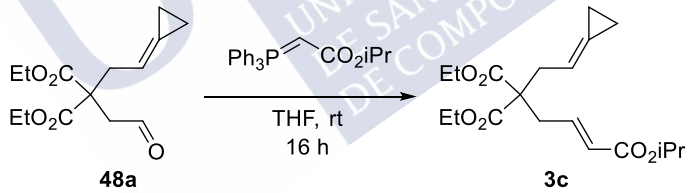

(Isopropyloxycarbonylmethylene)triphenylphosphorane (430 mg, 1.19 mmol) was added in one portion to a solution of aldehyde **48a**[163] (215 mg, 0.80 mmol) in THF (2 mL), and the mixture was stirred overnight. The solution was then poured into water and extracted with Et_2O (3 x 20 mL), the organic phases were dried, filtered and concentrated to give a crude oily residue that was purified by flash chromatography (3-5 % EtOAc/hexanes) to yield **3c** (246 mg, 0.70 mmol, 87%) as a colourless oil. **^{1}H-NMR** (300 MHz, $CDCl_3$) δ (ppm): 6.74 (1H, dt, *J* = 15.5, 7.7 Hz), 5.74 (1H, d, *J* = 15.4), 5.73 – 5.52 (1H, m), 4.98 (1H, p, *J* = 6.3 Hz), 4.14 (4H, q, *J* = 7.1 Hz), 2.77 (4H, dd, *J* = 13.4, 7.6 Hz), 1.21 – 1.18 (12H, m), 1.16 – 0.87 (4H, m); **^{13}C-NMR** (75.4 MHz, $CDCl_3$) δ (ppm): 170.5 (C), 165.4 (C), 142.6 (CH), 126.9 (C), 125.3 (CH), 111.7 (CH), 67.6 (CH_2), 61.4 (CH_2), 57.4 (C), 35.4 (CH_2), 21.9 (CH_3), 14.1 (CH_3), 3.0 (CH_2), 2.0 (CH_2); **LRMS** (m/z, ESI): 375 $(M+Na)^+$, 219, 191, 163, 145, 117. **HRMS** (ESI-TOF): *m/z* calculated for $C_{19}H_{28}NaO_6$ $[M+Na]^+$: *m/z* 375.1784, found 375.1778.

Triethyl (E)-6-cyclopropylidenehept-1-ene-1,4,4-tricarboxylate (3d)

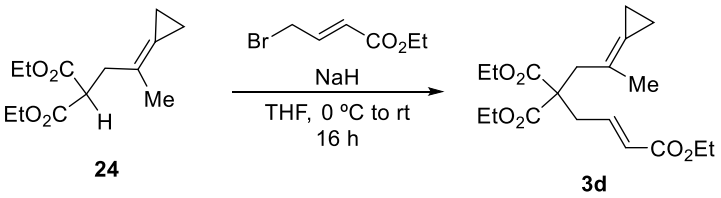

Obtained using the procedure described for the synthesis of **3a**[161] using NaH (55 mg, 1.37 mmol) **24**[175] (328 mg, 1.38 mmol) and *E*-ethyl-4-bromocrotonate (0.28 mL, 1.50 mmol). The compound **3d** was obtained as a colourless oil (353 mg, 1.00 mmol, 73% yield). **^{1}H-NMR** (300 MHz, $CDCl_3$) δ (ppm): 6.84 (1H, dt, *J* = 15.4, 7.6 Hz), 5.87 – 5.57 (1H, m), 4.20 – 4.08 (6H, m), 2.86 (2H, s), 2.69 (2H ,dd, *J* = 7.6, 1.5 Hz), 1.70 (3H, t, *J* = 1.8 Hz), 1.27 – 1.17 (9H, m), 1.00 (4H, br s).**^{13}C-NMR** (75.4 MHz, $CDCl_3$) δ (ppm): 171.0 (C), 165.9 (C), 143.5 (CH), 124.5 (CH), 122.0 (C), 119.3 (C), 61.5 (CH_2), 60.3 (CH_2), 57.1 (C), 39.8 (CH_2), 35.5 (CH_2), 21.3 (CH_3), 14.28 (CH_3), 14.06 (CH_3), 3.86 (CH_2), 2.76 (CH_2); **LRMS** (m/z, ESI): 375 $(M+Na)^+$, 233, 187, 159, 131, 119. **HRMS** (ESI-TOF): *m/z* calculated for $C_{19}H_{28}NaO_6$ $[M+H]^+$: *m/z* 375.1784, found 375.1778.

Triethyl (E)-6-cyclopropylidene-2-methylhex-1-ene-1,4,4-tricarboxylate (4e)

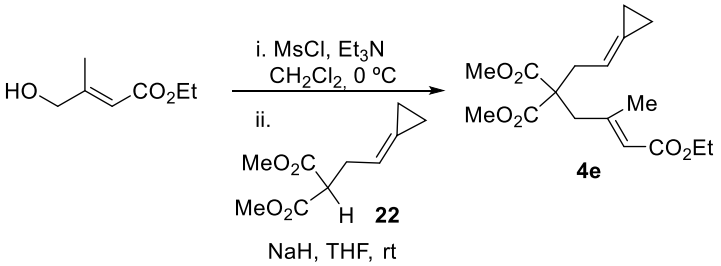

Methanesulfonyl chloride (0.32 mL, 3.21 mmol) was added dropwise to a solution of ethyl (E)-4-hydroxy-3-methylbut-2-enoate[176] (463 mg, 3.21 mmol) and Et_3N (0.67 mL, 4.82 mmol) in CH_2Cl_2 (20 mL) at 0 °C and the mixture was stirred 16 h at room temperature, then the mixture was poured into water (20 mL), extracted with Et_2O (2x20 mL), dried and concentrated to give a crude oil which was dissolved in THF (5 mL) and added dropwise to a preformed mixture of NaH (110 mg, 2.76 mmol) and diethyl 2-(2-cyclopropylideneethyl)malonate **22**[1] (521 mg, 2.63 mmol) in THF (10 mL) at 0 °C and finally stirred at room temperature for 16 h. The mixture was poured into water (40 mL), extracted with Et_2O (3x20 mL), dried and concentrated to give a crude oil which was purified by flash chromatography (3% Et_2O/hexanes) to give triethyl (E)-6-cyclopropylidene-2-methylhex-1-ene-1,4,4-tricarboxylate **4e** (418 mg, 1.18 mmol, 37% yield over two steps) as a colourless oil. **^{1}H-NMR** (300 MHz, $CDCl_3$) δ (ppm): 5.75 - 5.44 (2H, m), 4.21 - 4.04 (2H, m), 3.71 (6H, d, *J* = 0.6 Hz), 2.84 – 2.73 (4H, m), 2.07 (3H, dd, *J* = 1.3, 0.6 Hz), 1.39 - 1.17 (3H, m), 1.12 - 0.94 (4H, m). **^{13}C-NMR** (75 MHz, $CDCl_3$) δ (ppm): 171.4 (C), 166.3 (C), 154.0 (C), 127.0 (C), 120.4 (CH), 111.9 (CH), 59.8 (CH_2), 57.6 (C), 52.6 (CH_3), 43.3 (CH_2), 35.3

[175] A. M. Bernard, P. P. Piras, *Synth. Commun.* **1997**, *27*, 709–723.
[176] L. Geiger, M. Nieger, S. Brärse, *Chem. Select*, **2017**, *2*, 3268-3275.

(CH_2), 19.5 (CH_3), 14.4 (CH_3), 3.04 (CH_2), 2.12 (CH_2). **LRMS** (*m/z, I*): 324 (M^++1), 219, 191, 159, 131, 59; **HRMS** calculated for $C_{17}H_{24}O_6$ 324.1573, found 324.1573.

Triethyl (E)-7-cyclopropylidenehept-1-ene-1,5,5-tricarboxylate (3f)

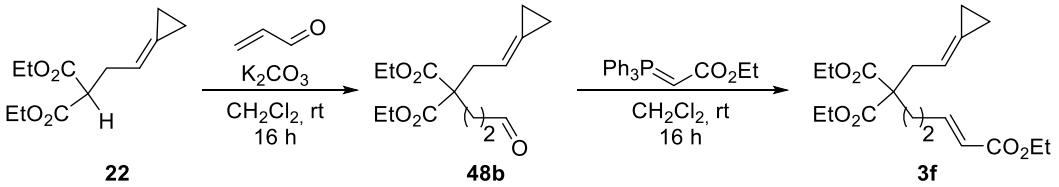

Malonate **22**[161] (0.5 g, 2.21 mmol, 1 equiv.) was added dropwise over a suspension of K_2CO_3 (1.22 g, 8.84 mmol, 4 eq.) in dry CH_2Cl_2 (5 mL) at room temperature. After 5 minutes, acrolein (246 µL, 3.32 mmol, 1.5 eq) was added dropwise and the mixture was stirred for 16 h. The reaction was quenched using $NaHCO_3(aq)_{sat}$ (50 mL) and the aqueous phase was extracted with Et_2O (3x20 mL). The combined organic layers were dried, filtered, concentred and purified by flash chromatography (10% EtOAc/Hexanes) affording diethyl 2-(2-cyclopropylideneethyl)-2-(3-oxopropyl)malonate **48b** as a colourless oil (424 mg, 1.20 mmol 68% yield). **^{1}H-NMR** (300 MHz, $CDCl_3$): δ (ppm) 9.69 (s, 1H), 5.57 (t, *J* = 7.3 Hz, 1H), 4.15 (q, *J* = 7.1 Hz, 4H), 2.74 (d, *J* = 7.3 Hz, 2H), 2.50 – 2.40 (m, 2H), 2.21 – 2.07 (m, 2H), 1.22 (t, *J* = 7.1 Hz, 6H), 1.12 – 0.91 (m, 4H); **^{13}C-NMR** (75 MHz, $CDCl_3$): δ (ppm) 201.4 (C), 171.5 (C), 127.2 (C), 112.2 (CH), 61.9 (CH_2), 57.3 (C), 39.7 (CH_2), 36.3 (CH_2), 25.4 (CH_2), 14.6 (CH_3), 3.5 (CH_2), 2.4 (CH_2); **LRMS** (m/z, ESI): 305 ([M^+ + Na]), 297, 191, 177, 163, 145, 117; **HRMS** (ESI-TOF): *m/z* calculated for $C_{15}H_{22}NaO_5$ [M + Na]$^+$: *m/z* 305.1365, found 305.1360.

(Carbethoxymethylene)triphenylphosphorane (733 mg, 2.00 mmol) was added in one portion to a solution containing the intermediate aldehyde **48b (**424 mg, 1.20 mmol) in dry CH_2Cl_2 (5 mL), and the mixture was stirred at rt for 16 h. Evaporation afforded a crude mixture that was purified by flash chromatography (3 – 4 % EtOAc/ Hexanes) to yield triethyl (E)-7-cyclopropylidenehept-1-ene-1,5,5-tricarboxylate **3f** (423 mg, 1.20 mmol, 80%) as a colourless oil. **^{1}H-NMR** (300 MHz, $CDCl_3$) δ (ppm): 6.89 (dt, *J* = 15.5, 6.5 Hz, 1H), 5.79 (d, *J* = 15.7 Hz, 1H), 5.58 (t, *J* = 7.3 Hz, 1H), 6.17 (q, *J* = 7.1 Hz, 20H), 2.79 (d, *J* = 7.4 Hz, 2H), 2.21 – 2.06 (m, 2H), 2.06 – 1.91 (m, 2H), 1.25 (dt, *J* = 14.4, 7.2 Hz, 9H), 1.14 – 0.89 (m, 4H); **^{13}C-NMR** (75.4 MHz, $CDCl_3$) δ (ppm): 170.8 (C), 166.2 (C), 147.4 (CH), 126.2 (C), 121.5 (CH), 111.5 (CH), 61.0 (CH_2), 59.9 (CH_2), 56.9 (C), 34.8 (CH_2), 30.2 (CH_2), 26.6 (CH_2), 14.0 (CH_3), 13.8 (CH_3), 2.7 (CH_2), 1.6 (CH_2); **LRMS** (m/z, ESI): 375 (M+Na)$^+$, 213, 187, 159, 131; **HRMS** (ESI-TOF): *m/z* calculated for $C_{19}H_{28}NaO_6$ [M+H]$^+$: *m/z* 375.1784, found 375.1778.

Ethyl (E)-4-(benzyl(2-cyclopropylideneethyl)amino)but-2-enoate (3i)

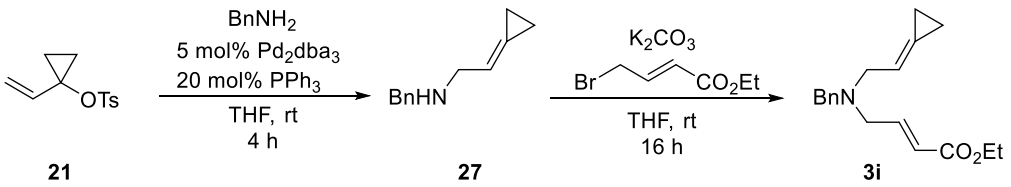

A solution of Pd_2dba_3 (576 mg, 0.63 mmol), triphenylphosphine (660 mg, 2.52 mmol), and 1-vinylcyclopropyltosylate **21**[1] (3.00 g, 12.6 mmol) in THF (30 mL) was stirred at rt for 15 min and then added dropwise to a solution of benzylamine (5.60 mL, 50.4 mmol) in THF (30 mL). The resulting mixture was stirred at rt for 3 h, poured into water and extracted with Et_2O (3x20 mL). The organic phases were dried, filtered and concentrated to give a crude oily residue that was purified by flash chromatography (20% EtOAc/hexanes) to yield N-Benzyl-2-cyclopropylidene-ethan-1-amine **27** (1.50 g, 8.67 mmol, 69% yield) as a yellow oil. **^{1}H-NMR** (300 MHz, $CDCl_3$) δ (ppm): 7.47 – 7.24 (5H, m), 5.99 – 5.83 (1H, m), 3.8 (2H, s), 3.42 (2H, d, *J* = 6.3 Hz), 1.07 (4H, br s); **^{13}C-NMR** (75.4 MHz, $CDCl_3$) δ (ppm): 131.0 (C), 128.9 (CH), 128.7 (CH), 127.4 (CH), 123.4 (C), 117.1 (CH), 54.0 (CH_2), 51.0 (CH_2), 2.6 (CH_2), 2.5 (CH_2); **LRMS** (m/z, ESI): 174 $(M)^+$, 155, 141, 128. **HRMS** (ESI-TOF): *m/z* calculated for $C_{12}H_{16}N$ $[M+H]^+$: *m/z* 174.1283, found 174.1277.

N-Benzyl-2-cyclopropylidene-ethan-1-amine **27** (500 mg, 2.89 mmol) was added dropwise to a suspension of K_2CO_3 (479 mg, 3.46 mmol) in THF (10 mL) at 0 ºC. After stirring for 15 min, *E*-ethyl 4-bromocrotonate (0.6 mL, 4.33 mmol) was added dropwise and the mixture was stirred overnight at rt. Then, the mixture was poured into water and extracted with Et_2O (3x20 mL). The organic phases were dried, filtered and concentrated to give a crude oily residue that was purified by flash chromatography (5 – 10 % Et_2O/hexanes) to yield **3i** (639 mg, 2.24 mmol, 78%) as a pale-yellow oil. **^{1}H-NMR** (300 MHz, $CDCl_3$) δ (ppm): 7.37 – 7.22 (5H, m), 6.99 (1H, dt, *J* = 15.6, 5.9 Hz), 6.00 (1H, d, *J* = 15.7 Hz), 5.95 – 5.79 (1H, m), 4.19 (2H, q, *J* = 7.1 Hz), 3.60 (2H, s), 3.27 – 3.17 (4H, m), 1.29 (3H, t, *J* = 7.1 Hz), 1.15 – 0.95 (4H, m); **^{13}C-NMR** (75.4 MHz, $CDCl_3$) δ (ppm): 166.1 (C), 145.3 (CH), 138.9 (C), 128.5 (CH), 128.0 (CH), 126.7 (CH), 125.4 (C), 122.4 (CH), 114.7 (CH), 60.0 (CH_2), 57.9 (CH_2), 55.0 (CH_2), 54.0 (CH_2), 14.0 (CH_3), 2.1 (CH_2), 1.7 (CH_2); **LRMS** (m/z, ESI): 286 $(M)^+$, 218, 190, 157, 142. **HRMS** (ESI-TOF): *m/z* calculated for $C_{18}H_{24}NO_2$ $[M+H]^+$: *m/z* 286.1807, found 286.1802.

Ethyl (E)-4-((N-(2-cyclopropylideneethyl)-4-methylphenyl)sulfonamido)but-2-enoate (3j)

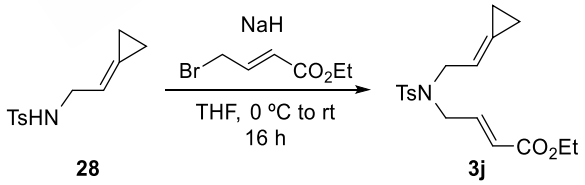

Obtained using the procedure described for the synthesis of **3a**[161] using NaH (67 mg, 1.67 mmol), **28**[161] (360 mg, 1.52 mmol) and *E*-ethyl-4-bromocrotonate (0.3 mL, 2.16 mmol). The compound **3j** was obtained as a pale yellow solid (332 mg, 0.95 mmol, 69% yield). **^{1}H NMR** (300 MHz, $CDCl_3$) δ (ppm): 7.66 (2H, d), 7.27 (2H, d), 6.68 (1H, dt, *J* = 15.6, 5.7 Hz), 5.83 (1H, dt, *J* = 15.7, 1.7 Hz), 5.61 – 5.53 (1H, m), 4.13 (2H, q, *J* = 7.1 Hz), 4.00 – 3.72 (4H, m), 2.39 (3H, s), 1.23 (3H, t, *J* = 7.1 Hz), 1.09 – 0.89 (4H, m); **^{13}C-NMR** (75.4 MHz, $CDCl_3$) δ (ppm): 165.7 (C), 143.5 (C), 142.7 (CH), 137.0 (C), 129.8 (CH), 128.2 (C), 127.2 (CH), 123.5 (CH), 112.3 (CH), 60.5 (CH_2), 49.2 (CH_2), 47.6 (CH_2), 21.5 (CH_3), 14.2 (CH_3), 2.6 (CH_2), 1.9 (CH_2); **LRMS** (m/z, ESI):

372 ([M⁺+ Na]); **HRMS** (ESI-TOF): *m/z* calculated for $C_{18}H_{23}NNaO_4S$ [M+Na]⁺: *m/z* 372.1240, found 372.1231.

Ethyl (E)-4-(2-cyclopropylideneethoxy)but-2-enoate (3k)

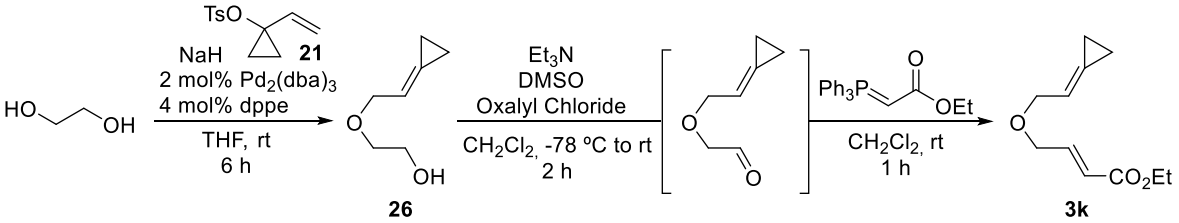

Ethyleneglycol (94 µL, 1.68 mmol) was added dropwise to a suspension of NaH (67 mg, 1.68 mmol) in THF (3 mL) at 0 °C. After stirring for 2h at rt, a solution of $Pd_2(dba)_3$ (15 mg, 0.02 mmol), dppe (13 mg, 0.03 mmol) and 1-vinylcyclopropyltosylate **21**[1] (200 mg, 0.84 mmol) in THF (3 mL), previously stirred for 10 minutes, was added via cannula. The resulting mixture was further stirred for 3h and then, the reaction was quenched with $NH_4Cl_{(sat)}$, extracted with Et_2O (3x30 mL) and dried. The resulting organic phase was evaporated under reduced pressure and the crude was purified by flash chromatography (5 - 10 % EtOAc/ Hexanes) to yield 2-(2-Cyclopropylideneethoxy)ethan-1-ol **26** (64 mg, 0.99 mmol, 59% yield) as a colourless oil. **¹H-NMR** (300 MHz, $CDCl_3$) *δ* (ppm): 5.93 (1H, tt, *J* = 6.7, 2.0 Hz), 4.15 (2H, dd, *J* = 6.4, 1.5 Hz), 3.73 (2H, dd, *J* = 5.4, 3.7 Hz), 3.54 (2H, dd, *J* = 5.4, 3.7 Hz), 2.20 (1H, s), 1.09 (4H, s); **¹³C-NMR** (75.4 MHz, $CDCl_3$) *δ* (ppm): 127.3 (C), 114.6 (CH), 71.4 (CH_2), 71.1 (CH_2), 62.0 (CH_2), 2.4 (CH_2), 1.9 (CH_2); **LRMS** (m/z, APCI): 129 (M+H), 127, 113, 105, 93; **HRMS** (APCI--TOF): *m/z* calculated for $C_7H_{12}O_2$ [M]⁺: *m/z* 129.0916, found 129.0910.

DMSO (277 µL, 3.9 mmol) was added to a solution of oxalyl chloride (187 µL, 2.19 mmol) in CH_2Cl_2 (5 mL) at -78 ºC, and the mixture was stirred at -78 ºC for 20 min. Then a solution of 2-(2-cyclopropylideneethoxy)ethan-1-ol **26** (200 mg, 1.56 mmol) in CH_2Cl_2 (3 mL) was added dropwise and the mixture was stirred for 20 minutes. Et_3N (1.09 mL, 7.80 mmol) was added dropwise and the mixture was stirred for 15 minutes before being warmed to rt and stirred for an additional hour. The reaction is then quenched with $NH_4Cl_{(sat)}$, extracted with CH_2Cl_2 (3x10 mL), dried and partially evaporated to a 10 -15 mL volume. (Carbethoxymethylene)triphenylphosphorane (1.09 g, 3.10 mmol) was added in one portion to this solution containing the intermediate aldehyde and the mixture was stirred at rt for 1 h. Evaporation afforded a crude mixture that was purified by flash chromatography (3 – 4 % EtOAc/ Hexanes) to yield **3k** (148 mg, 0.75 mmol, 48% over two steps) as a colourless oil. **¹H-NMR** (300 MHz, $CDCl_3$) δ (ppm): 6.94 (1H, dt, *J* = 15.8, 4.4 Hz), 6.05 (1H, dt, *J* = 15.7, 2.0 Hz), 5.90 (1H, ddt, *J* = 6.6, 4.3, 2.1 Hz), 4.25 – 4.08 (6H, m), 1.26 (3H, t, *J* = 7.2 Hz), 1.08 (4H, br); **¹³C-NMR** (75.4 MHz, $CDCl_3$) *δ* (ppm): 166.4 (C), 144.6 (CH), 127.5 (C), 121.3 (CH), 114.4 (CH), 71.0 (CH_2), 68.4 (CH_2), 60.4 (CH_2), 14.3(CH_3), 2.4 (CH_2), 1.9 (CH_2); **LRMS** (m/z, ESI): 219 (M+Na), 192, 184, 169, 140; **HRMS** (ESI-TOF): *m/z* calculated for $C_{11}H_{16}NaO_3$ [M+Na]⁺: *m/z* 219.0997, found 219.0949.

1.3. Representative procedure for the enantioselective (3+2) cycloaddition of alkylidenecyclopropanes and alkenes

Procedure A: exemplified for the reaction of **3b**.

Ethyl (1R*,3aS*,6aR*)-5,5-bis(benzyloxy)-3-methyleneoctahydropentalene-1-carboxylate (4b)

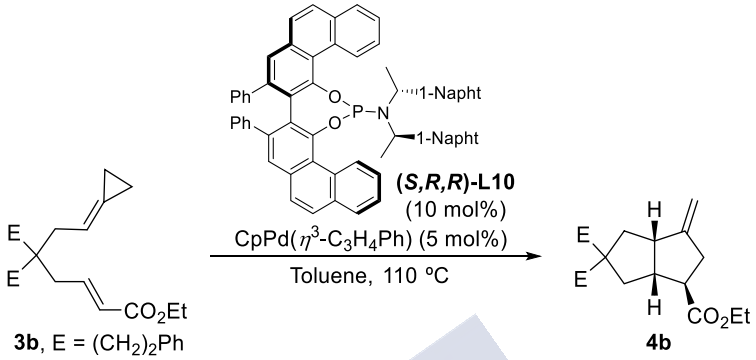

A solution of CpPd(η³-1-PhC$_3$H$_4$) (2.13 mg, 5 mol%), **(*S,R,R*)-L10** (13.2 mg, 10 mol%) and **3b** (50 mg, 0.148mmol) in freshly distilled toluene (3 mL) was degassed and heated under reflux for 6h. The mixture was cooled to rt, diluted with Et$_2$O and filtered through a short pad of florisil, eluting with Et$_2$O. The filtrate was concentrated and purified by flash chromatography (3% EtOAc/hexanes) to afford ethyl (1R*,3aS*,6aR*)-5,5-bis(benzyloxy)-3-methyleneoctahydropentalene-1-carboxylate **4b** as colourless oil (45 mg, 90% yield). **^{1}H-NMR** (300 MHz, $CDCl_3$) δ (ppm): 7.67 – 6.72 (10H, m), 4.98 – 4.79 (1H, m), 4.72 (1H, d, *J* = 2.4 Hz), 4.25 (4H, dt, *J* = 13.8, 6.9 Hz), 4.12 (2H, q, *J* = 7.1 Hz), 2.98 (1H, dd, *J* = 19.3, 10.3 Hz), 2.86 (6H, q, *J* = 7.2 Hz), 2.71 - 2.55 (3H, m), 2.55 - 2.39 (2H, m), 1.96 (2H, ddd, *J* = 13.4, 10.6, 7.7 Hz), 1.25 (3H, td, *J* = 7.2, 1.2 Hz). **^{13}C-NMR** (75.4 MHz, $CDCl_3$) δ (ppm): 175.1 (C), 171.7 (C), 171.4 (C), 153.2 (C), 137.6 (C), 129.0 (CH), 128.9 (CH), 128.6 (CH), 126.7 (CH), 107.0 (CH_2), 66.0 (CH_2), 62.8 (C), 60.6 (CH_2), 49.1 (CH), 47.6 (CH), 47.2 (CH), 40.0 (CH_2), 39.7 (CH_2), 38.0 (CH_2), 35.0 (CH_2), 14.4 (CH_3); **LRMS** (m/z, ESI): 491 ([M$^+$+H]), 444, 417, 369, 209, 105; **HRMS** (ESI-TOF): *m/z* calculated for $C_{30}H_{35}O_6$ [M+H]$^+$: *m/z* 491.2434 found 491.2422. The stereochemistry of **4b** was deduced from nOe experiments and by comparison with previously reported cycloadduct analog **2a**. Enantioselectivity was determined by chiral HPLC analysis on Chiralpak OZ-H at rt, (Hexane : iPrOH = 98 : 2, 0.5 mL/min), by comparison with an independently prepared racemic sample (see below).

Protocol used for obtaining a racemic samples (exemplified for **4b**):[1] A mixture of Pd_2dba_3 (8.12 mg, 6 mol%), and tris(2,4-di-*tert*-butylphenyl) phosphite (**L1**, 19.5 mg, 20 mol%) and **3b** (50 mg, 0.148mmol) were dissolved in freshly distilled dioxane (1.1 mL), The mixture was degassed and the reaction was heated under reflux for 4h. The mixture was cooled to rt, diluted with Et$_2$O and filtered through a short pad of florisil eluting with Et$_2$O. The filtrate was concentrated and purified by flash chromatography (3% EtOAc/hexanes) to afford **4b** as colourless oil (37 mg, 74% yield).

Racemic sample:

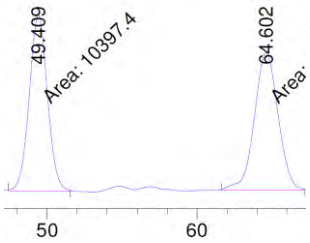

Signal 3: DAD1 C, Sig=210,8 Ref=360,100

Peak #	RetTime [min]	Type	Width [min]	Area [mAU*s]	Height [mAU]	Area %
1	49.409	MM	1.4107	1.03974e4	122.83980	49.6041
2	64.602	MM	1.8347	1.05634e4	95.95742	50.3959
Totals :				2.09608e4	218.79722	

Asymmetric sample (92% ee.):

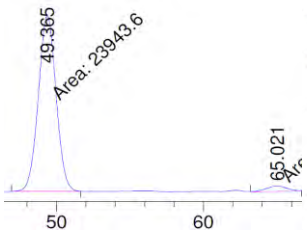

Signal 3: DAD1 C, Sig=210,8 Ref=360,100

Peak #	RetTime [min]	Type	Width [min]	Area [mAU*s]	Height [mAU]	Area %
1	49.365	MM	1.4036	2.39436e4	284.31830	96.4863
2	65.021	MM	1.6639	871.94910	8.73402	3.5137
Totals :				2.48155e4	293.05232	

Figure 28. HPLC traces and report for **4b**.

5,5-Diethyl 1-isopropyl (1R*,3aS*,6aR*)-3-methylenehexahydropentalene-1,5,5(1H)-tricarboxylate (4a)

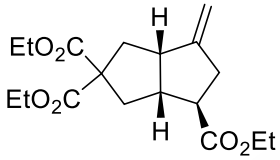

89% yield, colourless oil. The spectroscopic data are in agreement with those reported in literature.[1] **^{1}H-NMR** δ (ppm): 4.86 (1H, s), 4.76 (1H, s), 4.17-4.05 (6H, m), 3.19 – 3.02 (1H, m), 2.90 – 2.77 (1H, m), 2.69 - 2.55 (4H, m), 2.50 (1H, dd, *J* = 13.6 and 8.4 Hz), 2.05 - 1.97 (2H, m), 1.22 - 1.17 (9H, m). Enantioselectivity was determined by chiral HPLC analysis on Lux Cellulose-1 at rt (Hexane : iPrOH = 99:1, 1 ml/min).

Racemic sample (obtained in 71% yield following the racemic protocol):

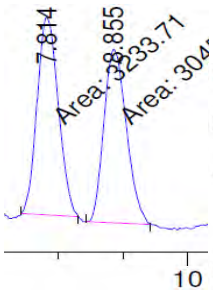

Signal 3: DAD1 C, Sig=210,8 Ref=360,100

Peak #	RetTime [min]	Type	Width [min]	Area [mAU*s]	Height [mAU]	Area %
1	7.814	MM	0.3796	3233.71216	141.99382	51.5027
2	8.855	MM	0.4058	3045.01025	125.06250	48.4973
Totals :				6278.72241	267.05632	

Asymmetric sample (94% ee):

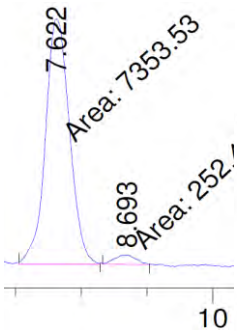

Signal 3: DAD1 C, Sig=210,8 Ref=360,100

Peak #	RetTime [min]	Type	Width [min]	Area [mAU*s]	Height [mAU]	Area %
1	7.622	MM	0.4231	7353.53027	289.66394	96.6806
2	8.693	MM	0.3906	252.47357	10.77193	3.3194
Totals :				7606.00385	300.43587	

Figure 29. HPLC traces and reports for **4a.**

5,5-Diethyl 1-isopropyl (1R*,3aS*,6aR*)-3-methylenehexahydropentalene-1,5,5(1H)-tricarboxylate (4c)

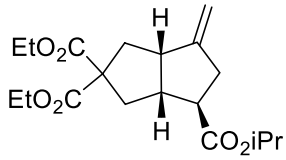

90% yield, Colourless oil. **^{1}H NMR** (300 MHz, $CDCl_3$) δ (ppm): 4.99 (1H, hept, *J* = 6.2 Hz), 4.90 (1H, s), 4.80 (1H, s), 4.30 – 4.04 (4H, m), 3.13 (1H, q, *J* = 10.3, 9.0 Hz), 2.93 – 2.78 (1 H, m), 2.73 – 2.49 (5H, m), 2.12 – 1.99 (2H, m), 1.28 – 1.20 (12H, m). **^{13}C-NMR** (75 MHz, $CDCl_3$) δ (ppm): 174.7 (C), 172.0 (C), 171.7 (C), 153.4 (C), 106.9 (CH_2), 67.9 (CH), 62.8 (C), 61.6 (CH_2), 49.3 (CH), 47.7 (CH), 47.3 (CH), 40.0 (CH_2), 39.7 (CH_2), 38.1 (CH_2), 22.0 (CH_3), 14.2 (CH_3). **LRMS** (m/z, ESI): 375 $(M+Na)^+$, 219, 191, 163, 145, 117. **HRMS** (ESI-TOF): *m/z* Calculated for $C_{19}H_{28}NaO_6$ $[M+Na]^+$: *m/z* 375,1784, found 375.1777. The stereochemistry was deduced from nOe experiments as well as by analogy with previously reported analog **4a**.[161] Enantioselectivity was determined by chiral HPLC analysis on Chiralpak OZ-H at rt, (Hexane : iPrOH = 99:1, 0.5 ml/min).

Racemic sample (obtained in 66% yield following the racemic protocol):

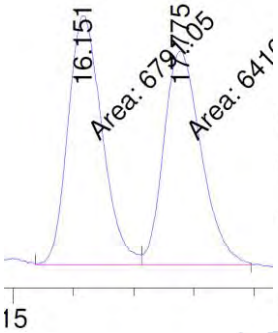

Signal 3: DAD1 C, Sig=210,8 Ref=360,100

Peak #	RetTime [min]	Type	Width [min]	Area [mAU*s]	Height [mAU]	Area %
1	16.151	MF	0.6607	6791.04980	171.32095	51.4190
2	17.775	FM	0.7270	6416.23486	147.09119	48.5810
Totals :				1.32073e4	318.41214	

Asymmetric sample (90% ee)

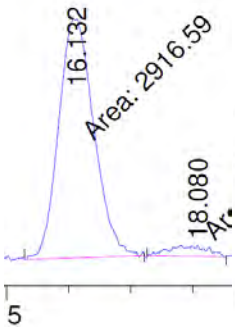

Signal 3: DAD1 C, Sig=210,8 Ref=360,100

Peak #	RetTime [min]	Type	Width [min]	Area [mAU*s]	Height [mAU]	Area %
1	16.132	MM	0.6584	2916.59497	73.82793	95.3675
2	18.080	MM	0.7088	141.67357	3.33123	4.6325
Totals :				3058.26854	77.15915	

Figure 30. HPLC traces and reports of **4c**.

Triethyl (1R*,3aS*,6aS*)-3a-methyl-3-methylenehexahydropentalene-1,5,5(1H)-tricarboxylate (4d)

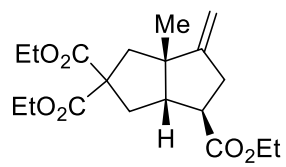

85% yield, colourless Oil. 1H NMR (300 MHz, CDCl3) δ (ppm): 4.86 (1H, s), 4.79 (1H, s), 4.26 – 4.08 (6H, m), 2.84 – 2.55 (4H, m), 2.53 – 2.40 (2H, m), 2.30 (1H, d, J = 14.1 Hz), 2.22 (1H, dd, J = 13.7, 4.6 Hz), 1.40 – 1.18 (9H, m), 1.16 (3H, s). 13C-NMR (75 MHz, CDCl3) δ (ppm): 175.3 (C), 172.4 (C), 172.3 (C), 158.4 (C), 105.3 (CH2), 61.7 (CH2), 61.6 (CH2), 60.7 (CH2), 55.3 (CH), 54.1 (C), 47.5 (CH), 46.9 (CH2), 39.4 (CH2), 36.6 (CH2), 27.2 (CH3), 14.4

(CH3), 14.2 (CH3), 14.1 (CH3). LRMS (m/z, ESI): 375 (M+Na)+. 233, 205, 159, 131. HRMS (ESI-TOF): m/z Calculated for $C_{19}H_{28}NaO_6$ [M+Na]+: m/z 375.1784, found 375.1777. The stereochemistry of the ring junction of **4d** was deduced by nOe experiments, (nOe between Me-1 and H-5). The stereochemistry at C-4 was further confirmed in the derivative **4d`** (nOe between H4 and H6), which as prepared by treatment of **4d** with pTsOH (CDCl3, 55 °C, 5h, 99% yield), following a reported procedure.[161]

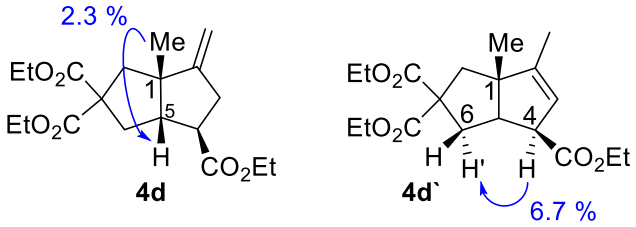

Figure 31. Significant nOe's observed for **4d** and **4d'.**

Enantioselectivity was determined by chiral HPLC analysis on Chiralpak IA3 at rt, (Hexane : iPrOH = 99:1, 0.5 ml/min).

Racemic sample (69% yield following the racemic protocol)

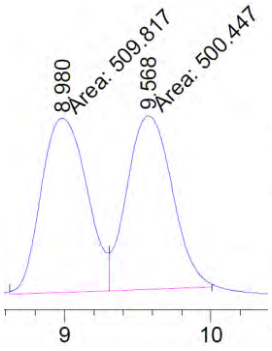

Peak #	RetTime [min]	Type	Width [min]	Area [mAU*s]	Height [mAU]	Area %
1	8.980	MF	0.3646	509.81677	23.30282	50.4637
2	9.568	FM	0.3589	500.44675	23.23809	49.5363
Totals :				1010.26352	46.54092	

Asymmetric sample (92% ee)

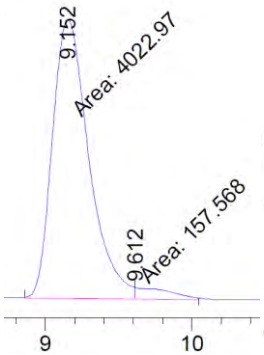

Peak #	RetTime [min]	Type	Width [min]	Area [mAU*s]	Height [mAU]	Area %
1	9.152	MF	0.2892	4022.97217	231.87950	96.2309
2	9.612	FM	0.2744	157.56842	9.57210	3.7691
Totals :				4180.54059	241.45160	

Figure 32. HPLC traces and reports of **4d**.

1-Ethyl 5,5-dimethyl (1R,*3aR,*6aR*)-6a-methyl-3-methylenehexahydropentalene-1,5,5(1H)-tricarboxylate (4e).

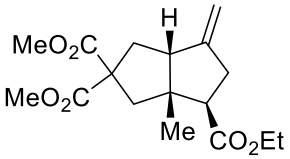

90% yield, colourless oil (obtained from a 12:1 mixture isomers). **^{1}H-RMN** (300 MHz, $CDCl_3$) δ (ppm): 4.95 – 4.88 (1H, m), 4.83 (1H, dt, J = 1.6, 0.8 Hz), 4.26 – 4.04 (2H, m), 3.74 (3H, s), 3.71 (3H, s), 2.91 – 2.51 (6H, m), 2.30 – 2.12 (2H, m), 1.33 – 1.20 (3H, m), 1.01 (3H, s). **^{13}C-RMN** (75.4 MHz, $CDCl_3$) δ (ppm): 173.6 (C), 172.9 (C), 172.6 (C), 151.4 (C), 107.6 (CH_2), 61.8 (C), 60.4 (CH_2), 57.0 (CH), 53.7 (CH), 53.0 (CH_3), 52.9 (CH_3), 52.5 (CH), 46.6 (CH_2), 40.7 (CH_2), 35.2 (CH_2), 22.8 (CH_3), 14.5 (CH_3). Enantioselectivity was determined by GC (FID detector) using a *Chiraldex* □*-DA* column (100 – 175 °C for 10 min, 175 °C for 50 min, 175-100 °C for 10 min).

Racemic sample (prepared following the racemic protocol)

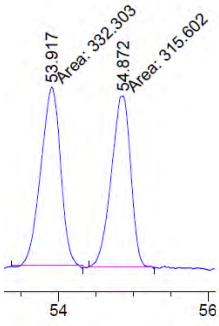

Peak #	RetTime [min]	Type	Width [min]	Area [pA*s]	Height [pA]	Area %
1	53.917	MM	0.3049	332.30347	18.16644	51.28886
2	54.872	MM	0.3018	315.60223	17.42768	48.71114
Totals :				647.90570	35.59412	

Asymmetric reaction (44% ee)

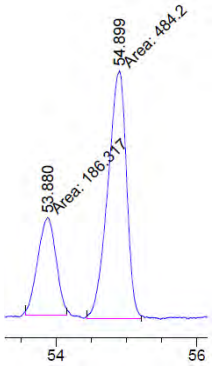

Peak #	RetTime [min]	Type	Width [min]	Area [pA*s]	Height [pA]	Area %
1	53.880	MM	0.2996	186.31656	10.36450	27.78703
2	54.899	MM	0.3052	484.19980	26.44003	72.21297
Totals :				670.51636	36.80453	

Figure 33. GC (FID detector) traces and reports of **4e**.

Triethyl (1R,7aR)-3-methyleneoctahydro-5H-indene-1,5,5-tricarboxylate (4f+4f`)

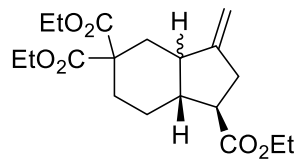

90% yield (dr = 1.1 : 1), colourless oil. **^{1}H-NMR** (300 MHz, CDCl3) δ (ppm): 4.90 (s, 0.45H), 4.87 – 4.75 (m, 1.65H), 4.28 – 4.04 (m, 6H), 2.87 (q, J = 9.8 Hz, 0.5H), 2.79 – 2.51 (m, 3H), 2.51 – 2.33 (m, 1.5H), 2.34 – 2.14 (m, 1H), 2.14 – 1.93 (m, 1H), 1.86 (td, J = 13.0, 4.0 Hz, 1.2H), 1.76 – 1.47 (m, 0.8H), 1.47 – 1.33 (m, 2H),1.23 (m, 9H); **^{13}C-NMR** (75 MHz, CDCl3) δ (ppm): 174.9 (C), 174.4 (C), 171.9 (C), 170.7 (C), 170.5 (C), 152.7 (C), 150.3 (C), 106.3 (CH_2), 103.6 (CH_2), 61.2 (CH_2), 61.1 (CH_2), 61.0 (CH_2), 60.9 (CH_2), 60.1 (CH_2), 54.8 (C), 53.8 (C), 48.4 (CH), 46.9 (CH_3), 45.9 (CH), 43.6 (CH_3), 41.3 (CH_3), 41.2 (CH_3), 34.8 (CH_2), 34.6 (CH_2), 33.3 (CH_2), 32.9 (CH_2), 31.0 (CH_2), 26.9 (CH_2), 25.6 (CH_2), 21.3 (CH_2), 14.0 (CH_3), 13.8 (CH_3), 13.7 (CH_3); **LRMS** (m/z, ESI): 375 $(M+Na)^+$. 233, 205, 189, 177, 159, 131; **HRMS** (ESI-TOF): m/z

Calculated for $C_{19}H_2NaO_6$ $[M+Na]^+$: m/z 375.1784, found 375.1789. Enantioselectivity was determined by chiral HPLC analysis on Chiralpak IA3 at rt, (Hexane : iPrOH = 99:1, 0.5 ml/min).

Racemic sample (Major isomer) (70% yield following the racemic protocol)

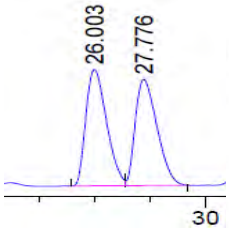

Peak #	RetTime [min]	Type	Width [min]	Area [mAU*s]	Height [mAU]	Area %
1	26.003	PV	0.8191	1.29839e4	250.35320	51.1115
2	27.776	VB	0.8358	1.24192e4	227.88565	48.8885
Totals :				2.54031e4	478.23885	

Asymmetric sample (47% ee)

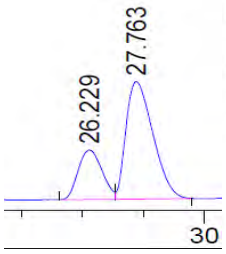

Signal 1: DAD1 A, Sig=220,8 Ref=360,100

Peak #	RetTime [min]	Type	Width [min]	Area [mAU*s]	Height [mAU]	Area %
1	26.233	PV	0.7976	1256.84216	23.29057	26.7323
2	27.762	VB	0.9252	3444.74829	56.99161	73.2677
Totals :				4701.59045	80.28218	

Figure 34. HPLC traces and reports of **4f**.

Diethyl (3aR,4R,6aS)-4-acetyl-6-methylenehexahydropentalene-2,2(1H)-dicarboxylate (4g)

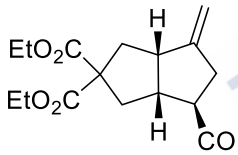

87% yield, colourless oil. Spectroscopic data is in agreement with the described in literature. **^{1}H-NMR** (300 MHz, CDCl3) δ (ppm): 4.89 (d, *J* = 2.1 Hz, 1H), 4.79 (t, *J* = 1.7 Hz, 1H), 4.20-4.08 (m, 4H), 3.09 (m, 1H), 2.80 (m, 2H), 2.70-2.49 (m, 4H), 2.16 (s, 3H), 2.07-2.01 (m, 2H), 1.28-1.19 (m, 6H).Enantioselectivity was determined by chiral GC analysis on ASTEC SUPELCO B-DA, (N_2, flow 0.2 mL/min, 150 °C, 100 min).

Racemic sample (70% yield following the racemic protocol)

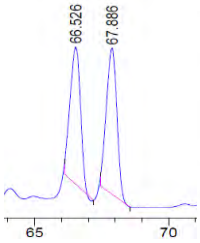

Peak #	RetTime [min]	Type	Width [min]	Area [pA*s]	Height [pA]	Area %
1	66.526	BB	0.3158	740.61322	27.50145	48.09146
2	67.886	BB	0.3220	799.39648	29.32771	51.90854
Totals :				1540.00970	56.82916	

Asymmetric sample (56% ee)

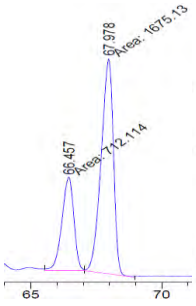

Peak #	RetTime [min]	Type	Width [min]	Area [pA*s]	Height [pA]	Area %
1	66.457	MM	0.5321	712.11438	22.30435	29.82991
2	67.978	MM	0.5429	1675.13489	51.42333	70.17009
Totals :				2387.24927	73.72768	

Figure 35. HPLC traces and reports of **4g**.

Ethyl (3aR*,4R*,6aS*)-2-benzyl-6-methyleneoctahydrocyclopenta[c]pyrrole-4-carboxylate (4i)

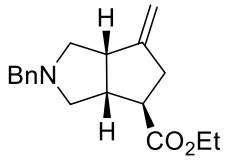

70% yield. Pale yellow oil. **^{1}H- NMR** (300 MHz, $CDCl_3$) δ (ppm): 7.18 – 7.38 (5H, m), 4.93 (1H, s), 4.77 (1H, s), 4.13 (2H, q, J = 7.1 Hz), 3.58 (2H, s), 3.08 (1H, t, J = 7.89 Hz), 2.95 – 2.83 (1H, m), 2.75 – 2.60 (4H, m), 2.59 – 5.26 (1H, m), 2.55 - 2.42 (2H, m), 1.26 (3H, t, J = 7.11 Hz); **^{13}C-NMR** (75.4 MHz, $CDCl_3$) δ (ppm): 175.4 (C), 154.7 (C), 139.3 (C), 128.6 (CH), 128.3 (CH), 126.9 (CH), 106.0 (CH_2), 60.9 (CH_2), 60.5 (CH_2), 60.2 (CH_2), 59.7 (CH_2), 49.33 (CH), 47.0 (CH), 46.9 (CH), 39.0 (CH_2), 14.37(CH_3); **LRMS** (m/z, ESI): 286 $(M+H)^+$, 212, 194, 183, 166, 148, 120; **HRMS** (ESI-TOF): *m/z* calculated for $C_{18}H_{24}NO_2$ $[M+H]^+$: *m/z* 286.1807, found 286.1802. The stereochemistry of the ring junction of **4i** was deduced by nOe experiments (nOe between H1 and H5) in **4a**: moreover, the alcohol derivative **4ib**, which was obtained according to the below described procedure, showed also nOe's between H1 - H5 and H5 – H9. Enantioselectivity was also determined on the corresponding derivative **4ib** (see below).

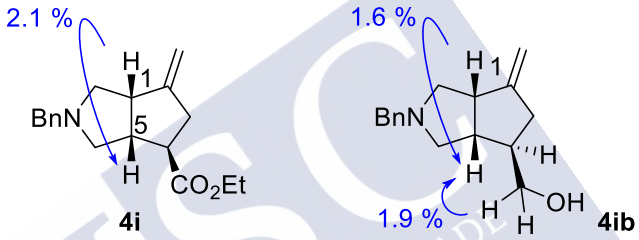

Figure 36 Significant nOes observed for **4i** and **4ib**.

((3aR*,4R*,6aS*)-2-Benzyl-6-methyleneoctahydrocyclopenta[c]pyrrol-4-yl)methanol (4ib)

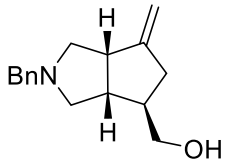

Synthesized following the same procedure for the synthesis of triol **4ab.** 63%. Pale yellow oil. **^{1}H- NMR** (300 MHz, $CDCl_3$) δ (ppm): 7.34 – 7.19 (5H, m), 4.89 (1H, s), 4.77 (1H, s), 3.64 - 3.43 (4H, m), 3.09 – 2.98 (1H, m), 2.74 – 2.56 (3H, m), 2.51 (1H, dd, J = 9.0, 4.4 Hz), 2.47 – 2.38 (2H, m), 2.15 (1H, dd, J = 14.9, 6.2 Hz), 2.06 – 1.94 (1H, m), 1.29 – 1.18 (1H, m); **^{13}C-NMR** (75.4 MHz, $CDCl_3$) δ (ppm): 155.4 (C), 139.2 (C), 128.6 (CH), 128.2 (CH), 126.8 (CH), 106.0 (CH_2), 66.0 (CH_2), 61.3 (CH_2), 60.7 (CH_2), 59.9 (CH_2), 47.0 (CH), 46.9 (CH), 45.6 (CH), 37.4 (CH_2); **LRMS** (m/z, ESI): 244$(M+H)^+$, 212, 168, 152, 134; **HRMS** (ESI-TOF): *m/z* calculated for $C_{16}H_{22}NO$ $[M+H]^+$: *m/z* 244.1701, found 244.1696. Enantioselectivity was determined by chiral HPLC analysis on Chiralpak IA3 at rt, (Hexane : iPrOH = 95:5, 0.5 ml/min).

Racemic sample **4ib** (obtained from *rac*-**4i**, which was obtained in 63% yield following the racemic cycloaddition protocol):

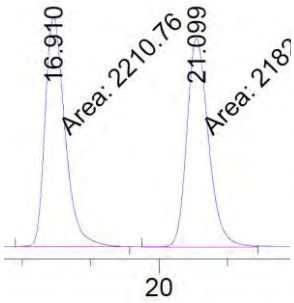

Signal 1: DAD1 A, Sig=220,8 Ref=360,100

Peak #	RetTime [min]	Type	Width [min]	Area [mAU*s]	Height [mAU]	Area %
1	16.910	MM	0.6760	2210.75928	54.50231	50.3269
2	21.099	MM	0.7351	2182.03687	49.47415	49.6731
Totals :				4392.79614	103.97646	

Asymmetric sample (84% ee):

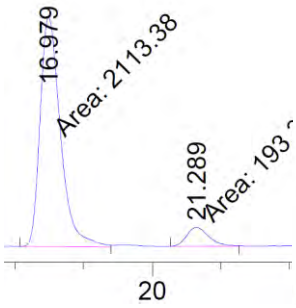

Peak #	RetTime [min]	Type	Width [min]	Area [mAU*s]	Height [mAU]	Area %
1	16.979	MM	0.6869	2113.37598	51.27949	91.6182
2	21.289	MM	0.7567	193.34502	4.25867	8.3818
Totals :				2306.72099	55.53815	

Figure 37. HPLC traces and reports of **4ib**.

Ethyl (3aR*,4R*,6aS*)-6-methylene-2-tosyloctahydrocyclopenta[c]pyrrole-4-carboxylate (4j)

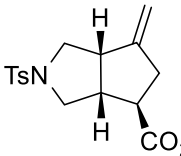

68% yield, Yellowish oil (isolated from a 5:1 mixture of *cis* and *trans* isomers at the ring fusion). **^{1}H-NMR** (300 MHz, $CDCl_3$) δ (ppm): 7.76 - 7.59 (2H, m), 7.41 - 7.28 (2H, m), 4.97 (1H, t, *J* = 2.0 Hz), 4.84 (1H, q, *J* = 1.8 Hz), 4.12 (2H, q, *J* = 7.1 Hz), 3.34 (1H, dd, *J* = 10.0, 2.4 Hz), 3.27 - 2.99 (4H, m), 2.92 - 2.81 (1H, m), 2.71 - 2.50 (3H, m), 2.44 (3H, s), 1.25 (3H, t, *J* = 7.1 Hz); **^{13}C-NMR** (75.4 MHz, $CDCl_3$) *δ* (ppm): 174.2 (C), 151.4 (C), 143.8 (C), 132.4 (C), 129.7 (CH), 128.1 (CH), 108.4 (CH_2), 60.9 (CH_2), 53.8 (CH_2), 53.1 (CH_2), 48.0 (CH), 46.8 (CH), 46.7 (CH), 37.9 (CH_2), 21.7 (CH_3), 14.4 (CH_3). **LRMS** (m/z, ESI): 372 $(M+Na)^+$, 350, 276, 194, 155, 119. **HRMS** (ESI-TOF): *m/z* Calculated for $C_{18}H_{23}NNaO_4S$ $[M+Na]^+$: *m/z* 372.1245, found 372.1242. The stereochemistry was deduced from nOe experiments as well as by analogy with **4i** and **4k**. Enantioselectivity was determined by chiral HPLC analysis on Chiralpak IA3 at rt, (Hexane : iPrOH = 95:5, 0.5 ml/min).

Racemic sample (obtained in 60% yield following the racemic protocol):

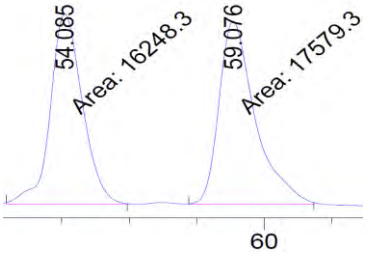

Peak #	RetTime [min]	Type	Width [min]	Area [mAU*s]	Height [mAU]	Area %
1	54.085	MM	1.1043	1.62483e4	245.23212	48.0327
2	59.076	MM	1.2423	1.75793e4	235.84320	51.9673
Totals :				3.38275e4	481.07532	

Asymmetric sample (74% ee)

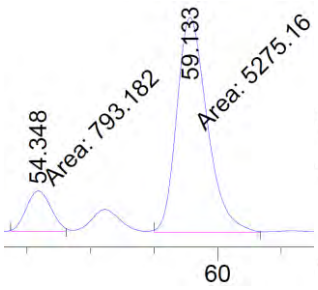

Peak #	RetTime [min]	Type	Width [min]	Area [mAU*s]	Height [mAU]	Area %
1	54.348	MM	0.8923	793.18250	14.81530	13.0708
2	59.133	MM	1.1086	5275.15625	79.30359	86.9292
Totals :				6068.33875	94.11889	

Figure 38. HPLC traces and reports of **4j**.

Ethyl (3aR*,4R*,6aS*)-6-methylenehexahydro-1H-cyclopenta[c]furan-4-carboxylate) (4k)

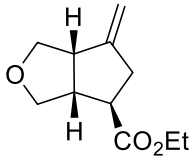

Prepared following a slightly modified procedure, using $Pd_2(dba)_3$ (2.5 mol%) instead of CpPd(η^3-1-PhC_3H_4) (5 mol%) and dioxane instead of toluene, at 130 ºC for 6h, under otherwise identical reaction conditions. 55% yield, colourless oil. **^{1}H- NMR** (300 MHz, $CDCl_3$) δ (ppm): 4.98 (1H, s), 4.85 (1H, s), 4.15 (2H, q, J = 7.2 Hz), 3.87 – 3.79 (4H, m), 3.27 – 3.16 (1H, m), 3.09 – 2.94 (1H, m), 2.72 – 2.59 (3H, m), 1.26 (3H, t, J = 7.2 Hz); **^{13}C-NMR** (75.4 MHz, $CDCl_3$) δ (ppm): 174.9 (C), 153.1 (C), 107.4 (CH_2), 74.9 (CH_2), 73.8 (CH_2), 60.8 (CH_2), 48.8 (CH), 48.7 (CH), 48.5 (CH), 38.6 (CH_2), 13.4 (CH_3); **LRMS** (m/z, ESI): 197 $(M+H)^+$, 167, 151, 123, 93; **HRMS** (ESI-TOF): *m/z* calculated for $C_{11}H_{17}O_3$ $[M+H]^+$: *m/z* 197.1178, found 197.1173. The stereochemistry of **4k** was deduced from nOe experiments and by comparison with previously reported analog **4a**. Enantioselectivity was determined by chiral HPLC analysis on Chiralpak IA3 at rt, (Hexane : iPrOH = 99:1, 0.5 ml/min).

Racemic sample (obtained in 35% yield following the racemic protocol):

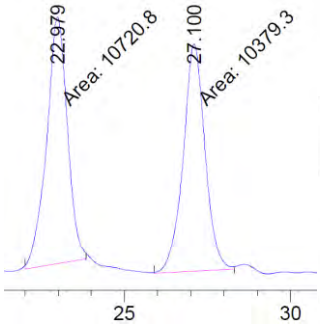

Peak #	RetTime [min]	Type	Width [min]	Area [mAU*s]	Height [mAU]	Area %
1	22.979	MM	0.7284	1.07208e4	245.30203	50.8091
2	27.100	MM	0.7657	1.03793e4	225.91330	49.1909
Totals :				2.11002e4	471.21533	

Asymmetric sample (78% ee):

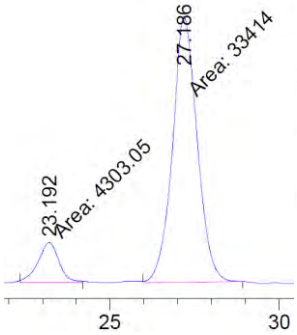

Signal 1: DAD1 A, Sig=210,4 Ref=off

Peak #	RetTime [min]	Type	Width [min]	Area [mAU*s]	Height [mAU]	Area %
1	23.192	MM	0.7259	4303.05420	98.79539	11.4088
2	27.186	MM	0.8483	3.34140e4	656.50415	88.5912
Totals :				3.77171e4	755.29954	

Figure 39. HPLC traces and reports of **4k**.

(3aR,6aS)-2-benzyl-6-methylenehexahydro-1H-spiro[cyclopenta[c]pyrrole-4,1'-cyclopropane] (4m)

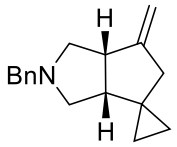

49% yield (75% Conv.), pale yellow oil. Spectroscopic data is in agreement with the described in literature. **^{1}H-NMR** (300 MHz, $CDCl_3$) δ (ppm): 7.34-7.30 (m, 4H), 7.25 (m, 1H), 4.83 (s, 1H), 4.80 (s, 1H), 3.57 (m, 2H), 4.22 (m, 1H) 2.91 (, d, J = 14.8 Hz, 1H), 2.88 (t, J = 8.5 Hz, 1H), 2.63 (t, J = 8.5 Hz, 1H), 2.45 (dd, J = 8.2 y 6.6 Hz, 1H), 2.41 (dd, J = 7.4 y 6.6 Hz, 1H), 2.21 (m, 1H), 0.52 (m, 1H), 0.47 (m, 1H), 0.43-0.40 (m, 2H). Enantioselectivity was determined by chiral GC analysis on ASTEC SUPELCO B-DA, (N_2, flow 0.2 mL/min, 150 ºC, 100 min).

Racemic sample (75% yield following the racemic protocol)

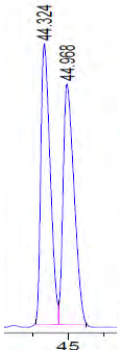

Peak #	RetTime [min]	Type	Width [min]	Area [pA*s]	Height [pA]	Area %
1	44.324	BV	0.2261	1133.57385	61.30854	49.96734
2	44.968	VB	0.2561	1135.05554	52.52047	50.03266
Totals :				2268.62939	113.82900	

Asymmetric sample (50% ee)

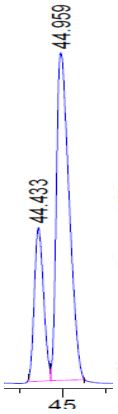

Peak #	RetTime [min]	Type	Width [min]	Area [pA*s]	Height [pA]	Area %
1	44.433	BV	0.2156	411.72571	27.22443	25.45336
2	44.959	VB	0.2815	1205.84375	58.06534	74.54664
Totals :				1617.56946	85.28977	

Figure 40. HPLC traces and reports of **4m**.

Diethyl (3aR,6aS)-4-ethylidene-6-methylenehexahydropentalene-2,2(1H)-dicarboxylate (4o)

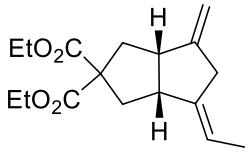

60% yield, colourless oil. Spectroscopic data is in agreement with the described in literature. **^{1}H-NMR** (300 MHz, $CDCl_3$) δ (ppm): 5.27 (m, 1H); 4.88 (s, 1H), 4.84 (s, 1H), 4.21 (q, J = 7.1 Hz, 2H), 4.14 (q, J = 7.1 Hz, 2H), 3.28-3.21 (m, 2H), 3.11 (q, J = 7.8 Hz, 1H), 2.93 (d, J = 19.5 Hz, 1H), 2.67-2.60 (m, 2H), 2.09 (dd, J = 13.5, 7.7 Hz, 1H), 1.87 (dd, J = 13.3, 9.5 Hz, 1H), 1.60 (d, J = 6.9 Hz, 3H), 1.27 (t, J = 7.1 Hz, 3H), 1.22 (t, J = 7.1 Hz, 3H). Enantioselectivity was determined by chiral HPLC analysis on Chiralpak IC at rt, (Hexane : iPrOH = 99:1, 0.5 ml/min).

Racemic sample (77% yield following the racemic protocol)

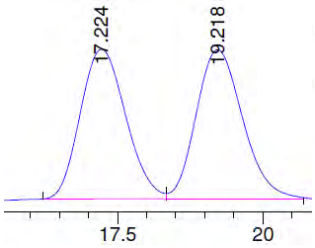

Signal 1: DAD1 A, Sig=220,8 Ref=360,100

Peak #	RetTime [min]	Type	Width [min]	Area [mAU*s]	Height [mAU]	Area %
1	17.224	BV	0.8469	3455.17065	63.69189	49.5914
2	19.218	VB	0.8680	3512.11304	63.43078	50.4086
Totals :				6967.28369	127.12267	

Asymmetric sample (24% ee)

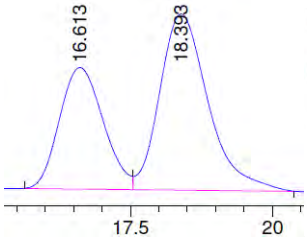

Signal 3: DAD1 C, Sig=210,8 Ref=360,100

Peak #	RetTime [min]	Type	Width [min]	Area [mAU*s]	Height [mAU]	Area %
1	16.613	BV	0.8374	4334.56934	80.86591	38.4575
2	18.393	VB	0.9040	6936.49023	117.27859	61.5425
Totals :				1.12711e4	198.14450	

Figure 41. HPLC traces and reports of **4o**.

1.4. Procedure for the derivatization of the cycloadducts

Procedure for the conversion of 4a into the ketone 4ac

Triethyl (1R*,3aS*,6aR*)-3-oxohexahydropentalene-1,5,5(1H)-tricarboxylate (4ac)

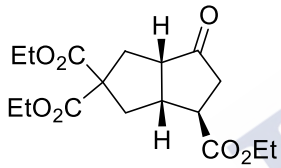

A solution of **4a** (40 mg, 0.118 mmol) in CH_2Cl_2 (5 mL) at -78 °C was bubbled with ozone for 5 minutes until the solution turns blue, then the excess of ozone was removed with an argon flow and PPh_3 (45 mg, 0.17 mmol) was added in one portion. The mixture was stirred at -78 °C for 2.5 h. Then the solvent was evaporated and the crude was purified by flash chromatography (15% Et_2O/ Hexanes) to obtain **4ac** (38 mg, 0.111 mmol, 95% yield) as a colourless oil. **^{1}H-NMR** (300 MHz, $CDCl_3$) δ (ppm): 4.20 – 4.07 (6H, m), 3.07 – 2.97 (1H, m), 2.92 – 2.85 (2H, m), 2.70 – 2.50 (4H, m), 2.31 (1H, dd, *J* = 14.3, 5.4 Hz), 2.10 (1H, dd, *J* = 13.9, 7.6 Hz), 1.30 – 1.03 (9H, m); **^{13}C-NMR** (75 MHz, $CDCl_3$) δ (ppm): 217.1 (C), 174.4 (C), 171.2 (C), 171.1 (C), 62.0 (CH_2), 61.4 (C), 61.3(CH_2), 51.3 (CH), 44.6 (CH), 44.1 (CH), 40.5 (CH_2), 40.4 (CH_2), 36.17 (CH_2), 14.6 (CH_3), 14.4 (CH_3), 14.3 (CH_3); **LRMS** (m/z, CI): 341 ([M^+ + H]), 295, 267, 239, 127; **HRMS** (CI): *m/z* calculated for $C_{17}H_{257}$ [M+H]$^+$: *m/z* 341.1600, found 341.1611.

Procedure for the reduction of esters to 4a, 4i and 4j to alcohols 4ab, 4ib and 4jb

((1R,3aS,6aR)-3-methyleneoctahydropentalene-1,5,5-triyl)trimethanol (4ab)

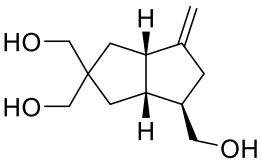

A solution of enantioenriched **4a** (70 mg, 0.19 mmol, 96:4 e.r.) in THF (2 mL) was added dropwise over a suspension of $LiAlH_4$ (66 mg, 1.75 mmol) in THF (2mL) at 0 °C under Argon. The mixture was heated to 70 °C for 1 h, then cooled to rt, and was carefully quenched with HCl (1N) and extracted with EtOAc. The organic phases are dried, concentrated and purified by flash chromatography (3% MeOH/EtOAc) to obtain **4ab** (30 mg, 0.13 mmol, 70%) as pale brown solid. **^{1}H-NMR** (300 MHz, $CDCl_3$) δ (ppm): 4.87 (1H, s), 4.77 (1H, s), 3.66 (2H, s), 3.59 (2H, s), 3.54 – 3.45 (2H, m), 3.00 (1H, q, *J* = 8.9 Hz), 2.68 – 2.56 (2H, m),

2.49 – 2.33 (2H, m), 2.17 (1H, dd, *J* = 15.8, 6.4 Hz), 2.03 – 1.87 (3H, m), 1.37 – 1.14 (3H, m); **^{13}C-NMR** (75 MHz, $CDCl_3$) δ (ppm): δ); 156.0 (C), 106.2 (CH_2), 72.1 (CH_2), 68.7 (CH_2), 66.4 (CH_2), 51.8 (C), 47.4 (CH), 47.1 (CH), 45.9 (CH), 38.6 (CH_2), 38.0 (CH_2), 36.6 (CH_2); **LRMS** (m/z, ESI): 213 ([M^+ + H]), 177, 159, 149, 133; **HRMS** (ESI-TOF): *m/z* calculated for $C_{12}H_{21}O_3$ [M+H]$^+$: *m/z* 213.1491, found 213.1485. **X-ray analysis**: Crystals of **4b** were grown from Chloroform. The molecule has crystallized in the chiral space group P212121. The absolute configuration has been established by anomalous dispersion effects in diffraction measurements on the crystal [Flack8 parameter = 0.02(5)].

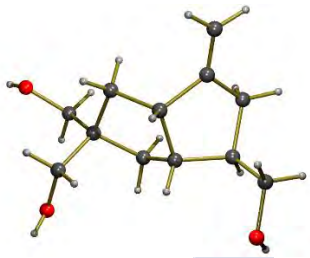

Figure 42. X-ray difraction analysis of **4ab** (CCDC 1844789); Cu-K radiation, Flack parameter: 0.02 (5)

((3aR*,4R*,6aS*)-2-Benzyl-6-methyleneoctahydrocyclopenta[c]pyrrol-4-yl)methanol (4ib)

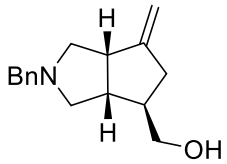

Obtained following the same procedure used for the synthesis of the alcohol **4ab**, to obtain **4ib** (41 mg, 63%) as pale yellow oil. **^{1}H- NMR** (300 MHz, $CDCl_3$) *δ* (ppm): 7.34 – 7.19 (5H, m), 4.89 (1H, s), 4.77 (1H, s), 3.64 - 3.43 (4H, m), 3.09 – 2.98 (1H, m), 2.74 – 2.56 (3H, m), 2.51 (1H, dd, *J* = 9.0, 4.4 Hz), 2.47 – 2.38 (2H, m), 2.15 (1H, dd, *J* = 14.9, 6.2 Hz), 2.06 – 1.94 (1H, m), 1.29 – 1.18 (1H, m); **^{13}C-NMR** (75.4 MHz, $CDCl_3$) δ (ppm): 155.4 (C), 139.2 (C), 128.6 (CH), 128.2 (CH), 126.8 (CH), 106.0 (CH_2), 66.0 (CH_2), 61.3 (CH_2), 60.7 (CH_2), 59.9 (CH_2), 47.0 (CH), 46.9 (CH), 45.6 (CH), 37.4 (CH_2); **LRMS** (m/z, ESI): 244(M+H)$^+$, 212, 168, 152, 134; **HRMS** (ESI-TOF): *m/z* calculated for $C_{16}H_{22}NO$ [M+H]$^+$: *m/z* 244.1701, found 244.1696.

((3aR*,4R*,6aS*)-6-methylene-2-tosyloctahydrocyclopenta[c]pyrrol-4-yl)metanol (4jb)

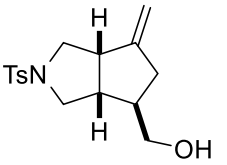

Obtained following the same procedure used for the synthesis of the alcohol **4ab**, using a 4 : 1 mixture of *cis* and *trans* diasteroisomers at the ring fusion of **4j** (48 mg, 0.14 mmol) to afford **4jb** (31 mg, 0.10 mmol, 74%) as a yellowish oil. NMR data of a 4 : 1 mixture of *cis* and *trans* diasteroisomers at the ring fusion of **4e**. **^{1}H-NMR** (300 MHz, $CDCl_3$) δ (ppm): 7.75 – 7.62 (2H, m), 7.37 – 7.27 (2H, m), 4.92 (0.8 H, q, *J* = 2.0 Hz), 4.80 (0.8 H, q, *J* = 2.0 Hz), 4.72 (0.2 H, *J* = 2.2 Hz), 4.64 (0.2H, q, *J* = 2.5 Hz), 3.66 – 3.35 (2H, m), 3.28 – 3.08 (3.6 H, m), 3.08 – 2.99 (1H, m), 2.97 – 2.88 (0.4H, m), 2.86 – 2.73 (0.4H, m), 2.57 – 2.39 (5.2H, m), 2.30 – 2.19 (0.2H, m), 2.30 – 2.19 (0.2H, m), 2.12 (1H, ddt, *J* = 15.8, 8.0, 2.2 Hz), 1.94 (1H, *J* = 14.5, 7.1 Hz); **^{13}C-NMR** (75 MHz, $CDCl_3$) δ (ppm): 152.7 (C), 145.5 (C), 143.7 (C), 143.4 (C), 132.4 (C), 129.9 (CH), 128.1 (CH), 127.8 (C), 127.3 (CH), 108.0 (CH_2), 105.1 (CH_2), 65.8 (CH_2), 65.4 (CH_2), 55.2 (C), 54.1 (CH_2), 53.7 (CH_2), 49.9 (CH_2), 47.4 (CH_2), 47.0 (CH), 46.1 (CH), 45.9 (CH), 41.7 (CH), 39.0 (CH_2), 36.8 (CH_2), 21.7 (CH_3), 21.7 (CH_3). **LRMS** (m/z, ESI): 308 ([M^+ + H]), 155, 107; **HRMS** (ESI-TOF): *m/z* calculated for $C_{16}H_{22}NO_3S$ [M+H]$^+$: *m/z* 308.1320, found 308.1313.

3,5-Dinitrobenzoyl derivative for X-ray analysis

((3aR,4R,6aS)-6-methylene-2-tosyloctahydro-2l4-cyclopenta[c]pyrrol-4-yl)methyl 3,5-dinitro benzoate (30)

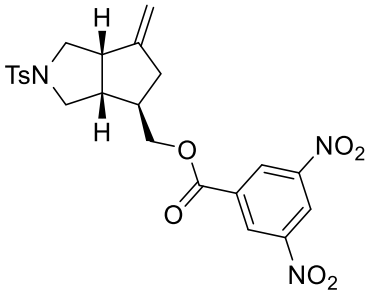

3,5-Dinitrobenzoyl chloride (9 mg, 0.04 mmol) was added in one portion over a solution of the alcohol **4jb** (10 mg, 0.03 mmol), DMAP (0.4 mg, 3 µmol) and Et_3N (5 µL) in dry CH_2Cl_2 (1 mL). The mixture was stirred at rt for 16 h, then dried and purified by flash chromatography (5% EtOAc/Hexanes) to obtain **30** (15 mg, 0.03 mmol, 90% yield) as a yellowish solid. NMR data corresponds to a 4 : 1 mixture of *cis* and *trans* diasteroisomers at the ring fusion of **30**. **^{1}H-NMR** (300 MHz, $CDCl_3$) δ (ppm): 9.30 – 9-20 (1H, m), 9.16 – 9.06 (2H, m), 7.77 – 7.61 (2H, m), 7.39 – 7.29 (2H, m), 5.01 (0.8 H, q, *J* = 1.9 Hz), 4.91 (0.8 H, q, *J* = 1.9 Hz), 4.82 (0.2 H, t, *J* = 2.2 Hz), 4.73 (0.2H, t, *J* = 2.5 Hz), 4.53 – 4.18 (2H, m), 3.78 – 3.38 (0.6H, m), 3.29 – 3.08 (4 H, m), 3.07 – 2.89 (0.6H, m), 2.74 – 2.63 (0.8 H, m), 2.54 (1H, dq, *J* = 11.6, 4.2, 3.2 Hz), 2.44 (3H, s), 2.40 – 2.15 (2H, m); **^{13}C-NMR** (75 MHz, $CDCl_3$) δ (ppm): δ 162.6 (C), 162.4 (C), 151.7 (C), 148.9 (C), 143.9 (C), 135.1 (C), 133.7 (C), 132.2 (C), 130.0 (CH), 129.8 (CH), 129.5 (CH), 128.1 (CH), 127.3 (CH), 122.8 (CH), 122.7 (CH), 109.0 (CH_2), 106.1 (CH_2), 69.3 (CH_2), 69.2 (CH_2), 55.2 (CH), 54.3 (CH_2), 53.5 (CH), 53.4 (CH_2), 49.2 (CH_2), 47.3 (CH_2), 47.0 (CH), 46.2 (CH), 43.0 (CH), 39.4 (CH_2), 38.3 (CH), 37.3 (CH_2), 21.7 (CH_3). **LRMS** (m/z, ESI): 502 ([M^+ + H]); **HRMS** (ESI-TOF): *m/z* calculated for $C_{23}H_{24}N_3O_8S$ [M+H]$^+$: *m/z* 502.1284, found 502.1281. **X-ray analysis**: Crystals of the major isomer were grown from an Et_2O/ hexane solution. The molecule has crystallized in the chiral space group P212121. The absolute configuration has been established by anomalous dispersion effects in diffraction measurements on the crystal [Flack8 parameter = -0.04(3)].

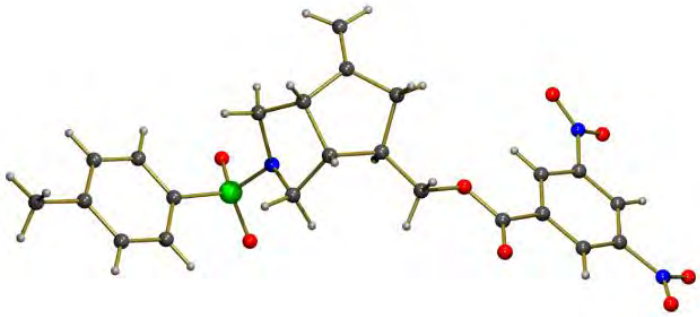

Figure 43. X-ray diffraction analysis of **30** (CCDC 1844790); Flack parameter -0.04 (3)

1.5. Synthesis of (4+3) cycloaddition precursors

Triethyl (1E,3E)-8-cyclopropylidenenona-1,3-diene-1,6,6-tricarboxylate (9b)

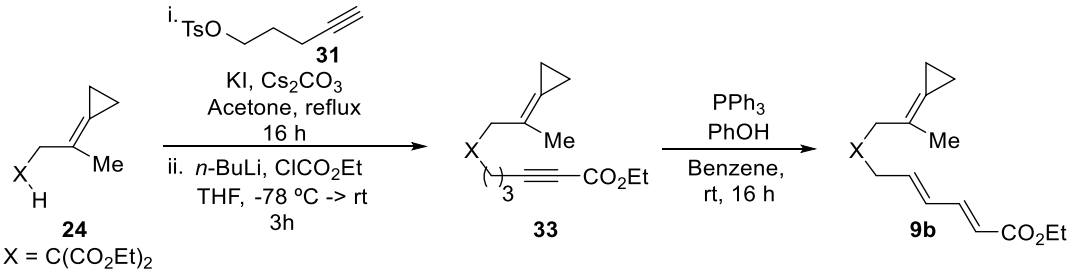

A mixture of **24**[175] (670 mg, 2.79 mmol), 4-pentynyl *p*-tosylate **31**[2] (1.4 g, 6.13 mmol), KI (1.0 g, 6.13 mmol) and Cs_2CO_3 (2.0 g, 5.58 mmol) in acetone (15 mL) was refluxed for 12h. The solvent was partially removed under reduced pressure and the crude was diluted in water (50 mL), extracted with Et_2O (3x30 mL), dried, and concentrated. The residue was purified by chromatography (5 - 10 % Et_2O/hexanes) to give diethyl 2-(2-cyclopropylidenepropyl)-2-(pent-4-yn-1-yl)malonate (751 mg, 2.45 mmol, 88% yield) as a colourless oil. **^{1}H-NMR** (300 MHz, $CDCl_3$): δ (ppm) 4.23 – 4.04 (4H, m), 2.81 (2H, s), 2.09 (2H, td, *J* = 7.0, 2.7 Hz), 1.99 – 1.83 (3H, m), 1.70 – 1.66 (3H, m), 1.48 – 1.33 (2H, m), 1.20 (6H, t, *J* = 7.1 Hz), 1.05 – 0.90 (4H, m) **^{13}C-NMR** (75.4 MHz, $CDCl_3$): δ (ppm) 171.8 (C), 121.3 (C), 119.6 (C), 83.64 (C), 68.7 (C), 61.2 (CH_2), 57.0 (C), 39.3 (CH_2), 31.6 (CH_2), 23.4 (CH_2), 21.3 (CH), 18.7 (CH_2), 14.2 (CH_3), 3.7 (CH_2), 2.6 (CH_2) **LRMS** (*m/z*, *I*): 329 ([M$^+$ +Na]), 187, 159, 131, 119; **HRMS** (ESI-TOF): *m/z* calculated for $C_{18}H_{26}NaO_6$ [M+Na]$^+$: *m/z* 329.1729, found 329.1725.

n-BuLi (0.94 mL, 2.35 mmol) was added to a solution of diethyl 2-(2-cyclopropylidenepropyl)-2-(pent-4-yn-1-yl)malonate (600 mg, 1.96 mmol) in dry THF (32 mL) at -78 ºC. After stirring the mixture for 15 minutes, ethyl chloroformiate (0.35 mL, 3.52 mmol) was added dropwise and the resulting solution was further stirred for 30 minutes at -78 ºC and allowed to warm slowly to rt. The mixture was poured into water (50 mL), extracted with Et_2O (3x30 mL), dried and concentrated to give a crude oil which was purified by flash chromatography (10% Et_2O/hexanes) to give triethyl 8-cyclopropylidenenon-1-yne-1,6,6-tricarboxylate **33** (513 mg , 1.36 mmol, 69% yield) as a colourless oil. **^{1}H-NMR** (300 MHz, $CDCl_3$) δ (ppm): 4.28 – 4.04 (6H, 2.83 (2H, br s), 2.26 (2H, t, *J* = 7.1 Hz), 2.00 – 1.83 (2H, m), 1.69 (3H, s), 1.59 – 1.37 (2H, m), 1.34 – 1.15 (9H, m), 1.05 – 0.90 (4H, m) **^{13}C-NMR** (75.4 MHz, $CDCl_3$): δ (ppm) 171.7 (C), 153.7 (C), 121.5 (C), 119.5 (C), 88.2 (C), 73.6 (C), 61.8 (CH_2), 61.3 (CH_2), 57.0 (C), 39.4 (CH_2), 31.7 (CH_2), 23.2 (CH_2), 22.8 (CH_3), 19.0 (CH_2), 14.1 (CH_3), 3.8 (CH_2), 2.7 (CH_2) **LRMS** (m/z, ESI): 401 (M+H)$^+$, 309, 271, 259, 213, 185, 157; **HRMS** (ESI-TOF): *m/z* (ESI-TOF): *m/z* calculated for $C_{21}H_{30}NaO_6$ [M+Na]$^+$: *m/z* 401.1940, found 401.1934.

Triphenylphosphine (291 mg, 1.1 mmol) and phenol (104 mg, 1.1 mmol) were added to a solution of **33** (420 mg, 1.1 mmol) in dry benzene (1 mL). The resulting solution was stirred at rt for 12h, poured into NaOH (1M) and extracted with Et_2O (3x20 mL). The organic phases

were dried, filtered and concentrated. The resulting crude oil was purified by chromatography (10% Et_2O/hexanes) to give **9b** (400 mg, 1.05 mmol, 95% yield) as a colourless oil. **^{1}H-NMR** (300 MHz, $CDCl_3$): δ (ppm) 7.19 (1H, dd, *J* = 15.4, 10.0 Hz), 6.21 – 5.92 (2H, m), 5.75 (1H, d, *J* = 15.4 Hz), 4.28 – 4.00 (6H, m), 2.85 (2H, s), 2.68 (2H, d, *J* = 6.6 Hz), 1.72 (1H, s), 1.36 – 1.13 (9H, m), 1.00 (4H, br s); **^{13}C-NMR** (75.4 MHz, $CDCl_3$) δ (ppm): 171.2 (C), 167.1 (C), 144.2 (CH), 138.2 (CH), 131.6 (CH), 121.9 (C), 120.6 (CH), 119.5 (C), 61.4 (CH_2), 60.4 (CH_2), 57.5 (C), 39.9 (CH_2), 36.4 (CH_2), 21.4 (CH_3), 14.38 (CH_3), 14.0 (CH_3), 3.9 (CH_2), 2.8 (CH_2) **LRMS** (m/z, ESI): 401 ([M^++H]), 381, 335, 294, 232, 213, 185; **HRMS** (ESI-TOF): *m/z* calculated for $C_{21}H_{30}NaO_6$ [M+Na]$^+$: *m/z* 401.1940, found 401.1933.

1.6. Representative procedure for the enantioselective (3+2) cycloaddition of alkylidenecyclopropanes and alkenes

Procedure A: exemplified for the reaction of ***9a***.

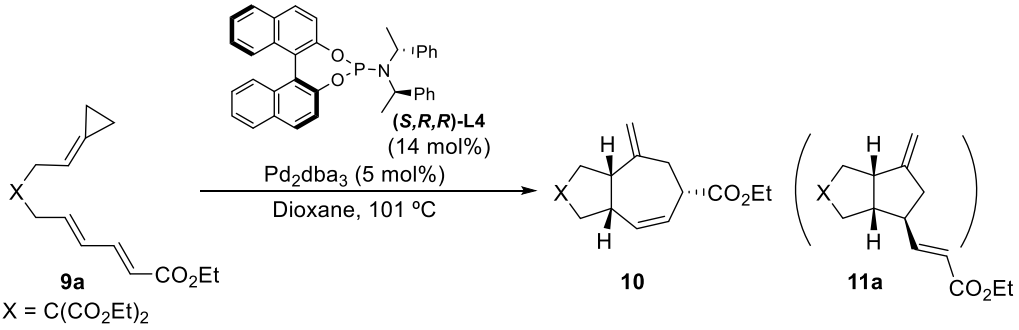

A solution of $Pd_2(dba)_3$ (6.3 mg, 5 mol%), **(*S,R,R*)-L4** (8.9 mg, 14 mol%) and **9a** (50 mg, 0.14mmol) in freshly distilled dioxane (2.7 mL) was carefully degassed and heated under reflux for 4h. The mixture was cooled to rt, diluted with Et_2O and filtered through a short pad of florisil, eluting with Et_2O. The filtrate was concentrated and purified by flash chromatography (3% EtOAc/hexanes) to afford triethyl (3aS*,6S*,8aS*)-4-methylene-3,3a,4,5,6,8a-hexahydroazulene-2,2,6(1H)-tricarboxylate **10a** as colourless oil (45 mg, 90% yield, 6a : 7a = 20 : 1). The spectroscopic data are in agreement with those reported in literature.[163] 1H-NMR (500 MHz, $CDCl_3$): δ (ppm) 5.73 (1H, ddd, J = 11.2, 5.4, 2.9 Hz), 5.47 (1H, ddd, J = 11.0, 3.4, 2.2 Hz), 4.86 (1H, s), 4.82 (1H, s), 4.21 - 4.12 (6H, m), 3.45 – 3.28 (1H, m), 3.09 – 2.92 (1H, m), 2.91 – 2.83 (1H, m), 2.66 (1H, dd, J = 14.1, 5.9 Hz), 2.51-2.42 (3H, m), 2.34 – 2.21 (1H, m), 2.13 (1H, dd, J = 13.1, 8.5 Hz), 1.27 - 1.21 (9H, m). Enantioselectivity was determined by transforming the cycloadduct 6a into the corresponding □,□-unsaturated ester 6a', by treatment with a base, according to the following previously reported procedure: [163]

Isomerization process: To a solution of **10a** (60 mg, 0.165 mmol) in THF (6 mL) was added DBU (140 μL). The resulting mixture was refluxed for 20h, poured into 3% HCl aqueous solution (30 mL) and extracted with Et_2O (3x20 mL). The combined organic phases were washed with water, dried, filtered and concentrated. The crude oil was purified by silica gel chromatography (10 % Et_2O/hexanes) to give 55 mg of **10a'** (92 %) as a colourless oil.

Triethyl (3aS*,8aR*)-4-methylene-3,3a,4,5,8,8a-hexahydroazulene-2,2,6(1H)-tricarboxylate (10a')

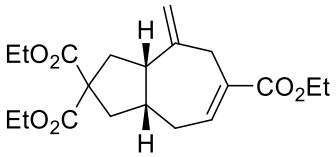

The spectroscopic data are in agreement with those reported in literature.[163] **^{1}H-NMR** (250 MHz, $CDCl_3$): *δ* (ppm) 7.01 – 8.86 (1H, m), 4.93 (1H, s), 4.83 (1H, s), 4.23 - 4.12 (6H, m), 3.31 (1H, d, *J* = 17.2 Hz), 3.05 (1H, d, *J* = 17.2 Hz), 2.94 – 2.81 (1H, m), 2.59 - 2.42 (3H, m), 2.32 - 2.21 (2H, m), 2.07 (1H, ddd, *J* = 15.9, 8.0, 1.5 Hz), 1.92 – 1.77 (1H, m), 1.31 - 1.19 (9H, m); Enantioselectivity was determined by chiral HPLC analysis on (a) Chiralpak OZ-H at rt, (Hexane : iPrOH = 98 : 2, 0.5 mL/min) or on (b) Chiralpak IA3 at rt (Hexane : iPrOH = 99 : 1, 0.5 ml/min) by comparison with an independently prepared racemic sample (see below).

Protocol used for obtaining a racemic samples (exemplified for the cycloaddition of **9a**):[2] A mixture of Pd_2dba_3 (8.12 mg, 6 mol%), **L2** (11.2 mg, 24 mol%) and **9a** (50 mg, 0.137 mmol) were dissolved in freshly distilled dioxane (2.7 mL), The mixture was degassed and the reaction was heated under reflux for 4h. The mixture was cooled to rt, diluted with Et_2O and filtered through a short pad of florisil eluting with Et_2O. The filtrate was concentrated and purified by flash chromatography (3% EtOAc/hexanes) to afford a 8: 1 mixture of **10a** and **11a** mixture as colourless oil (37 mg, 74% yield, **10a** : **11a** = 8 : 1). The mixture was submitted to the based-promoted isomerization so that a racemic sample of **10a'** could be isolated from column chromatography.

Racemic sample **10a'** (analysed in Chiralpak OZ-H, Hexane : iPrOH = 90 : 10, 0.5 ml/min):

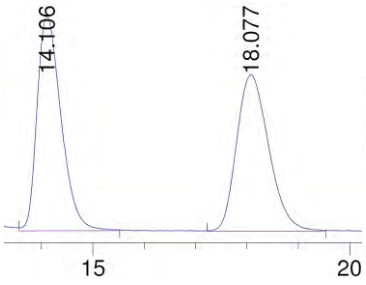

Signal 1: DAD1 A, Sig=220,8 Ref=360,100

Peak #	RetTime [min]	Type	Width [min]	Area [mAU*s]	Height [mAU]	Area %
1	14.106	VB	0.5156	5737.84229	176.36760	50.8087
2	18.077	BB	0.6730	5555.18457	128.34871	49.1913
Totals :				1.12930e4	304.71631	

Asymmetric sample **10a'** (86% ee):

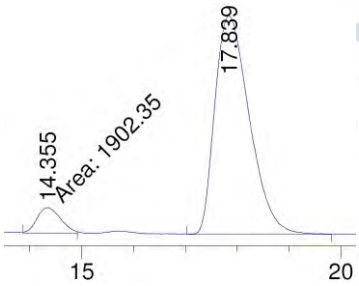

Signal 1: DAD1 A, Sig=220,8 Ref=360,100

Peak #	RetTime [min]	Type	Width [min]	Area [mAU*s]	Height [mAU]	Area %
1	14.355	MM	0.5203	1902.35046	60.94112	7.2366
2	17.839	BB	0.7318	2.43856e4	527.03198	92.7634
Totals :				2.62880e4	587.97310	

Asymmetric sample **10a'** (92% ee):

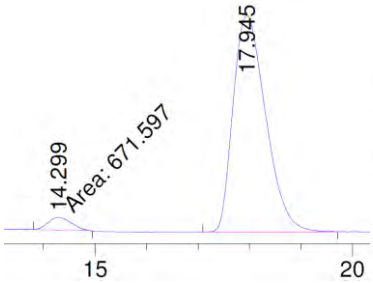

Signal 1: DAD1 A, Sig=220,8 Ref=360,100

Peak #	RetTime [min]	Type	Width [min]	Area [mAU*s]	Height [mAU]	Area %
1	14.299	MM	0.5189	671.59723	21.57003	4.0016
2	17.945	PB	0.7022	1.61114e4	365.56207	95.9984
Totals :				1.67830e4	387.13210	

Figure 44. HPLC traces and reports of **10a`**.

Triethyl (3aR*,6S*,8aS*)-8a-methyl-4-methylene-3,3a,4,5,6,8a-hexahydroazulene-2,2,6(1H)-tricarbo-xylate (10b)

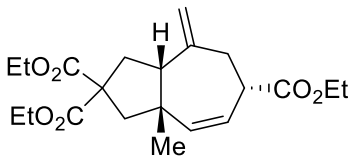

(90 % yield, **10b** : **11b** = 4 : 1) Colourless oil. The spectroscopic data are in agreement with those reported in literature.[163] **^{1}H-NMR** (500 MHz, $CDCl_3$): □ (ppm) 5.72 (1H, dd, *J* = 12.1, 3.5 Hz), 5.50 (1H, ddd, *J* = 12.1, 2.7, 0.9 Hz), 4.97 (1H, d, *J* = 1.9 Hz), 4.90 (1H, d, *J* = 2.2 Hz), 4.24 - 4.13 (6H, m), 3.06 (1H, dq, *J* = 11.9, 3.05 Hz), 2.64 (1H, d, *J* = 13.5 Hz), 2.55 - 2.45 (3H, m), 2.41 (1H, t, *J* = 12.2 Hz), 2.31 (1H, dd, *J* = 12.3, 5.8 Hz), 1.96 (1H, d, *J* = 13.5 Hz), 1.28 - 1.21 (9H, m), 1.08 (3H, s). Enantioselectivity was determined by transforming the cycloadduct **10b** into the corresponding α,β-unsaturated ester **10b'**, by treatment with a base, according to the previously reported procedure.[2]

(3a*R, 8a*R**, *E*)-Triethyl 8a-methyl-4-methylene-3,3a,4,5,8,8a-hexahydroazulene-2,2,6(1*H*)-tricarboxylate (10b`)**

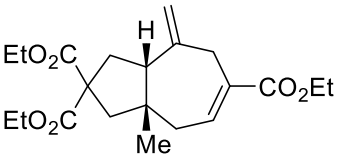

Colourless oil. The spectroscopic data are in agreement with those reported in literature.[163] 1H-NMR (250 MHz, CDCl3): δ (ppm) 6.83 (1H, t, J = 6.4 Hz), 4.83 (1H, s), 4.74 (1H, d, J = 1.8 Hz), 4.20 - 4.07 (6H, m), 3.20 (1H, d, J = 15.9 Hz), 3.08 (1H, d, J = 15.9 Hz), 2.50 - 2.35 (4H, m), 2.20 (2H, s), 1.97 (1H, dd, J = 14.5, 8.0 Hz), 1.28 - 1.18 (9H, m), 0.98 (3H, s); Enantioselectivity was determined by chiral SFC analysis on Lux Cellulose-2 column at 40 °C, (CO2 : MeOH = 95:5, 1 ml/min).

Racemic Sample of **10b'** (obtained from the isomerization of a 3.3 : 1 mixture of **10b** and **11b**, obtained in from the cycloaddition of **9b** according to the racemic protocol, 56% yield)

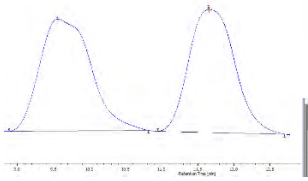

#	Peak Name	CH	tR	Area	Height	Area%	Height%
1	Unknown	6	9,560	11926956	241799	50,448	47,716
2	Unknown	6	11,653	11715214	264942	49,552	52,284

Asymmetric sample (82% ee):

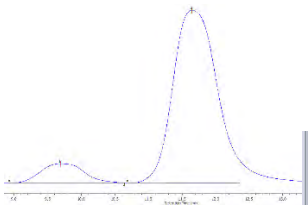

#	Peak Name	CH	tR	Area	Height	Area%	Height%
1	Unknown	6	9,687	3057525	68237	9,373	9,928
2	Unknown	6	11,647	29562278	619070	90,627	90,072

Figure 45. SFC traces and reports of **6c'**.

Triethyl (3aS*,6S*,8aS*)-3a-methyl-6-methylene-3,3a,4,5,6,8a-hexahydroazulene-2,2,6(1H)-tricarboxylate (10c)

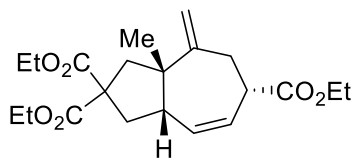

90% global yield (**10c** : **11c** = 2.4 : 1), Colourless oil. NMR data of **10c** deduced from a 2.4 : 1 mixture of **10c** and **11c**. **^{1}H-NMR** (300 MHz, $CDCl_3$) *δ* (ppm): 5.98 – 5.94 (1H, m), 5.85 (1H, ddd, *J* = 11.4, 5.1, 2.6 Hz), 5.04 (1H, t, *J* = 1.1 Hz), 4.93 (1H, d, *J* = 1.3 Hz), 4.14 –

3.92 (6H, m), 3.37 – 3.31 (1H, m), 2.95 (1H, ddt, *J* = 13.9, 5.3, 0.9 Hz), 2.91 – 2.85 (2H, m), 2.81 (1H, dd, *J* = 13.7, 1.1 Hz), 2.76 – 2.71 (1H, m), 2.67 - 2.62 (1H, m), 2.59 – 2.54 (1H, m), 1.23 (3H, s), 1.06 – 0.95 (9H, m); **^{13}C-NMR** (75 MHz, $CDCl_3$) δ (ppm): 173.9 (C), 172.9 (C), 134.4 (CH), 127.2 (CH), 112.6 (CH_2), 102.9 (C), 61.7 (CH_2), 59.4 (C), 54.0 (C), 47.3 (CH_2), 47.2 (CH), 45.4 (CH), 45.1 (CH_2), 39.9 (CH_2), 38.05 (CH_2), 34.47 (CH_2), 24.02 (CH_3), 14.37 (CH_3), 14.15 (CH_3). **LRMS** (m/z, ESI): 401 ([M^+ +Na]), 361, 317, 185, 157, 141, 128; **HRMS** (ESI-TOF): *m/z* calculated for $C_{21}H_{30}NaO_6$ [M+Na]$^+$: *m/z* 401.1940, found 401.1934. The stereochemistry of **10c** was deduced by nOe experiments, in particular nOe between Me-1 and H-4 and between H-4 and H-7.

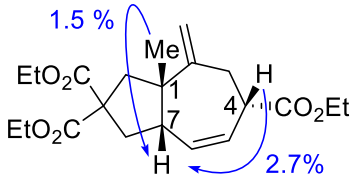

Figure 46. Significant nOes observed for **10c**.

Enantioselectivity was determined by transforming the cycloadduct **10c** into the corresponding *α,β*-unsaturated ester **10c'**, by treatment with a base, according to the previously reported procedure.[163]

Triethyl (3aS*,8aR*)-3a-methyl-4-methylene-3,3a,4,5,8,8a-hexahydroazulene-2,2,6(1H)-tricarboxy-late (10c')

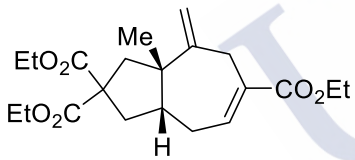

Obtained in 90% yield following the isomerization protocol,[163] colourless oil. **^{1}H-NMR** (500 MHz, $CDCl_3$) *δ* (ppm): 6.88 (1H, ddd, *J* = 7.7, 3.8, 2.5 Hz), 4.87 (1H, s), 4.84 (1H, d, *J* = 1.2 Hz), 4.23 – 4.15 (6H, m), 3.27 (1H, dd, *J* = 17.0, 1.5 Hz), 3.13 (1H, dt, *J* = 17.0, 3.0 Hz), 2.77 – 2.67 (2H, m), 2.38 (1H, d, *J* = 14.1 Hz), 2.35 – 2.23 (1H, m), 2.16 – 2.10 (1H, m), 2.09 – 2.01 (2H, m), 1.31 – 1.22 (9H, m), 1.15 (3H, s); **^{13}C-NMR** (75 MHz, $CDCl_3$) δ (ppm): 173.0 (C), 172.9 (C), 167.7 (C), 152.5 (C), 140.5 (CH), 132.5 (C), 112.3 (CH_2), 61.8 (CH_2), 60.8 (CH_2), 58.9 (C), 51.9 (C), 47.7 (CH), 43.2 (CH_2), 40.0 (CH_2), 34.0 (CH_2), 32.2 (CH_2), 27.2 (CH_3), 14.4 (CH_3), 14.2 (CH_3). **LRMS** (m/z, ESI): 401.19 ([M^+ +Na]), 333, 259, 241, 213, 185, 157; **HRMS** (ESI-TOF): *m/z* calculated for $C_{21}H_{30}NaO_6$ [M+Na]$^+$: *m/z* 401.1940, found 401.1923. Stereochemistry if **10c'** was determined by nOe experiments.

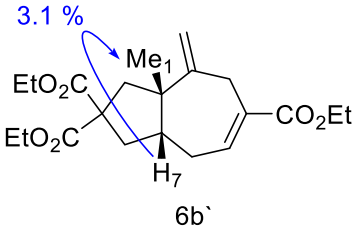

Figure 47. Significant nOes observed for **10c'**.

Enantioselectivity was determined by chiral SFC analysis on Lux Cellulose-2 column at 40 °C, (CO_2 : MeOH = 95:5, 1 ml/min).

Racemic sample of **10c`** (Obtained from the isomerization of a 2.5 : 1 mixture of **10c`** and **11c`**, obtained in from the cycloaddition of **9c** according to the racemic protocol using *rac*-**L4**, 90% yield):

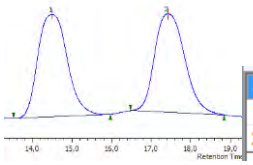

#	Peak Name	CH	tR	Area	Height	Area%	Height%
1	Unknown	6	14,490	14383026	279282	50,409	50,950
2	Unknown	6	17,420	14149558	268865	49,591	49,050

Asymmetric sample (94% ee.):

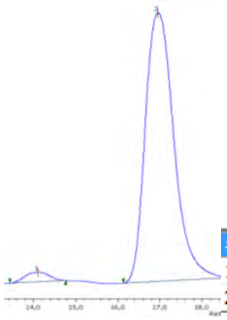

#	Peak Name	CH	tR	Area	Height	Area%	Height%
1	Unknown	6	14,107	398369	9634	3,002	3,415
2	Unknown	6	16,950	12870786	272436	96,998	96,585

Figure 48. SFC traces and reports of **10c'**.

Diethyl (3aS*,6S*,6aS*)-6-((E)-3-ethoxy-3-oxoprop-1-en-1-yl)-3a-methyl-4-methylene-hexahydro pentalene-2,2(1H0020)-dicarboxylate (11c)

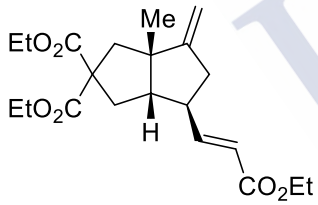

NMR data obtained from a pure sample of **11c** isolated by column chromatography. Colourless oil. **^{1}H-NMR** (300 MHz, $CDCl_3$) δ (ppm): 6.84 (1H, dd, *J* = 15.5, 7.9 Hz), 5.83 (1H, d, *J* = 15.5 Hz), 4.87 (1H, s), 4.80 (1H, s), 4.25 – 4.11 (6H, m), 2.78 – 2.59 (2H, m), 2.59 – 2.53 (1H, m), 2.52 – 2.45 (1H, m), 2.43 (1 H, d, *J* = 14.3 Hz), 2.32 (1H, d, *J* = 14.3 Hz), 2.16 (1H, dd, *J* = 14.1, 3.8 Hz), 2.11 – 2.00 (1H, m), 1.38 – 1.18 (9H, m), 1.16 (3H, s); **^{13}C-NMR** (75 MHz, $CDCl_3$) δ (ppm): 172.5 (C), 166.8 (C), 158.8 (C), 151.2 (CH), 120.9 (CH), 105.4 (CH_2), 61.7 (CH_2), 60.4 (CH_2), 57.9 (CH), 54.1 (C), 47.3 (CH_2), 46.0 (CH), 39.5 (CH_2), 37.8 (CH_2), 29.9 (C), 27.2 (CH_3), 14.4 (CH_3), 14.2 (CH_3). **LRMS** (m/z, ESI): 401 ([M^+ +Na]), 363, 259, 213, 182, 157, 141; **HRMS** (ESI-TOF): *m/z* calculated for $C_{21}H_{30}NaO_6$ [M+Na]$^+$: *m/z* 401.1940, found 401.1932. The stereochemistry was deduced from nOe experiments as well as by analogy with previously reported analog **4d**.

Diethyl (3aS*,8aS*)-4-methylene-3,3a,4,5,6,8a-hexahydroazulene-2,2(1H)-dicarboxylate (10d)

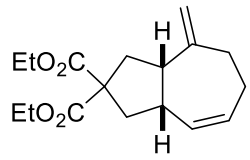

(64 % yield, **10d** : **11d** = 1 : 0) Colourless oil. The spectroscopic data are in agreement with those reported in literature.[163] **^{1}H-NMR** (400 MHz, $CDCl_3$): □ (ppm) 5.57 – 5.49 (1H, m), 5.37 (1H, dd, *J* = 11.4, 2.4 Hz), 4.82 (1H, s), 4.77 (1H, s), 4.19 - 4.13 (4H, m), 3.10 – 3.02 (1H, m), 3.00 – 2.90 (1H, m), 2.49 (1H, dd, *J* = 13.8, 7.2 Hz), 2.41 (1H, dd, *J* = 13.9, 7.2 Hz), 2.38 - 2.10 (6H, m), 1.24 -

1.20 (6H, m). Enantioselectivity was determined by transforming the cycloadduct **10d** into the corresponding diol **10d''**, by treatment with $LiAlH_4$, according to the previously reported procedure.[2]

((3aS*,8aS*)-4-methylene-1,2,3,3a,4,5,6,8a-octahydroazulene-2,2-diyl)dimethanol (10d'')

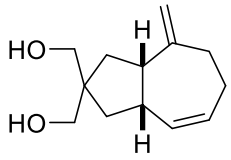

White solid. The spectroscopic data are in agreement with those reported in literature.[163] **^{1}H-NMR** (500 MHz, $CDCl_3$) δ (ppm): 5.65 – 5.44 (1H, m), 5.35 (1H, dt, *J* = 11.5, 2.7 Hz), 4.80 (1H, s), 4.75 (1H, t, *J* = 1.7 Hz), 3.72 - 3.59 (m, 4H), 3.16 – 2.98 (1H, m), 2.97 – 2.82 (1H, m), 2.51 - 2.11 (6H, m), 1.80 - 1.71 (1H, m), 2.38 - 2.10 (6H, m), 1.57-1.48 (4H, m); Enantioselectivity was determined by chiral HPLC analysis on Chiralpak IF3 at rt, (Hexane : iPrOH = 95:5, 0.5 ml/min).

Racemic sample

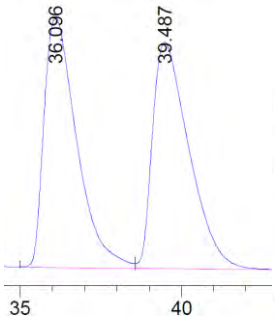

Peak #	RetTime [min]	Type	Width [min]	Area [mAU*s]	Height [mAU]	Area %
1	36.096	BV	1.0143	3.71382e4	525.60779	49.7967
2	39.487	VB	1.0913	3.74415e4	476.20010	50.2033
Totals :				7.45797e4	1001.80789	

Asymmetric sample (54% ee)

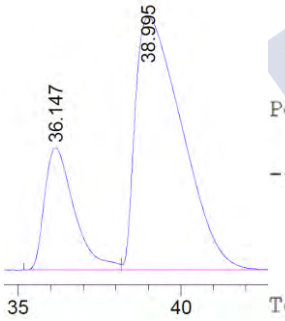

Peak #	RetTime [min]	Type	Width [min]	Area [mAU*s]	Height [mAU]	Area %
1	36.147	BV	0.9141	2.39135e4	373.92819	23.6096
2	38.995	VB	1.3127	7.73735e4	775.01764	76.3904
Totals :				1.01287e5	1148.94583	

Figure 49. HPLC traces and reports of **10d''**.

Ethyl (3aS*,6S*,8aS*)-4-methylene-3,3a,4,5,6,8a-hexahydro-1H-cyclohepta[c]furan-6-carboxylate (10e)

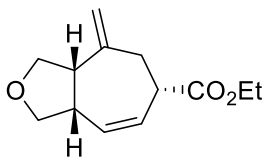

(74 % yield, **10e** : **11e** = 20 : 1) Colourless oil. The spectroscopic data are in agreement with those reported in literature.[163] **^{1}H-NMR** (500 MHz, $CDCl_3$): δ (ppm) 5.92 – 5.77 (1H, m), 5.44 (1H, ddd, *J* = 11.2, 3.1, 2.4 Hz), 4.89 (1H, s), 4.83 (1H, d, *J* = 1.8 Hz), 4.15 (2H, q, *J* = 7.1 Hz), 4.04 (1H, t, *J* = 7.8 Hz), 3.97 (1H, dd, *J* = 8.8, 6.9 Hz), 3.87 (1H, dd, *J* = 8.8, 5.3 Hz), 3.53 (1H, t, *J* = 8.1 Hz), 3.47 (1H, m), 3.11 - 3.02 (2H, m), 2.74 (1H, dd, *J* = 14.1, 6.1 Hz), 2.52 (1H, dd, *J* = 14.1, 12.1 Hz), 1.25 (3H, t, *J* = 7.1 Hz). Enantioselectivity was determined by transforming the cycloadduct **10e** into the corresponding *a,β*-unsaturated ester **10e'**, by treatment with a base, according to the previously reported procedure.[163]

Methyl (3aS*,8aS*)-4-methylene-3,3a,4,5,8,8a-hexahydro-1H-cyclohepta[c]furan-6-carboxylate (10e')

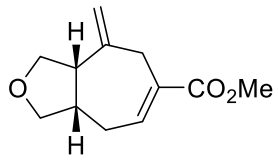

Colourless oil. The spectroscopic data are in agreement with those reported in literature.[163] **^{1}H-NMR** (500 MHz, $CDCl_3$): δ (ppm) 7.05 – 6.93 (1H, m), 4.98 (1H, s), 4.80 (1H, s), 4.01 - 3.96 (2H, m), 3.84 (1H, t, *J* = 8.2 Hz), 3.73 (3H, s), 3.48 (1H, dd, *J* = 8.5 and 5.4 Hz), 3.30 (1H, d, *J* = 17.3 Hz), 3.17 (1H, d, *J* = 17.3 Hz), 3.06 (1H, q, *J* = 7.7 Hz), 2.69 – 2.58 (1H, m), 2.50 – 2.29 (1H, m), 2.16 (1H, ddd, *J* = 15.5, 8.0, 2.6 Hz); Enantioselectivity was determined by chiral HPLC analysis on (a) Chiralpak IF3 at rt, Hexane : iPrOH = 98 : 2, 0.5 ml/min or on (b) Chiralpak IA3 at rt Hexane : iPrOH = 99 : 1, 0.5 ml/min.

Racemic Sample of **10e'** (obtained from the isomerization of a 10 : 1 mixture of **10e** and **11e**, previously obtained in 70% yield following the racemic cycloaddition protocol for **9e**). Chiralpak IF3

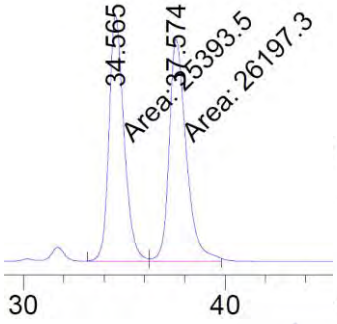

Peak #	RetTime [min]	Type	Width [min]	Area [mAU*s]	Height [mAU]	Area %
1	34.565	MM	0.8619	2.53935e4	491.05078	49.2210
2	37.574	MM	0.9865	2.61973e4	442.59033	50.7790
Totals :				5.15908e4	933.64111	

Asymmetric sample (60% ee), Chiralpak IF3:

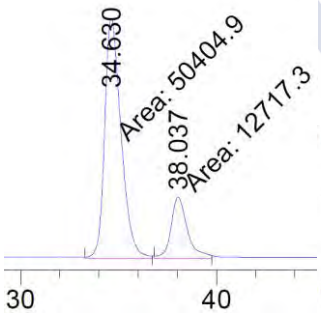

Peak #	RetTime [min]	Type	Width [min]	Area [mAU*s]	Height [mAU]	Area %
1	34.630	MM	0.9681	5.04049e4	867.77142	79.8529
2	38.037	MM	0.9616	1.27173e4	220.42941	20.1471
Totals :				6.31222e4	1088.20084	

Figure 50. SFC traces and reports of **10e'**.

USC
UNIVERSIDADE
DE SANTIAGO
DE COMPOSTELA

CHAPTER II: Palladium catalyzed (3+2) heterocycloadditions of alkylidenecyclopropanes

2.1. Synthesis of oxime substrates

Procedure exemplified for the reaction of **45b**.

Diethyl 2-(2-cyclopropylideneethyl)-2-(2-(methoxyimino)ethyl)malonate (45b)

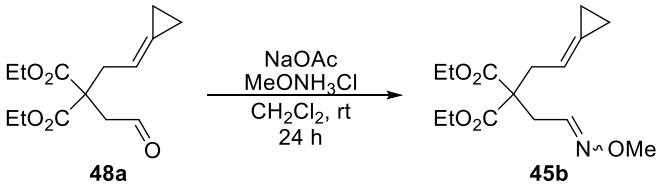

48a **45b**

Aldehyde **48a**[163] (1.30 g, 15.25 mmol, 1 equiv.) was added dropwise over a suspension of NaOAc (2.50 g, 30.51 mmol, 2 eq.) in dry CH_2Cl_2 (30 mL) at room temperature. After 5 minutes, methoxyamine hydrochloride (3.67 g, 15.25 mmol, 1 eq) was added in one portion and the mixture was stirred for 16 h. The reaction was quenched using $NaHCO_3(aq)_{sat}$ (50 mL) and the aqueous phase was extracted with Et_2O (3x20 mL). The combined organic layers were dried, filtered, concentred and purified by flash chromatography (5% EtOAc/Hexanes) affording diethyl 2-(2-cyclopropylideneethyl)-2-(2-(methoxyimino)ethyl)malonate **45b** as a pale-yellow oil (**45b**, *E:Z* ratio 2 : 1, 78% yield). **^{1}H-NMR** (300 MHz, $CDCl_3$): δ (ppm) 6.90 (t, *J* = 6.4 Hz, 0.66 H), 6.27 (t, *J* = 5.3 Hz, 0.33H), 5.28 – 5.08 (m, 1H), 3.89 – 3.63 (m, 4H), 3.41 (s, 1H), 3.35 (s, 2H), 2.43 (d, *J* = 5.3 Hz, 0.66H), 2.37 (d, *J* = 7.4 Hz, 2H), 2.28 (d, *J* = 6.4 Hz, 1.34H), 0.82 (t, *J* = 7.1 Hz, 6H), 0.74 – 0.50 (m, 4H); **^{13}C-NMR** (75 MHz, $CDCl_3$): δ (ppm) 170.7 (C), 170.5 (C), 146.9 (CH), 146.8 (CH), 127.6 (C), 127.4 (C), 111.6 (CH), 111.5 (CH), 61.8, 61.8, 61.7, 61.6, 61.5, 56.1, 56.0, 52.7, 36.4 (CH_2), 36.1 (CH_2), 32.9 (CH_2), 29.1 (CH_2), 14.2 (CH_3), 3.1 (CH_2), 2.0 (CH_2); **LRMS** (m/z, ESI): 298 ([M^+ + H]), 288, 195, 118, 117, 105; **HRMS** (ESI-TOF): *m/z* calculated for $C_{15}H_{24}NO_5$ [M + H]$^+$: *m/z* 298.1654, found 298.1646.

Diethyl 2-(2-((benzyloxy)imino)ethyl)-2-(2-cyclopropylideneethyl)malonate (45a)

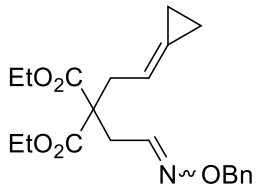

^{1}H NMR (300 MHz, $CDCl_3$) δ 7.36 (t, J = 6.4 Hz, 0.15H), 7.29 – 7.18 (m, 5H), 6.68 (t, J = 5.2 Hz, 0.85H), 5.60 – 5.48 (m, 1H), 5.02 (s, 1.7H), 4.96 (s, 0.3H), 4.14 – 4.02 (m, 4H), 2.87 (d, J = 5.2 Hz, 1.7H), 2.74 (dt, J = 7.4, 1.3 Hz, 2H), 2.66 (d, J = 6.4 Hz, 0.3H), 1.16 (t, J = 7.2 Hz, 6H), 1.03 – 0.84 (m, 4H). **^{13}C NMR** (75 MHz, $CDCl_3$) δ 170.7 (C), 170.5 (C), 147.5 (CH), 137.9 (C), 137.7 (C), 128.4 (CH), 128.3 (CH), 128.1 (CH), 127.9 (CH), 127.4 (C), 127.3 (C), 111.5 (CH), 76.0 (CH2), 75.8 (CH2), 61.7 (CH2), 61.6 (CH2), 56.8 (C), 55.9 (C), 36.3 (CH2), 36.0 (CH2), 32.9 (CH2), 29.26 (CH2), 14.11 (CH3), 3.09 (CH2), 1.97 (CH2). EMAR (ESI-TOF): m/z calculada para $C_{22}H_{27}NO_5$ [M+H]$^+$: 374.1967; encontrada 374.1963.

Diethyl 2-(3-((benzyloxy)imino)propyl)-2-(2-cyclopropylideneethyl)malonate (45c)

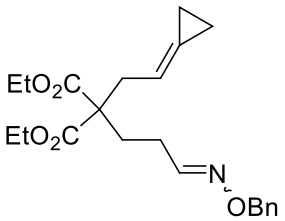

90 % yield, (*E* : *Z* = 1.5 : 1) colourless oil. **^{1}H-NMR** (300 MHz, CD_2Cl_2): δ (ppm) 7.44 – 7.21 (m, 5.6H), 6.62 (t, *J* = 5.3 Hz, 0.4H), 5.66 – 5.53 (m, 1H), 5.07 (s, 0.8H), 5.01 (s, 1.2H), 4.25 – 4.06 (m, 4H), 2.78 (dq, *J* = 7.4, 1.2 Hz, 2H), 2.36 – 2.22 (m, 0.8H), 2.18 – 2.08 (m, 1.2H), 2.07 – 1.95 (m, 2H), 1.32 – 1.14 (m, 6H), 1.14 – 0.91 (m, 4H); **^{13}C-NMR** (75 MHz, CD_2Cl_2): δ (ppm) 171.5 (C), 151.4 (CH), 150.7 (CH), 138.9 (C), 138.6 (C), 128.9 (CH), 128.7 (CH), 128.5 (CH), 128.3 (CH), 128.2 (CH), 127.1 (C), 127.0 (C), 112.4 (CH), 76.3 (CH_2), 76.0 (CH_2), 61.9 (CH_2), 57.7 (C), 57.6 (C), 35.5 (CH_2), 35.3 (CH_2), 29.6 (CH_2), 29.2 (CH_2), 25.3 (CH_2), 21.5 (CH_2), 14.4 (CH_3), 3.3 (CH_2), 2.3 (CH_2), 2.2 (CH_2); **LRMS** (m/z, ESI): 388 ([M^+ + H]), 360, 314; **HRMS** (ESI-TOF): *m/z* calculated for $C_{22}H_{30}NO_5$ [M + H]$^+$: *m/z* 388.2124, found 388.2119.

Diethyl (E)-2-(2-cyclopropylideneethyl)-2-(2-(methoxyimino)propyl)malonate (45d)

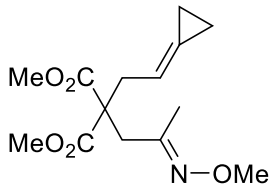

Pale-yellow oil, ratio *E*:*Z* 1:0, 66% yield. **^{1}H NMR** (300 MHz, $CDCl_3$) δ 5.62 – 5.24 (m, 1H), 3.59 (s, 3H), 3.52 (s, 6H), 2.71 (d, *J* = 7.5 Hz, 2H), 2.62 (s, 2H), 1.57 (s, 3H), 1.03 – 0.60 (m, 4H). **^{13}C NMR** (75 MHz, CD_3OD) δ 170.88 (C), 152.27 (C), 126.19 (C), 111.91 (CH), 60.97 (CH_3), 56.30 (C), 52.07 (CH_3), 37.64 (CH_2), 34.88 (CH_2), 14.78 (CH_3), 2.57 (CH_2), 1.44 (CH_2). **HRMS** (ESI-TOF): *m/z* calculated for $C_{14}H_{22}NO_5^+$ [M+H]$^+$: *m/z* 284.1492, found 284.1490.

(E)-2-(2-cyclopropylideneethoxy)acetaldehyde O-methyl oxime (45e)

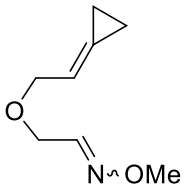

Pale-yellow oil, *E*:*Z* ratio 1.4:1, 57% yield. **^{1}H NMR** (300 MHz, $CDCl_3$) δ 7.44 (t, *J* = 5.7 Hz, 0.6H), 6.84 (t, *J* = 3.7 Hz, 0.4H), 5.92 (m, 1H), 4.25 (d, *J* = 3.7 Hz, 0.8H), 4.14 (m, 2H), 4.07 (d, *J* = 5.7 Hz, 1.2H), 3.86 (s, 1.7H), 3.86 (s, 1.3H), 1.18 – 1.01 (m, 4H). **^{13}C NMR** (75 MHz, $CDCl_3$) δ 150.28 (CH), 147.08 (CH), 127.68 (C), 114.12 (CH), 114.04 (CH), 71.11 (CH_2), 70.54 (CH_2), 66.26 (CH_2), 63.87 (CH_2), 61.85 (CH_3), 61.48 (CH_3), 2.23 (CH_2), 1.68 (CH_2), 1.65 (CH_2). **HRMS** (ESI-TOF): *m/z* calculated for $C_8H_{14}NO_2^+$ [M+H]$^+$: *m/z* 156.1019, found 156.1020.

N-(2-cyclopropylideneethyl)-N-(2-(methoxyimino)ethyl)-4-methylbenzenesulfonamide (45f)

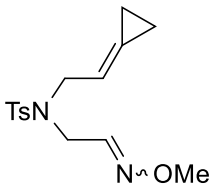

70 % yield (*E*/*Z* = 1.2 : 1), colourless oil. **^{1}H-NMR** (300 MHz, $CDCl_3$): δ (ppm) 7.67 (d, *J* = 7.4 Hz, 2H), 7.34 – 7.23 (m, 2H), 7.13 (t, *J* = 6.0 Hz, 0.6H), 6.58 (t, *J* = 4.2 Hz, 0.4H), 5.70 – 5.49 (m, 1H), 3.94 (d, *J* = 4.2 Hz, 0.9H), 3.89 (dd, *J* = 6.9, 1.2 Hz, 2H), 3.82 (d, *J* = 6.0 Hz, 1.1H), 3.77 (s, 1.4H), 3.72 (s, 1.6H), 2.39 (s, 3H), 1.11 – 0.87 (m, 4H).**^{13}C-NMR** (75 MHz, $CDCl_3$): δ (ppm) 148.3 (CH), 145.7 (CH), 143.6 (C), 143.5 (C), 136.8 (C), 136.2 (C), 129.8 (CH), 129.7 (CH), 129.0 (C), 128.5 (C), 127.1 (CH), 112.0 (CH), 111.8 (CH), 61.9 (CH_3), 61.5 (CH_3), 50.5 (CH_2), 49.2 (CH_2),

45.7 (CH_2), 42.8 (CH_2), 21.4 (CH_3), 2.6 (CH_2), 2.5 (CH_2), 1.8 (CH_2), 1.6 (CH_2); **LRMS** (m/z, ESI): 309 ([M^+ + H]), 250, 184, 155; **HRMS** (ESI-TOF): *m/z* calculated for $C_{15}H_{21}N_2O_3S$ [M + H]$^+$: *m/z* 309.1273, found 309.1270.

5-cyclopropylidenepentanal O-methyl oxime (45g)

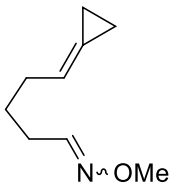

Pale-yellow oil, *E*:*Z* ratio 1.4:1, 57% yield. **^{1}H NMR** (300 MHz, $CDCl_3$) δ 7.36 (t, *J* = 6.2 Hz, 0.6H), 6.63 (t, *J* = 5.5 Hz, 0.4H), 5.80 – 5.65 (m, 1H), 3.85 (s, 1.2H), 3.80 (s, 1.8H), 2.38 – 2.26 (m, 1H), 2.29 – 2.12 (m, 3H), 1.73 – 1.54 (m, 2H), 1.13 – 0.97 (m, 4H);**^{13}C NMR** (75 MHz, $CDCl_3$) δ 151.8 (CH), 150.9 (CH), 122.2 (C), 117.3 (CH), 61.6 (CH_3), 61.2 (CH_3), 31.6 (CH_2), 31.3 (CH_2), 29.1 (CH_2), 26.5 (CH_2), 26.0 (CH_2), 25.2 (CH_2), 2.3 (CH_2), 2.0 (CH_2), 1.9 (CH_2); **LRMS** (m/z, ESI): 154 ([M+ H]), 143, 128; HRMS (ESI-TOF): m/z calculated for $C_9H_{16}NO$ [M + H]$^+$: m/z 154.1232, found 154.1225.

2.2. Representative procedure for the enantioselective intramolecular (3+2) cycloaddition of alkylidenecyclopropanes and oximes.

Procedure exemplified for the reaction of **46b**.

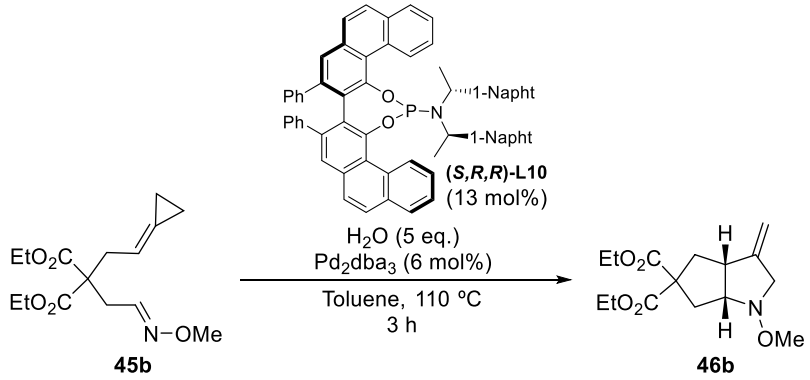

A solution of Pd_2dba_3 (7.4 mg, 6 mol%), **(*S,R,R*)-L10** (16.4 mg, 10 mol%), water (12 µL, 5 eq.) and **45b** (40 mg, 0.135 mmol) in freshly distilled toluene (2.7 mL) was degassed and heated under reflux for 3h. The mixture was cooled to rt, diluted with EtOAc and filtered through a short pad of florisil, eluting with EtOAc. The filtrate was concentrated and purified by flash chromatography (5% EtOAc/hexanes) to afford ethyl (diethyl (3aR,6aR)-1-methoxy-3-methylenehexahydrocyclopenta[b]pyrrole-5,5(1H)-dicarboxylate **46b** as colourless oil (36 mg, 90% yield). **^{1}H-NMR** (300 MHz, $CDCl_3$) δ (ppm): δ 5.00 (s, 1H), 4.93 (s, 1H), 4.31 – 4.04 (m, 4H), 3.85 (d, J = 14.2 Hz, 1H), 3.70 (dt, J = 10.4, 5.7 Hz, 1H), 3.53 (s, 3H), 3.43 (d, J = 13.5 Hz, 1H), 3.16 (q, J = 7.9, 7.4 Hz, 1H), 2.56 – 2.38 (m, 2H), 2.31 (dd, J = 13.5, 6.8 Hz, 1H), 1.24 (t, J = 7.1 Hz, 6H); **^{13}C NMR** (75 MHz, $CDCl_3$) δ 172.2 (C), 171.3 (C), 149.5 (C), 107.6 (CH2), 72.9 (CH), 61.7 (CH2), 61.5 (CH2), 61.0 (CH), 60.8 (CH2), 45.0 (CH3), 40.2 (CH2), 38.8 (CH2), 14.2 (CH3), 14.1 (CH3). HRMS (ESI-TOF): m/z calculated for $C_{15}H_{24}NO_5^+$ $[M+H]^+$: m/z 298.1654, found 298.1646. . Stereochemistry of **46b** was determined by nOe experiments. Enantioselectivity was determined by chiral HPLC analysis on Chiralpak OZ-H at rt, (Hexane : iPrOH = 98 : 2, 0.5 mL/min), by comparison with an independently prepared racemic sample (see below).

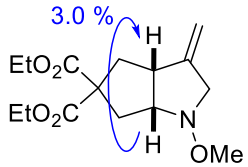

Figure 51. Significant nOes observed for **46b**.

Protocol used for obtaining a racemic samples (exemplified for **46b**): A mixture of Pd_2dba_3 (7.4 mg, 6 mol%), and tris(2,4-di-*tert*-butylphenyl) phosphite (**L1**, 11.9 mg, 20 mol%) and (40 mg, 0.135mmol) were dissolved in freshly distilled dioxane (1.1 mL). The mixture was degassed and the reaction was heated under reflux for 4h. The mixture was cooled to rt, diluted with EtOAc and filtered through a short pad of florisil eluting with EtOAc. The filtrate was concentrated and purified by flash chromatography (5% EtOAc/hexanes) to afford **46b** as colourless oil (28 mg, 74% yield). Enantioselectivity was determined by chiral HPLC analysis

on Chiralpak OZ-H at rt, (Hexane : iPrOH = 98 : 2, 1 mL/min), by comparison with an independently prepared racemic sample (see below).

Racemic sample:

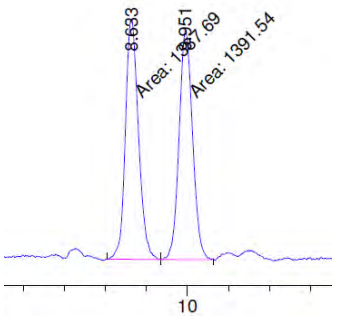

Signal 1: DAD1 A, Sig=220,8 Ref=360,100

Peak #	RetTime [min]	Type	Width [min]	Area [mAU*s]	Height [mAU]	Area %
1	8.633	MF	0.3641	1387.69446	63.52994	49.9308
2	9.951	FM	0.3830	1391.54285	60.55071	50.0692
Totals :				2779.23730	124.08065	

Asymmetric sample (94% ee.):

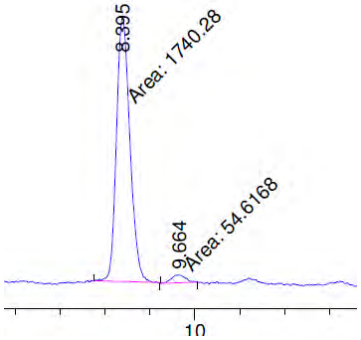

Signal 1: DAD1 A, Sig=220,8 Ref=360,100

Peak #	RetTime [min]	Type	Width [min]	Area [mAU*s]	Height [mAU]	Area %
1	8.395	MM	0.3468	1740.27795	83.62944	96.9571
2	9.664	MM	0.3699	54.61684	2.46096	3.0429
Totals :				1794.89479	86.09040	

Figure 52. HPLC traces and reports of **46b**.

Diethyl (3aR,6aR)-1-(benzyloxy)-3-methylenehexahydrocyclopenta[b]pyrrole-5,5(1H)-dicarboxylate (46a)

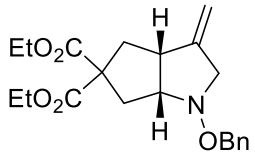

Pale yellow oil. **^{1}H-NMR** (300 MHz, $CDCl_3$) δ (ppm): δ 7.29 – 7.17 (m, 5H), 4.87 (dq, *J* = 16.2, 2.2 Hz, 2H), 4.73 – 4.58 (m, 2H), 4.21 – 3.98 (m, 4H), 3.74 – 3.61 (m, 2H), 3.39 (dt, *J* = 13.5, 2.4 Hz, 1H), 3.09 (q, *J* = 8.4 Hz, 1H), 2.50 – 2.18 (m, 4H), 1.17 (tdd, *J* = 7.1, 4.0, 0.8 Hz, 6H). **^{13}C-NMR** (75 MHz, $CDCl_3$) δ 172.2 (C), 171.**4** (C), 149.**3** (C), 13**8.0** (C), 128.7 (CH), 128.4 (CH), 127.9 (CH), 107.4 (CH2), 7**6.0** (CH2), 73.**1** (CH), 61.7 (CH2), 61.6 (CH2), 61.6 (C), 61.5 (CH2), 45.0 (CH), 40.**2** (CH2), 38.7 (CH2), 14.**2** (CH3), 14.1 (CH3). **HRMS** (ESI-TOF): *m/z* calculated for $C_{21}H_{27}NO_5$ $[M+H]^+$: 374,4570; found 374.1958. Stereochemistry of **46a** was determined by nOe experiments.

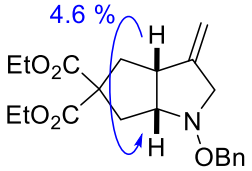

Figure 53. Significant nOes observed for **46a**.

Enantioselectivity was determined by chiral HPLC analysis on Chiralpak IE-3 at rt, (Hexane : iPrOH = 98 : 2, 0.5 mL/min), by comparison with an independently prepared racemic sample (see below).

Racemic sample:

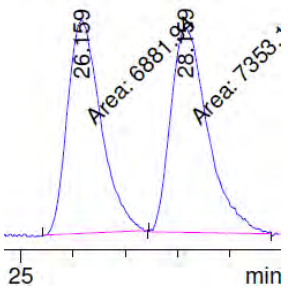

Signal 3: DAD1 C, Sig=210,8 Ref=360,100

Peak #	RetTime [min]	Type	Width [min]	Area [mAU*s]	Height [mAU]	Area %
1	26.159	MM	0.7410	6881.93848	154.79091	48.3449
2	28.159	MM	0.8265	7353.16162	148.28255	51.6551
Totals :				1.42351e4	303.07346	

Asymmetric sample (88% ee)

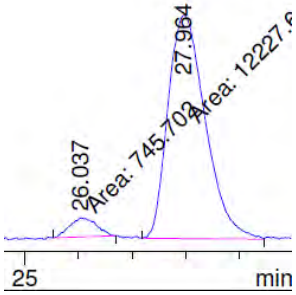

Signal 3: DAD1 C, Sig=210,8 Ref=360,100

Peak #	RetTime [min]	Type	Width [min]	Area [mAU*s]	Height [mAU]	Area %
1	26.037	MM	0.5831	745.70197	21.31582	5.7480
2	27.964	MM	0.8087	1.22276e4	252.00256	94.2520
Totals :				1.29733e4	273.31839	

Figure 54. SFC traces and reports of **46a**.

2.3. Synthesis of aldehydes for the intramolecular cycloaddition

Diethyl 2-(2-cyclopropylideneethyl)-2-(3-oxopropyl)malonate

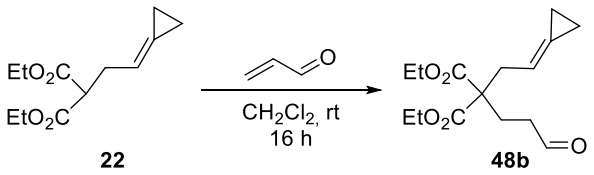

Malonate **22**[161] (0.5 g, 2.21 mmol, 1 equiv.) was added dropwise over a suspension of K_2CO_3 (1.22 g, 8.84 mmol, 4 eq.) in dry CH_2Cl_2 (5 mL) at room temperature. After 5 minutes, acrolein (246 µL, 3.32 mmol, 1.5 eq) was added dropwise and the mixture was stirred for 16 h. The reaction was quenched using $NaHCO_3(aq)_{sat}$ (50 mL) and the aqueous phase was extracted with Et_2O (3x20 mL). The combined organic layers were dried, filtered, concentred and purified by flash chromatography (10% EtOAc/Hexanes) affording diethyl 2-(2-cyclopropylideneethyl)-2-(3-oxopropyl)malonate **48b** as a colourless oil (68% yield). **^{1}H-NMR** (300 MHz, $CDCl_3$): δ (ppm) 9.69 (s, 1H), 5.57 (t, *J* = 7.3 Hz, 1H), 4.15 (q, *J* = 7.1 Hz, 4H), 2.74 (d, *J* = 7.3 Hz, 2H), 2.50 – 2.40 (m, 2H), 2.21 – 2.07 (m, 2H), 1.22 (t, *J* = 7.1 Hz, 6H), 1.12 – 0.91 (m, 4H); **^{13}C-NMR** (75 MHz, $CDCl_3$): δ (ppm) 201.4 (C), 171.5 (C), 127.2 (C), 112.2 (CH), 61.9 (CH_2),

57.3 (C), 39.7 (CH_2), 36.3 (CH_2), 25.4 (CH_2), 14.6 (CH_3), 3.5 (CH_2), 2.4 (CH_2); **LRMS** (m/z, ESI): 305 ([M^+ + Na]), 297, 191, 177, 163, 145, 117; **HRMS** (ESI-TOF): *m/z* calculated for $C_{15}H_{22}NaO_5$ [M + Na]$^+$: *m/z* 305.1365, found 305.1360.

Dimethyl 2-(2-cyclopropylidenepropyl)-2-(3-oxopropyl)malonate (48c)

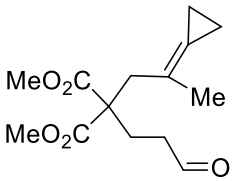

Was synthesized following the same procedure than **48b**, using malonate **24**[175] as precursor. 42% yield, colourless oil. **^{1}H-NMR** (300 MHz, $CDCl_3$): δ (ppm) 9.66 (s, 1H), 3.68 (s, 6H), 2.83 (s, 2H), 2.47 – 2.35 (m, 2H), 2.18 – 2.06 (m, 2H), 1.66 (t, *J* = 1.7 Hz, 3H), 0.98 (s, 4H); **^{13}C-NMR** (75 MHz, $CDCl_3$): δ (ppm) 200.9 (), 171.9 (C), 122.0 (C), 119.0 (C), 56.3 (C), 52.6 (CH_3), 40.2 (CH_2), 39.4 (CH_2), 24.9 (CH_2), 21.2 (CH_3), 3.7 (CH_2), 2.8 (CH_2); **LRMS** (m/z, ESI): 291 ([M^+ + Na]), 269, 251, 219, 191, 159, 131; **HRMS** (ESI-TOF): *m/z* calculated for $C_{14}H_{20}NaO_5$ [M + Na]$^+$: *m/z* 291.1208, found 291.1202.

3,3-bis((benzyloxy)methyl)-5-cyclopropylidenepentanal (48d)

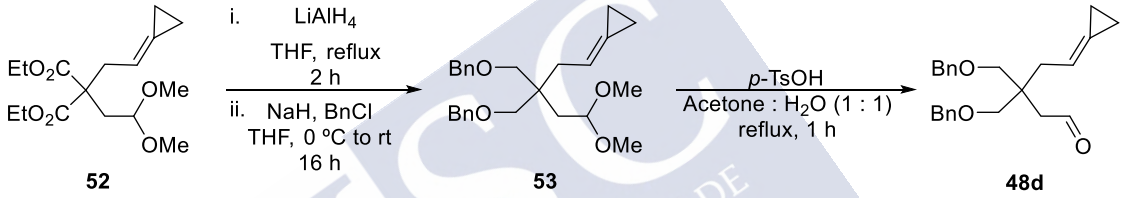

Over a suspension of lithium aluminum hydride (795.3 mg, 20.96 mmol, 3 eq.) in THF (20 mL) was added a solution of diethyl 2-(2-cyclopropylideneethyl)-2-(2,2-dimethoxyethyl)malonate **52**[163] (2.00 g, 6.36 mmol, 1 eq.) in THF (12 mL) dropwise and reaction is gently heated to reflux and stirred for 2 h. the mixture is then cooled to 0 ºC and the reaction is carefully quenched with 30 ml of a $NH_4Cl_{(sat)}$ solution and the mixture is extracted with Et_2O (3x30 mL). The combined organic layers were dried, filtered, concentred and purified by flash chromatography (30% EtOAc/Hexanes) affording 2-(2-cyclopropylideneethyl)-2-(2,2-dimethoxyethyl)propane-1,3-diol as a pale-yellow solid (952 mg, 4.13 mmol, 65%).**^{1}H-NMR** (300 MHz, $CDCl_3$): δ (ppm) 5.81 – 5.67 (m, 1H), 4.69 – 4.59 (m, 1H), 3.62 – 3.43 (m, 4H), 3.37 – 3.30 (m, 6H), 3.02 – 2.91 (m, 2H), 2.12 (d, J = 7.8 Hz, 2H), 1.76 (dt, J = 5.3, 1.6 Hz, 2H), 1.20 – 0.86 (m, 4H). **^{13}C-NMR** (75 MHz, $CDCl_3$): δ (ppm) 125.60 (C), 113.01 (CH), 102.13 (CH), 68.43 (CH_2), 52.96 (CH_3), 42.12 (C), 35.48 (CH_2), 34.76 (CH_2), 3.08 (CH_2), 1.95 (CH2).**LRMS** (m/z, ESI): 387 ([M^+ + Na]), 347, 311, 271, 221, 181, 117, 91; **HRMS** (ESI-TOF): *m/z* calculated for $C_{12}H_{22}NaO_4$ [M + Na]$^+$: *m/z* 253.1416, found 253.1409.

Over a suspension of sodium hydride (265.0 mg, 6.63 mmol, 3 eq.) in THF (20 mL) at 0ºC was added 2-(2-cyclopropylideneethyl)-2-(2,2-dimethoxyethyl)propane-1,3-diol (500.0 mg, 4.21 mmol, 1 eq.) dropwise. After 15 minutes, benzyl bromide (671 µL, 5.53 mmol, 2.5 eq.) was added dropwise and the mixture was stirred at room temperature for 16 h. The reaction was then quenched with 200 mL of a $NH_4Cl_{(sat)}$ solution and the mixture was extracted with Et_2O (3x30 mL). The combined organic layers were dried, filtered, and evaporated to be used

without further purification in the next step. The resulting crude containing **53** was dissolved in a mixture of acetone : H_2O (1:1), (15 mL) and *p*-Toluenesulphonic acid (100 mg, 0.6 mmol, 40 mol%) was added in one portion. The mixture was heated to reflux for 1 h and then was cooled to rt. Acetone was then removed under vacuum and the resulting aqueous phase was then extracted with Et_2O (3x30 mL). The combined organic layers were dried, filtered, concentred and purified by flash chromatography (5% EtOAc/Hexanes) affording 3,3-bis((benzyloxy)methyl)-5-cyclopropylidenepentanal **48d** as a colourless oil (474 mg, 1.30 mmol, 60%). **^{1}H-NMR** (300 MHz, $CDCl_3$): δ (ppm) 9.84 (s, 1H), 7.42 – 7.23 (m, 10H), 5.83 – 5.67 (m, 1H), 4.50 (s, 4H), 3.58 – 3.40 (m, 4H), 2.43 (s, 4H), 1.28 – 0.82 (m, 4H); **^{13}C-NMR** (75 MHz, $CDCl_3$): δ (ppm) 202.70 (CH), 138.45 (C), 128.47 (CH), 127.68 (CH), 127.60 (CH), 125.88 (C), 113.08 (CH), 73.48 (CH_2), 73.17 (CH_2), 47.74 (CH_2), 43.63 (C), 35.97 (CH_2), 3.02 (CH_2), 2.09 (CH_2); **LRMS** (m/z, ESI): 387 ([M^+ + Na]), 347, 311, 271, 221, 181, 117, 91; **HRMS** (ESI-TOF): *m/z* calculated for $C_{24}H_{28}NaO_3$ [M + Na]$^+$: *m/z* 387.1936, found 387.1930.

N-(2-cyclopropylideneethyl)-4-methyl-N-(2-oxoethyl)benzenesulfonamide (48e)

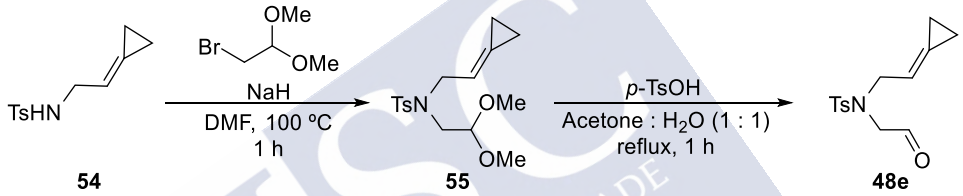

Over a suspension of sodium hydride (185 mg, 4.64 mmol, 1.1 eq.) in DMF (17 mL) at 0ºC is added N-(2-cyclopropylideneethyl)-4-methylbenzenesulfonamide **54**[161] (1.00 g, 4.21 mmol, 1 eq.) in one portion. After 15 minutes, 2-Bromo-1,1-dimethoxyethane (1.5 mL, 12.64 mmol, 3 eq.) is added dropwise and the mixture is heated at 100 ºC for 1 h. The reaction is then quenched with 200 mL of a $NH_4Cl_{(sat)}$ solution and the mixture is extracted with Et_2O (3x30 mL). The combined organic layers were dried, filtered, concentred and purified by flash chromatography (5% EtOAc/Hexanes) affording N-(2-cyclopropylideneethyl)-N-(2,2-dimethoxyethyl)-4-methylbenzenesulfonamide **55** as a pale-yellow solid (1.23 g, 4.18 mmol, 90%). **^{1}H-NMR** (300 MHz, $CDCl_3$): δ (ppm) 7.67 (d, *J* = 6.9 Hz, 2H), 7.25 (d, *J* = 7.5 Hz, 2H), 5.49 (tq, *J* = 6.6, 2.0 Hz, 1H), 4.47 (t, *J* = 5.4 Hz, 1H), 4.01 (d, *J* = 6.8 Hz, 2H), 3.31 (s, 6H), 3.17 (d, *J* = 5.4 Hz, 2H), 2.36 (s, 3H), 1.04 – 0.81 (m, 4H); **^{13}C-NMR** (75 MHz, $CDCl_3$): δ (ppm) 143.0 (C), 137.4 (C), 129.5 (CH), 127.3 (C), 127.0 (CH), 112.5 (CH), 104.0 (CH), 54.5 (CH_3), 50.1 (CH_2), 48.1 (CH_2), 21.3 (CH_3), 2.3 (CH_2), 1.7 (CH_2); **LRMS** (m/z, ESI): 348 ([M^+ + Na]), 294, 262, 138; **HRMS** (ESI-TOF): *m/z* calculated for $C_{16}H_{23}NNaO_4S$ [M + Na]$^+$: *m/z* 348.1245, found 348.1242.

Over a solution of *p*-Toluenesulphonic acid (526 mg, 2.77 mmol, 3 eq.) in a mixture of acetone : H_2O (1:1), (9 mL) was added N-(2-cyclopropylideneethyl)-N-(2,2-dimethoxyethyl)-4-methylbenzenesulfonamide **55** (300 mg, 0.92 mmol, 1 eq.) in one portion, and the mixture is then heated to reflux for 1 h. The mixture is cooled to rt, and the acetone is removed under vacuum and the resulting aqueous phase is then extracted with Et_2O (3x30 mL). The combined organic layers were dried, filtered, concentred and purified by flash chromatography (10%

EtOAc/Hexanes) affording N-(2-cyclopropylideneethyl)-4-methyl-N-(2-oxoethyl)benzene sulfonamide **48e** as a pale-yellow solid (205 mg, 0.74 mmol, 80%). **^{1}H-NMR** (300 MHz, $CDCl_3$): δ (ppm) 9.55 (t, *J* = 1.7 Hz, 1H), 7.71 (d, *J* = 8.3 Hz, 2H), 7.35 (d, *J* = 8.4 Hz, 2H), 5.75 – 5.55 (m, 1H), 3.93 (d, *J* = 7.2 Hz, 2H), 3.71 (s, 2H), 2.45 (s, 3H), 1.18 – 0.82 (m, 4H). **^{13}C-NMR** (75 MHz, $CDCl_3$): δ (ppm) 198.6 (CH), 144.0 (C), 135.4 (C), 130.4 (C), 129.9 (CH), 127.3 (CH), 111.6 (CH), 56.3 (CH_2), 51.1 (CH_2), 21.5 (CH_3), 2.7 (CH_2), 1.8 (CH_2);**LRMS** (m/z, ESI): 280 ([M^+ + H]), 262, 155, 125; **HRMS** (ESI-TOF): *m/z* calculated for $C_{14}H_{18}NO_3S$ [M + H]$^+$: *m/z* 280.1007, found 280.1003.

2.4. Representative procedure for the intramolecular (3+2) cycloaddition of alkylidenecyclopropanes and aldehydes

Procedure exemplified for the reaction of ***48a***.[163]

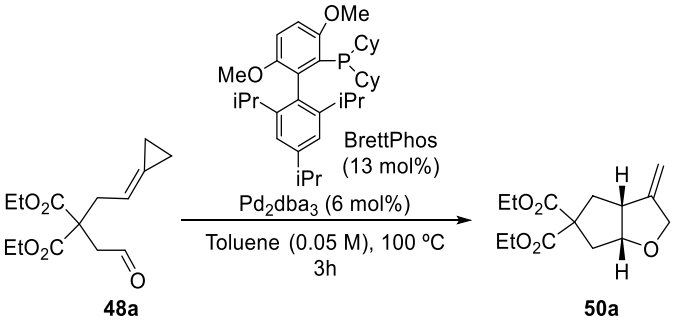

A solution of Pd_2dba_3 (10.3 mg, 6 mol%), BrettPhos (11.0 mg, 13 mol%) and **48a**[163] (40 mg, 0.149mmol) in freshly distilled toluene (3 mL) heated under reflux for 3h. The mixture was cooled to rt, diluted with EtOAc and filtered through a short pad of florisil, eluting with EtOAc. The filtrate was concentrated and purified by flash chromatography (8% EtOAc/hexanes) to afford Ethyl (diethyl (3aR,6aR)-3-methylenehexahydro-5H-cyclopenta[b]furan-5,5-dicarboxylate **50a** as colourless oil (30 mg, 75% yield). **^{1}H-NMR** (300 MHz, $CDCl_3$) δ (ppm): **^{1}H-NMR** (300 MHz, $CDCl_3$): δ (ppm) 4.97 (q, *J* = 2.2 Hz, 1H), 4.90 (q, *J* = 2.0 Hz, 1H), 4.54 (ddd, *J* = 6.3, 4.9, 2.1 Hz, 1H), 4.36 (dd, *J* = 13.0, 1.9 Hz, 1H), 4.24 – 4.07 (m, 5H), 3.24 – 3.08 (m, 1H), 2.55 (dd, *J* = 14.4, 2.2 Hz, 1H), 2.51 – 2.24 (m, 3H), 1.23 (t, *J* = 7.1 Hz, 6H); **^{13}C-NMR** (75 MHz, $CDCl_3$): δ (ppm) 172.1 (C), 171.0 (C), 152.8 (C), 104.8 (CH_2), 85.5 (CH), 72.0 (CH_2), 61.7 (CH_2), 61.5 (CH_2), 61.2 (C), 48.0 (CH), 40.9 (CH_2), 40.3 (CH_2), 14.1 (CH_3), 14.1 (CH_3);); **LRMS** (m/z, ESI): 269 ([M^+ + H]), 223, 195, 149, 121; **HRMS** (ESI-TOF): *m/z* calculated for $C_{14}H_{21}O_5$ [M + H]$^+$: *m/z* 269.1389, found 269.1382. Stereochemistry of **50a** was determined by nOe experiments:

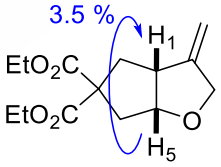

Figure 55. Significant nOes observed for **50a**.

Diethyl (3aR,7aR)-3-methylenehexahydrobenzofuran-5,5(4H)-dicarboxylate (50b)

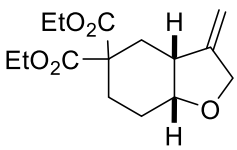

43% Colourless oil. **^{1}H-NMR** (300 MHz, $CDCl_3$): δ (ppm) 5.00 (s, 1H), 4.84 (s, 1H), 4.50 (d, *J* = 13.6 Hz, 1H), 4.30 – 4.06 (m, 5H), 3.87 (s, 1H), 2.72 (dt, *J* = 11.6, 5.2 Hz, 1H), 2.23 (ddd, *J* = 13.7, 6.5, 2.2 Hz, 1H), 2.15 – 1.92 (m, 3H), 1.79 – 1.53 (m, 2H), 1.33 – 1.17 (m, 6H); **^{13}C-NMR** (75 MHz, $CDCl_3$): δ (ppm) 172.1 (C), 170.9 (C), 153.1 (C), 104.3 (CH_2), 76.3 (CH), 70.1 (CH_2), 61.6 (CH_2), 61.3 (CH_2), 54.1 (C), 41.1 (CH), 32.4 (CH_2), 25.0 (CH_2), 24.3 (CH_2), 14.2 (CH_3), 14.2 (CH_3); **LRMS** (m/z, ESI): 283 ([M^+ + H]), 237, 209, 191, 163, 135; **HRMS** (ESI-TOF): *m/z* calculated for $C_{15}H_{23}O_5$ [M + H]$^+$: *m/z* 283.1545, found 283.1544. Stereochemistry of **50b** was determined by nOe experiments:

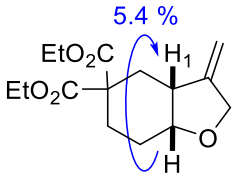

Figure 56. Significant nOes observed for **50b**.

Diethyl (3aR,7aS)-3-methylenehexahydrobenzofuran-5,5(4H)-dicarboxylate (50b`)

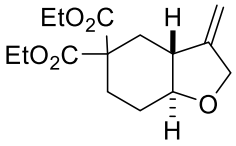

33% Colourless oil. **^{1}H-NMR** (300 MHz, $CDCl_3$): δ (ppm) 4.87 (s, 1H), 4.84 (s, 1H), 4.49 (d, *J* = 13.4 Hz, 1H), 4.35 – 4.11 (m, 5H), 3.12 (td, *J* = 10.5, 3.7 Hz, 1H), 2.75 (d, *J* = 13.2 Hz, 1H), 2.56 (d, *J* = 11.9 Hz, 1H), 2.13 (d, *J* = 10.8 Hz, 1H), 1.99 (t, *J* = 11.9 Hz, 1H), 1.77 – 1.55 (m, 3H), 1.32 – 1.19 (m, 6H); **^{13}C-NMR** (75 MHz, $CDCl_3$): δ (ppm) 171.9 (C), 170.8 (C), 149.7 (C), 102.1 (CH_3), 82.9 (CH), 71.5 (CH_3), 61.8 (CH_3), 61.7 (CH_3), 55.2 (C), 46.1 (CH), 31.7 (CH_3), 30.0 (CH_3), 28.5 (CH_3), 14.2 (CH_3), 14.1 (CH_3); **LRMS** (m/z, ESI): 305 ([M^+ + H]), 237, 191, 163,135; **HRMS** (ESI-TOF): *m/z* calculated for $C_{15}H_{22}O_5Na$ [M + Na]$^+$: *m/z* 305.1365, found 305.1363. Stereochemistry of **50b`** was determined by nOe experiments:

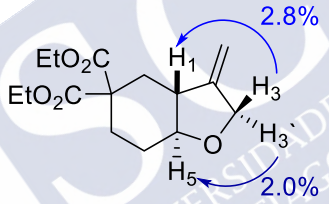

Figure 57. Significant nOes observed for **50b`**.

Dimethyl (3aR,7aR)-3a-methyl-3-methylenehexahydrobenzofuran-5,5(4H)-dicarboxylate (50c)

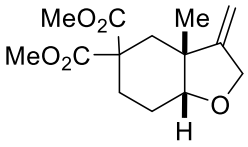

43% yield, white solid. **^{1}H-NMR** (300 MHz, $CDCl_3$): δ (ppm) 4.81 (q, *J* = 2.4 Hz, 2H), 4.58 (dt, *J* = 13.7, 2.4 Hz, 1H), 4.29 (dt, *J* = 13.6, 2.4 Hz, 1H), 3.73 (s, 3H), 3.67 (s, 3H), 3.49 (t, *J* = 3.3 Hz, 1H), 2.17 – 2.04 (m, 2H), 2.05 – 1.91 (m, 3H), 1.81 (ddd, *J* = 12.6, 11.1, 5.6 Hz, 1H), 0.97 (s, 3H); **^{13}C-NMR** (75 MHz, $CDCl_3$): δ (ppm) 172.5 (C), 172.3 (C), 157.9 (C), 102.3 (CH_2), 81.7 (CH), 69.8 (CH_2), 52.9 (CH_3), 52.6 (C), 52.4 (CH_3), 42.6 (C), 36.5 (CH_2), 25.1 (CH_2), 22.8 (CH_2), 20.3 (CH_3); **LRMS** (m/z, ESI): 269 ([M^+ + H]), 237, 209, 191, 177; **HRMS** (ESI-TOF): *m/z* calculated for $C_{14}H_{21}O_5$ [M + H]$^+$: *m/z* 269.1389, found 269.1384. Stereochemistry of **50c** was determined by nOe experiments:

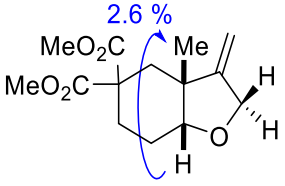

Figure 58. Significant nOes observed for **50c**.

Dimethyl (3aR,7aS)-3a-methyl-3-methylenehexahydrobenzofuran-5,5(4H)-dicarboxylate (50c`)

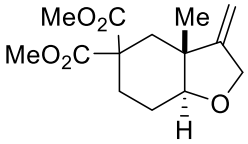

42% yield, white solid. **^{1}H-NMR** (300 MHz, $CDCl_3$): δ (ppm) 4.78 (dt, *J* = 9.7, 2.3 Hz, 2H), 4.51 (dt, *J* = 13.4, 2.4 Hz, 1H), 4.25 (dt, *J* = 13.4, 2.2 Hz, 1H), 3.76 (s, 3H), 3.70 (s, 3H), 3.20 (dd, *J* = 11.0, 5.0 Hz, 1H), 2.76 – 2.63 (m, 2H), 2.06 (d, *J* = 14.0 Hz, 1H), 2.02 – 1.78 (m, 2H), 1.60 – 1.44 (m, 1H), 0.75 (s, 3H); **^{13}C-NMR** (75 MHz, $CDCl_3$): δ (ppm) 172.7 (C), 172.6 (C), 156.2 (C), 100.8 (CH_2), 85.0 (CH), 70.3 (CH_2), 53.5 (C), 53.1 (CH_3), 52.8 (CH_3), 43.36 (C), 37.8 (CH_2), 30.72 (CH_2), 23.1 (CH_2), 17.5 (CH_3); **LRMS** (m/z, ESI): 269 ([M^+ + H]), 137, 209, 177, 151; **HRMS** (ESI-TOF): *m/z* calculated for $C_{14}H_{21}O_5$ [M + H]$^+$: *m/z* 269.1389, found 269.1381. Stereochemistry of **50c`** was determined by nOe experiments:

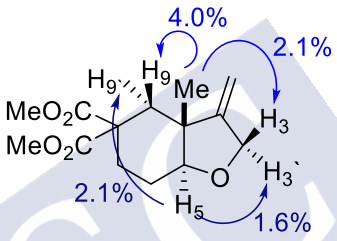

Figure 59. Significant nOes observed for **50c`**.

(3aR,6aR)-5,5-bis((benzyloxy)methyl)-3-methylenehexahydro-2H-cyclopenta[b]furan (50d)

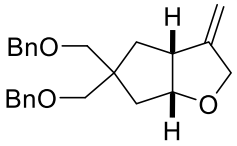

70%, colourless oil. **^{1}H-NMR** (300 MHz, $CDCl_3$): δ 7.39 – 7.21 (m, 10H), 4.88 (q, *J* = 2.1 Hz, 1H), 4.85 (q, *J* = 2.0 Hz, 1H), 4.58 – 4.48 (m, 3H), 4.48 (d, *J* = 1.9 Hz, 2H), 4.41 (dq, *J* = 13.0, 1.6 Hz, 1H), 4.22 (dtd, *J* = 13.0, 2.3, 0.9 Hz, 1H), 3.43 (d, *J* = 1.2 Hz, 2H), 3.37 (s, 2H), 3.10 (q, *J* = 7.6 Hz, 1H), 2.00 (dd, *J* = 13.4, 9.5 Hz, 1H), 1.96 – 1.76 (m, 2H), 1.60 (dd, *J* = 13.5, 7.2 Hz, 1H); **^{13}C-NMR** (75 MHz, $CDCl_3$): δ (ppm) 153.9 (C), 139.0 (C), 138.9 (C), 128.5 (CH), 128.4 (CH), 128.4 (CH), 127.6 (CH), 127.6 (CH), 127.5 (CH), 127.5 (CH), 127.5 (CH), 103.8 (CH_2), 86.8 (CH), 74.7 (CH_2), 74.3 (CH_2), 73.4 (CH_2), 73.3 (CH_2), 72.0 (CH_2), 50.3 (C), 48.3 (CH), 39.3 (CH_2), 38.9 (CH_2); **LRMS** (m/z, ESI): 365 ([M^+ + H]), 257, 181, 91; **HRMS** (ESI-TOF): *m/z* calculated for $C_{24}H_{29}O_3$ [M + H]$^+$: *m/z* 365.2117, found 265.2110. Stereochemistry of **50d** was determined by nOe experiments:

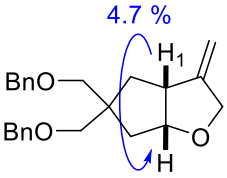

Figure 60. Significant nOes observed for **50d**.

(3aS,6aS)-3-methylene-5-tosylhexahydro-2H-furo[2,3-c]pyrrole (50e)

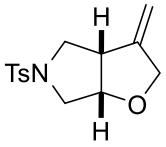

60% yield, pale Orange solid. **^{1}H-NMR** (300 MHz, $CDCl_3$): δ (ppm) 7.69 (d, *J* = 8.0 Hz, 2H), 7.32 (d, *J* = 7.9 Hz, 2H), 5.00 (s, 1H), 4.97 (s, 1H), 4.57 (t, *J* = 5.6 Hz, 1H), 4.35 (d, *J* = 12.8 Hz, 1H), 4.22 (d, *J* = 13.0 Hz, 1H), 3.47 (d, *J* = 11.1 Hz, 1H), 3.40 – 3.06 (m, 4H), 2.43 (s, 3H); **^{13}C-NMR** (75 MHz, $CDCl_3$): δ (ppm) 149.6 (C), 143.9 (C), 132.7 (C), 129.8 (CH), 128.1 (CH), 106.6 (CH_2), 83.1 (CH), 72.2 (CH_2), 54.8 (CH_2), 53.7 (CH_2), 47.6 (CH), 21.7 (CH_3); **LRMS** (m/z, ESI): 280 ([M^+ + H]), 222, 155, 119; **HRMS** (ESI-TOF): *m/z* calculated for $C_{14}H_{18}NO_3S$ [M + H]$^+$: *m/z* 280.1007, found 280.1003. Stereochemistry of **50e** was determined by nOe experiments:

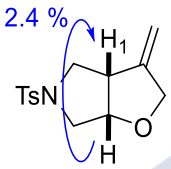

Figure 61. Significant nOes observed for **50e**.

2.5. Synthesis of ketones for the intramolecular cycloaddition

Dimethyl 2-(2-cyclopropylideneethyl)-2-(2-oxopropyl)malonate (49a)

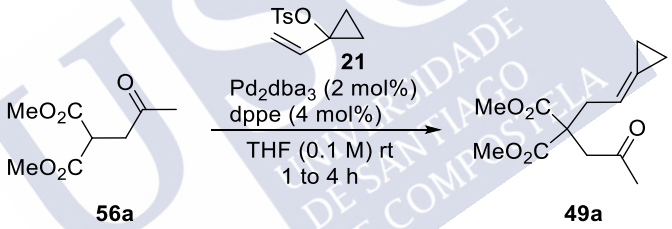

Dimethyl 2-(2-oxopropyl)malonate **56a**[177] (1.00 g, 5.31 mmol, 1.0 eq) was added dropwise to a suspension of NaH (234 mg, 5.85 mmol, 1.1 eq) in THF (53 mL) at 0 °C. After stirring for 10 min at rt, a solution of $Pd_2(dba)_3$ (97 mg, 0.11 mmol, 2 mol%), dppe (85 mg, 0.21 mmol, 4 mol%) and 1-vinylcyclopropyltosylate **21**[161] (1.52 g, 6.38 mmol, 1.2 eq) in THF (15 mL), previously stirred for 10 minutes, was added via cannula. The resulting mixture was further stirred for 3h and then, the reaction was quenched with $NH_4Cl_{(sat)}$, extracted with Et_2O (3x30 mL) and dried. The resulting organic phase was evaporated under reduced pressure and the crude was purified by flash chromatography (5 - 10 % EtOAc/ Hexanes) to yield Diethyl 2-(2-cyclopropylideneethyl)-2-(2,2-dimethoxyethyl)malonate **49a** (1.06 g, 4.17 mmol, 79% yield) as a colourless oil. **^{1}H-NMR** (300 MHz, $CDCl_3$): δ (ppm) 5.56 (tt, *J* = 7.5, 2.0 Hz, 1H), 3.89 – 3.60 (m, 6H), 3.08 (s, 2H), 2.87 (dt, *J* = 7.5, 1.2 Hz, 2H), 2.09 (s, 3H), 1.14 – 0.98 (m, 2H), 0.97 – 0.84 (m, 2H); **^{13}C-NMR** (75 MHz, $CDCl_3$): δ (ppm) 205.2 (C), 171.1 (C), 127.1 (C), 112.3 (CH), 55.5 (C), 52.8 (CH_3), 46.0 (CH_2), 36.1 (CH_2), 30.3 (CH_3), 3.1 (CH_2), 1.9 (CH_2); **LRMS** (m/z, ESI): 277

[177] J. Muñoz-Bascõn, C. Hernández-Cervantes, N. M. Padial, M. Álvarez-Corral, A. Rosales, I. Rodríguez-García, J. E. Oltra, *Chem. - A Eur. J.* **2014**, *20*, 801–810.

([M⁺ + Na]), 272, 255, 223, 195; **HRMS** (ESI-TOF): *m/z* calculated for $C_{13}H_{18}NaO_5$ [M + Na]⁺: *m/z* 277.1052, found 277.1047.

N-(2-cyclopropylideneethyl)-4-methyl-N-(2-oxopropyl)benzenesulfonamide (49c)

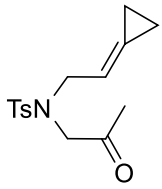

Was synthesized following the procedure used for **49a**. using N-tosylacetamide instead malonate as nucleophile, and was purified by flash chromatography (5 – 10 % EtOAc/ Hexane) to afford **49c** as a pale yellow solid. **¹H-NMR** (300 MHz, $CDCl_3$): δ (ppm) 7.67 (d, *J* = 8.3 Hz, 2H), 7.28 (d, *J* = 8.3 Hz, 2H), 5.67 – 5.51 (m, 1H), 3.88 (d, *J* = 7.1 Hz, 2H), 3.78 (s, 2H), 2.39 (s, 3H), 2.14 (s, 3H), 1.12 – 0.80 (m, 4H); **¹³C-NMR** (75 MHz, $CDCl_3$): δ 204.6 (C), 143.6 (C), 136.0 (C), 129.7 (CH), 129.4 (C), 127.3 (CH), 111.8 (CH), 56.1 (CH_2), 50.4 (CH_2), 26.9 (CH_3), 21.5 (CH_3), 2.6 (CH_2), 1.6 (CH_2); **LRMS** (m/z, ESI): (294 [M⁺ + H]), 276, 221, 139, 96 ; **HRMS** (ESI-TOF): *m/z* calculated for $C_{15}H_{20}NO_3S$ [M + H]⁺: 294.1164 *m/z* , found 294.1159.

1-(2-cyclopropylideneethoxy)propan-2-one (49d)

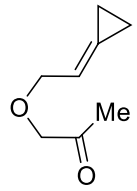

Was prepared following the procedure used for **49a**. using Hydroxyacetone instead malonate as nucleophile, and was purified by flash chromatography (8% Et_2O/ Pentane) to afford **49d** (30% yield) as a pale yellow oil. **¹H-NMR** (300 MHz, CD_2Cl_2): δ (ppm) 5.94 – 5.77 (m, 1H), 4.12 (d, *J* = 6.7 Hz, 1H), 3.96 (s, 2H), 2.07 (s, 3H), 1.14 – 1.00 (m, 4H); **¹³C-NMR** (75 MHz, CD_2Cl_2): δ (ppm) 207.2 (C), 128.1 (C), 114.6 (CH), 75.5 (CH_2), 71.7 (CH_2), 26.6 (CH_3), 2.6 (CH_2), 2.1 (CH_2); **LRMS** (m/z, ESI): 163 ([M⁺ + Na]), 119, 105; **HRMS** (ESI-TOF): *m/z* calculated for $C_8H_{12}NaO_2$ [M + Na]⁺: *m/z* 163.0735, found 163.0735.

Dimethyl 2-(2-cyclopropylideneethyl)-2-(3-oxobutyl)malonate (49e)

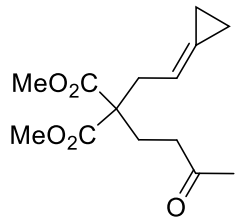

Was synthesized following the procedure used for **49a**. 80% yield, as a white solid oil. **¹H-NMR** (300 MHz, $CDCl_3$): δ (ppm) 5.57 – 5.45 (m, 1H), 3.65 – 3.60 (m, 6H), 2.69 (d, *J* = 7.5 Hz, 2H), 2.44 – 2.33 (m, 2H), 2.10 – 2.01 (m, 5H), 1.04 – 0.86 (m, 4H); **¹³C-NMR** (75 MHz, $CDCl_3$): δ (ppm) 207.2 (C), 171.5 (C), 126.7 (C), 111.6 (CH), 56.9 (C), 52.4 (CH_3), 38.6 (CH_2), 36.0 (CH_2), 29.9 (CH_3), 26.5 (CH_2), 2.9 (CH_2), 1.8 (CH_2); **LRMS** (m/z, ESI): 291 ([M⁺ + Na]), 193, 167, 135; **HRMS** (ESI-TOF): *m/z* calculated for $C_{14}H_{20}O_5Na$ [M + Na]⁺: *m/z* 291.1208, found 291.1205.

Dimethyl 2-(2-cyclopropylidenepropyl)-2-(2-oxopropyl)malonate (49f)

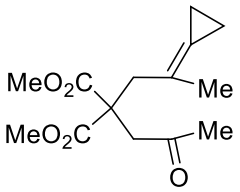

Was synthesized following the procedure used for **49a**. using (2-cyclopropylidenepropoxy)benzene **23** instead vinylcyclopropyltosylate **21** as electrophile, at 50 ºC for 6 h. The compound was purified by flash chromatography (8% Et_2O/ Pentane) to afford **49f** (50% yield) as a white solid. **^{1}H-NMR** (300 MHz, $CDCl_3$): δ (ppm) 3.68 (s, 6H), 3.07 (s, 2H), 2.94 (s, 2H), 2.04 (s, 3H), 1.64 (t, *J* = 1.7 Hz, 3H), 1.03 – 0.83 (m, 4H).; **^{13}C-NMR** (75 MHz, $CDCl_3$): δ (ppm) 205.2 (C), 171.5 (C), 122.0 (C), 119.8 (C), 54.7 (C), 52.8 (CH_3), 45.64 (CH_2), 40.0 (CH_2), 30.0 (CH_3), 21.2 (CH_3), 3.5 (CH_2), 2.7 (CH_2); **LRMS** (m/z, ESI): 291 ([M^+ + Na]), 191, 159, 131; **HRMS** (ESI-TOF): *m/z* calculated for $C_{14}H_{20}NaO_5$ [M + Na]$^+$: *m/z* 291.1208, found 291.1204.

Dimethyl 2-(2-cyclopropylideneethyl)-2-(2-oxobutyl)malonate (49g)

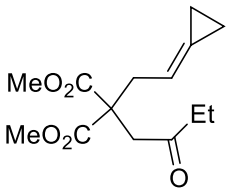

Was synthesized following the procedure used for **49a**. 70% yield, colourless oil. **^{1}H-NMR** (300 MHz, $CDCl_3$): δ (ppm) 5.63 – 5.36 (m, 1H), 3.63 (s, 6H), 2.98 (s, 2H), 2.79 (d, *J* = 7.5 Hz, 2H), 2.30 (q, *J* = 7.3 Hz, 2H), 1.07 – 0.72 (m, 7H); **^{13}C-NMR** (75 MHz, $CDCl_3$): δ (ppm) 207.8 (C), 171.0 (C), 126.8 (C), 112.2 (CH), 55.3 (C), 52.6 (CH_3), 44.6 (CH_2), 36.0 (CH_2), 7.5 (CH_3), 2.9 (CH_2), 1.7 (CH_2); **LRMS** (m/z, ESI): 269 ([M^+ + H]), 237, 205, 177, 121; **HRMS** (ESI-TOF): *m/z* calculated for $C_{14}H_{21}O_5$ [M + H]$^+$: *m/z* 269.1389, found 269.1382.

Dimethyl 2-(2-cyclopropylideneethyl)-2-(3,3-dimethyl-2-oxobutyl)malonate (49h)

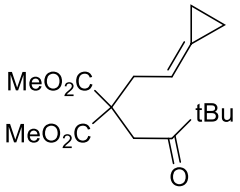

Was synthesized following the procedure used for **49a**. 83% yield, colourless oil. **^{1}H-NMR** (300 MHz, $CDCl_3$): δ (ppm) 5.58 – 5.43 (m, 1H), 3.62 (s, 6H), 3.11 (s, 2H), 2.80 (d, *J* = 7.2 Hz, 2H), 1.03 (s, 9H), 1.01 – 0.80 (m, 4H).**^{13}C-NMR** (75 MHz, $CDCl_3$): δ (ppm) 212.5 (C), 171.2 (C), 126.6 (C), 112.3 (CH), 55.1 (C), 52.5 (CH_3), 43.9 (C), 40.0 (CH_2), 35.9 (CH_2), 26.4 (CH_3), 2.8 (CH_2), 1.8 (CH_2); **LRMS** (m/z, ESI): 297 ([M^+ + H]), 265, 233, 189, 159; **HRMS** (ESI-TOF): *m/z* calculated for $C_{16}H_{25}O_5$ [M + H]$^+$: *m/z* 297.1702, found 297.1696.

Dimethyl 2-(2-cyclopropylideneethyl)-2-(2-oxo-2-phenylethyl)malonate (49i)

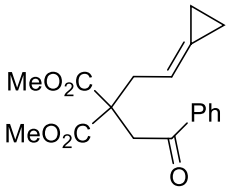

Was synthesized following the procedure used for **49a**. 82% yield, colourless oil. **^{1}H-NMR** (300 MHz, $CDCl_3$): δ (ppm) 7.88 (d, *J* = 7.2 Hz, 1H), 7.51 (t, *J* = 7.3 Hz, 1H), 7.39 (t, *J* = 7.6 Hz, 2H), 5.63 – 5.51 (m, 1H), 3.70 (s, 6H), 3.63 (s, 2H), 2.95 (d, *J* = 7.6 Hz, 2H), 0.96 – 0.82 (m, 2H), 0.73 – 0.66 (m, 2H); **^{13}C-NMR** (75 MHz, $CDCl_3$): δ (ppm) 196.7 (C), 171.1 (C), 136.5 (C), 133.3 (CH), 128.6 (CH), 127.9 (CH), 127.2 (C), 112.2 (CH), 55.4 (C), 52.7 (CH_3), 41.1 (CH_2), 35.6 (CH_2), 2.8 (CH_2), 1.6 (CH_2); **LRMS** (m/z, ESI): 317 ([M^+ + H]), 285, 253, 225; **HRMS** (ESI-TOF): *m/z* calculated for $C_{18}H_{21}O_5$ [M + H]$^+$: *m/z* 317.1389, found 317.1381.

Dimethyl 2-(2-cyclopropylideneethyl)-2-(2-oxocyclopentyl)malonate (49j)

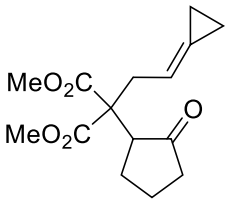

Was synthesized following the procedure used for **49a**. 95% yield, colourless oil. **^{1}H-NMR** (300 MHz, $CDCl_3$): δ (ppm) 5.86 – 5.72 (m, 1H), 3.66 (s, 3H), 3.65 (s, 3H), 2.85 – 2.62 (m, 3H), 2.26 – 2.02 (m, 3H), 2.00 – 1.87 (m, 1H), 1.77 – 1.57 (m, 2H), 1.10 – 0.84 (m, 4H); **^{13}C-NMR** (75 MHz, $CDCl_3$): δ (ppm) 216.4 (C), 171.0 (C), 170.4 (C), 125.8 (C), 113.2 (CH), 59.5 (C), 52.7 (CH_3), 52.3 (CH), 37.7 (CH_2), 36.8 (CH_2), 26.2 (CH_2), 20.4 (CH_2), 2.7 (CH_2), 1.6 (CH_2); **LRMS** (m/z, ESI): 281 ([M^+ + H]), 221, 189, 161, 143; **HRMS** (ESI-TOF): *m/z* calculated for $C_{15}H_{21}O_5$ [M + H]$^+$: *m/z* 281.1389, found 281.1382.

6-cyclopropylidene-1-phenylhexan-2-one (49b)

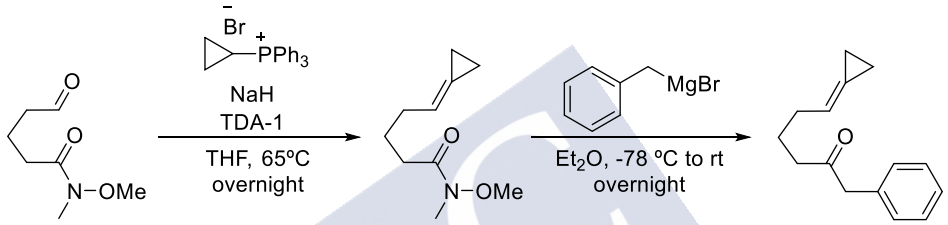

Over a suspension of NaH (863 mg, 21.5 mmol, 2.0 eq) in THF (63 mL) was added Cyclopropyltriphenylphosphonium bromide (8.27 g, 21.5 mmol, 2.0 eq) and the mixture was heated to 65 °C and stirred for 16h, then a mixture of N-methoxy-N-methyl-5-oxopentanamide **58** (1.77 g, 10.7 mmol, 1.0 eq), Tris[2-(2-methoxyethoxy)ethyl]amine (TDA-1) (1.8 mL, 5.4 mmol, 0.5 eq) in THF (10 mL) was added dropwise, maintaining the gentle reflux. The resulting mixture was further stirred for 3h and then, the reaction was quenched with $NH_4Cl_{(sat)}$, extracted with Et_2O (3x30 mL) and dried. The resulting organic phase was evaporated under reduced pressure and the crude was purified by flash chromatography (10 - 15 % EtOAc/ Hexanes) to yield 5-cyclopropylidene-N-methoxy-N-methylpentanamide **59** (760 mg, 4.15 mmol, 38% yield) as a pale yellow oil. **^{1}H-NMR** (300 MHz, $CDCl_3$): δ (ppm) 5.73 – 5.60 (m, 1H), 3.58 (s, 3H), 3.08 (s, 3H), 2.34 (t, *J* = 7.6 Hz, 2H), 2.15 (q, *J* = 7.7, 6.7 Hz, 2H), 1.71 (p, *J* = 7.6 Hz, 2H), 0.93 (q, *J* = 1.6 Hz, 4H).; **^{13}C-NMR** (75 MHz, $CDCl_3$): δ (ppm) 174.5 (C), 121.8 (C), 117.4 (CH), 61.1 (CH_3), 32.1 (CH_3), 31.4 (CH_2), 31.2 (CH_2), 24.2 (CH_2), 2.1 (CH_2), 1.8 (CH_2); **LRMS** (m/z, ESI): 184 ([M^+ + H]), 152, 142, 124, 95; **HRMS** (ESI-TOF): *m/z* calculated for $C_{10}H_{18}NO_2$ [M + H]$^+$: *m/z* 184.1338, found 184.1334.

Over a solution of 5-cyclopropylidene-N-methoxy-N-methylpentanamide **59** (160 mg, 0.87 mmol, 1 eq) in dry Et_2O (6 mL) at -78 °C was added dropwise a solution of Benzylmagnesium bromide (2.9 mL, 2.62 mmol, 3 eq, 3M in Et_2O) then the mixture was warmed at room temperature and the resulting mixture was further stirred for 16h and then, Rochelle´s $Salt_{(sat)}$ (10 mL) was added at 0 °C. The organic phase was washed with $NH_4Cl_{(sat)}$, extracted with Et_2O (3x30 mL), dried and evaporated under reduced pressure and the crude was purified by flash chromatography (5 - 10 % EtOAc/ Hexanes) to yield 6-cyclopropylidene-1-phenylhexan-2-one

49b (145 mg, 0.68 mmol, 78% yield) as a white solid. **^{1}H-NMR** (300 MHz, $CDCl_3$): δ (ppm) 7.29 – 7.13 (m, 3H), 7.15 – 7.07 (m, 2H), 5.67 – 5.48 (m, 1H), 3.57 (s, 2H), 2.37 (t, *J* = 7.4 Hz, 2H), 2.05 (q, *J* = 7.0 Hz, 2H), 1.63 (p, *J* = 7.4 Hz, 2H), 1.00 – 0.81 (m, 4H); **^{13}C-NMR** (75 MHz, $CDCl_3$): δ (ppm) 208.5 (C), 134.5 (C), 129.5 (CH), 128.7 (CH), 127.0 (CH), 122.1 (C), 117.3 (CH), 50.2 (CH_2), 41.5 (CH_2), 31.2 (CH_2), 23.3 (CH_2), 2.3 (CH_2), 1.9 (CH_2); **LRMS** (m/z, ESI): 215 ([M^+ + H]), 197, 155, 131, 91; **HRMS** (ESI-TOF): *m/z* calculated for $C_{15}H_{19}O$ [M + H]$^+$: *m/z* 215.1436, found 215.1432.

2.6. Representative procedure for the intramolecular (3+2) cycloaddition of alkylidenecyclopropanes and ketones

Procedure exemplified for the reaction of **49a**.

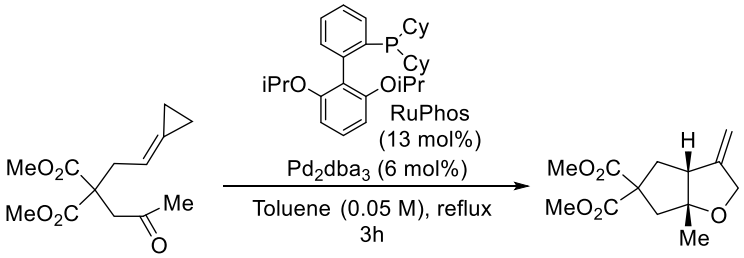

49a **51a**

A solution of Pd_2dba_3 (8.6 mg, 6 mol%), RuPhos (10.2 mg, 13 mol%) and **9a** (40 mg, 0.157mmol) in freshly distilled toluene (3 mL) heated under reflux for 3h. Then the mixture was cooled to rt, diluted with EtOAc and filtered through a short pad of florisil, eluting with EtOAc. The filtrate was concentrated and purified by flash chromatography (8% EtOAc/hexanes) to afford dimethyl (3aR,6aR)-6a-methyl-3-methylenehexahydro-5H-cyclopenta[b]furan-5,5-dicarboxylate **51a** as colourless oil (36 mg, 90% yield). ***NOTE:*** *For compounds **51b**, **51f**, **51i** and **51j** were necessary degassing the mixture in order to obtain the best results. The degassing process was carried out by freezing the reaction mixture using liquid nitrogen and removing the gas phase under high vacuum, then the flask was refilled with argon. This procedure was carried out twice. In the synthesis of **51f** that involve the use of sealed tube, the mixture must be at rt before sealing the tube, to avoid over-pressure at high temperatures.* **^{1}H-NMR** (300 MHz, $CDCl_3$): δ (ppm) 4.98 (dt, *J* = 2.5, 1.3 Hz, 1H), 4.90 (q, *J* = 2.0 Hz, 1H), 4.39 – 4.20 (m, 2H), 3.71 (s, 3H), 3.70 (s, 3H), 2.82 (dd, *J* = 10.3, 5.0 Hz, 1H), 2.69 (dd, *J* = 14.0, 1.2 Hz, 1H), 2.55 (ddd, *J* = 13.7, 5.1, 1.3 Hz, 1H), 2.46 – 2.31 (m, 2H), 1.28 (s, 3H).; **^{13}C-NMR** (75 MHz, $CDCl_3$): δ (ppm) 172.6 (C), 171.5 (C), 153.0 (C), 105.3 (CH_2), 92.4 (C), 70.3 (CH_2), 53.3 (CH), 53.0 (CH_3), 52.7 (CH_3), 46.8 (CH_2), 41.1 (CH_2), 22.8 (CH_3); **LRMS** (m/z, ESI): 255 ([M^+ + H]), 195, 177, 163, 135, 107; **HRMS** (ESI-TOF): *m/z* calculated for $C_{13}H_{19}O_5$ [M + H]$^+$: *m/z* 255.1232, found 255.1227. Stereochemistry of **51a** was determined by nOe experiments:

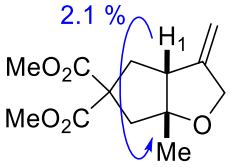

Figure 62. Significant nOes observed for **51a**.

(3aR,6aS)-6a-benzyl-3-methylenehexahydro-2H-cyclopenta[b]furan (51b)

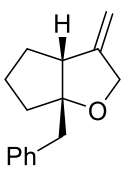

40% yield, colourless oil. **^{1}H-NMR** (300 MHz, $CDCl_3$): δ (ppm) 7.37 – 7.16 (m, 5H), 4.86 (dq, *J* = 4.3, 2.1 Hz, 2H), 4.39 (dq, *J* = 13.0, 1.8 Hz, 1H), 4.27 (dq, *J* = 13.0, 1.3 Hz, 1H), 2.97 (d, *J* = 13.6 Hz, 1H), 2.90 – 2.73 (m, 2H), 1.95 – 1.49 (m, 6H); **^{13}C-NMR** (75 MHz, $CDCl_3$): δ (ppm) 154.8 (C), 138.7 (C), 130.4 (CH), 128.1 (CH), 126.3 (CH), 103.8 (CH_2), 95.9 (C), 71.6 (CH_2), 51.8 (CH), 44.0 (CH_2), 38.7 (CH_2), 34.5 (CH_2), 24.6 (CH_2);

LRMS (m/z, ESI): 215 ([M⁺ + H]), 197, 155, 129; **HRMS** (ESI-TOF): *m/z* calculated for $C_{15}H_{19}O$ [M + H]⁺: *m/z* Stereochemistry of **51b** was determined by analogy with previously reported analogues **51c**.

(3aS,6aS)-6a-methyl-3-methylene-5-tosylhexahydro-2H-furo[2,3-c]pyrrole (51c)

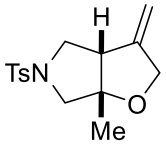

80% yield, pale yellow solid. **¹H-NMR** (300 MHz, $CDCl_3$): δ (ppm) 7.69 (d, *J* = 8.3 Hz, 2H), 7.32 (d, *J* = 8.0 Hz, 2H), 4.97 (q, *J* = 2.1 Hz, 1H), 4.94 (q, *J* = 2.0 Hz, 1H), 4.38 – 4.18 (m, 2H), 3.43 (dd, *J* = 10.2, 8.4 Hz, 2H), 3.20 (dd, *J* = 9.9, 5.1 Hz, 1H), 3.04 (d, *J* = 10.8 Hz, 1H), 2.82 (t, *J* = 6.5 Hz, 1H), 2.43 (s, 3H), 1.26 (s, 3H); **¹³C-NMR** (75 MHz, $CDCl_3$): δ (ppm) 149.7 (C), 143.8 (C), 132.8 (C), 129.7 (CH), 128.0 (CH), 106.9 (CH_2), 90.3 (C), 70.9 (CH_2), 59.0 (CH_2), 53.9 (CH), 53.1 (CH_2), 22.8 (CH_3), 21.7 (CH_3); **LRMS** (m/z, ESI): 294 ([M⁺ + H]), 276, 236, 155, 139; **HRMS** (ESI-TOF): *m/z* calculated for $C_{15}H_{20}NO_3S$ [M + H]⁺: *m/z* 294.1164, found 294.1160. Stereochemistry of **51c** was determined by nOe experiments:

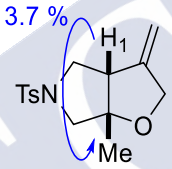

Figure 63. Significant nOes observed for **51c**.

(3aS,6aS)-6a-methyl-3-methylenehexahydrofuro[3,4-b]furan (51d)

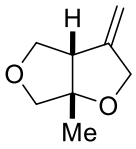

90% yield, pale yellow oil. **¹H-NMR** (300 MHz, CD_2Cl_2): δ (ppm) 5.00 – 4.91 (m, 2H), 4.43 (dq, *J* = 12.8, 1.9 Hz, 1H), 4.33 (dt, *J* = 12.8, 2.1 Hz, 1H), 3.94 – 3.85 (m, 2H), 3.80 (dd, *J* = 8.9, 3.5 Hz, 1H), 3.41 (d, *J* = 9.7 Hz, 1H), 2.93 – 2.80 (m, 1H), 1.34 (s, 3H); **¹³C-NMR** (75 MHz, CD_2Cl_2): δ (ppm) 152.8 (C), 105.5 (CH_2), 92.4 (C), 79.6 (CH_2), 75.8 (CH_2), 72.3 (CH_2), 55.4 (CH), 21.6 (CH_3); **LRMS** (m/z, APCI): 141 ([M⁺ + H]), 123, 111, 95, 83; **HRMS** (APCI-TOF): *m/z* calculated for $C_8H_{13}O_2$ [M + H]⁺: *m/z* 141.0916, found 141.0908. Stereochemistry of **51d** was determined by analogy with previously reported **51c**.

Dimethyl (3aR,7aR)-7a-methyl-3-methylenehexahydrobenzofuran-5,5(4H)-dicarboxylate (51e)

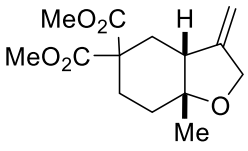

85% yield, colourless oil. **¹H-NMR** (300 MHz, $CDCl_3$): δ (ppm) 5.01 (s, 1H), 4.86 (s, 1H), 4.45 (d, *J* = 13.4 Hz, 1H), 4.28 (dt, *J* = 13.6, 2.2 Hz, 1H), 3.74 (s, 3H), 3.68 (s, 3H), 2.48 (dd, *J* = 11.0, 6.4 Hz, 1H), 2.26 (ddd, *J* = 14.0, 6.6, 1.8 Hz, 1H), 2.14 – 1.88 (m, 3H), 1.62 (dd, *J* = 13.9, 10.9 Hz, 1H), 1.56 – 1.38 (m, 1H), 1.08 (s, 3H); **¹³C-NMR** (75 MHz, $CDCl_3$): δ (ppm) 172.4 (C), 171.6 (C), 152.8 (C), 104.9 (CH_2), 79.8 (C), 68.0 (CH_2), 53.9 (C), 52.8 (CH_3), 52.7 (CH_3), 46.3 (CH), 33.4 (CH_2), 30.9 (CH_2), 26.6 (CH_2), 25.8 (CH_3); **LRMS** (m/z, ESI): 251 ([M⁺ + H]), 237, 209, 191, 177, 151, 131, 121; **HRMS** (ESI-TOF): *m/z* calculated for $C_{14}H_{21}O_5$ [M + H]⁺: *m/z* 269.1389, found 269.1386. Stereochemistry of **51e** was determined by nOe experiments:

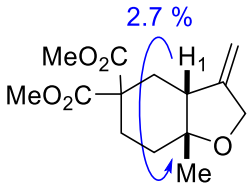

Figure 64. Significant nOes observed for **51e**.

Dimethyl (3aR,6aR)-3a,6a-dimethyl-3-methylenehexahydro-5H-cyclopenta[b]furan-5,5-dicarboxylate (51f)

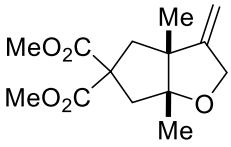

50 % yield, colourless oil. **^{1}H-NMR** (300 MHz, $CDCl_3$): δ (ppm) 4.87 (dt, *J* = 4.0, 2.3 Hz, 2H), 4.36 (dt, *J* = 13.3, 2.4 Hz, 1H), 4.24 (dt, *J* = 13.4, 2.3 Hz, 1H), 3.71 (s, 3H), 3.70 (s, 3H), 2.88 (dd, *J* = 14.3, 1.2 Hz, 1H), 2.75 (dd, *J* = 14.2, 1.1 Hz, 1H), 2.43 (d, *J* = 14.1 Hz, 1H), 1.97 (d, *J* = 14.3 Hz, 1H), 1.09 (s, 3H), 1.09 (s, 3H); **^{13}C-NMR** (75 MHz, $CDCl_3$): δ (ppm) 173.0 (C), 171.9 (C), 157.0 (C), 103.1 (CH_2), 93.7 (C), 69.1 (CH_2), 58.7 (C), 54.0 (C), 53.1 (CH_3), 52.8 (CH_3), 48.2 (CH_2), 45.5 (CH_2), 21.8 (CH_3), 18.8 (CH_3); **LRMS** (m/z, ESI): 269 ([M^+ + H]), 237, 209, 191, 179, 151; **HRMS** (ESI-TOF): *m/z* calculated for $C_{14}H_{21}O_5$ [M + H]$^+$: *m/z* 269.1389, found 269.1383. Stereochemistry of **51f** was determined X-Ray crystallography. **X-ray analysis**: Crystals were grown from CH_2Cl_2/Hexane solution.

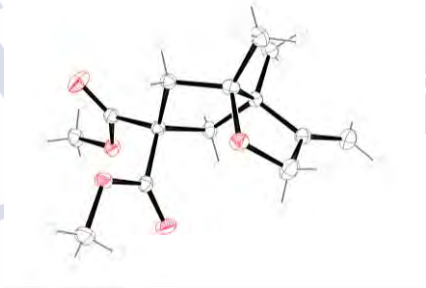

Figure 65. Crystal structure of **51f**.

Dimethyl (3aR,6aR)-6a-ethyl-3-methylenehexahydro-5H-cyclopenta[b]furan-5,5-dicarboxylate (51g)

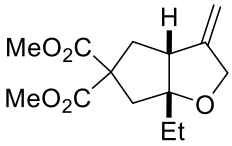

90% Colourless oil. **^{1}H-NMR** (300 MHz, $CDCl_3$): δ (ppm) 4.97 (q, *J* = 2.5 Hz, 1H), 4.87 (q, *J* = 2.0 Hz, 1H), 4.39 – 4.19 (m, 2H), 3.71 (s, 3H), 3.70 (s, 3H), 2.86 (dd, *J* = 10.5, 4.8 Hz, 1H), 2.63 (d, *J* = 14.1 Hz, 1H), 2.54 (ddd, *J* = 13.6, 4.8, 1.3 Hz, 1H), 2.44 – 2.28 (m, 2H), 1.70 – 1.44 (m, 2H), 0.92 (t, *J* = 7.4 Hz, 3H); **^{13}C-NMR** (75 MHz, $CDCl_3$): δ (ppm) 172.6 (C), 171.6 (C), 153.4 (C), 104.9 (CH_2), 95.7 (C), 70.6 (CH_2), 60.5 (C), 53.0 (CH_3), 52.7 (CH_3), 51.9 (CH), 44.4 (CH_2), 41.0 (CH_2), 29.5 (CH_2), 9.1 (CH_3); **LRMS** (m/z, ESI): 291 ([M^+ + H]), 193, 167; **HRMS** (ESI-TOF): *m/z* calculated for $C_{14}H_{20}O_5Na$ [M + Na]$^+$: *m/z* 291.1208, found 291.1205. Stereochemistry of **51g** was determined by nOe experiments:

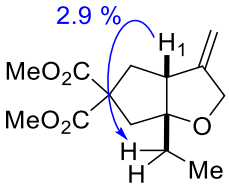

Figure 66. Significant nOes observed for **51g**.

Dimethyl (3aR,6aR)-6a-(tert-butyl)-3-methylenehexahydro-5H-cyclopenta[b]furan-5,5 dicarboxylate (51h)

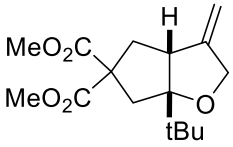

86% yield, white solid. **^{1}H-NMR** (300 MHz, $CDCl_3$): δ (ppm) 4.95 (q, *J* = 2.6 Hz, 1H), 4.81 (q, *J* = 2.0 Hz, 1H), 4.39 – 4.24 (m, 2H), 3.70 (s, 6H), 3.15 (d, *J* = 10.3 Hz, 1H), 2.66 – 2.52 (m, 2H), 2.48 (d, *J* = 14.3 Hz, 1H), 2.31 (dd, *J* = 13.6, 10.3 Hz, 1H), 0.93 (s, 9H); **^{13}C-NMR** (75 MHz, $CDCl_3$): δ (ppm) 172.5 (C), 171.5 (C), 155.3 (C), 103.7 (CH_2), 101.6 (C), 73.0 (CH_2), 60.1 (C), 53.0 (CH_3), 52.7 (CH_3), 48.3 (CH), 43.0 (CH_2), 42.4 (CH_2), 37.8 (C), 26.1 (CH_3); **LRMS** (m/z, ESI): 297 ([M^+ + H]), 265, 237, 205, 181; **HRMS** (ESI-TOF): *m/z* calculated for $C_{16}H_{25}O_5$ [M + H]$^+$: *m/z* 297.1702, found 297.1693. Stereochemistry of **51h** was determined X-Ray crystallography. **X-ray analysis**: Crystals were grown from CH_2Cl_2/Hexane solution.

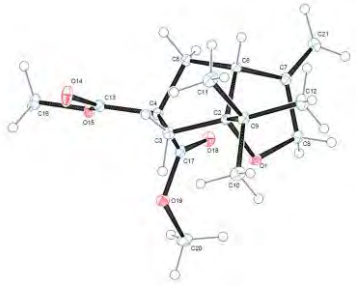

Figure 67. Crystal structure of **51h**.

Dimethyl (3aR,6aR)-3-methylene-6a-phenylhexahydro-5H-cyclopenta[b]furan-5,5-dicarboxylate (51i)

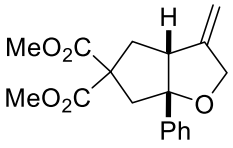

60 % yield, white solid. **^{1}H-NMR** (300 MHz, $CDCl_3$): δ (ppm) 7.46 – 7.21 (m, 5H), 4.99 (q, *J* = 2.5 Hz, 1H), 4.87 (q, *J* = 1.9 Hz, 1H), 4.46 (dq, *J* = 13.2, 2.0 Hz, 1H), 4.28 (dt, *J* = 13.3, 2.6 Hz, 1H), 3.78 (s, 3H), 3.76 (s, 3H), 3.44 (dd, *J* = 10.8, 4.4 Hz, 1H), 2.99 (d, *J* = 13.9 Hz, 1H), 2.78 (ddd, *J* = 13.7, 4.5, 1.4 Hz, 1H), 2.70 (d, *J* = 14.3 Hz, 1H), 2.60 (dd, *J* = 13.7, 10.6 Hz, 1H); **^{13}C-NMR** (75 MHz, $CDCl_3$): δ (ppm) 172.4 (C), 171.5 (C), 152.7 (C), 142.5 (C), 128.5 (CH), 127.3 (CH), 125.3 (CH), 105.1 (CH_2), 96.1 (C), 70.9 (CH_2), 61.1 (C), 55.1 (CH), 53.1 (CH_3), 52.8 (CH_3), 49.4 (CH_2), 41.7 (CH_2); **LRMS** (m/z, ESI): 317 ([M^+ + H]), 299, 257, 239, 179; **HRMS** (ESI-TOF): *m/z* calculated for $C_{18}H_{21}O_5$ [M + H]$^+$: *m/z* 317.1389, found 317.1382. Stereochemistry of **51i** was determined by nOe experiments:

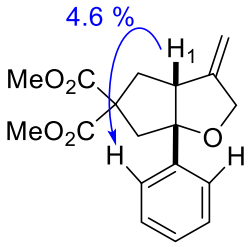

Figure 68. Significant nOes observed for **51i**.

Dimethyl (3aR,5aS,8aS)-3-methyleneoctahydro-5H-pentaleno[6a,1-b]furan-5,5-dicarboxylate (51j)

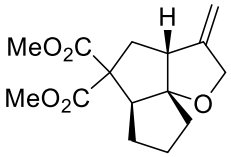

86% yield, white solid. **^{1}H-NMR** (300 MHz, $CDCl_3$): δ (ppm) 4.89 (p, *J* = 2.3 Hz, 2H), 4.48 – 4.32 (m, 2H), 3.69 (s, 3H), 3.64 (s, 3H), 3.26 (t, *J* = 8.7 Hz, 1H), 2.87 (d, *J* = 7.1 Hz, 1H), 2.68 (dd, *J* = 13.9, 7.4 Hz, 1H), 2.45 (ddd, *J* = 13.9, 2.9, 1.2 Hz, 1H), 2.04 – 1.95 (m, 1H), 1.94 – 1.84 (m, 1H), 1.79 – 1.61 (m, 3H), 1.22 – 1.07 (m, 1H); **^{13}C-NMR** (75 MHz, $CDCl_3$): δ (ppm) 172.2 (C), 171.0 (C), 152.1 (C), 104.9 (CH_2), 103.4 (C), 71.8 (CH_2), 63.5 (C), 54.4 (CH), 52.9 (CH_3), 52.6 (CH_3), 51.7 (CH), 39.0 (CH_2), 38.35 (CH_2), 30.0 (CH_2), 26.5 (CH_2); **LRMS** (m/z, ESI): 281 ([M^+ + H]), 249, 221, 203, 163; **HRMS** (ESI-TOF): *m/z* calculated for $C_{15}H_{21}O_5$ [M + H]$^+$: *m/z* 281.1389, found 281.1383. Stereochemistry of **51j** was determined X-Ray crystallography. **X-ray analysis**: Crystals were grown from CH_2Cl_2/Hexane solution.

Figure 69. Crystal structure of **51j**.

2.7. Procedure for the derivatization of the cycloadducts

*Synthesis of a,β-unsaturated Lactones **63a**, **63e** and **63j** (Exemplified for **63a**).*

Dimethyl (3aR,6aR)-6a-methyl-3-methylene-2-oxohexahydro-5H-cyclopenta[b]furan-5,5-dicarboxylate (63a)

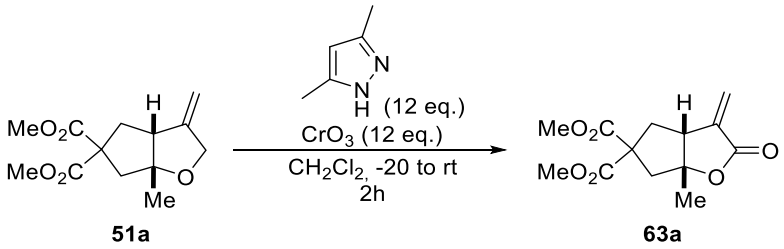

51a **63a**

Over a suspension of Chromium Trioxide (235.9 mg, 2.36 mmol, 12 eq.) in dry CH_2Cl_2 (1 mL) at -20 °C was added 2,5-dimethylpyrazole (226.8 mg, 2.36 mmol, 12 eq) in one portion. After stirring 15 minutes at the same temperature, a solution of malonate **51a** (50.0 mg, 0.197 mmol, 1 eq.) dissolved in CH_2Cl_2 (0.5 mL) was added dropwise, then the resulting mixture is stirred for 1h and a solution of NaOH (5M, 2mL) was added and the mixture was further stirred at 0 °C for 1h. The crude was poured into 1M HCl, extracted with EtOAc (3x10 mL) and dried with anhydrous Na_2SO_4. The organic phase was then evaporated and purified by flash chromatography (15% EtOAc/ Hexanes) to afford **63a** (35 mg, 130 mmol, 66%) as a colourless oil. **^{1}H-NMR** (300 MHz, $CDCl_3$): δ (ppm) 6.23 (d, *J* = 2.0 Hz, 1H), 5.65 (d, *J* = 1.8 Hz, 1H), 3.73 (s, 3H), 3.70 (s, 3H), 3.17 (ddd, *J* = 7.6, 4.1, 1.8 Hz, 1H), 2.82 (d, *J* = 14.8 Hz, 1H), 2.59 (dd, *J* = 13.7, 9.5 Hz, 1H), 2.52 – 2.43 (m, 2H), 1.47 (s, 3H); **^{13}C-NMR** (75 MHz, $CDCl_3$): δ (ppm) 171.4 (C), 170.9 (C), 169.3 (C), 140.1 (C), 123.3 (CH_2), 91.3 (C), 60.6 (C), 53.3 (CH_3), 53.2 (CH_3), 49.0 (CH), 46.2 (CH_2), 41.5 (CH_2), 26.1 (CH_3); **LRMS** (m/z, ESI): 269 ([M^+ + H]), 223, 209, 191, 177, 163; **HRMS** (ESI-TOF): *m/z* calculated for $C_{13}H_{17}O_6$ [M + H]$^+$: *m/z* 269.1025, found 269.1020.

Dimethyl (3aR,7aR)-7a-methyl-3-methylene-2-oxohexahydrobenzofuran-5,5(4H)-dicarboxylate (63e)

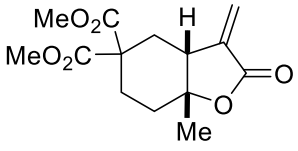

The product was obtained following the abovementioned procedure for the synthesis of **63a**, using **51e**. 71% yield, colourless oil. **^{1}H-NMR** (300 MHz, $CDCl_3$): δ (ppm) 6.18 (d, *J* = 1.7 Hz, 1H), 5.62 (d, *J* = 1.5 Hz, 1H), 3.76 (s, 3H), 3.69 (s, 3H), 2.97 (ddt, *J* = 9.9, 6.6, 1.6 Hz, 1H), 2.42 (dd, *J* = 14.5, 6.6 Hz, 1H), 2.13 – 1.99 (m, 3H), 1.74 (dd, *J* = 14.5, 10.0 Hz, 1H), 1.65 – 1.50 (m, 1H), 1.31 (s, 3H); **^{13}C-NMR** (75 MHz, $CDCl_3$): δ (ppm) 171.6 (C), 171.4 (C), 169.7 (C), 141.1 (C), 122.0 (CH_2), 81.3 (C), 53.0 (CH_3), 53.0 (CH_3), 52.7 (C), 43.0 (CH), 32.9 (CH_2), 30.8 (CH_2), 27.7, 26.0 (CH_2); **LRMS** (m/z, ESI): 283 ([M^+ + H]), 265, 237, 205, 177; **HRMS** (ESI-TOF): *m/z* calculated for $C_{14}H_{19}O_6$ [M + H]$^+$: *m/z* 283.1182, found 283.1176.

Dimethyl (3aR,5aS,8aS)-3-methylene-2-oxooctahydro-5H-pentaleno[6a,1-b]furan-5,5-dicarboxylate (63j)

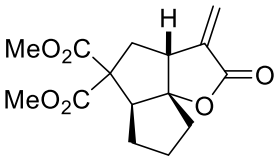

The product was obtained following the abovementioned procedure for the synthesis of **63a**, using **51j**. 70%, white solid. **^{1}H-NMR** (300 MHz, $CDCl_3$): δ (ppm) 6.17 (d, *J* = 3.1 Hz, 1H), 5.53 (d, *J* = 2.7 Hz, 1H), 3.69 (s, 3H), 3.60 (s, 3H), 3.37 (t, *J* = 9.1 Hz, 1H), 3.16 (dq, *J* = 8.0, 2.8 Hz, 1H), 2.85 (dd, *J* = 14.2, 8.0 Hz, 1H), 2.44 (dt, *J* = 14.2, 1.7 Hz, 1H), 2.36 – 2.18 (m, 1H), 1.98 – 1.86 (m, 1H), 1.87 – 1.67 (m, 3H), 1.29 – 1.10 (m, 1H); **^{13}C-NMR** (75 MHz, $CDCl_3$): δ (ppm) 171.5 (C), 169.8 (C), 169.5 (C), 139.6 (C), 122.2 (CH_2), 100.6 (C), 62.6 (C), 54.7 (CH), 53.0 (CH_3), 52.7 (CH_3), 48.0 (CH), 39.6 (CH_2), 39.0 (CH_2), 29.7 (CH_2), 26.0 (CH_2); **LRMS** (m/z, ESI): 295 ([M^+ + H]), 277, 235, 217, 203, 189; **HRMS** (ESI-TOF): *m/z* calculated for $C_{15}H_{19}O_6$ [M + H]$^+$: *m/z* 2295.1182, found 295.1177.

Synthesis of Ketone 62a.

Dimethyl (3aS,6aR)-6a-methyl-3-oxohexahydro-5H-cyclopenta[b]furan-5,5-dicarboxylate (62a)

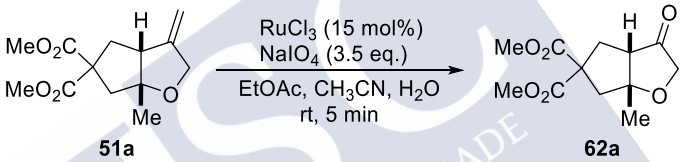

A solution of $NaIO_4$ (147.2 mg, 0.69 mmol, 3.5 eq) in water (1.2 mL) was added to a solution of $RuCl_3$ (6.1 mg, 0.03 mmol, 15 mol%) in CH_3CN (1.5 mL). After 2 minutes of stirring, a solution of malonate **51a** (50.0 mg, 0.197 mmol, 1 eq.) in EtOAc (1.5 mL) was added dropwise. The mixture was stirred for 5-10 minutes until TLC indicates complete consumption of the starting material. $MgSO_4$ was added and the resulting heterogeneous mixture was washed with EtOAc. The combined organic phases were carefully evaporated and the crude residue was purified by flash chromatography (15% EtOAc/ Hexanes) to afford **62a** (30.0 mg, 118 mmol, 60%) as a white solid.**^{1}H-NMR** (300 MHz, $CDCl_3$): δ (ppm) 3.91 (s, 2H), 3.74 (s, 3H), 3.72 (s, 3H), 2.86 – 2.68 (m, 2H), 2.55 (dd, *J* = 11.9, 2.6 Hz, 1H), 2.48 (d, *J* = 14.1 Hz, 1H), 2.27 (dd, *J* = 13.7, 11.9 Hz, 1H), 1.44 (s, 3H); **^{13}C-NMR** (75 MHz, $CDCl_3$): δ (ppm) 216.5 (C), 171.4 (C), 171.3 (C), 91.2 (C), 70.2 (CH_2), 60.2 (C), 54.7 (CH), 53.1 (CH_3), 52.9 (CH_3), 48.0 (CH_2), 37.7 (CH_2), 29.8, 22.9 (CH_3); **LRMS** (m/z, ESI): 257 ([M^+ + H]), 239, 225, 197, 165; **HRMS** (ESI-TOF): *m/z* calculated for $C_{12}H_{17}O_6$ [M + H]$^+$: *m/z* 257.1025, found 257.1018.

Procedure for the hydrogenation of compound ***60a+60a`***

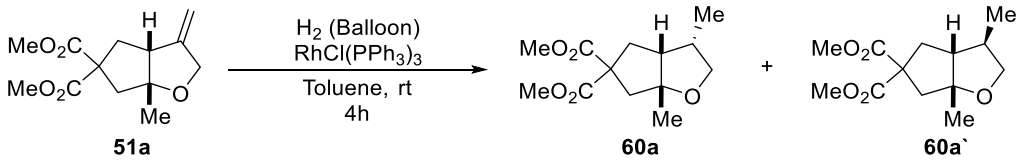

Over a solution of olefin **51a** (75.0 mg, 0.30 mmol) in toluene (7.4 mL) was added Wilkinson's catalyst, $RhCl(PPh_3)_3$ (40.9 mg, 0.04 mmol, 15 mol%). The resulting solution was then placed under a hydrogen atmosphere and stirred for 4 h. The solution was filtered on a Fluorisil pad, and the pad was rinsed with EtOAc. After the evaporation of the solvent the crude residue was purified by flash chromatography (8% EtOAc/ Hexanes) to afford **60a+60a`** (68.0 mg, 0.27 mmol, 90%, d.r = 6 : 1 in crude, measured by GC-MS) as a colourless oil.

Dimethyl (3S,3aR,6aR)-3,6a-dimethylhexahydro-5H-cyclopenta[b]furan-5,5-dicarboxylate (60a)

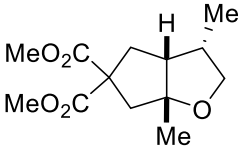

Colourless oil. **^{1}H-NMR** (300 MHz, $CDCl_3$): δ (ppm) 3.88 (t, *J* = 8.0 Hz, 1H), 3.72 (s, 3H), 3.71 (s, 3H), 3.37 (dd, *J* = 10.6, 8.4 Hz, 1H), 2.59 – 2.37 (m, 3H), 2.35 – 2.11 (m, 3H), 1.27 (s, 3H), 0.98 (d, *J* = 6.8 Hz, 3H); **^{13}C-NMR** (75 MHz, $CDCl_3$): δ (ppm) 172.7 (C), 171.9 (C), 91.9 (C), 72.6 (CH_2), 60.3 (C), 52.9 (CH_3), 52.8 (CH_3), 52.1 (CH), 47.6 (CH_2), 35.9 (CH), 33.9 (CH_2), 26.1 (CH_3), 11.8 (CH_3); **LRMS** (m/z, ESI): 257 ([M^+ + H]), 225, 181, 107; **HRMS** (ESI-TOF): *m/z* calculated for $C_{13}H_{21}O_5$ [M + H]$^+$: *m/z* 257.1389, found 257.1386. Stereochemistry of **60a** was determined by nOe experiments:

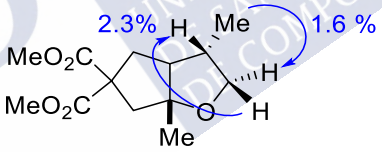

Figure 70. Significant nOes observed for **60a**.

Dimethyl (3aR,6aR)-3,6a-dimethylhexahydro-5H-cyclopenta[b]furan-5,5-dicarboxylate (60a+60a`)

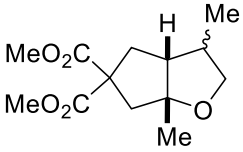

Mixture of diastereoisomers (*E*/*Z* = 3.3 : 1). **^{1}H-NMR** (300 MHz, $CDCl_3$): δ (ppm) 3.93 – 3.82 (m, 1H), 3.74 – 3.67 (m, 6H), 3.37 (ddd, *J* = 10.6, 7.3, 5.1 Hz, 1H), 2.57 – 2.35 (m, 2.8H), 2.32 – 2.09 (m, 3H), 1.97 (ddd, *J* = 9.1, 5.5, 3.4 Hz, 0.2H), 1.29 (s, 0.7H), 1.25 (s, 2.3H), 1.02 (d, *J* = 7.0 Hz, 0.7H), 0.97 (d, *J* = 6.8 Hz, 2.3H).; **^{13}C-NMR** (75 MHz, $CDCl_3$): δ (ppm) 172.7 (C), 172.5 (C), 171.8 (C), 91.9 (C), 91.5 (C), 73.5 (CH_2), 72.5 (CH_2), 60.7 (C), 60.3 (C), 56.0 (CH), 52.9 (CH_3), 52.8 (CH_3), 52.7 (CH_3), 52.1 (CH), 47.6 (CH_2), 46.9 (CH_2), 42.2 (CH), 40.6 (CH_2), 35.9 (CH), 33.8 (CH_2), 26.1 (CH_3), 25.6 (CH_3), 19.1 (CH_3), 11.7 (CH_3); **LRMS** (m/z, ESI): 257 ([M^+ + H]), 225, 207, 181, 147, 119, 107; **HRMS** (ESI-TOF): *m/z* calculated for $C_{13}H_{21}O_5$ [M + H]$^+$: *m/z* 257.1389, found 257.1385.

Procedure for the oxidation of compound ***51a***

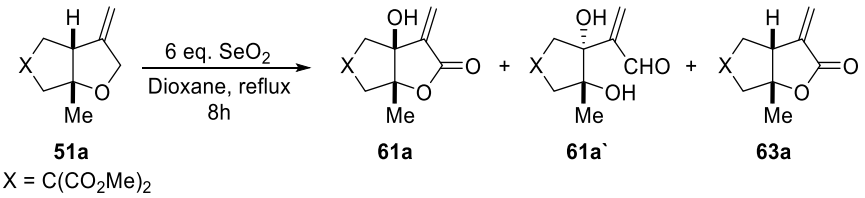

A mixture of the malonate **51a** (50.0 mg, 0.2 mmol) and SiO_2 (93.8 mg, 0.85 mmol, 4.3 eq.) in dioxane (3.0 mL) was refluxed for 4h. The solvent was carefully evaporated and the crude residue was purified by flash chromatography (20% EtOAc/ Hexanes) to afford a mixure of **61a** (24.0 mg, mmol, 42%) and **61a** (14 mg, mmol, 26%) and **63a** (4 mg, 8%) as white solids.

Dimethyl (3aS,6aR)-3a-hydroxy-6a-methyl-3-methylene-2-oxohexahydro-5H-cyclopenta[b]furan-5,5-dicarboxylate (61a)

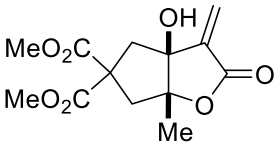

^{1}H-NMR (300 MHz, $CDCl_3$): δ (ppm) 6.35 (s, 1H), 5.93 (s, 1H), 3.75 (s, 3H), 3.71 (s, 3H), 3.59 – 3.20 (br, 0.8H), 2.86 (ddd, *J* = 22.4, 14.9, 1.2 Hz, 2H), 2.57 (dd, *J* = 17.0, 14.9 Hz, 2H), 1.40 (s, 3H); **^{13}C-NMR** (75 MHz, $CDCl_3$): δ (ppm) 172.0 (C), 170.6 (C), 167.7 (C), 142.2 (C), 124.5 (CH_2), 94.0 (C), 83.8 (C), 58.4 (C), 53.5 (CH_3), 53.3 (CH_3), 47.9 (CH_2), 45.0 (CH_2), 20.9 (CH_3); **LRMS** (m/z, ESI): 285 ([M^+ + H]), 267, 235, 217, 203, 189, 175; **HRMS** (ESI-TOF): *m/z* calculated for $C_{13}H_{17}O_7$ [M + H]$^+$: *m/z* 285.0974, found 285.0970. Stereochemistry of the alcohol in the ring fusion of compound **61a** was determined by nOe experiments:

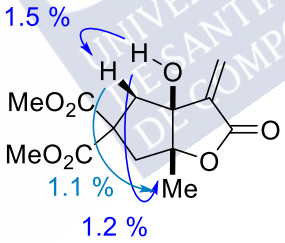

Figure 71. Significant nOes observed for 61a.

Dimethyl (3R,4S)-3,4-dihydroxy-3-methyl-4-(3-oxoprop-1-en-2-yl)cyclopentane-1,1-dicarboxylate (61a`)

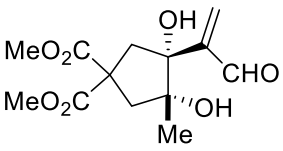

^{1}H-NMR (300 MHz, $CDCl_3$): δ (ppm) 9.50 (s, 1H), 6.67 (s, 1H), 6.27 (s, 1H), 4.14 (br, 0.9H), 4.01 (br, 0.8H), 3.76 (s, 3H), 3.74 (s, 3H), 3.00 (d, *J* = 14.7 Hz, 1H), 2.91 – 2.73 (m, 2H), 2.28 (d, *J* = 14.6 Hz, 1H), 1.13 (s, 3H); **^{13}C-NMR** (75 MHz, $CDCl_3$): δ (ppm) 197.0 (C), 172.7 (C), 172.6 (C), 150.1 (C), 139.1 (CH_2), 82.6 (C), 80.2 (C), 56.2 (C), 53.3, 53.2, 46.0 (CH_2), 42.9 (CH_2), 25.6 (CH_3); **LRMS** (m/z, ESI): 287 ([M^+ + H]), 269, 255, 219, 193, 161, 133; **HRMS** (ESI-TOF): *m/z* calculated for $C_{13}H_{19}O_7$ [M + H]$^+$: *m/z* 287.1131, found 287.1131. Stereochemistry of the alcohol in the ring fusion of compound **61a'** was determined was determined X-Ray crystallography. **X-ray analysis**: Crystals were grown from CH_2Cl_2.

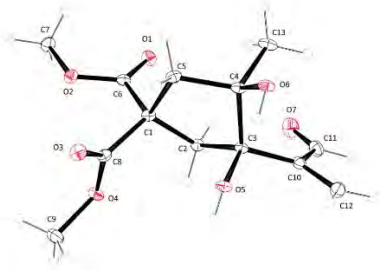

Figure 72. Crystal structure of aldehyde **61a`**.

2.8. Synthesis of substrates for the intermolecular reaction

Tert-butyl(2-(2-cyclopropylideneethoxy)ethoxy)diphenylsilane (65a)

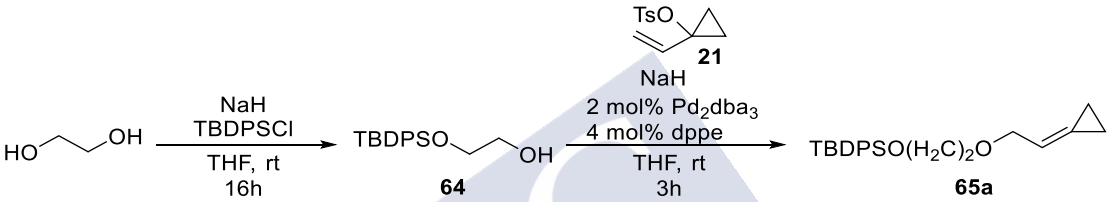

Ethylenglycol (0.9 mL, 16.1 mmol) was added dropwise over a suspension of NaH (0.58 g, 14.5 mmol) in THF (16 mL). After stirring for 10 minutes, tert-butyldiphenylchlorosilane (5.4 mL, 20.9 mmol) was added and the reaction was stirred for 16 h. The reaction was quenched with $NH_4Cl_{(sat)}$, extracted with Et_2O (3x40 mL) and the organic layers were dried using Na_2SO_4, the organic phase was then filtered and evaporated to give a residue that was purified by flash column chromatography (5 % AcOEt/Hexane) to yield 2-((tert-butyldiphenylsilyl)oxy)ethan-1-ol **64** (2.74 g, 9.0 mmol, 65%) as a colourless oil. The spectroscopic data is in agreement with the described in bibliography. **^{1}H-NMR** (300 MHz, $CDCl_3$) δ (ppm): 7.73 – 7.64 (m, 4H), 7.50 – 7.33 (m, 6H), 3.82 – 3.75 (m, 2H), 3.71 – 3.64 (m, 2H), 1.07 (s, 9H).

Over a suspension of NaH (0.127 g, 3.163 mmol) in THF (3.8 mL) at 0°C it was added dropwise 2-((tert-butyldiphenylsilyl)oxy)ethan-1-ol **64**. After stirring for 10 min at rt, a solution of Pd_2dba_3 (50.3 mg, 0.058 mmol), dppe (46.0 mg, 0.115 mmol) and 1-vinylcyclopropyltosylate **21** (0.685 g, 2.9 mmol) in THF (11 mL), previously stirred for 10 minutes, was added via cannula. The resulting mixture was further stirred for 3h and then the reaction was quenched with $NH_4Cl_{(sat)}$, extracted with Et_2O (3x30 mL) and the organic layers were dried with Na_2SO_4 and the organic phase was evaporated under reduced pressure. The crude was purified by flash chromatography (5% Et_2O/ Hexane) to yield tert-butyl(2-(2-cyclopropylideneethoxy)ethoxy)diphenylsilane **65a** (0.948 g, 0.347 mol, 89% yield) as a colourless oil. **^{1}H-NMR** (300 MHz, $CDCl_3$) δ (ppm): 7.79 – 7.74 (m, 2H), 7.52 – 7.36 (m, 6H), 6.25 – 5.48 (m, 1H), 4.33 – 4.09 (m, 2H), 3.89 (t, *J* = 5.5 Hz, 2H), 3.63 (t, *J* = 5.4 Hz, 2H), 1.13 (s, 13H). **^{13}C-NMR** (75.4 MHz, $CDCl_3$) *δ* (ppm) δ 135.74 (CH), 133.84 (C), 129.70 (CH), 127.73 (CH), 126.60 (C), 115.13 (CH), 71.50 (CH_2), 71.21 (CH_2), 63.64 (CH_2), 26.94 (CH_3), 19.32 (C), 2.37 (CH_2), 1.85 (CH_2). **HRMS** (ESI-TOF): m/z calculated for $C_{23}H_{30}O_2Si$ $[M+H]^+$: *m/z* 367.2087, found 367.2088

Tert-butyl(2-cyclopropylideneethoxy)dimethylsilane (64b)

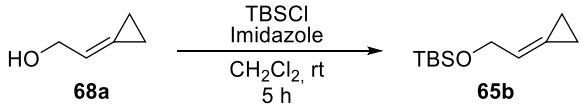

68a **65b**

Over a solution of 2-cyclopropylideneethan-1-ol[178] (1.5 g, 10.69 mmol) in DCM (10.7 mL) at 0°C was added imidazole (1.093 g, 14.05 mmol) and tert-butyldimethylilyl chloride (2.04 mL, 11.769 mmol) was added and the reaction was stirred for 5 h. The reaction was quenched with $NH_4Cl_{(sat)}$, extracted with Et_2O (3x60 mL) and the organic layers were dried using Na2SO4, filtered and concentrated to give a residue that was purified by flash column chromatography (5 % AcOEt/Hexane) to yield tert-butyl(2-cyclopropylideneethoxy)dimethylsilane **65b** (2.12 g, 10.7 mmol, 99%) as a colourless oil. **^{1}H-NMR** (300 MHz, $CDCl_3$) δ (ppm): 5.95 – 5.85 (m, 1H), 4.30 (d, *J* = 6.3 Hz, 2H), 1. 05 (s, 4H), 0.91 (s, 9H), 0.07 (s, 6H). **^{13}C-NMR** (75.4 MHz, $CDCl_3$) *δ* (ppm) δ 123.6 (C), 117.8 (CH), 63.9 (CH_2), 26.0 (CH_3), 18.5 (C), 1.99 (CH2), 1.72 (CH2) -5.08 (CH3) . **HRMS** (APCI-TOF): m/z calculated for $C_{11}H_{22}OSi$ $[M+H]^+$: *m/z* 199.1513, found 199.1513.

Tert-butyl(2-cyclopropylidenepropoxy)dimethylsilane (65c)

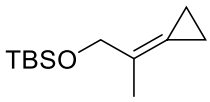

Was synthesized following the procedure used for **65c**[178], using 2-cyclopropylidenepropan-1-ol.[178] 60% yield, colourless oil. **^{1}H-NMR** (300 MHz, $CDCl_3$) δ (ppm): 4.27 (s, 2H), 1.87 (s, 3H), 1.1-0.95 (m, 4H), 0.94 (s, 9H), 0.09 (s, 6H). **^{13}C-NMR** (75.4 MHz, $CDCl_3$) *δ* (ppm) δ 123.9 (C), 117.4 (C), 67.1 (CH_2), 25.9(CH_3), 18.4 (C), 17.7 (CH_3), 2.43 (CH_2), 1.21 (CH_2) -5.3 (CH_3) . **HRMS** (APCI-TOF): m/z calculated for $C_{11}H_{22}OSi$ $[M+H]^+$: *m/z* 213.1669, found 213.1669.

[178] H. Hori, S. Arai, A. Nishida, *Adv. Synth. Catal.* **2017**, *359*, 1170–1176.

2.9. Representative procedure for the intramolecular (3+2) cycloaddition of alkylidenecyclopropanes and ketones

Procedure exemplified for the reaction of **65a**.

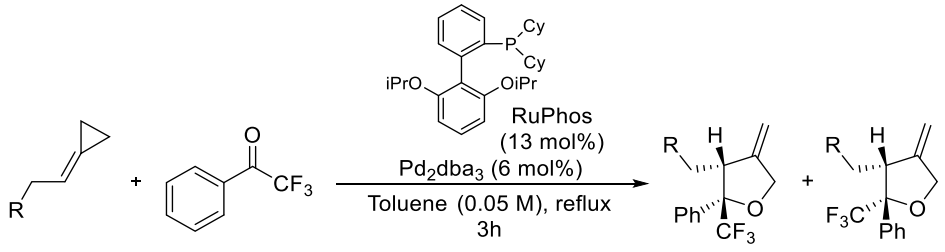

In a dried schlenck it was dissolved Pd_2dba_3 (7.8 mg, 6 mol %), RuPhos (9.1 mg, 13 mol%), tert-butyl(2-(2-cyclopropylideneethoxy)ethoxy)diphenylsilane **65a** (50.0 mg, 0.143 mmol) and 2,2,2-trifluroacetophenone (43 µL , 0.285 mmol) in freshly distilled toluene (2.9 mL, 0.05 M) and the mixture was stirred for 3 h at reflux. Then the reaction was cooled to room temperature and diluted with Et_2O and filtered through a short pad of Fluorisil®. Finally the residue was evaporated and purified by flash column chromatography (1% EtOAc/Hexane) to afford **66a+66a`** (73 mg, 0.129 mmol, 95 %, d.r = 1 : 1.3) as a colourless oil. **^{1}H-NMR** (300 MHz, $CDCl_3$) δ (ppm): 7.71 (m, 5H), 7.55 (m, 1H), 7.50-7.30 (m, 9H), 5.28 (dd, *J* = 30.6, 2.3 Hz, 1H) 5.05 (dd, *J* = 27.7, 2.3 Hz, 1H), 4.70 (m, 2H), 4.15 (dd, *J* = 9.7, 5.0 Hz, 0.5H), 3.88 (q, *J* = 5.1 Hz, 1.5H), 3.70 (dd, *J* = 5.9, 4.4 Hz, 1H) 3.63 (t, *J* = 5.2 Hz, 1H), 3.43 (d, *J* = 5.9 Hz, 1H), 3.32 (dd, *J* = 9.5, 4.9 Hz, 0.5H), 3.19 (m, 1.5H), 1.10 (s, 4.5H), 1.05 (s, 4.5H). **^{13}C-NMR** (75.4 MHz, $CDCl_3$) *δ* (ppm): ^{13}C NMR (75 MHz, cdcl$_3$) δ 147.3 (C), 147.2 (C), 135.6 (CH), 135.6 (CH),129.6 (CH), 128.6 (CH), 128.3 (CH), 128.2 (CH), 127.8 (CH), 127.7 (CH), 127.6 (CH), 126.8 (CH), 126.8 (CH), 126.6 (CH), 106.8 (CH_2), 106.2 (CH_2), 87.5 ($J_{C\text{-}F}$ = 27.5 Hz), 86.6 ($J_{C\text{-}F}$ = 28.1 Hz), 72.7 (CH_2), 72.5 (CH_2), 72.2 (CH_2), 71.5 (CH_2), 71.1 (CH_2), 70.2 (CH_2), 63.5 (CH_2), 63.2 (CH_2), 52.4 (CH), 47.9 (CH), 29.74, 26.8 (CH_3), 26.7 (CH_3), 19.2 (C), 19.1 (C). **^{19}F NMR** (282 MHz, $CDCl_3$) δ (ppm) -73.37, -76.86 **HRMS** (APCI-TOF): *m/z* found for $[M+NH_4]^+$: *m/z* 576.293.

Tert-butyldimethyl((4-methylene-2-phenyl-2-(trifluoromethyl)tetrahydrofuran-3-yl) methoxy)silane (66b+66b`)

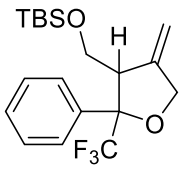

95% yield, as an inseparable mixture of **66b** and **66b`** (1 : 1.2) as a colourless oil . **^{1}H-NMR** (300 MHz, $CDCl_3$) δ (ppm): 7.90 (d, *J* = 7.9 Hz, 2H), 7.72 (d, *J* = 8.0 Hz, 2H), 7.33 – 7.24 (m, 5H), 7.24 – 7.16 (m, 2H), 5.20 (q, *J* = 2.4 Hz, 1H), 5.14 – 5.09 (m, 1.2H), 4.92 – 4.88 (m, 1.2H), 4.76 (q, *J* = 2.2 Hz, 1H), 4.74 – 4.65 (m, 2H), 4.59 (dq, *J* = 12.8, 1.9 Hz, 1H), 4.49 – 4.42 (m, 1H), 4.37 (ddt, *J* = 12.8, 2.3, 1.1 Hz, 1H), 4.13 (ddd, *J* = 10.3, 7.8, 1.2 Hz, 1H), 3.48 (dd, *J* = 10.0, 4.0 Hz, 1.2H), 3.45 (td, *J* = 6.7, 5.6, 2.9 Hz, 1H), 3.40 (dd, *J* = 10.0, 5.4 Hz, 1.2H), 3.29 (dddd, *J* = 6.4, 4.0, 1.5, 0.7 Hz, 1.2zH), 1.09 (s, 9H), 0.94 (s, 10.5H), 0.17 (d, *J* = 1.2 Hz, 6H), -0.10 (s, 3.4H), -0.19 (s, 3.4H);**^{13}C-NMR** (75.4 MHz, $CDCl_3$) *δ* (ppm): 148.8 (C), 147.3 (C), 138.4 (C), 135.1 (C), 128.8 (CH), 128.5 (CH), 128.4

(CH), 128.1 (CH), 128.0 (CH), 127.9 (CH), 127.7 (CH), 127.5 (CH), 127.4 (CH), 127.3 (CH), 124.9 (C), 124.0 (C), 106.6 (CH_2), 105.9 (CH_2), 87.6 (m, C) 72.9 (CH_2), 71.3 (CH_2), 63.7 (CH_2), 62.4 (CH_2), 62.4, 55.5 (CH), 50.3 (CH), 26.0 (CH_3), 25.9 (CH_3), 18.4 (C), 18.3 (C), -5.4 (CH_3), -5.5 (CH_3), -5.9 (CH_3); **^{19}F NMR** (282 MHz, $CDCl_3$) δ -73.09, -77.27; **HRMS** (APCI-TOF): m/z calculated for $C_{19}H_{28}F_3O_2Si$ $[M+H]^+$: 373.1805, found 373.1805

Dimethyl 2-((4-methylene-2-phenyl-2-(trifluoromethyl)tetrahydrofuran-3-yl)methyl)malonate (66c+66c`)

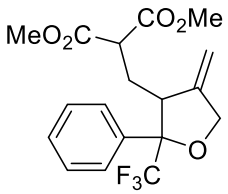

74% yield (d.r = 1.8 : 1) as a colourless oil**. ^{1}H-NMR** (300 MHz, $CDCl_3$) δ (ppm): 7.56 - 7.47 (m, 2H), 7.47 – 7.32 (m, 3H), 5.10 (s, 0.7H), 5.06 (s, 0.7H), 4.97 – 4.89 (m, 0.6H), 4.78 – 4.60 (m, 1.7H), 4.47 (d, *J* = 12.7 Hz, 0.3H), 3.79 (s, 2.1H), 3.75 (s, 0.9H), 3.72 (s, 0.9H), 3.62 (s, 2.1H), 3.57 – 3.44 (m, 1H), 3.21 – 3.03 (m, 1H), 2.63 (t, *J* = 12.4 Hz, 0.3H), 2.24 (t, *J* = 11.4 Hz, 0.3H), 1.90 (t, *J* = 11.9 Hz, 0.7H), 1.29 (t, *J* = 12.4 Hz, 0.7H). **^{13}C-NMR** (75.4 MHz, $CDCl_3$) *δ* (ppm): 169.6 (C), 169.4 (C), 147.4 (C), 146.4 (C), 137.6 (C), 134.2 (C), 128.8 (CH), 128.7, 128.5 (CH), 128.4 (CH), 127.2 (CH), 126.4 (CH), 108.2 (CH_2), 107.9 (CH_2), 89.1 (C) 71.7 (CH_2), 70.7 (CH_2), 52.9 (CH_3), 52.8 (CH_3), 52.8 (CH_3), 51.3 (CH), 49.8 (CH), 48.8 (CH), 46.0 (CH), 28.9 (CH_2), 27.5 (CH_2).**^{19}F NMR** (282 MHz, $CDCl_3$) δ -71.85, -76.41. **HRMS** (APCI-TOF): m/z calculated for $C_{17}H_{20}F_3NO_2$ [M+H]+: 373.1254, found 373.1257

Tert-butyl((2-(4-fluorophenyl)-3-methyl-4-methylene-2-(trifluoromethyl)tetrahydrofuran-3-yl)methoxy)dimethylsilane (66d+66d`)

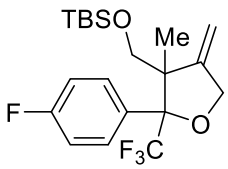

60% yield (d.r = 1 : 2) as an inseparable mixture of **66d** and **66d`** (1 : 2) as a colourless oil**. ^{1}H-NMR** (300 MHz, $CDCl_3$) δ (ppm): 7.89 – 7.78 (m, 2H), 7.12 – 6.95 (m, 3H), 5.02 (t, *J* = 2.1 Hz, 0.7H), 4.93 (dt, *J* = 5.1, 2.5 Hz, 3.3H), 4.84 – 4.65 (m, 4H), 4.08 (d, *J* = 10.8 Hz, 0.7H), 3.86 (d, *J* = 10.3 Hz, 0.7H), 3.05 (d, *J* = 9.6 Hz, 0.3H), 2.90 (d, *J* = 9.6 Hz, 0.3H), 0.96 (s, 9H), 0.76 (s, 3H), 0.14 (s, 6H). **^{13}C-NMR** (75.4 MHz, $CDCl_3$) *δ* (ppm): 153.4 (C), 151.8 (C), 130.1 (CH), 130.0 (CH), 114.7 (CH), 114.4 (CH), 104.6 (CH_2), 103.3 (CH_2), 72.0 (CH_2), 71.2 (CH_2), 68.2 (CH_2), 65.8 (CH_2), 52.2 (C), 51.8 (C), 26.1 (CH_3), 26.0 (CH_3), 25.9 (CH_3), 24.0 (CH_3), 18.6 (C), 18.3 (C), 16.5 (CH_3);**^{19}F NMR** (282 MHz, $CDCl_3$) δ -72.6, -76.8. **HRMS** (APCI-TOF): *m/z* calculated for $C_{14}H_{14}F_4O_2$ $[M+NH_4]^+$: 420.1258 found, 420.1260

USC
UNIVERSIDADE
DE SANTIAGO
DE COMPOSTELA

Addendum: Palladium catalyzed Tandem cycloisomerization reactions of alkylidenecyclopropanes

2.10. Representative procedure for the tandem annulation reaction of alkylidenecyclopropanes and boronic acids.

Procedure exemplified for the reaction of **72ca**.

(3S,4S)-4-(3-(4-methoxyphenyl)prop-1-en-2-yl)-1-tosylpyrrolidin-3-ol (72ca)

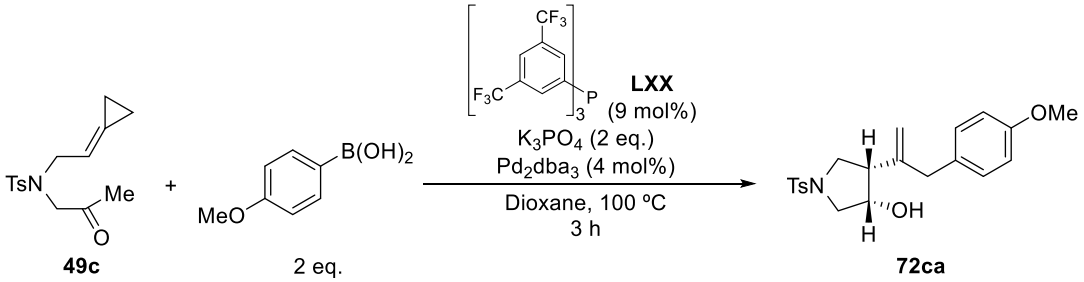

A solution of Pd_2dba_3 (4.4 mg, 4 mol%), $P(3,5\text{-}CF_3\text{-}C_6H_4)_3$ (7.6 mg, 9 mol%), 4-Methoxyphenylboronic acid (50,9 mg, 0.24 mmol, 2 eq.), K_3PO_4 (51 mg, 0.24 mmol, 2 eq.) and **49c** (35.2 mg, 0.12 mmol) in dry dioxane (2.4 mL) was heated under reflux for 3h. The mixture was then cooled to rt, diluted with EtOAc and filtered through a short pad of florisil, eluting with EtOAc. The filtrate was concentrated and purified by flash chromatography (10% EtOAc/hexanes) to afford (3S,4S)-4-(3-(4-methoxyphenyl)prop-1-en-2-yl)-1-tosylpyrrolidin-3-ol **72ca** as a pale brown oil (44.9 mg, 90% yield). **^{1}H-NMR** (300 MHz, $CDCl_3$): δ (ppm) 7.74 – 7.61 (m, 2H), 7.35 – 7.21 (m, 2H), 7.05 – 6.93 (m, 2H), 6.90 – 6.79 (m, 2H), 5.06 (q, *J* = 1.3 Hz, 1H), 4.96 (s, 1H), 3.80 (s, 3H), 3.45 – 3.34 (m, 3H), 3.33 – 3.18 (m, 3H), 2.42 (s, 4H), 1.20 (s, 3H); **^{13}C-NMR** (75 MHz, $CDCl_3$): δ (ppm) 158.5 (C), 143.9 (C), 143.5 (C), 134.1 (C), 130.3 (C), 130.0 (CH), 129.7 (CH), 127.6 (CH), 115.8 (CH_2), 114.11 (CH), 60.6 (CH_2), 55.4 (CH_3), 51.9 (CH), 51.7 (CH_2), 44.1 (CH_2), 24.9 (CH_3), 21.7 (CH_3); **LRMS** (m/z, ESI): 363 ([M^+ + H]), 228, 175, 119; **HRMS** (ESI-TOF): *m/z* calculated for $C_{22}H_{28}NO_4S$ [M + H]$^+$: *m/z* 402.1739, found 402.1730. Stereochemistry if **72ca** was determined by nOe experiments.

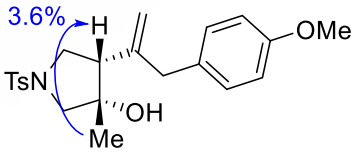

Figure 73. Significant nOes observed for **72ca**.

Dimethyl (3R,4R)-3-hydroxy-4-(3-(4-methoxyphenyl)prop-1-en-2-yl)-3-methylcyclopentane -1,1-dicarboxylate (72aa)

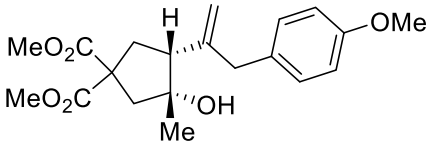

The compound was purified by flash chromatography (10% EtOAc/Hexane) to afford **72aa** (90% yield) as a White solid. **^{1}H-NMR** (300 MHz, $CDCl_3$): δ (ppm) 7.07 (d, *J* = 8.5 Hz, 2H), 6.83 (d, *J* = 8.6 Hz, 2H), 5.13 (s, 1H), 4.98 (s, 1H), 3.79 (s, 3H), 3.74 (s, 3H), 3.68 (s, 3H), 3.43 (d, *J* = 15.6 Hz, 1H), 3.31 (d, *J* = 15.6 Hz, 1H), 2.70 – 2.54 (m, 2H), 2.46 (dd, *J* = 12.2, 7.2 Hz, 1H), 2.37 – 2.23 (m, 2H), 1.30 (s, 3H); **^{13}C-NMR** (75 MHz, $CDCl_3$): δ (ppm) 173.2 (C), 158.3 (C), 146.7 (C), 131.2 (C), 130.2 (CH), 114.9 (CH_2), 114.0 (CH), 79.0 (C), 57.1 (C), 55.4 (CH_3), 53.7 (CH), 53.1 (CH_3), 53.0 (CH_3), 48.4 (CH_2), 43.75 (CH_2),

38.6 (CH_2), 26.4 (CH_3); **LRMS** (m/z, ESI): 363 ([M^+ + H]), 345, 313, 285; **HRMS** (ESI-TOF): *m/z* calculated for $C_{20}H_{27}O_6$ [M + H]$^+$: *m/z* 363.1808, found 363.1806. Stereochemistry if **72aa** was determined by nOe experiments.

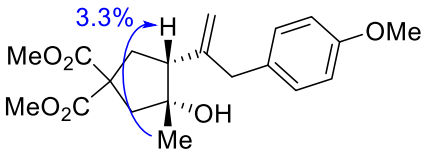

Figure 74. Significant nOes observed for **72aa**.

Dimethyl (3R,4R)-4-(3-(4-fluorophenyl)prop-1-en-2-yl)-3-hydroxy-3-methylcyclopentane-1,1-dicarboxylate (72ac)

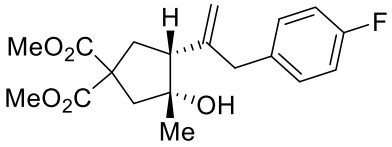

The compound was purified by flash chromatography (10% EtOAc/Hexane) to afford **72ac** (96% yield) as a White solid. **^{1}H-NMR** (300 MHz, $CDCl_3$): δ (ppm) 7.17 – 7.06 (m, 2H), 7.02 – 6.92 (m, 2H), 5.14 (s, 1H), 4.95 (q, *J* = 1.4 Hz, 1H), 3.74 (s, 3H), 3.68 (s, 3H), 3.46 (d, *J* = 15.0 Hz, 1H), 3.35 (d, *J* = 15.6 Hz, 1H), 2.66 – 2.53 (m, 2H), 2.43 (dd, *J* = 12.1, 7.2 Hz, 1H), 2.35 – 2.24 (m, 2H), 1.90 (br, 1H), 1.29 (s, 3H)..; **^{13}C-NMR** (75 MHz, $CDCl_3$): δ (ppm) 173.3 (C), 173.2 (C), 161.7 (d, *J* = 244.1 Hz), 146.2 (C), 134.8 (d, *J* = 3 Hz), 130.7 (d, *J* = 8.0 ppm), 115.3 (d, *J* = 21.0 Hz), 115.3 (CH_2), 79.1 (C), 57.0 (C), 53.8 (CH), 53.1 (CH_3), 53.0 (CH_3), 48.5, 43.6, 38.5, 26.3 (CH_3); **LRMS** (m/z, ESI): 373 ([M^+ + Na]), 273, 163, 109; **HRMS** (ESI-TOF): *m/z* calculated for $C_{19}H_{23}FNaO_5$ [M + Na]$^+$: *m/z* 373.1427, found 373.1422. Stereochemistry if **72ac** was determined by nOe experiments.

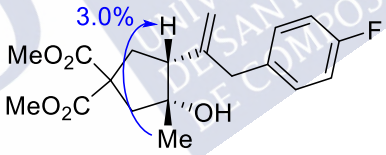

Figure 75. Significant nOes observed for **72ac**.

Dimethyl (3R,4R)-3-hydroxy-4-(3-(4-methoxyphenyl)prop-1-en-2-yl)-3-methylcyclopentane -1,1-dicarboxylate (72ab)

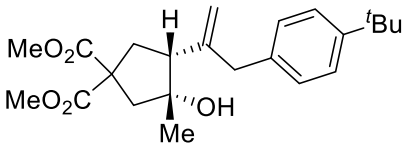

The compound was purified by flash chromatography (20% EtOAc/Hexane) to afford **72ab** (95% yield) as a White solid. **^{1}H-NMR** (300 MHz, $CDCl_3$): δ (ppm) 7.41 – 7.28 (m, 2H), 7.19 – 7.02 (m, 2H), 5.15 (d, *J* = 1.2 Hz, 1H), 5.01 (q, *J* = 1.4 Hz, 1H), 3.74 (s, 3H), 3.67 (s, 3H), 3.51 – 3.43 (m, 1H), 3.41 – 3.31 (m, 1H), 2.72 – 2.54 (m, 2H), 2.48 (dd, *J* = 12.2, 7.3 Hz, 1H), 2.34 (s, 1H), 2.29 (dd, *J* = 7.2, 5.8 Hz, 1H), 1.31 (d, *J* = 2.8 Hz, 12H); **^{13}C-NMR** (75 MHz, $CDCl_3$): δ (ppm) 173.2 (C), 173.2 (C), 149.2 (C), 146.4 (C), 136.0 (C), 128.9 (CH), 125.4 (CH), 115.0 (CH_2), 78.9 (C), 57.1 (C), 53.7 (CH), 53.0 (CH_3), 52.9 (CH_3), 48.4 (CH_2), 44.1 (CH_2), 38.6 (CH_2), 34.5 (C), 31.5 (CH_3), 26.4 (CH_3); **LRMS** (m/z, ESI): 389 ([M^+ + H]), 311, 195, 119; **HRMS** (ESI-TOF): *m/z* calculated for $C_{23}H_{33}O_5$ [M + H]$^+$: *m/z* 389.2328, found 389.2323. Stereochemistry of **72ab** was determined by nOe experiments.

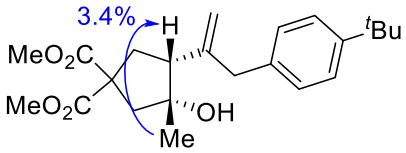

Figure 76. Significant nOes observed for **72ab**.

Dimethyl (3R,4R)-3-hydroxy-3-methyl-4-(4-phenylpenta-1,4-dien-2-yl)cyclopentane-1,1-dicarboxylate (72ad)

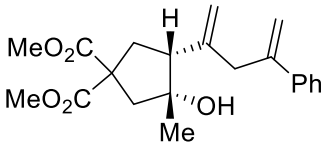

The compound was purified by flash chromatography (10% EtOAc/Hexane) to afford **72ad** (88% yield) as a pale orange oil. **^{1}H-NMR** (300 MHz, $CDCl_3$): δ (ppm) 7.47 – 7.38 (m, 2H), 7.38 – 7.23 (m, 3H), 5.47 (d, *J* = 1.4 Hz, 1H), 5.12 (s, 3H), 3.75 (s, 3H), 3.74 (s, 3H), 3.40 (d, *J* = 16.7 Hz, 1H), 3.30 (d, *J* = 16.6 Hz, 1H), 2.67 – 2.51 (m, 3H), 2.40 – 2.27 (m, 2H), 1.89 (br, 1H), 1.32 (s, 3H).; **^{13}C-NMR** (75 MHz, $CDCl_3$): δ (ppm) 173.2 (C), 145.8 (C), 144.3 (C), 141.0 (C), 128.3 (CH), 127.6 (CH), 126.3 (CH), 115.7 (CH_2), 115.1 (CH_2), 79.1 (C), 57.1 (C), 53.9 (CH), 53.0 (CH_3), 52.9 (CH_3), 48.4 (CH_2), 43.8 (CH_2), 38.4 (CH_2), 26.3 (CH_3); **LRMS** (m/z, ESI): 381 ([M$^+$ + Na]), 327, 251, 171; **HRMS** (ESI-TOF): *m/z* calculated for $C_{21}H_{26}NaO_5$ [M + Na]$^+$: *m/z* 381.1678, found 381.1671. Stereochemistry of **72ad** was determined by nOe experiments.

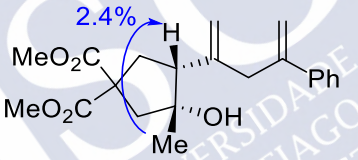

Figure 77. Significant nOes observed for **72ad**.

Dimethyl (3R,4R)-4-(3-(cyclopent-1-en-1-yl)prop-1-en-2-yl)-3-hydroxy-3-methylcyclo pentane -1,1-dicarboxylate (72ae)

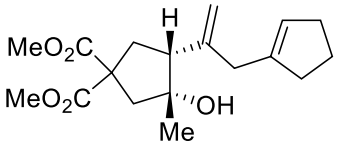

The compound was purified by flash chromatography (10% EtOAc/Hexane) to afford **72ae** (36% yield) as a pale orange oil. **^{1}H-NMR** (300 MHz, $CDCl_3$): δ (ppm) 5.43 – 5.36 (m, 1H), 5.12 – 5.04 (m, 2H), 3.75 (d, *J* = 0.8 Hz, 3H), 3.72 (d, *J* = 0.8 Hz, 3H), 2.87 (br, 2H), 2.66 – 2.46 (m, 3H), 2.40 – 2.28 (m, 4H), 2.24 – 2.14 (m, 2H), 1.94 – 1.81 (m, 3H), 1.27 (s, 3H); **^{13}C-NMR** (75 MHz, $CDCl_3$): δ (ppm) 173.4 (C), 173.1 (C), 144.8 (C), 142.1 (C), 126.6 (CH), 114.3 (CH_2), 78.8 (C), 57.2 (C), 53.6 (CH), 53.0 (CH_3), 48.3 (CH_2), 40.3 (CH_2), 38.5 (CH_2), 35.0 (CH_2), 32.7 (CH_2), 26.4 (CH_3), 23.7 (CH_2); **LRMS** (m/z, ESI): 345 ([M$^+$ + Na]), 305, 245, 135; **HRMS** (ESI-TOF): *m/z* calculated for $C_{18}H_{26}NaO_5$ [M + Na]$^+$: *m/z* 345.1678, found 345.1677. Stereochemistry if **72ae** was determined by nOe experiments.

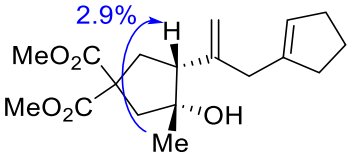

Figure 78. Significant nOes observed for **72ae**.

Methyl (1R,6R)-6-(3-(cyclopent-1-en-1-yl)prop-1-en-2-yl)-1-methyl-3-oxo-2-oxabicyclo[2.2.1]heptane-4-carboxylate (70ae)

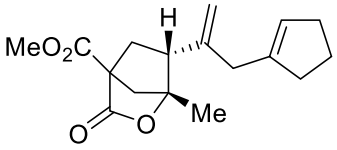

The compound was purified by flash chromatography (10% EtOAc/Hexane) to afford **70ae** (54% yield) as a pale orange oil. **^{1}H-NMR** (300 MHz, $CDCl_3$): δ (ppm) 5.43 – 5.34 (m, 1H), 5.05 – 4.98 (m, 2H), 3.80 (s, 3H), 2.80 (p, *J* = 1.2 Hz, 2H), 2.74 (dd, *J* = 11.1, 5.4 Hz, 1H), 2.56 (dd, *J* = 13.3, 11.2 Hz, 1H), 2.38 (dd, *J* = 10.4, 2.4 Hz, 1H), 2.35 – 2.26 (m, 2H), 2.23 – 2.13 (m, 2H), 2.12 (d, *J* = 10.4 Hz, 1H), 2.00 (ddd, *J* = 13.3, 5.3, 2.4 Hz, 1H), 1.93 – 1.77 (m, 2H), 1.53 (s, 3H); **^{13}C-NMR** (75 MHz, $CDCl_3$): δ (ppm) 173.5 (C), 168.6 (C), 143.0 (C), 142.1 (C), 126.7 (CH), 115.3 (CH_2), 90.5 (C), 58.2 (C), 52.8 (CH_3), 49.8 (CH), 49.3 (CH_2), 38.9 (CH_2), 34.8 (CH_2), 34.7 (CH_2), 32.7 (CH_2), 23.7 (CH_2), 17.5 (CH_3); **LRMS** (m/z, ESI): 291 ([M^+ + H]), 247, 245, 231; **HRMS** (ESI-TOF): *m/z* calculated for $C_{17}H_{23}O_4$ [M + H]$^+$: *m/z* 291.1596, found 291.1592. Stereochemistry if **70ae** was determined by nOe experiments.

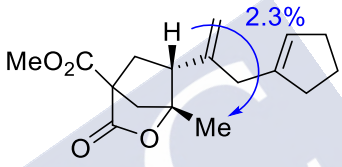

Figure 79. Significant nOes observed for **70ae**.

Methyl (1R,6R)-1-methyl-3-oxo-6-(prop-1-en-2-yl)-2-oxabicyclo[2.2.1]heptane-4-carboxylate (70aa)

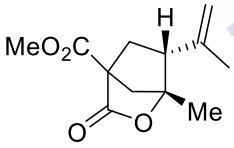

The compound was purified by flash chromatography (10% EtOAc/Hexane) to afford **70aa** (70% yield) as pale brown oil. **^{1}H-NMR** (300 MHz, $CDCl_3$): δ (ppm) 4.98 (s, 1H), 4.85 (s, 1H), 3.81 (s, 3H), 2.79 (dd, *J* = 11.1, 5.3 Hz, 1H), 2.51 (dd, *J* = 13.4, 11.1 Hz, 1H), 2.38 (dd, *J* = 10.4, 2.3 Hz, 1H), 2.14 – 1.99 (m, 2H), 1.74 (s, 3H), 1.51 (s, 3H); **^{13}C-NMR** (75 MHz, $CDCl_3$): δ (ppm) 173.5 (C), 168.6 (C), 141.3 (C), 116.2 (CH_2), 90.9 (C), 58.2 (C), 52.8 (CH_3), 52.3 (CH), 48.8 (CH_2), 32.8 (CH_2), 20.8 (CH_3), 17.3 (CH_3); **LRMS** (m/z, ESI): 247 ([M^+ + Na]), 225, 179, 165, 147, 119; **HRMS** (ESI-TOF): *m/z* calculated for $C_{12}H_{16}NaO_4$ [M + Na]$^+$: *m/z* 247.0946, found 247.0937. The stereochemistry of lactone **70aa** was confirmed by comparison with analogue **70ae**.

(3S,4S)-4-(3-(cyclopent-1-en-1-yl)prop-1-en-2-yl)-3-methyl-1-tosylpyrrolidin-3-ol (72ce)

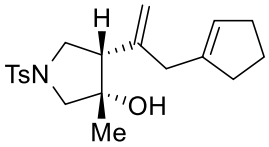

The compound was purified by flash chromatography (20% EtOAc/Hexane) to afford **72ce** (63% yield) as a pale orange oil. **^{1}H-NMR** (300 MHz, $CDCl_3$): δ (ppm) 7.72 (d, *J* = 8.0 Hz, 2H), 7.31 (d, *J* = 7.9 Hz, 2H), 5.33 (s, 1H), 5.09 (s, 1H), 4.90 (s, 1H), 3.52 (dd, *J* = 9.4, 7.6 Hz, 1H), 3.41 (d, *J* = 11.0 Hz, 1H), 3.34 – 3.21 (m, 2H), 2.81 (s, 2H), 2.53 (dd, *J* = 11.3, 7.6 Hz, 1H), 2.42 (s, 3H), 2.37 – 2.25 (m, 2H), 2.12 (d, *J* = 7.7 Hz, 2H), 1.85 (p, *J* = 7.4 Hz, 2H), 1.22 (s, 3H); **^{13}C-NMR** (75 MHz, $CDCl_3$): δ (ppm) 143.5 (C), 142.1 (C), 141.5 (C), 134.3 (C), 129.7 (CH), 127.7 (CH), 127.0 (CH), 115.4 (CH_2), 60.6 (CH_2), 52.1 (CH), 51.5 (CH_2), 40.6 (CH_2), 34.9 (CH_2), 32.6 (CH_2), 24.9 (CH_3), 23.6 (CH_2), 21.7 (CH_3); **LRMS** (m/z, ESI): 362 ([M^+ + H]), 344, 228, 135;

HRMS (ESI-TOF): *m/z* calculated for $C_{20}H_{28}NO_3S$ [M + H]$^+$: *m/z* 362.1790, found 362.1785. Stereochemistry if **72ce** was determined by nOe experiments.

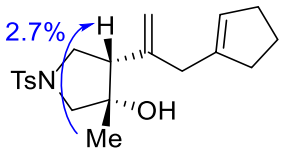

Figure 80. Significant nOes observed for **72ce**.

Dimethyl (3R,3aS,6aS)-3a-hydroxy-3-(3-(4-methoxyphenyl)prop-1-en-2-yl)hexahydro pentalene-1,1(2H)-dicarboxylate (72ja)

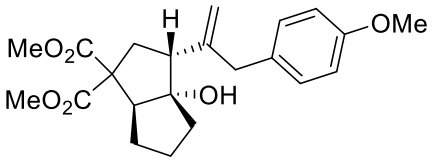

The compound was purified by flash chromatography (20% EtOAc/Hexane) to afford **72ja** (88% yield) as a pale orange oil. **^{1}H-NMR** (300 MHz, $CDCl_3$): δ (ppm) 7.14 – 7.00 (m, 2H), 6.88 – 6.79 (m, 2H), 5.00 (t, *J* = 1.1 Hz, 1H), 4.91 (q, *J* = 1.4 Hz, 1H), 3.79 (s, 3H), 3.72 (s, 3H), 3.66 (s, 3H), 3.42 (d, *J* = 15.7 Hz, 1H), 3.33 (d, *J* = 15.7 Hz, 1H), 3.22 (dd, *J* = 9.9, 8.4 Hz, 1H), 2.85 (dd, *J* = 12.6, 6.5 Hz, 1H), 2.59 (dd, *J* = 13.1, 6.4 Hz, 1H), 2.30 (br, 1H), 2.06 (d, *J* = 14.2 Hz, 1H), 1.98 – 1.79 (m, 2H), 1.78 – 1.65 (m, 2H), 1.32 – 1.06 (m, 2H); **^{13}C-NMR** (75 MHz, $CDCl_3$): δ (ppm) 173.0 (C), 171.7 (C), 158.2 (C), 147.0 (C), 131.1 (C), 130.2 (CH), 114.4 (CH_2), 114.0 (CH), 90.1 (C), 60.3 (C), 59.3 (CH), 55.3 (CH_3), 52.9 (CH), 52.8 (CH_3), 52.20 (CH_3), 42.9 (CH_2), 40.3 (CH_2), 40.2 (CH_2), 29.7 (CH_2), 27.2 (CH_2); **LRMS** (m/z, ESI): 389 ([M$^+$ + H]), 311, 175, 121; **HRMS** (ESI-TOF): *m/z* calculated for $C_{22}H_{29}O_6$ [M + H]$^+$: *m/z* 389.1964, found 389.1956. Stereochemistry if **72ja** was determined by nOe experiments.

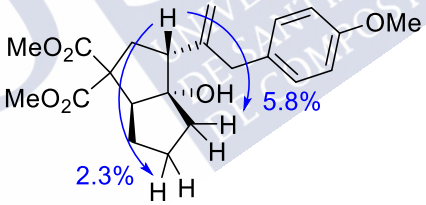

Figure 81. Significant nOes observed for **72ja**.

(3S,4S)-4-(3-(4-methoxyphenyl)prop-1-en-2-yl)-3-methyl-1-tosylpyrrolidin-3-ol (72ca)

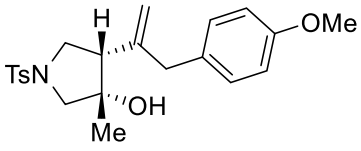

The compound was purified by flash chromatography (20% EtOAc/Hexane) to afford **72ca** (90% yield) as a pale orange oil. **^{1}H-NMR** (300 MHz, $CDCl_3$): δ (ppm) 7.74 – 7.61 (m, 2H), 7.35 – 7.21 (m, 2H), 7.05 – 6.93 (m, 2H), 6.90 – 6.79 (m, 2H), 5.06 (q, *J* = 1.3 Hz, 1H), 4.96 (s, 1H), 3.80 (s, 3H), 3.45 – 3.34 (m, 3H), 3.33 – 3.18 (m, 3H), 2.42 (s, 4H), 1.20 (s, 3H); **^{13}C-NMR** (75 MHz, $CDCl_3$): δ (ppm) 158.5 (C), 143.9 (C), 143.5 (C), 134.1 (C), 130.3 (C), 130.0 (CH), 129.7 (CH), 127.6 (CH), 115.8 (CH_2), 114.11 (CH), 60.6 (CH_2), 55.4 (CH_3), 51.9 (CH), 51.7 (CH_2), 44.1 (CH_2), 24.9 (CH_3), 21.7 (CH_3); **LRMS** (m/z, ESI): 363 ([M$^+$ + H]), 228, 175, 119; **HRMS** (ESI-TOF): *m/z* calculated for $C_{22}H_{28}NO_4S$ [M + H]$^+$: *m/z* 402.1739, found 402.1730. Stereochemistry if **72ca** was determined by nOe experiments.

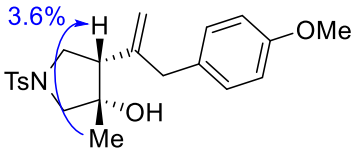

Figure 82. Significant nOes observed for **72ca**.

(3S,4S)-4-(3-(4-methoxyphenyl)prop-1-en-2-yl)-3-methyltetrahydrofuran-3-ol (72da)

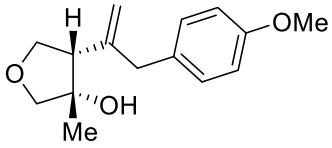

The compound was purified by flash chromatography (20% EtOAc/Hexane) to afford **72da** (63% yield) as a pale orange oil. **^{1}H-NMR** (300 MHz, $CDCl_3$): δ (ppm) 7.11 – 7.05 (m, 2H), 6.88 – 6.81 (m, 2H), 5.14 – 5.08 (m, 2H), 3.93 – 3.82 (m, 3H), 3.80 (s, 3H), 3.67 (dd, *J* = 9.1, 0.9 Hz, 1H), 3.47 (d, *J* = 15.3 Hz, 1H), 3.33 (d, *J* = 15.3 Hz, 1H), 2.63 (t, *J* = 8.8 Hz, 1H), 1.33 (s, 3H); **^{13}C-NMR** (75 MHz, $CDCl_3$): δ (ppm) 158.4 (C), 144.8 (C), 130.7 (C), 130.1 (CH), 115.2 (CH_2), 114.1 (CH), 80.4 (CH_2), 72.4 (CH_2), 55.4 (CH_3), 53.5 (CH), 44.3 (CH_2), 24.7 (CH_3); **LRMS** (m/z, ESI): 363 ([M^+ + Na]), 175, 160; **HRMS** (ESI-TOF): *m/z* calculated for $C_{15}H_{20}NaO_3$ [M + Na]$^+$: *m/z* 271.1310, found 271.1301. Stereochemistry if **72da** was determined by nOe experiments.

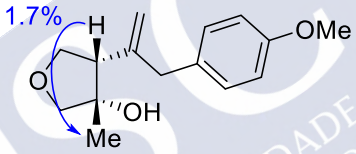

Figure 83. Significant nOes observed for **72da**.

(1S,2R)-1-benzyl-2-(3-(4-methoxyphenyl)prop-1-en-2-yl)cyclopentan-1-ol (72ca)

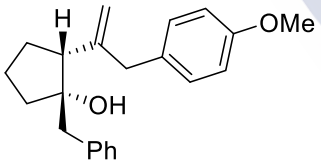

The compound was purified by flash chromatography (5% EtOAc/Hexane) to afford **72ca** (50% yield) as a pale yellow oil. **^{1}H-NMR** (300 MHz, $CDCl_3$): δ (ppm) 7.36 – 7.20 (m, 5H), 7.16 – 7.09 (m, 2H), 6.91 – 6.84 (m, 2H), 5.18 – 5.12 (m, 1H), 5.04 (q, *J* = 1.5 Hz, 1H), 3.83 (s, 3H), 3.48 (d, *J* = 15.4 Hz, 1H), 3.37 (d, *J* = 15.5 Hz, 1H), 2.95 (d, *J* = 13.4 Hz, 1H), 2.71 (d, *J* = 13.4 Hz, 1H), 2.40 (dd, *J* = 10.7, 8.0 Hz, 1H), 1.98 – 1.68 (m, 4H), 1.59 – 1.46 (m, 2H); **^{13}C-NMR** (75 MHz, $CDCl_3$): δ (ppm) 158.2 (C), 149.3 (C), 138.6 (C), 131.7 (C), 130.3 (CH), 130.2 (CH), 128.2 (CH), 126.4 (CH), 114.3 (CH_2), 113.9 (CH), 81.7 (C), 55.4 (CH_3), 53.8 (CH), 47.0 (CH_2), 43.9 (CH_2), 38.8 (CH_2), 30.9 (CH_2), 21.2 (CH_2); **LRMS** (m/z, ESI): 323 ([M^+ + H]), 305, 235, 213, 121; **HRMS** (ESI-TOF): *m/z* calculated for $C_{22}H_{27}O_2$ [M + H]$^+$: *m/z* 323.2011, found 323.2002. Stereochemistry if **72ca** was determined by nOe experiments.

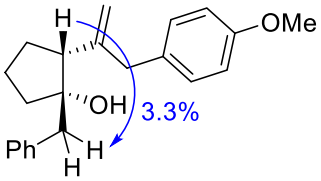

Figure 84. Significant nOes observed for **72ca**.

2.11. Representative procedure for the tandem annulation reaction of alkylidenecyclopropanes and malonates.

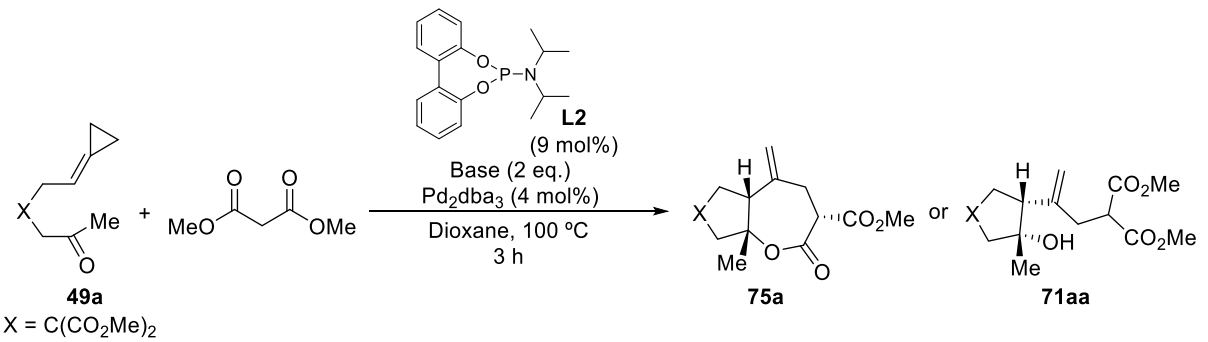

A solution of Pd_2dba_3 (4.4 mg, 4 mol%), N,N-diisopropyldibenzo[d,f][1,3,2]dioxaphosphepin-6-amine (3.6 mg, 9 mol%), dimethyl malonate (27 µL, 0.24 mmol, 2 eq.) base (50,9 mg, 0.24 mmol, 2 eq.) and **49a** (30.5 mg, 0.12 mmol) in dry dioxane (2.4 mL) was heated under reflux for 3h. The mixture was then cooled to rt, diluted with EtOAc and filtered through a short pad of florisil, eluting with EtOAc. The filtrate was concentrated and the crude was further purified by flash chromatography (10-20%% EtOAc/hexanes).

Trimethyl (3R,5aR,8aR)-8a-methyl-5-methylene-2-oxooctahydro-7H-cyclopenta[b]oxepine-3,7,7-tricarboxylate (75a)

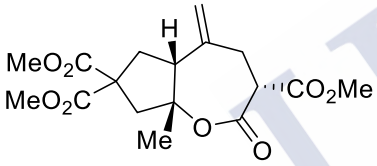

89%, colourless oil. Obtained using K_3PO_4 as base. **^{1}H-NMR** (300 MHz, $CDCl_3$): δ (ppm) 5.03 (s, 1H), 4.99 (d, *J* = 1.5 Hz, 1H), 3.81 (s, 3H), 3.73 (s, 3H), 3.72 (s, 3H), 3.64 (t, *J* = 7.8 Hz, 1H), 2.76 (dd, *J* = 11.1, 5.2 Hz, 1H), 2.68 – 2.53 (m, 3H), 2.40 (dd, *J* = 10.5, 2.4 Hz, 1H), 2.13 (d, *J* = 10.5 Hz, 1H), 2.03 (ddd, *J* = 13.4, 5.3, 2.4 Hz, 1H), 1.53 (s, 3H). **^{13}C-NMR** (75 MHz, $CDCl_3$): δ (ppm) 173.2 (C), 169.3 (C), 169.3 (C), 168.4 (C), 141.8 (C), 115.2 (CH_2), 90.2 (C), 58.2 (C), 52.9 (CH_3), 52.8 (CH_3), 51.0 (CH), 50.7 (CH), 49.2 (CH_2), 34.6 (CH_2), 34.5 (CH_2), 17.5 (CH_3); **LRMS** (m/z, ESI): 355 ([M^+ + H]), 311, 279, 247, 219, 179; **HRMS** (ESI-TOF): *m/z* calculated for $C_{17}H_{23}O_8$ [M + H]$^+$: *m/z* 355.1393, found 355.1387. Stereochemistry if **75a** was determined by nOe experiments.

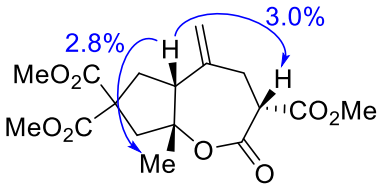

Figure 85. Significant nOes observed for **75a**.

Dimethyl (3R,4R)-3-hydroxy-4-(5-methoxy-4-(methoxycarbonyl)-5-oxopent-1-en-2-yl)-3-methylcyclopentane-1,1-dicarboxylate (71a)

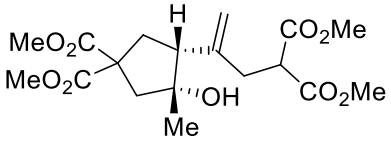

87%, colourless oil. Obtained using K_2CO_3 as base. **^{1}H-NMR** (300 MHz, $CDCl_3$): δ (ppm) 5.03 (s, 1H), 4.99 (s, 1H), 3.78 – 3.68 (m, 13H), 2.83 – 2.66 (m, 2H), 2.67 – 2.53 (m, 2H), 2.46 (dd, *J* = 12.0, 7.1 Hz, 1H), 2.40 – 2.22 (m, 3H), 1.29 (s, 3H); **^{13}C-NMR**

(75 MHz, $CDCl_3$): δ (ppm) 173.3 (C), 173.0 (C), 169.8 (C), 169.5 (C), 143.2 (C), 114.07 (CH_2), 79.5 (C), 57.1 (C), 55.1 (CH), 53.0 (CH_3), 52.9 (CH_3), 52.8 (CH_3), 52.7 (CH_3), 50.5 (CH), 48.2 (CH_2), 37.4 (CH_2), 34.5 (CH_2), 25.9 (CH_3); **LRMS** (m/z, ESI): 409 ([M^+ + Na]), 369, 337, 309, 277, 237; **HRMS** (ESI-TOF): *m/z* calculated for $C_{18}H_{26}NaO_9$ [M + Na]$^+$: *m/z* 409.1475, found 409.1472. Stereochemistry if **71a** was determined by nOe experiments.

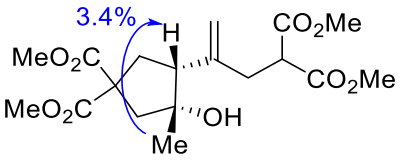

Figure 86. Significant nOes observed for **71a**.

USC
UNIVERSIDADE
DE SANTIAGO
DE COMPOSTELA

CHAPTER III: Cyclometallated alkenyl-gold(III) species by proximal ring-opening of 2-(cyclopropylidenemethyl)pyridines

3.1. Synthesis of alkylidenecyclopropane precursors

Procedure for the obtention of 79a

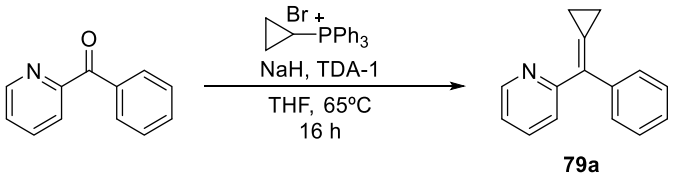

79a

Over a suspension of NaH (1.3, 31.77 mmol, 3 eq.) in dry THF (35 mL) at rt is added Cyclopropyltriphenylphosphonium bromide in one portion (12.2 g, 31.77 mmol, 3 eq.) and the mixture is heated to gentle reflux for 16 h. Then, a solution of 2-benzoylpyridine (2.0 g, 10.69 mmol, 1 eq.) and TDA-1 (1.8 g, 5.30 mmol, 0.5 eq.) in dry THF (20 mL) are added dropwise. The mixture is stirred at 65 ºC for 5 hours, then the mixture is cooled to rt and quenched with a $NH_4Cl_{(sat)}$ solution (100 mL), extracted with Et_2O (3x40 mL) and the organic layers were dried using Na_2SO_4. The organic phase was then filtered and evaporated to give a residue that was purified by flash column chromatography (10 % AcOEt/Hexane) to yield 2-(cyclopropylidene(phenyl)methyl)pyridine **79a** (1.9 g, 9.17 mmol, 87%) as a pale yellow solid. **^{1}H-RMN** (500 MHz, CD_2Cl_2) δ (ppm): 8.57 (ddd, *J* = 4.9, 1.9, 1.0 Hz, 1H), 7.72 (td, *J* = 7.7, 1.9 Hz, 1H), 7.64 (dt, *J* = 8.0, 1.1 Hz, 1H), 7.52 – 7.44 (m, 2H), 7.39 – 7.33 (m, 2H), 7.31 – 7.25 (m, 1H), 7.19 (ddd, *J* = 7.4, 4.8, 1.3 Hz, 1H), 1.49 (s, 4H);); **^{13}C-NMR** (126 MHz, CD_2Cl_2) δ (ppm): 159.7 (C), 149.4 (CH), 140.8 (C), 136.6 (CH), 131.0 (C), 129.1 (CH), 128.8 (C), 128.7 (CH), 128.5 (CH), 127.4 (CH), 123.7 (CH), 122.1 (CH_2), 4.3, 4.1 (CH_2). The exact mass of this compound was not available at the date of writing this doctoral thesis.

2-(1-cyclopropylideneethyl)pyridine (79b)

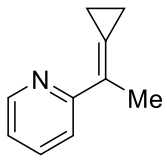

23% yield, as a yellowish oil. The spectroscopic data is in agreement with those reported in literature.[168] **^{1}H-RMN** (300 MHz, CD_2Cl_2) δ (ppm): 8.54 (ddd, *J* = 4.9, 1.9, 1.0 Hz, 1H), 7.82 (d, *J* = 8.1 Hz, 1H), 7.62 (ddd, *J* = 8.1, 7.4, 1.9 Hz, 1H), 7.10 (ddd, *J* = 7.4, 4.9, 1.2 Hz, 1H), 2.29 (p, *J* = 1.7 Hz, 3H), 1.53 – 1.43 (m, 2H), 1.25 – 1.12 (m, 2H).

2-(cyclopropylidenemethyl)pyridine (79c)

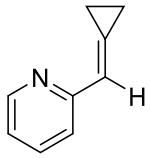

28% yield, as a yellowish oil. The spectroscopic data is in agreement with those reported in literature.[168] **^{1}H-RMN** (300 MHz, CD_2Cl_2) δ (ppm): 8.51 (ddd, *J* = 4.9, 1.8, 1.0 Hz, 1H), 7.73 – 7.68 (m, 1H), 7.64 (ddd, *J* = 7.4, 1.8, 0.6 Hz, 1H), 7.10 (ddd, *J* = 7.3, 4.9, 1.3 Hz, 1H), 6.93 – 6.89 (m, 1H), 1.53 – 1.40 (m, 2H), 1.29 – 1.19 (m, 2H).

3.2. Procedure for the obtention of Au (III)-chloride complexes

Procedure for the obtention of 79a-$AuCl_3$

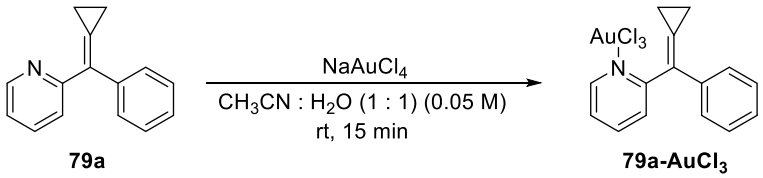

79a **79a-$AuCl_3$**

Over a solution of 2-(cyclopropylidene(phenyl)methyl)pyridine **79a** (50.0 mg, 0.24 mmol, 1 eq.) in CH_3CN (2.4 mL) was rapidly added a solution of sodium tetrachloroaureate (87.3 mg, 0.24 mmol, 1 eq.) and the mixture was stirred at room temperature for 15 minutes. An orange solid was then formed, which was filtrated and dried under vacuum to afford coordinated complex **79a-$AuCl_3$** (63.5 mg, 0.13 mmol, 52%) as an orange solid. **^{1}H-RMN** (500 MHz, CD_2Cl_2) δ (ppm): 8.77 (dd, *J* = 6.1, 1.9 Hz, 1H), 8.14 (td, *J* = 7.7, 1.5 Hz, 1H), 7.83 (dd, *J* = 8.0, 1.6 Hz, 1H), 7.63 (ddd, *J* = 7.6, 6.0, 1.7 Hz, 1H), 7.44 (m, 5H), 1.73 (m, 2H), 1.54 (m, 2H); **^{13}C-NMR** (126 MHz, CD_2Cl_2) δ (ppm): 161.2, 150.5, 142.6, 137.2, 137.0, 131.1, 129.8, 129.4, 129.2, 128.6, 126.4, 5.9, 4.8. The exact mass of this compound was not available at the date of writing this doctoral thesis.

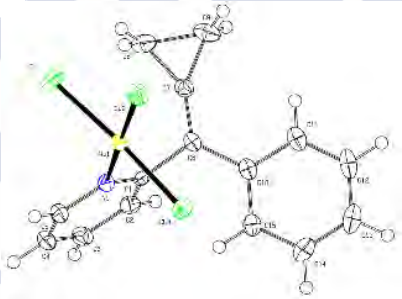

Figure 87. Crystal structure of complex **79a-$AuCl_3$**.

Procedure for the obtention of (C^N) cyclometallated complexes

*(Exemplified with the synthesis of **82a**)*

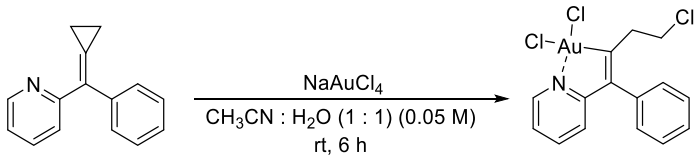

79a **82a**

Over a solution of 2-(cyclopropylidene(phenyl)methyl)pyridine **79a** (50.0 mg, 0.24 mmol, 1 eq.) in CH_3CN (2.4 mL) was rapidly added a solution of sodium tetrachloroaurate (87.3 mg, 0.24 mmol, 1 eq.) and the mixture was stirred at room temperature for 6 h. The CH_3CN was then evaporated and the aqueous phase was diluted with water (20 mL), then was extracted with CH_2Cl_2 (3x20 mL). The combined organic layers were dried, filtered, concentred and purified by flash chromatography (100% CH_2Cl_2) affording cyclometallated complex [(N^C)$AuCl_2$] **82a** as a pale yellow solid (91 mg, 0.18 mmol, 75%) as an yellow solid. **^{1}H-RMN** (500 MHz, CD_2Cl_2) δ (ppm): 9.65 (ddd, *J* = 5.9, 1.5, 0.6 Hz, 1H), 7.94 (td, *J* = 7.8, 1.6 Hz, 1H), 7.56 – 7.47 (m, 3H),

7.42 (ddd, *J* = 7.6, 6.0, 1.6 Hz, 1H), 7.35 – 7.22 (m, 2H), 6.80 (ddd, *J* = 8.0, 1.6, 0.6 Hz, 1H), 3.77 (t, *J* = 7.0 Hz, 2H), 2.74 (t, *J* = 7.0 Hz, 2H); **^{13}C-NMR** (126 MHz, CD_2Cl_2) δ (ppm): 172.9, 168.5, 149.4, 149.2, 143.7, 134.1, 129.9, 129.7, 124.9, 124.0 , 43.5, 39.0. The exact mass of this compound was not available at the date of writing this doctoral thesis.

Cyclometallated complex [(N^C)AuCl$_2$] (82b)

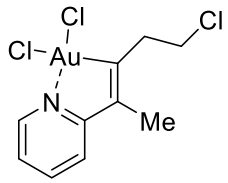

60%, yellow solid.**^{1}H-RMN** (500 MHz, CD_2Cl_2) δ (ppm): 9.63 (ddd, *J* = 6.0, 1.6, 0.6 Hz, 1H), 8.10 (td, *J* = 7.7, 1.6 Hz, 1H), 7.43 (ddd, *J* = 7.6, 6.0, 1.5 Hz, 1H), 7.34 (ddd, *J* = 7.6, 6.0, 1.5 Hz, 1H), 3.86 (t, *J* = 6.6 Hz, 2H), 2.98 (td, *J* = 6.6, 0.7 Hz, 1H), 2.12 (s, 3H); **^{13}C-NMR** (126 MHz, CD_2Cl_2) δ (ppm): 170.8, 168.8, 149.0, 143.8, 142.4, 124.0, 122.8, 44.1, 38.0, 14.8; **HRMS** calculated for C10H13AuCl3NNa $[M+Na]^+$: *m/z* 469.9520, found 469.9513.

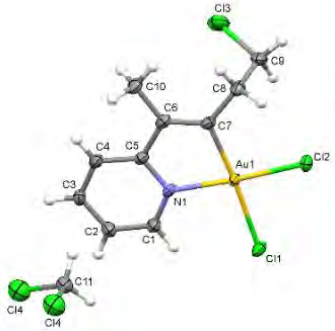

Figure 88. Crystal structure of complex **82b**.

Cyclometallated complex [(N^C)AuCl$_2$] (82c)

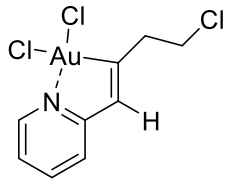

40%, yellow solid. **^{1}H-RMN** (500 MHz, CD_2Cl_2) δ (ppm): 9.51 (d, *J* = 6.0 Hz, 1H), 8.04 (td, *J* = 7.8, 1.6 Hz, 1H), 7.44 (d, *J* = 7.8 Hz, 1H), 7.41 (dd, *J* = 10.0, 3.6 Hz, 1H), 6.38 (s, 1H), 3.86 (t, *J* = 6.3 Hz, 2H), 2.93 (td, *J* = 6.2, 1.0 Hz, 2H); **^{13}C-NMR** (126 MHz, CD_2Cl_2) δ (ppm): 175.9, 166.9, 149.1, 143.9, 136.5, 123.1, 122.6, 43.2, 42.3; **HRMS** calculated for $C_9H_9AuCl_3NNa$ $[M+Na]^+$: *m/z* 455.9364, found 455.9358.

Cyclometallated cyclopropanic complex [(N^C)AuCl$_2$] (83b)

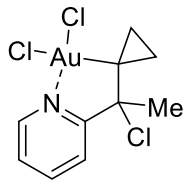

30%, white solid.**^{1}H-RMN** (500 MHz, CD_2Cl_2) δ (ppm): 9.65 (ddd, *J* = 6.0, 1.5, 0.8 Hz, 1H), 8.20 (t, *J* = 7.7 Hz, 1H), 7.80 (ddd, *J* = 7.9, 1.6, 0.8 Hz, 1H), 7.66 (ddd, *J* = 7.6, 5.9, 1.6 Hz, 1H), 1.48 (dt, *J* = 10.5, 6.7 Hz, 1H), 0.94 (dt, *J* = 10.4, 7.1 Hz, 2H), 0.39 (dt, *J* = 10.6, 7.3 Hz, 1H); **^{13}C-NMR** (126 MHz, CD_2Cl_2) δ (ppm): 170.8 (C), 168.8 (C), 149.0 (CH), 143.8 (CH), 142.4 (C), 124.0 (CH), 122.8 (CH), 44.1(CH_2), 38.0 (CH_2), 14.8 (CH_3). The exact mass of this compound was not available at the date of writing this doctoral thesis.

Cyclometallated cyclopropanic complex [(N^C)AuCl$_2$] (83c)

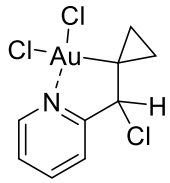

18%, white solid.**^{1}H-RMN** (500 MHz, CD_2Cl_2) δ (ppm): 9.75 (dd, *J* = 6.0, 0.9 Hz, 1H), 8.24 (td, *J* = 7.8, 1.5 Hz, 1H), 7.88 (d, *J* = 7.7 Hz, 1H), 7.74 (ddd, *J* = 7.5, 6.0, 1.4 Hz, 1H), 4.65 (s, 1H), 1.65 (dt, *J* = 10.6, 6.8 Hz, 1H), 1.41 (ddd, *J* = 10.6, 7.4, 6.3 Hz, 1H), 0.92 (dt, *J* = 10.4, 6.5 Hz, 1H), 0.69 (dt, *J* = 10.4, 7.2 Hz, 1H); **^{13}C-NMR** (126 MHz, CD_2Cl_2) δ (ppm): 165.13, 149.82, 143.85, 127.09, 124.17, 75.86, 58.88, 17.13, 12.87**HRMS** calculated for $C_9H_9AuCl_3NNa$ [M+Na]$^+$: *m/z* 455.9364, found 455.9358.

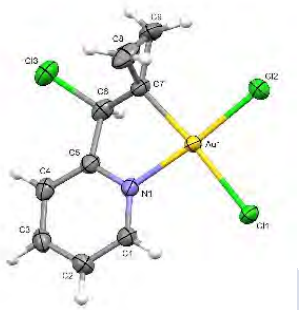

Figure 89. Crystal structure of complex **83c**.

3.3. Procedure for the obtention of cyclometallated complexes [(C^N)-AuBr$_2$]

*Procedure exemplified for the formation of complex **82a`***

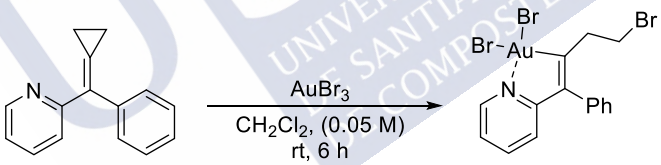

79a **82a`**

A solution of 2-(cyclopropylidene(phenyl)methyl)pyridine **79a** (20.7 mg, 0.10 mmol, 1 eq.) and $AuBr_3$ (43.7 mg, 0.10 mmol, 1 eq.) in CH_2Cl_2 (2.4 mL) was stirred at room temperature for 6 h. The mixture was then evaporated and the crude was purified by flash chromatography (100% CH_2Cl_2) affording cyclometallated complex [(N^C)AuBr$_2$] **82a`** as a white solid (52 mg, 0.08 mmol, 80%) as a white solid. **^{1}H-RMN** (500 MHz, CD_2Cl_2) δ (ppm): 9.85 (d, *J* = 6.0 Hz, 1H), 7.91 (t, *J* = 7.8 Hz, 1H), 7.56 - 7.48 (m, 3H), 7.41 (t, *J* = 6.7 Hz, 1H), 7.31-7.23 (m, 2H), 6.77 (d, *J* = 8.0 Hz, 1H), 3.58 (t, *J* = 7.5 Hz, 2H), 2.98 (t, *J* = 7.5 Hz, 2H); **^{13}C-NMR** (126 MHz, CD_2Cl_2) δ (ppm): 174.5, 168.3, 150.2, 149.8, 143.3, 134.4, 130.0, 129.8, 124.7, 125.0, 124.11, 40.7, 31.3; **HRMS** calculated for $C_{15}H_{13}AuBr_3NNa$ [M+Na]$^+$: *m/z* 663.8161, found 663.8154.

Cyclometallated complex [(N^C)AuBr$_2$] (82b`)

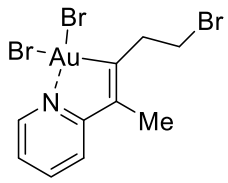

60%, white solid. **^{1}H-RMN** (500 MHz, CD_2Cl_2) δ (ppm): 9.84 (d, *J* = 6.0 Hz, 1H), 8.08 (t, *J* = 7.8 Hz, 1H), 7.47 - 7.35 (m, 1H), 7.33 (d, *J* = 8.0 Hz, 1H), 3.69 (t, *J* = 7.0 Hz, 2H), 3.26 (t, *J* = 7.0 Hz, 2H), 2.09 (m, 3H); **^{13}C-NMR** (126 MHz, CD_2Cl_2) δ (ppm): 172.6, 168.6, 150.0, 143.4, 142.7, 124.1, 123.0, 39.8, 31.9, 15.0; **HRMS** calculated for $C_{10}H_{11}AuBr_3NNa$ [M+Na]$^+$: *m/z* 601.8005, found 601.7990.

Cyclometallated complex [(N^C)AuBr$_2$] (82c`)

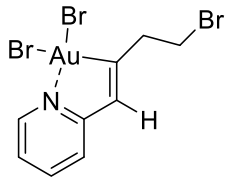

13%, white solid.**^{1}H-RMN** (500 MHz, CD_2Cl_2) δ (ppm): 9.84 (d, *J* = 6.1 Hz, 1H), 8.09 (td, *J* = 7.7, 1.5 Hz, 1H), 7.60 (td, *J* = 7.8, 2.7 Hz, 2H), 4.28 (td, *J* = 9.3, 1.9 Hz, 1H), 3.38 (ddt, *J* = 14.6, 8.4, 2.2 Hz, 1H), 2.78 (ddd, *J* = 14.7, 11.1, 9.1 Hz, 1H), 2.67 – 2.42 (m, 2H); **^{13}C-NMR** (126 MHz, CD_2Cl_2) δ (ppm): 177.15, 166.8, 150.1, 143.6, 137.2, 123.3, 122.5, 44.2, 31.8. **HRMS** calculated for $C_9H_9AuBr_3NNa$ [M+Na]$^+$: *m/z* 587.7848, found 587.7846.

Cyclometallated cyclobutanic complex [(N^C)AuBr$_2$] (84c`)

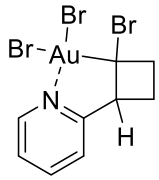

15%, white solid.**^{1}H-RMN** (500 MHz, CD_2Cl_2) δ (ppm): 9.84 (ddd, *J* = 6.0, 1.4, 0.8 Hz, 1H), 8.09 (td, *J* = 7.7, 1.5 Hz, 1H), 7.48 - 7.69 (m, 2H), 4.29 (td, *J* = 9.2, 1.6 Hz, 1H), 3.38 (ddt, *J* = 14.5, 8.3, 2.1 Hz, 1H), 2.78 (ddd, *J* = 14.9, 11.1, 9.5 Hz, 1H) 2.63-2.46 (m, 2H); **^{13}C-NMR** (126 MHz, CD_2Cl_2) δ (ppm): 170.9, 150.9, 142.9, 125.7, 123.4, 80.6, 67.3, 44.7, 29.6 **HRMS** calculated for $C_9H_9AuBr_3NNa$ [M+Na]$^+$: *m/z* 587.7848, found 587.7839.

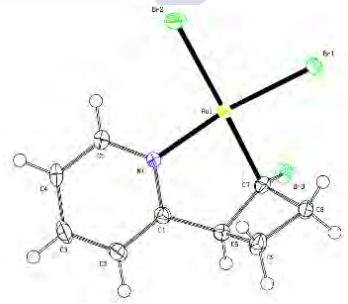

Figure 90. Crystal structure of complex **84c`**.

3.4. Procedure for the obtention of transmetallated complexes [(C^N)-Au-Ar_xCl_y]

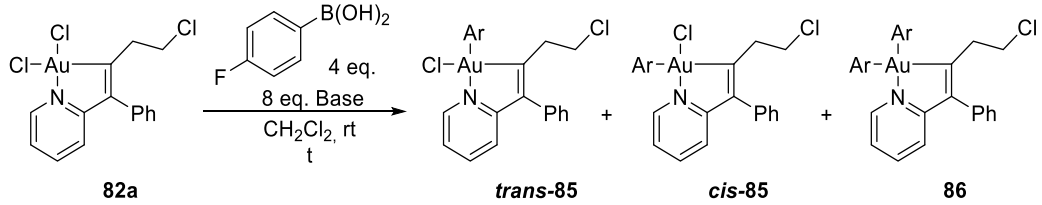

A solution of cyclometallated complex [(N^C)$AuCl_2$] **82a** (21.1 mg, 0.04 mmol, 1 eq.) K_3PO_4 (67.9 mg, 0.32 mmol, 8 eq.), 4-fluorophenylboronic acid (22.4 mg, 0.16 mmol, 4 eq.) in CH_2Cl_2 (1 mL) was stirred at room temperature. The mixture was then evaporated and the crude was purified by flash chromatography (5-20% CH_2Cl_2/Hexanes) affording transmetallated complexes ***cis*-85**, ***trans*-85** and **86** as white solids.

Monotransmetallated complex *trans*-[(N^C)AuCl-C_6H_4F] (*trans*-85)

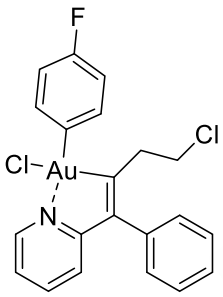

83%, white solid. **^{1}H-RMN** (500 MHz, CD_2Cl_2) δ (ppm): 9.31 (m, 1H),7.84 (td, *J* = 7.9, 1.7 Hz, 1H), 7.53 - 7.42 (m, 6H), 7.24 (dd, *J* = 8.0, 1.5 Hz, 2H), 7.00 (m, 2H), 6.79 (d, *J* = 8.0 Hz, 1H), 3.06 (t, *J* = 7.5 Hz, 2H), 2.42 (t, *J* = 7.5 Hz, 2H); **^{13}C-NMR** (126 MHz, CD_2Cl_2) δ 165.7, 163.2, 161.3, 161.1, 149.9, 148.3, 142.2, 136.5, 135.1 (d, *J* = 3.0 Hz), 134.6 (d, *J* = 6.6 Hz), 130.3, 129.9, 129.2, 123.6 (d, *J* = 8.9 Hz), 116.4 (d, *J* = 20.4 Hz), 42.5, 38.5; **HRMS** calculated for $C_{21}H_{17}AuCl_2FNNa$ $[M+Na]^+$: *m/z* 592.0285, found 592.0280.

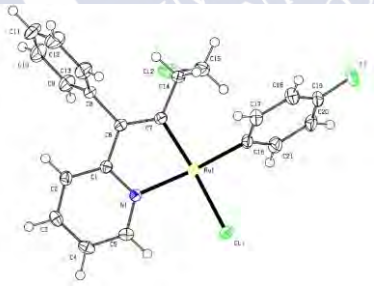

Figure 91. Crystal structure of complex ***trans*-85**.

Monotransmetallated complex *cis*-[(N^C)AuCl-C_6H_4F] (*cis*-85)

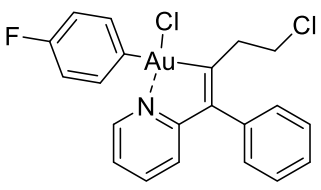

40%, white solid. **^{1}H-RMN** (500 MHz, CD_2Cl_2) δ (ppm): 8.10 (ddd, *J* = 6.0, 1.5, 0.6 Hz, 1H), 7.79 (ddd, *J* = 8.1, 7.6, 1.6 Hz, 1H), 7.53 - 7.41 (m, 5H), 7.26-7.22 (m, 2H), 7.11-7.00 (m, 3H), 6.82 (ddd, *J* = 8.1, 1.5, 0.5 Hz, 1H), 3.74 (m, 2H), 2.91 (m, 2H); **^{13}C-NMR** (126 MHz, CD_2Cl_2) δ (ppm) 189.0, 172.3, 163.1, 162.2 (d, *J* = 3.3 Hz), 161.2, 149.8, 149.7, 142.6, 136., 135.3 (d, *J* = 6.0 Hz), 129.9 (d, *J* = 44.5 Hz), 128.6, 124.3, 122.8, 116.3 (d, *J* = 18.9 Hz), 43.9, 38.2.; **HRMS** calculated for $C_{21}H_{17}AuCl_2FNNa$ $[M+Na]^+$: *m/z* 592.0285, found 592.0280.

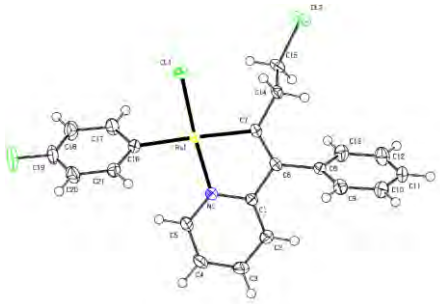

Figure 92. Crystal structure of complex cis-85.

Bistransmetallated complex [(N^C)Au($C_6H_4F)_2$] (86)

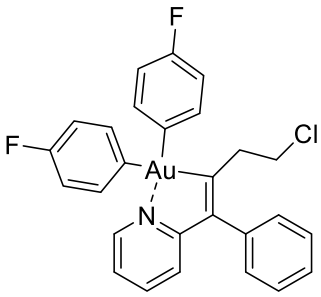

17%, white solid. **^{1}H-RMN** (500 MHz, CD_2Cl_2) δ (ppm): 7.91 (ddd, *J* = 5.6, 1.7, 0.8 Hz, 1H), 7.71 (ddd, *J* = 8.1, 7.5, 1.7 Hz, 1H), 7.51-7.44 (m, 2H), 7.44-7.36 (m, 5H), 7.23 – 7.19 (m, 2H), 7.08 (ddd, *J* = 7.6, 5.6, 1.4 Hz, 1H), 6.98 (dd, *J* = 9.8, 8.6 Hz, 2H), 6.89 (dd, *J* = 9.4, 8.8 Hz, 2H), 6.76 (dt, *J* = 8.1, 1.2 Hz, 1H), 3.13 – 2.96 (m, 2H), 2.51 (m, 2H); **^{13}C-NMR** (126 MHz, CD_2Cl_2) δ (ppm): 183.3, 169.6, 162.3 (d, *J* = 73.5 Hz), 161.1 (d, *J* = 3.7 Hz), 160.4 (d, *J* = 73.5 Hz), 151.2, 149.0, 141.3, 138.6, 136.0 (d, *J* = 5.9 Hz), 135.0 (d, *J* = 3.1 Hz), 133.5 (d, *J* = 6.3 Hz), 130.5, 129.5, 128.1, 123.2, 122.6, 116.0 (d, *J* = 15.7 Hz), 115.9 (d, *J* = 14.4 Hz), 43.2, 38.9.**HRMS** calculated for $C_{27}H_{21}AuClF_2NNa$ $[M+Na]^+$: *m/z 652,0894*.

Selected NMR spectra[179]

[179] In this section we only include the NMR spectra of the most representative compounds. In the attached CD-ROM, the corresponding NMR spectra of all the compounds of this thesis can be found.

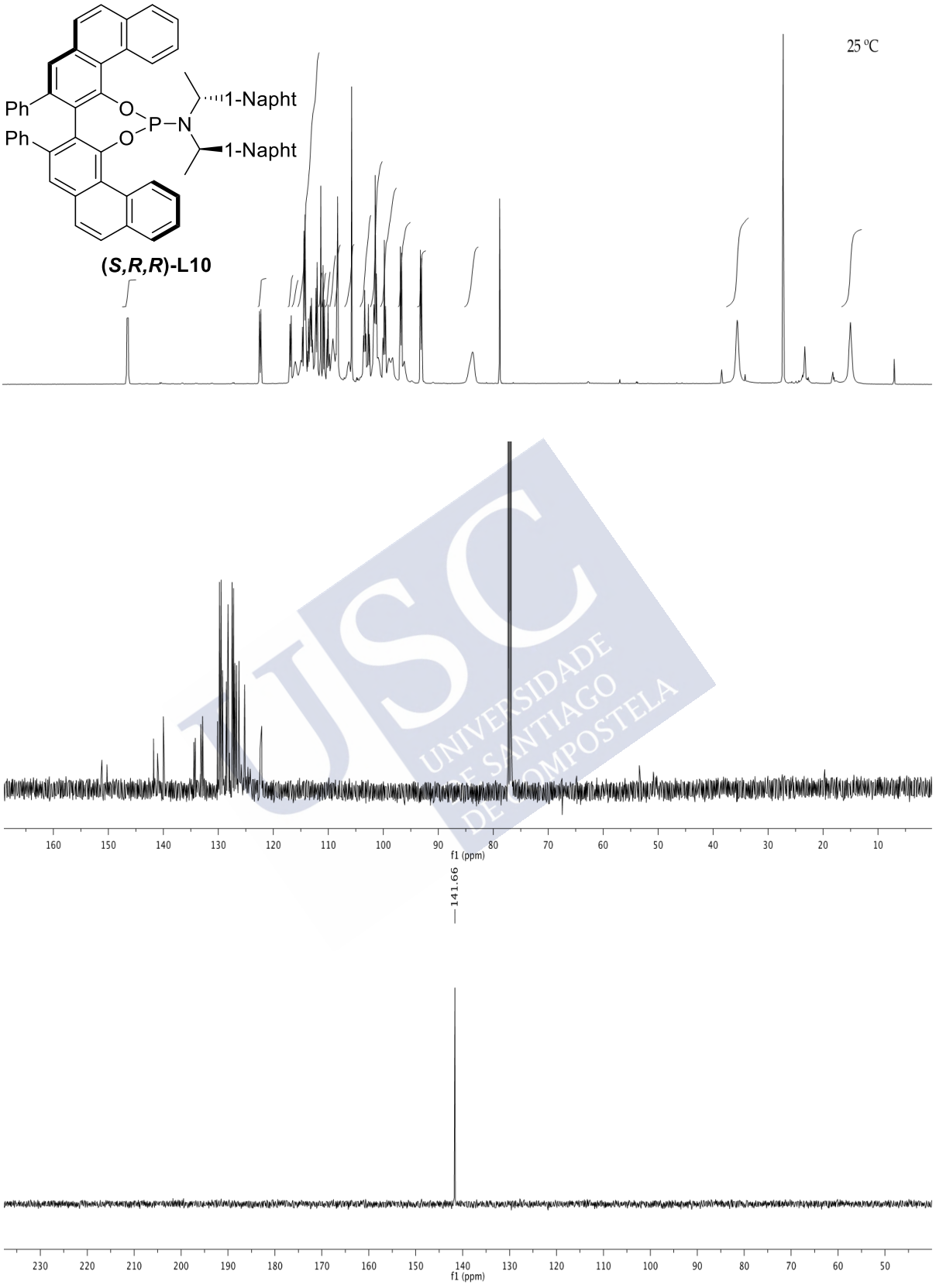

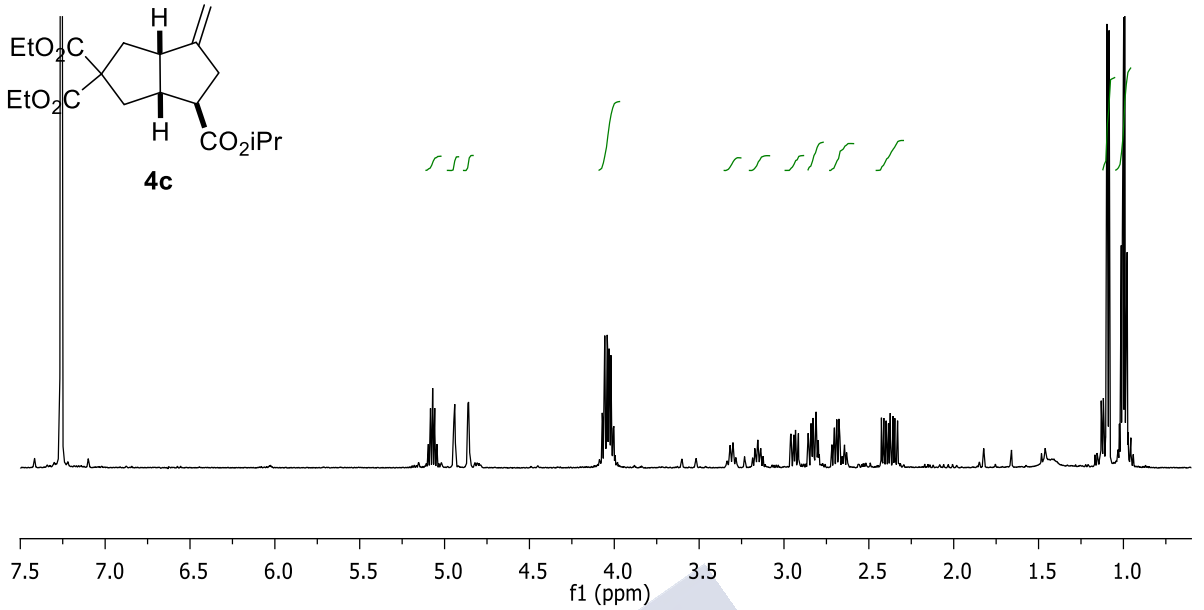
EtO2C
EtO2C
H
H
CO2iPr
4c
7.5 7.0 6.5 6.0 5.5 5.0 4.5 4.0 3.5 3.0 2.5 2.0 1.5 1.0
f1 (ppm)

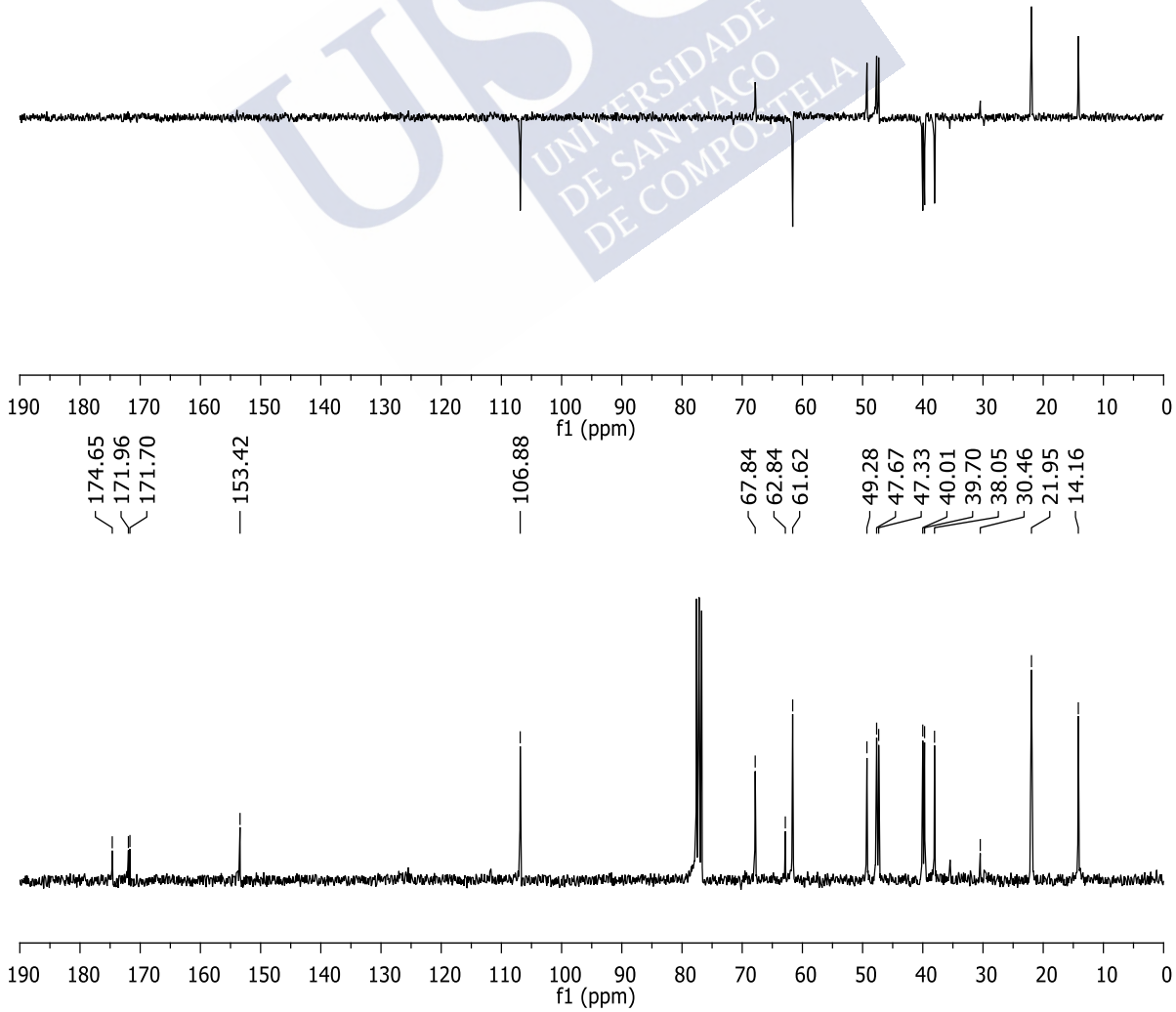
190 180 170 160 150 140 130 120 110 100 90 80 70 60 50 40 30 20 10 0
f1 (ppm)
174.65
171.96
171.70
153.42
106.88
67.84
62.84
61.62
49.28
47.67
47.33
40.01
39.70
38.05
30.46
21.95
14.16

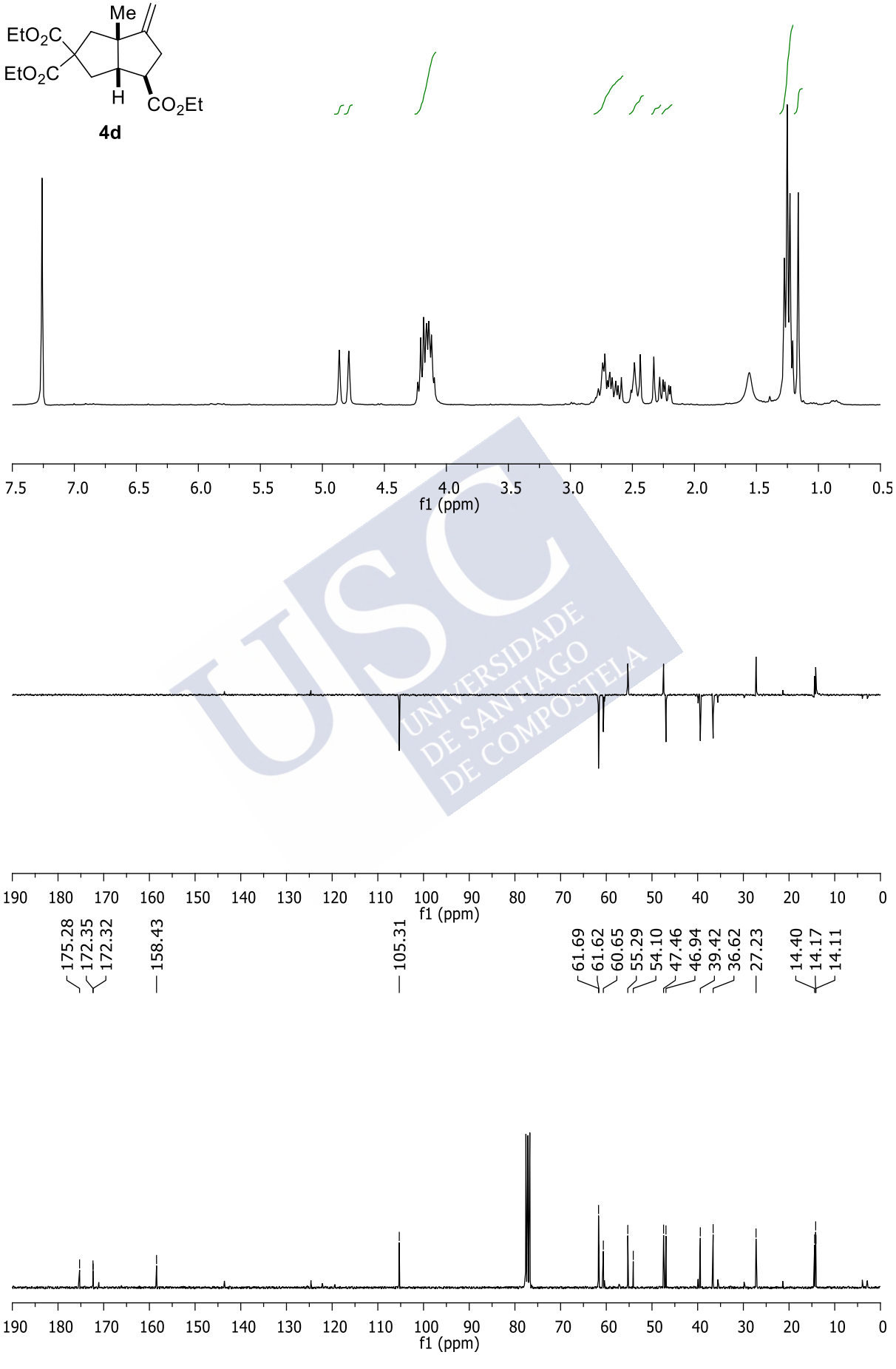
Me
EtO2C
EtO2C
H
CO2Et
4d
7.5 7.0 6.5 6.0 5.5 5.0 4.5 4.0 3.5 3.0 2.5 2.0 1.5 1.0 0.5
f1 (ppm)
190 180 170 160 150 140 130 120 110 100 90 80 70 60 50 40 30 20 10 0
f1 (ppm)
175.28
172.35
172.32
158.43
105.31
61.69
61.62
60.65
55.29
54.10
47.46
46.94
39.42
36.62
27.23
14.40
14.17
14.11
190 180 170 160 150 140 130 120 110 100 90 80 70 60 50 40 30 20 10 0
f1 (ppm)

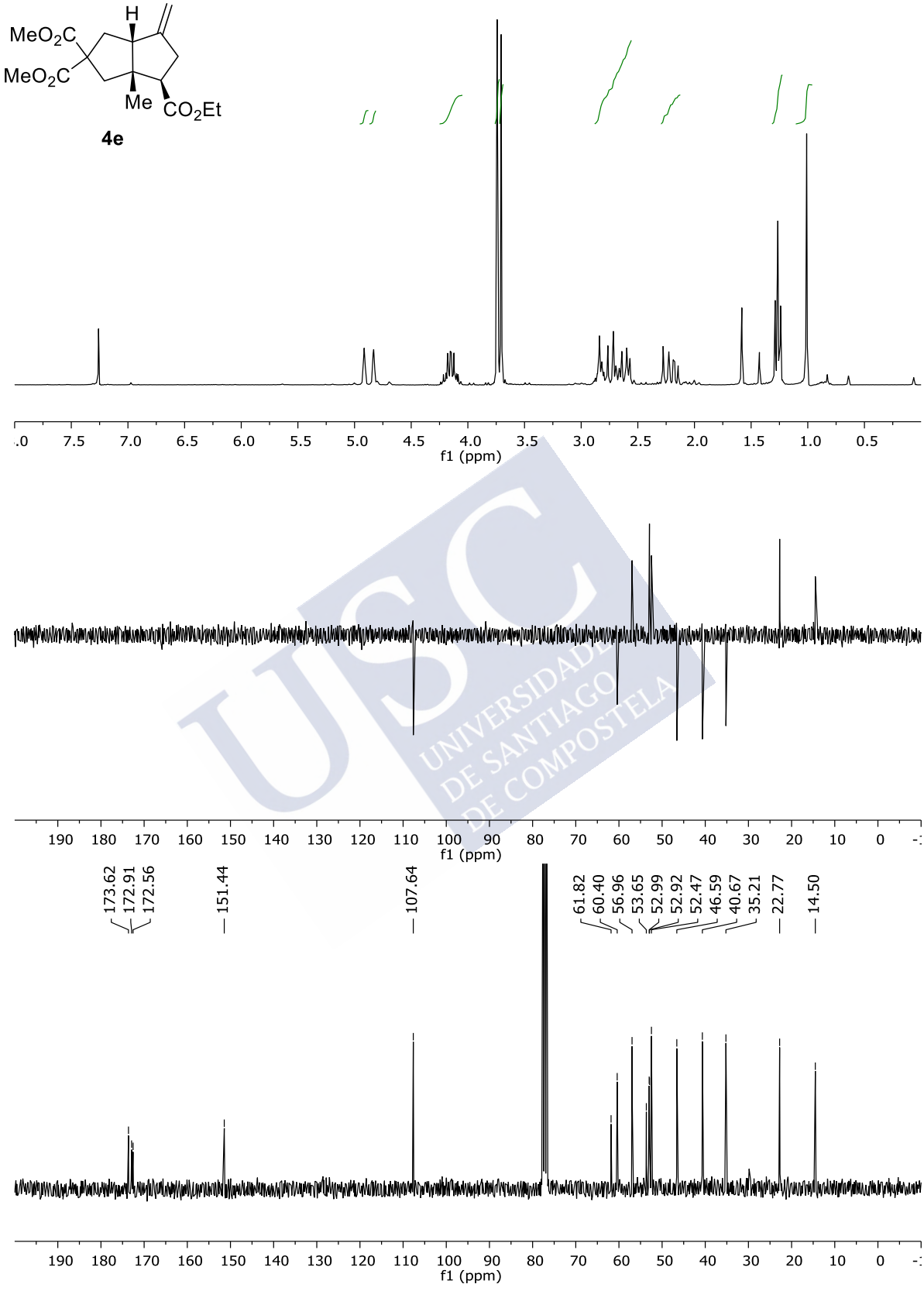
MeO2C
MeO2C
H
Me
CO2Et
4e
f1 (ppm)
173.62
172.91
172.56
151.44
107.64
61.82
60.40
56.96
53.65
52.99
52.92
52.47
46.59
40.67
35.21
22.77
14.50

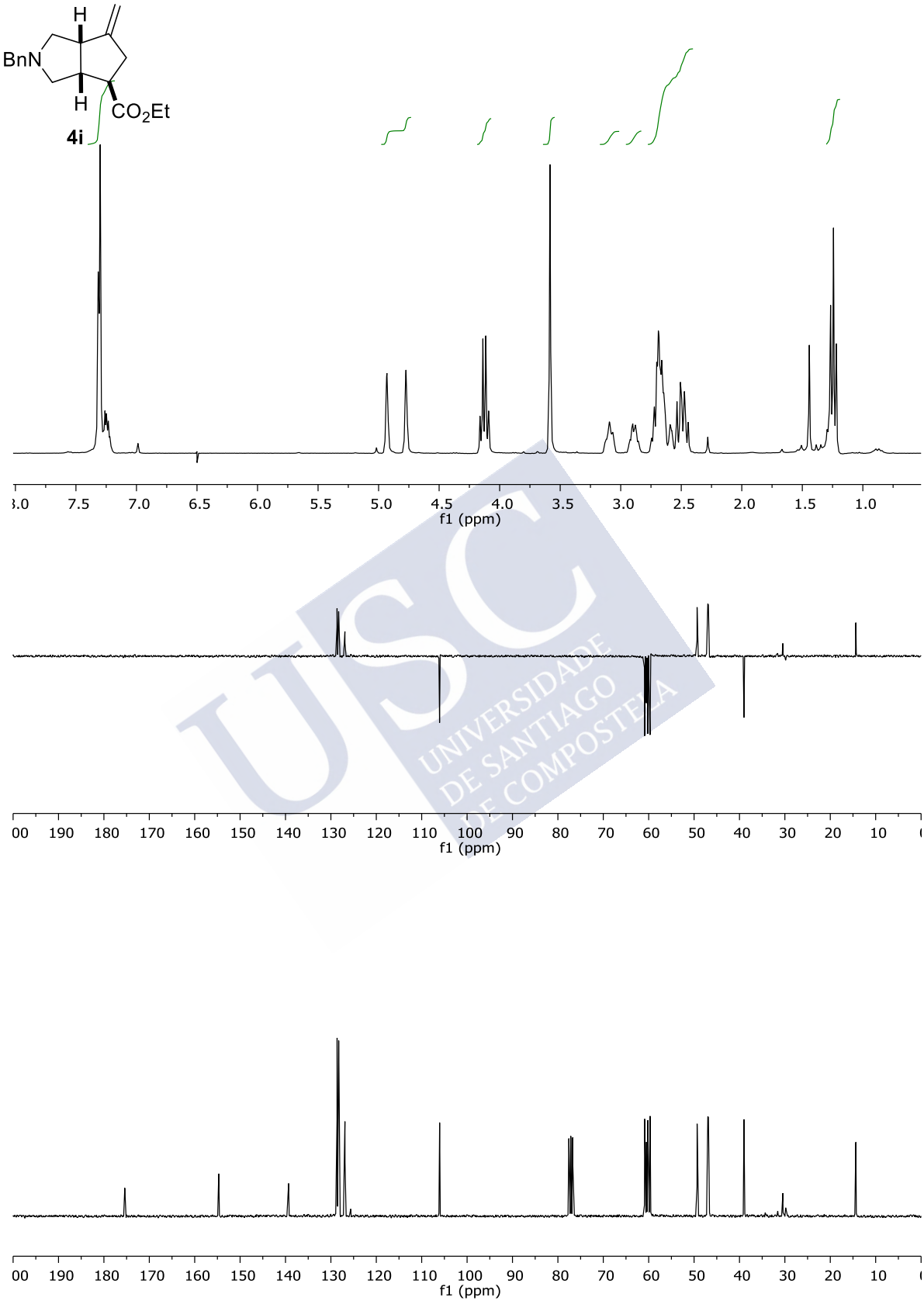
H
BnN
H
CO2Et
4i
f1 (ppm)
f1 (ppm)
f1 (ppm)

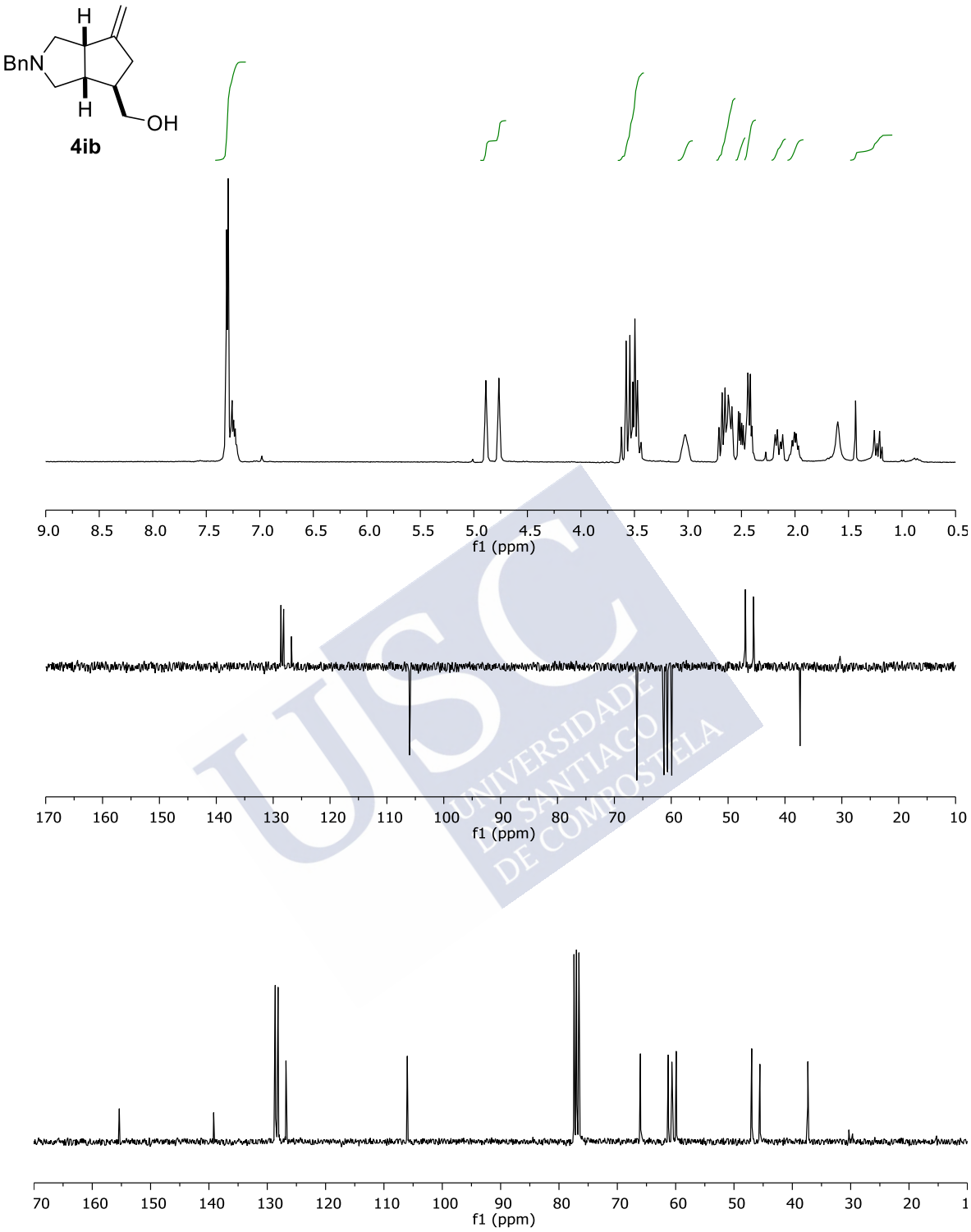
H
BnN
H
OH
4ib
9.0 8.5 8.0 7.5 7.0 6.5 6.0 5.5 5.0 4.5 4.0 3.5 3.0 2.5 2.0 1.5 1.0 0.5
f1 (ppm)
170 160 150 140 130 120 110 100 90 80 70 60 50 40 30 20 10
f1 (ppm)
70 160 150 140 130 120 110 100 90 80 70 60 50 40 30 20 1
f1 (ppm)

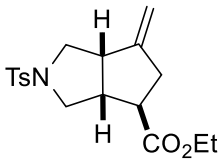
H
TsN
H
CO_2Et

4j

9.0
8.5
8.0
7.5
7.0
6.5
6.0
5.5
5.0
4.5
4.0
3.5
3.0
2.5
2.0
1.5
1.0
0.5
f1 (ppm)

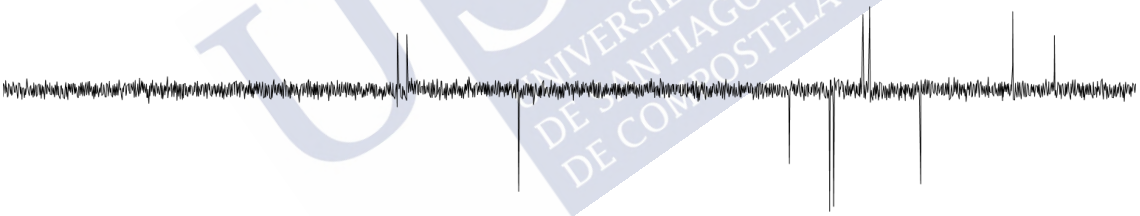

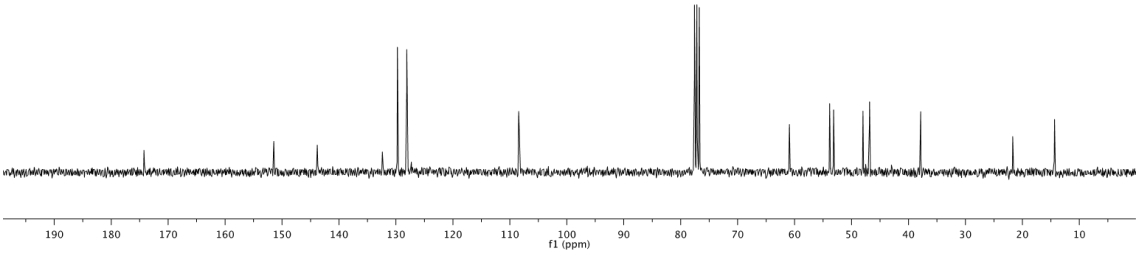
190
180
170
160
150
140
130
120
110
100
90
80
70
60
50
40
30
20
10
f1 (ppm)

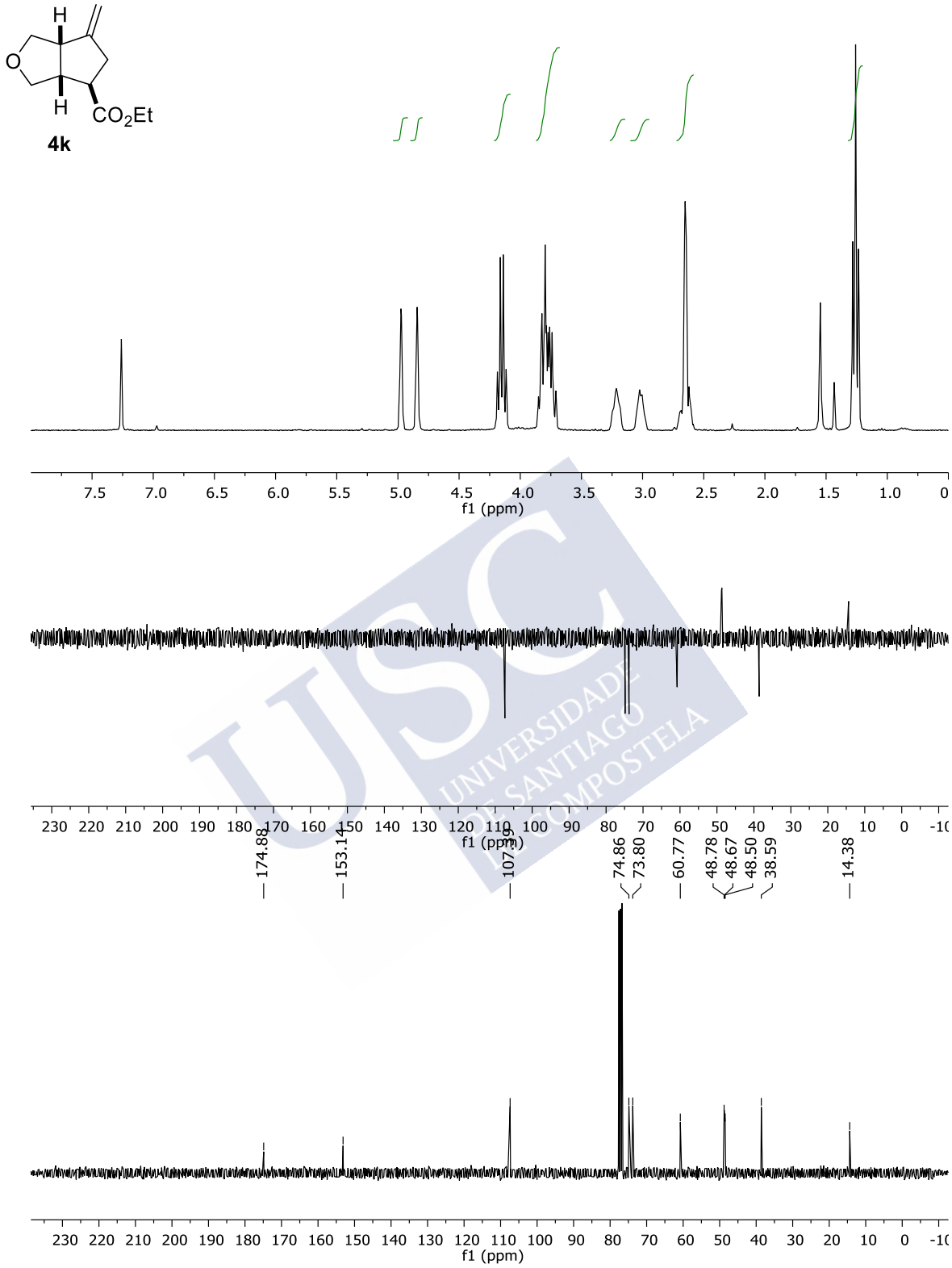
H
O
H
CO2Et
4k
7.5 7.0 6.5 6.0 5.5 5.0 4.5 4.0 3.5 3.0 2.5 2.0 1.5 1.0 0
f1 (ppm)
230 220 210 200 190 180 170 160 150 140 130 120 110 100 90 80 70 60 50 40 30 20 10 0 -10
f1 (ppm)
174.88
153.14
107.99
74.86
73.80
60.77
48.78
48.67
48.50
38.59
14.38
230 220 210 200 190 180 170 160 150 140 130 120 110 100 90 80 70 60 50 40 30 20 10 0 -10
f1 (ppm)

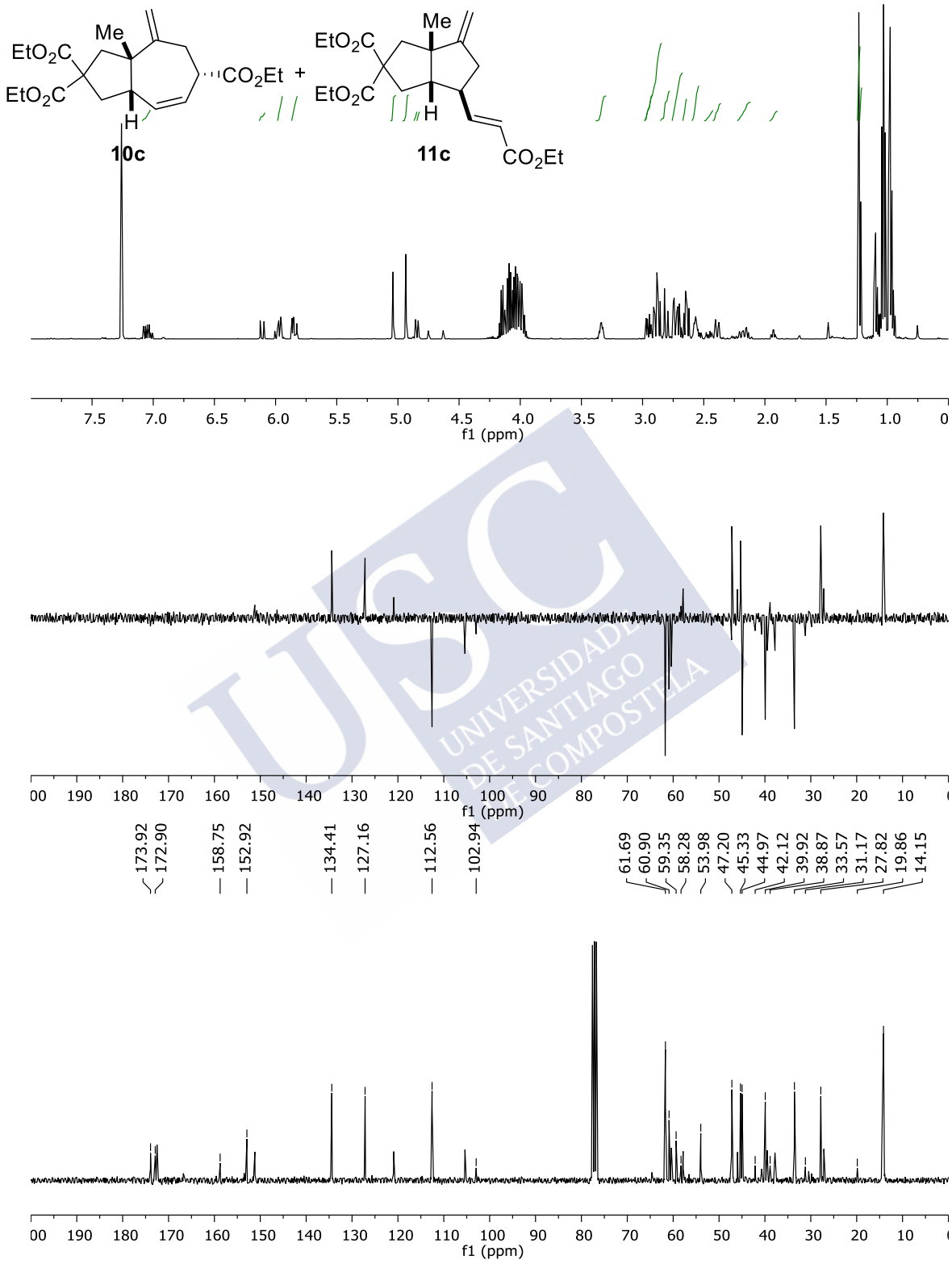
Me
EtO2C
EtO2C
CO2Et
H
10c
+
Me
EtO2C
EtO2C
H
11c
CO2Et
7.5 7.0 6.5 6.0 5.5 5.0 4.5 4.0 3.5 3.0 2.5 2.0 1.5 1.0 0
f1 (ppm)
00 190 180 170 160 150 140 130 120 110 100 90 80 70 60 50 40 30 20 10
f1 (ppm)
173.92
172.90
158.75
152.92
134.41
127.16
112.56
102.94
61.69
60.90
59.35
58.28
53.98
47.20
45.33
44.97
42.12
39.92
38.87
33.57
31.17
27.82
19.86
14.15
00 190 180 170 160 150 140 130 120 110 100 90 80 70 60 50 40 30 20 10
f1 (ppm)

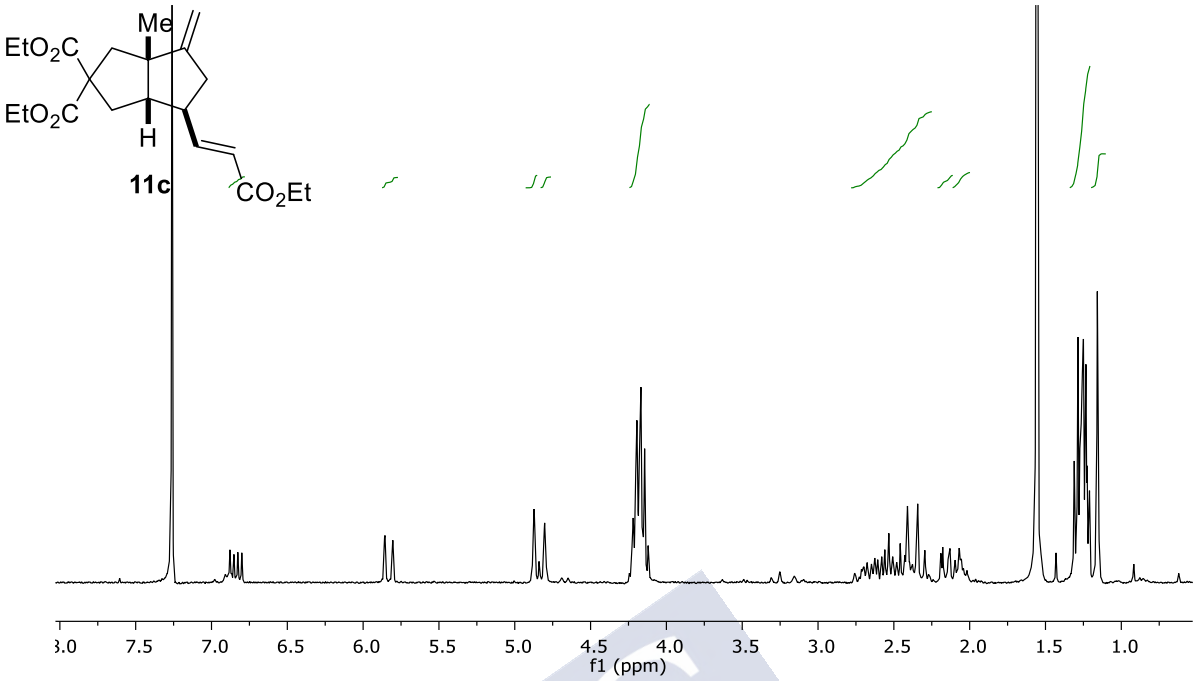

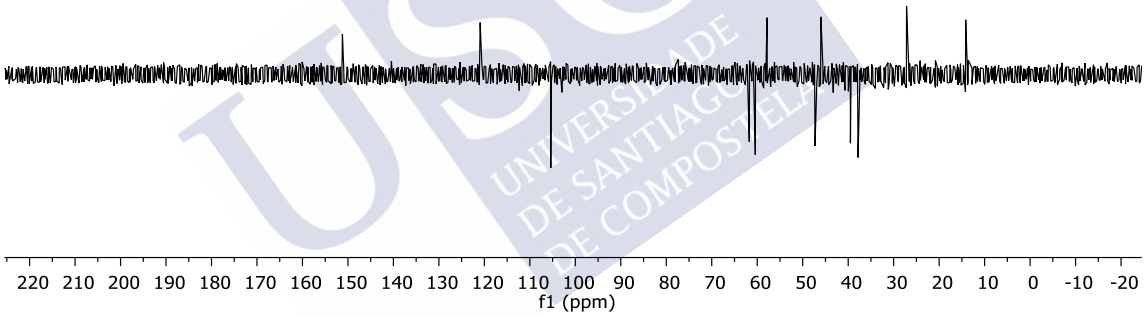

4c

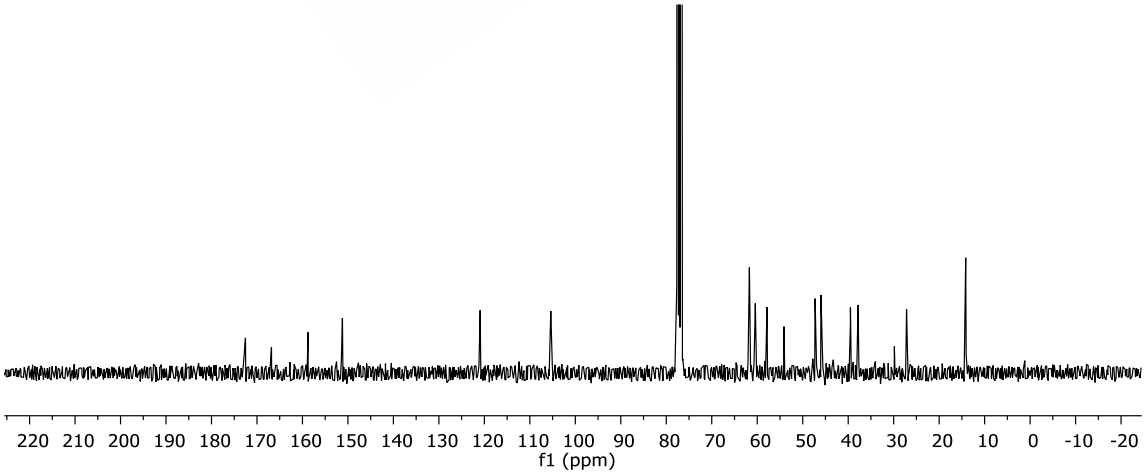

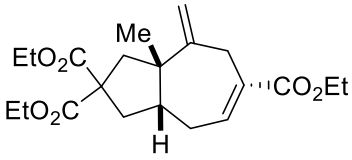

10c'

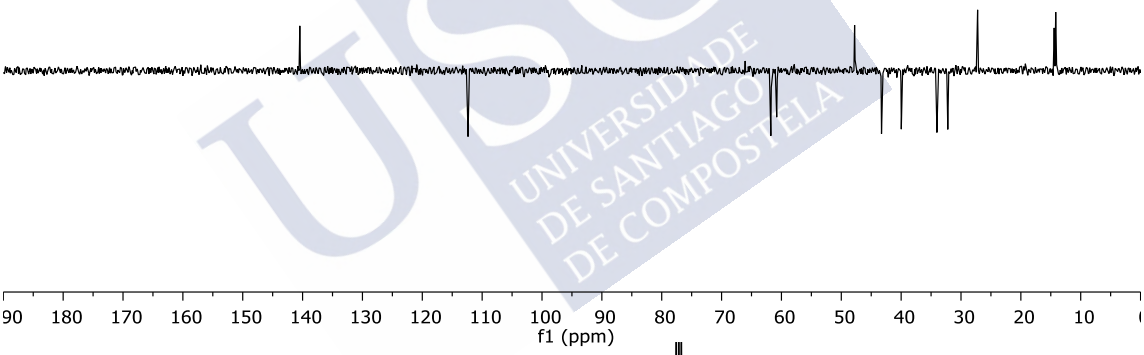

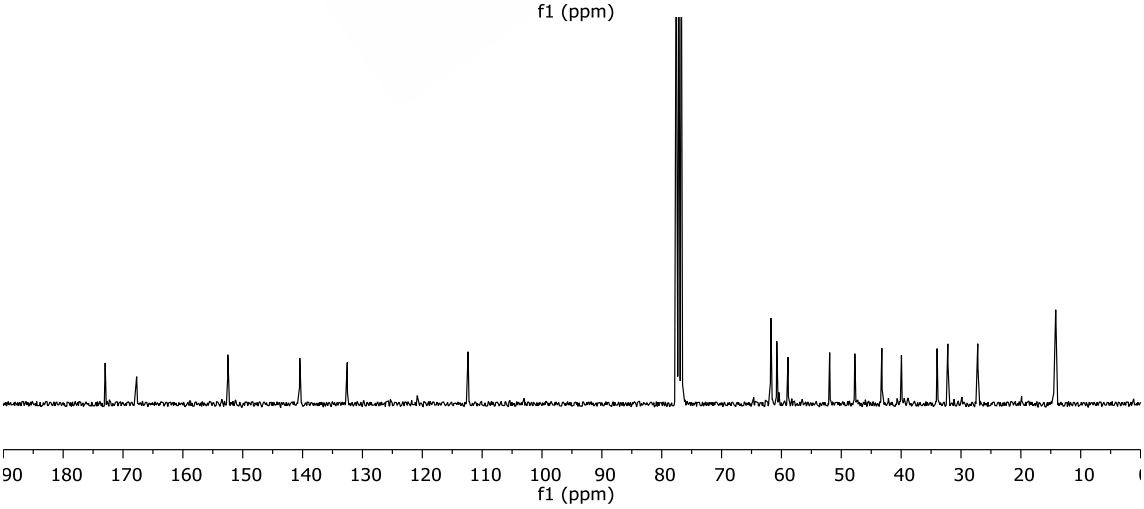

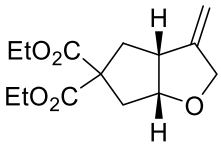
H
EtO2C
EtO2C
O
H

50a

7.5 7.0 6.5 6.0 5.5 5.0 4.5 4.0 3.5 3.0 2.5 2.0 1.5 1.0 0.5 0
f1 (ppm)

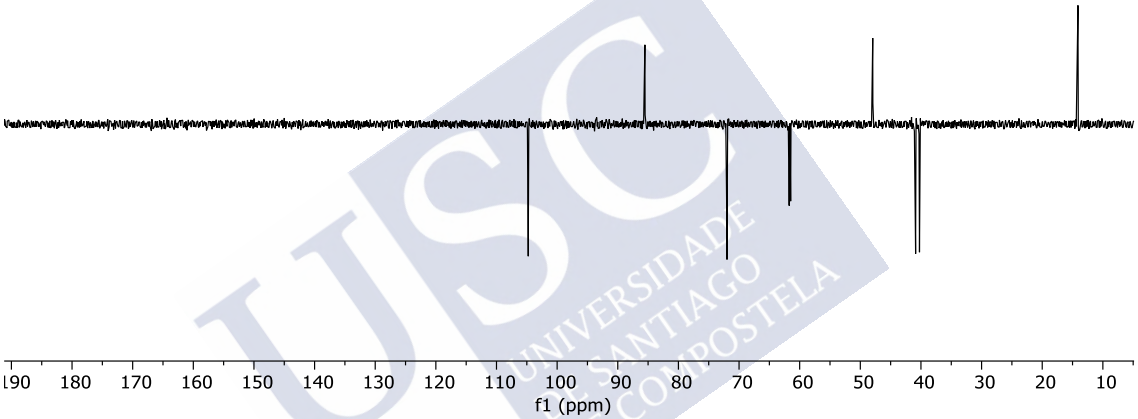
190 180 170 160 150 140 130 120 110 100 90 80 70 60 50 40 30 20 10
f1 (ppm)

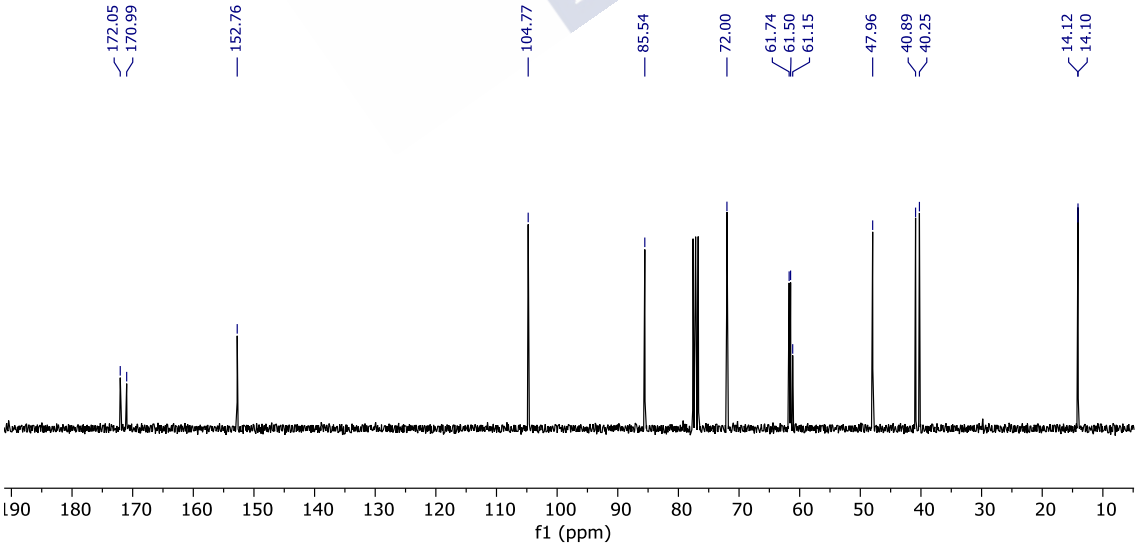
172.05
170.99
152.76
104.77
85.54
72.00
61.74
61.50
61.15
47.96
40.89
40.25
14.12
14.10
190 180 170 160 150 140 130 120 110 100 90 80 70 60 50 40 30 20 10
f1 (ppm)

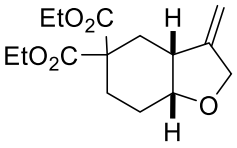
EtO2C
H
EtO2C
O
H

50b

7.5
7.0
6.5
6.0
5.5
5.0
4.5
4.0
3.5
3.0
2.5
2.0
1.5
1.0
0.
f1 (ppm)

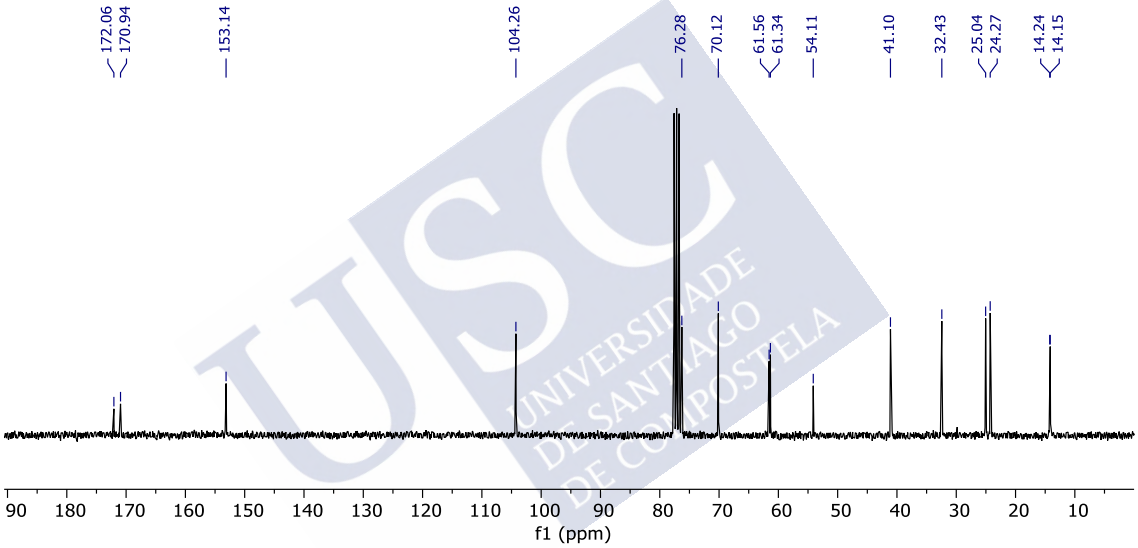
172.06
170.94
153.14
104.26
76.28
70.12
61.56
61.34
54.11
41.10
32.43
25.04
24.27
14.24
14.15
90
180
170
160
150
140
130
120
110
100
90
80
70
60
50
40
30
20
10
f1 (ppm)

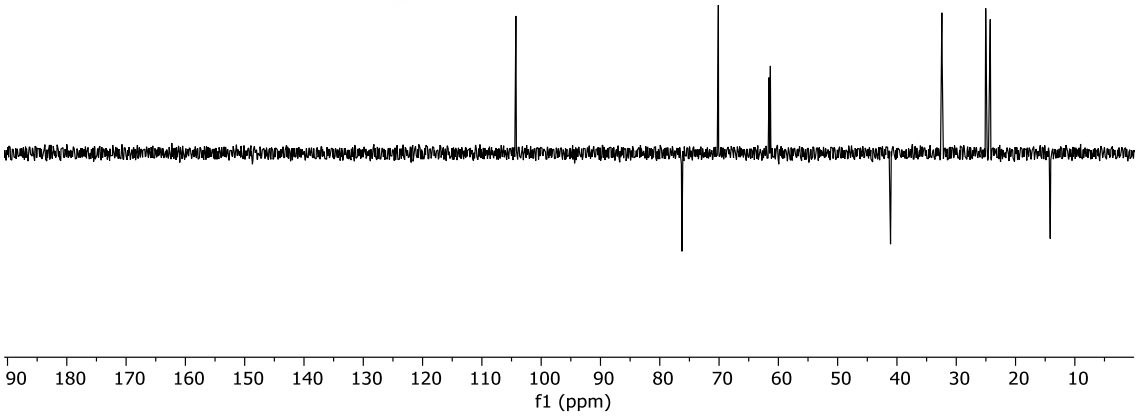
90
180
170
160
150
140
130
120
110
100
90
80
70
60
50
40
30
20
10
f1 (ppm)

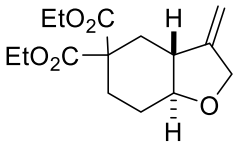
EtO2C
EtO2C
H
O
H

50b`

7.5
7.0
6.5
6.0
5.5
5.0
4.5
4.0
3.5
3.0
2.5
2.0
1.5
1.0
f1 (ppm)

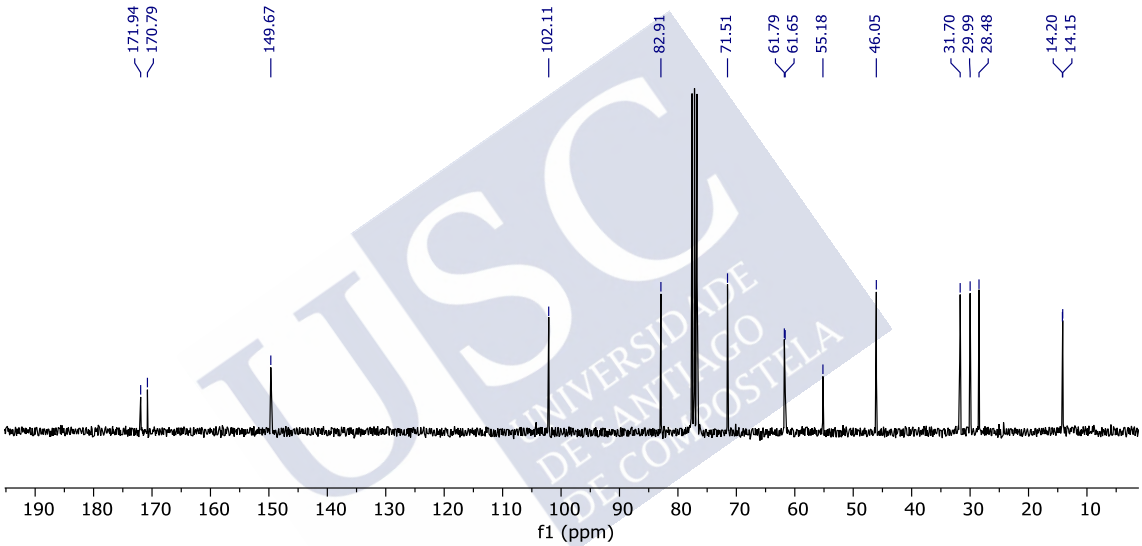
171.94
170.79
149.67
102.11
82.91
71.51
61.79
61.65
55.18
46.05
31.70
29.99
28.48
14.20
14.15
190
180
170
160
150
140
130
120
110
100
90
80
70
60
50
40
30
20
10
f1 (ppm)

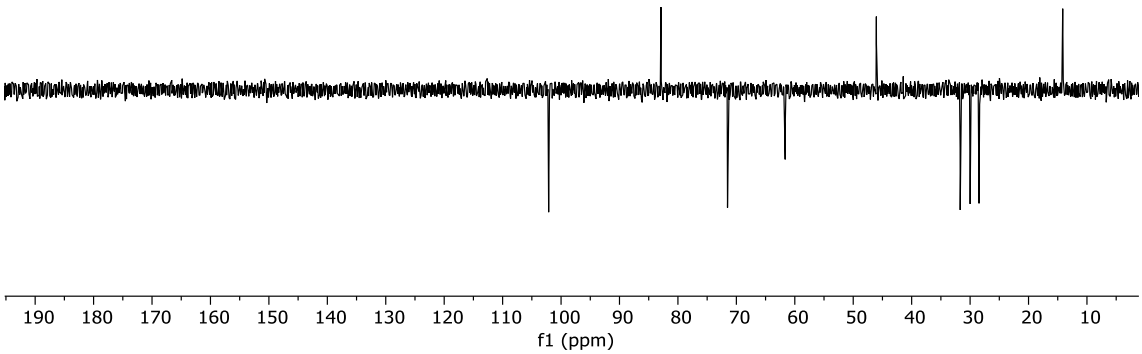
190
180
170
160
150
140
130
120
110
100
90
80
70
60
50
40
30
20
10
f1 (ppm)

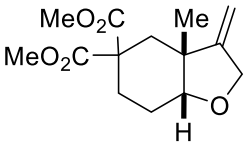
MeO2C
Me
MeO2C
O
H

50c

7.5 7.0 6.5 6.0 5.5 5.0 4.5 4.0 3.5 3.0 2.5 2.0 1.5 1.0 0.5
f1 (ppm)

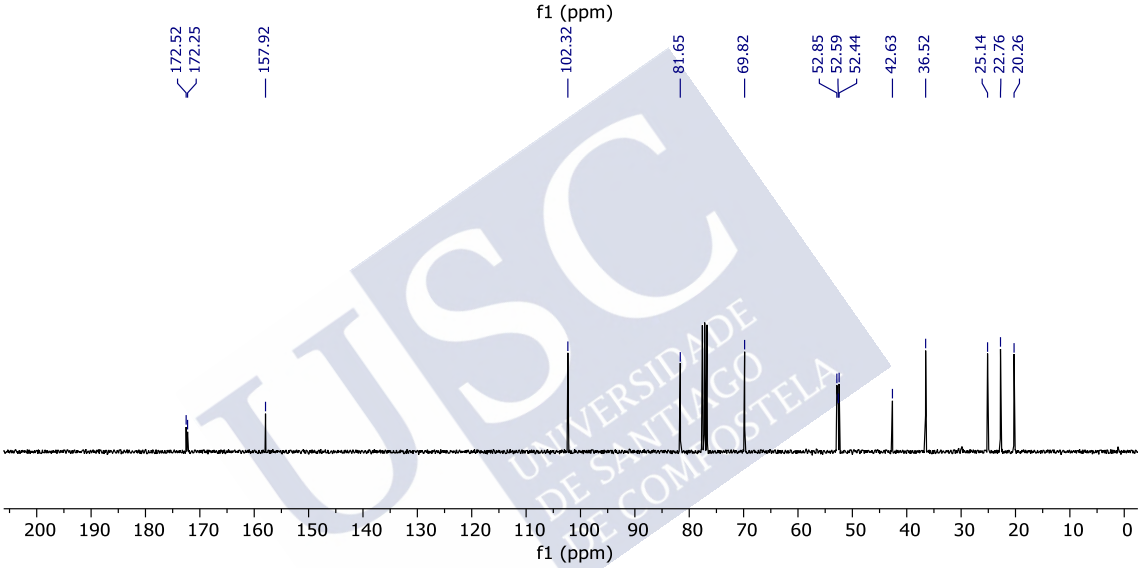
172.52
172.25
157.92
102.32
81.65
69.82
52.85
52.59
52.44
42.63
36.52
25.14
22.76
20.26
200 190 180 170 160 150 140 130 120 110 100 90 80 70 60 50 40 30 20 10 0
f1 (ppm)

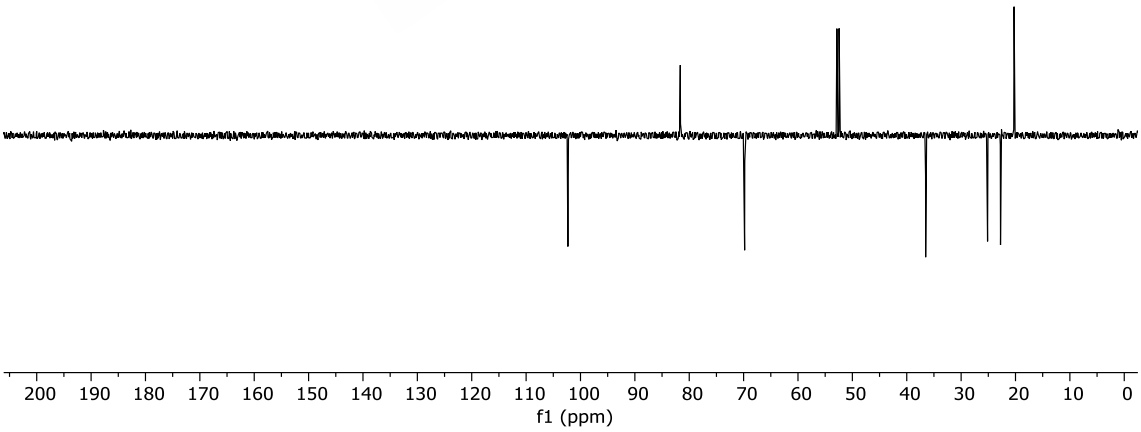
200 190 180 170 160 150 140 130 120 110 100 90 80 70 60 50 40 30 20 10 0
f1 (ppm)

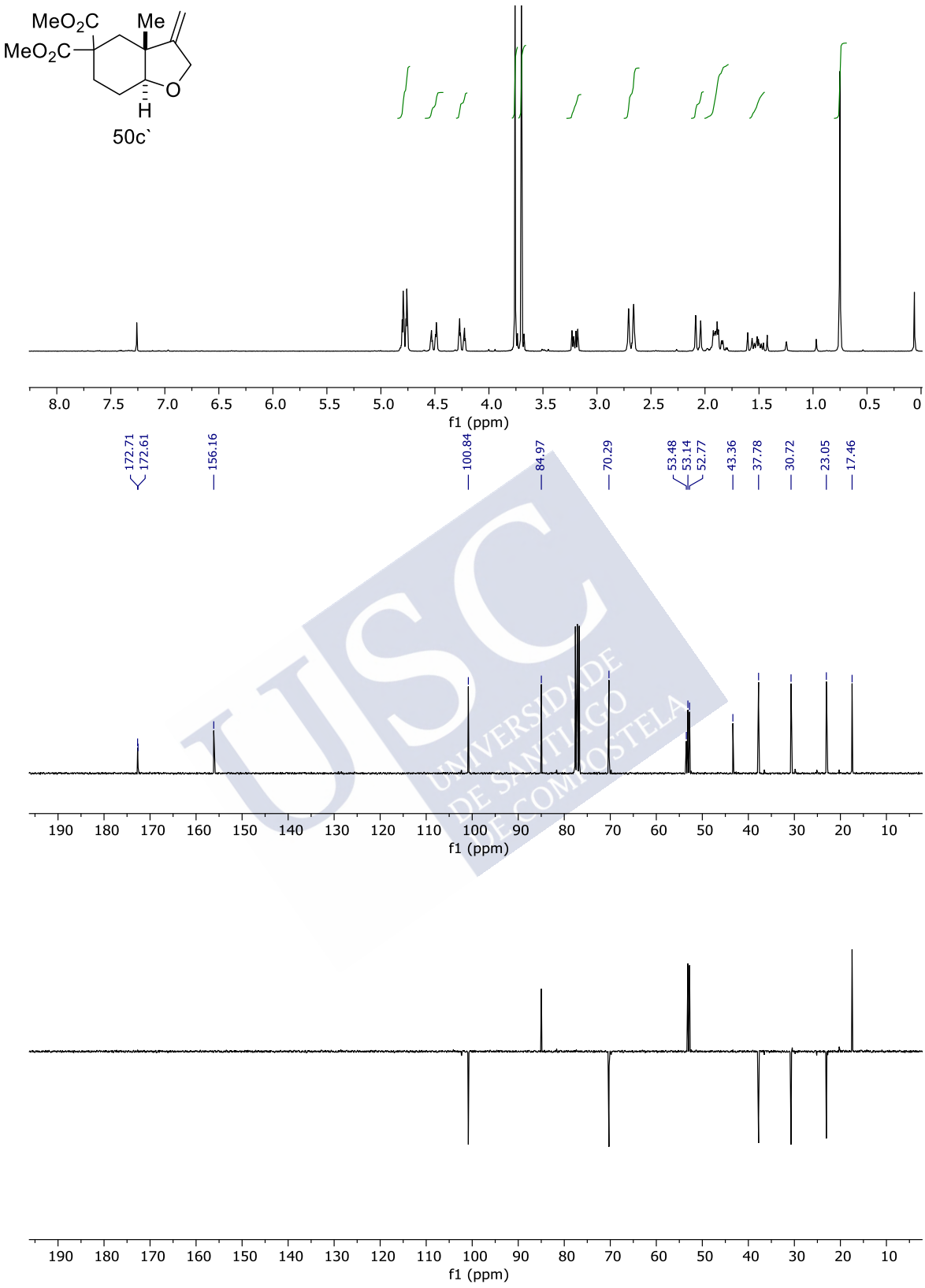
MeO2C
Me
MeO2C
O
H
50c`
f1 (ppm)
172.71
172.61
156.16
100.84
84.97
70.29
53.48
53.14
52.77
43.36
37.78
30.72
23.05
17.46
f1 (ppm)
f1 (ppm)

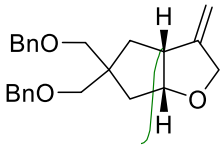
BnO
BnO
H
O
H

50d

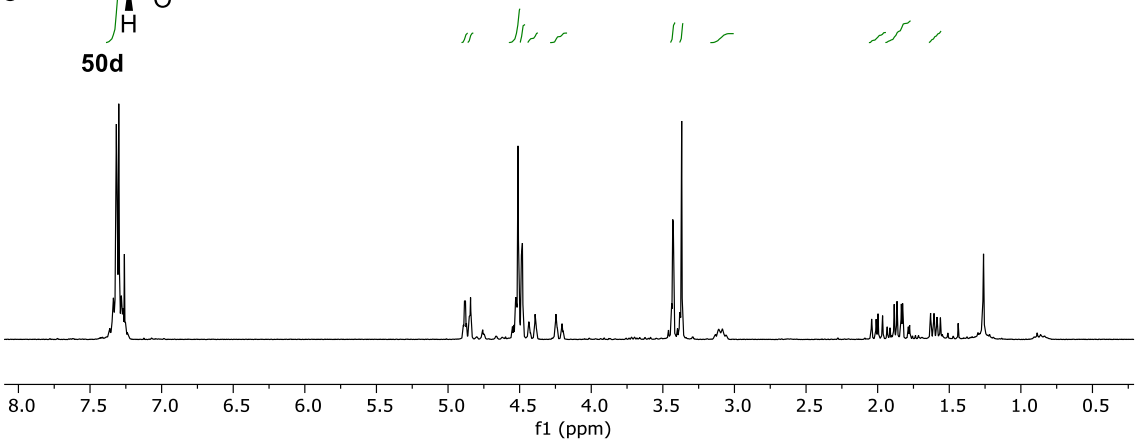
8.0
7.5
7.0
6.5
6.0
5.5
5.0
4.5
4.0
3.5
3.0
2.5
2.0
1.5
1.0
0.5
f1 (ppm)

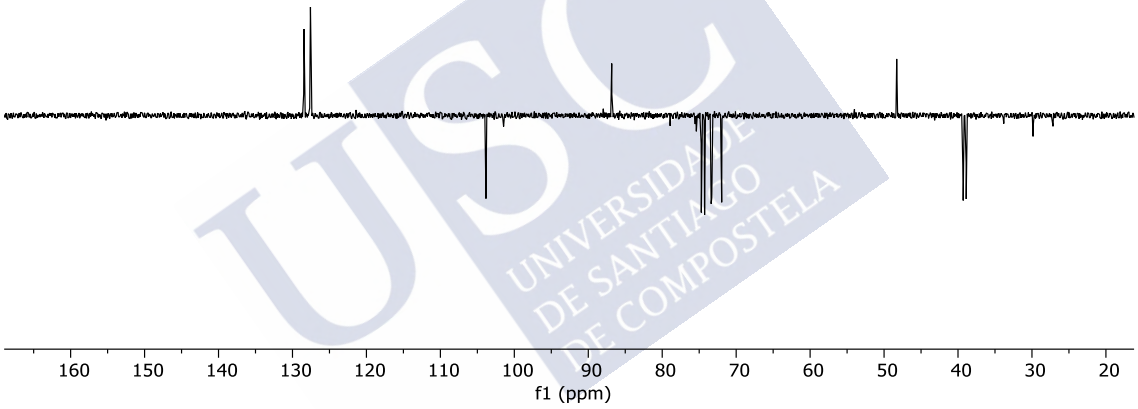
160
150
140
130
120
110
100
90
80
70
60
50
40
30
20
f1 (ppm)


153.87
139.02
138.96
128.47
128.44
128.37
127.61
127.57
127.54
127.52
127.46
103.83
86.83
74.71
74.27
73.39
73.29
71.96
50.34
48.29
39.29
38.89

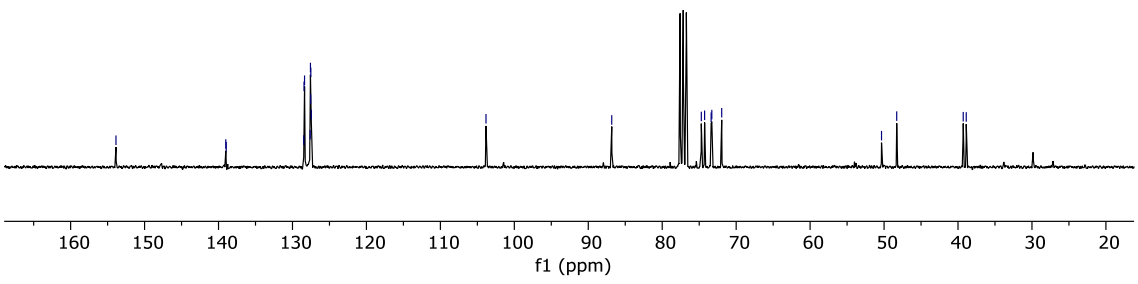
160
150
140
130
120
110
100
90
80
70
60
50
40
30
20
f1 (ppm)

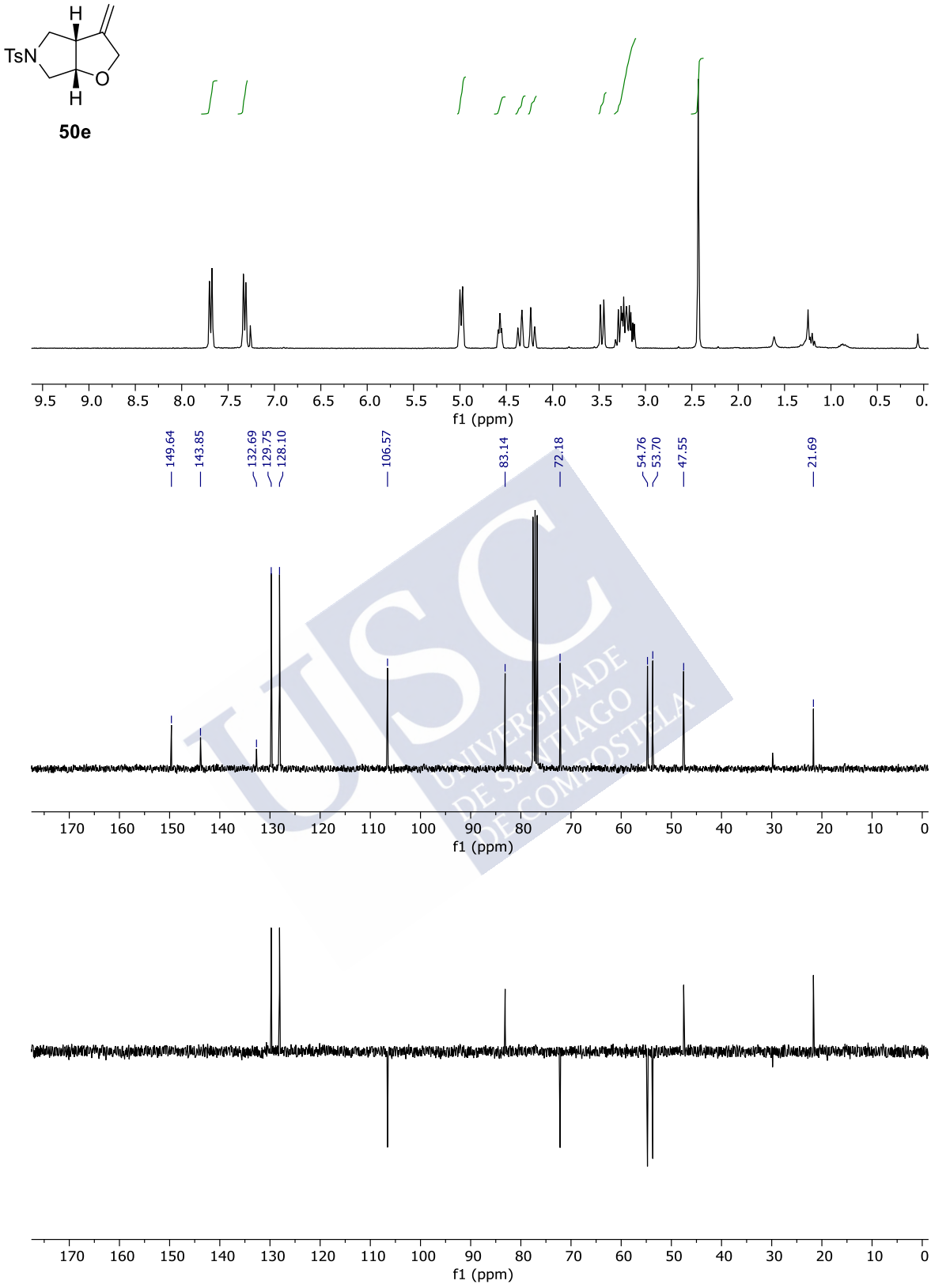
H
TsN
O
H
50e
f1 (ppm)
149.64
143.85
132.69
129.75
128.10
106.57
83.14
72.18
54.76
53.70
47.55
21.69
f1 (ppm)
f1 (ppm)

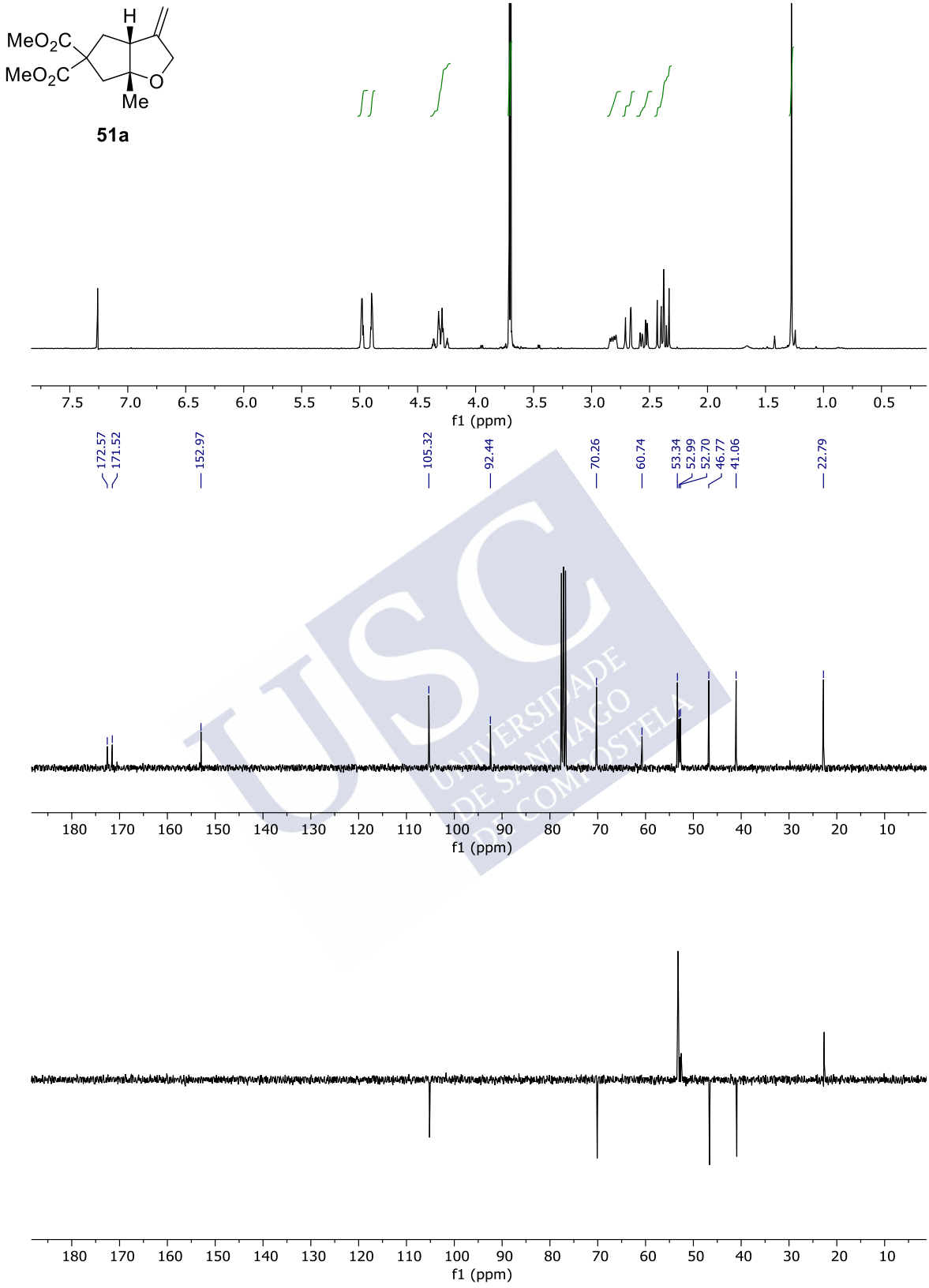
MeO2C
MeO2C
H
O
Me
51a
f1 (ppm)
172.57
171.52
152.97
105.32
92.44
70.26
60.74
53.34
52.99
52.70
46.77
41.06
22.79

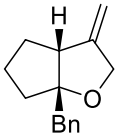
H
O
Bn

51b

8.0
7.5
7.0
6.5
6.0
5.5
5.0
4.5
4.0
3.5
3.0
2.5
2.0
1.5
1.0
0.5
f1 (ppm)

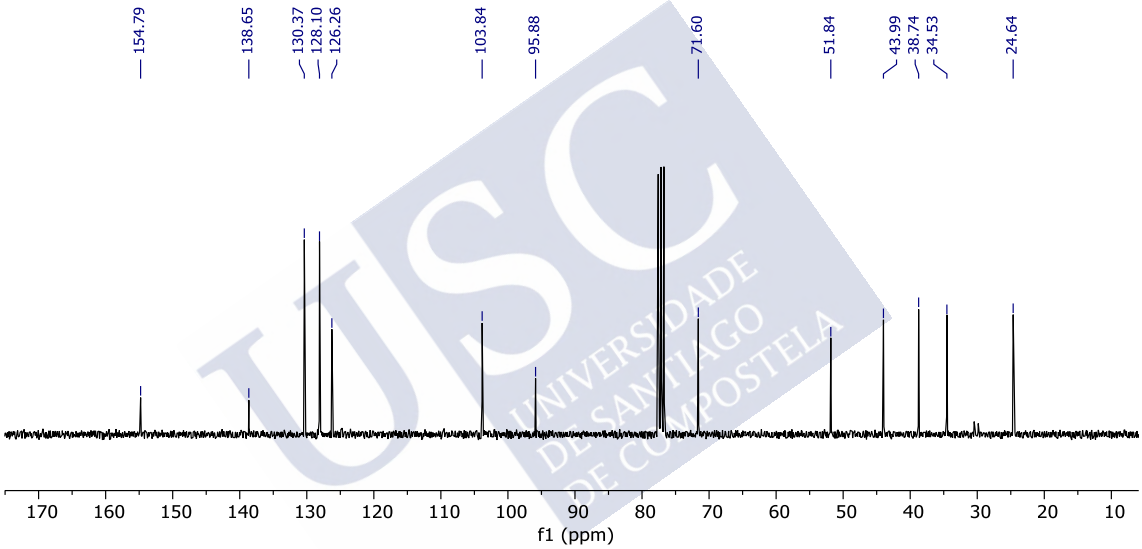
154.79
138.65
130.37
128.10
126.26
103.84
95.88
71.60
51.84
43.99
38.74
34.53
24.64
170
160
150
140
130
120
110
100
90
80
70
60
50
40
30
20
10
f1 (ppm)

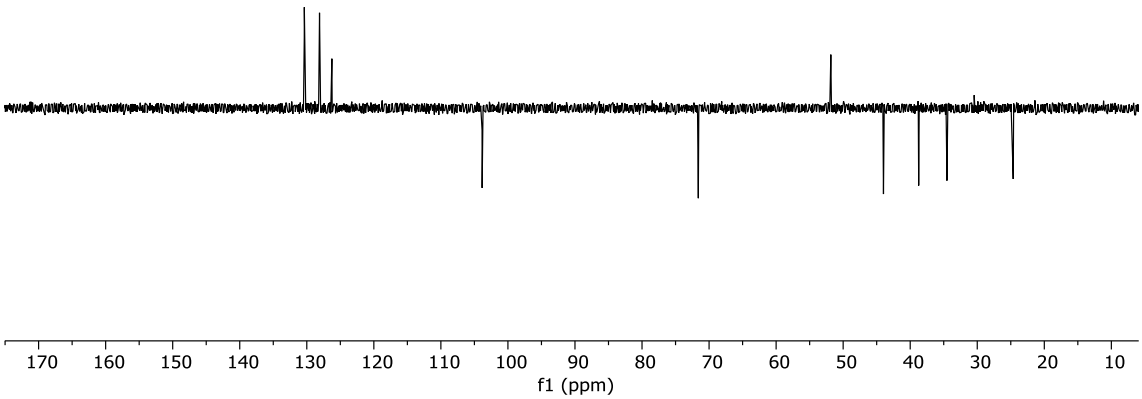
170
160
150
140
130
120
110
100
90
80
70
60
50
40
30
20
10
f1 (ppm)

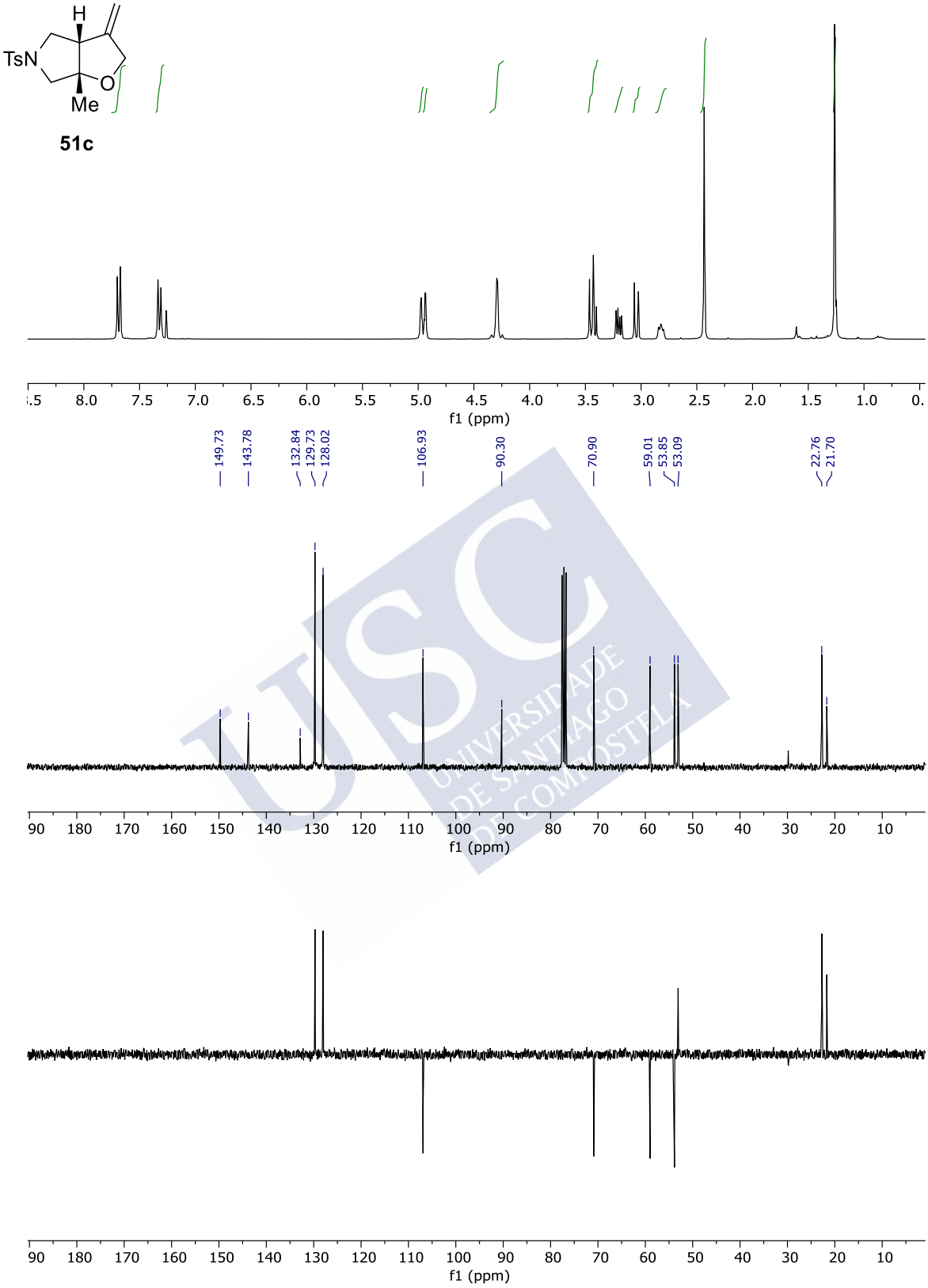
H
TsN
O
Me
51c
f1 (ppm)
149.73
143.78
132.84
129.73
128.02
106.93
90.30
70.90
59.01
53.85
53.09
22.76
21.70
f1 (ppm)
f1 (ppm)

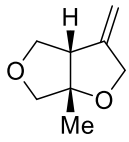
H
O
O
Me

51d

6.5
6.0
5.5
5.0
4.5
4.0
3.5
3.0
2.5
2.0
1.5
1.0
0.5
f1 (ppm)

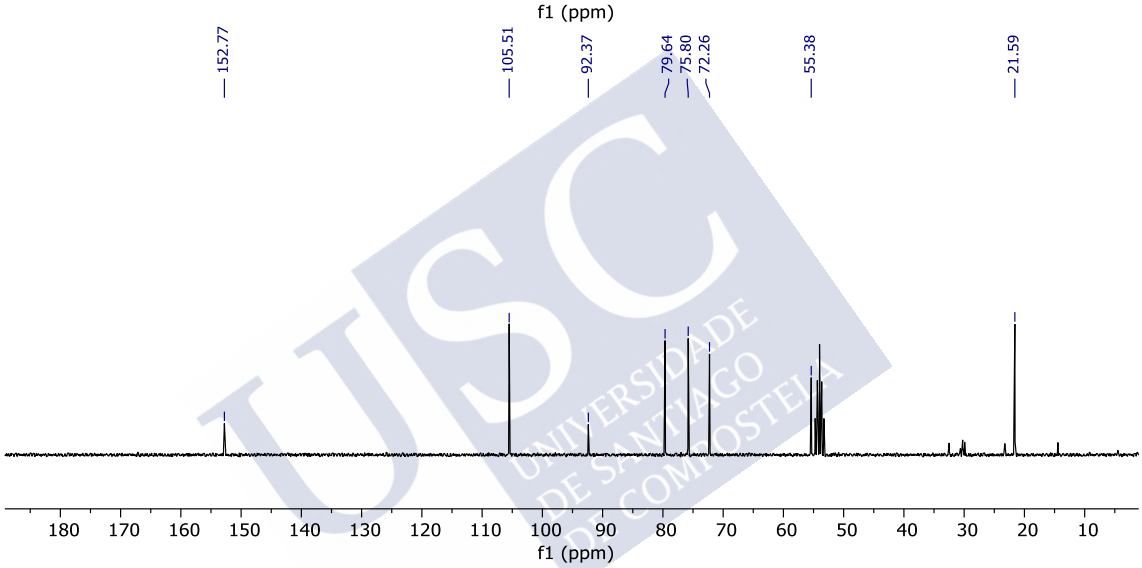
152.77
105.51
92.37
79.64
75.80
72.26
55.38
21.59
180
170
160
150
140
130
120
110
100
90
80
70
60
50
40
30
20
10
f1 (ppm)

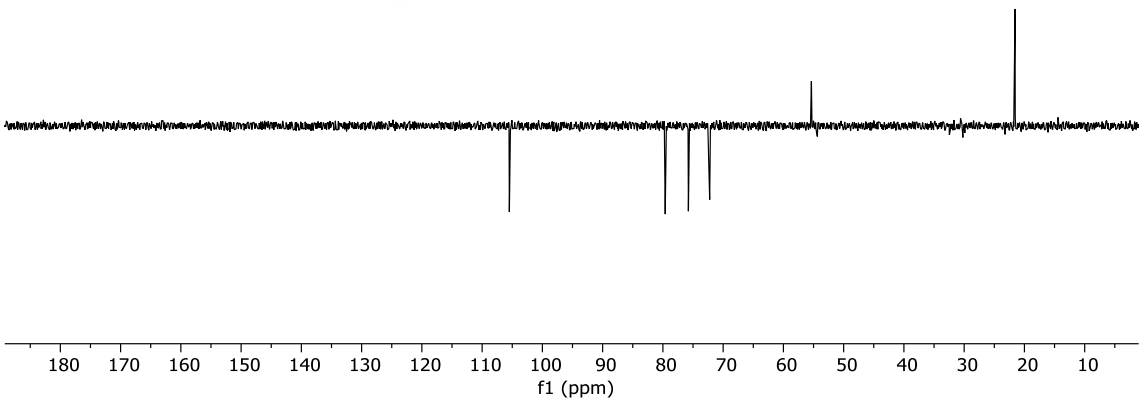
180
170
160
150
140
130
120
110
100
90
80
70
60
50
40
30
20
10
f1 (ppm)

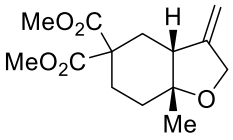
MeO2C
MeO2C
H
O
Me

51e

7.5 7.0 6.5 6.0 5.5 5.0 4.5 4.0 3.5 3.0 2.5 2.0 1.5 1.0 0.5
f1 (ppm)

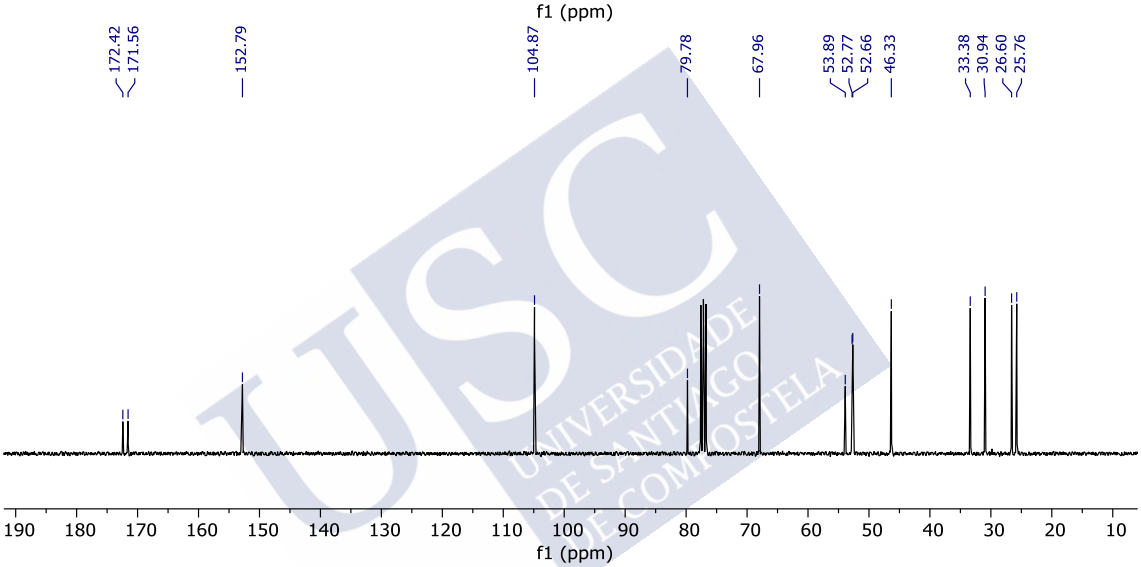
172.42
171.56
152.79
104.87
79.78
67.96
53.89
52.77
52.66
46.33
33.38
30.94
26.60
25.76
190 180 170 160 150 140 130 120 110 100 90 80 70 60 50 40 30 20 10
f1 (ppm)

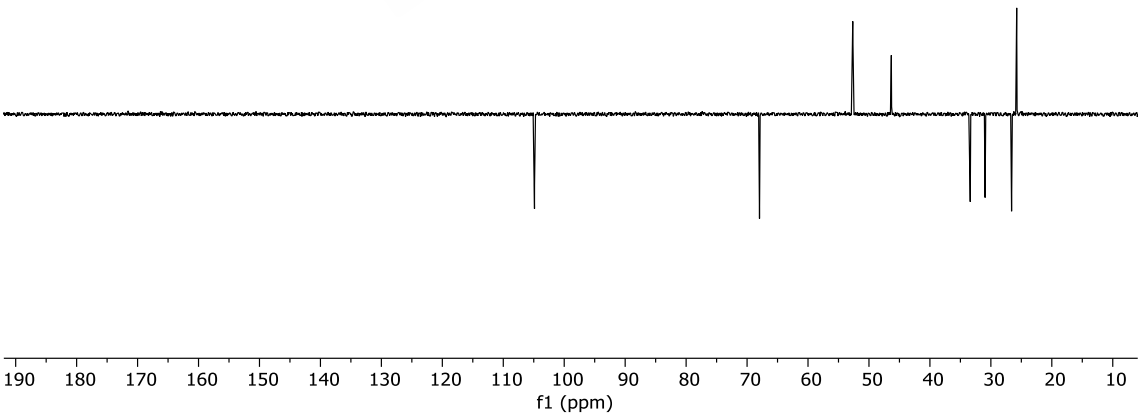
190 180 170 160 150 140 130 120 110 100 90 80 70 60 50 40 30 20 10
f1 (ppm)

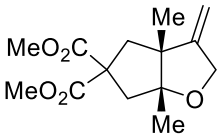
Me
MeO2C
MeO2C
O
Me

51f

7.5 7.0 6.5 6.0 5.5 5.0 4.5 4.0 3.5 3.0 2.5 2.0 1.5 1.0 0.5
f1 (ppm)

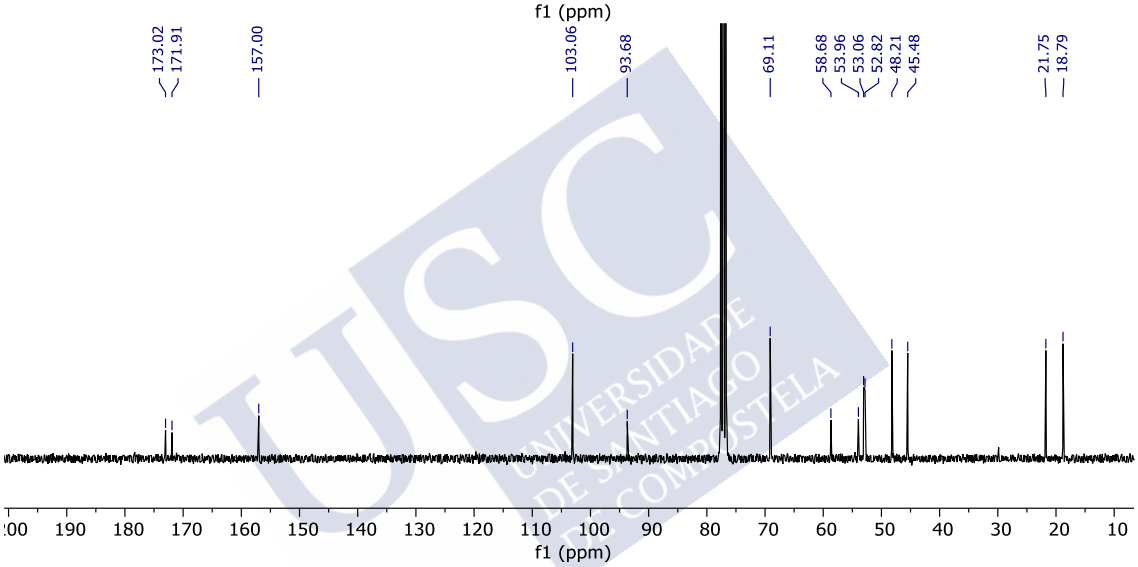
173.02
171.91
157.00
103.06
93.68
69.11
58.68
53.96
53.06
52.82
48.21
45.48
21.75
18.79
190 180 170 160 150 140 130 120 110 100 90 80 70 60 50 40 30 20 10
f1 (ppm)

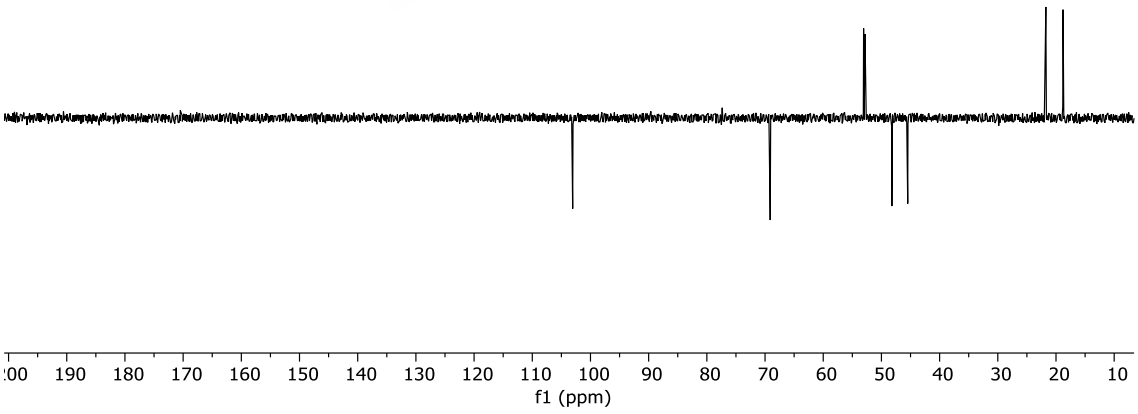
190 180 170 160 150 140 130 120 110 100 90 80 70 60 50 40 30 20 10
f1 (ppm)

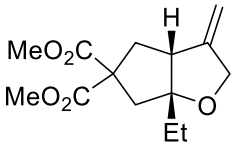
H
MeO2C
MeO2C
O
Et

51g

8.0 7.5 7.0 6.5 6.0 5.5 5.0 4.5 4.0 3.5 3.0 2.5 2.0 1.5 1.0 0.5 0
f1 (ppm)

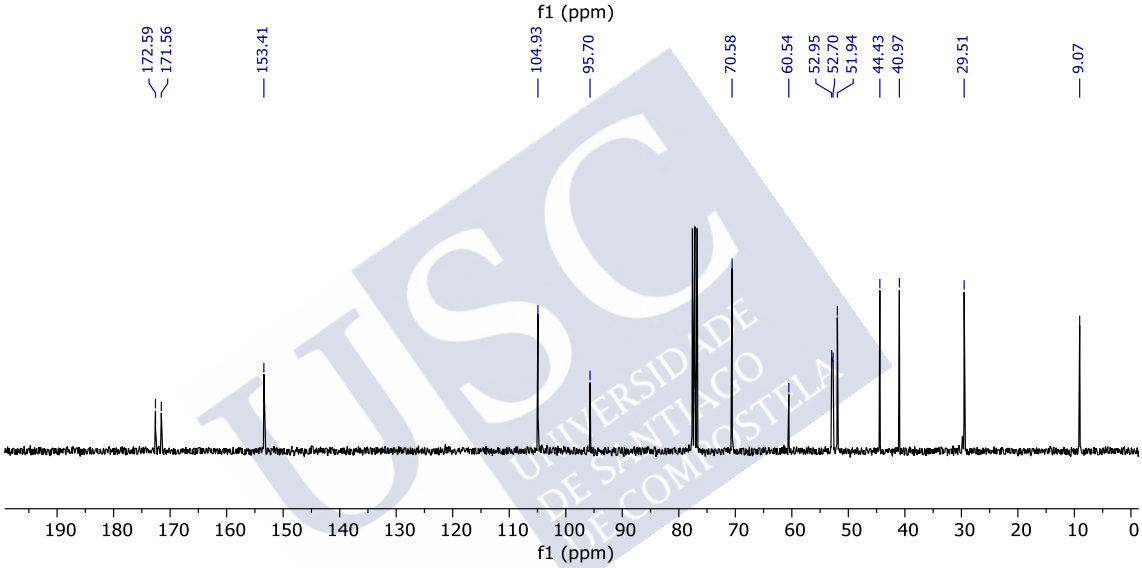
172.59
171.56
153.41
104.93
95.70
70.58
60.54
52.95
52.70
51.94
44.43
40.97
29.51
9.07
190 180 170 160 150 140 130 120 110 100 90 80 70 60 50 40 30 20 10 0
f1 (ppm)

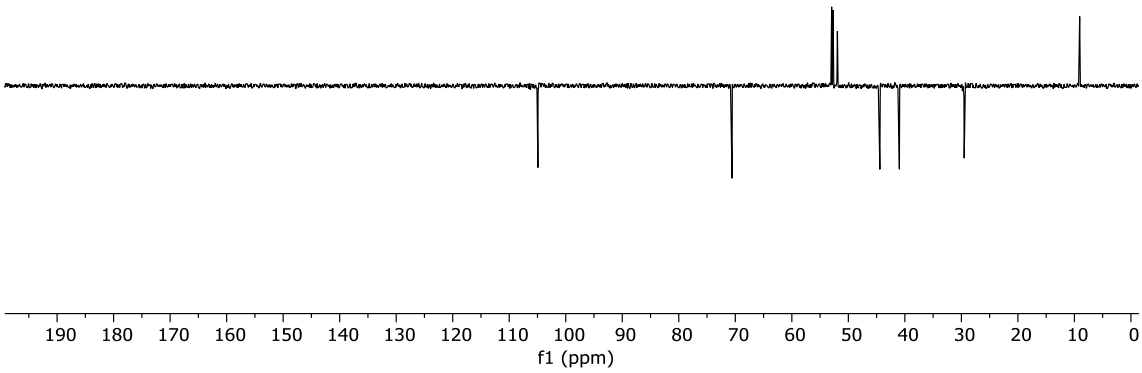
190 180 170 160 150 140 130 120 110 100 90 80 70 60 50 40 30 20 10 0
f1 (ppm)

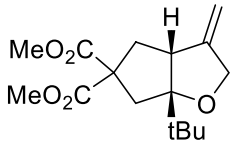
H
MeO2C
MeO2C
O
tBu

51h

7.5 7.0 6.5 6.0 5.5 5.0 4.5 4.0 3.5 3.0 2.5 2.0 1.5 1.0 0.5
f1 (ppm)

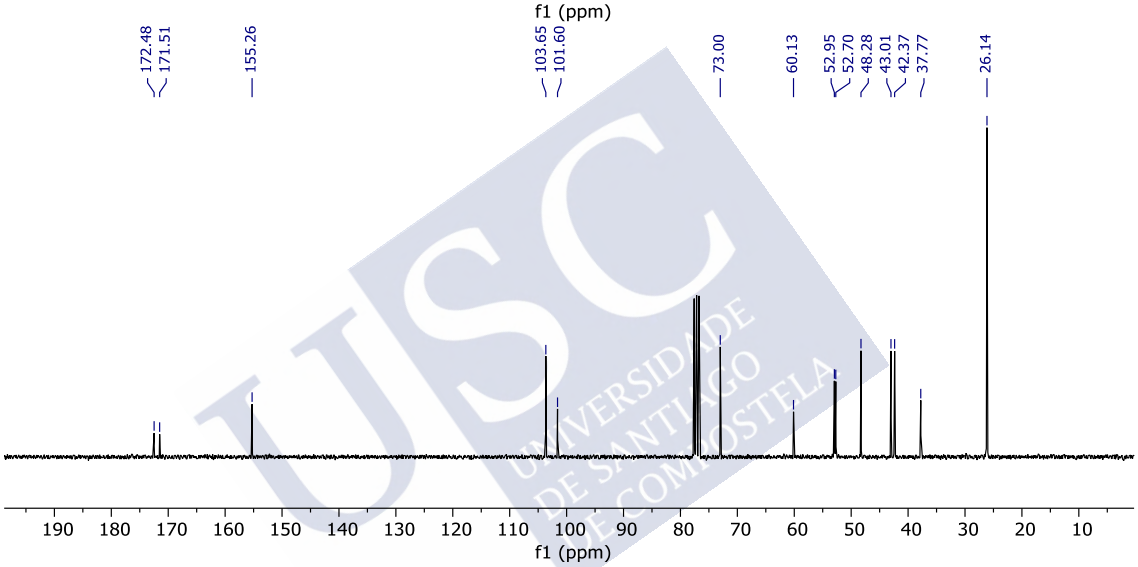
172.48
171.51
155.26
103.65
101.60
73.00
60.13
52.95
52.70
48.28
43.01
42.37
37.77
26.14
190 180 170 160 150 140 130 120 110 100 90 80 70 60 50 40 30 20 10
f1 (ppm)

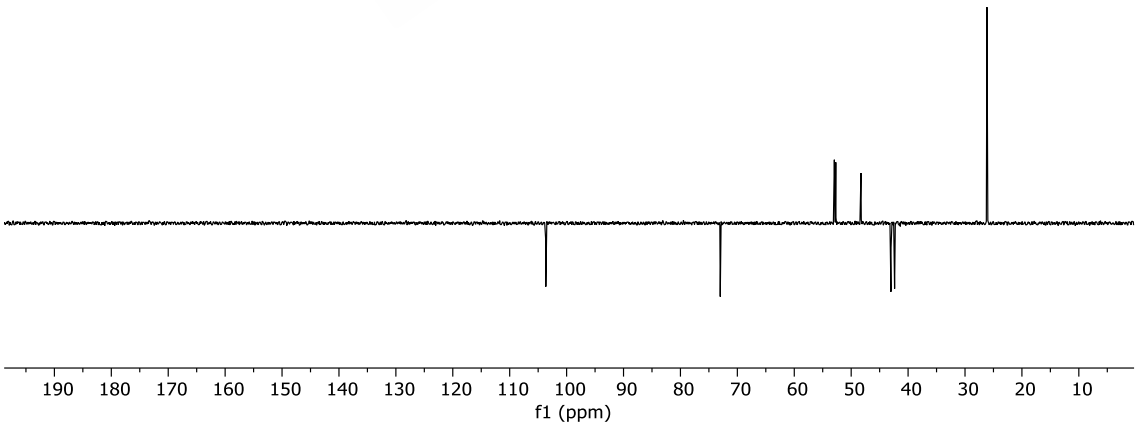
190 180 170 160 150 140 130 120 110 100 90 80 70 60 50 40 30 20 10
f1 (ppm)

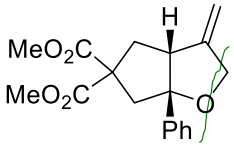
H
MeO2C
MeO2C
O
Ph

51i

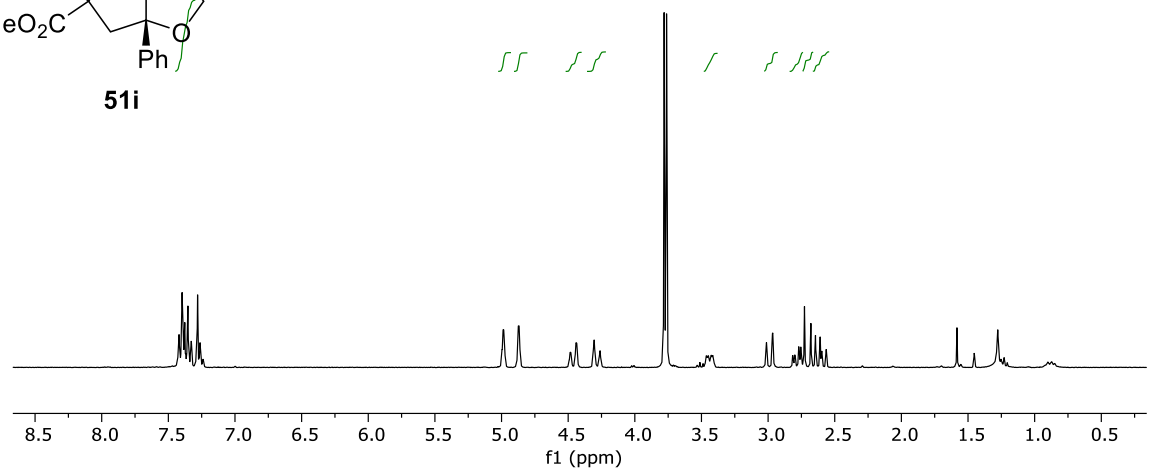
8.5
8.0
7.5
7.0
6.5
6.0
5.5
5.0
4.5
4.0
3.5
3.0
2.5
2.0
1.5
1.0
0.5
f1 (ppm)

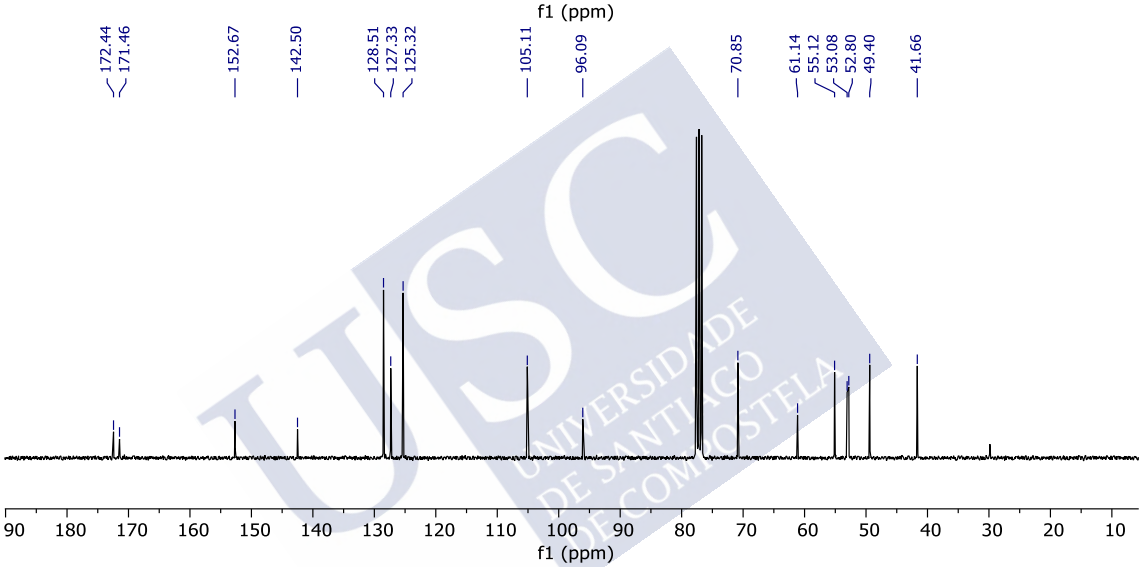
172.44
171.46
152.67
142.50
128.51
127.33
125.32
105.11
96.09
70.85
61.14
55.12
53.08
52.80
49.40
41.66
90
180
170
160
150
140
130
120
110
100
90
80
70
60
50
40
30
20
10
f1 (ppm)

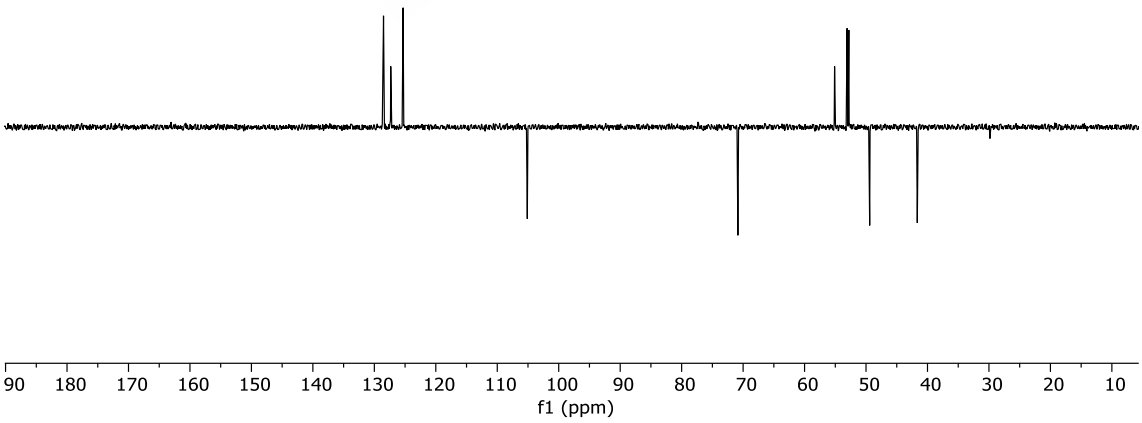
90
180
170
160
150
140
130
120
110
100
90
80
70
60
50
40
30
20
10
f1 (ppm)

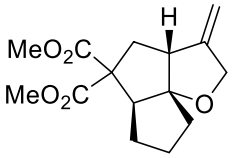
H
MeO2C
MeO2C
O

51j

7.5 7.0 6.5 6.0 5.5 5.0 4.5 4.0 3.5 3.0 2.5 2.0 1.5 1.0 0.5
f1 (ppm)

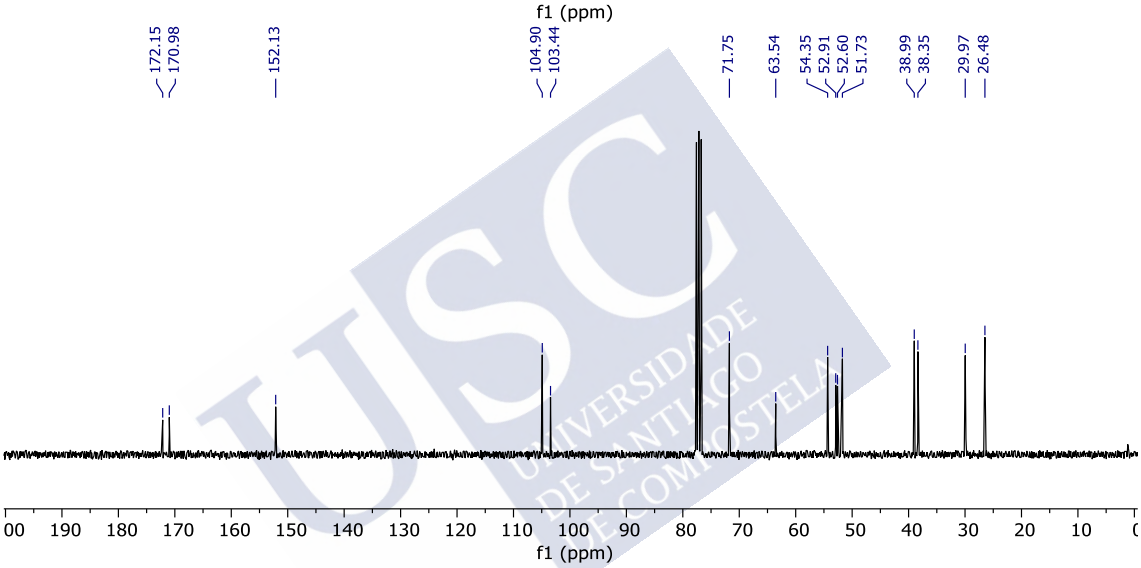
172.15
170.98
152.13
104.90
103.44
71.75
63.54
54.35
52.91
52.60
51.73
38.99
38.35
29.97
26.48
00 190 180 170 160 150 140 130 120 110 100 90 80 70 60 50 40 30 20 10 0
f1 (ppm)

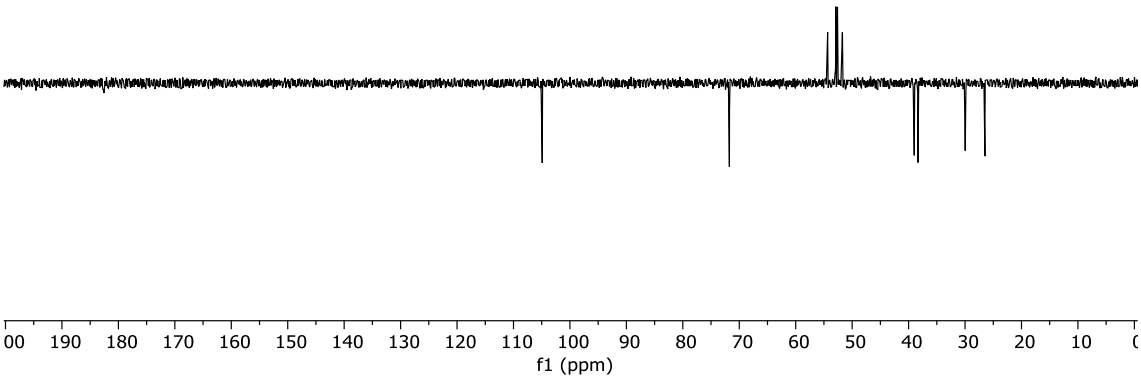
00 190 180 170 160 150 140 130 120 110 100 90 80 70 60 50 40 30 20 10 0
f1 (ppm)

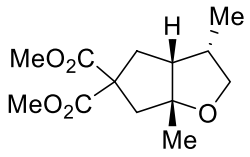
H
Me
MeO2C
MeO2C
O
Me

60a

8.0
7.5
7.0
6.5
6.0
5.5
5.0
4.5
4.0
3.5
3.0
2.5
2.0
1.5
1.0
0.5
f1 (ppm)

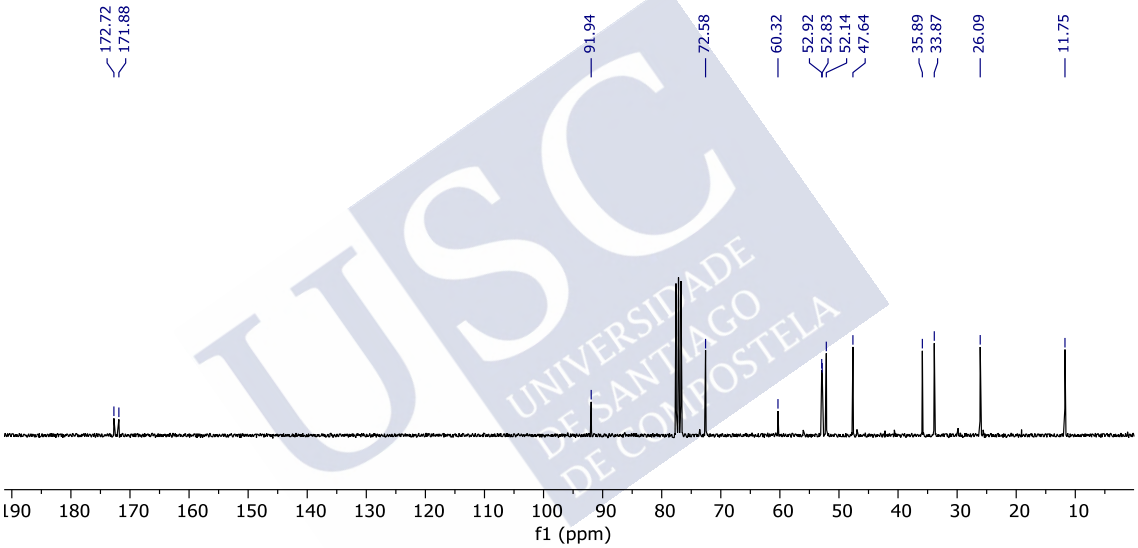
172.72
171.88
91.94
72.58
60.32
52.92
52.83
52.14
47.64
35.89
33.87
26.09
11.75
190
180
170
160
150
140
130
120
110
100
90
80
70
60
50
40
30
20
10
f1 (ppm)

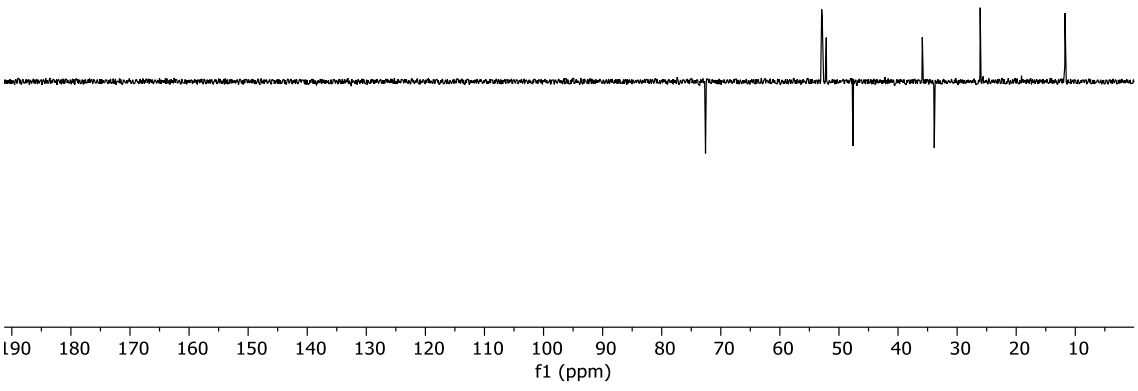
190
180
170
160
150
140
130
120
110
100
90
80
70
60
50
40
30
20
10
f1 (ppm)

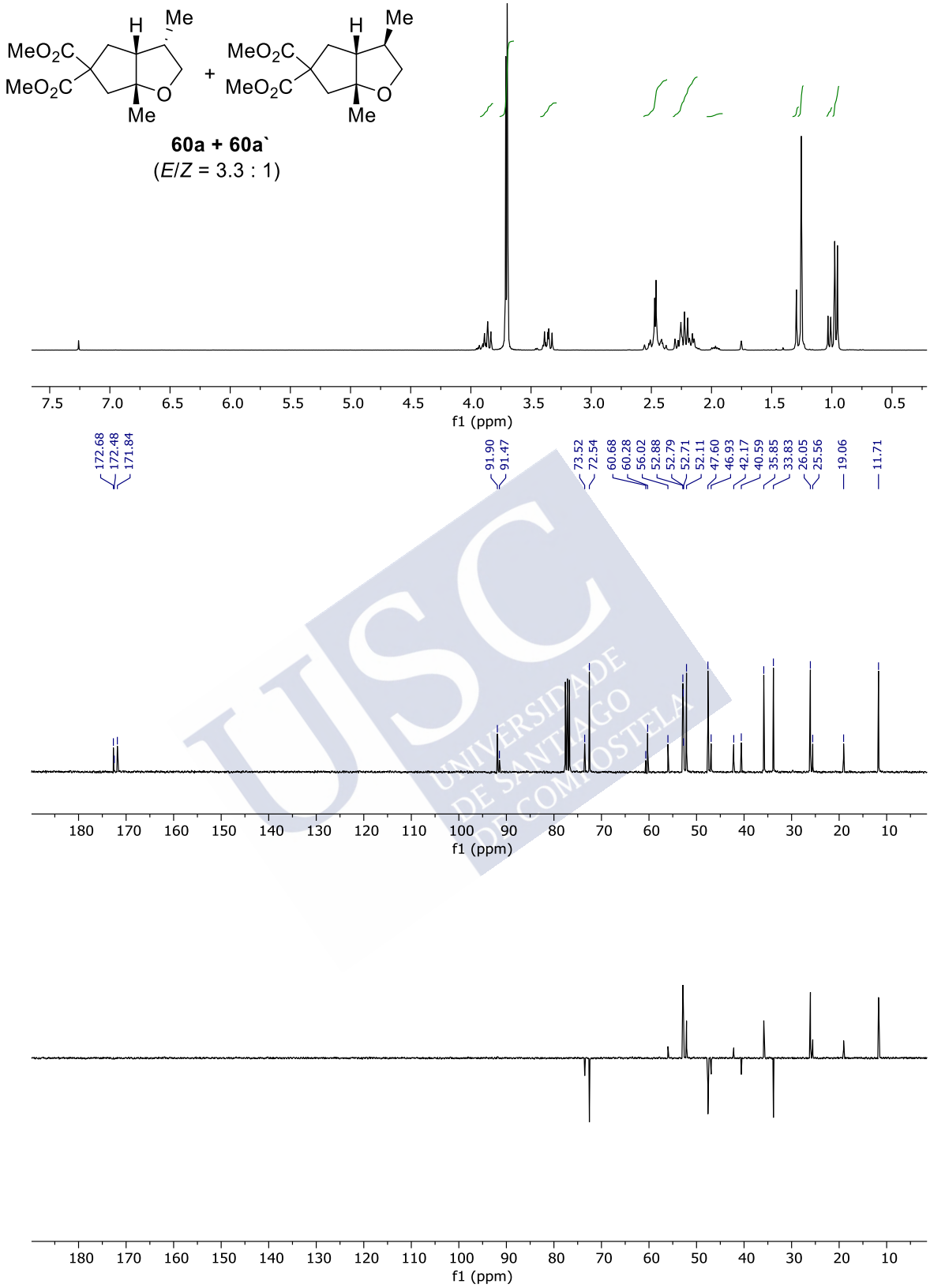
MeO2C
MeO2C
H
Me
O
Me
+
MeO2C
MeO2C
H
Me
O
Me
60a + 60a`
(E/Z = 3.3 : 1)
f1 (ppm)
172.68
172.48
171.84
91.90
91.47
73.52
72.54
60.68
60.28
56.02
52.88
52.79
52.71
52.11
47.60
46.93
42.17
40.59
35.85
33.83
26.05
25.56
19.06
11.71
f1 (ppm)
f1 (ppm)

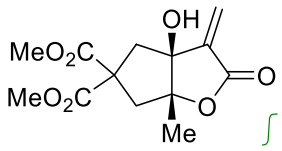
OH
MeO2C
MeO2C
O
O
Me

61a

7.5
7.0
6.5
6.0
5.5
5.0
4.5
4.0
3.5
3.0
2.5
2.0
1.5
1.0
f1 (ppm)

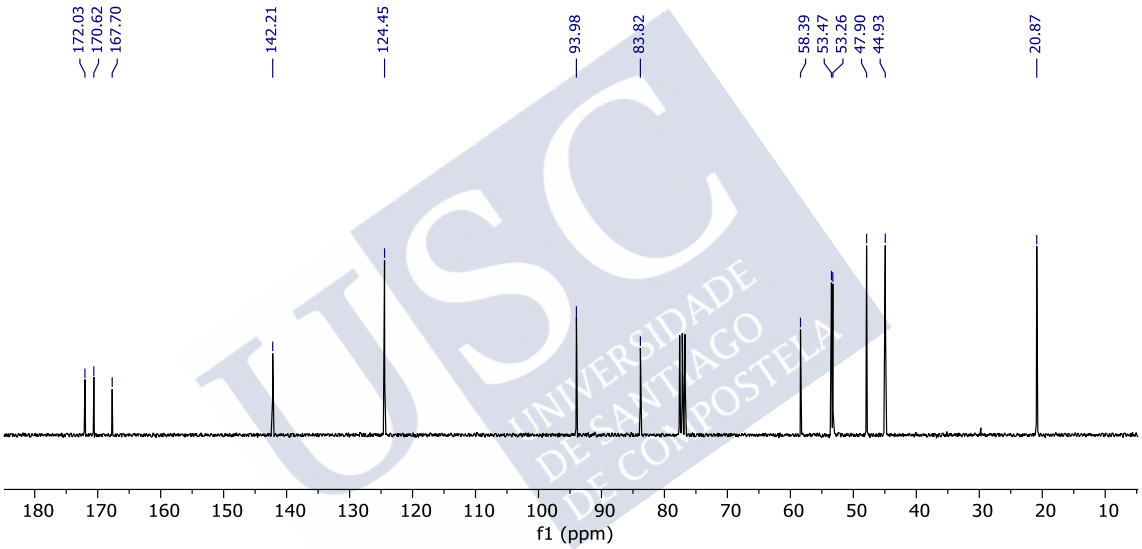
172.03
170.62
167.70
142.21
124.45
93.98
83.82
58.39
53.47
53.26
47.90
44.93
20.87
180
170
160
150
140
130
120
110
100
90
80
70
60
50
40
30
20
10
f1 (ppm)

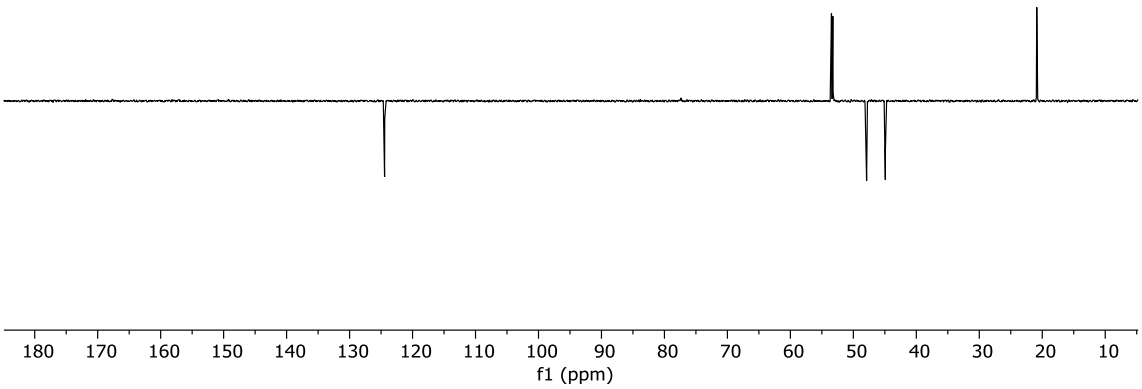
180
170
160
150
140
130
120
110
100
90
80
70
60
50
40
30
20
10
f1 (ppm)

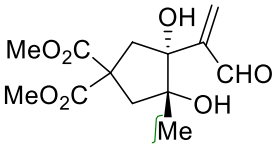
OH
MeO2C
CHO
MeO2C
OH
Me

61a`

10.5 10.0 9.5 9.0 8.5 8.0 7.5 7.0 6.5 6.0 5.5 5.0 4.5 4.0 3.5 3.0 2.5 2.0 1.5 1.0 0.5
f1 (ppm)

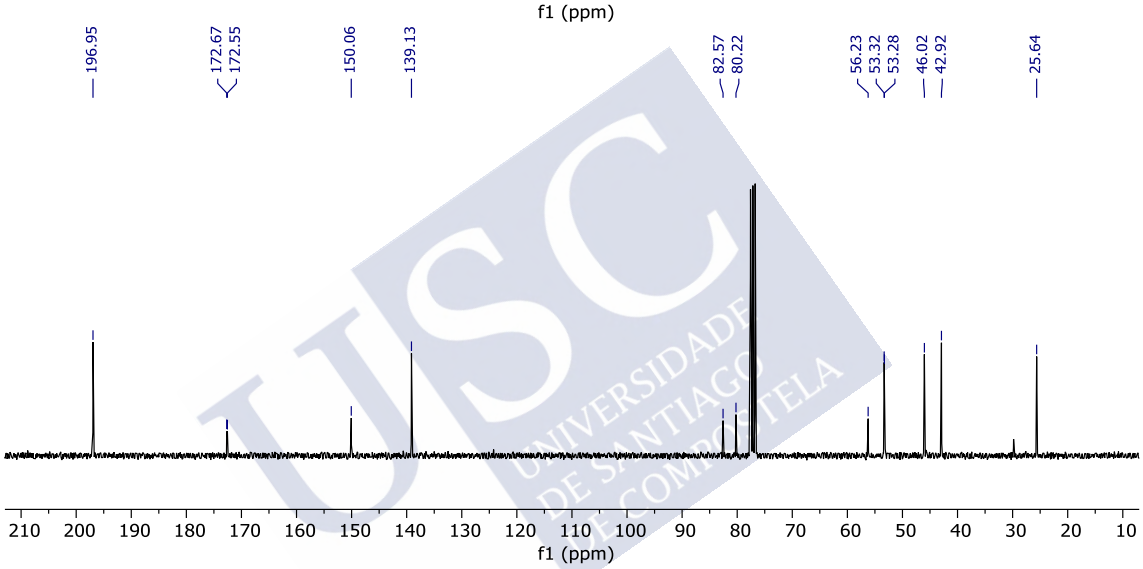
196.95
172.67
172.55
150.06
139.13
82.57
80.22
56.23
53.32
53.28
46.02
42.92
25.64
210 200 190 180 170 160 150 140 130 120 110 100 90 80 70 60 50 40 30 20 10
f1 (ppm)

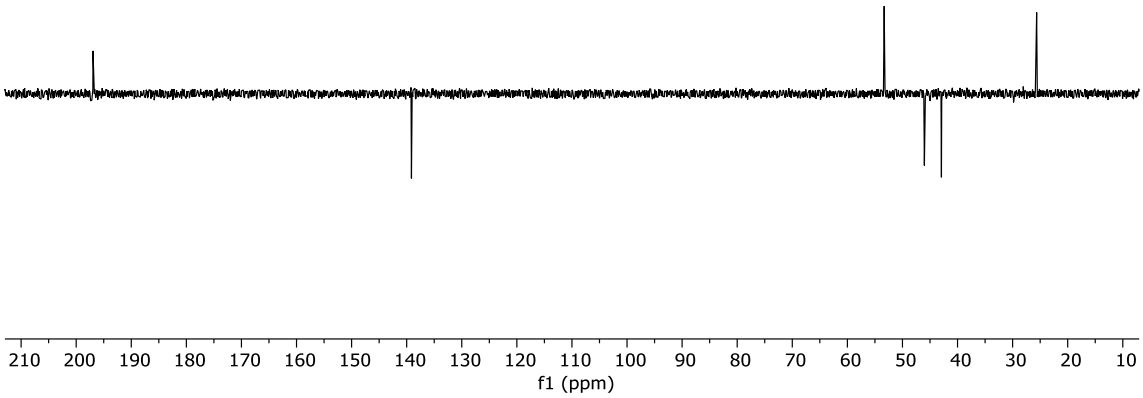
210 200 190 180 170 160 150 140 130 120 110 100 90 80 70 60 50 40 30 20 10
f1 (ppm)

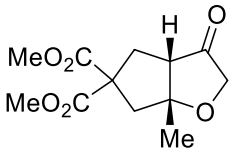
H
O
MeO2C
MeO2C
O
Me

62a

7.5 7.0 6.5 6.0 5.5 5.0 4.5 4.0 3.5 3.0 2.5 2.0 1.5 1.0 0.5
f1 (ppm)

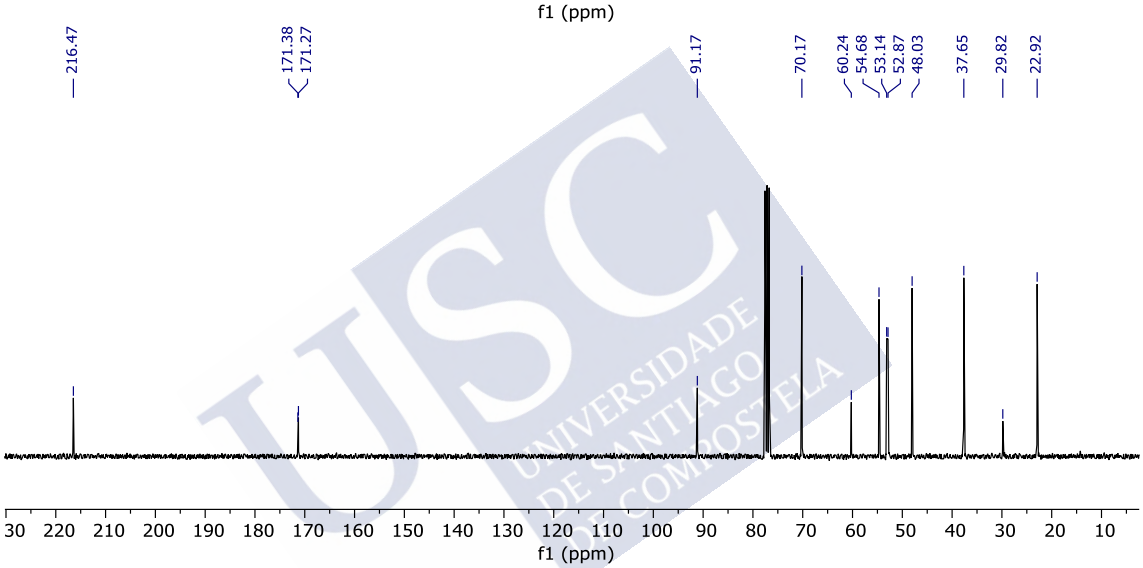
216.47
171.38
171.27
91.17
70.17
60.24
54.68
53.14
52.87
48.03
37.65
29.82
22.92
30 220 210 200 190 180 170 160 150 140 130 120 110 100 90 80 70 60 50 40 30 20 10
f1 (ppm)

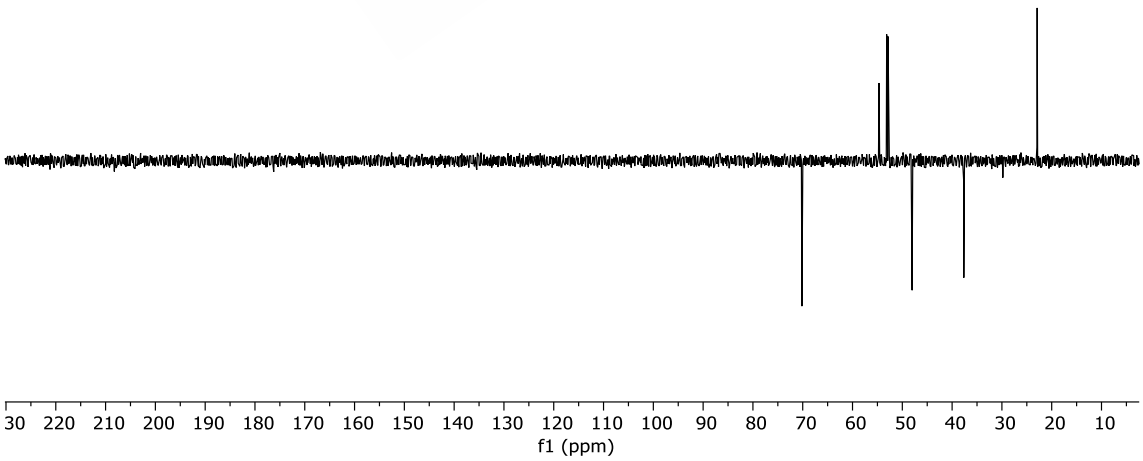
30 220 210 200 190 180 170 160 150 140 130 120 110 100 90 80 70 60 50 40 30 20 10
f1 (ppm)

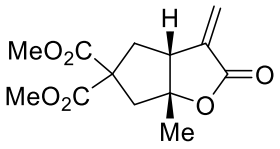
H
MeO2C
MeO2C
O
O
Me

63a

7.5
7.0
6.5
6.0
5.5
5.0
4.5
4.0
3.5
3.0
2.5
2.0
1.5
1.0
0.5
f1 (ppm)

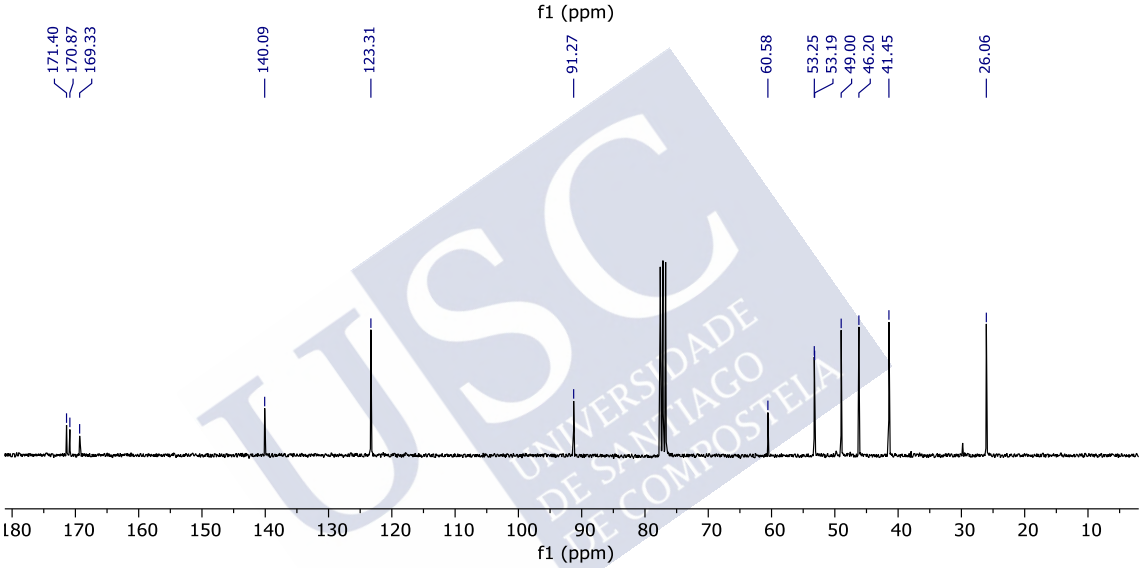
171.40
170.87
169.33
140.09
123.31
91.27
60.58
53.25
53.19
49.00
46.20
41.45
26.06
180
170
160
150
140
130
120
110
100
90
80
70
60
50
40
30
20
10
f1 (ppm)

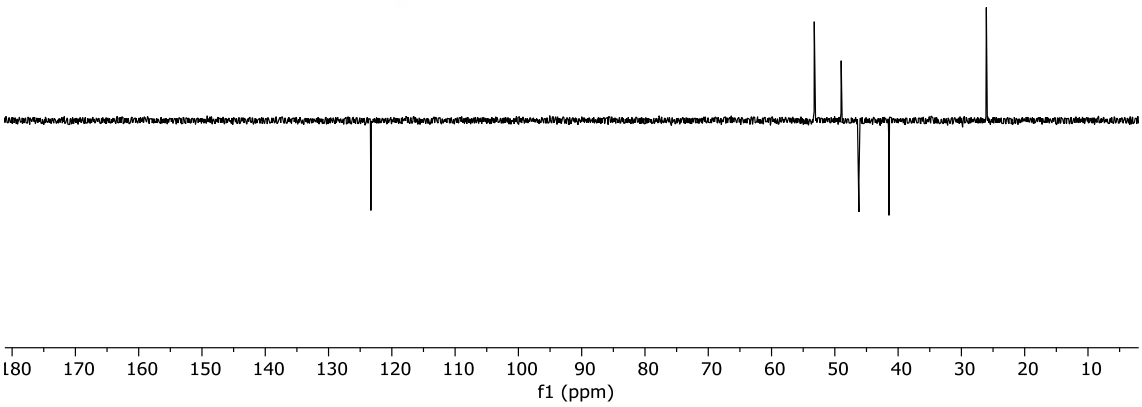
180
170
160
150
140
130
120
110
100
90
80
70
60
50
40
30
20
10
f1 (ppm)

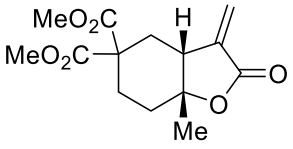

63e

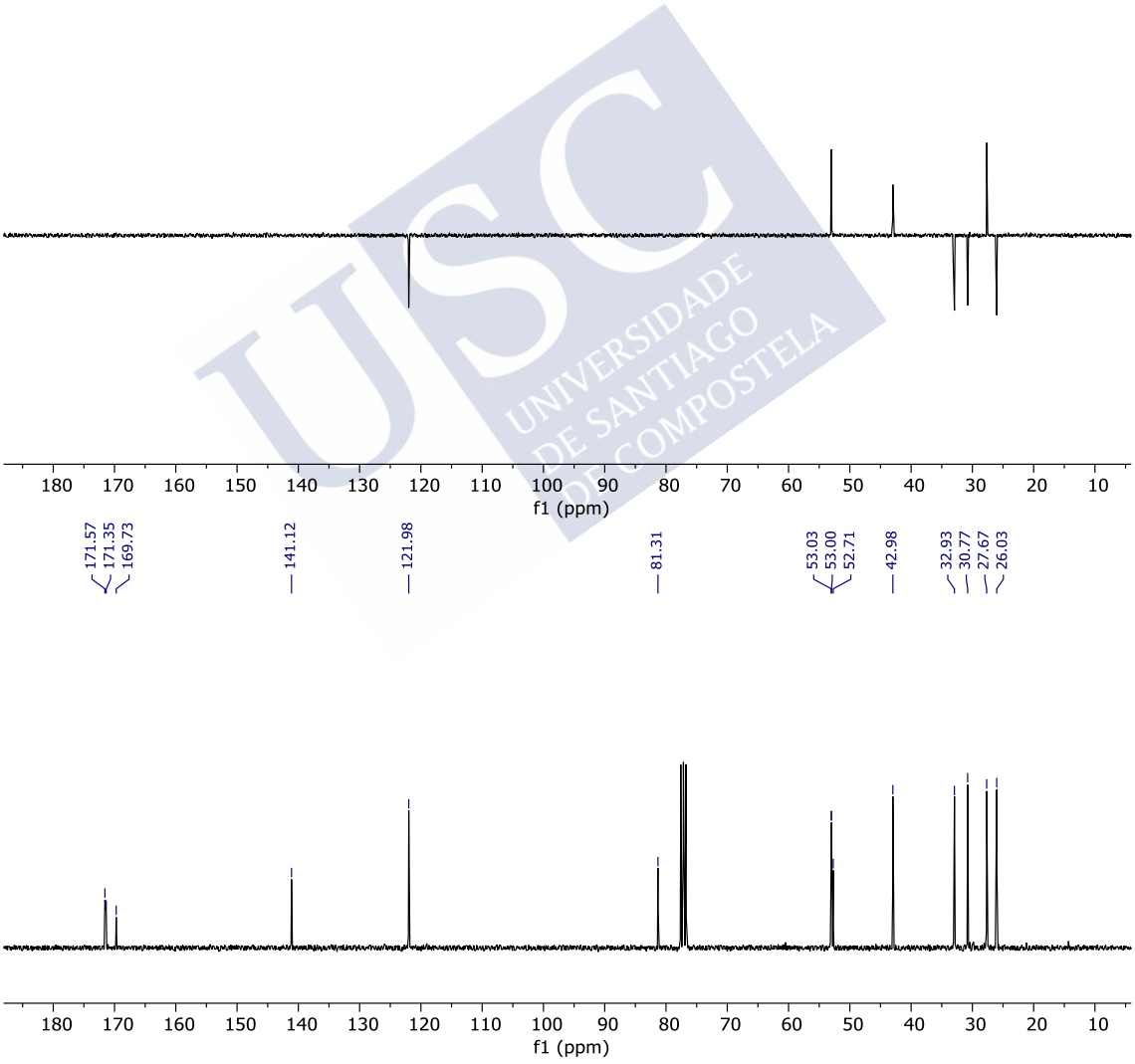

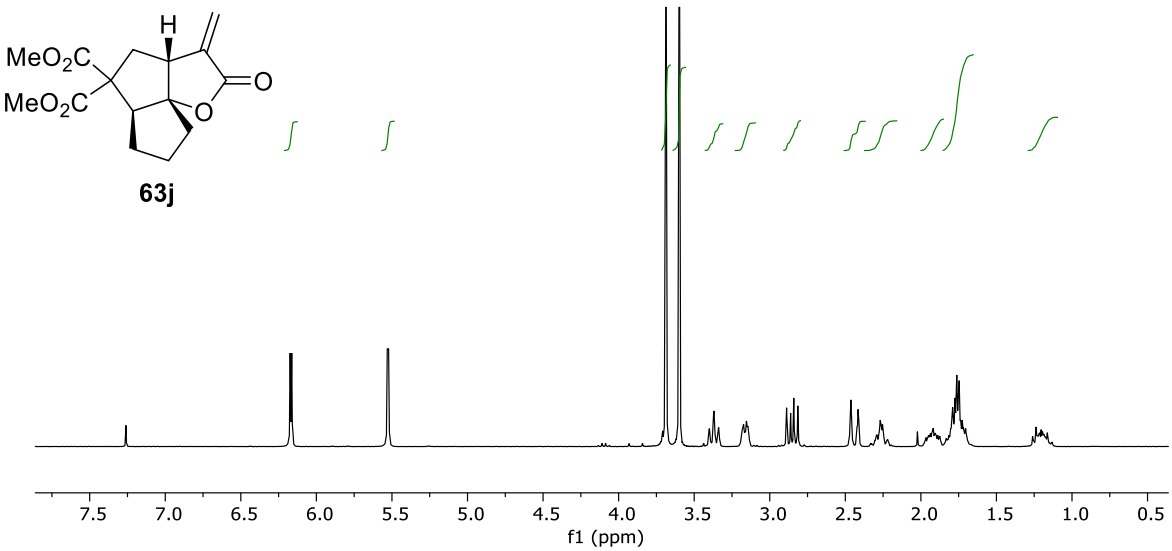
MeO2C
MeO2C
H
O
O

63j

7.5 7.0 6.5 6.0 5.5 5.0 4.5 4.0 3.5 3.0 2.5 2.0 1.5 1.0 0.5
f1 (ppm)

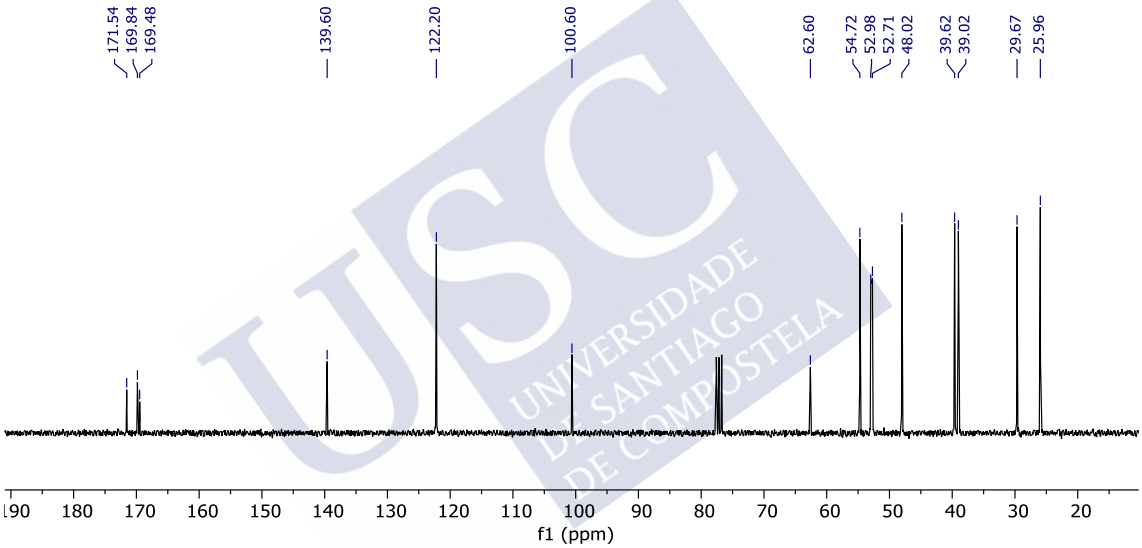
171.54
169.84
169.48
139.60
122.20
100.60
62.60
54.72
52.98
52.71
48.02
39.62
39.02
29.67
25.96
190 180 170 160 150 140 130 120 110 100 90 80 70 60 50 40 30 20
f1 (ppm)

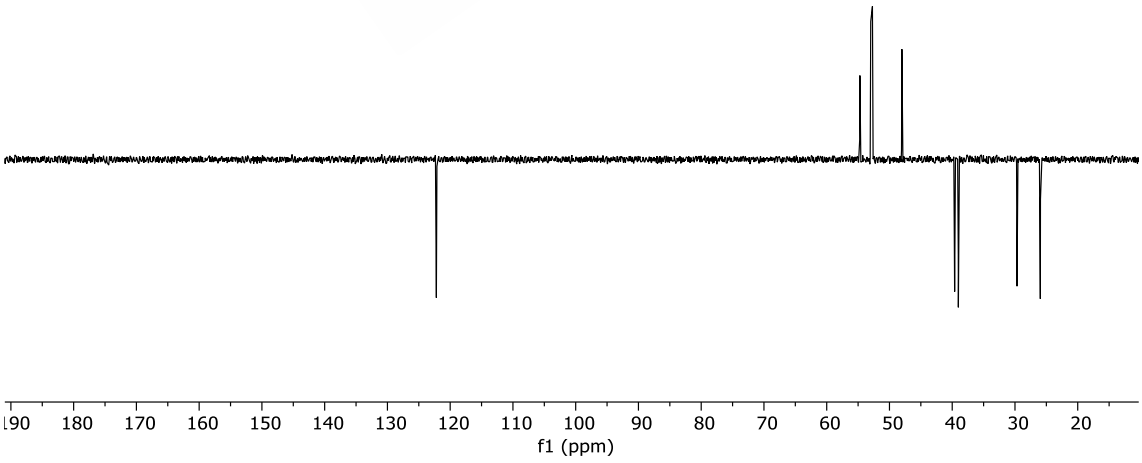
190 180 170 160 150 140 130 120 110 100 90 80 70 60 50 40 30 20
f1 (ppm)

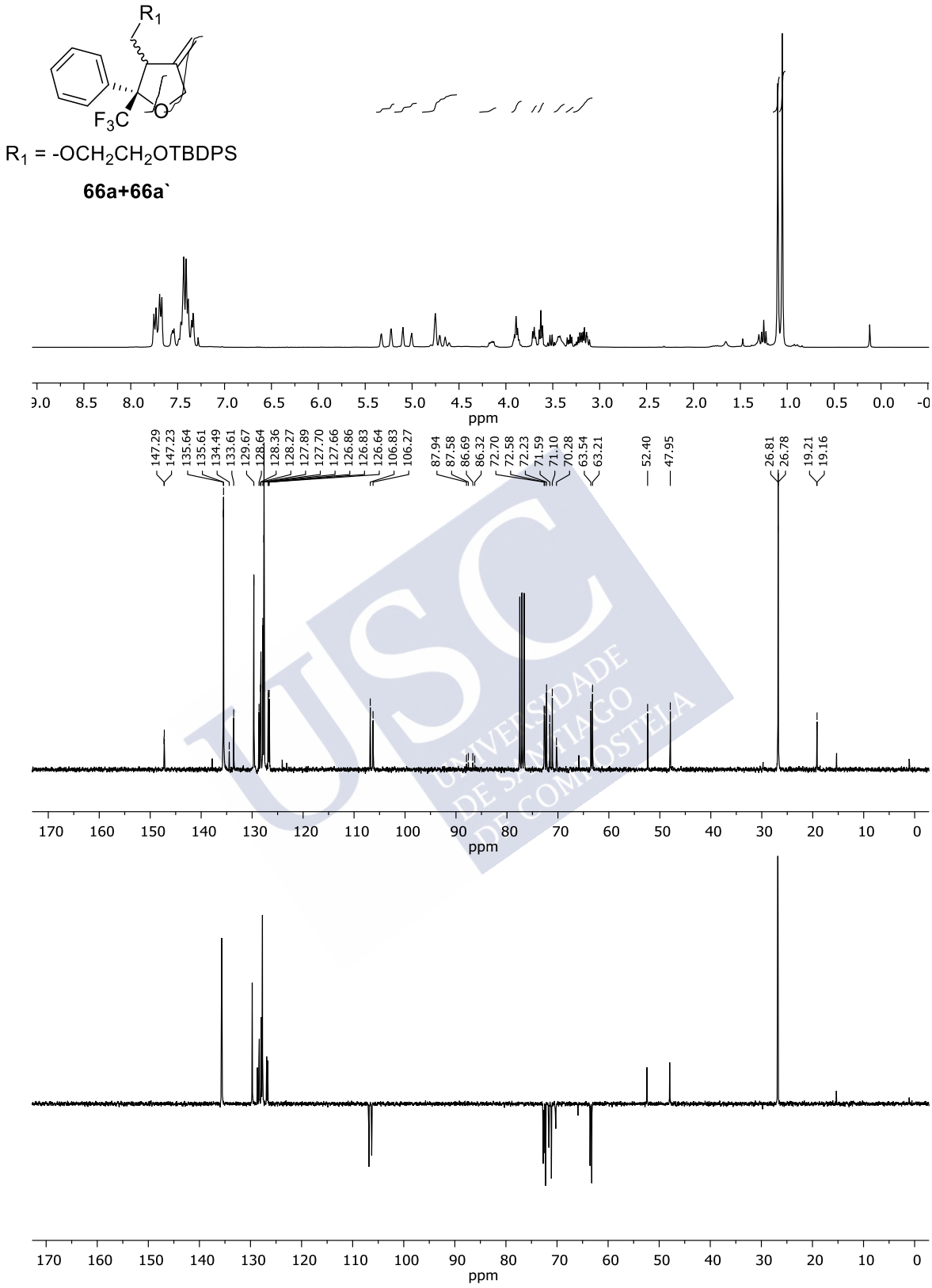
R1
F3C
O
R1 = -OCH2CH2OTBDPS
66a+66a`
ppm
147.29
147.23
135.64
135.61
134.49
133.61
129.67
128.64
128.36
128.27
127.89
127.70
127.66
126.86
126.83
126.64
106.83
106.27
87.94
87.58
86.69
86.32
72.70
72.58
72.23
71.59
71.10
70.28
63.54
63.21
52.40
47.95
26.81
26.78
19.21
19.16

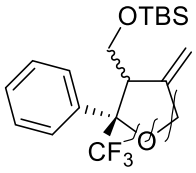
OTBS
CF3
O

66b+66b`

8.0 7.5 7.0 6.5 6.0 5.5 5.0 4.5 4.0 3.5 3.0 2.5 2.0 1.5 1.0 0.5 0.0 -0.5 -1
ppm

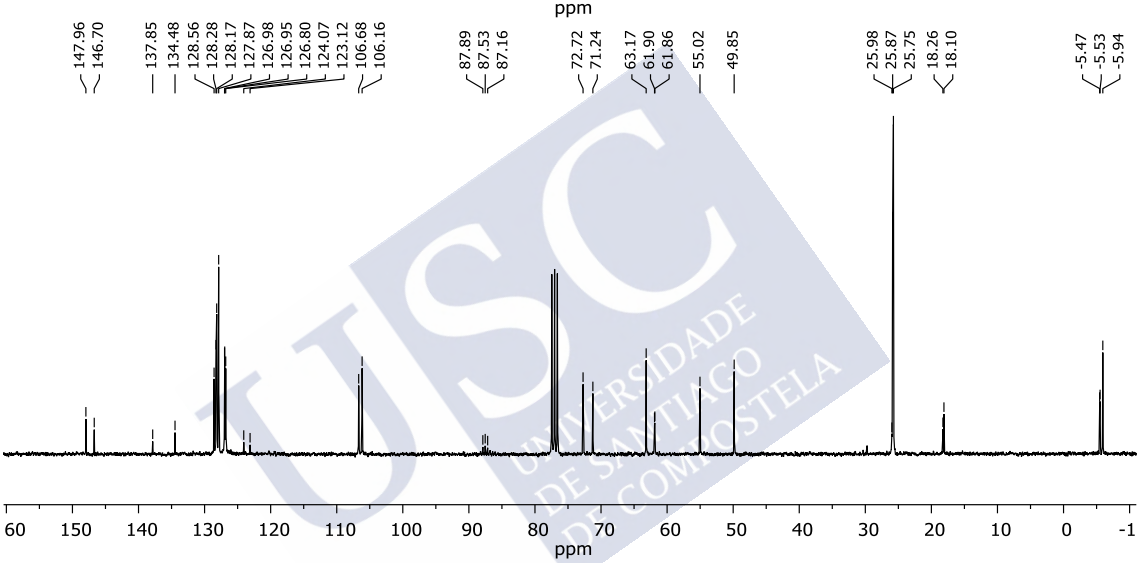
147.96
146.70
137.85
134.48
128.56
128.28
128.17
127.87
126.98
126.95
126.80
124.07
123.12
106.68
106.16
87.89
87.53
87.16
72.72
71.24
63.17
61.90
61.86
55.02
49.85
25.98
25.87
25.75
18.26
18.10
-5.47
-5.53
-5.94
60 150 140 130 120 110 100 90 80 70 60 50 40 30 20 10 0 -1
ppm

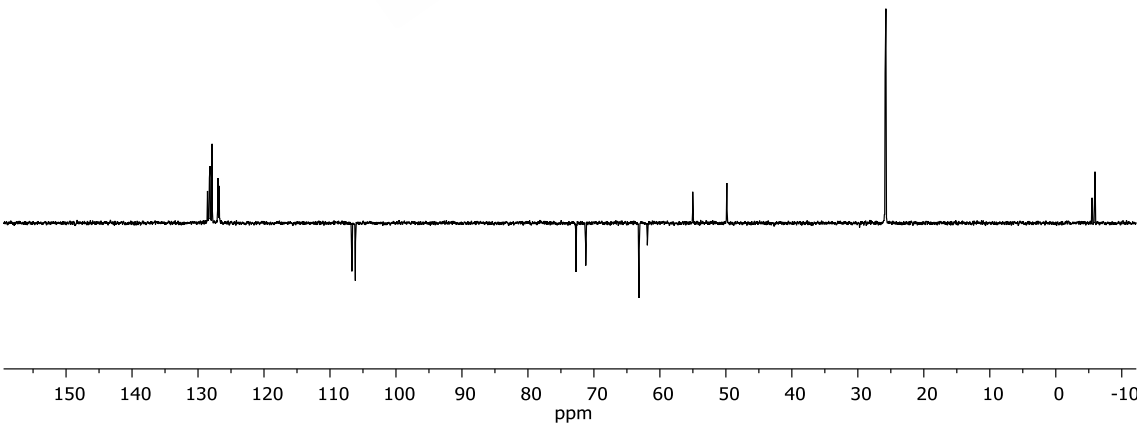
150 140 130 120 110 100 90 80 70 60 50 40 30 20 10 0 -10
ppm

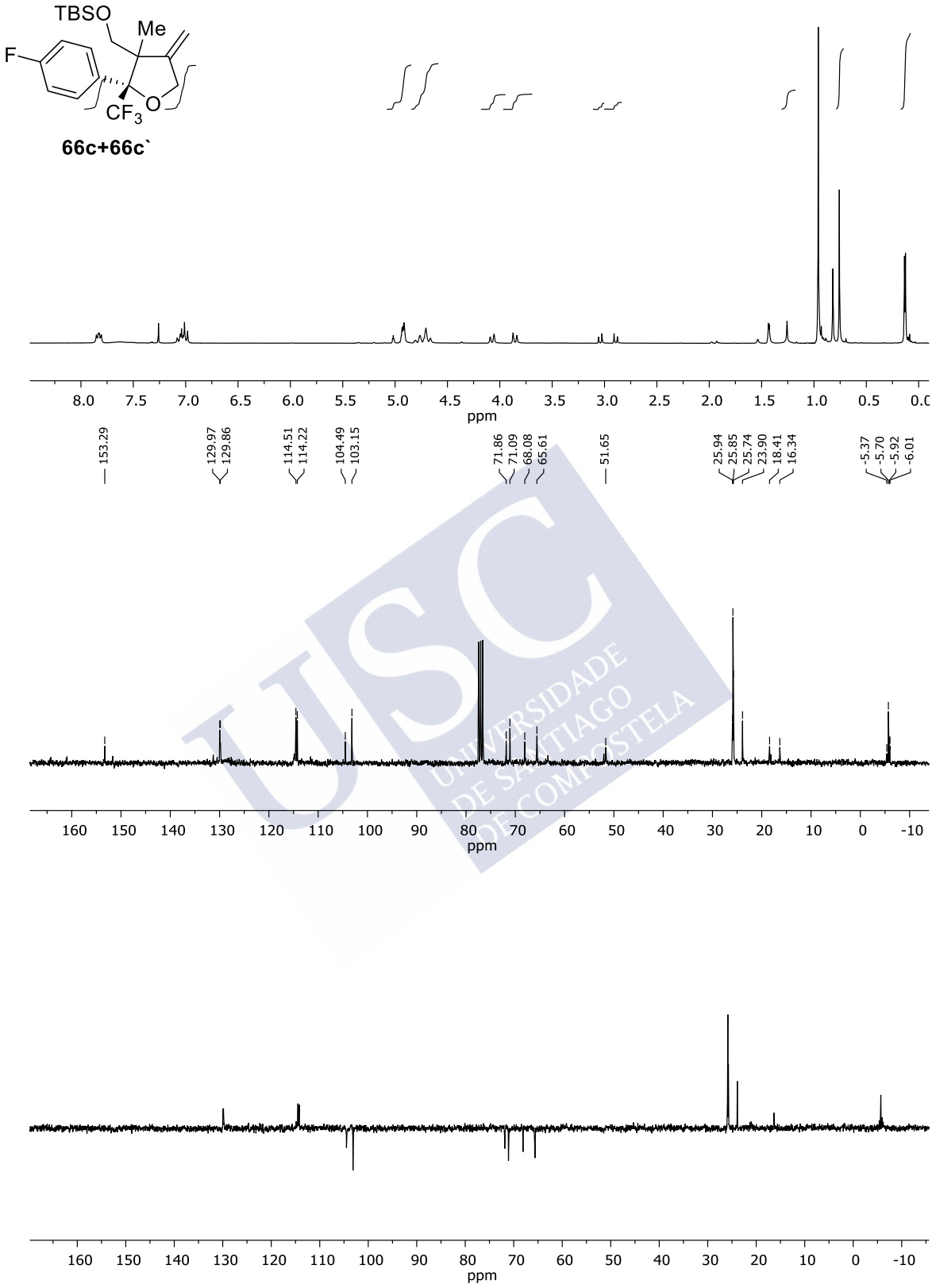
TBSO
Me
F
CF3
O
66c+66c`
ppm
153.29
129.97
129.86
114.51
114.22
104.49
103.15
71.86
71.09
68.08
65.61
51.65
25.94
25.85
25.74
23.90
18.41
16.34
-5.37
-5.70
-5.92
-6.01

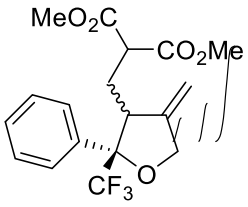
MeO2C
CO2Me
CF3
O

66d+66d`

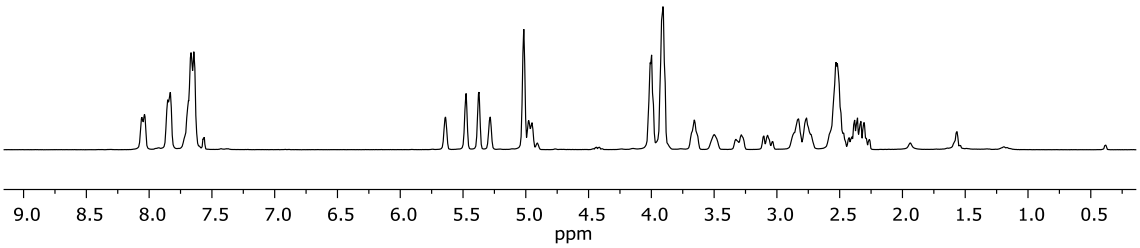
9.0
8.5
8.0
7.5
7.0
6.5
6.0
5.5
5.0
4.5
4.0
3.5
3.0
2.5
2.0
1.5
1.0
0.5
ppm

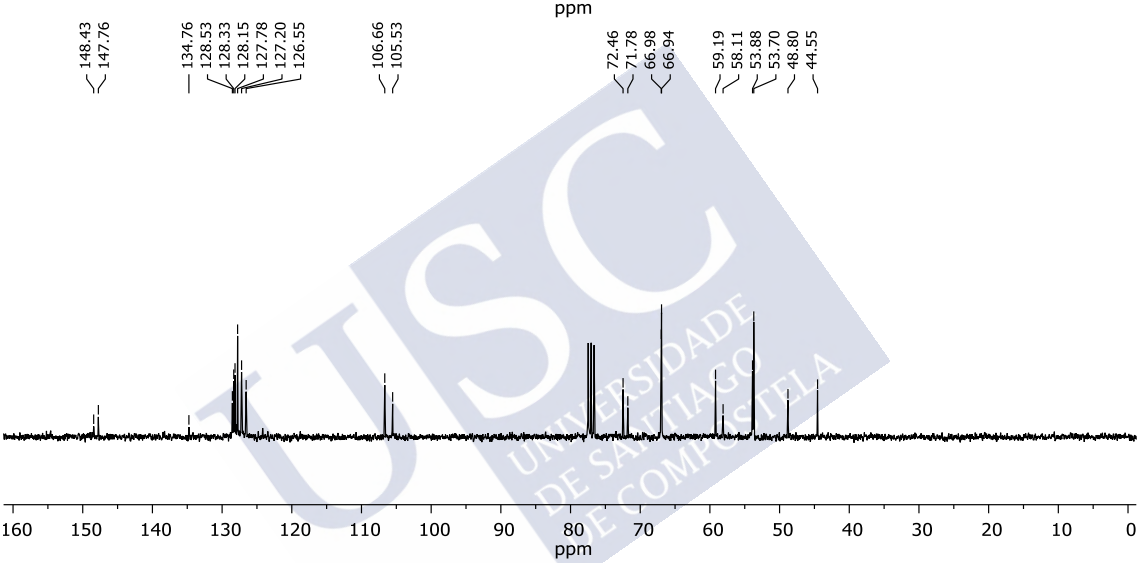
148.43
147.76
134.76
128.53
128.33
128.15
127.78
127.20
126.55
106.66
105.53
72.46
71.78
66.98
66.94
59.19
58.11
53.88
53.70
48.80
44.55
160
150
140
130
120
110
100
90
80
70
60
50
40
30
20
10
0
ppm

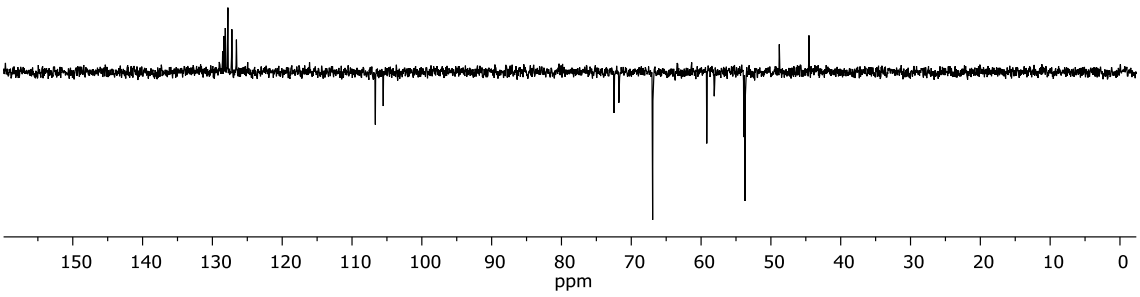
150
140
130
120
110
100
90
80
70
60
50
40
30
20
10
0
ppm

^{19}F-NMR

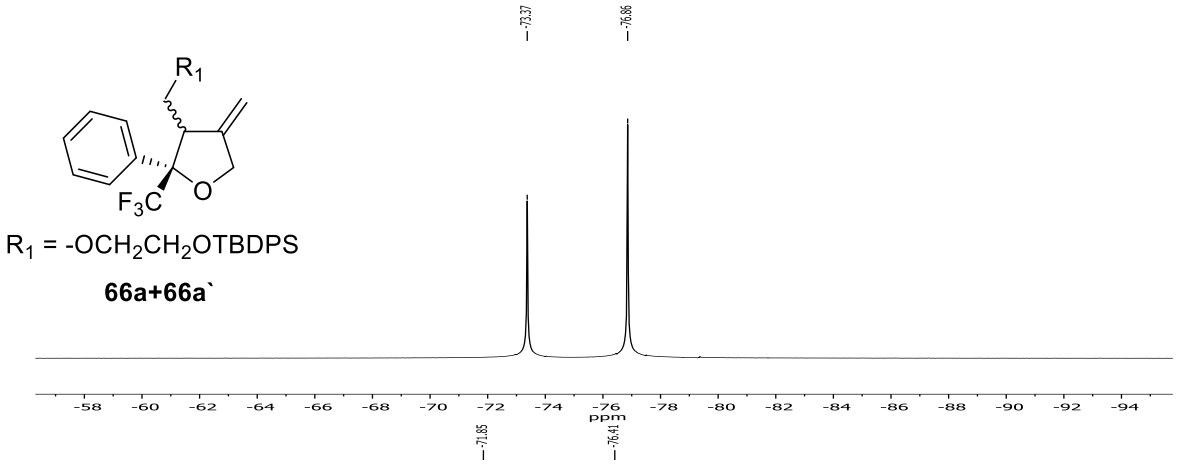

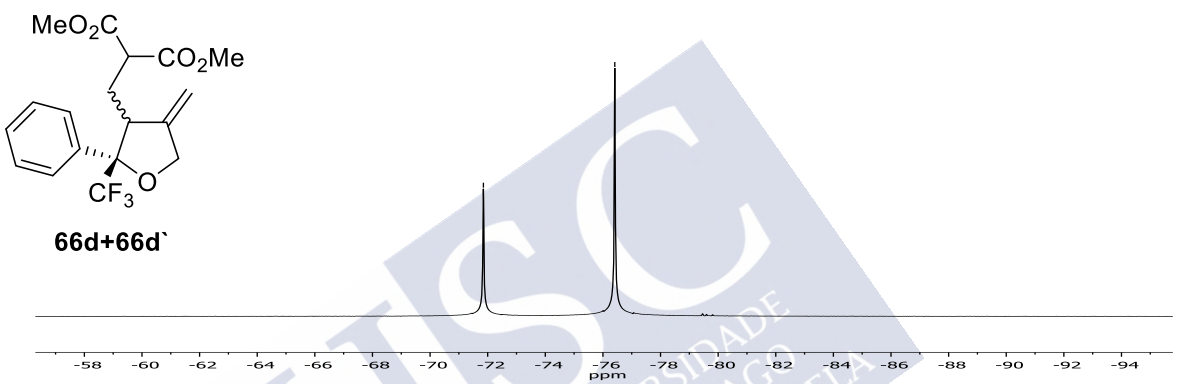

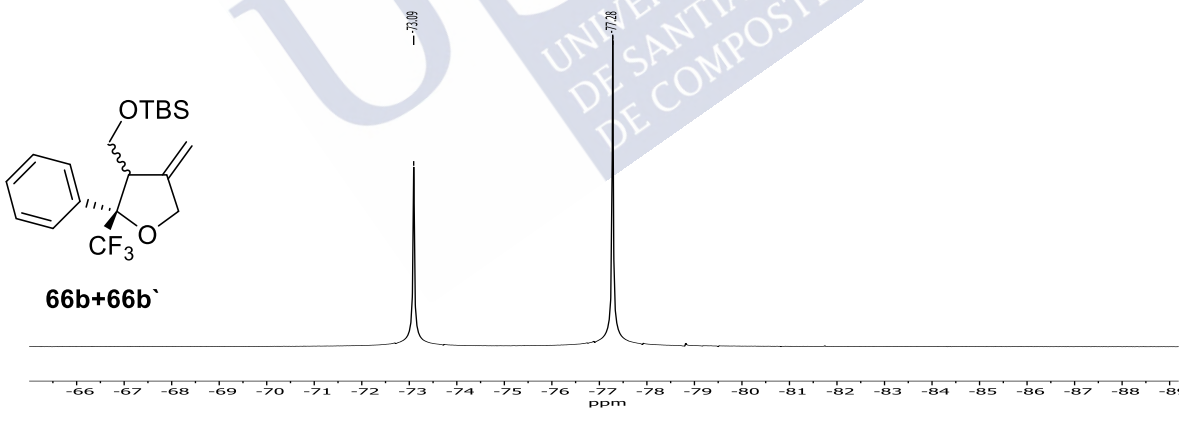

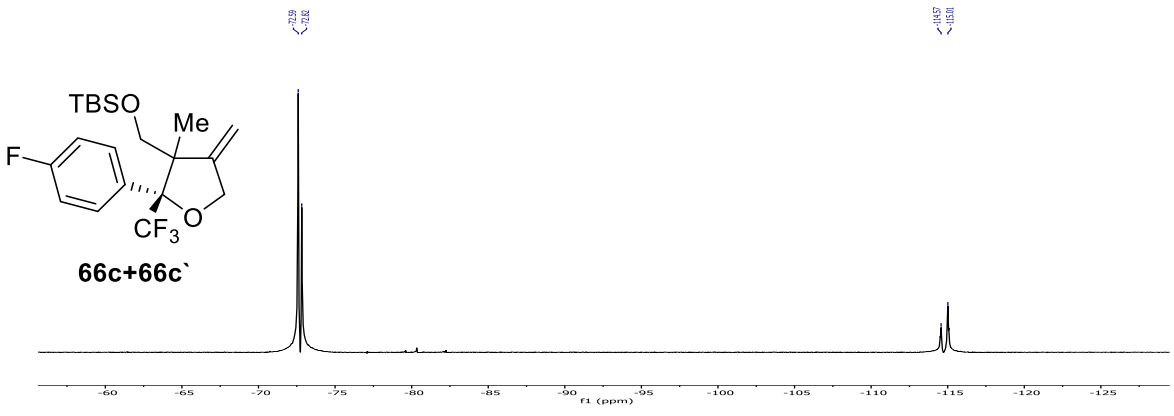

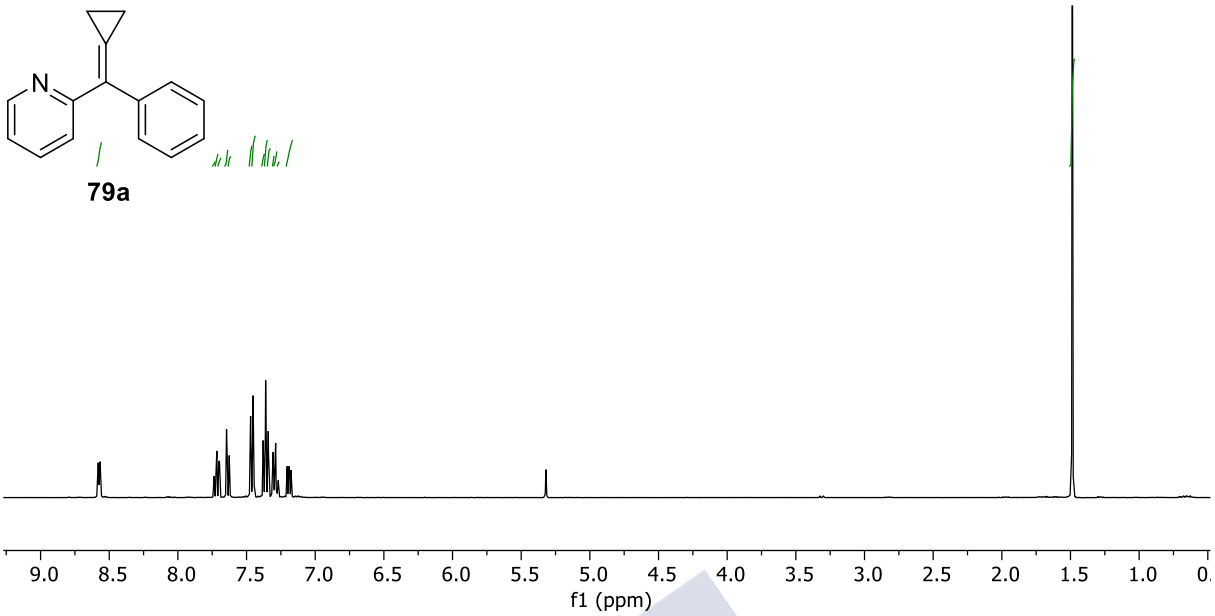

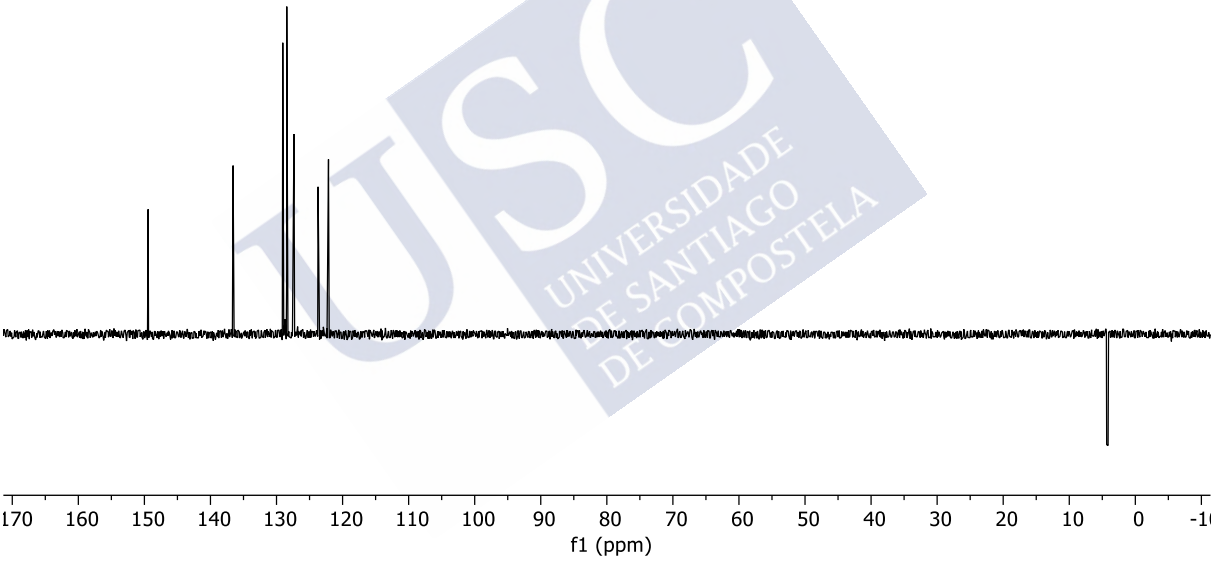

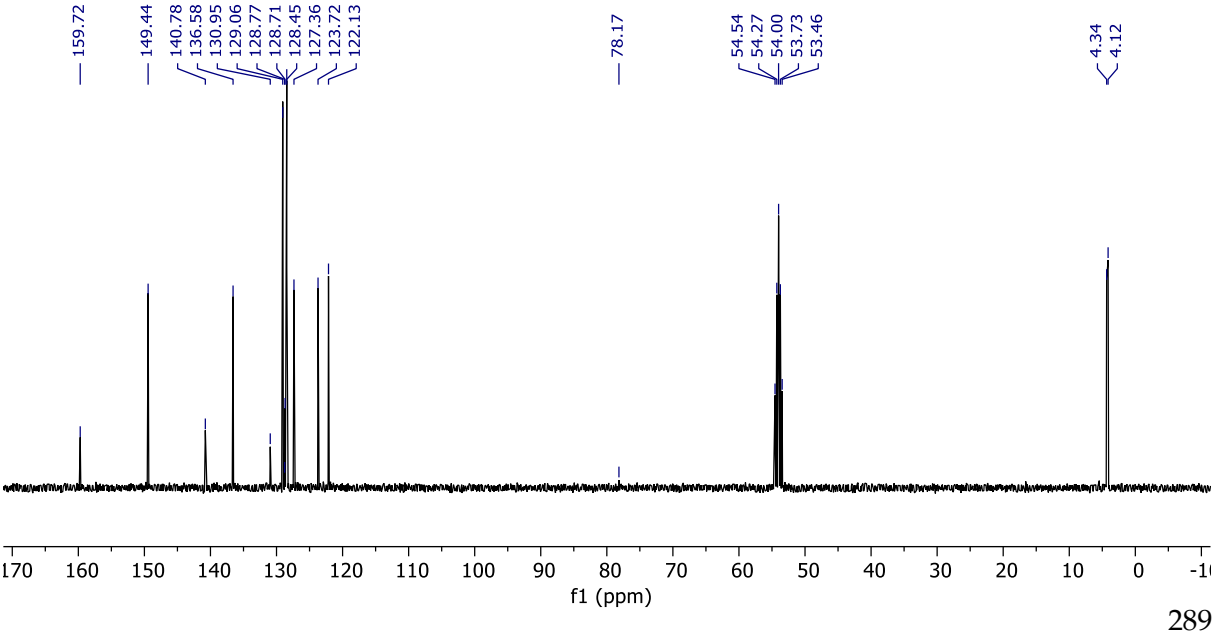

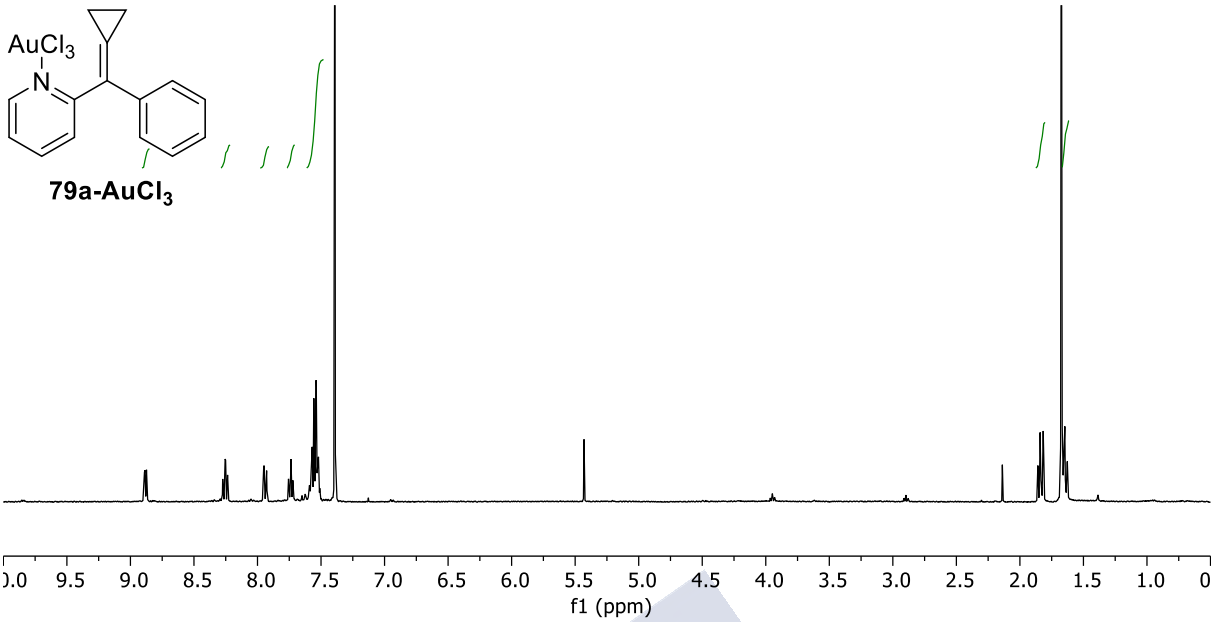
AuCl3
N
79a-AuCl3
f1 (ppm)

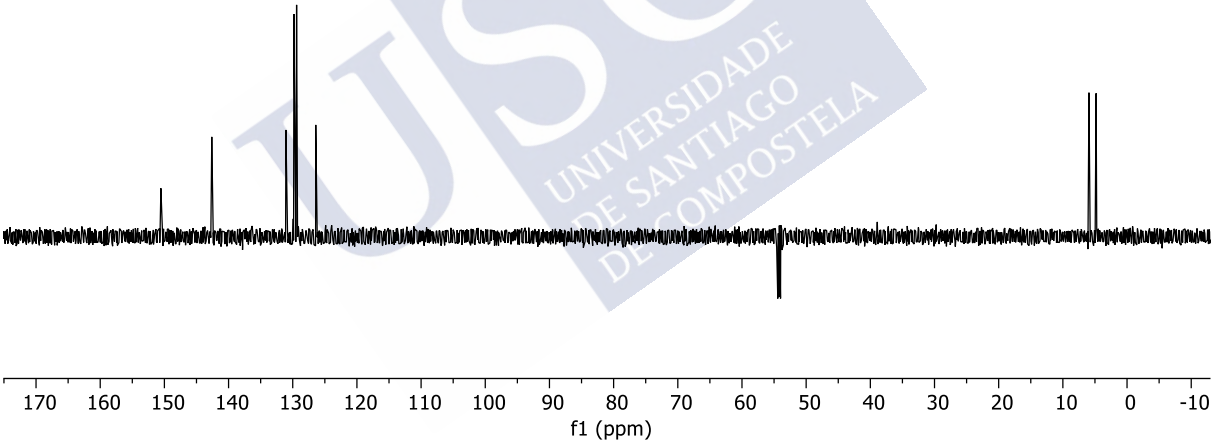
f1 (ppm)

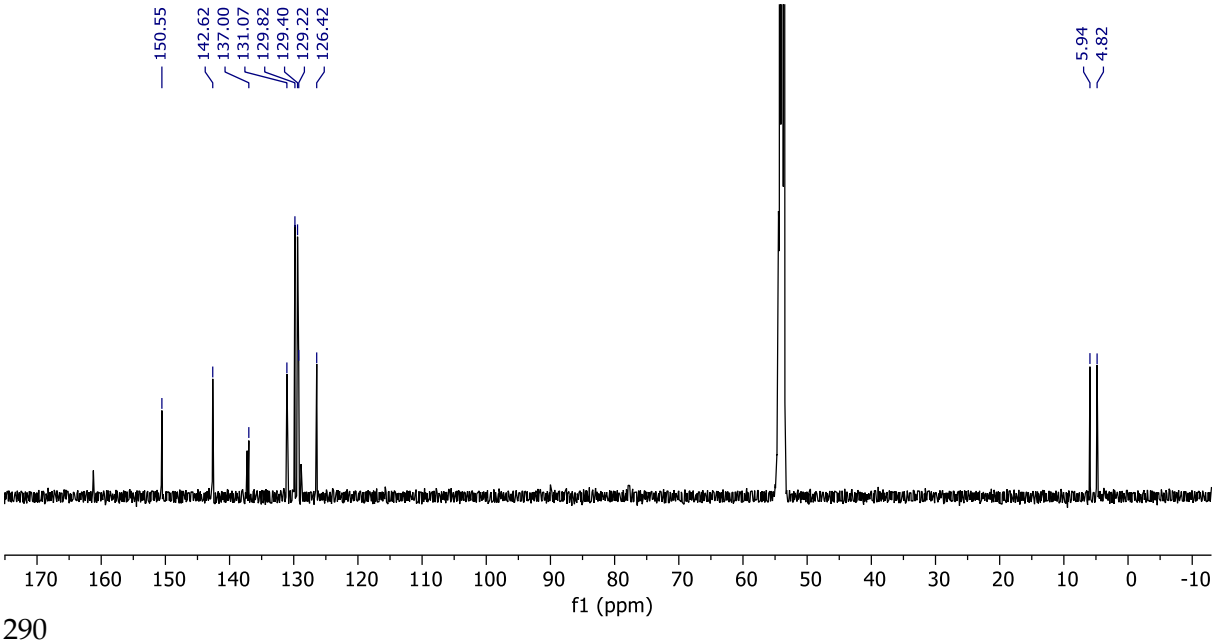
150.55
142.62
137.00
131.07
129.82
129.40
129.22
126.42
5.94
4.82
f1 (ppm)

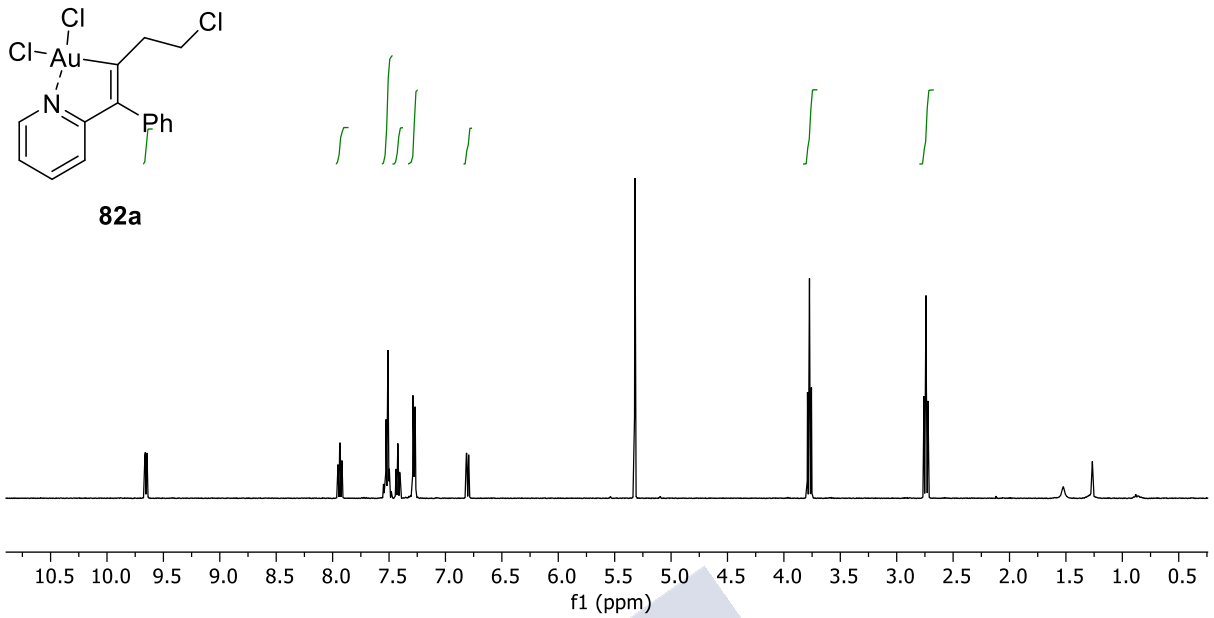

82a

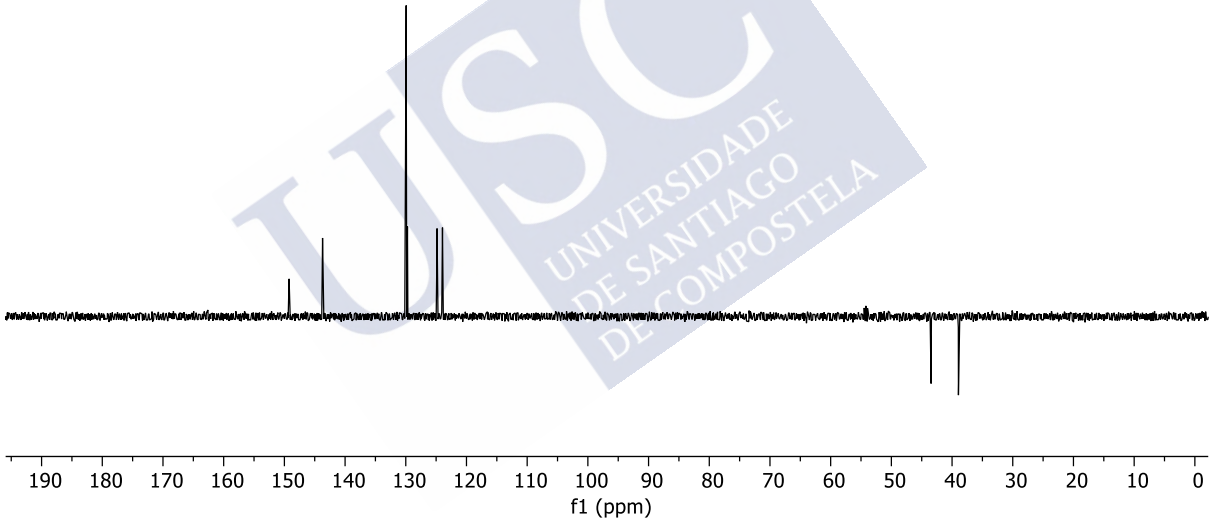

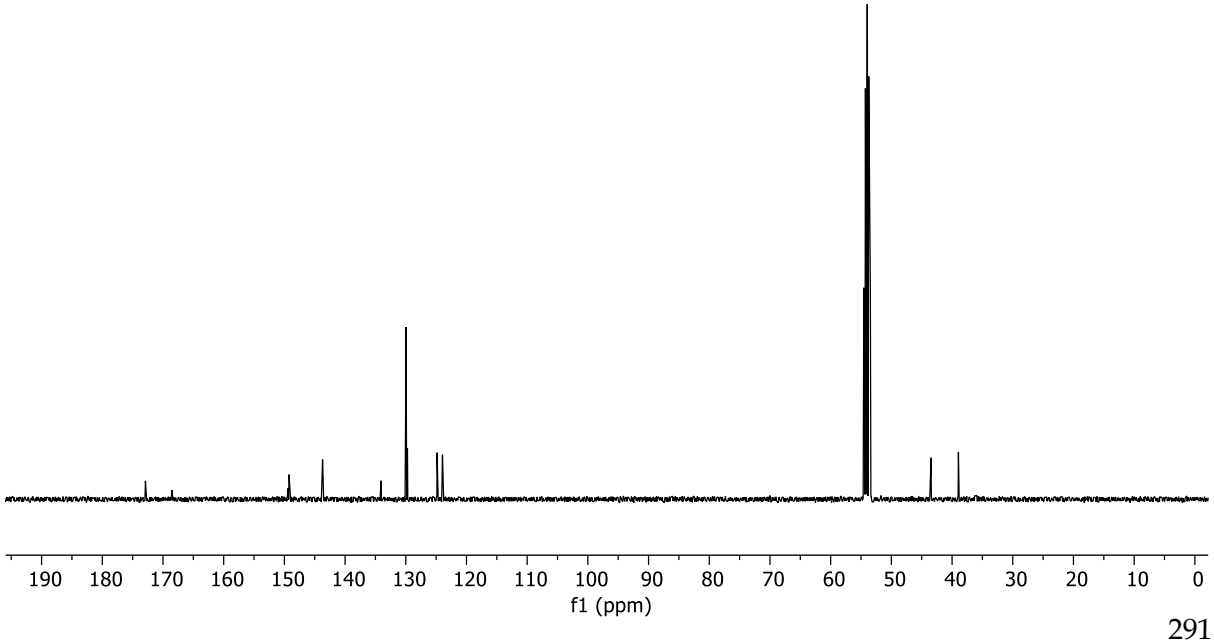

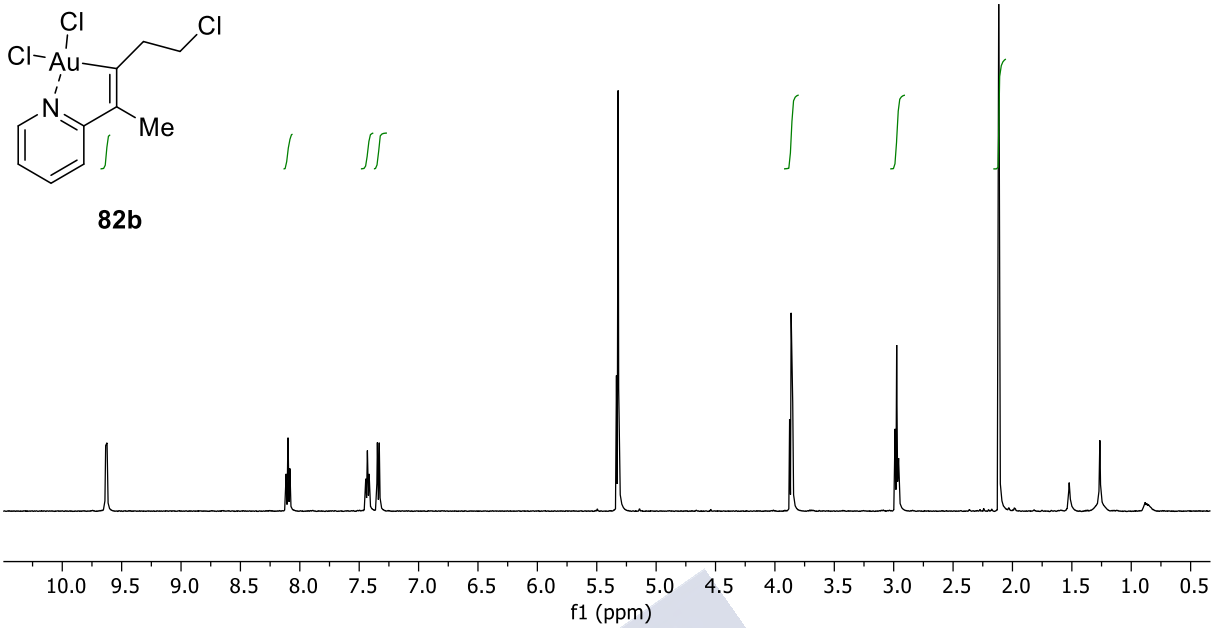

82b

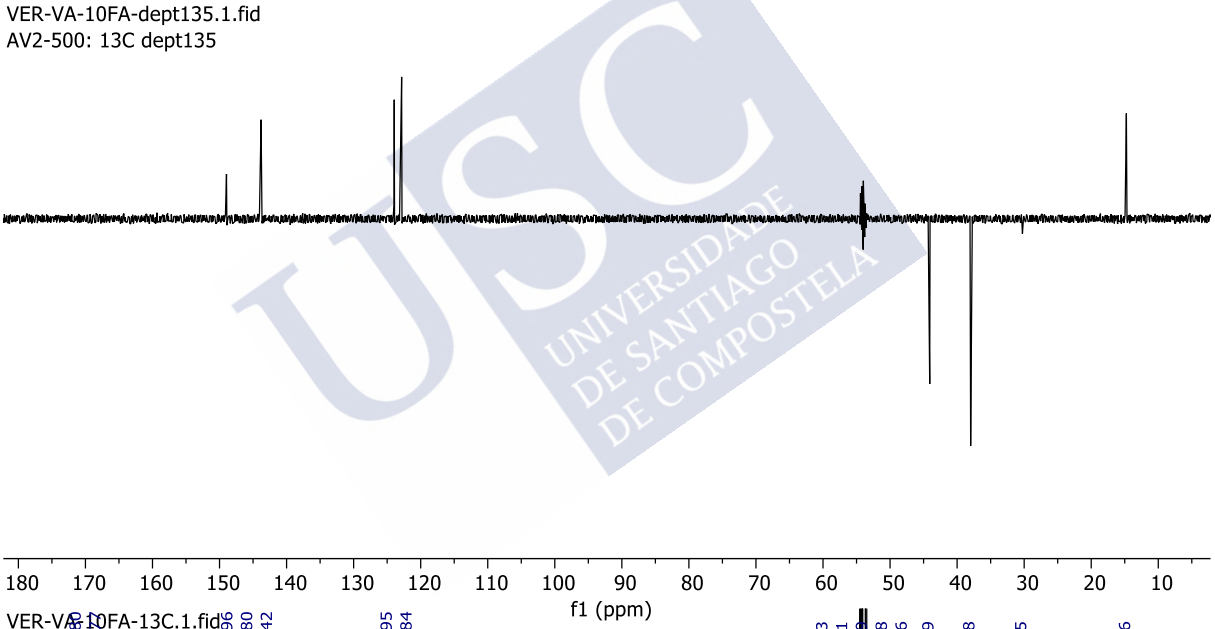

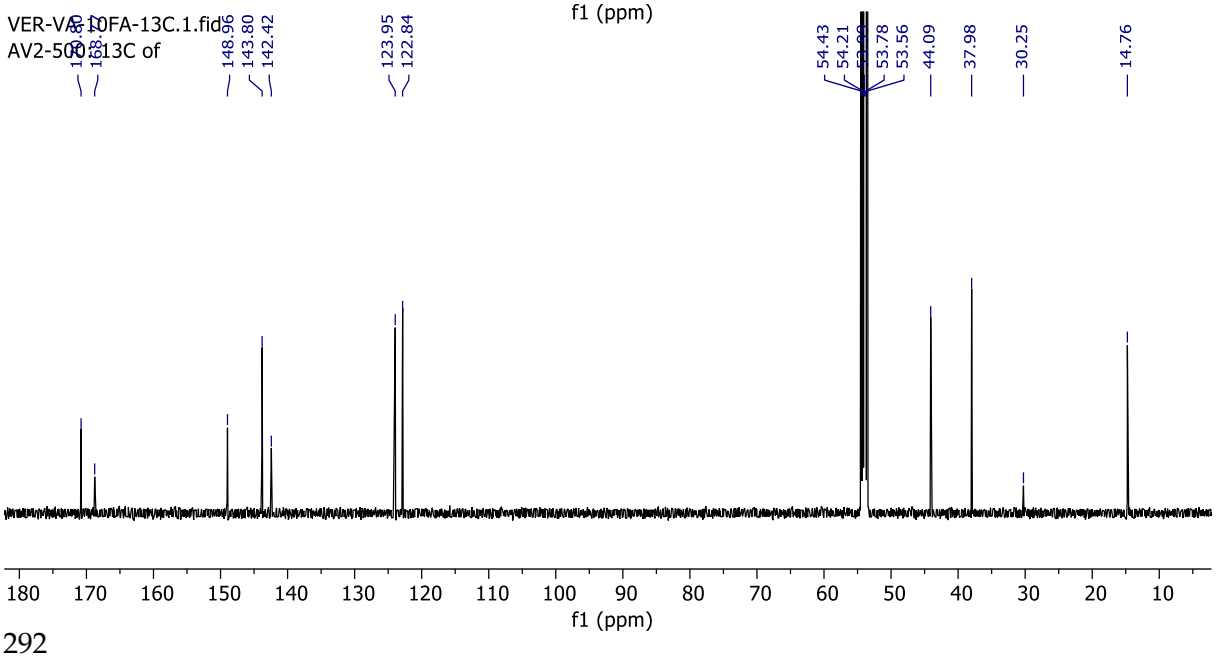

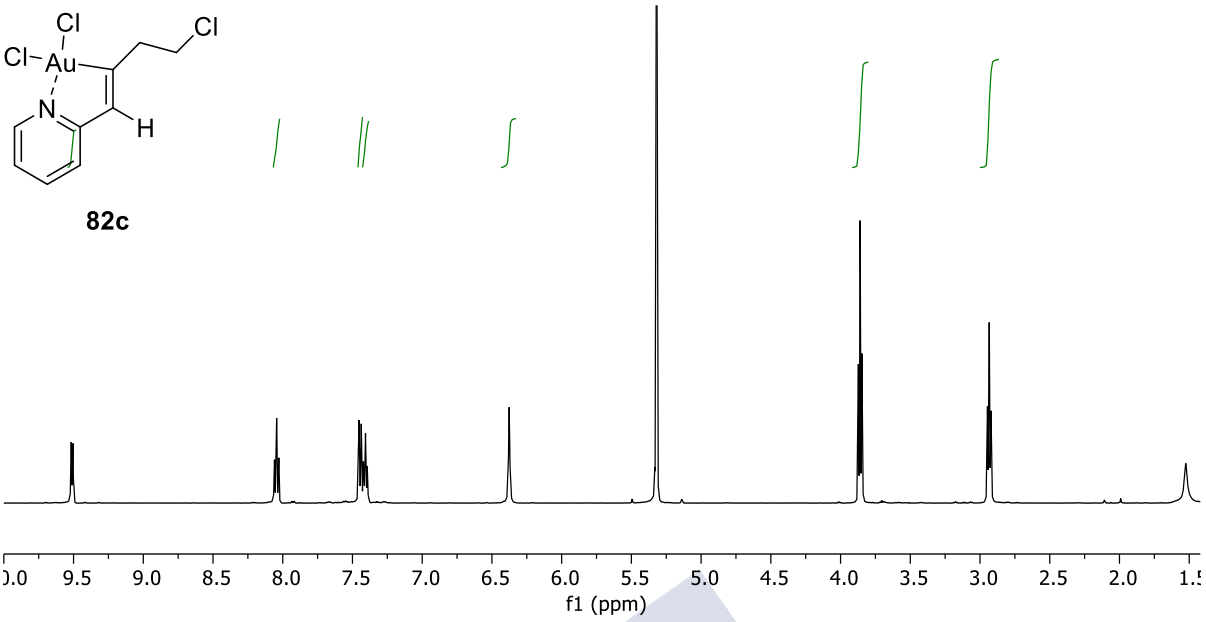

VER-VA-09-opench REPETIR

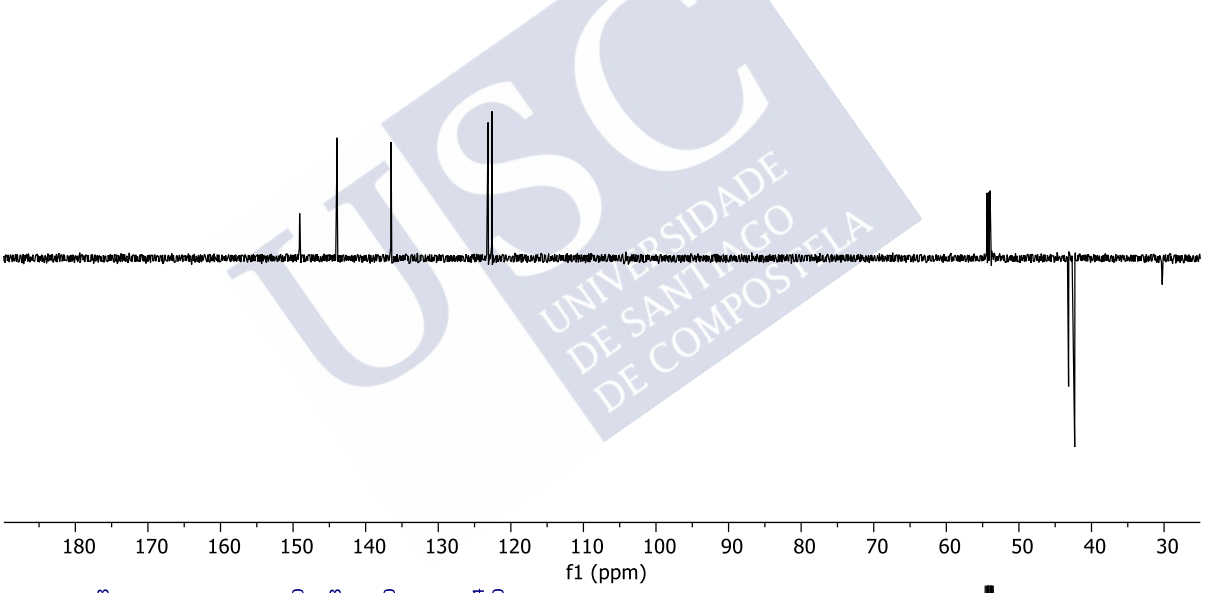

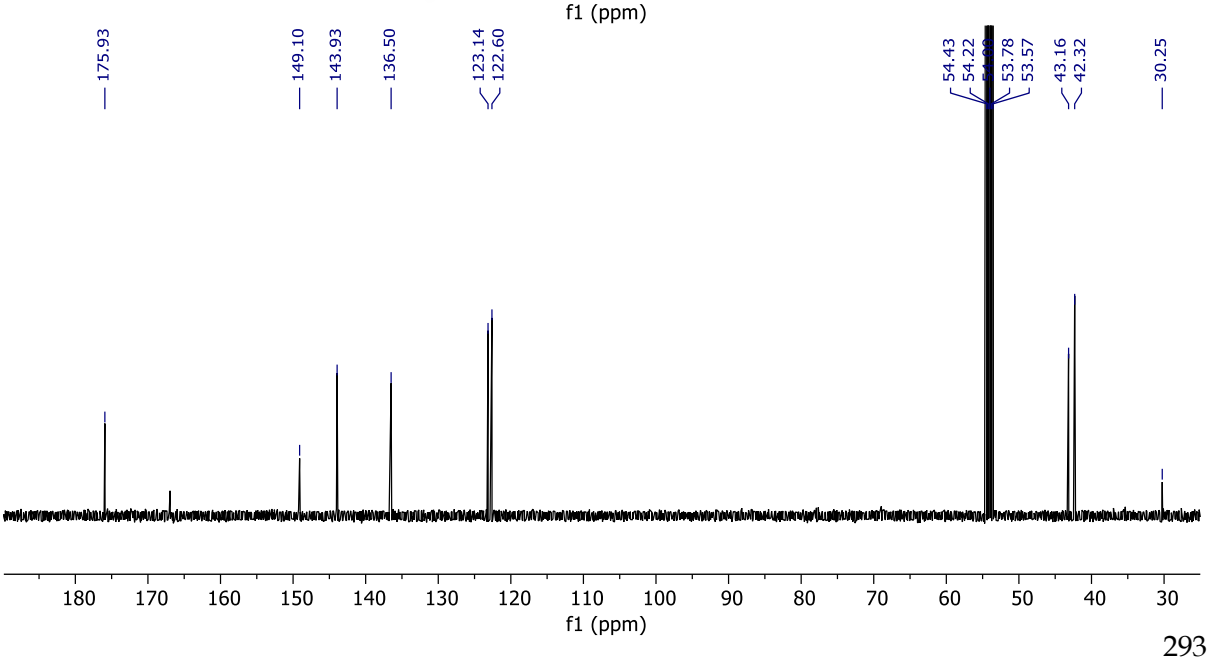

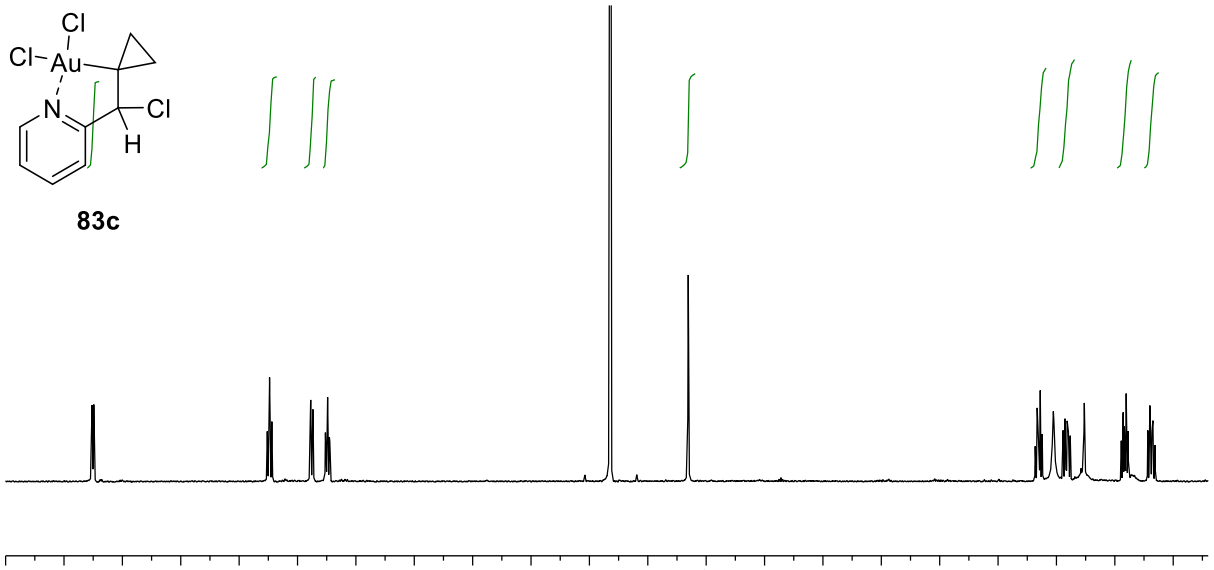

83c

H-Cycloc-Cl VER-VA-09

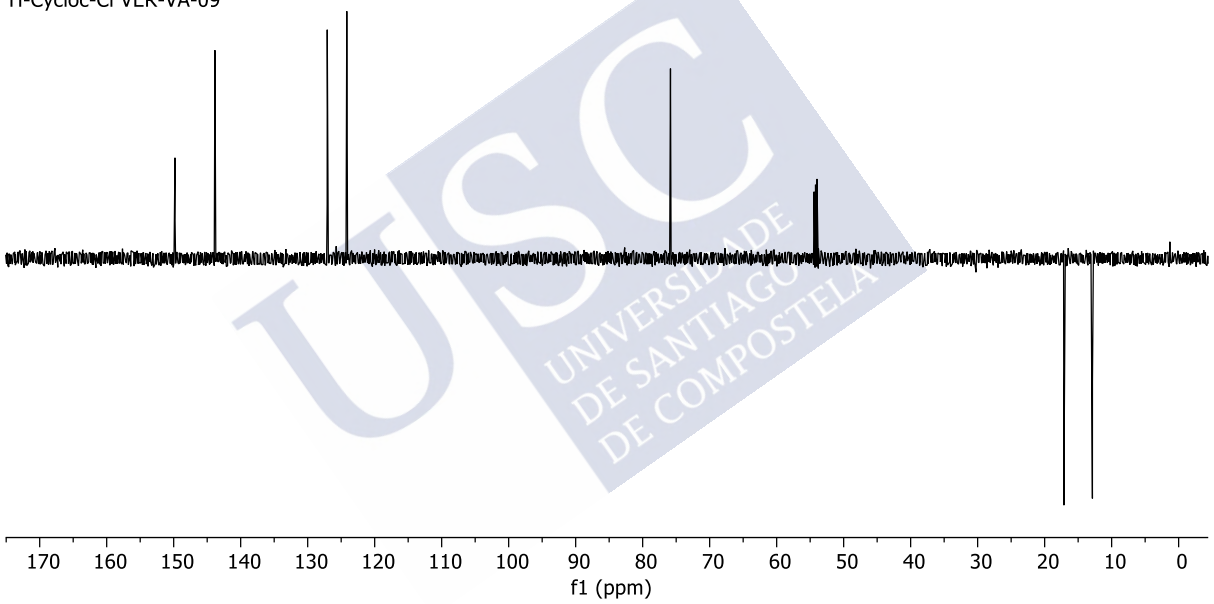

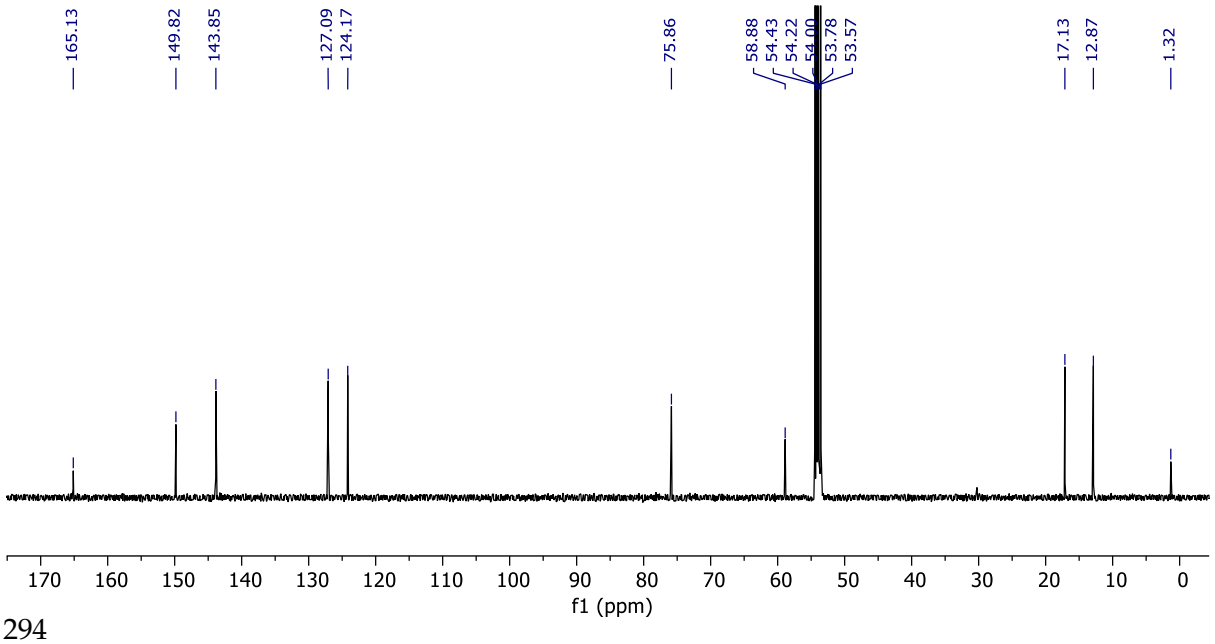

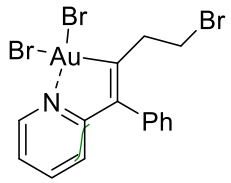

82a`

VER-VA-63-carDEPT

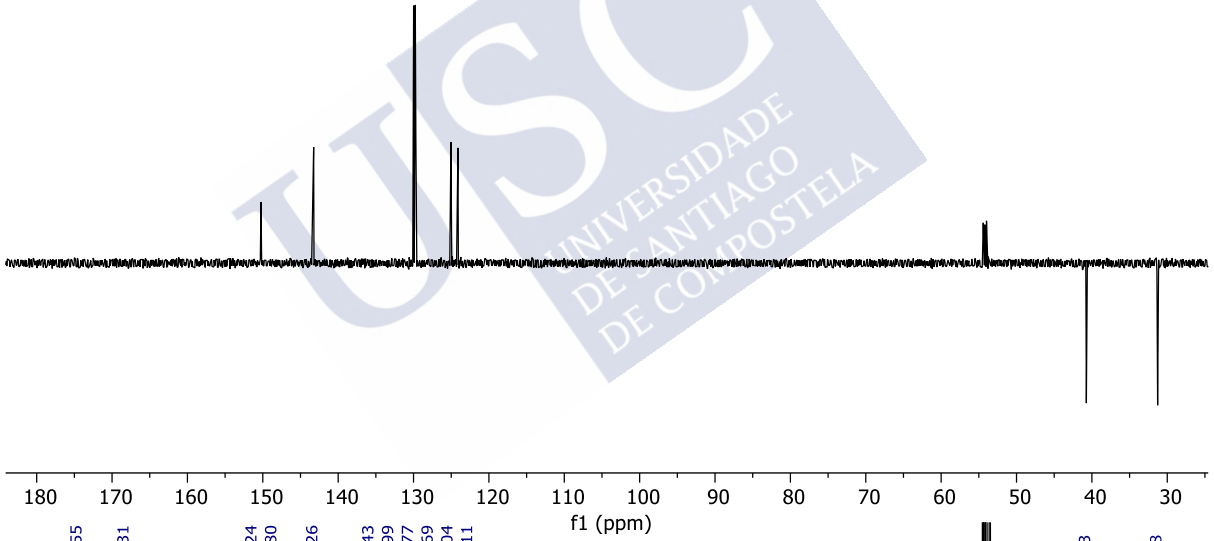

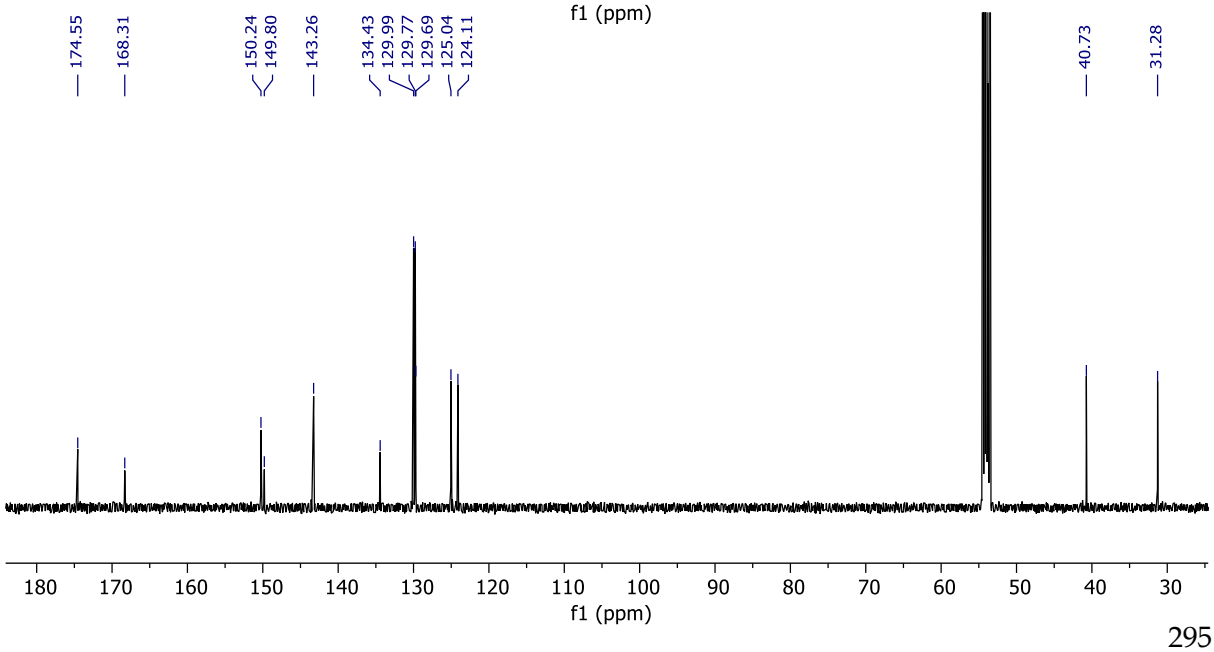

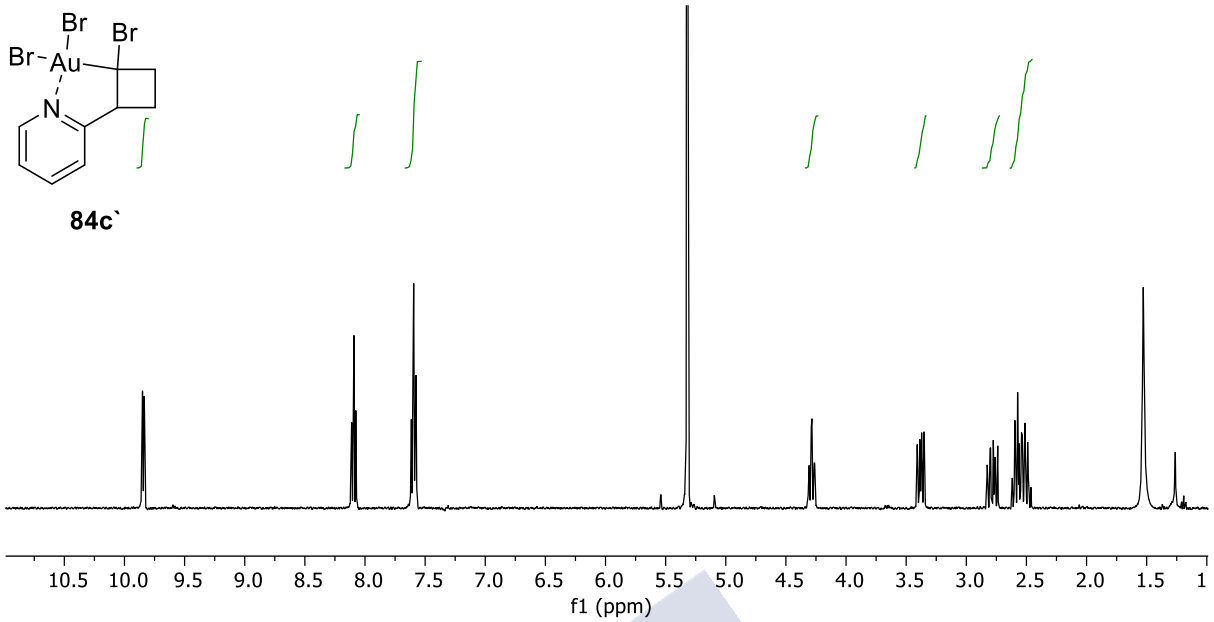

84c`

VER-VA-66-caract
AV2-500: 1H of cyclobutane

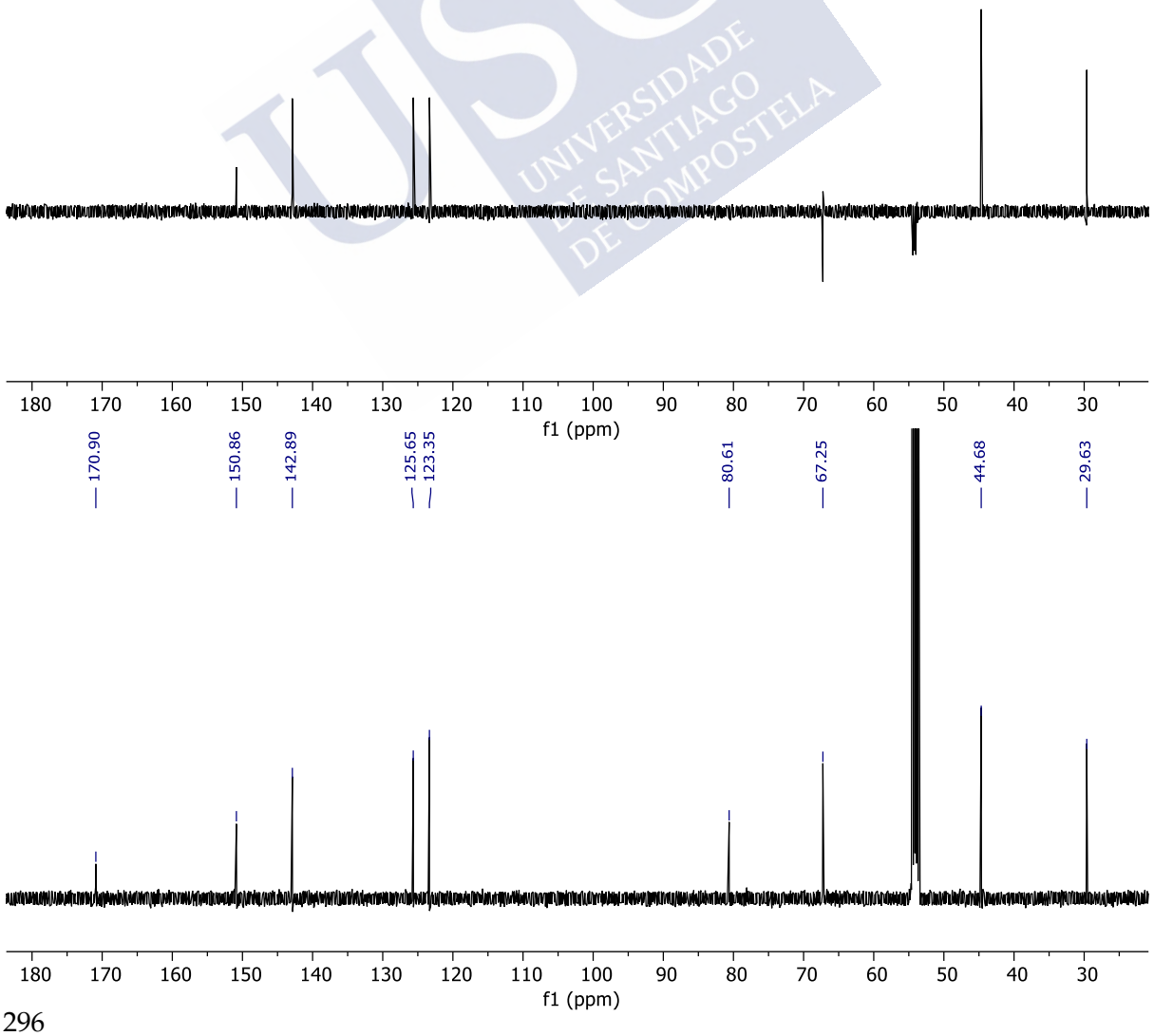

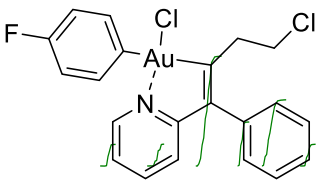

***cis*-85**

VER-VC-39-FA-caract
AV2-500: 1H of transmetal cis N

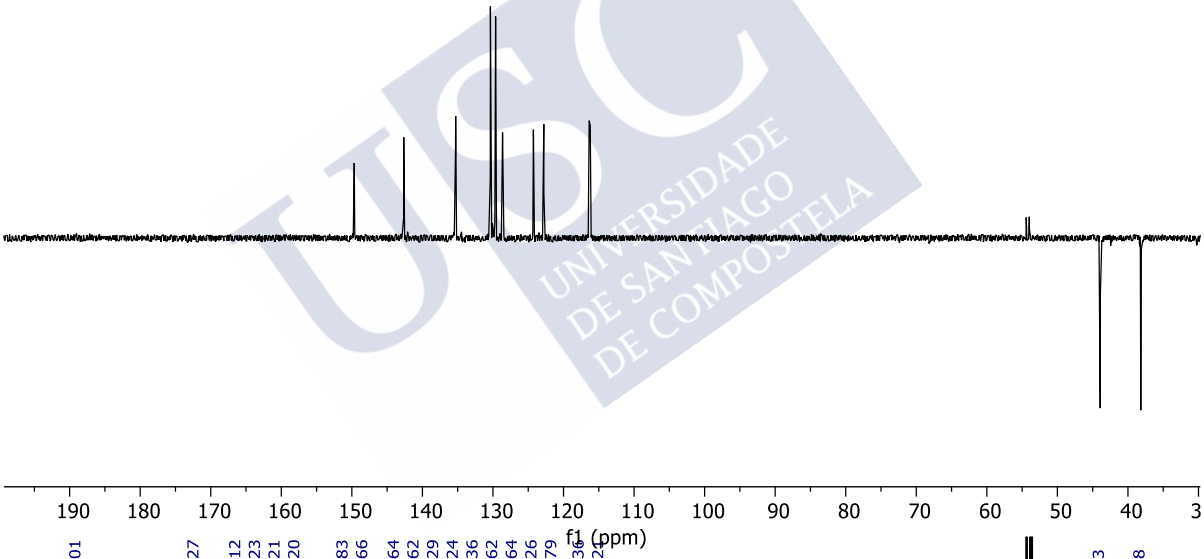

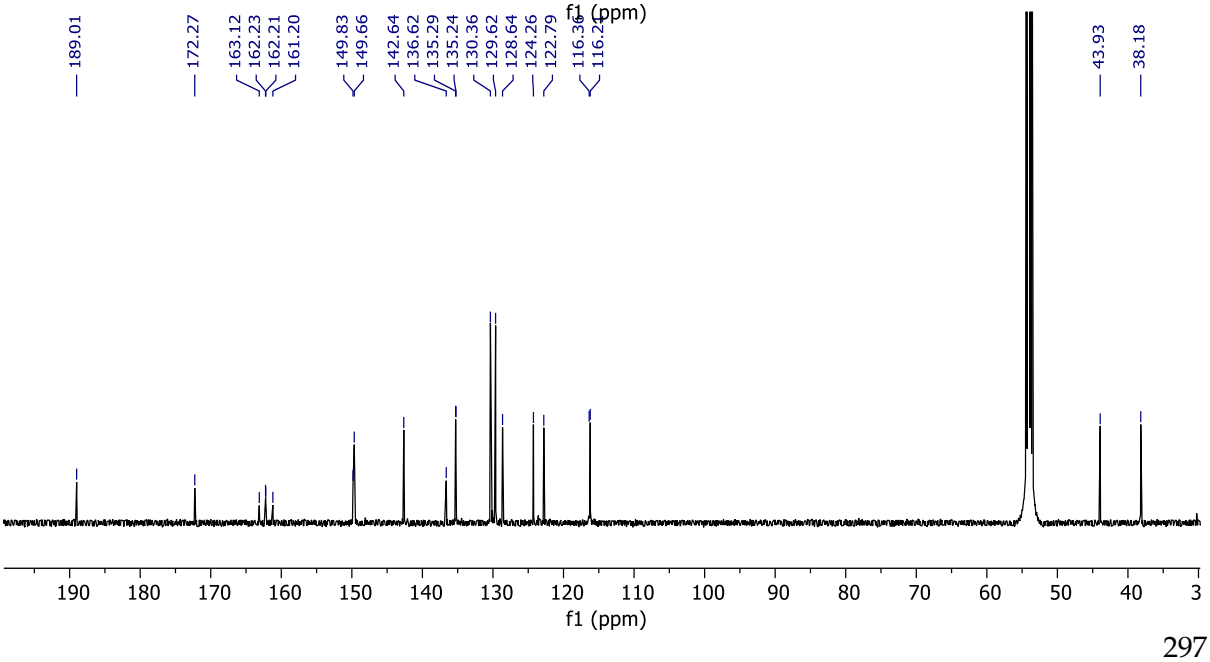

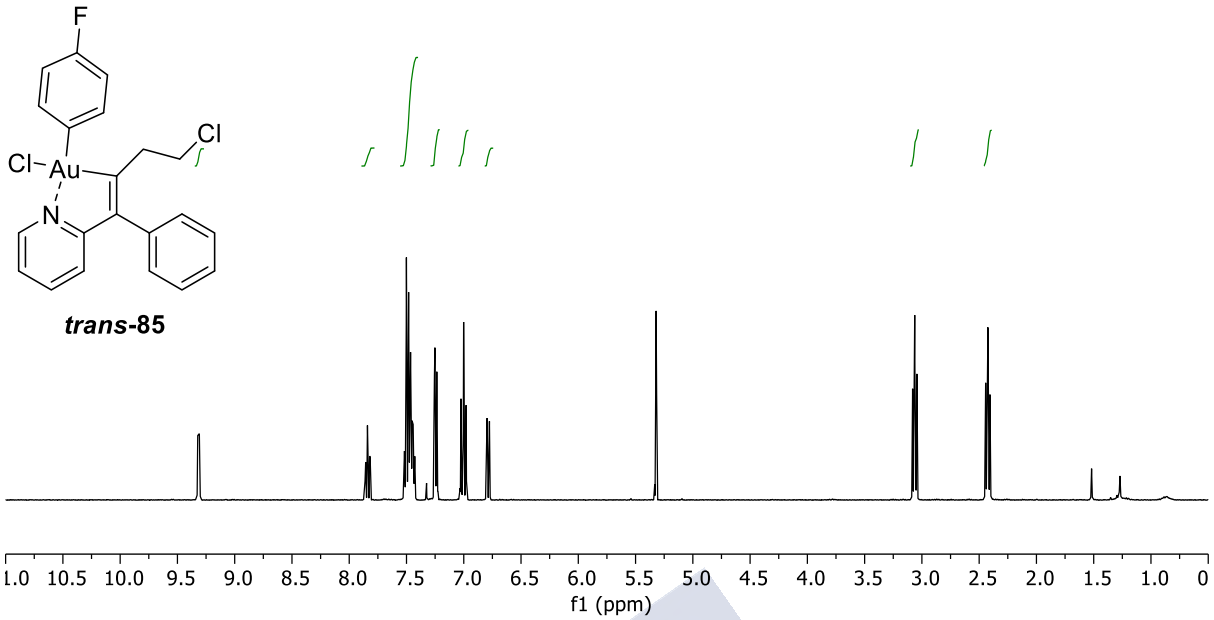
F
Cl
Cl–Au
N
f1 (ppm)

***trans*-85**

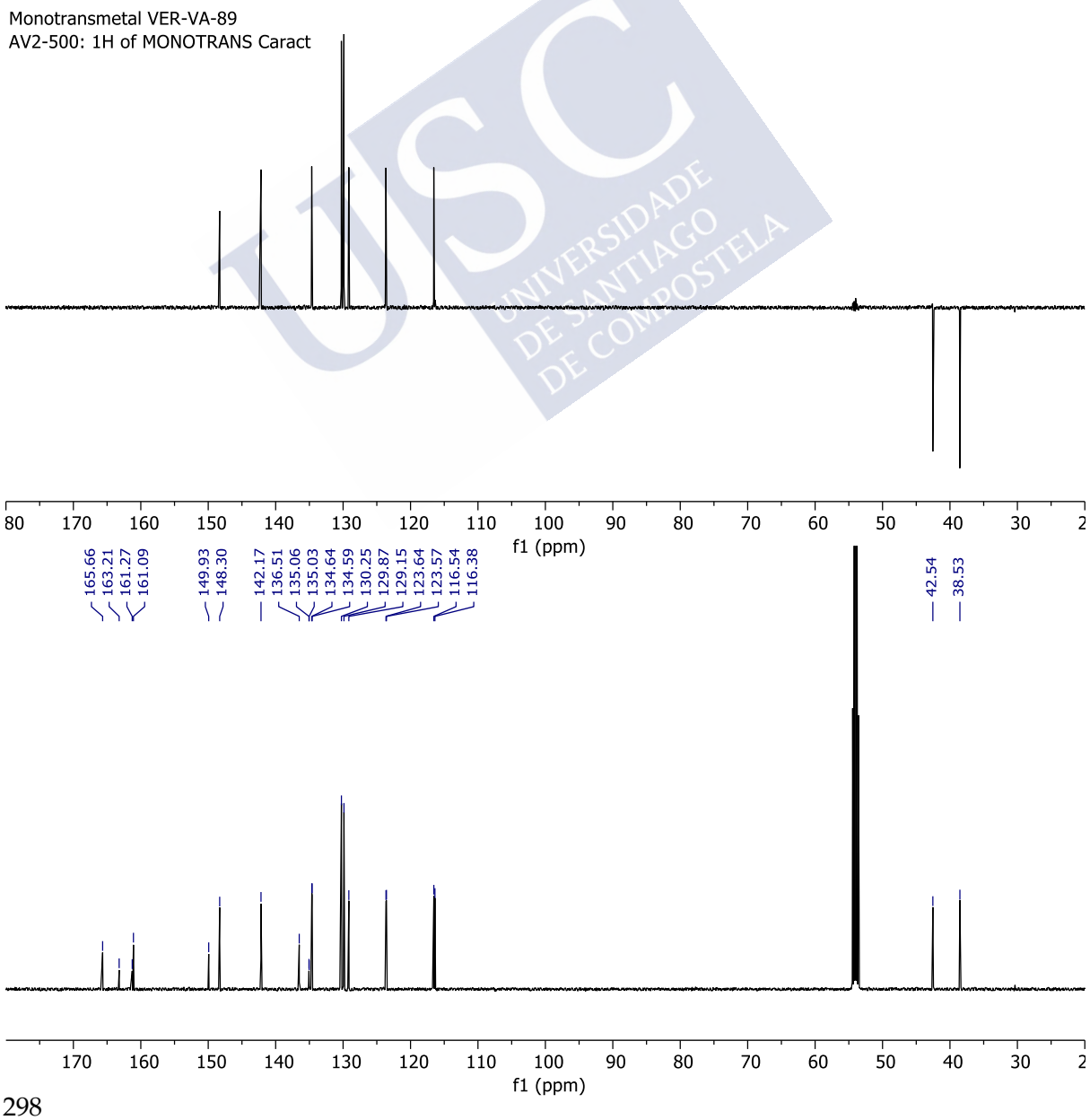
Monotransmetal VER-VA-89
AV2-500: 1H of MONOTRANS Caract
f1 (ppm)
165.66
163.21
161.27
161.09
149.93
148.30
142.17
136.51
135.06
135.03
134.64
134.59
130.25
129.87
129.15
123.64
123.57
116.54
116.38
42.54
38.53
f1 (ppm)

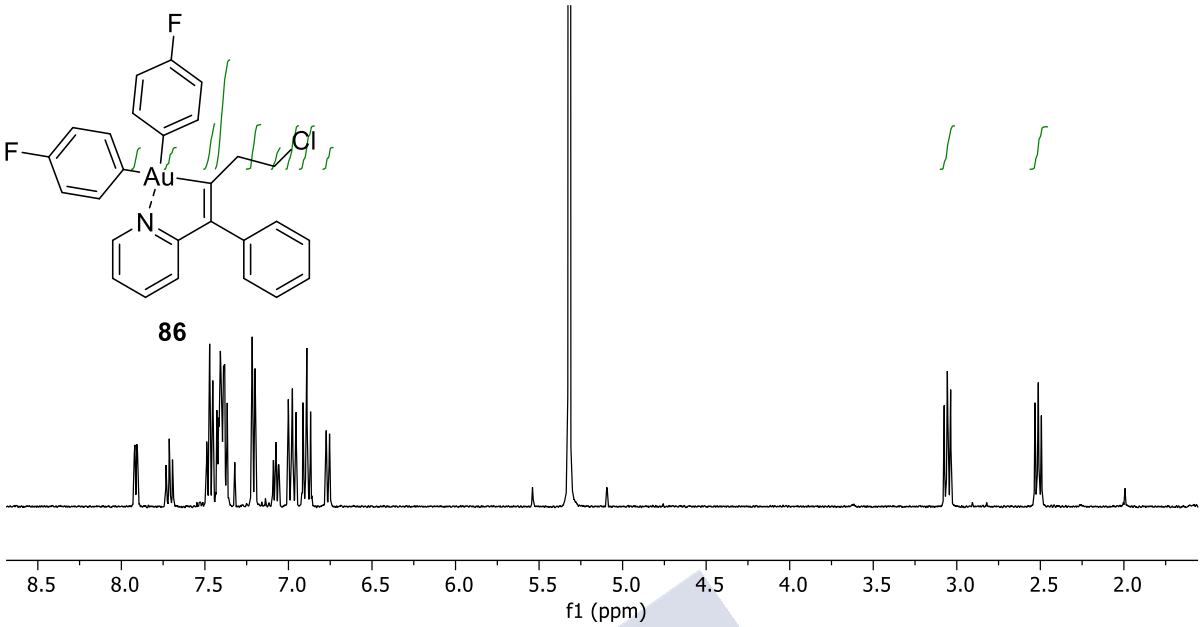

VER-VC-37-FA-carac
AV2-500: 13C{1H} bistransmetal

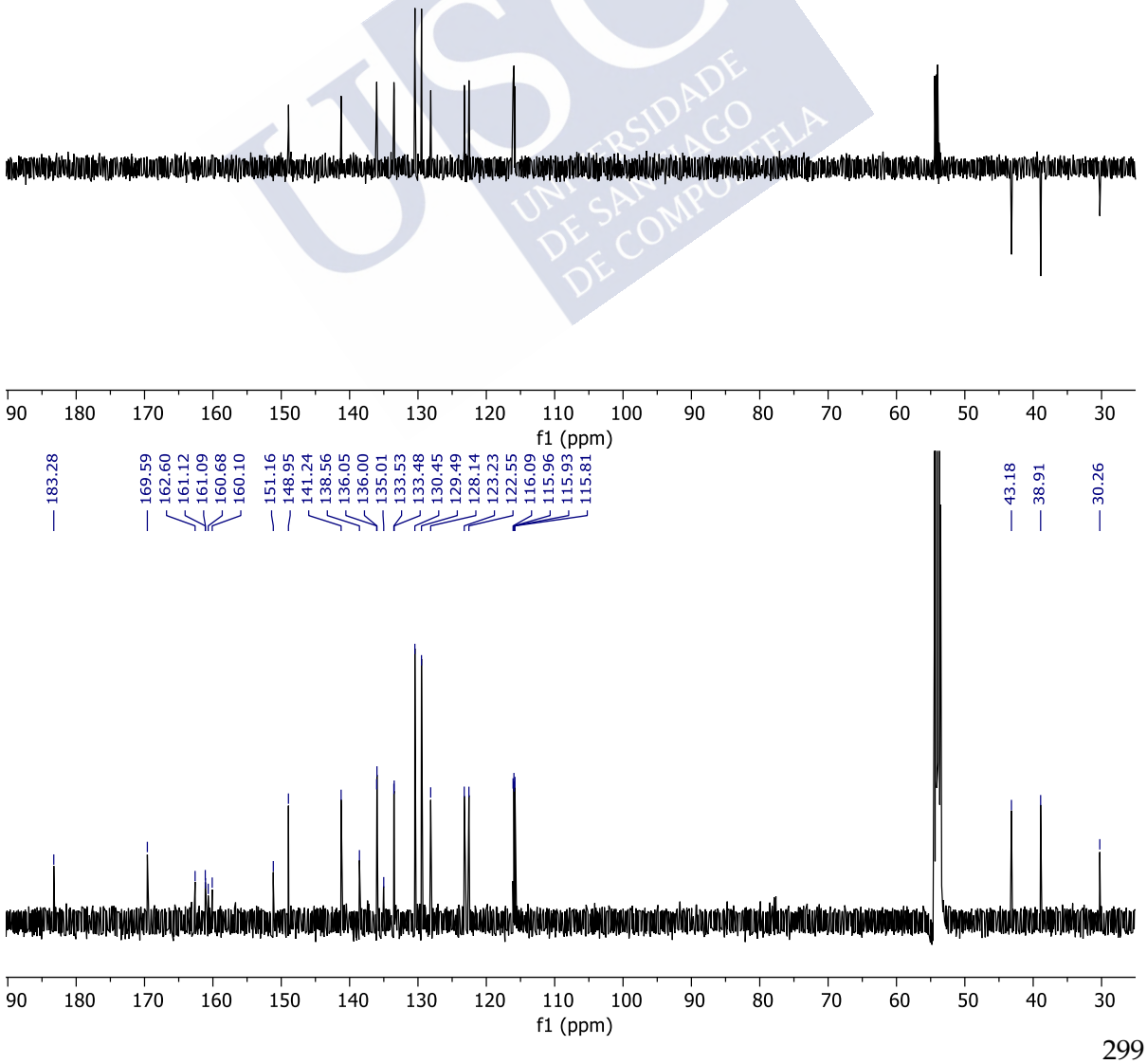

Resumen de la tesis doctoral

En esta memoria de investigación se recogen los resultados obtenidos en los estudios sobre el desarrollo de nuevas reacciones de alquilidenciclopropanos promovidas por metales de transición. Concretamente, el *capítulo I* estudia el desarrollo de reacciones de cicloadición enantioselectiva (3C+2C) y (4C+3C) catalizada por paladio. El *capítulo II* extiende la reacción (3+2) a procesos de heterocicloadición catalizados por paladio para la obtención de diversos sistemas heterocíclicos. En el *capítulo III*, se presentan los resultados obtenidos durante una estancia de investigación realizada el año 2017 en el grupo de la Prof. Cristina Nevado, donde se estudió la reactividad de alquilidenciclopropanos en presencia de precursores de oro (I) y oro (III) de manera estequiométrica.

En primer lugar, en la introducción de esta memoria de tesis se explica el potencial de los alquilidenciclopropanos en procesos de cicloadición. Estas moléculas sencillas, estables, y fáciles de preparar, son capaces de ensamblar una amplia variedad de moléculas complejas en presencia de catalizadores metálicos. Esto es posible por medio de la "activación" de enlaces C-C tradicionalmente inertes, y generar como consecuencia especies reactivas intermedias, las cuales se pueden ensamblar a sistemas insaturados generando estructuras policíclicas diversas. Además, estas reacciones tienen el potencial de formar centros quirales durante el proceso, y si el catalizador metálico es quiral, el proceso de cicloadición puede ser *enantioselectivo*.

Esta tesis doctoral se centra en el uso de reacciones de cicloadición de alquilidenciclopropanos catalizadoras por paladio, por lo que la descripción bibliográfica se centra en procesos que utilizan este metal como promotor. Se hace hincapié en los procesos intramoleculares, que son generalmente menos explorados, más complejos, pero con el potencial de ensamblar esqueletos con múltiples centros quirales. En este sentido, nuestro grupo ha explorado fructíferamente esta química, en particular en reacciones intramoleculares con componentes C-C insaturados, como por ejemplo las reacciones de alquilidenciclopropanos intramoleculares (3+2) con alquenos y (4+3) con dienos. Estas reacciones son capaces de ensamblar moléculas bicíclicas 5-5 y 5-7 de manera rápida y eficiente a partir de precursores lineales de fácil acceso.

Estas reacciones de cicloadición catalizadas por metales de transición son herramientas poderosas para la síntesis de moléculas biológicamente relevantes. Sin embargo, dichos compuestos generalmente tienen utilidad en su forma enantiopura, por lo que el desarrollo de reacciones catalíticas enantioselectivas es fundamental. De manera similar, el desarrollo de metodologías que permitan el ensamblaje de moléculas policíclicas complejas que contienen heteroátomos, es otro desafío importante en la actualidad. Ambas metas son difíciles de conseguir, debido a la inherente complejidad involucrada en dichos procesos.

A continuación, se realiza una breve descripción de los resultados más relevantes obtenidos en esta tesis doctoral.

CAPITULO I: Cicloadiciones enantioselectivas (3C+2C) y (4C+3C) de alquilidenciclopropanos catalizadas por paladio

Reacción de cicloadición enantioselectiva (3+2)

El primer capítulo de esta tesis explora, en primer lugar, el alcance de la cicloadición asimétrica (3+2) entre alquilidenciclopropanos y alquenos catalizada por complejos de paladio-fosforamidito quiral previamente desarrollada por el grupo, en particular por los doctores Juan Durán y Lara Villarino. Estos estudios preliminares se enfocaron en la optimización de las condiciones de reacción y diseñar un ligando quiral fosforamidito adecuado. Así, el complejo formado por el ligando derivado de VAPOL **(S,R,R)-L10** (6 mol%) y el catalizador CpPd(η^3-1-PhC_3H_4) (5 mol%) demostró ser el más eficiente para esta transformación, alcanzando un excelente 90% de rendimiento y 94% ee.

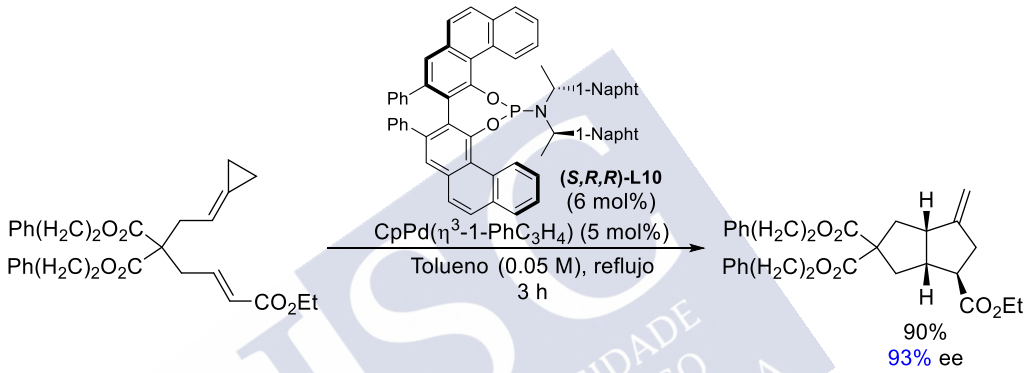

Inicialmente, intentamos reproducir estos resultados reportados sin éxito, alcanzando los excelentes niveles de enantioselectividad reportados, pero con un rendimiento significativamente menor. Pruebas control permitieron identificar el problema: la presencia de trazas de oxígeno afecta la disponibilidad en el medio de reacción del ligando quiral, afectando la eficiencia del proceso. Por esta razón, la previa desoxigenación de la mezcla de reacción, y el aumento de la carga del ligando desde un 6% a un 10% permitieron solucionar los problemas de reproducibilidad.

Con estas nuevas condiciones de reacción, evaluamos el alcance de esta metodología utilizando sustratos con distintas modificaciones estructurales. Los sustratos con un *gem*-diester y un grupo ester en la posición terminal del alqueno (R^3), demostraron ser claves para alcanzar excesos enantioméricos excelentes, alcanzando enantioselectividades superiores al 90%. El uso de alquenos trisustituidos o cadenas de conexión más largas también son compatibles con la reacción, pero la diastereo- y enantioselectividad disminuyeron notoriamente. El uso de otros grupos activantes en la posición terminal del alqueno, como cetonas o amidas, demostró disminuir significativamente la eficiencia del proceso. La reacción mostró una muy buena tolerancia a la presencia de heteroátomos en la cadena, alcanzando buenos rendimientos y excesos enantioméricos. Curiosamente, la ausencia de grupos activantes en el alqueno mostró afectar de manera relevante la reactividad de la reacción. Es importante destacar que la reacción muestra, en general, una alta selectividad *syn* en la fusión de los anillos.

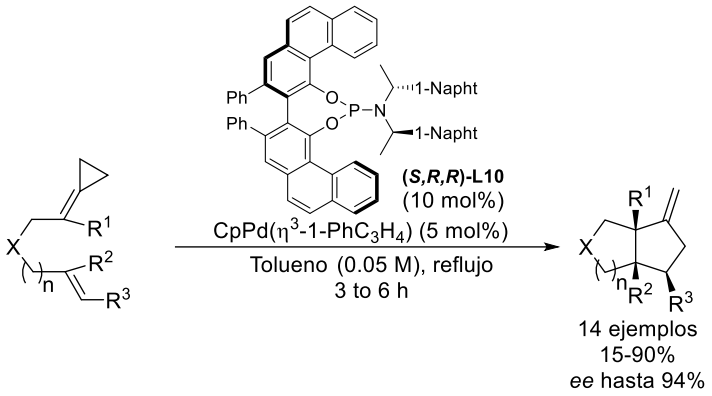

Reacción de cicloadición enantioselectiva (4+3)

La segunda parte del capítulo I explora el desarrollo de una variable enantioselectiva de la reacción (4+3) entre alquilidenciclopropanos y dienos conjugados, previamente desarrollada por el grupo. Este trabajo, reportado en 2007, explora principalmente la reacción de manera racémica, pero reporta tres ejemplos enantioselectivos utilizando un ligando fosforamidito quiral de estructura sencilla, alcanzando buenos rendimientos pero enantioselectividades moderadas de hasta un 64%.

La investigación en esta tesis doctoral se enfocó principalmente en encontrar un ligando fosforamidito quiral que sea capaz de proveer los biciclos 5-7 tipo de manera selectiva con respecto al subproducto competitivo (3+2), y con alta enantioselectividad. Después de una extensa evaluación de ligandos y condiciones de reacción encontramos que, a diferencia de la reacción (3+2), este proceso requiere un ligando mucho más sencillo. Así, el uso de un catalizador formado por Pd_2dba_3 (5 mol%) el fosforamidito **(*S,R,R*)-L4** (14 mol%) en dioxano a reflujo, permitió obtener los cicloaductos fusionados de siete miembros con alta selectividad, rendimiento y exceso enantiomérico

El alcance de esta reacción fue evaluado usando distintos alquilidenciclopropanos. Similar a la reacción asimétrica (3+2), esta cicloadición funciona de manera eficiente alcanzando excelentes rendimientos y excesos enantiomericos cuando un grupo *gem*-diester une la cadena y un ester en la posición terminal actúa como grupo activante. Es posible sintetizar sintetizar productos fusionados con centros cuaternarios en la fusión de anillos con hasta un 94% ee (R^1 = Me). La reacción tambien tolera heteroátomos (O) y el uso de dienos no activados, sin embargo los rendimientos y enantioselectividades son menores.

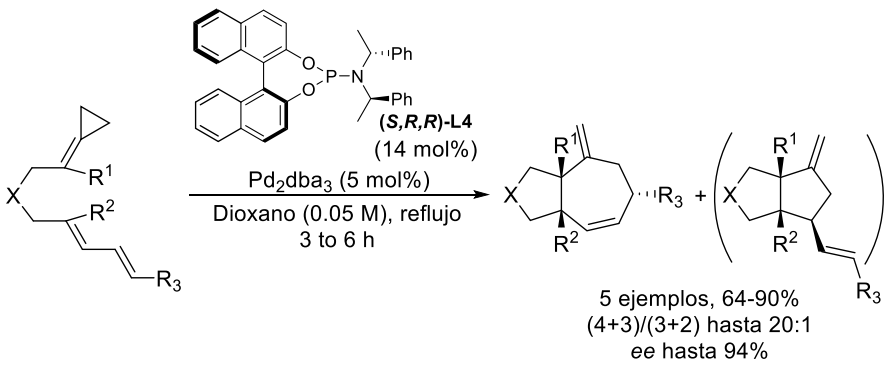

CAPÍTULO II: Heterocicloadiciones (3+2) de alquilidenciclopropanos catalizadas por paladio

Cicloadición (3+2) para formar anillos nitrogenados de 5 miembros

En este segundo capítulo se aborda la síntesis de sistemas cíclicos nitrogenados u oxigenados por medio de reacciones de cicloadición de alquilidenciclopropanos catalizadas por paladio. Esto es de particular importancia, ya que amplia variedad de moléculas biológicamente relevantes posee sistemas policíclicos complejos con anillos heterocíclicos de cinco miembros.

En primer lugar, se describen las metodologías descritas en la literatura donde, a pesar de existir variados métodos para el ensamblaje de este tipo de moléculas, estos están limitadas mayoritariamente a versiones intermoleculares que permiten la construcción de un único anillo. En este contexto, existen cuatro reportes de reacciones de heterocicloadición (3+2) de alquilidenciclopropanos, utilizando aldehídos para sistemas oxacíclicos e iminas, aziridinas o azocarboxilatos para sistemas azacíclicos. Todos estos precedentes son intermoleculares, y presentan limitantes importantes, exhibiendo muy baja eficiencia y alcance limitado.

La cicloadición intramolecular de alquilidenciclopropanos es una alternativa atractiva para el ensamblaje de sistemas policíclicos, como se mostró en el capítulo I, ya que son moléculas estables y fáciles de sintetizar. En principio, el uso de alquilidenciclopropanos conectados a sistemas insaturados nitrogenados u oxigenados, permitiría acceder directamente a pirrolidinas y tetrahidrofuranos fusionados, de manera análoga a la reacción con alquenos.

Primero se evaluó la versión nitrogenada de la cicloadición utilizando las condiciones óptimas reportadas para la cicloadición (3+2) entre alquilidenciclopropanos y alquenos. Este estudio se realizó en colaboración con el estudiante de doctorado Ricardo Rodiño. Las iminas demostraron no ser grupos funcionales adecuados para esta reacción, formando mezclas de subproductos diénicos indeseados. Por otra parte, el uso de éteres de oxima permitió obtener las pirrolidinas fusionadas deseadas, alcanzando rendimientos cercanos al 70% bajo condiciones óptimas de reacción (6 mol% Pd_2dba_3, 13 mol% L1, tolueno, 90 ^oC). Curiosamente, el ligando tipo dialquil biarilfosfina RuPhos también promueve la reacción con una eficiencia similar a **L1**.

El alcance de esta metodología se evaluó utilizando distintos sustratos análogos con variaciones estructurales, bajo las óptimas de reacción. Lamentablemente el proceso demostró ser extremadamente sensible a variaciones estructurales, mostrando en todos los casos bajas conversiones y la formación de subproductos no deseados. De forma paralela al desarrollo de la versión racémica, se estudió la variante asimétrica de esta reacción. El uso de condiciones muy similares a la descritas para la reacción asimétrica (3+2) con alquenos (Capítulo I) mostró promover la cicloadición enantioselectiva de manera eficiente. Rendimientos y excesos enantioméricos excelentes fueron observados al utilizar el isómero *E* de la oxima, alcanzando hasta un 94% ee. Lamentablemente, al evaluar el alcance de esta variante asimétrica, la metodología mostró similares limitaciones observadas a la reacción racémica.

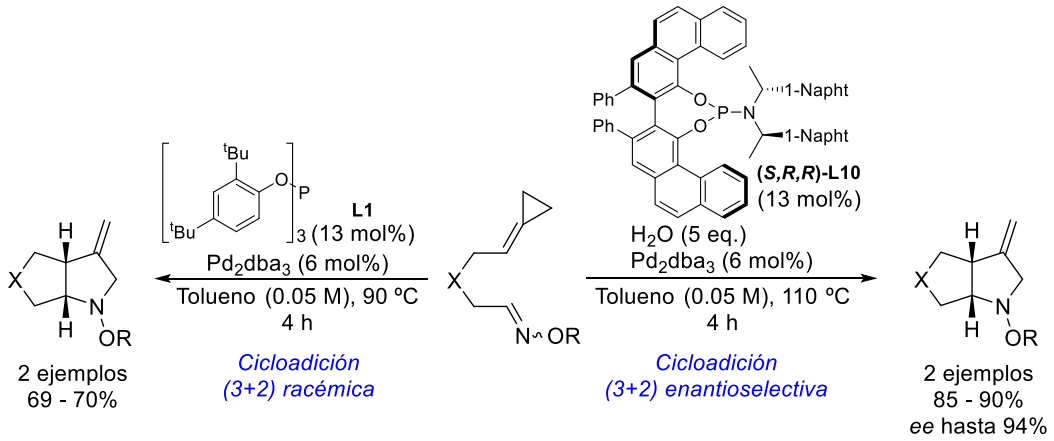

Cicloadición (3+2) para formar anillos oxigenados de 5 miembros

La síntesis de sistemas tetrahidrofuránicos fusionados fue estudiada preliminarmente utilizando alquilidenciclopropanos enlazados a aldehídos en presencia de precatalizadores de paladio y ligandos de distintas características electrónicas. Curiosamente, a diferencia de las reacciones previamente descritas, esta cicloadición requiere el uso de ligandos de tipo dialquil biaril fosfina (BrettPhos para aldehídos) para formar los correspondientes cicloaductos tetrahidrofuránicos de manera eficiente, alcanzando rendimientos y selectividad excelentes. Por otra parte, sustratos análogos de tipo cetona también reaccionaron eficientemente, pero en este caso, ligando RuPhos fue necesario. Esta última reacción demostró ser más robusta que la cicloadición con aldehídos, exhibiendo una gran tolerancia a distintos grupos funcionales. Así, una amplia variedad de tetrahidrofuranos fusionados con centros quirales cuaternarios en la posición alfa al oxígeno fue obtenida con altos rendimientos y una diastereoselectividad excepcional.

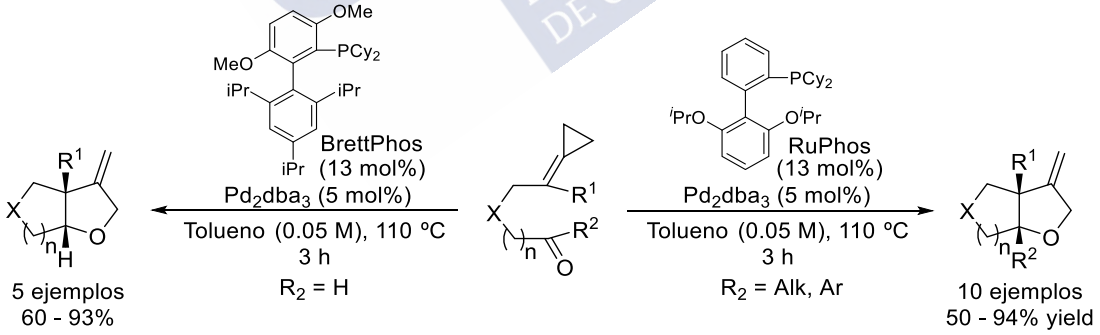

Para evaluar la utilidad práctica de los productos obtenidos, algunos de los cicloaductos obtenidos fueron sometidos a diversas manipulaciones sintéticas. En particular, la hidrogenación catalizada por rodio permitió la obtención de un producto con tres centros quirales con excelente rendimiento y buena selectividad (90%, dr = 6 : 1). Por otra parte, una ruptura oxidativa permitió la obtención de una cetona (60%) y la oxidación utilizando selenio o cromo permitió la síntesis de una atractiva variedad de α-metilenbutirolactonas fusionadas en buenos rendimientos. Estos compuestos son muy interesantes desde un punto de vista biológico, pero su síntesis es en general muy compleja por métodos tradicionales.

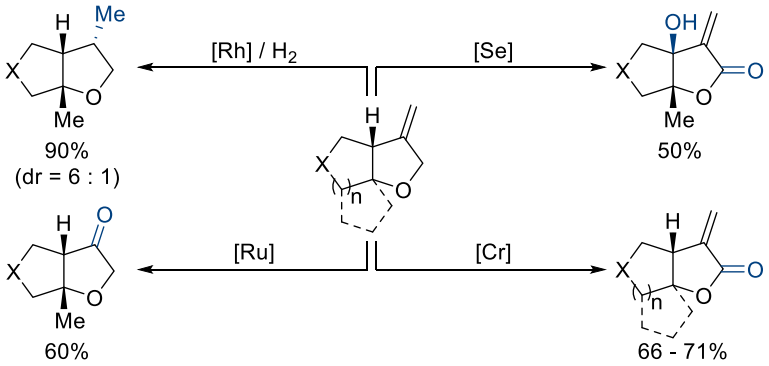

De manera preliminar, también se estudió la cicloadición (3+2) intermolecular entre alquilidenciclopropanos y compuestos carbonílicos, en colaboración con el estudiante de doctorado Eduardo Da Concepción. Después de una extensa investigación, encontramos que el mismo sistema catalítico utilizado para la cicloadicion (3+2) intramolecular con cetonas (Pd_2dba_3 (5 mol%) y RuPhos (13 mol%)), es capaz de promover de manera eficiente la reacción intermolecular con 2,2,2-trifluorocetonas. Sin embargo, a pesar de los excelentes rendimientos globales observados, los productos obtenidos fueron obtenidos como mezclas de diastereoisómeros con una baja selectividad, alcanzando como máximo un dr = 1.8 : 1.

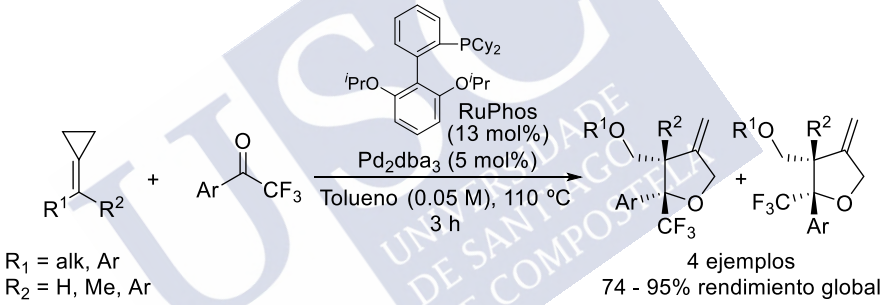

ANEXO: Reacciones Tandem de cicloisomerización de alquilidenciclopropanos catalizadas por paladio

Durante la exploración preliminar de la variante enantioselectiva de la reacción (3+2) con aldehídos y cetonas, se obtuvieron subproductos de cicloisomerización que sugieren la formación de especies zwitterionicas de tipo **A**. Estos intermedios podrían reaccionar de diversas maneras. Por una parte, el alcóxido formado puede actuar como base o como nucleófilo y, por otra parte, el π-alilo de paladio puede actuar como electrófilo siendo útiles para la adición de distintos nucleófilos en procesos tándem.

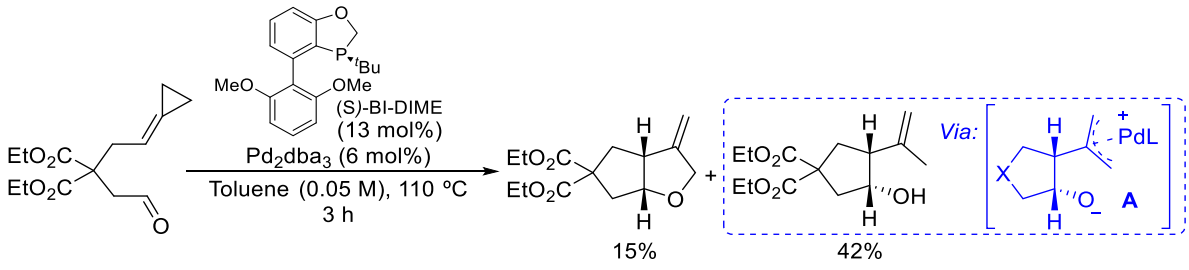

En base a esta hipótesis, se estudió la viavilidad de desarrollar reacciones tandem de cicloisomerización de alquilidenciclopropanos catalizadoras por paladio. En primer lugar, se intentó acoplar esta cicloisomerización a una reacción de acomplamiento cruzado de tipo Suzuki con ácidos borónicos. La reacción mostró una gran eficiencia, y curiosamente en este caso, se requiere el uso de ligandos electrodeficientes a diferencia de la cicloadición (3+2). La optimización de la reacción demostró que una combinación de Pd_2dba_3, la fosfina **L18**, y K_3PO_4 en dioxano a reflujo, la reacción transcurre con una alta eficiencia, formando los productos cíclicos en rendimientos de buenos a excelentes.

Una vez optimizada la reacción, se evaluó el alcance de la reacción utilizando distintos ácidos borónicos y sustratos de tipo cetona-alquilidenciclopropano. La reacción mostró tener una alta tolerancia a ácidos borónicos de distinta naturaleza y al uso de distintos sustratos con distintas características estructurales. Los productos son obtenidos en buenos rendimientos y con diastereoselectividad total en todos los casos.

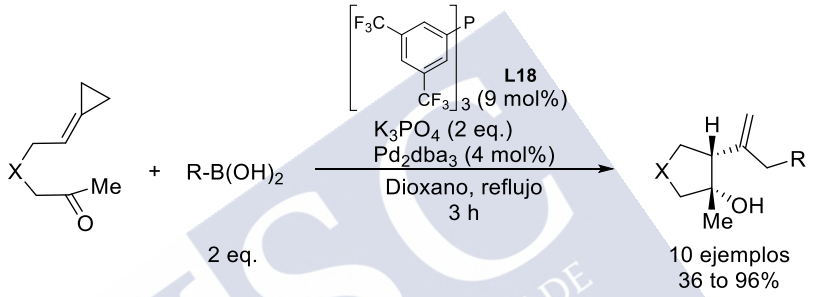

De manera preliminar, se estudió también el uso de distintos nucleófilos para reacciones de tipo cicloisomerización/adición nucleofílica. Despues de un extenso estudio utilizando diversos nucleófilos (haluros, aminas, amidas, alcóxidos, etc.), encontramos que los malonatos son capaces de adicionarse al sistema π-alílico de paladio de manera eficiente, obteniéndose el producto de adición esperado cuando K_2CO_3 es usado como base. Curiosamente, un producto lactónico con tres estereocentros es formado de manera totalmente diastereoselectiva y con buen rendimiento cuando K_3PO_4 fue utilizado. Pruebas control demostraron que estos productos están relacionados, donde el producto de adición evoluciona hacia la lactona a través de una transesterificación intramolecular.

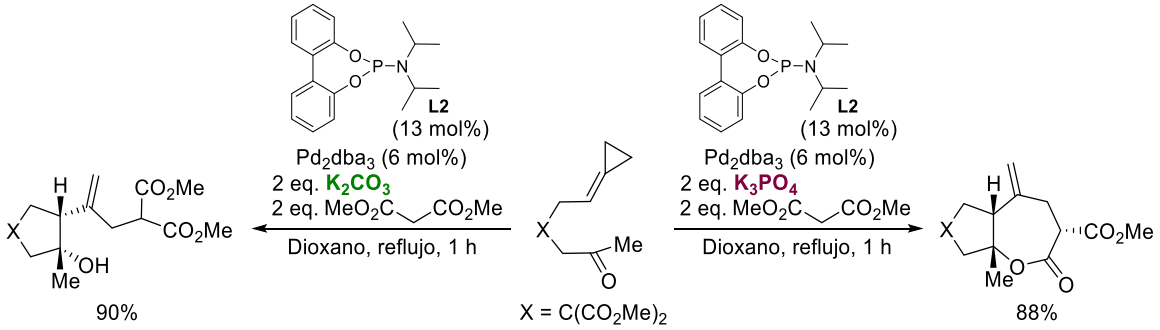

Los resultados obtenidos preliminarmente en estas nuevas cicloisomerizaciones tándem son prometedores. En este sentido, la investigación estará dirigida a la extensión del alcance de ámbos procesos tándem, así como también extender esta reactividad a aldehídos. Por otra

parte, se estudiará el uso de otros nucleófilos más complejos, como también el desarrollo de variantes asimétricas de estas nuevas transformaciones.

CAPITULO III: Especies ciclometaladas de oro (III) por medio de la apertura de anillo de 2-(ciclopropilidenmetil)piridinas

En el tercer capítulo se describe la relevancia de la química de oro, y los avances significativos que ha presentado este campo durante las últimas décadas. En este contexto, se hace hincapié en el estudio de la reactividad de diversos complejos de oro (I), en particular en sus caracteríscticas carbofílicas excepcionales en catálisis homogénea, y en como las especie de oro (III) han sido significativamente menos exploradas. Esto, en particular por su menor carbofilia, dificil acceso y alta inestabilidad. En efecto, los complejos de oro (III) más estudiados utilizan ligandos tipo pinza capaces de estabilizar fuertemente estos compuestos metálicos, y sus aplicaciones más destacadas son en el campo de química de materiales, química biológica y química organometálica.

En esta última área de estudio, la Dra. Cristina Nevado de la universidad de Zürich tiene amplia experiencia, utilizando estos complejos para estudiar procesos químicos complejos relacionados a reacciones organometálicas. Durante 2017, realicé una estancia de investigación en este grupo, donde nos propusimos como objetivos estudiar la reactividad de 2-(ciclopropilidenmetil)- piridinas en reacciones de C-H y C-C activación utilizando precursores de oro (I) y oro (III) respectivamente.

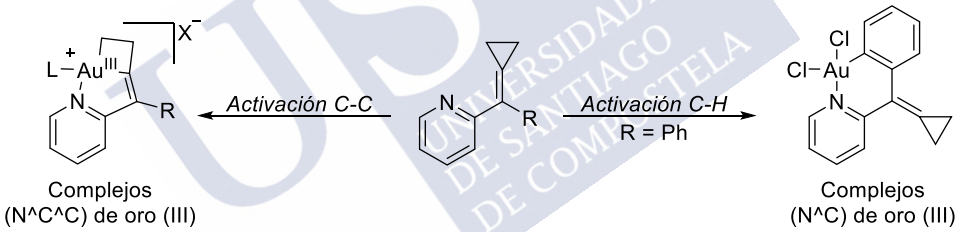

Los alquilidenciclopropanos en presencia de precursores de oro (I) no dieron los resultados esperados, observandose solo la coordinación a la piridina o descomposición en el caso de generar especies catiónicas más reactivas. Sin embargo, los precursores de oro (III) mostraron una reactividad inesperada, formando tres tipos diferentes de ciclometalados de oro (III), obtenidos en buenos rendimientos y en condiciones suaves de reacción. En este sentido, es importante destacar que en la literatura actual los métodos disponibles para la síntesis de complejos ciclometalados de oro (III) implican el uso de metales pesados de forma estequiométrica o condiciones agresivas de reacción, mientras que la reacción con alquilidenciclopropanos requiere el uso de simples sales de oro a temperatura ambiente.

De esta manera, complejos de oro (III) cadena abierta, son obtenidos por medio de un mecanismo no descrito, que está siendo estudiado en profundidad por el grupo de la Dr. Nevado. Por otra parte, los complejos espirociclicos son formados por medio de un mecanismo carbocatiónico previamente reportado en la literatura para vinilpiridinas, que ha sido reportado como un caso aislado e involucra el uso de altas temperaturas y la obtención de bajos rendimientos. Finalmente, un complejo ciclobutánico de oro fue también aislado en bajo rendimiento, producto de una reacción de expansión de anillo del alquilidenciclopropano. La mayoría de estos compuestos fueron cristalizados y caracterizados por análisis de RMN y

difracción de rayos X. Adicionalmente, experimentos control demostraron que esta reactividad es exclusiva de los alquilidenciclopropanos, sugiriendo que la liberación de la tensión anular del sistema ciclopropánico conduce la reacción.

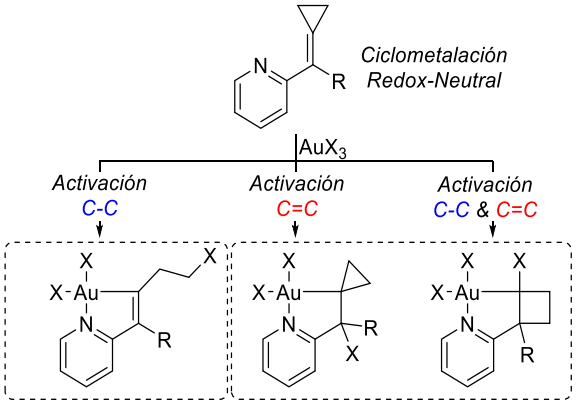

De manera preliminar, se estudió la reactividad de los complejos ciclometalados de cadena abierta en reacciones de transmetalación con ácidos borónicos. El uso del ácido 4-fluorofenil borónico en combinación con fosfato potásico tribásico (K_3PO_4) permitió la obtención de distintas especies ciclometaladas en buenos rendimientos. Estudios control sugieren que existe una relación directa en la formación de ambos compuestos monotransmetalados, donde el isómero *cis* está cinéticamente favorecido en la primera transmetalación, a partir del cual se obtiene el isómero *trans* por medio de una reacción de isomerización. Además, la evidencia experimental apunta a que este isómero (*trans*) es el que evoluciona más favorablemente hacia la especie bisciclometalada. Estos se pueden explicar por el fuerte efecto *trans* de los complejos reactivos en cada etapa, que fue confirmado por medio del análisis de la estructura cristalina de los complejos implicados en estas reacciones.

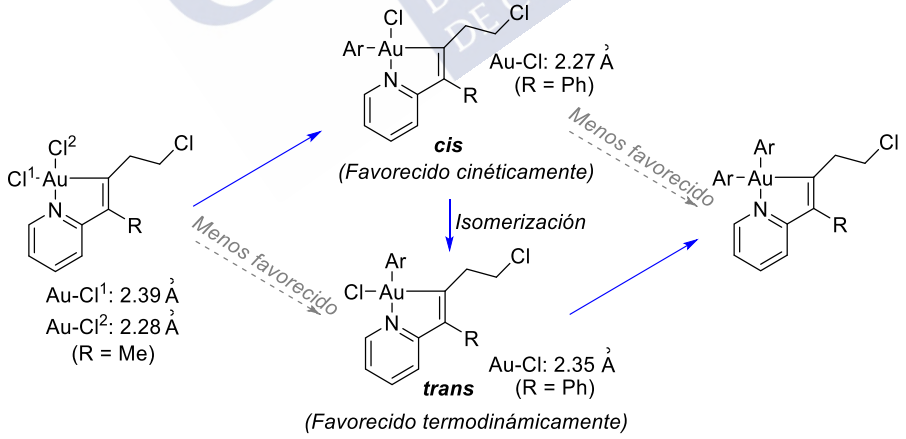

Finalmente, se estudió de manera preliminar la etapa de eliminación reductora a partir del complejo monotransmetalado *trans* y el bistransmetalado. Ambos, de manera separada, formaron el producto de acoplamiento cruzado en rendimientos bajos. Sin embargo, este estudio demuestra la factibilidad del potencial de esta química en el eventual desarrollo de reacciones catalíticas oro (I) – oro (III) de acomplamiento cruzado mediante reacciones de C-C activación, proceso que hasta el día de hoy no ha sido reportado.

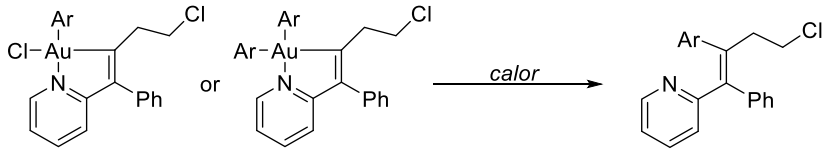

Conclusión general

El primer capítulo de esta tesis describe el desarrollo de cicloadiciones enantioselectivas (3+2) y (4+3) utilizando alquilidenciclopropanos en presencia de catalizadores de paladio (0) - fosforamidito quiral. Productos bicíclicos de tipo 5-5 y 5-7 son obtenidos con rendimientos y excesos enantiomericos excelentes en varios casos, sin embargo la eficiencia de estos proceso depende significativamente de la arquitectura de los sustratos.

El segundo capítulo describe el desarrollo de reacciones de heterocicloadición intramolecular (3+2) de alquilidenciclopropanos. El uso de oximas en presencia de un catalizador de paladio (0) – fosfito permite obtener pirrolidinas bicíclicas con buen rendimiento, pero el alcance está limitado a 2 ejemplos. Una variable enantioselectiva también fue desarrollada utilizando fosforamiditos quirales, pero exhibe las mismas limitaciones que la variante racémica. En contraste, la síntesis de tetrahidrofuranos fusionados es posible de manera eficiente utilizando aldehídos y cetonas en combinación con un sistema de paladio (0) – dialquil biaril fosfina, y ha demostrado ser una reacción robusta y de amplio alcance. Adicionalmente, una variante intermolecular fue preliminarmente desarrollada, alcanzando muy buenos rendimientos, pero una diastereoselectividad pobre.

Durante el desarrollo de una variante enantioselectiva de la reacción de (3+2) intramolecular con aldehídos y cetonas, se identificaron subproductos que dieron indicios sobre la participación de intermedios zwitteriónicos no vistos previamente en esta química. Como anexo al capítulo II, se estudió la reactividad de estos intermedios hipotéticos por medio de la adición de distintos nucleófilos, de manera exitosa. Dos nuevos tipos de reacciones de cicloisomerización tándem han sido preliminarmente desarrolladas, y se encuentran en la actualidad en pleno desarrollo.

Finalmente, el capitulo III explora la reactividad de alquilidenciclopropanos de tipo 2-(ciclopropilidenmetil)piridinas en presencia de sales de oro (III) de manera estequiométrica. De manera inesperada, nuevas reacciones de ciclometalación fueron descubiertas, en condiciones inesperadamente suaves de reacción. Particularmente interesantes, complejos de cadena abierta son obtenidos, los cuales son formados por medio de un mecanismo no reportado que es en la actualidad, estudiado por el grupo de la Dr. Nevado. Se ha estudiado de manera preliminar la reactividad de estos complejos en procesos de transmetalación y eliminación reductora, demostrando la viabilidad del potencial desarrollo de reacciones de acoplamiento cruzado.